

**Mobile-to-Mobile Cooperative
Communication Systems: Channel Modeling
and System Performance Analysis**

Batool Talha

**Mobile-to-Mobile Cooperative
Communication Systems: Channel Modeling
and System Performance Analysis**

Doctoral Dissertation for the Degree *Philosophiae Doctor (PhD)* in
Information and Communication Technology

University of Agder
Faculty of Engineering and Science
2010

Doctoral Dissertation by the University of Agder 26

ISBN: 978-82-7117-674-7

ISSN: 1504-9272

©Batoool Talha, 2010

Printed in the Printing Office, University of Agder
Kristiansand

Preface and Acknowledgements

This dissertation is a result of the three and half years (September 2006 - May 2010) research carried out at the Information and Communication Technology (ICT) Department, Mobile Communications Group of University of Agder (UiA) in Grimstad, Norway. This work is the part of the project entitled “Mobile-to-Mobile Communication Systems (M2M)” funded by the Norges Forskningsråd (NFR, Norwegian Research Council).

The monumental task of crossing the finishing line of this dissertation involved the technical and emotional contribution of many individuals. I would, therefore, like to take this opportunity to express my gratitude to those.

First of all, I would like to thank Almighty Allah for giving me enough strength to stay on the path going towards the completion of this work. HE provided me with favorable conditions to bring this effort to a good end. The successful conclusion of my dissertation is one of HIS blessings for which I am obliged.

The excellent guidance, active involvement, extensive cooperation, encouragement, and constant support of my supervisor Prof. Matthias Pätzold during the course of my dissertation deserve special appreciation. I am thankful to the members of my evaluation committee, Professor Claes Beckman (University of Gävle, Sweden), Dr. Mischa Dohler (Centre Tecnològic de Telecomunicacions de Catalunya, Spain), and Associate Professor Frank Li (UiA, Norway) for their time to give my dissertation a thorough reading. Their constructive feedback helped in improving the overall quality of the manuscript. I would like to acknowledge all the help provided in administrative matters by the Project Secretary of the MCG, Mrs. Katharina Pätzold. It would be unfair if I do not mention the assistance provided by the Coordinator of the PhD program in the ICT department of UiA, Mrs. Trine Tønnessen, in several formalities associated with our PhD program.

While I was in Norway for my doctoral studies, my family (i.e., parents and sisters) was in Pakistan. However, during my stay in Norway, I have made such great friends who seem to be my family in Norway. I'll start with my friends/fellow doctoral students who are and were members of MCG, i.e., Adrian Gutierrez, Akmal Fayziyev, Ali Chelli, Bjørn Olav Hogstad, Dmitry Umansky, Gulzaib Rafiq, Nurilla Avazov, and Yuanyuan Ma. Their lovely, friendly, and un-selfish personalities created a very comfortable working environment around me. They were always available to answer my questions and I have learnt a lot from the extremely beneficial technical discussions with them. All of them are worthy of a very special round of applause. A bunch of friends with whom I was enjoying different recreational activities include Chee Lim Nge, Liping Mu, Martin Choux, Morten Kollerup Bak,

and Ram Kumar along with Adrian, Dmitry, Nurilla as well as Yuanyuan. I can not forget to mention the hospitality of Anis Yazidi and Zia-ul-Haq Abbas. The credit of translating the press release from English to Norwegian for me goes to Terje Gjørseter. My sincere gratitude goes to all the doctoral fellows at the ICT department of UiA especially to those mentioned above. Thank you all for being such wonderful friends!!!

Professor Hayder Radha and Professor Mostafa Kaveh hosted me for summer internships at Michigan State University, U.S.A. and University of Minnesota, U.S.A., respectively. I want to thank both these professors for giving me the chance to have an immense learning experience. A note of appreciation goes to Professor Serguei Primak (University of Western Ontario, Canada) for his inspiring ideas and thought-provoking questions in the context of my research, which compelled me to see different sides of the picture. I am grateful to the wishes and support of all my friends from De-21 Electrical along with Gävle Masters Class of 2004-05.

The loving, encouraging, and supporting role of my parents, Shahla and Talha; and my sisters, Monazza and Sanaa; throughout my life in general and during my doctoral studies in particular, can not go without being praised. Earnest thanks to them for having confidence in me and praying for my success all the time. I give a lot of credit to Ammi (my mother), Shahla, for who I am and where I am in my life. Thank you and love you, Ammi!!!

Batool Talha
September 2010
Rawalpindi, PAKISTAN

Summary

In recent years, there has been an upsurge of interest towards two wireless communication technologies, namely cooperative communications and mobile-to-mobile (M2M) communications. The reason being that cooperative systems bring with them many advantages such as enhanced performance in terms of increased pathloss, diversity as well as multiplexing gains, balanced quality of service (QoS), infrastructure-less deployment, and reduced operational costs. On the other hand, applications targeted to reduce traffic accidents as well as to facilitate the flow of traffic, provision of in-vehicle internet access, support for convoy driving, automatic driving, and speed regulation etc are to name some few utilities of M2M communications. The efforts to profit from the benefits of both technologies have resulted in the emergence of M2M cooperative communication systems.

The design, development, performance analysis, and test of such communication systems, however, call for a profound insight of the most important characteristics of real-world propagation environments. It is widely acknowledged that field trails for performance evaluation purposes are both expensive and time inefficient. It is therefore, inevitable to find cost effective alternative. Reproduction of the desired channel characteristics by computer simulations is one such option. It is, nonetheless, imperative as well as highly desirable that the channel models are accurate enough to reflect the fading statistics of real-world channels. For this reason, a major portion of this dissertation presents the state-of-the-art regarding the modeling and analysis of a large variety of M2M fading channels in cooperative systems.

We model and analyze narrowband M2M fading channels in cooperative networks under non-line-of-sight (NLOS) as well as line-of-sight (LOS) propagation conditions. The motivation behind modeling M2M channels with LOS components comes from the fact that such models are flexible enough to accommodate asymmetric channel conditions associated with many practical propagation scenarios. Besides, LOS fading channel models easily reduce to those models that correspond to NLOS propagation conditions. In addition, two different kinds of channel models, i.e., geometry-based models and non-geometrical models are studied. The statistical characterization of geometry-based channel models is carried out in terms of the temporal autocorrelation function (ACF) and space-time cross-correlation functions (CCFs). For non-geometrical models statistical quantities, such as the probability density function (PDF), cumulative distribution function (CDF), level-crossing rate (LCR), and average duration of fades (ADF) are discussed in detail.

An interesting idea has started to gain recognition is that in addition to the

knowledge of the propagation channel characteristics, a sound understanding of the channel capacity is also indispensable to meet the data rate requirements of future mobile communication systems. Recently, some researchers have demonstrated techniques to optimize the network performance with the help of the LCR of the channel capacity. Inspired by this work, we include, in this dissertation, a thorough evaluation of the channel capacity statistics of M2M fading channels in cooperative networks.

Without discussing the performance of M2M cooperative communication systems under different propagation environments, this study seems to be unfinished. Thus, for the sake of completeness, we utilize several measures such as the statistics of the instantaneous signal-to-noise ratio (SNR), average bit error probability (BEP), amount of fading (AOF), and outage probability to determine the performance of the said systems. We believe that the performance assessment reported here bridges the gap between the derived M2M channel models and their impact on the performance of the deployed cooperative systems.

Contents

List of Figures	xviii
Abbreviations	xix
1 Introduction	1
1.1 Cooperative Communication Systems	1
1.2 M2M Communication Systems	3
1.3 Organization of the Dissertation	5
2 Statistical Modeling and Analysis of Narrowband M2M Fading Channels Under NLOS Propagation Conditions	9
2.1 Introduction	9
2.1.1 Statistical Characterization of Geometry-Based Channel Models	9
2.1.2 Statistical Characterization of Fading Channels	11
2.1.2.1 Fading Channels in Systems without Diversity Combining	12
2.1.2.2 Fading Channels in Diversity Systems	13
2.2 The Geometrical Three-Ring-Based Channel Model	13
2.3 Statistical Modeling and Analysis of K -Parallel Dual-Hop Relay Channels	15
2.4 Statistical Analysis of EGC over Multiple Double Rayleigh Fading Channels	18
2.5 Chapter Summary and Conclusion	21
3 Statistical Modeling and Analysis of Narrowband M2M Fading Channels Under LOS Propagation Conditions	23
3.1 Introduction	23
3.2 Statistical Modeling and Analysis of Double Rice Channels	25
3.3 Statistical Modeling and Analysis of SLDS Channels	27

3.4	Statistical Modeling and Analysis of MLSS Channels	30
3.5	Statistical Analysis of EGC over M2M Fading Channels with LOS Components	33
3.6	Chapter Summary and Conclusion	36
4	Channel Capacity of M2M Links in Cooperative Communication Systems	39
4.1	Introduction	39
4.2	Statistical Analysis of the Channel Capacity of NLOS M2M Relay Links with EGC	41
4.3	Chapter Summary and Conclusion	43
5	Performance Analysis of M2M Cooperative Communication Systems	45
5.1	Introduction	45
5.2	Performance Analysis of Cooperative Systems with EGC in NLOS M2M Fading Channels	46
5.3	Performance Analysis of Cooperative Systems with EGC in LOS M2M Fading Channels	49
5.4	Chapter Summary and Conclusion	52
6	Summary of Contributions and Outlook	55
6.1	Major Contributions	55
6.2	Outlook	57
	References	59
A	List of Publications	79
A.1	Articles Included in this Dissertation	79
A.2	Articles Not Included in this Dissertation	81
B	Paper I	83
C	Paper II	117
D	Paper III	133
E	Paper IV	149
F	Paper V	169
G	Paper VI	189

H Paper VII	211
H.A Proof of (30)	237
H.B Proof of (35)	238
H.C Proof of (40)	239
H.D Proof of (46)	240
H.E Proof of (51)	241
I Paper VIII	251
J Paper IX	267
K Paper X	285
L Paper XI	301
M Paper XII	319

List of Figures

2.1	The propagation scenario behind K -parallel dual-hop relay fading channels.	17
2.2	The propagation scenario behind dual-hop multi-relay NLOS M2M fading channels.	19
3.1	Scenario 1 – The overall mobile fading channel as a result of a concatenation of fixed-to-mobile and mobile-to-mobile fading channels.	26
3.2	Scenario 2 – The overall mobile fading channel as a result of a concatenation of mobile-to-fixed and fixed-to-mobile fading channels.	26
3.3	The propagation scenario behind SLDS fading channels.	29
3.4	The propagation scenario behind MLSS fading channels.	31
3.5	The propagation scenario behind dual-hop multi-relay LOS M2M fading channels.	34
5.1	The propagation scenario behind dual-hop multi-relay NLOS M2M fading channels.	47
5.2	The propagation scenario behind dual-hop multi-relay LOS M2M fading channels.	51
B.1	The geometrical three-ring scattering model for a $2 \times 2 \times 2$ MIMO M2M channel with local scatterers on rings around the source mobile station, the mobile relay, and the destination mobile station.	108
B.2	A simplified diagram describing the overall MIMO M2M channel from the source mobile station to the destination mobile station via the mobile relay.	109
B.3	The source CF $\rho_s(\delta_s, \tau)$ of the $2 \times 2 \times 2$ MIMO M2M reference channel model under isotropic scattering conditions.	109
B.4	The source CF $\hat{\rho}_s(\delta_s, \tau)$ of the $2 \times 2 \times 2$ MIMO M2M stochastic channel simulator under isotropic scattering conditions.	110

B.5	Absolute error $e_s(\delta_s, \tau) = \rho_s(\delta_s, \tau) - \hat{\rho}_s(\delta_s, \tau) $ by using the MMEA with $M = 40$ (isotropic scattering).	110
B.6	The relay CF $\rho_R(\delta_R, \tau)$ of the $2 \times 2 \times 2$ MIMO M2M reference channel model under isotropic scattering conditions.	111
B.7	The relay CF $\hat{\rho}_R(\delta_R, \tau)$ of the $2 \times 2 \times 2$ MIMO M2M stochastic channel simulator under isotropic scattering conditions.	111
B.8	Absolute error $e_R(\delta_R, \tau) = \rho_R(\delta_R, \tau) - \hat{\rho}_R(\delta_R, \tau) $ by using the MMEA with $K = L = 23$ (isotropic scattering).	112
B.9	Absolute value of the source CF $ \rho_s(\delta_s, \tau) $ of the $2 \times 2 \times 2$ MIMO M2M reference channel model under non-isotropic scattering conditions (von Mises density with $\phi_s^{(0)} = 60^\circ$ and $\kappa_s = 40$).	112
B.10	Absolute value of the source CF $ \hat{\rho}_s(\delta_s, \tau) $ of the $2 \times 2 \times 2$ MIMO M2M stochastic channel simulator designed by applying the MMEA with $M = 40$ (non-isotropic scattering, von Mises density with $\phi_s^{(0)} = 60^\circ$ and $\kappa_s = 40$).	113
B.11	Absolute error $e_s(\delta_s, \tau) = \rho_s(\delta_s, \tau) - \hat{\rho}_s(\delta_s, \tau) $ by using the MMEA with $M = 40$ (non-isotropic scattering, von Mises density with $\phi_s^{(0)} = 60^\circ$ and $\kappa_s = 40$).	113
B.12	Absolute value of the relay CF $ \rho_R(\delta_R, \tau) $ of the $2 \times 2 \times 2$ MIMO M2M reference channel model under non-isotropic scattering conditions (von Mises density with $\phi_{S-R}^{(0)} = \phi_{R-D}^{(0)} = 60^\circ$ and $\kappa_{S-R} = \kappa_{R-D} = 40$).	114
B.13	Absolute value of the relay CF $ \hat{\rho}_R(\delta_R, \tau) $ of the $2 \times 2 \times 2$ MIMO M2M stochastic channel simulator designed by applying the MMEA with $K = L = 23$ (non-isotropic scattering, von Mises density with $\phi_{S-R}^{(0)} = \phi_{R-D}^{(0)} = 60^\circ$ and $\kappa_{S-R} = \kappa_{R-D} = 40$).	114
B.14	Absolute error $e_R(\delta_R, \tau) = \rho_R(\delta_R, \tau) - \hat{\rho}_R(\delta_R, \tau) $ by using the MMEA with $K = L = 23$ (non-isotropic scattering, von Mises density with $\phi_{S-R}^{(0)} = \phi_{R-D}^{(0)} = 60^\circ$ and $\kappa_{S-R} = \kappa_{R-D} = 40$).	115
C.1	The propagation scenario describing K -parallel dual-hop relay fading channels.	122
C.2	The PDF $p_{\Xi}(r)$ of the envelope $\Xi(t)$ of K -parallel dual-hop relay fading channels.	128
C.3	The mean value m_{Ξ} of the envelope $\Xi(t)$ of K -parallel dual-hop relay fading channels.	128
C.4	The standard deviation σ_{Ξ} of the envelope $\Xi(t)$ of K -parallel dual-hop relay fading channels.	129

D.1	The propagation scenario describing K -parallel dual-hop relay M2M fading channels.	138
D.2	The LCR $N_{\Xi}(r)$ of the envelope $\Xi(t)$ of K -parallel dual-hop relay M2M fading channels.	144
D.3	The CDF $F_{\Xi-}(r)$ of the envelope $\Xi(t)$ of K -parallel dual-hop relay M2M fading channels.	145
D.4	The ADF $T_{\Xi-}(r)$ of the envelope $\Xi(t)$ of K -parallel dual-hop relay M2M fading channels.	145
E.1	The propagation scenario describing K -parallel dual-hop relay M2M fading channels.	155
E.2	The PDF $p_{\Xi}(x)$ of the received signal envelope at the output of the EG combiner $\Xi(t)$ for a different number of diversity branches K	161
E.3	The CDF $F_{\Xi-}(r)$ of the received signal envelope at the output of the EG combiner $\Xi(t)$ for a different number of diversity branches K	162
E.4	The LCR $N_{\Xi}(r)$ of the received signal envelope at the output of the EG combiner $\Xi(t)$ for a different number of diversity branches K	162
E.5	The ADF $T_{\Xi-}(r)$ of the received signal envelope at the output of the EG combiner $\Xi(t)$ for a different number of diversity branches K	163
F.1	Scenario A: The overall mobile fading channel as a result of a concatenation of fixed-to-mobile and mobile-to-mobile fading channels.	174
F.2	Scenario B: The overall mobile fading channel as a result of a concatenation of mobile-to-fixed and fixed-to-mobile fading channels.	174
F.3	The PDF $p_{\eta}(z)$ of the envelope of the double Rice process $\eta(t)$	182
F.4	The PDF $p_{\vartheta}(\theta)$ of the phase of the double Rice process $\eta(t)$	183
F.5	The LCR $N_{\eta}(r)$ of the double Rice process $\eta(t)$ for various values of ρ	183
F.6	The LCR $N_{\eta}(r)$ of the double Rice process $\eta(t)$ for various values of $f_{\rho_{MR}}$ and $f_{\rho_{MS}}$	184
F.7	The ADF $T_{\eta-}(r)$ of the double Rice process $\eta(t)$ for various values of ρ	184
F.8	The ADF $T_{\eta-}(r)$ of the double Rice process $\eta(t)$ for various values of $f_{\rho_{MR}}$ and $f_{\rho_{MS}}$	185
G.1	The propagation scenario behind single-LOS double-scattering fading channels.	193
G.2	A comparison of the PDF $p_{\Xi}(z)$ of SLDS processes $\Xi(t)$ with that of various other stochastic processes.	203

G.3	Approximation of the PDF $p_{\Xi}(z)$ of SLDS processes $\Xi(t)$ to the Laplace distribution.	204
G.4	A comparison of the mean value m_{Ξ} of SLDS processes $\Xi(t)$ with that of various other stochastic processes.	204
G.5	A comparison of the standard deviation σ_{Ξ} of SLDS processes $\Xi(t)$ with that of various other stochastic processes.	205
G.6	A comparison of the CDF $F_{\Xi}(r)$ of SLDS processes $\Xi(t)$ with that of various other stochastic processes.	205
G.7	A comparison of the PDF $p_{\Theta}(\theta)$ of the phase process $\Theta(t)$ with that of various other stochastic processes.	206
G.8	A comparison of the LCR $N_{\Xi}(r)$ of SLDS processes $\Xi(t)$ for various values of ρ with that of various other stochastic processes.	207
G.9	A comparison of the ADF $T_{\Xi}(r)$ of SLDS processes $\Xi(t)$ for various values of ρ with that of various other stochastic processes.	207
H.1	The propagation scenario describing MLSS fading channels.	247
H.2	A comparison of the PDF $p_{\Xi}(x)$ of the MLSS process $\Xi(t)$ with that of various other stochastic processes.	248
H.3	A comparison of the CDF $F_{\Xi}(r)$ of the MLSS process $\Xi(t)$ with that of various other stochastic processes.	248
H.4	A comparison of the PDF $p_{\Theta}(\theta)$ of the phase of the MLSS process $\Theta(t)$ with that of various other stochastic processes.	249
H.5	A comparison of the LCR $N_{\Xi}(r)$ of the MLSS process $\Xi(t)$ with that of various other stochastic processes.	249
H.6	A comparison of the ADF $T_{\Xi}(r)$ of the MLSS process $\Xi(t)$ with that of various other stochastic processes.	250
I.1	The propagation scenario illustrating K -parallel dual-hop relay M2M fading channels.	256
I.2	The PDF $p_{\Xi_{\rho}}(x)$ of the received signal envelope $\Xi_{\rho}(t)$ at the output of the EG combiner for a different number of diversity branches K	261
I.3	The LCR $N_{\Xi_{\rho}}(r)$ of the received signal envelope $\Xi_{\rho}(t)$ at the output of the EG combiner for a different number of diversity branches K	262
I.4	The ADF $T_{\Xi_{\rho}}(r)$ of the received signal envelope $\Xi_{\rho}(t)$ at the output of the EG combiner for a different number of diversity branches K	262
J.1	The PDF $p_{\Xi}(x)$ of the received signal envelope at the output of the EG combiner $\Xi(t)$ for a different number K of diversity branches.	278

J.2	The PDF $p_C(r)$ of the channel capacity $C(t)$ of the double Rayleigh fading channels with EGC for a different number K of diversity branches.	278
J.3	The CDF $F_C(r)$ of the channel capacity $C(t)$ of the double Rayleigh fading channels with EGC for a different number K of diversity branches.	279
J.4	The LCR $N_C(r)$ of the channel capacity $C(t)$ of the double Rayleigh fading channels with EGC for a different number K of diversity branches.	280
J.5	The ADF $T_C(r)$ of the channel capacity $C(t)$ of the double Rayleigh fading channels with EGC for a different number K of diversity branches.	280
K.1	The propagation scenario describing K -parallel dual-hop relay M2M fading channels.	290
K.2	The PDF $p_{\Xi}(x)$ of the received signal envelope $\Xi(t)$ at the output of the EG combiner for a different number of diversity branches K having the same variance.	296
K.3	The PDF $p_{\Xi}(x)$ of the received signal envelope $\Xi(t)$ at the output of the EG combiner for a different number of diversity branches K having different variances.	297
K.4	The average BEP P_b of M -ary PSK modulation schemes over double Rayleigh processes with EGC.	297
K.5	A comparison of the average BEP P_b of M -ary PSK modulation schemes over double Rayleigh processes with EGC and MRC.	298
L.1	The propagation scenario describing K -parallel dual-hop relay M2M fading channels.	306
L.2	The PDF $p_{\Xi_\rho}(x)$ of the received signal envelope $\Xi_\rho(t)$ at the output of the EG combiner for a different number of diversity branches K under FLOS, PLOS, and NLOS propagation conditions.	313
L.3	The average BEP P_b of M -ary PSK modulation schemes over double Rice processes with EGC under FLOS propagation conditions.	314
L.4	The average BEP P_b of M -ary PSK modulation schemes over M2M fading channels with EGC under FLOS, PLOS, and NLOS propagation conditions.	314

L.5	The average BEP P_b of M -ary PSK modulation schemes over double Rice processes with EGC and MRC under FLOS propagation conditions.	315
M.1	The propagation scenario describing K -parallel dual-hop relay M2M fading channels.	345
M.2	The PDF $p_{\Xi_\rho}(x)$ of the received signal envelope at the output of the EG combiner $\Xi_\rho(t)$ for $K + 1$ diversity branches under different propagation conditions.	345
M.3	The LCR $N_{\Xi_\rho}(r)$ of the received signal envelope at the output of the EG combiner $\Xi_\rho(t)$ for $K + 1$ diversity branches under different propagation conditions.	346
M.4	The ADF $T_{\Xi_\rho}(r)$ of the received signal envelope at the output of the EG combiner $\Xi_\rho(t)$ for $K + 1$ diversity branches under different propagation conditions.	346
M.5	The average BEP P_b of M -ary PSK modulation schemes over M2M fading channels with EGC under full-LOS propagation conditions. .	347
M.6	The average BEP P_b of M -ary PSK modulation schemes over M2M fading channels with EGC for $LOS_{K,K}$ scenario.	347
M.7	The average BEP P_b of M -ary PSK modulation schemes over M2M fading channels with EGC under different propagation conditions. .	348
M.8	The outage probability $P_{out}(\gamma_{th})$ in M2M fading channels with EGC under different propagation conditions.	348

Abbreviations

2D	two-dimensional
3D	three-dimensional
4D	four-dimensional
2G	second generation
3G	third generation
4G	fourth generation
ACF	autocorrelation function
ADF	average duration of fades
AHSRA	Advanced Cruise-Assist Highway Systems Research Association
AOA	angle of arrival
AOD	angle of departure
AOF	amount of fading
AWGN	additive white Gaussian noise
BS	base station
BEP	bit error probability
BPSK	binary phase shift keying
C2C	car-to-car
CCF	cross-correlation function
CF	characteristic function
CDF	cumulative distribution function
CSI	channel state information
CVIS	Cooperative Vehicle-Infrastructure Systems
DQPSK	differentially encoded quadrature phase shift keying
DSRC	dedicated short-range communications
EG	equal gain
EGC	equal gain combining
EMEDS	extended method of exact Doppler spread
F2F	fixed-to-fixed
F2M	fixed-to-mobile

FCC	Federal Communications Commission
BFSK	binary frequency shift keying
GMEDS	generalized method of exact Doppler spread
GSM	global system for mobile communications
IMT-Advanced	International Mobile Telecommunications Advanced
LCR	level-crossing rate
LOS	line-of-sight
LPNM	L_p -norm method
M2M	mobile-to-mobile
M2F	mobile-to-fixed
MAC	medium access control
MIMO	multiple-input multiple output
MMEA	modified method of equal areas
MRC	maximal ratio combining
NLOS	non-line-of-sight
PDF	probability density function
PSD	power spectral density
PSK	phase shift keying
QPSK	quadrature phase shift keying
SC	selection combining
SISO	single-input single-output
SNR	signal-to-noise ratio
SOS	sum-of-sinusoids
V2V	vehicle-to-vehicle
TDMA	time-division multiple-access
UMTS	Universal Mobile Telecommunications System

Chapter 1

Introduction

1.1 Cooperative Communication Systems

The provision of very high data rates (> 100 Mbps) and higher spectral efficiency (> 10 b/s/Hz) envisioned for fourth generation (4G) wireless communication systems in reasonably large areas requires significant development of new wireless network technologies. This has in turn resulted in an upsurge of interest towards cooperative communications. Without any extra cost resulting from the deployment of a new infrastructure and by utilizing the existing resources of the network, cooperative relaying promises increased capacity, improved connectivity, and a larger coverage range [1, 2, 3]. It is worth stating that cooperative relaying has found applications in various networks ranging from cellular, ad hoc, and sensor networks to mobile-to-mobile (M2M) communication systems [4, 5, 6, 7, 8, 9, 10, 11, 12].

The growing popularity of cooperative diversity [4, 7, 13] in wireless networks is also due to its ability to mitigate the deleterious fading effects by achieving a spatial diversity gain. This diversity gain is attained when several single-antenna mobile stations in a multi-user scenario collaborate together and share their antennas to create a virtual multiple-input multiple-output (MIMO) system [14]. Such a network permits mobile stations to relay signals from another mobile station to a final destination. That is, each mobile station in a cooperative communication system is assumed to transmit its own data as well as acts as a cooperative agent for another mobile station.

The relays in cooperative communication systems are categorized as non-regenerative and regenerative relays. Non-regenerative relays just amplify the received signal and forward it towards the destination mobile station. The regenerative relays however first decode the received signal, encode it again and then forward it to the final destination. Both amplify-and-forward as well as decode-and-forward

relaying belong to the class of cooperative protocols referred to as fixed relaying [7]. Among many possible adaptive strategies, selection relaying is built upon fixed relaying, where the transmitting mobile stations are allowed to select a suitable cooperative (or non-cooperative) action based upon the received signal-to-noise ratio (SNR) [7]. Incremental relaying protocols intend to improve the spectral efficiency of both fixed and selection relaying by exploiting limited feedback from the destination mobile station. In addition, relaying can take place only when absolutely necessary [7]. Amplify-and-forward relay type cooperative communication systems are the center of attention of this dissertation.

In the simplest configuration, an amplify-and-forward relay system consists of a source mobile station, a destination mobile station, and a relaying node. However, depending upon the gains we aim to achieve from the cooperative system, multiple relays can be connected in different configurations. These configurations are inclusive of multi-relay multi-hop and multi-relay dual-hop. The multi-relay multi-hop configuration is associated with the scenario where the relaying nodes are connected in series between the source mobile station and the destination mobile station, whereas in multi-relay dual-hop configuration the relays are operating in parallel. It has been cited in the literature that increasing the number of serial relaying nodes results in an increase in the pathloss gain [3]. An increase in the number of parallel relaying nodes, on the other hand, boosts the diversity gain [3]. In this dissertation, we are focusing on single- and multi-relay dual-hop amplify-and-forward relay type cooperative systems.

As mentioned above, cooperative systems come with many advantages such as enhanced performance in terms of increased pathloss, diversity as well as multiplexing gains, balanced quality of service (QoS), infrastructure-less deployment, and reduced operational costs [3]. However, there is no such thing as a perfect system and every system brings with it some disadvantages also. In multi-relay cooperative systems, whether they are dual-hop or multi-hop, complex schedulers and advanced algorithms for choosing partner nodes are required. Besides, the relay traffic, signaling overhead, end-to-end latency as well as interference increases in such systems [3]. It is thus, imperative for the cooperative system designers to cautiously analyze shortcomings of cooperative relaying. They should propose those strategies which facilitate in exploiting the benefits of cooperative communication to their full extend. The development of such cooperative communication systems is, nonetheless, not possible without a profound knowledge of the wireless channel. A major portion of this dissertation is therefore dedicated to the modeling and analysis of the fading channels in the relay links. It is out of the scope of this dis-

sertation to provide solutions to the problems pertaining to the protocol level and system level implementation of amplify-and-forward relay networks. The results presented here are, however, advantageous to resolve the design issues related to cooperative networks.

1.2 M2M Communication Systems

During the last two decades, the trend in wireless communication technologies has shifted from the traditional voice-centric “man-to-man” mobile communications (2G, GSM)¹ to today’s data-centric “man-to-machine” mobile communications (3G, UMTS)². A further shift towards “machine-to-machine” wireless communications (4G, IMT-Advanced³) is expected in near future. A typical example of machine-to-machine mobile communications is car-to-car (C2C) or equivalently vehicle-to-vehicle (V2V) communications. Moreover, C2C or V2V communications fall under the broader umbrella of what is called M2M communications. As the name refers, in M2M communication systems, all entities in the network are in motion. These entities can either be mobile users and/or vehicles. Throughout this dissertation, the terms C2C, V2V, and M2M would be used interchangeably.

C2C communications has recently gained a fair share of attention by researchers, standardization bodies, and industrial companies, since it offers many applications. Some of these applications are targeted to reduce traffic accidents and to facilitate the flow of traffic [15, 16]. While others include availability of in-vehicle internet access and support for convoy driving, automatic driving, as well as speed regulation etc. Several countries have allocated a dedicated frequency band for C2C communications. For instance, in the US, a 75 MHz band in the 5.9 GHz range has been allocated for short-range communications by the Federal Communications Commission (FCC). On the standardization level, the dedicated short-range communications (DSRC) [17] standard has been developed to support C2C communication systems. Several task groups within the IEEE, such as IEEE 802.11p, IEEE 1609.2, .3, and .4, are contributing to the development of C2C communications. On the industrial level, a number of projects can be found in Europe, USA, and Asia. Among the large-scale European projects, CAR 2 CAR Communication Consortium (see <http://www.car-to-car.org>), Cooperative Vehicle-Infrastructure

¹2G corresponds to second generation, whereas Global System for Mobile Communications is abbreviated as GSM

²3G corresponds to third generation, whereas Universal Mobile Telecommunications System is abbreviated as UMTS

³IMT-Advanced stands for International Mobile Telecommunications Advanced

Systems (CVIS) (see <http://www.cvisproject.org>), SAFESPOT (see <http://www.safe-spot-eu.org/>), and CALM (see <http://www.isotc204wg16.org/>) are to name a few. In the US, the Driver Workload Metrics Project, the Forward Collision Warning Requirement Project, and the Vehicle Safety Communications Project make use of C2C communications. In Asia, the Advanced Cruise-Assist Highway Systems Research Association (AHSRA) (see http://www.ahsra.or.jp/index_e.html) is one of the main associations contributing to the development of C2C communications.

As for any other communication system, the development of M2M communication systems requires the knowledge of the propagation channel characteristics. It is widely accepted now that the properties of M2M channels are considerably different from those of classical cellular channels (see, e.g., [18] and the references therein). These differences originate because the dominant propagation mechanisms of the multipath components associated with M2M communications and cellular radio communications are different. In V2V systems, the transmitter (Tx) and the receiver (Rx) are at the same height and in similar environments. Furthermore, propagation in the horizontal plane with diffraction and reflection, around street corners is more important. By contrast to the classical cellular systems, both the Tx and the Rx along with the scatterers are moving in M2M systems. This implies that the propagation conditions are highly dynamic and the fluctuations in M2M channels are much faster. Therefore, assumptions pertaining to the stationarity of M2M channels should be made carefully. It should also be pointed out that M2M channel characteristics are influenced by the properties of the environment around the communicating cars as well as the typical traffic characteristics [18].

The number of cars on roads is increasing day by day as a consequence of the ever increasing population on the face of the earth. This increase in the number of cars can, however, be utilized in a constructive manner by forming a network that relays information from one car to another. In other words, by deploying cooperative techniques in V2V systems, we can profit from the benefits of both systems, i.e., cooperative systems and V2V systems. Similar is the case of mobile users in ad hoc as well as wireless sensor networks and cooperative relaying. As it follows from the title, in this dissertation, we have devoted all our efforts to investigate various aspects of M2M cooperative communication systems. The topics covered range from the modeling of M2M fading channels in relay links to the overall performance analysis of cooperative communication systems.

1.3 Organization of the Dissertation

This dissertation is organized as a plurality of twelve technical papers. The connection between different papers on which the whole dissertation is built up is elaborated. Papers addressing similar topics are collected together to form chapters. The structure of this dissertation is as follows:

- **Chapter 2** reports on the modeling and analysis of narrowband M2M fading channels in cooperative networks under non-line-of-sight (NLOS) propagation conditions. Two different kinds of channel models, i.e., geometry-based models and non-geometrical models are introduced in the current chapter. Furthermore, first the statistical characterization of geometry-based channel models in terms of the temporal autocorrelation function (ACF) and space-time cross-correlation functions (CCFs) is discussed. Afterwards, we go through statistical quantities, such as the probability density function (PDF), cumulative distribution function (CDF), level-crossing rate (LCR), and average duration of fades (ADF). These quantities possess an important place in the modeling and analysis of fading channels in general. Papers I – IV (Appendices B – E) that are summarized in subsequent sections of Chapter 2 reveal key results pertaining to the statistical properties of the geometrical three-ring-based channel model, K -parallel dual-hop channels, and NLOS M2M fading channels with equal gain combining (EGC).
- **Chapter 3** contains a comprehensive overview of the modeling and analysis of narrowband M2M fading channels with line-of-sight (LOS) components in cooperative networks. The motivation behind modeling M2M channels with LOS components comes from the fact that such models are flexible enough to accommodate asymmetric channel conditions associated with many practical propagation scenarios. Besides, LOS fading channel models easily reduce to those models that correspond to NLOS propagation conditions. It is necessary to point out here that the M2M fading channel models illustrated in this chapter are not just straight forward extensions with respect to (w.r.t.) LOS conditions of the ones presented in Chapter 2. These models are in fact developed considering propagation scenarios and environments that are different from those used in Chapter 2. An insightful review of Papers V – VIII and XII (Appendices F – I and M) is included in Chapter 3. In these papers, we have studied the statistics in terms of the PDF, CDF, LCR, and ADF of double Rice, single-LOS double scattering (SLDS) and multiple-LOS second-order scattering (MLSS) channels along with LOS M2M channels with EGC.

- **Chapter 4** presents the state of the art regarding the analysis of the statistical properties of the channel capacity of M2M links in cooperative communication systems. A sound understanding of the channel capacity is also indispensable to meet the data rate requirements of future mobile communication systems, in addition to the knowledge about the propagation channel characteristics. A brief overview of Paper IX (Appendix J) is given in this chapter, which deals with the derivation and analysis of theoretical expressions for the PDF, CDF, LCR, and ADF of the channel capacity of NLOS M2M relay links with EGC.
- **Chapter 5** is a synopsis of the performance evaluation of M2M cooperative communication systems including those where EGC is deployed at the destination mobile station. This performance analysis is carried out assuming different propagation environments. A number of performance measures, inclusive the statistics of the instantaneous SNR at the output of the equal gain (EG) combiner, the average bit error probability (BEP), the amount of fading (AOF), and the outage probability are detailed in Chapter 5. Papers X – XII (Appendices K – M) outlined in subsections of the current chapter, actually contain the entire performance analysis.
- **Chapter 6** summarizes the main contributions of this dissertation. We close this chapter by highlighting some open problems pertaining to the design and development of M2M cooperative communication systems that call for further attention.

Each chapter comprises several sections. The organization of the chapters is given in the following.

- **Introduction** presents the background and the state of art regarding the main topic of the chapter.
- **Section N** details the related papers jointly.
- **Chapter Summary and Conclusion** summarizes the main findings of the chapter.

The sections outlining the papers are further organized in paragraphs. We used the following organization scheme as a road map for these sections.

- Each section opens with a brief introduction along with the motivation to address a particular problem. The key problems handled are the modeling of

M2M fading channels and their analysis, the channel capacity analysis, and the performance evaluation of M2M cooperative communication systems.

- Topic(s) that describe(s) what is the paper about.
- Main results include what has been achieved.
- Discussion covers the advantages and disadvantages of the proposed solution to the problem that is dealt with.

Chapter 2

Statistical Modeling and Analysis of Narrowband M2M Fading Channels Under NLOS Propagation Conditions

2.1 Introduction

Chapter 2 introduces different channel modeling approaches to describe M2M channels under NLOS propagation conditions. It is known that channel models can be developed based on the geometry of the scattering environment. On the other hand, without going into the details of the geometry of the scattering environment, statistical methods can also be employed to model fading channels. In the following, the statistical characterization of geometry-based channel models is explicitly discussed. In addition, accentuating those statistical quantities, which can usually characterize fading channels and provide an insight into the fading behavior of channels, is also the topic of the current section.

2.1.1 Statistical Characterization of Geometry-Based Channel Models

The design, development, performance analysis, and test of mobile radio communication systems call for a profound insight of the most important characteristics of real-world propagation environments. The attempts to avoid field trials for performance assessment purposes, which are neither cost nor time efficient, have compelled the communication systems' designers to find cost effective resorts. One

such alternative is to reproduce the desired channel characteristics by computer simulations. It is however, imperative as well as highly desirable that the channel simulation models are accurate enough to reflect the fading statistics of real-world channels.

Various studies have revealed that geometrical channel models are a good starting point for deriving simulation models for MIMO channels. Geometry-based narrowband MIMO channel models are usually characterized by their temporal as well as their spatial correlation properties. Besides, the drive to conduct research on MIMO systems is based on the well-established results that the gains in terms of channel capacity are larger for MIMO channels as compared to single-input single-output (SISO) channels [19, 20]. A number of narrowband MIMO channel models based on geometrical scattering models for isotropic environments have been proposed so far [21, 22, 23, 24, 25, 26, 27, 28]. The design of geometry-based MIMO channel models for non-isotropic scattering conditions is addressed in [29, 30], whereas wideband MIMO channel models are discussed in [31, 32]. The common feature in the works [21, 22, 23, 24, 25, 26, 27, 28, 29, 30, 31, 32] is that they model MIMO fixed-to-mobile (F2M) and/or fixed-to-fixed (F2F) channels.

The idea of M2M communication came in the limelight by the work of Akki and Haber [33, 34]. Their work deals with the study of the statistical properties of narrowband SISO M2M fading channels under NLOS propagation conditions. Some few techniques for simulating narrowband SISO M2M fading channels have been presented in [35]. The geometrical two-ring-based model for MIMO F2M channels originally proposed in [24], was extended to a narrowband MIMO M2M channel model by the authors of [36]. Extensions of MIMO M2M reference and simulation models under LOS propagation conditions have been reported in [37]. The geometrical street model [38] and the geometrical T-junction model [39] for MIMO M2M fading channels are also worth mentioning. All the geometry-based channel models referred to this point in the current section are two-dimensional (2-D) channel models. The credit of extending 2-D MIMO M2M channel models to three-dimensional (3-D) models based on geometrical cylinders goes to the authors of [40]. Quite a few articles dealing with wideband MIMO M2M channels have been published recently, see, e.g., [41, 42, 43, 44] and the references therein. In contrast to the MIMO M2M channel models mentioned thus far, where isotropic scattering conditions were assumed, a recent work [45] introduces a geometry-based model for non-isotropic MIMO M2M channels.

Motivated by the need for proper MIMO M2M fading channel models, in this dissertation, we are addressing modeling and simulation approaches for such chan-

nels in amplify-and-forward relay type cooperative networks. Additionally, there was not a single M2M channel model for cooperative networks available in the literature, which assumes multiple antennas on the source mobile station, the destination mobile station or the mobile relays. This gap in the research propelled us to introduce a geometry-based model for MIMO M2M channels in relay-based systems. Therein, the scattering environment around the source mobile station, the mobile relay, and the destination mobile station is modeled by a geometrical three-ring scattering model. In Section 2.2, a brief overview of this proposed geometrical three-ring model is given.

2.1.2 Statistical Characterization of Fading Channels

The development of M2M cooperative communication systems requires the knowledge of the propagation channel characteristics. In this regard, precise information about the PDF of the envelope and phase of the received signal, the LCR and ADF is of utmost importance.

Mobile radio fading channels are usually described by statistical quantities, such as the mean value, variance, and PDF of the envelope as well as the phase of the received signal. In addition to the statistical characterization of the fading channel, the significance of the PDF of the received signal envelope also lies in the fact that it can easily be utilized in the link level performance analysis of M2M cooperative communication systems. The average BEP or the symbol error probability (SEP) and the channel capacity are a few measures to evaluate the performance of communication systems at the link level. For the evaluation of the average BEP, SEP, and channel capacity, we usually need the PDF of the instantaneous SNR at the output of the receiver. Thus, given the PDF of the received signal envelope, the computation of the PDF of the instantaneous SNR is simply a transformation of random variables.

Unfortunately, the envelope and phase distributions do not provide any information pertaining to the rate of fading of the channel. The LCR of the envelope of fading channels is an important statistical quantity, revealing information about how fast the received signal changes with time. It is basically a measure to describe the average number of times the signal envelope crosses a certain threshold level from up to down (or from down to up) per second. In the same context as the LCR, another important statistical quantity is the ADF, which is defined as the expected value of the time intervals over which the fading signal envelope remains below a certain threshold level. In view of the fact that M2M fading is caused because of the time-variant multipath propagation, M2M fading channels exhibit bursty error

characteristics [46]. The fading channel often causes the signal to fall below a certain threshold noise level, which in turn results in error bursts. The error bursts produced as a consequence of fading have strong statistical connections with each other [47]. However, these errors can be combated by using interleaving techniques [46, 48] and coding techniques [49, 50]. The PDF of the received signal envelope is insufficient to be employed in developing robust interleaving and coding schemes, as it does not give any insight into the rate of fading. However, the LCR and the ADF describe the fading behavior of M2M channels. Studies pertaining to the LCR and the ADF are thus quite useful in the design as well as optimization of coding and interleaving schemes for M2M fading channels in the relay links in cooperative networks.

2.1.2.1 Fading Channels in Systems without Diversity Combining

As mentioned earlier, the multipath propagation channel in any mobile and wireless communication system can efficiently be described with the help of proper statistical models. For example, the Rayleigh distribution is considered suitable to model fading channels under NLOS propagation conditions in classical cellular networks [51, 52, 53], a Suzuki process represents a reasonable model for land mobile terrestrial channels [54, 55], and the generalized- K distribution is widely accepted in radar systems [56, 57]. Furthermore, cascaded distributions such as double Rayleigh, double Nakagami, or cascaded Weibull distributions find their applications in modeling keyhole fading channels [58, 59, 60]. Higher order statistics of Rayleigh, Nakagami- m , Suzuki, Nakagami-lognormal, double Rayleigh and double Nakagami channels are thoroughly studied in [61, 62, 63, 54, 64, 65, 66]. In various studies pertaining to M2M fading channels in single-relay dual-hop cooperative systems under NLOS propagation conditions, it has been shown that a double Rayleigh process is a simple and yet a well-suited statistical model for such channels [67, 66]. The analysis of experimental measurement data for outdoor-to-indoor M2M fading channels presented in [68], verifies the existence of double Rayleigh processes in real-world environments. In addition to dual-hop cooperative systems, several papers dealing with the statistical modeling and analysis of multi-hop cooperative systems having K relays connected in series between the source and the destination terminals are available in the literature [69, 70, 71, 72].

Section 2.3 provides us with vital information on the statistics of M2M fading channels in multi-relay dual-hop cooperative systems. The system considered therein assumes that K mobile relays are connected in parallel between the source mobile station and the destination mobile station, which in turn makes this system

different from multi-hop systems in [69, 70, 71, 72].

2.1.2.2 Fading Channels in Diversity Systems

Transmission links in mobile wireless communication systems are particularly vulnerable to multipath fading effects. Therefore, for decades, the development of new and robust techniques [73] to mitigate the adverse fading effects has been a topic of interest in the field of mobile communication systems design. In this context, diversity combining schemes are widely acknowledged for effectively combating fading. Diversity can be achieved in time, frequency, space, and through antenna polarization [73]. Some well-studied diversity combining techniques that have exhibited their potential in providing spatial diversity gain include selection combining (SC) [74], maximal ratio combining (MRC) [74], and EGC [74]. MRC has been proved to be the optimum scheme, whereas the suboptimal EGC scheme is more popular for its simplicity in implementation [74]. Statistical analysis of SC, EGC as well as MRC over Rayleigh, Nakagami, Hoyt, and Nakagami-lognormal channels can be found in the literature, see, e.g., [75, 76, 77, 78, 79, 80, 81].

It is noticeable that hardly any results have been reported that illustrate the statistical properties of any type of combining over M2M fading channels in cooperative networks. Our work summarized in Section 2.4 intends to fill in this gap by evaluating the statistics of M2M fading channels with EGC under NLOS propagation conditions.

2.2 The Geometrical Three-Ring-Based Channel Model

Section 2.1.1 sheds light on the scarcity of appropriate MIMO M2M channel models for transmission links in cooperative networks. Motivated by this discussion, we are addressing in Paper I, modeling and simulation approaches for MIMO M2M fading channels in amplify-and-forward relay type cooperative networks. Paper I, in Appendix B [82] of this dissertation, deals with the derivation of a stochastic narrowband MIMO M2M reference channel model as well as the corresponding channel simulation model. In addition, the analysis of both the reference and simulation models under isotropic and non-isotropic scattering conditions is reported. Paper I is in fact an extension of [83] to form a journal article. This section outlines Paper I, which is included in Appendix B [82] of this dissertation.

In Paper I, a new geometry-based model for narrowband MIMO M2M channels

in amplify-and-forward relay type cooperative networks is proposed. For ease of analysis, we have considered an elementary $2 \times 2 \times 2$ antenna configuration, meaning thereby, the source mobile station, the mobile relay, and the destination mobile station are equipped with two antennas each. For simplicity, NLOS propagation conditions are considered in all the transmission links. It is further assumed that there is no direct transmission link from the source mobile station to the destination mobile station. The scattering environment around the source mobile station, the mobile relay, and the destination mobile station is modeled by a geometrical three-ring scattering model. The advanced geometrical three-ring scattering model is an extension of the geometrical two-ring scattering model presented in [36], where the source mobile station and the destination mobile station are surrounded by rings of scatterers. However, in the suggested extension of the two-ring model, we have a separate ring of scatterers around the mobile relay along with a ring each around the source mobile station and the destination mobile station. Due to high path loss, the contribution of signal power from remote scatterers to the total received power is usually negligible. Therefore, in the proposed three-ring scattering model, we have only assumed local scattering.

The reference and stochastic simulation models are then derived employing the three-ring scattering model in Paper I. It is noteworthy that the developed reference model is a theoretical model, which is based on the assumption that the number of local scatterers around the source mobile station, the mobile relay, and the destination mobile station is infinite. The assumption of an infinite number of local scatterers prevents the realization of the reference model. However, a realizable stochastic simulation model can be derived from the reference model subject to certain conditions [36]. The development of reference and simulation models leads to the fact that the suggested three-ring scattering model is actually a concatenation of two separate two-ring models. Temporal as well as spatial correlation properties of the reference and simulation models are investigated in detail by evaluating their general analytical expressions. The derived four-dimensional (4-D) space-time CCF of the reference and simulation models can be expressed as a product of the correlation function at the source mobile station, the mobile relay, and the destination mobile station. It can further be inferred from the 4-D space-time CCF that the source mobile station and the destination mobile station are interchangeable. The 3-D spatial CCF and the temporal ACF can easily be obtained from the 4-D space-time CCF.

In Paper I, the correlation properties of the reference model are studied under isotropic and non-isotropic scattering conditions. Isotropic scattering around the

source mobile station (the destination mobile station) is determined by assuming uniformly distributed angles of departure (AOD) (angles of arrival (AOA)) over the interval $[0, 2\pi)$. Similarly, isotropic scattering around the mobile relay is characterized by a uniform distribution of the associated AOA as well as the AOD over $[0, 2\pi)$. By contrast, for characterizing non-isotropic scattering around the source mobile station, the mobile relay, and the destination mobile station, the von Mises distribution has been used for the corresponding AOD and AOA over $[0, 2\pi)$. The reason for using the von Mises distribution is its flexibility to closely approximate the Gaussian as well as the cardioid distribution and to have the uniform distribution as a special case [84]. Furthermore, the authors of [85] made a proposition of employing the von Mises distribution to model AOA statistics of mobile radio fading channels. They supported their proposal by matching the von Mises distribution to the measured data.

The results presented in Paper I show that various CCFs describing the simulation model closely approximate the corresponding CCFs of the reference model. It is worth mentioning that instead of using the complex Lp -norm method (LPNM) [61] to compute the required parameters of the developed M2M channel simulator, a relatively simple method, i.e., the modified method of equal areas (MMEA) [86] has been utilized in this work. The MMEA is known to be a high-performance parameter computation method for M2M channel simulators in non-isotropic scattering. Besides, it reduces to the best solution of the parameter computation problem in M2M channel simulators in isotropic scattering, known as the extended method of exact Doppler spread (EMEDS).

The significance of the work presented in Paper I comes from the fact that the realized channel simulator can be employed in analyzing the dynamic behavior of the MIMO channel capacity of relay-based M2M communication systems. In addition, the proposed geometrical three-ring scattering model for narrowband MIMO M2M fading channels can be considered as a starting point for the development and analysis of new channels models for wideband MIMO M2M fading channels in cooperative networks.

2.3 Statistical Modeling and Analysis of K -Parallel Dual-Hop Relay Channels

Paper I (Appendix B), summarized in Section 2.2, proposed the geometrical three-ring-based model for MIMO M2M fading channels in cooperative networks. This model is developed for M2M links in a single-relay cooperative network. In prac-

tise, there can be many relays available to form an M2M cooperative network. Papers II and III therefore, give an account of statistical properties of NLOS M2M fading channels in multi-relay dual-hop amplify-and-forward relay type systems. In light of the discussion concerning the importance of studying the PDF, LCR, and ADF of fading channels in Section 2.1.2, Papers II and III confer the findings about these statistical quantities associated with K -parallel dual-hop relay fading channels. A short overview of Paper II and III is given in this section, whereas these papers are available in full in Appendices C [87] and D [88], respectively.

In contrast to the fading channels considered in [69, 70, 71, 72] for multi-hop multi-relay cooperative networks, Papers II and III study the overall M2M fading channel in a dual-hop multi-relay cooperative network. Here, we have an amplify-and-forward relay system consisting of a source mobile station, a destination mobile station, and K mobile relays. The direct link between the source mobile station and the destination mobile station is blocked by obstacles. However, because of the parallel connection of the K mobile relays between the source mobile station and the destination mobile station, the resulting overall M2M channel is referred to as the K -parallel dual-hop relay M2M fading channel (see Fig. 2.1). The K -parallel dual-hop relay fading channel model caters for narrowband channels under NLOS propagation conditions. It is important to point out that the limitations posed on the physical implementation of all the mobile stations in the network restrict their mode of operation mostly to half-duplex. The half-duplex operation ensures that all the mobile stations do not transmit and receive a signal at the same time in the same frequency band.

Papers II and III aim at the statistical characterization of K -parallel dual-hop relay fading channels. Each individual transmission link from the source mobile station to the destination mobile station via the k th relay is modeled as a zero-mean complex double Gaussian process. These K zero-mean complex double Gaussian processes are independent but not necessarily identically distributed processes. Consequently, the overall M2M fading channel taking into account K parallel relay links is modeled as a sum of K zero-mean complex double Gaussian processes. Analytical expressions having integral forms for the characteristic function (CF), PDFs of the envelope as well as the phase, the mean value along with the variance, the LCR and ADF of K -parallel dual-hop relay M2M fading channels are derived. Furthermore, it has been shown that the complicated integral expressions can be reduced to simple and closed-form expressions when the underlying stochastic processes are assumed to be independent and identically distributed (i.i.d.). The correctness of the derived theoretical results is validated with the help of simula-

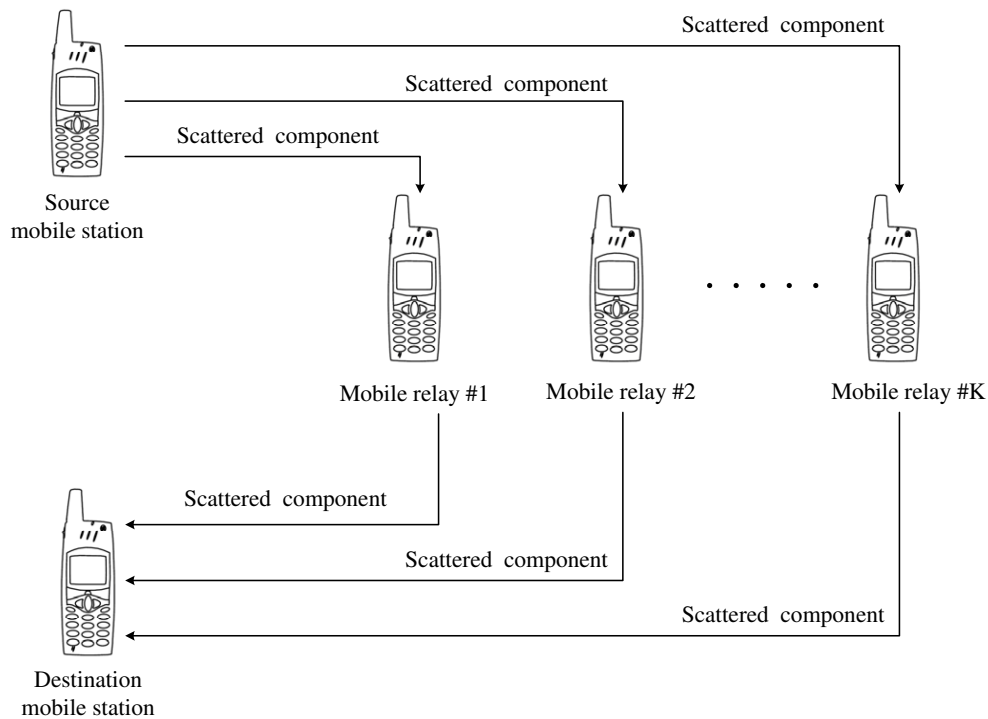


Figure 2.1: The propagation scenario behind K -parallel dual-hop relay fading channels.

tions. In this work, the underlying uncorrelated Gaussian noise processes making up the overall K -parallel dual-hop relay channel are simulated using the sum-of-sinusoids (SOS) principle [89, 90]. According to the SOS principle, a stochastic Gaussian process results as a consequence of the superposition of an infinite number of weighted harmonic functions. These harmonic functions are defined with the help of constant gains, constant frequencies, and random phases. The motivation to select an SOS-based channel simulator is that such simulators are widely acknowledged to be simple and efficient for simulating mobile radio fading channels under isotropic scattering conditions [61]. In addition, the concept of SOS has found its application in the design of channel simulators for temporally correlated frequency-nonselective channels [35, 61], frequency-selective channels [91, 92], and space-selective channels [22, 28, 36, 93]. However, in order to reproduce the desired channel characteristics in simulations, a careful selection of the simulator parameters (i.e., gains, frequencies, and phases) is essential. For this reason, several methods for an accurate computation of the model parameters of SOS simulators have been developed [91, 92, 94, 95, 96, 97]. One such method for the parameter computation, which is referred to as the generalized method of exact Doppler spread (GMEDS₁) [98], has been employed in this work. Using the GMEDS₁, it is possible to generate theoretically an unlimited number of uncorrelated Gaussian

waveforms without increasing the complexity of the channel simulator. The results presented in Papers II and III show a good fitting of the analytical and simulation results.

It can be concluded from this study that there is no significant increase in the mean value of K -parallel dual-hop relay channels, while keeping the variances of the underlying stochastic processes as well as the relay gains constant and increasing the number of mobile relays K in the network. On the contrary, increasing the relay gains increases both the mean value and standard deviation of K -parallel dual-hop relay channels. Similarly, the LCR as well as the ADF of K -parallel dual-hop relay channels is influenced by the number of the mobile relays considered, relay gains, and maximum Doppler frequencies caused by the motion of K mobile relays. For example, keeping the relay gains and the maximum Doppler frequencies associated with K mobile relays constant, the LCR decreases with the increase in the number K of mobile relays in the network. An increase in either the relay gains or the maximum Doppler frequencies, however, increases the LCR.

The work presented in Papers II and III does not completely take advantage of the concept of diversity. Here, signals reaching the destination mobile stations from K fading branches are linearly combined together. However, co-phasing is not applied on the branch signals before combining. Without co-phasing, the branch signals would not add up coherently. Thus, the resulting signal can still show signs of fading as a consequence of constructive and destructive superposition of the signals from K different branches [99]. This shortcoming of K -parallel dual-hop relay channel models is removed by deploying EGC at the destination mobile station in the following section.

2.4 Statistical Analysis of EGC over Multiple Double Rayleigh Fading Channels

In the final remarks of Section 2.3, it was brought to our attention that K -parallel dual-hop relay channel models do not entirely exploit the concept of diversity. It is nevertheless, absolutely necessary to make the most of the K -parallel dual-hop relay links in order to attain an improved systems performance. Therefore, for our study in Paper IV, we take a multi-relay M2M cooperative system, where EGC is deployed at the destination mobile station. In this section, we go over the analysis procedure followed in Paper IV along with the main contributions of this paper. Paper IV is included in full in Appendix E [100] of this dissertation.

In Paper IV, a multi-relay dual-hop amplify-and-forward relay configuration has

been taken into account. The selected system operates on amplify-and-forward relay protocols based on time-division multiple-access (TDMA) [8, 101], where the operational mode of all the mobile stations is half-duplex. It is further assumed that K mobile relays are arranged in parallel between the source mobile station and the destination mobile station. Since the direct link from the source mobile station to the destination mobile station is obstructed, the considered configuration gives rise to K diversity branches. Thus, the signals from these K diversity branches can be combined at the destination mobile station using EGC. For ease in understanding the considered propagation scenario, Fig. 2.2 has been included.

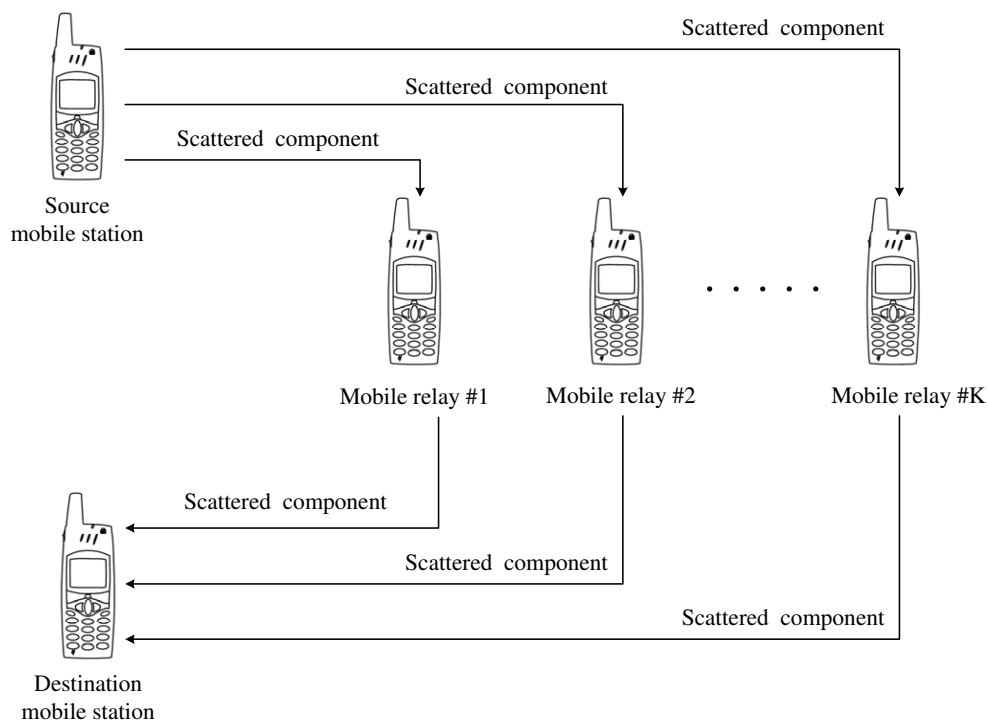


Figure 2.2: The propagation scenario behind dual-hop multi-relay NLOS M2M fading channels.

We intend to derive and analyze the statistical properties of EGC over NLOS M2M fading channels in cooperative networks in Paper IV. Although, the PDF can widely describe a fading channel, the LCR and the ADF, on the other hand, provide vital information about how fast the fading channel is changing with time. For this reason, studies pertaining to the PDF, CDF, LCR, and ADF along with the CF of the received signal envelope at the output of the equal gain (EG) combiner are included in this article. The output signal of the EG combiner is modeled as a sum of K i.i.d. double Rayleigh processes. It has been illustrated that the computation of the PDF of the sum of K double Rayleigh processes is rather intractable when it comes

to the evaluation of the inverse Fourier transform of the CF. An alternate approach is to approximate the target PDF either by another but a simpler expression or by a series. Depending upon the purpose for which the approximated PDF has to be used, several methods of approximation have been proposed so far such as Gaussian approximation, moment matching, Pearson type distribution fitting, approximation using orthogonal series expansion etc. [102, 103, 104, 105].

The approximation approach using orthogonal series expansion has been exploited in Paper IV. From various options of such series, like, e.g., the Edgeworth series [103], the Gram-Charlier series [103], the Laguerre series [103], etc., we proceed in our analysis using the Laguerre series expansion. The Laguerre series provides a good approximation for PDFs that are unimodal (i.e., having single maximum) with fast decaying tails and positive defined random variables. Furthermore, the Laguerre series is often used when the first term of the series provides a good enough statistical accuracy [103]. It turns out that the first term in the Laguerre series equals the gamma distribution. This enables us to show that the PDF of the sum of K double Rayleigh processes can be well approximated by the gamma distribution. Besides, the gamma distribution has demonstrated the potential to approximate other distributions with reasonable accuracy, including the lognormal distribution [106] and the generalized- K distribution [107]. Exploiting the properties of the gamma distribution, closed-form approximations are presented for the CDF, LCR, and ADF of the sum process. Furthermore, the close fitting of the approximated theoretical results with those of the exact simulation results shows that the approximation approach followed here is valid. Here, the simulations results are generated with the help of an SOS-based channel simulator [89, 90]. In order to ensure that the simulated waveforms possess the desired characteristics, the parameters of the channel simulator are computed by using GMEDS₁.

This study includes a discussion regarding the influence of the number of diversity branches K on the statistical properties of the received signal envelope at the output of the EG combiner. The presented results show that for $K = 1$ and unity relay gain, the approximated PDF maps to the double Rayleigh distribution, confirming that our approximation is valid. In addition, the PDF of the sum process tends to a Gaussian distribution if K increases. This observation is in accordance with the central limit theorem (CLT) [108]. Another important result is that for $K = 1$ and unity relay gain, our proposed solution for the LCR of the sum process provides us with a very close approximation to the exact LCR of a double Rayleigh distributed process given in [66]. Additionally, increasing K while keeping the relay gain constant, decreases the LCR at both lower and higher signal levels. Lastly,

the analysis of the obtained ADF reveals that keeping the relay gain constant and increasing K result in an increase of the ADF at higher signal levels, whereas it decreases at low signal levels.

With the intention to demonstrate the usefulness of this work, a BEP analysis of M -ary phase shift keying (PSK) modulation schemes over M2M fading channels under NLOS conditions with EGC in cooperative networks is reviewed in Section 5.2.

2.5 Chapter Summary and Conclusion

M2M cooperative communication systems aim to exploit the benefits of both M2M and cooperative communications. However, to cope with the problems faced within the development and performance investigation of these future communication systems, a solid knowledge of the underlying multipath fading channel characteristics is essential. For this reason, the current chapter was dedicated to model and analyze narrowband M2M fading channels in cooperative networks under NLOS propagation conditions. It is worth remembering that the topics covered in this chapter are not straightforwardly related. This chapter talked about both geometry-based and non-geometrical channel models. Furthermore, statistical characterization of MIMO M2M fading channels as well as M2M channels with and without diversity was addressed.

The chapter began with highlighting the need for proper MIMO M2M fading channel models. It was then illustrated that there is not a single M2M channel model for cooperative networks available in the literature, which assumes multiple antennas on the source mobile station, the destination mobile station or the mobile relays. These reasons provided us with a strong argument to propose a new geometry-based model for MIMO M2M channels in relay-based systems. The idea was to model the scattering environment around the source mobile station, the mobile relay, and the destination mobile station by a geometrical three-ring scattering model. The geometrical three-ring-based model is the topic of Paper I (Appendix B). The main contributions of the paper were, however, detailed in this chapter.

The chapter proceeds by bringing attention to the significance of evaluating the PDF, LCR, and ADF of fading channels. Motivated by this discussion, the key results for the aforementioned statistical quantities associated with K -parallel dual-hop fading channels were then conferred. These results were originally reported in Papers II and III (Appendices C and D). Afterwards, necessary background information was provided in the current chapter to conclude that investigations pertaining to the statistical properties of any type of diversity combining over M2M channels

in cooperative networks calls for further work. The chapter ends by summarizing the work presented in Paper IV (Appendix E), where the statistics of M2M fading channels with EGC under NLOS propagation conditions were evaluated.

Chapter 3

Statistical Modeling and Analysis of Narrowband M2M Fading Channels Under LOS Propagation Conditions

3.1 Introduction

Chapter 2 convincingly introduced the topic of channel modeling by addressing the needs, advantages, and utilization of channel models. A variety of models inclusive of the geometrical and non-geometrical models were proposed for narrowband M2M fading channels under NLOS conditions in cooperative networks. In contrast, Chapter 3 accentuates the modeling and analysis of narrowband M2M fading channels with LOS components in relay-based cooperative networks. The drive behind modeling M2M channels with LOS components is the flexibility such models provide to cater for asymmetric channel conditions associated with many practical propagation scenarios. Besides, LOS fading channel models easily reduce to those models that correspond to NLOS propagation conditions.

M2M fading channels in cooperative networks can be modeled as a sum of multiplicative fading channels. This sum of multiplicative fading channels is also called the multiple scattering radio propagation channel [109]. In a multiple scattering radio propagation environment, the received signal is composed of single, double, and in general multiple scattered components [109]. The multiple scattering concept provides a good starting point for modeling the signal envelope fluctuations of various types of M2M channels, so that their statistical properties are in agreement with measurement data [67, 68, 109]. In a single-relay dual-hop amplify-and-forward system, where the direct link from the source mobile station to the destination mobile station is obstructed, the multiple scattering results in double scattering. The

distribution of the received signal envelope at destination mobile station follows the double Rayleigh distribution under NLOS propagation conditions [66, 68]. In amplify-and-forward relay systems, profiting from cooperative diversity schemes require an extension of the double Rayleigh channel model by adding a direct link from the source mobile station to the destination mobile station. The newly added direct link between the source mobile station and the destination mobile station having no LOS component, is modeled as a zero-mean complex Gaussian process. The resulting channel, obtained by combining the direct link from the source mobile station to the destination mobile station and the link via the mobile relay is named as the NLOS second-order scattering (NLSS) channel model. The signal received after traversing through NLSS channels is composed of a sum of a single and a double scattered component [110, 111]. Extensions of NLSS channel models when a significant LOS component is only present in the direct link from the source mobile station to the destination mobile station results in single-LOS second-order scattering (SLSS) channels [110, 111]. In this case, the direct link is modeled as a non-zero-mean complex Gaussian process. It is worth indicating that even for a single-relay dual-hop configuration, SLSS channel models do not accommodate for all possible and unbalanced propagation conditions. This implies that there is still room for further research.

Statistical analysis in terms of the PDF, CDF, LCR, and ADF of double Rayleigh channels can be found in [66], whereas the distributions associated with the envelope of NLSS and SLSS channels are given in [110, 111]. The authors of [70] have studied the LCR and ADF of Rice channels in multi-hop multi-relay cooperative systems. Very few results pertaining to the statistics of Rice channels with SC, EGC, and MRC have been reported in [112, 113].

The lack of proper channel models describing the fading statistics of M2M channels with LOS components in cooperative networks has led to the work presented in this chapter. Statistical characterization of M2M fading channels under LOS propagation conditions in several different amplify-and-forward relay systems is covered in this chapter. The studied systems range from very simple configurations, such as, a single-relay dual-hop arrangement with no direct link between the source mobile station and the destination mobile station, to quite demanding situations, i.e., dual-hop multi-relay configuration in which a direct link is also available.

The remaining part of the chapter is organized as follows: Section 3.2 addresses the statistical modeling and analysis of double Rice channels. An extension of double Rayleigh channels to SLDS channels is discussed in Section 3.3. In Section 3.4, a summary of interesting results pertaining to the statistics of MLSS channels is

presented. The statistical analysis of EGC over M2M fading channels with LOS components is dealt with in Section 3.5. Finally, Section 3.6 presents the chapter summary.

3.2 Statistical Modeling and Analysis of Double Rice Channels

Statistical modeling and analysis of M2M fading channels under NLOS propagation conditions is addressed in detail in Papers I – IV (Appendices B – E). The NLOS M2M fading channel models proposed in Papers I – IV are not flexible enough to comply with the asymmetric channel conditions in many practical propagation scenarios. However, this flexibility is available in LOS M2M channel models. Ergo, Paper V aims at the statistical characterization and analysis of M2M fading channel under LOS propagation conditions. A summary of Paper V is given in this section, whereas the paper is available in Appendix F [114] of this dissertation.

Paper V presents the very first problem that was solved during the course of this PhD dissertation. Therefore, in this paper, a very simple amplify-and-forward relay fading channel is considered. This channel is in fact a concatenation of either F2M [74] and M2M channels [33] or M2F [74] and F2M channels. This kind of relay fading channel was first proposed in [66]. However, the novelty in our approach is that we have modeled the relay fading channel taking into account LOS propagation conditions. Accommodating LOS components in relay links allows us to model the overall fading channel from Tx to Rx via the relay (R) as the product of two non-zero-mean complex Gaussian processes. Thus, the envelope of the overall fading channel follows the double Rice distribution. Two typical communication scenarios, where double Rice fading comes into play, are discussed in Paper V. In one scenario, the overall Tx–R–Rx link corresponds to the downlink from the base station (BS) to the destination mobile station (MS) via a mobile relay (MR). The direct link between the BS and the MS is assumed to be blocked or can be neglected due to high path loss. See Fig. 3.1 for a better understanding of the propagation scenario. Since an MR is considered in the system, the channel from the BS to the MR is analogous to the F2M fading channel, whereas from the MR to the MS, it is an M2M fading channel. However, in the second scenario, as shown in Fig. 3.2, the Tx–R and R–Rx links correspond to the uplink from the MS to the BS and the downlink from the BS to another MS, respectively. It is assumed that the direct link between the two MSs is obstructed. Since the BS is considered to be a stationary relay, it can be seen that the overall relay fading channel from the first MS to the

second MS via the BS is a concatenation of M2F and F2M fading channels.

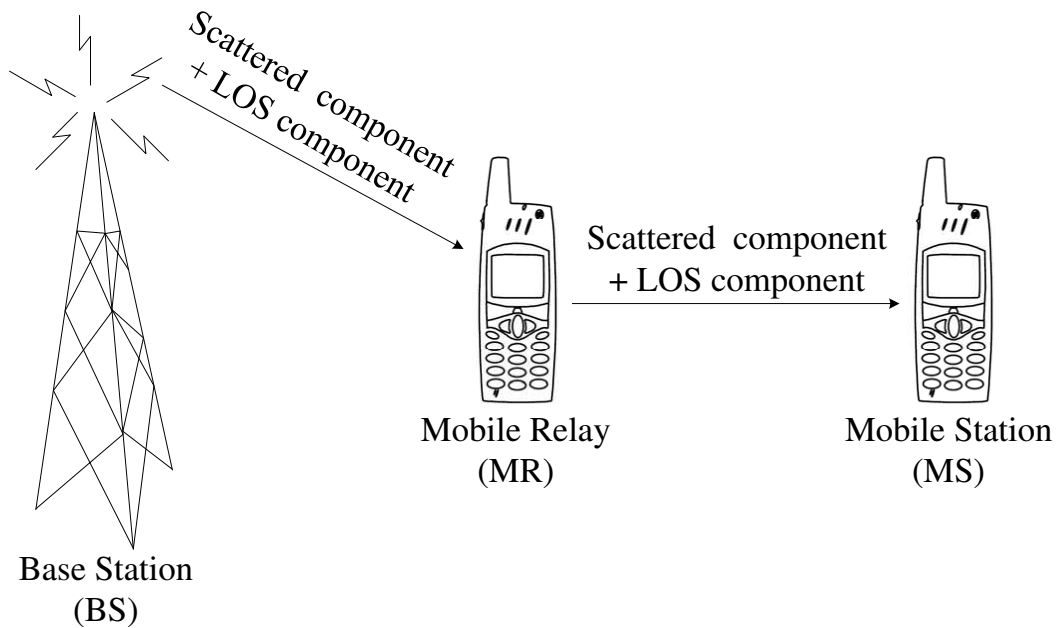


Figure 3.1: Scenario 1 – The overall mobile fading channel as a result of a concatenation of fixed-to-mobile and mobile-to-mobile fading channels.

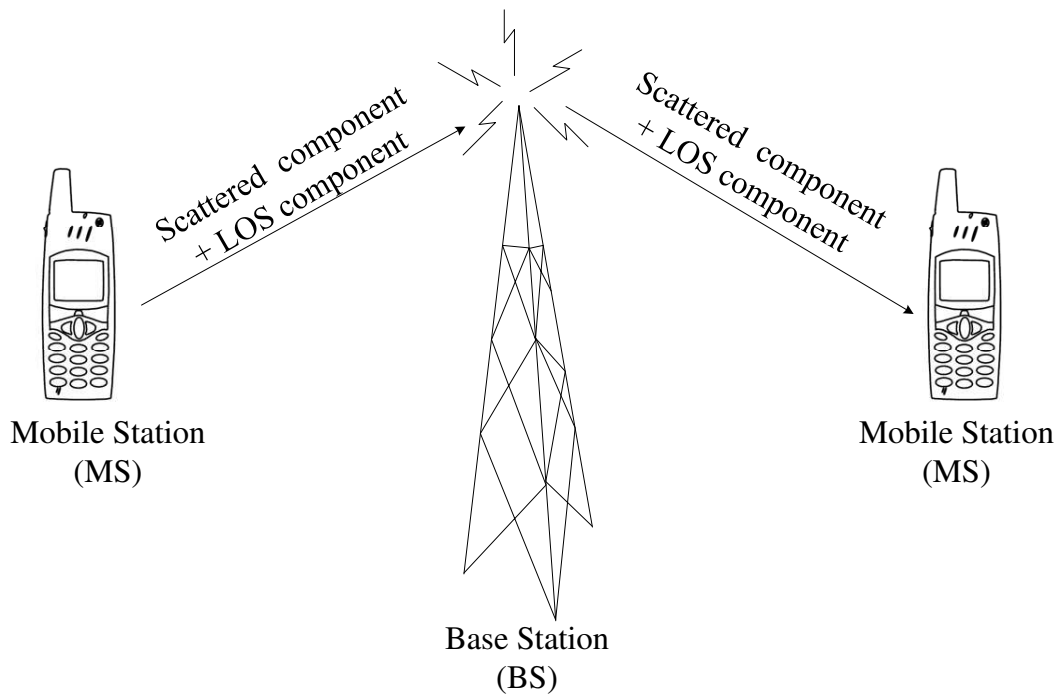


Figure 3.2: Scenario 2 – The overall mobile fading channel as a result of a concatenation of mobile-to-fixed and fixed-to-mobile fading channels.

In Paper V, we are interested in attaining a deep understanding of double Rice fading channels' statistics. For this reason, exact analytical expressions for the mean value, variance, envelope PDF, phase PDF, LCR, and ADF of double Rice channels are derived and thoroughly analyzed. The derived analytical expressions hold for the two types of double Rice fading scenarios described earlier. Additionally, they can easily be reduced to those of double Rayleigh channels by setting the amplitudes of LOS components in the expressions to zero. All numerical solutions of the integral expressions for the PDFs (envelope and phase), the LCR, and the ADF are verified by simulations. A high-performance channel simulator has been employed to obtain the simulation results. This channel simulator operates on the SOS concept [89, 90] to simulate the uncorrelated Gaussian noise processes making up the overall double Rice process. The parameters of the simulation model are designed using the GMEDS₁ [115].

In Paper V, the statistical properties of double Rice channels are compared with those of classical Rayleigh, classical Rice, and double Rayleigh channels. The presented results provide sufficient evidence to conclude that the statistics of double Rice channels are quite different from any of the other mentioned channels. It has been illustrated that the variance of the envelope PDF increases with increasing amplitudes of LOS components, whereas it decreases in case of the phase PDF. Studying the LCR at low levels reveals that keeping the Doppler frequencies of the LOS components constant, the LCR of double Rice channels with higher amplitudes of the LOS components is lower as compared to that with lower LOS amplitudes. However, at high signal levels, the LCR increases with the increase in amplitudes of the LOS components. Furthermore, keeping the amplitudes of the LOS components constant results in an increase in the LCR for all signal levels when the Doppler frequencies of the LOS components are increased. Discussions on the influence of the amplitudes and Doppler frequencies of the LOS components on the ADF of double Rice channels have been included in Paper V. This work can be utilized with ease in conducting the link-level performance analysis of communication systems in double Rice fading channels.

3.3 Statistical Modeling and Analysis of SLDS Channels

Paper V throws light on a channel model, classified as the double Rice model for M2M fading channels, assuming LOS conditions in the transmission links of amplify-and-forward relay type systems. Double Rice channel models are devel-

oped based on the assumption that the direct Tx-Rx link is blocked. This is, however, not always the case in real-world M2M cooperative communication systems. For this reason, in Paper VI, another LOS M2M fading channel model is proposed, which takes into account this direct Tx-Rx link. It is, nonetheless, assumed that the LOS component exists only in the direct link between the source mobile station and the destination mobile station. This model is referred to as the SLDS channel model. Paper VI is an extension of [116] to form a journal article. In order to cope with the demands of quality as well as comprehensiveness put on journal articles, Paper VI includes further explanations and improved figures to demonstrate the statistics of SLDS channels. This section presents a brief summary of Paper VI that can be found in full in Appendix G [117].

In Paper VI, a single-relay amplify-and-forward relay type cooperative system is studied. Meaning thereby, the considered system consists of a source mobile station, a destination mobile station, and a mobile relay. The transmission link from the source mobile station to the mobile relay and that from the mobile relay to the destination mobile station assumes NLOS propagation conditions. Therefore, the overall M2M fading channel between the source mobile station and the destination mobile station via the mobile relay is modeled as a zero-mean complex double Gaussian channel. The existence of an LOS component in the direct link from the source mobile station to the destination mobile station, makes the propagation scenario different from that behind double Rayleigh and double Rice channels. The corresponding overall M2M fading channel at the destination mobile station is then modeled as the superposition of a deterministic LOS component and the zero-mean complex double Gaussian channel. Such M2M channels are named as SLDS fading channels. Figure 3.3 illustrates the propagation scenario behind SLDS channels.

Statistical properties of SLDS fading channels are thoroughly investigated here. Analytical expressions for the mean value, variance, PDFs, LCR, and ADF of SLDS channels are derived. The derived expressions are verified using numerical techniques in simulations. An SOS-based channel simulator [89, 90] has been utilized to simulate the uncorrelated Gaussian noise processes making up the overall SLDS process. The required simulation model parameters are obtained with the help of the GMEDS₁ [115]. The close fitting of the presented theoretical and the simulation results validates the correctness of our analytical expressions. It has been shown that the properties of SLDS processes are quite different from classical Rayleigh, classical Rice, double Rayleigh, and double Rice processes. For example, the PDF of SDLS processes approaches the symmetrical Laplace distribution when the amplitude of the LOS component increases. Furthermore, for a particular value of

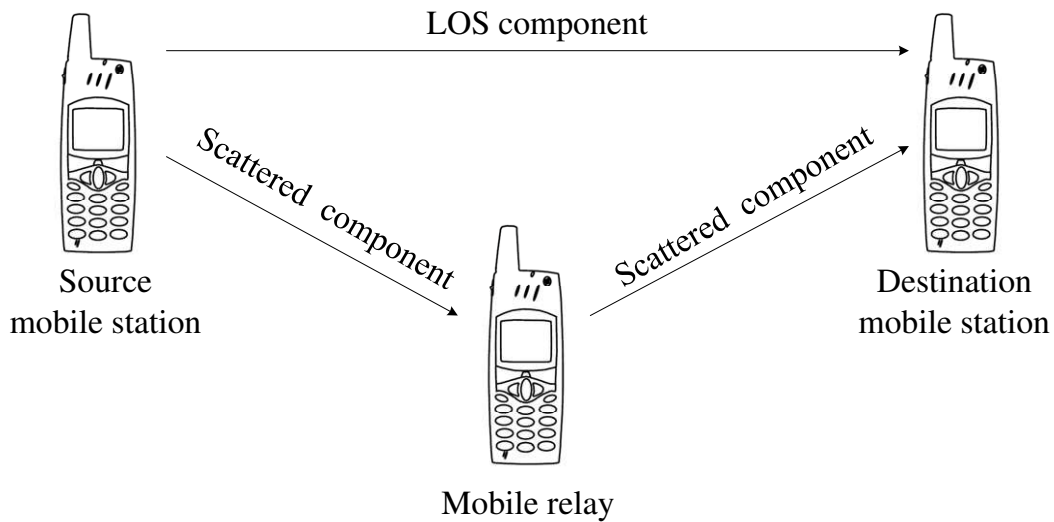


Figure 3.3: The propagation scenario behind SLDS fading channels.

the amplitude of the LOS component, the spread of the PDF of SLDS processes follows the same trend as that of classical Rayleigh and classical Rice processes. However, the PDF of SLDS processes has a narrower spread as compared to the spread of double Rice processes. With the increasing values of the amplitude of the LOS component, the PDF of the phase process associated with SLDS processes acquires a higher maximum value and narrow spread. A detailed analysis of the LCR of SLDS processes unveils that at low signal levels, the LCR decreases when the amplitude of the LOS component increases. However, the LCR of SLDS processes increases with increasing amplitudes of the LOS component at low signal levels, when compared with the LCR of double Rice processes. At medium and high signal levels, the LCR of SLDS processes is always lower than that of double Rice processes for the same value of the amplitude of the LOS component. The ADF of SLDS processes shows a behavior opposite to the LCR of SLDS processes. It has also been illustrated in Paper VI that SLDS processes reduce to double Rayleigh processes in the absence of the LOS component.

The drawback of SLDS channel models is that they cannot be justified physically. The reason is that the scattered component of the direct link between the source mobile station and the destination mobile station is ignored while modeling the M2M fading channels. This shortcoming of SLDS channel models is removed by introducing MLSS channel models in the next section.

3.4 Statistical Modeling and Analysis of MLSS Channels

Section 3.3, summarizing Paper VI (Appendix G), was concluded on the remark that the physical justification of SLDS channel models is not possible. This limitation of SLDS channel models motivated us to develop flexible channel models for realistic and more practical M2M communication scenarios. One such attempt is presented in [118] and [119], where MLSS channel models are proposed. It is assumed that in addition to the scattered components in the direct link between the source mobile station and the destination mobile station as well as in the links via the mobile relay, LOS components exist in all the transmission links. The findings of [118] and [119] are combined together, along with detailed explanations to justify our assumptions, better figures, and additional proofs, to form a journal article, i.e., Paper VII. A short overview of Paper VII is given in this section, where this paper is present in Appendix H [120] of this dissertation.

Taking into consideration the limitations on the physical implementation of the mobile stations, i.e., the source mobile station, the mobile relay, and the destination mobile station in an amplify-and-forward relay communication system, the mentioned mobile stations mostly operate in half-duplex. This means that the mobile stations cannot transmit and receive a signal in the same frequency band at the same time. Here, it is assumed that the source mobile station continuously communicates with the destination mobile station, i.e., the signal transmitted by the source mobile station in each time slot is received by the destination mobile station. The mobile relay however, receives a signal from the source mobile station in the first time slot and re-transmits it to the source mobile station in the second time slot [8, 101, 121]. For this communication scenario, a proposition for a new flexible M2M amplify-and-forward relay fading channel model under LOS conditions is made in Paper VII. The novelty in the model is that we are considering LOS components in all the transmission links, i.e., the direct link between the source mobile station and the destination mobile station as well as the two links via the mobile relay (see Fig. 3.4). Thus, by analogy to multiple scattering radio propagation channels [109], we have introduced a new narrowband M2M channel referred to as the MLSS fading channel. These channels belong to the class of second-order scattering channels, where the received signal is modeled in the complex baseband as a sum of a single and double scattered component. The flexibility of the MLSS channel model comes from the fact that it includes several other channel models as special cases, e.g., double Rayleigh, double Rice, SLDS, NLSS, and SLSS chan-

nel models. Furthermore, the MLSS channel model is general enough to cater for asymmetric channel conditions in the transmission links.

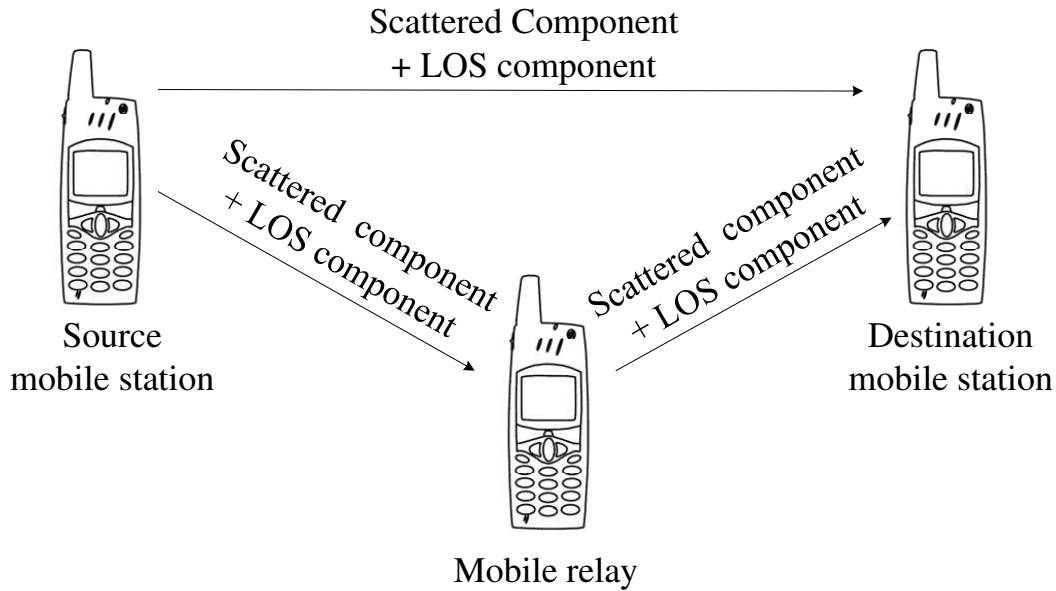


Figure 3.4: The propagation scenario behind MLSS fading channels.

Paper VII presents an insightful analysis pertaining to the statistical behavior of MLSS channels. Analytical expressions for the most important statistical properties like the mean, variance, PDF, CDF, LCR, and ADF of MLSS fading channels along with the PDF of the corresponding phase process are derived. The theory is verified for many different propagation scenarios and the presented results show a good fit between the analytical and the simulation results. The concept of SOS [89, 90] was exploited to simulate the underlying uncorrelated Gaussian noise processes of the overall MLSS process. In this work, the GMEDS₁ [115] has been employed for the computation of the simulation model parameters. In addition, the obtained results illustrate that the statistics of MLSS fading channels corresponding to various propagation scenarios vary in a wide range. This in turn leads to the fact that the proposed model is highly flexible, since we expect that its statistics can be fitted to measurement data.

It has been shown that under certain assumptions, the derived analytical expressions for the PDF, CDF, and LCR of MLSS processes reduce to the corresponding expressions of double Rayleigh, double Rice, SLDS, NLSS, and SLSS processes. A quantitative analysis is imperative to show how the channel and system parameters such as the relay gain, the amplitudes as well as the Doppler frequencies of LOS components, etc. affect the statistics of the channel and to what extent. Thus, classifying the studied fading channels as NLOS M2M channels (i.e., double Rayleigh

and NLSS channels) and LOS M2M channels (i.e., double Rice, SLDS, SLSS, and MLSS channels), we can conclude that LOS M2M channels have higher mean values and variances compared NLOS M2M channels. Furthermore, the fading behavior of LOS M2M channels can be described by a higher LCR at higher signal levels (a lower LCR at lower signal levels) but a lower ADF when compared to that of NLOS M2M channels. The relay gain influences the statistics of both NLOS and LOS M2M fading channels in the same way, i.e., increasing the relay gain increases the mean value, variance, and LCR of M2M fading channels. An increase in the relay gain, on the other hand, decreases the ADF of the channels under discussion.

Although, the problems pertaining to the protocol level and system level implementation of amplify-and-forward relay networks are out of scope of the current paper, our novel M2M channel model is useful for the system level performance evaluation of M2M communication systems in different M2M propagation scenarios. Furthermore, the theoretical results presented in this paper are beneficial for designers of the physical layer of M2M cooperative wireless networks. Based on our studies about the dynamics of MLSS fading channels, robust modulation, coding, and interleaving schemes can be developed and analyzed for M2M communication systems under LOS and NLOS propagation conditions. The obtained theoretical results have complicated integral forms, which is inherent in the nature of the problem. However, that is not a serious drawback since nowadays there are several efficient ways to solve multi-fold integrals numerically. Modern day computers and computer softwares such as Matlab can give very accurate numerical results of integrals. Furthermore, using functions available in Matlab for numerical integration like e.g., `trapz`, we managed to evaluate the derived analytical expressions with high accuracy and precision.

The limitation of MLSS channel models is that they are applicable for single-relay systems only. However, in practical cooperative systems, more than one relay can exist. In addition, in Paper VII, the relay gain assumes a constant value that does not depend on the channel and noise powers in the link from the source mobile station to the k th mobile relay. In contrast, for all practical purposes the relay gain is basically a power normalization factor [8]. In the next section, we summarize papers where we have endeavored to overcome these limitations.

3.5 Statistical Analysis of EGC over M2M Fading Channels with LOS Components

Paper VII in Appendix H was a modest attempt towards the development of flexible channel models for realistic and more practical M2M communication scenarios. Unfortunately, it was not adequate enough to cater for fading channels in multi-relay M2M communication systems. Paper IV (Appendix E) dealt with the statistical analysis of NLOS M2M channels in multi-relay cooperative systems. Therefore, in Paper VIII (Appendix I [122]), we have made an effort to extend the model discussed in Paper IV for LOS propagation conditions. However, in both Papers IV and VIII, it is supposed that the direct transmission link between the source mobile station and the destination mobile station is obstructed. It is also imperative to stress here that in order to achieve the optimum performance in a relay-based system, the selection of the relay gain is of critical importance. This crucial issue remained unaddressed in Papers IV, VII, and VIII. We have included in Appendix M [123] of this dissertation Paper XII that eliminates the drawbacks of the work presented in Paper VII. Moreover, Paper XII is a further extension of Paper VIII to form a journal article by considering the direct link from the source mobile station to the destination mobile station is unobstructed. In addition, with respect to the relay gain, the contribution of Paper XII is the derivation and verification of the optimal relay gain associated with LOS propagation scenarios. The current section outlines the statistical analysis covered in Paper XII. The performance analysis of M2M cooperative communication systems is also the subject of Paper XII, which will be reviewed in Section 5.3.

In Paper XII, we study a dual-hop amplify-and-forward relay network, where K mobile relays are connected in parallel between the source mobile station and the destination mobile station. Furthermore, the direct link from the source mobile station to the destination mobile station also exists. The propagation scenario is presented in Fig. 3.5. It is assumed that all mobile stations in the network, i.e., the source mobile station, the destination mobile station, and the K mobile relays do not transmit and receive a signal at the same time in the same frequency band. This can be achieved by using the TDMA-based amplify-and-forward relay protocols proposed in [8, 101]. Thus, the signals from the $K + 1$ diversity branches in different time slots can be combined at the destination mobile station using EGC.

Here, we are interested in analyzing the statistical properties of EGC over M2M fading channels under LOS propagation conditions. In many practical propagation scenarios, asymmetric fading conditions can be observed in different relay links.

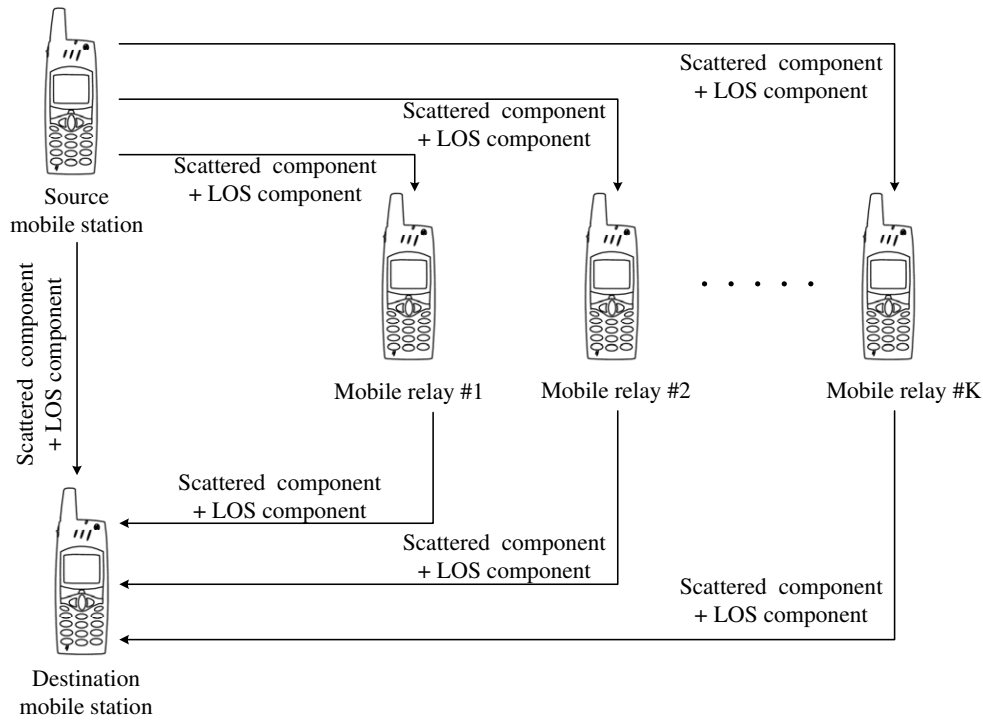


Figure 3.5: The propagation scenario behind dual-hop multi-relay LOS M2M fading channels.

Meaning thereby, LOS components can exist in all or just in some few transmission links between the source mobile station and the destination mobile station via K mobile relays. Similarly, the LOS component can be present in the direct link from the source mobile station to the destination mobile station. Thus, in order to accommodate the direct link along with the unbalanced relay links, the received signal envelope at the output of the EG combiner is modeled as a sum of a classical Rice process and K double Rice processes. Furthermore, the classical Rice process and double Rice processes are independent. Besides, these double Rice processes are independent but not necessarily identically distributed. Utilizing the derived relay gain in our analysis, the PDF, CDF, LCR, and ADF of the sum process are thoroughly investigated. The analysis of these statistical quantities gives us a complete picture of the fading channel, since the PDF can well characterize the channel, and the LCR along with the ADF provide an insight into the fading behavior of the channel. Exploiting the findings of Paper IV, analytical approximations for the aforementioned statistical quantities of the sum of a classical Rice process and K double Rice processes are derived in Paper XII. The correctness of the approximated analytical results is confirmed by evaluating the statistics of the waveforms generated by utilizing the SOS method [89, 90]. These simulation results correspond to

the true (exact) results here. The model parameters of the channel simulator are found by using the GMEDS₁ [115]. The results presented in Paper XII display a good fit of the approximated analytical and the exact simulated solutions.

This work includes a discussion on the influence of the number $K + 1$ of diversity branches as well as the presence of LOS components in the transmission links on the statistics of double Rice processes with EGC. It is necessary to keep in mind that there is also a direct link between the source mobile station and the destination mobile station, in addition to the links via K mobile relays. Therefore, the total number of diversity branches available is $K + 1$. Besides, for highlighting the effect of an LOS component on the statistics of EGC over M2M fading channels, three propagation scenarios called the full-LOS, the partial-LOS, and the NLOS scenario are considered. In the full-LOS scenario, we have LOS components in all the transmission links between the source mobile station and the destination mobile station via K mobile relays. The scenario in which LOS components are present in only some few relay links from the source mobile station to the destination mobile station via K mobile relays is referred to as the partial-LOS scenario. When LOS components do not exist in any of the transmission links, we have the NLOS scenario.

The presented results demonstrate that for any number $K + 1$ of diversity branches, the presence of LOS components increases both the mean value and variance of the received signal envelope at the output of the EG combiner. Furthermore, considering a single-relay cooperative system, where the direct transmission link from the source mobile station to the destination mobile station is blocked, under full-LOS conditions the approximated PDF maps to the double Rice distribution [114], whereas it reduces to the double Rayleigh distribution [68, 66] under NLOS conditions. It is worth mentioning that as the number of diversity branches increases, the approximated PDF tends to a Gaussian distribution. This result is in agreement with the CLT [108]. From the results obtained for the LCR of the received signal envelope at the output of the EG combiner, we can draw some conclusions. For example, LOS components facilitate in decreasing the LCR at low signal level, for any number of diversity branches. However, at high signal levels, the presence of LOS components contributes towards its increase. We can further deduce from these results that by increasing the number of diversity branches, the LCR can be reduced for lower signal values, whereas it increases for higher signal values. Finally, the results associated with the ADF clearly indicate that for all propagation scenarios, i.e., full-LOS, partial-LOS, and NLOS scenarios, increasing K results in a decrease of the ADF at all signal levels. Moreover, the presence of the LOS components in all the transmission links lowers the ADF for all signal levels

and any number of the diversity branches.

The utilization of the results discussed in this section is demonstrated in performance evaluation of M2M cooperative systems. This performance analysis is documented in the remaining part of Paper XII and Paper XI (Appendix L [124]) in Section 5.3.

3.6 Chapter Summary and Conclusion

Modeling M2M fading channels with LOS components is more reasonable, since such models can be reduced to those associated with NLOS propagation conditions with ease. Furthermore, in many practical propagation scenarios, asymmetric fading conditions can be observed in different relay links in dual-hop amplify-and-forward relay type cooperative networks. It is not necessary that LOS propagation conditions are available in all the transmission links. However, LOS M2M models provide reasonable flexibility to accommodate mixed LOS and NLOS conditions in different relay links. Therefore, Chapter 3 was devoted to modeling and analyzing narrowband M2M fading channels under LOS propagation conditions in relay-based cooperative networks.

The chapter began by discussing double Rice fading channels. Double Rice fading comes into play in single-relay dual-hop cooperative networks, where the direct transmission between the source mobile station and the destination mobile station is blocked by obstacles. It was illustrated that under NLOS propagation conditions, double Rice channels reduce to double Rayleigh channels. In addition, the differences between the statistical properties of double Rice channels and classical Rice channels are quite obvious. These results were first presented in Paper V (Appendix F), however its summary was included in this chapter.

The chapter proceeds with the proposition of another LOS M2M fading model referred to as the SLDS model for channels in single-relay dual-hop cooperative networks. This model takes into account an LOS component only in the direct link between the source mobile station and the destination mobile station, while it ignores the scattered component of this direct link. Since the scattered component of the direct link is ignored while modeling SLDS fading channels, this makes SLDS channels physically unjustifiable. This work can be found in Papers VI (Appendix G) in full.

The limitation of SLDS channel models was then removed with the introduction of MLSS channel models as we further proceeded in the chapter. M2M fading channels in single-relay dual-hop amplify-and-forward relay type cooperative sys-

tems are modeled as MLSS channels. For such channels, scattered components in the direct link between the source mobile station and the destination mobile station as well as in the links via the mobile relay are not ignored. In addition, it is assumed that LOS components exist in all the transmission links. MLSS channel models are highly flexible, since, they include several other channel models as special cases, e.g., double Rayleigh, double Rice, SLDS, NLSS, and SLSS channel models. It was argued that in practical cooperative systems, more than one relay can exist. This limits the application of MLSS channel models, which are applicable for single-relay systems only. This chapter gave a brief overview of Paper VII (Appendix H) that has been included in this dissertation in the context of MLSS channels.

The chapter ended by summing up the main findings of Papers VIII and XII (Appendices I and M), where the statistics of M2M fading channels with EGC under LOS propagation conditions were evaluated. With this study, we managed to model and analyze M2M fading channels in multi-relay dual-hop cooperative communication systems.

Chapter 4

Channel Capacity of M2M Links in Cooperative Communication Systems

4.1 Introduction

The provision of very high data rates (> 100 Mbps) is a challenging goal for future 4G mobile communication systems. In simple words, the aim is to achieve the maximum possible information transfer rate with minimum probability of error, in M2M communication links (channels) that are inherently highly dynamic in nature. This defines what is referred to as the channel capacity. According to Shannon's theory, the channel capacity serves as the upper bound to the maximum amount of information that can be reliably transmitted over a communication channel keeping the probability of error negligible [125, 126]. Statistical analysis of the channel capacity of M2M links in cooperative communication systems is the main topic of Chapter 4.

It is widely acknowledged that to cope with the problems faced within the development and performance investigation of these future communication systems, a solid knowledge of the underlying multipath fading channel characteristics is essential. It is, nonetheless, gaining recognition that in addition to the knowledge of the propagation channel characteristics, a sound understanding of the channel capacity is also indispensable to meet the data rate requirements of future mobile communication systems. For this reason, researchers are currently devoting their time and efforts to investigate various aspects of the channel capacity.

From the discussion in previous chapters, we know that M2M fading channels belong to the class of time-variant multipath propagation and fading channels. Additionally, these channels can be well characterized with the help of proper statistical models. It is therefore imperative to stress that as a consequence of the time-varying

nature of M2M channels, the channel capacity of such channels, in a general practice, is a random quantity. The channel capacity can thus also be described by appropriate statistical models. Statistical quantities such as the mean, variance, PDF, and CDF are adequate to characterize the channel capacity. The LCR and ADF, on the other hand, serve the purpose of describing the dynamic behavior of the channel capacity [127]. Recalling the discussions presented in Chapters 2 and 3, we can see that the statistical quantities mentioned here are exactly those which are important to get a complete picture of the fading channel.

Since recently, a lot of work can be found in the open literature that addresses the statistical characterization of the channel capacity of different fading channels including Rayleigh, Suzuki, Nakagami-lognormal, and Rice- m channels (see, e.g., [128, 127, 129, 130, 131, 132, 133, 134, 135] and the references therein). In addition, the statistical analysis of the channel capacity of MIMO systems with orthogonal space-time block code (OSTBC) transmission over Rayleigh and Nakagami- m channels can be found in [136] and [137], respectively. Studies pertaining to the capacity of spatially correlated Nakagami- m and Rice MIMO channels are reported in [133, 138]. In recent works [139, 140], the channel capacity statistics of fading channels in diversity systems have been analyzed. More specifically, [139] deals with the capacity analysis of Rayleigh channels with EGC, whereas the evaluation of the capacity statistics of Nakagami- m channels with EGC as well as MRC is available in [140]. The authors of [141] have presented in their work the capacity fades analysis of MIMO M2M Rician fading channels. With the increasing popularity of M2M cooperative communications, researchers are now focusing attention on exploring the statistics of the channel capacity in such systems as well. For this reason, the channel capacity statistics of double Rice and double Nakagami- m channels have thoroughly been investigated in [142, 143]. These works, however, cater for the channel capacity of SISO channels in single-relay amplify-and-forward networks only. To the best of the authors' knowledge, the analysis of the statistical properties of the channel capacity of M2M fading channels with diversity combining in dual-hop multi-relay amplify-and-forward networks is still an open problem that calls for further work. In addition, the innovative idea of utilizing the LCR of the channel capacity in cross-layer optimization of network performance over MIMO wireless channels [144] has motivated us enough to explore the capacity statistics of M2M channels in cooperative networks.

This chapter discusses the statistical properties of the channel capacity of M2M channels under NLOS conditions in V2V systems, where EGC is deployed at the destination mobile station. By using an appropriate relay gain, these results can

easily be extended for dual-hop multi-relay amplify-and-forward relay networks. An extension of the capacity analysis carried out for M2M channels under NLOS conditions to that for M2M channels with LOS components is also possible. Lastly, this capacity analysis can be employed in solving the cross-layer design and optimization problems related to M2M cooperative communication systems.

This chapter has the following structure. Section 4.2 summarizes important findings pertaining to the capacity statistics of M2M channels with EGC under NLOS conditions in V2V systems. In Section 4.3, the chapter summary is given.

4.2 Statistical Analysis of the Channel Capacity of NLOS M2M Relay Links with EGC

The authors of [144] have demonstrated the significance of knowing the channel capacity statistics. They optimized the network performance by taking advantage of the LCR of the channel capacity. Inspired by their work, in Paper IX, we evaluate the statistical properties of the channel capacity of M2M fading channels under NLOS conditions with EGC. We can, however, not proceed with the statistical analysis of the channel capacity without the knowledge of the corresponding fading channel statistics. Papers I – VIII (Appendices B – I) dealt with the statistical characterization of M2M fading channels for several different propagation scenarios assuming both NLOS and LOS conditions. Therefore, the studies presented in Papers I – VIII, especially the findings in Paper IV have been utilized in Paper IX. In this section, we summarize Paper IX that can be found in Appendix J [145].

In Paper IX, a V2V communication system is considered, where the destination mobile station is equipped with K receive antennas. The signal reaching the destination mobile station through K diversity branches is then combined using EGC. Since, the double Rayleigh distribution is considered to be the most suitable distribution to model fading channels under NLOS propagation conditions in V2V communication systems (see, e.g., [68, 36] and the references therein). Therefore, the received signal envelope at the output of the EG combiner is modeled as a sum of K double Rayleigh processes, under the assumption that perfect CSI is available at the destination mobile station. These double Rayleigh processes are assumed to be independent but not necessarily identically distributed. Here, we are interested in analyzing the statistical properties of the channel capacity of double Rayleigh fading channels with EGC. It is worth highlighting that the statistical analysis of the channel capacity documented in Paper IX is the first of its kind when it comes to M2M fading channels with diversity combining. The statistical quantities included

in our study are the PDF, CDF, LCR, and ADF of the channel capacity. The motivation to derive an expression for the PDF of the channel capacity lies in the fact that it allows us to deduce information about the mean channel capacity and the capacity variance. In addition, to obtain an insight into the temporal variations of the channel capacity, an analysis of the LCR and ADF of the channel capacity is unavoidable [127].

The derivation of the expressions for the statistical properties of the channel capacity requires information about the fading channel characteristics. It has been illustrated in Paper IV that the PDF of the sum of K double Rayleigh processes can efficiently be approximated using the Laguerre series expansion [103]. The first term in the Laguerre series expansion turns out to be the gamma distribution. This made it possible to show in Paper IV that the PDF of the sum process can be approximated by the gamma distribution. Exploiting the properties of the gamma distribution, other statistical properties of the sum process can be evaluated. Ergo, given the analytical expression for the statistical properties of the received signal envelope at the output of the EG combiner, the theoretical results associated with the statistics of the channel capacity just involve the transformation of random variables. Consequently, simple and closed-form analytical approximations for the PDF, CDF, LCR, and ADF of the channel capacity of double Rayleigh fading channels with EGC have been derived here. It is important to mention that these analytical approximations are quite general as they can accommodate unbalanced power in the diversity branches and any number K of the diversity branches. The obtained approximate analytical results are compared with the exact simulation results. Here, the simulation results are considered as the true results. This allows us to confirm the correctness and to study the accuracy of our approximate solution. An SOS-based channel simulator [61] has been employed to obtain the simulation results. Meaning thereby, the SOS concept [89, 90] has been exploited to simulate the uncorrelated Gaussian noise processes making up the received signal envelope at the output of the EG combiner. The model parameters of the channel simulator are computed by utilizing the GMEDS₁ [115].

In Paper IX, the results demonstrating the influence of the number K of diversity branches on the PDF, CDF, LCR, and ADF of the channel capacity of double Rayleigh fading channels with EGC are discussed. It has been shown that the mean channel capacity increases and the capacity variance decreases with an increase in the value of K . In addition, at low signal levels, the LCR of the channel capacity decreases as the value of K increases. The LCR however, remains the same at high signal levels for all values of K . A decrease in the ADF of the channel capacity can

be observed if the number of diversity branches K increases.

The results presented in this article can be utilized to optimize the spatial diversity receivers employed in future V2V MIMO communication systems. Furthermore, the channel capacity analysis discussed for NLOS M2M fading channels with EGC can easily be extended to cater for LOS propagation conditions. This extension is, however, quite straightforward and does not involve any new as well as innovative ideas to reach the final solution. For this reason, we have not compiled the results related to the channel capacity statistics for LOS M2M fading channels with EGC to publish a new paper.

4.3 Chapter Summary and Conclusion

The perception that a solid knowledge of the channel capacity is cardinal to meet the data rate requirements of future communication systems is gradually gaining acceptance. For this reason, this chapter focused on analyzing the statistical properties of the channel capacity of M2M links in cooperative communication systems.

The chapter began by providing necessary background information to believe that studies pertaining to the channel capacity statistics are worth spending time on. Moreover, the capacity fades analysis can be employed in the cross-layer design and to provide network performance optimization solutions. The chapter proceeds by reporting the statistical analysis of the channel capacity of NLOS M2M links with EGC in cooperative communication systems. Statistical quantities such as the PDF, CDF, LCR and ADF of the channel capacity are explored in detail. This chapter is, in short, a summary of the work presented in Paper IX (Appendix J).

Chapter 5

Performance Analysis of M2M Cooperative Communication Systems

5.1 Introduction

Chapter 5 aims to assess the performance of M2M cooperative communication systems under different propagation environments. Special emphasis is given to those M2M systems where EGC is deployed at the destination mobile station. In order to fulfill the task at hand, several performance measures such as the statistics of the instantaneous SNR, average BEP, AOF, and outage probability are discussed here.

The SNR measured at the output of the receiver is usually of interest as it is thought to be a good indicator of the overall fidelity of the considered communication system [146]. Furthermore, the PDF of the instantaneous SNR serves as the basis for the evaluation of the average BEP, AOF, and outage probability in addition to the channel capacity. In the context of diversity combining over fading channels, the outage probability and AOF are important performance criteria. The outage probability is defined as the probability that the output SNR falls below a certain specified threshold [146], whereas the AOF is a measure to quantify the severity of fading experienced by a particular channel [147].

Performance analysis of diversity systems operating over multipath fading channels is a well-explored area. For instance, performance evaluation of EGC along with MRC in terms of the bit error and outage probability over Rayleigh as well as Rice fading channels can be found in [148, 149, 150, 151, 152]. Results associated with the performance analysis of EGC over Nakagami channels and MRC over $\eta - \mu$ channels are reported in [152, 153] and [154], respectively. Several papers have been published so far concerning the AOF over multipath fading channels in diversity systems (see, e.g., [155, 156, 157, 158] and the references therein). During

the last decade, a large number of researchers devoted their efforts to analyze the performance of cooperative networks. For example, the performance of dual-hop amplify-and-forward relay networks has extensively been investigated for different types of fading channels in [159, 160, 161, 162, 163, 164, 165, 166, 167, 168, 169, 170, 171, 172, 173]. A performance analysis in terms of the average BEP as well as the outage probability of single-relay dual-hop configuration over Rayleigh and generalized- K fading channels is presented in [159, 160, 161] and [163], respectively. Studies pertaining to the asymptotic outage behavior of amplify-and-forward dual-hop multi-relay systems with Nakagami fading channels are available in [166], whereas the diversity order is addressed in [170]. The common denominator in the works [159, 160, 161, 162, 165, 164, 166, 167, 168, 169, 170, 171] is that they consider MRC at the destination mobile station, where the authors of [171] have also included in their analysis results when EGC is deployed. Performance related issues in multi-relay dual-hop non-regenerative relay systems with EGC over Nakagami- m channels are investigated in [172, 173]. The authors of [174] have explored the performance of intervehicular cooperative schemes and they proposed optimum power allocation strategies assuming cascaded Nakagami fading. The performance of several digital modulation schemes over double Nakagami- m channels with MRC diversity has been studied in [175].

This chapter focuses on analyzing the performance of multi-relay dual-hop amplify-and-forward cooperative systems with EGC over M2M fading channels under both NLOS and LOS conditions. As far as we are aware, investigations on the performance of M2M cooperative systems with EGC under different propagation environments have not been carried out yet. Thus, a performance analysis in terms of the statistics of the instantaneous SNR at the output of the EG combiner, average BEP, AOF, and outage probability is presented in the following.

The remaining part of the chapter is structured as follows: Section 5.2 deals with the average BEP analysis over multiple double Rayleigh fading channels with EGC. Section 5.3 summarizes the conclusions that can be drawn after exploring the performance of cooperative systems with EGC over M2M fading channels with LOS components. Finally, the chapter summary is given in Section 5.4.

5.2 Performance Analysis of Cooperative Systems with EGC in NLOS M2M Fading Channels

A number of models for narrowband M2M fading channels under NLOS as well as LOS propagation conditions are introduced in Papers I – VIII (Appendices B – I).

In addition, several important statistical properties have thoroughly been investigated. Paper IX (AppendixJ) is dedicated to the analysis of statistics of the channel capacity. Realizing the necessity of performance assessment in the design and development of relay-based cooperative communication systems, in Paper X, we have drawn our attention towards evaluating the performance of such systems. Here, the system performance is studied in narrowband, NLOS M2M fading channels with EGC. However, this performance analysis is not possible without a deep understanding of how the associated fading channel behaves. Thus, Paper X readily exploits the results obtained in Paper IV. In this section, we present a brief overview of Paper X, which is given in Appendix K [176].

In Paper X, we have a dual-hop amplify-and-forward relay type cooperative network (see Fig. 5.1). It is assumed that K mobile relays are connected in parallel between the source mobile station and the destination mobile. Furthermore, it is supposed that the direct transmission link between the source mobile station and the destination mobile has been obstructed. Consequently, this kind of config-

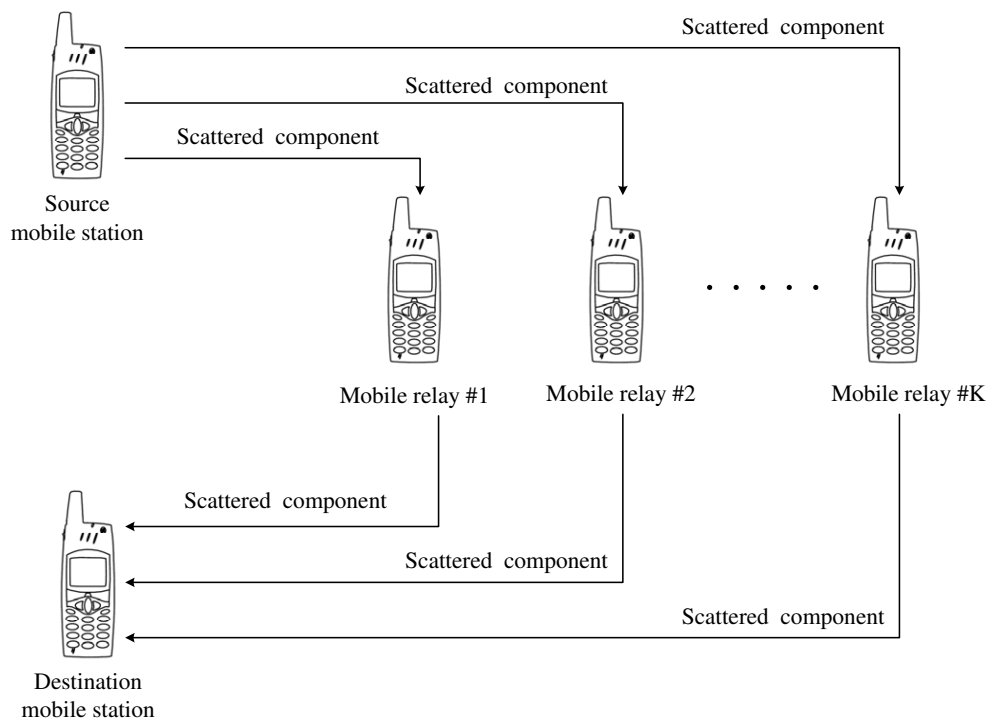


Figure 5.1: The propagation scenario behind dual-hop multi-relay NLOS M2M fading channels.

uration gives rise to K diversity branches. All the mobile stations in the network, i.e., the source mobile station, the destination mobile station, and the K mobile re-

band. An EG combiner is deployed at the destination mobile station in the system under consideration. Given that the LOS components in all the relay links are blocked and perfect CSI is available at the destination mobile station, the received signal envelope at the output of the EG combiner is modeled as a sum of K double Rayleigh processes. It can easily be found in the literature that under NLOS propagation conditions, the overall M2M fading channel between the source mobile station and the destination mobile station via k th mobile relay follows the double Rayleigh distribution [66, 111]. The double Rayleigh processes in the sum process are independent but not necessarily identically distributed. It is important to note that in a real amplify-and-forward relay system, the noise component present in the link between the source mobile station and k th mobile relay is also amplified and forwarded along with the signal to the destination mobile station. Plus to that, on its way to the destination mobile station, this noise acquires a contribution from the fading in the relay link from the k th mobile relay to the destination mobile station. Thus, the total noise in the k th relay link is a sum of the noise component inherently present in the transmission link between the k th mobile relay and the destination mobile (i.e., AWGN) and the noise component that is amplified by the k th mobile relay and then is forwarded. However, for reasons of simplicity, we have modeled the total noise in the link from the source mobile station to the destination mobile station via the k th mobile relay as a zero-mean AWGN process with variance $N_0/2$, where N_0 is the noise power spectral density. Here, the aim is to study the performance of M -ary PSK modulation schemes over double Rayleigh fading channels with EGC assuming K diversity branches (mobile relays). For this reason, the average BEP is evaluated.

In order to obtain an expression for the average BEP, there is a need to first define the instantaneous SNR per bit at the output of the EG combiner and then derive its PDF. The required SNR can be expressed as the ratio of the squared received signal envelope at the output of the EG combiner and the total received noise. Using the approximation for the PDF of the received signal envelope at the output of the EG combiner presented in Paper IV and the concept of transformation of random variable, the PDF of the required SNR is computed. This approximation of the PDF of the instantaneous SNR per bit at the output of the EG combiner in turn leads to a simple approximation for the average BEP.

The derived average BEP approximation for double Rayleigh channels with EGC is evaluated for the QPSK, 8-PSK, and 16-PSK modulation schemes in Paper X. Furthermore, the average BEP for these modulation schemes is compared for a different number of diversity branches K . It is quite obvious from the obtained

results that for all modulation schemes, a remarkable improvement in the diversity gain can be achieved when the number of diversity branches increases, say e.g., from $K = 1$ to $K = 6$. For the sake of completeness of our performance analysis, we have included in our discussion the average BEP results when MRC is deployed at the destination mobile station.

Although, the average BEP approximation is evaluated for the M -ary PSK modulation schemes in Paper X, this approximation can easily be employed in evaluating other modulation schemes, such as coherent binary frequency shift keying (BFSK), coherent M -ary amplitude shift keying (MASK), coherent differentially encoded PSK, coherent $\frac{\pi}{4}$ differentially encoded QPSK etc. Moreover, it is possible to extend the average BEP analysis carried out for M -ary PSK modulation schemes over double Rayleigh fading channels with EGC in Paper X to the average BEP analysis over M2M fading channels with EGC and LOS components. The average BEP along with several other performance measures are discussed in the following section, in context with LOS M2M fading channels with EGC.

5.3 Performance Analysis of Cooperative Systems with EGC in LOS M2M Fading Channels

Paper X (Appendix K) analyzes the performance of M -ary PSK over multiple M2M fading channels with EGC under NLOS propagation conditions. Paper XI in Appendix L [124] is an extension of Paper X, which evaluates the performance of cooperative communication systems in M2M fading channels with EGC under LOS conditions. This system performance analysis over LOS M2M fading channels was attractive for us since we gained additional degrees of freedom to take into account several propagation scenarios. It is worth mentioning that the performance of dual-hop amplify-and-forward relay systems is highly dependent on the appropriate selection of the relay gain. Moreover, the assessment of the performance of such systems, without considering the actual noise component associated with real-world amplify-and-forward relay systems can lead to incorrect conclusions about the achievable performance gains. Therefore, Paper XI gives special consideration to the selection of proper relay gains. Afterwards, these optimum relay gains are applied to calculate the true noise power in the relay links, which in turn forms the basis for our performance analysis in Paper XI. The actual noise is modeled as a sum of the noise component inherently existing in the transmission link between the k th mobile relay and the destination mobile (i.e., AWGN) and the noise component that is amplified by the k th mobile relay and then is forwarded. This is in contrast to the

analysis presented in Paper X. The problem, which still remains in Paper XI is, the analysis is performed assuming that the direct transmission link between the source mobile station and the destination mobile station is blocked by obstacles. This calls for further work in order to move one step ahead towards analyzing M2M cooperative communication systems in more practical propagation scenarios. For this reason, we have included in Appendix M [123] of this dissertation, Paper XII. This paper is an upgrade of Papers IV and XI to form a journal article. It is considered that the transmission links between the source mobile station and the destination mobile station include the direct link along with the links via K mobile relays in Paper XII. It is further assumed that an LOS component can exist in any of the transmission links. The presence of $K + 1$ transmission links each having a scattered component along with an LOS component, the utilization of optimum relay gains as well as the actual noise component in our analysis, make this work novel. The part of Paper XII dealing with the statistical analysis of M2M fading channels with LOS components and EGC has been discussed in Section 3.5. However, this section details the part of Paper XII pertaining to the performance analysis of M2M cooperative communication systems in such channels.

Recall from Section 3.5 that in Paper XII, the system under investigation is a dual-hop amplify-and-forward relay system, where K mobile relays are arranged in parallel between the source mobile station and the destination mobile station. It is further assumed that the direct link from the source mobile station to the destination mobile station is not blocked by any obstacles. The propagation scenario is illustrated in Fig. 5.2. All the mobile stations in the network, i.e., the source mobile station, the destination mobile station, and the K mobile relays operate in half-duplex mode. Such a configuration gives rise to $K + 1$ diversity branches. The signals received from $K + 1$ diversity branches are then combined at the destination mobile station using EGC to achieve the spatial diversity gain. For quickly refreshing further details about the system model as well as the procedures followed to derive analytical expressions for different statistical properties of M2M fading channels with LOS components and EGC, we refer the reader to Section 3.5.

As mentioned earlier in Paper XII, a major section is devoted to assess the performance of dual-hop amplify-and-forward relay systems in M2M fading channels with LOS components and EGC. Several performance measures inclusive of the statistics of the instantaneous SNR at the output of the EG combiner, AOF, average BEP, and outage probability are explored in detail. The derivation and analysis of these performance measures however, specifically require the knowledge of the PDF of the sum of a classical Rice process and K double Rice processes. It has

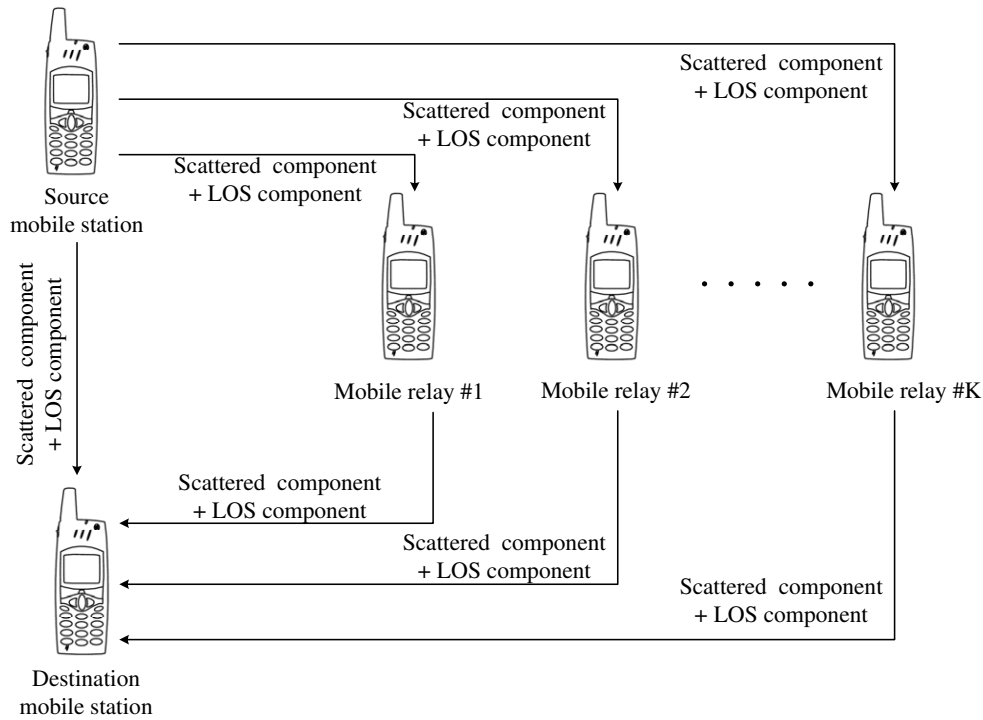


Figure 5.2: The propagation scenario behind dual-hop multi-relay LOS M2M fading channels.

been illustrated in Paper XII that the PDF of this sum process can efficiently be approximated with the help of the Laguerre series expansion. The advantage of using the Laguerre series is that this makes it possible to approximate the PDF of the sum process by a gamma distribution with reasonable accuracy. The PDF of the instantaneous SNR is then obtained using the approximated PDF of the sum process and a simple transformation of random variables. Given the PDF of the instantaneous SNR, the computation of the moments of SNR, AOF, the average BEP, and the outage probability is rather straightforward.

The accuracy of the derived theoretical approximations is assessed by simulations. The presented results display a good fit between the approximated theoretical and the exact simulation results confirming the correctness of our approximation. This work aims to provide vital information about the influence of LOS components on the overall performance of relay-based cooperative systems in different propagation conditions. For this reason, three propagation scenarios namely full-LOS, partial-LOS, and NLOS scenarios are considered. The full-LOS scenario corresponds to the situation where LOS components are present in the direct link as well as all the transmission links between the source mobile station and the destination mobile station via K mobile relays. In the partial-LOS scenario, we have LOS com-

ponents only in some few links from the source mobile station to the destination mobile station via K mobile relays. The absence of LOS components in all the transmission links leads to the NLOS scenario.

The approximated average BEP over M2M fading channels with EGC under full-LOS, partial-LOS, and NLOS conditions is evaluated for QPSK, 8-PSK, and 16-PSK modulation schemes in Paper XII. A comparison of the average BEP of these modulation schemes is shown by taking into account $K + 1$ diversity branches for each modulation scheme. The obtained results show that for all modulation schemes, a significant enhancement in the diversity gain in a single-relay system can be observed with the availability of just one extra transmission link. For example, when the direct link from the source mobile station to the destination mobile station is not blocked by obstacles and a single relay is present in the system, then at the average BEP of 10^{-3} , it is possible to attain a diversity gain of approximately 21 dB. The illustrated results show a decrease in the outage probability as the number of diversity branches increases. This is due to EGC deployed at the destination mobile station and the resulting performance advantage is the diversity gain. It has also been demonstrated that for $K \geq 10$, the dual-hop amplify-and-forward system with M2M fading channels has a lower error probability than an AWGN channel with the same SNR. This improved performance is due to the array gain of the EG combiner. It can also be concluded from the presented results that generally, in a dual-hop relay system with EGC, the presence of LOS components in the transmission links improves the systems' performance.

5.4 Chapter Summary and Conclusion

In the design and development of any new communication system, rigorous evaluation of its performance is imperative. This chapter therefore, draws attention towards analyzing the performance of M2M cooperative communication systems in different propagation environments.

The chapter began by introducing some important performance measures such as the instantaneous SNR at the output of a receiver, AOF, average BEP, and outage probability. Arguments were included to justify the importance of these performance measures. Motivated by the scarce availability of studies pertaining to the performance assessment of M2M cooperative systems especially those where EGC is deployed at the destination mobile station, performance results of significant importance were detailed in this chapter. The performance of such systems was evaluated over M2M fading channels under NLOS propagation conditions. These

results were originally presented in Paper X (Appendix K). The chapter ends by summarizing the work reported in Paper XII (Appendix M), where the performance of dual-hop multi-relay cooperative systems over M2M fading channels with EGC under LOS propagation conditions was evaluated. As a result, it was concluded that generally, in a dual-hop relay system with EGC, the presence of LOS components in the transmission links improves the systems' performance.

Chapter 6

Summary of Contributions and Outlook

6.1 Major Contributions

This dissertation dealt with the exploration of various aspects of M2M cooperative communication systems. The topics covered range from the modeling of M2M fading channels in relay links under different propagation conditions to the overall performance analysis of the system. In the following, the contributions of this doctoral dissertation are summarized.

- A new geometry-based model for MIMO M2M channels in relay-based systems was proposed, where the scattering environment around the source mobile station, the mobile relay, and the destination mobile station is modeled by a geometrical three-ring scattering model.
- A stochastic narrowband MIMO M2M reference channel model and the corresponding channel simulation model were derived based on the geometrical three-ring scattering models. Spatial and temporal correlation functions of the reference and the simulation model were analyzed for isotropic as well as non-isotropic scattering scenarios.
- We have extended the double Rayleigh channel model to the double Rice channel model for M2M fading channels under LOS conditions in single-relay dual-hop amplify-and-forward relay systems. A profound statistical analysis of double Rice channels is presented by deriving analytical expressions for their mean, variance, PDFs of the envelope as well as the associated phase process, CDF, LCR, and ADF.

- The double Rice channel model was further extended to the MLSS model for M2M fading channels with LOS components in single-relay dual-hop amplify-and-forward relay systems. Interesting findings pertaining to statistical properties, such as, the mean, variance, PDFs of the envelope as well as the associated phase process, CDF, LCR, and ADF of MLSS fading channels were documented.
- In practical cooperative systems, more than one relay can exist. Since MLSS channel models are developed for single-relay systems only, their application in practical cooperative systems is limited. For this reason, we modeled M2M fading channels with EGC under NLOS in multi-relay dual-hop amplify-and-forward relay systems, as a sum of double Rayleigh processes.
- We demonstrated that the statistical properties, such as the PDF, CDF, LCR, and ADF of a sum of double Rayleigh processes can be well approximated by the corresponding statistical quantities of a gamma process.
- In order to accommodate the asymmetric propagation conditions and to have some flexibility in the model, we studied M2M fading channels with EGC under LOS in multi-relay dual-hop amplify-and-forward relay systems. Thus, we extended the sum of double Rayleigh to a sum of double Rice processes. A further extension was made to cater for the direct transmission link from the source mobile station to the destination mobile station. The resulting overall M2M fading channel with LOS components was then modeled as a sum of classical Rice and multiple double Rice processes.
- In order to meet the data rate requirements of future communication systems, it is thought that a sound understanding of the channel capacity is indispensable. Therefore, we explored the statistical characteristics of the channel capacity of M2M links under NLOS conditions in cooperative communication systems. The statistical quantities of interest included the PDF, CDF, LCR, and ADF of the channel capacity.
- Keeping in view the necessity of performance evaluation in the design and development of any new communication system, we analyzed the performance of M2M cooperative communication systems in different propagation environments. The statistics of the instantaneous SNR, average BEP, AOF, and outage probability are those performance measures which were thoroughly investigated.

6.2 Outlook

This dissertation was an attempt to probe into the issues related to the modeling and analysis of M2M fading channels considering different propagation conditions in cooperative communication systems. Statistical characterization of the channel capacity and the performance analysis of the mentioned systems were also included. However, there are still problems that remain unaddressed. Some few problems are highlighted in the following.

- The experimental validation of any channel model no doubt gives stronger grounds to believe that the channel model reliably represents the reality. However, to the best of our knowledge, real-world measurement data for M2M fading channels in cooperative networks have never been studied, as no measurements are available. Spending resources to obtain the measurement data is a good investment if the priority is to guarantee the reliability of the channel model. The unavailability of measurements restricted us to verify the results presented here by measurement data.
- Geometrical and non-geometrical channel models for M2M cooperative communication systems were introduced. However, there is a lack of measurement-based channel models for such systems. The design of measurement-based channel models requires other parameter computation methods, such as those in [177, 178]. This topic was, nevertheless, beyond the scope of the current dissertation.
- The entire analysis presented in this dissertation is based on the assumption that the stochastic processes making up M2M fading channels in different propagation scenarios are uncorrelated. Therefore, our analysis can be extended while taking into account spatially and/ or temporally correlated MIMO channels.
- We have only discussed narrowband M2M fading channels throughout this work. Efforts are required to extend our studies to frequency selective M2M fading channels.
- Although, we managed to provide simple and closed-form analytical expressions for the statistical properties of M2M channels with EGC and their capacity, these expressions are, nevertheless, just approximations. Therefore, there is a need of further research to obtain exact, simple, and closed-form solution.

- It is known that the performance of dual-hop amplify-and-forward relay systems is highly dependent on the appropriate selection of the relay gain. We employed blind and semi-blind relaying with fixed and average relay gain, respectively, in our studies. CSI-assisted relaying that utilizes variable relay gain has not been explored by us. It is important to investigate the pros and cons of blind, semi-blind, and CSI-assisted relaying over M2M fading channels.
- It is available in the literature that the LCR of the channel capacity can be utilized in cross-layer design and optimization of network performance. We have derived the LCR of the channel capacity of M2M channels with EGC, which can be employed in cross-layer design and optimization of cooperative communication systems.
- M2M cooperative communication systems profit from the principle of adaptability. There is, nonetheless, a need to develop adaptive algorithms for efficient radio resource management (RRM). These RRM algorithms should be dynamic in nature in order to take advantage of the favorable channel conditions to increase the system's spectral efficiency (capacity).

REFERENCES

- [1] R. Pabst, B. Walke, D. Schultz, et al., “Relay-based deployment concepts for wireless and mobile broadband radio,” *IEEE Communications Magazine*, vol. 42, no. 9, pp. 80–89, Sept. 2004.
- [2] Y. Fan and J. S. Thompson, “MIMO configurations for relay channels: Theory and practice,” *IEEE Trans. Wireless Commun.*, vol. 6, no. 5, pp. 1774–1786, May 2007.
- [3] M. Dohler and Y. Li, *Cooperative Communications: Hardware, Channel, and PHY*. Chichester: John Wiley & Sons, 1st edition, 2010.
- [4] A. Sendonaris, E. Erkip, and B. Aazhang, “User cooperation diversity — Part I: System description,” *IEEE Trans. Commun.*, vol. 51, no. 11, pp. 1927–1938, Nov. 2003.
- [5] C. Weijun, L. Zheng, and J. Hu, “Performance analysis of cooperative macro-diversity in mobile cellular networks,” in *Proc. IEEE 6th Circuits and Systems Symp. on Emerging Technologies: Frontiers of Mobile and Wireless Communication*, Shanghai, China, Jun. 2004, vol. 1, pp. 133–136.
- [6] A. Scaglione, D. L. Goeckel, and J. N. Laneman, “Cooperative communications in mobile ad hoc networks,” *IEEE Signal Processing Magazine*, vol. 23, no. 5, pp. 18–29, Sept. 2006.
- [7] J. N. Laneman, D. N. C. Tse, and G. W. Wornell, “Cooperative diversity in wireless networks: Efficient protocols and outage behavior,” *IEEE Trans. Inform. Theory*, vol. 50, no. 12, pp. 3062–3080, Dec. 2004.
- [8] R. U. Nabar, H. Bölcskei, and F. W. Kneubühler, “Fading relay channels: Performance limits and space-time signal design,” *IEEE J. Select. Areas Commun.*, vol. 22, no. 6, pp. 1099–1109, Aug. 2004.
- [9] J. N. Laneman and G. W. Wornell, “Distributed space-time-coded protocols for exploiting cooperative diversity in wireless networks,” *IEEE Trans. Inform. Theory*, vol. 49, no. 10, pp. 2415–2425, Oct. 2003.
- [10] A. Stefanov and E. Erkip, “Cooperative space-time coding for wireless networks,” *IEEE Trans. Commun.*, vol. 53, no. 11, pp. 1804–1809, Nov. 2005.

- [11] S. Barbarossa and G. Scutari, “Distributed space time codes for regenerative relays,” *IEEE Trans. Wireless Commun.*, vol. 4, no. 5, pp. 2387–2399, Sept. 2005.
- [12] C. Lee and S. C. Vishwanath, “Cooperative communication strategies for sensor networks,” in *Proc. IEEE Military Comm. Conf., (MILCOM)*, Atlantic City, NJ, USA, Oct. 2005, vol. 2, pp. 698–704.
- [13] A. Sendonaris, E. Erkip, and B. Aazhang, “User cooperation diversity — Part II: Implementation aspects and performance analysis,” *IEEE Trans. Commun.*, vol. 51, no. 11, pp. 1939–1948, Nov. 2003.
- [14] M. Dohler, *Virtual Antenna Arrays*. Ph.D. dissertation, King’s College, London, United Kingdom, 2003.
- [15] J. Zhu and S. Roy, “MAC for dedicated short range communications in intelligent transport system,” *IEEE Communications Magazine*, vol. 41, no. 12, pp. 60–67, Dec. 2003.
- [16] V. Gradinescu et al., “Adaptive traffic lights using car-to-car communication,” in *Proc. IEEE 65th Veh. Technol. Conf., VTC’07-Spring*, Dublin, Ireland, Apr. 2007, pp. 21–25, DOI 10.1109/VETECS.2007.17.
- [17] C. P. Young, “A highway traffic simulator with Dedicated Short Range Communications based cooperative collision prediction and warning mechanism,” in *Proc. 1st IEEE Intelligent Vehicles Symposium*, Eindhoven, Holland, Jun. 2008, pp. 114–119.
- [18] A. F. Molisch, F. Tufvesson, J. Karedal, and C. F. Mecklenbräuker, “A survey on vehicle-to-vehicle propagation channels,” *IEEE Trans. Commun.*, vol. 16, no. 6, pp. 12–22, Dec. 2009.
- [19] G. J. Foschini and M. J. Gans, “On limits of wireless communications in a fading environment when using multiple antennas,” *Wireless Pers. Commun.*, vol. 6, pp. 311–335, Mar. 1998.
- [20] I. E. Telatar, “Capacity of multi-antenna Gaussian channels,” *European Trans. Telecommun. Related Technol.*, vol. 10, pp. 585–595, 1999.
- [21] D. S. Shiu, G. J. Foschini, M. J. Gans, and J. M. Kahn, “Fading correlation and its effect on the capacity of multielement antenna systems,” *IEEE Trans. Commun.*, vol. 48, no. 3, pp. 502–513, Mar. 2000.

- [22] M. Pätzold and B. O. Hogstad, “A space-time channel simulator for MIMO channels based on the geometrical one-ring scattering model,” *Wireless Communications and Mobile Computing, Special Issue on Multiple-Input Multiple-Output (MIMO) Communications*, vol. 4, no. 7, pp. 727–737, Nov. 2004.
- [23] M. Pätzold and B. O. Hogstad, “Design and performance of MIMO channel simulators derived from the two-ring scattering model,” in *Proc. 14th IST Mobile & Communications Summit, IST 2005*, Dresden, Germany, Jun. 2005, paper no. 121.
- [24] G. J. Byers and F. Takawira, “Spatially and temporally correlated MIMO channels: modelling and capacity analysis,” *IEEE Trans. Veh. Technol.*, vol. 53, no. 3, pp. 634–643, May 2004.
- [25] Z. Tang and A. S. Mohan, “A correlated indoor MIMO channel model,” in *Canadian Conference on Electrical and Computer Engineering 2003, IEEE CCECE 2003*, Venice, Italy, May 2003, vol. 3, pp. 1889 – 1892.
- [26] R. B. Ertel, P. Cardieri, K. W. Sowerby, T. S. Rappaport, and J. H. Reed, “Overview of spatial channel models for antenna array communication systems,” *IEEE Personal Communications*, vol. 5, no. 1, pp. 10–22, Feb. 1998.
- [27] R. B. Ertel and J. H. Reed, “Angle and time of arrival statistics for circular and elliptical scattering models,” *IEEE J. Select. Areas Commun.*, vol. 17, no. 11, pp. 1829–1840, Nov. 1999.
- [28] M. Pätzold and N. Youssef, “Modelling and simulation of direction-selective and frequency-selective mobile radio channels,” *International Journal of Electronics and Communications*, vol. AEÜ-55, no. 6, pp. 433–442, Nov. 2001.
- [29] A. Abdi and M. Kaveh, “A space-time correlation model for multielement antenna systems in mobile fading channels,” *IEEE J. Select. Areas Commun.*, vol. 20, no. 3, pp. 550–560, Apr. 2002.
- [30] T. A. Chen, M. P. Fitz, W. Y. Kuo, M. D. Zoltowski, and J. H. Grimm, “A space-time model for frequency nonselective Rayleigh fading channels with applications to space-time modems,” *IEEE J. Select. Areas Commun.*, vol. 18, no. 7, pp. 1175–1190, Jul. 2000.

- [31] Y. Ma and M. Pätzold, "A wideband one-ring MIMO channel model under non-isotropic scattering conditions," in *Proc. IEEE 67th Vehicular Technology Conference, IEEE VTC 2008-Spring*, Marina Bay, Singapore, May 2008, pp. 424–429.
- [32] M. Pätzold and B. O. Hogstad, "A wideband MIMO channel model derived from the geometrical elliptical scattering model," *Wireless Communications and Mobile Computing*, vol. 8, pp. 597–605, May 2008.
- [33] A. S. Akki and F. Haber, "A statistical model of mobile-to-mobile land communication channel," *IEEE Trans. Veh. Technol.*, vol. 35, no. 1, pp. 2–7, Feb. 1986.
- [34] A. S. Akki, "Statistical properties of mobile-to-mobile land communication channels," *IEEE Trans. Veh. Technol.*, vol. 43, no. 4, pp. 826–831, Nov. 1994.
- [35] C. S. Patel, G. L. Stüber, and T. G. Pratt, "Comparative analysis of statistical models for the simulation of Rayleigh faded cellular channels," *IEEE Trans. Commun.*, vol. 53, no. 6, pp. 1017–1026, Jun. 2005.
- [36] M. Pätzold, B. O. Hogstad, and N. Youssef, "Modeling, analysis, and simulation of MIMO mobile-to-mobile fading channels," *IEEE Trans. Wireless Commun.*, vol. 7, no. 2, pp. 510–520, Feb. 2008.
- [37] A. G. Zajić and G. L. Stüber, "Space-time correlated mobile-to-mobile channels: modelling and simulation," *IEEE Trans. Veh. Technol.*, vol. 57, no. 2, pp. 715–726, Mar. 2008.
- [38] A. Chelli and M. Pätzold, "A MIMO mobile-to-mobile channel model derived from a geometric street scattering model," in *Proc. 4th IEEE International Symposium on Wireless Communication Systems, ISWCS 2007*, Trondheim, Norway, Oct. 2007, pp. 792–797.
- [39] A. Chelli and M. Pätzold, "A non-stationary MIMO vehicle-to-vehicle channel model based on the geometrical T-junction model," in *Proc. International Conference on Wireless Communications and Signal Processing, WCSP 2009*, Nanjing, China, Nov. 2009.
- [40] A. G. Zajić and G. L. Stüber, "Three-dimensional modeling, simulation, and capacity analysis of space-time correlated mobile-to-mobile channels," *IEEE Trans. Veh. Technol.*, vol. 57, no. 4, pp. 2042–2054, Jul. 2008.

- [41] Y. Ma and M. Pätzold, “Wideband two-ring MIMO channel models for mobile-to-mobile communications,” in *Proc. 10th International Symposium on Wireless Personal Multimedia Communications, WPMC 2007*, Jaipur, India, Dec. 2007, pp. 380–384.
- [42] A. Chelli and M. Pätzold, “A wideband multiple-cluster MIMO mobile-to-mobile channel model based on the geometrical street model,” in *Proc. IEEE International Symposium on Personal, Indoor and Mobile Radio Communications, PIMRC 2008*, Cannes, France, Sept. 2008, pp. 1–6.
- [43] A. G. Zajić, G. L. Stüber, T. G. Pratt, and S. Nguyen, “Wideband MIMO mobile-to-mobile channels: Geometry-based statistical modeling with experimental verification,” *IEEE Trans. Veh. Technol.*, vol. 58, no. 2, pp. 517–534, Feb. 2009.
- [44] A. G. Zajić and G. L. Stüber, “Three-dimensional modeling and simulation of wideband MIMO mobile-to-mobile channels,” *IEEE Trans. Wireless Commun.*, vol. 8, no. 3, pp. 1260–1275, Mar. 2009.
- [45] X. Cheng et al., “An adaptive geometry-based stochastic model for non-isotropic MIMO mobile-to-mobile channels,” *IEEE Trans. Wireless Commun.*, vol. 8, no. 9, pp. 4824–4835, Sept. 2009.
- [46] J. Proakis and M. Salehi, *Digital Communications*. New York: McGraw-Hill, 5th edition, 2008.
- [47] R. E. Blahut, *Theory and Practice of Error Control Codes*. Reading, Massachusetts: Addison-Wesley, 1984.
- [48] K. Y. Tsie, P. Fines, and A. H. Aghvami, “Concatenated code and interleaver design for data transmission over fading channels,” in *Proc. 9th International Conference on Digital Satellite Communications, ICDS-9*, Copenhagen, Denmark, May 1992, pp. 253–259.
- [49] E. Biglieri, D. Divsalar, P. J. McLane, and M. K. Simon, *Introduction to Trellis-Coded Modulation with Applications*. New York: Macmillan Publishing Company, 1991.
- [50] J. M. Morris, “Burst error statistics of simulated Viterbi decoded BPSK on fading and scintillating channels,” *IEEE Trans. Commun.*, vol. 40, no. 1, pp. 34–41, Jan. 1992.

- [51] W. R. Young, "Comparison of mobile radio transmission at 150, 450, 900, and 3700 MHz," vol. 31, pp. 1068–1085, Nov. 1952.
- [52] H. W. Nylund, "Characteristics of small-area signal fading on mobile circuits in the 150 MHz band," *IEEE Trans. Veh. Technol.*, vol. 17, pp. 24–30, Oct. 1968.
- [53] Y. Okumura, E. Ohmori, T. Kawano, and K. Fukuda, "Field strength and its variability in VHF and UHF land mobile radio services," *Rev. Elec. Commun. Lab.*, vol. 16, pp. 825–873, Sept./Oct. 1968.
- [54] M. Pätzold, U. Killat, and F. Laue, "An extended Suzuki model for land mobile satellite channels and its statistical properties," *IEEE Trans. Veh. Technol.*, vol. 47, no. 2, pp. 617–630, May 1998.
- [55] H. Suzuki, "A statistical model for urban radio propagation," *IEEE Trans. Commun.*, vol. 25, no. 7, pp. 673–680, Jul. 1977.
- [56] S. Chitroub, A. Houacine, and B. Sansal, "Statistical characterisation and modelling of SAR images," *Elsevier, Signal Processing*, vol. 82, no. 1, pp. 69–92, DOI [http://dx.doi.org/10.1016/S0165-1684\(01\)00158-X](http://dx.doi.org/10.1016/S0165-1684(01)00158-X), Jan. 2002.
- [57] P. M. Shankar, "Error rates in generalized shadowed fading channels," *Wireless Personal Communications (WPC)*, vol. 28, no. 3, pp. 233–238, DOI <http://dx.doi.org/10.1023/B:wire.0000032253.68423.86>, Feb. 2004.
- [58] P. Almers, F. Tufvesson, and A. F. Molisch, "Keyhole effect in MIMO wireless channels: measurements and theory," *IEEE Trans. Wireless Commun.*, vol. 5, no. 12, pp. 3596–3604, Dec. 2006.
- [59] H. Shin and J. H. Lee, "Performance analysis of space-time block codes over keyhole Nakagami- m fading channels," *IEEE Trans. Veh. Technol.*, vol. 53, no. 2, pp. 351–362, Mar. 2004.
- [60] N. C. Sagias and G. S. Tombras, "On the cascaded Weibull fading channel model," *J. Franklin Inst.*, vol. 344, pp. 1–11, Elsevier Ltd., Jan. 2007.
- [61] M. Pätzold, *Mobile Fading Channels*. Chichester: John Wiley & Sons, 2002.
- [62] M. D. Yacoub, J. E. V. Bautista, and L. G. de Rezende Guedes, "On higher order statistics of the Nakagami- m distribution," *IEEE Trans. Veh. Technol.*, vol. 48, no. 3, pp. 790–794, May 1999.

- [63] A. F. Ramos, Y. V. Kontorovitch, and M. Lara, "High order fading distributions in Nakagami wireless channels," in *Proc. IEEE 65th Veh. Technol. Conf., VTC'07-Spring*, Dublin, Ireland, Apr. 2007, pp. 564–568, DOI 10.1109/VETECS.2007.17.
- [64] T. T. Tjhung and C. C. Chai, "Fade statistics in Nakagami-lognormal channels," *IEEE Trans. Commun.*, vol. 47, no. 12, pp. 1769–1772, Dec. 1999.
- [65] N. Zlatanov, Z. Hadzi-Velkov, and K. G. Karagiannidis, "Level crossing rate and average fade duration of the double Nakagami-m random process and application in MIMO keyhole fading channels," *IEEE Communications Letters*, vol. 12, no. 11, pp. 2042–2054, Jul. 2008.
- [66] C. S. Patel, G. L. Stüber, and T. G. Pratt, "Statistical properties of amplify and forward relay fading channels," *IEEE Trans. Veh. Technol.*, vol. 55, no. 1, pp. 1–9, Jan. 2006.
- [67] V. Ercerg, S. J. Fortune, J. Ling, A. J. Rustako Jr., and R. A. Valenzuela, "Comparison of a computer-based propagation prediction tool with experimental data collected in urban microcellular environment," *IEEE J. Select. Areas Commun.*, vol. 15, no. 4, pp. 677–684, May 1997.
- [68] I. Z. Kovacs, P. C. F. Eggers, K. Olesen, and L. G. Petersen, "Investigations of outdoor-to-indoor mobile-to-mobile radio communication channels," in *Proc. IEEE 56th Veh. Technol. Conf., VTC'02-Fall*, Vancouver BC, Canada, Sept. 2002, vol. 1, pp. 430–434.
- [69] G. K. Karagiannidis, N. C. Sagias, and P. T. Mathiopoulos, "N*Nakagami: A novel stochastic model for cascaded fading channels," *IEEE Trans. Commun.*, vol. 55, no. 8, pp. 1453–1458, Aug. 2007.
- [70] A. Y. Chau, Y. K. Huang, and C. Yao-Hua, "Level-crossing rates of envelope processes for multihop fading channels with amplify-and-forward relays," in *Proc. IEEE Wireless Commun. Networking Conf., (WCNC 2007)*, Xiamen, Hong Kong, Mar. 2007, pp. 2338–2343, DOI 10.1109/WCNC.2007.437.
- [71] A. Y. Chau and K. Yung-Ta Huang, "Evaluation of level crossing rates and fade durations for multihop Nakagami fading channels with an amplify-and-forward relay," in *Int. Symp. on Intelligent Signal Processing and Communication Systems, ISPACS 2007*, Xiamen, China, Mar. 2007, pp. 36–39, DOI 10.1109/ISPACS.2007.4445817.

- [72] Z. Hadzi-Velkov, N. Zlatanov, and G. K. Karagiannidis, "On the second order statistics of the multihop Rayleigh fading channel," *IEEE Trans. Commun.*, vol. 57, no. 6, pp. 1815–1823, Jun. 2009.
- [73] T. S. Rappaport, *Wireless Communications: Principles and Practice*. Upper Saddle River, New Jersey: Prentice-Hall, 2nd edition, 1996.
- [74] W. C. Jakes, Ed., *Microwave Mobile Communications*. Piscataway, NJ: IEEE Press, 1994.
- [75] M. D. Yacoub, C. R. C. Monterio da Silva, and J. E. V. Bautista, "Second-order statistics for diversity-combining techniques in Nakagami fading channels," *IEEE Trans. Veh. Technol.*, vol. 50, no. 6, pp. 1464–1470, Nov. 2001.
- [76] P. Ivanis, D. Drajić, and B. Vucetic, "The second order statistics of maximal ratio combining with unbalanced branches," *IEEE Communications Letters*, vol. 12, no. 7, pp. 508–510, Jul. 2008.
- [77] Z. Hadzi-Velkov, "Level crossing rate and average fade duration of EGC systems with cochannel interference in Rayleigh fading," *IEEE Communications Letters*, vol. 10, no. 9, pp. 649–651, Sept. 2006.
- [78] Z. Hadzi-Velkov, N. Zlatanov, and G. K. Karagiannidis, "An accurate approximation to the distribution of the sum of equally correlated Nakagami- m envelopes and its application in equal gain diversity receivers," in *Proc. IEEE Int. Conf. Communications (ICC'09)*, Dresden, Germany, Jun. 2009, pp. 1–5, DOI 10.1109/ICC.2009.5198714.
- [79] G. Fraidenraich, J. C. S. S. Filho, and M. D. Yacoub, "Second-order statistics of maximal-ratio and equal-gain combining in Hoyt fading," *IEEE Communications Letters*, vol. 9, no. 1, pp. 19–21, Jan. 2005.
- [80] X. Wang, W. Wang, and Z. Bu, "Fade statistics for selection diversity in Nakagami-lognormal fading channels," *IEEE Electronics Letters*, vol. 42, no. 18, pp. 1046–1047, Aug. 2006.
- [81] C. D. Iskander and P. T. Mathiopoulos, "Analytical level crossing rate and average fade durations for diversity techniques in Nakagami fading channels," *IEEE Trans. Commun.*, vol. 50, no. 8, pp. 1301–1309, Aug. 2002.
- [82] B. Talha and M. Pätzold, "A geometrical three-ring-based model for MIMO mobile-to-mobile fading channels in cooperative networks," *EURASIP Journal on Advances in Signal Processing*, submitted for publication, 2010.

- [83] B. Talha and M. Pätzold, “A geometrical channel model for MIMO mobile-to-mobile fading channels in cooperative networks,” in *Proc. IEEE 69th Vehicular Technology Conference, IEEE VTC 2009-Spring*, Barcelona, Spain, Apr. 2009.
- [84] K. V. Mardia and P. E. Jupp, *Directional Statistics*. Chichester: John Wiley & Sons, 1999.
- [85] A. Abdi, J. A. Barger, and M. Kaveh, “A parametric model for the distribution of the angle of arrival and the associated correlation function and power spectrum at the mobile station,” *IEEE Trans. Veh. Technol.*, vol. 51, no. 3, pp. 425–434, May 2002.
- [86] C. A. Gutiérrez and M. Pätzold, “Sum-of-sinoids-based simulation of flat fading wireless propagation channels under non-isotropic scattering conditions,” in *Proc. 50th IEEE Global Telecommunications Conference, GLOBECOM 2007*, Washington DC, USA, Nov. 2007, pp. 3842–3846.
- [87] B. Talha and M. Pätzold, “On the statistical characterization of mobile-to-mobile fading channels in dual-hop distributed cooperative multi-relay systems,” in *Proc. 12th Int. Symp. on Wireless Personal Multimedia Communications, WPMC 2009*, Sendai, Japan, Sept. 2009.
- [88] B. Talha and M. Pätzold, “Level-crossing rate and average duration of fades of the envelope of mobile-to-mobile fading channels in K -parallel dual-hop relay networks,” in *IEEE Int. Conf. on Wireless Communications & Signal Processing, WCSP 2009*, Nanjing, China, Nov. 2009, DOI 10.1109/WCSP.2009.5371574 .
- [89] S. O. Rice, “Mathematical analysis of random noise,” *Bell Syst. Tech. J.*, vol. 23, pp. 282–332, Jul. 1944.
- [90] S. O. Rice, “Mathematical analysis of random noise,” *Bell Syst. Tech. J.*, vol. 24, pp. 46–156, Jan. 1945.
- [91] P. Höher, “A statistical discrete-time model for the WSSUS multipath channel,” *IEEE Trans. Veh. Technol.*, vol. 41, no. 4, pp. 461–468, Nov. 1992.
- [92] K. W. Yip and T. S. Ng, “Efficient simulation of digital transmission over WSSUS channels,” *IEEE Trans. Commun.*, vol. 43, no. 12, pp. 2907–2913, Dec. 1995.

- [93] J. K. Han, J. G. Yook, and H. K. Park, "A deterministic channel simulation model for spatially correlated Rayleigh fading," *IEEE Communications Letters*, vol. 6, no. 2, pp. 58–60, Feb. 2002.
- [94] M. Pätzold, U. Killat, and F. Laue, "A deterministic digital simulation model for Suzuki processes with application to a shadowed Rayleigh land mobile radio channel," *IEEE Trans. Veh. Technol.*, vol. 45, no. 2, pp. 318–331, May 1996.
- [95] M. Pätzold, U. Killat, F. Laue, and Y. Li, "On the statistical properties of deterministic simulation models for mobile fading channels," *IEEE Trans. Veh. Technol.*, vol. 47, no. 1, pp. 254–269, Feb. 1998.
- [96] Y. R. Zheng and C. Xiao, "Improved models for the generation of multiple uncorrelated Rayleigh fading waveforms," *IEEE Communications Letters*, vol. 6, no. 6, pp. 256–258, Jun. 2002.
- [97] M. Pätzold, B. O. Hogstad, and D. Kim, "A new design concept for high-performance fading channel simulators using set partitioning," *Wireless Personal Communications (WPC)*, vol. 40, no. 2, pp. 267–279, Feb. 2007.
- [98] M. Pätzold and B. O. Hogstad, "Two new methods for the generation of multiple uncorrelated Rayleigh fading waveforms," in *Proc. IEEE 63rd Semianual Veh. Tech. Conf., VTC'06-Spring*, Melbourne, Australia, May 2006, vol. 6, pp. 2782–2786.
- [99] A. Goldsmith, *Wireless Communications*. New York: Cambridge University Press, 2005.
- [100] B. Talha, S. Primak, and M. Pätzold, "On the statistical properties of equal gain combining over mobile-to-mobile fading channels in cooperative networks," in *Proc. IEEE Int. Conf. Communications (ICC'10)*, Cape Town, South Africa, May 2010, DOI 10.1109/ICC.2010.5501898.
- [101] K. Azarian, H. E. Gamal, and P. Schniter, "On the achievable diversity-multiplexing tradeoff in half-duplex cooperative channels," *IEEE Trans. Inform. Theory*, vol. 51, no. 12, pp. 4152–4172, Dec. 2005.
- [102] O. E. Barndorff-Nielsen and D. R. Cox, *Asymptotic Techniques for use in Statistics*. New York: Chapman and Hall, 1989.

- [103] S. Primak, V. Kontorovich, and V. Lyandres, Eds., *Stochastic Methods and their Applications to Communications: Stochastic Differential Equations Approach*. Chichester: John Wiley & Sons, 2004.
- [104] A. Ord, *Families of Frequency Distributions*. London: Griffin, 1972.
- [105] A. Stuart and J. K. Ord, *Kendall's Advanced Theory of Statistics*, vol. I. London: Arnold, 6th edition, 1994.
- [106] A. Abdi and M. Kaveh, "On the utility of gamma PDF in modeling shadow fading (slow fading)," in *Proc. IEEE 49th Veh. Technol. Conf., VTC 1999*, Houston, USA, May 1999, pp. 2308 – 2312.
- [107] S. Al-Ahmadi and H. Yanikomeroglu, "On the approximation of the generalized-K distribution by a gamma distribution for modeling composite fading channels," *IEEE Trans. Wireless Commun.*, vol. 9, no. 2, pp. 706–713, Feb. 2010.
- [108] A. Papoulis and S. U. Pillai, *Probability, Random Variables and Stochastic Processes*. New York: McGraw-Hill, 4th edition, 2002.
- [109] J. B. Andersen, "Statistical distributions in mobile communications using multiple scattering," in *Proc. 27th URSI General Assembly*, Maastricht, Netherlands, Aug. 2002.
- [110] J. Salo, J. Salmi, and P. Vainikainen, "Distribution of the amplitude of a sum of singly and doubly scattered fading radio signal," in *Proc. IEEE 61st Semi-annual Veh. Tech. Conf., VTC'05-Spring*, Stockholm, Sweden, May /Jun. 2005, vol. 1, pp. 87–91.
- [111] J. Salo, H. M. El-Sallabi, and P. Vainikainen, "Statistical analysis of the multiple scattering radio channel," *IEEE Trans. Antennas Propagat.*, vol. 54, no. 11, pp. 3114–3124, Nov. 2006.
- [112] N. C. Beaulieu and X. Dong, "Level crossing rate and average fade duration of MRC and EGC diversity in Ricean fading," *IEEE Trans. Commun.*, vol. 51, no. 5, pp. 722–726, May 2003.
- [113] Z. Hadzi-Velkov, "Level crossing rate and average fade duration of selection diversity with Rician-faded cochannel interferers," *IEEE Trans. Commun.*, vol. 55, no. 11, pp. 2104–2113, Nov. 2007.

- [114] B. Talha and M. Pätzold, “On the statistical properties of double Rice channels,” in *Proc. 10th Int. Symp. on Wireless Personal Multimedia Communications, WPMC 2007*, Jaipur, India, Dec. 2007, pp. 517–522.
- [115] M. Pätzold, C. X. Wang, and B. O. Hogstad, “Two new sum-of-sinusoids-based methods for the efficient generation of multiple uncorrelated Rayleigh fading waveforms,” *IEEE Trans. Wireless Commun.*, vol. 8, no. 6, pp. 3122–3131, Jun. 2009.
- [116] B. Talha and M. Pätzold, “On the statistical properties of mobile-to-mobile fading channels in cooperative networks under line-of-sight conditions,” in *Proc. 10th Int. Symp. on Wireless Personal Multimedia Communications, WPMC 2007*, Jaipur, India, Dec. 2007, pp. 388–393.
- [117] B. Talha and M. Pätzold, “Statistical modeling and analysis of mobile-to-mobile fading channels in cooperative networks under line-of-sight conditions,” *Wireless Personal Communications (WPC)*, Springer Netherlands, DOI 10.1007/s11277-009-9721-4, Apr. 2009.
- [118] B. Talha and M. Pätzold, “A novel amplify-and-forward relay channel model for mobile-to-mobile fading channels under line-of-sight conditions,” in *Radio Communications*, pp. 307 – 319, IN-TECH Education and Publishing, Vienna, Austria, 2009, ISBN 978-953-307-091-9.
- [119] B. Talha and M. Pätzold, “Level-crossing rate and average duration of fades of the envelope of mobile-to-mobile fading channels in cooperative networks under line-of-sight conditions,” in *Proc. 51st IEEE Globecom 2008*, New Orleans, USA, Nov. /Dec. 2008, pp. 1–6, DOI 10.1109/GLOCOM.2008.ECP.860.
- [120] B. Talha and M. Pätzold, “Mobile-to-mobile fading channels in amplify-and-forward relay systems under line-of-sight conditions: statistical modeling and analysis,” *Annals of Telecommunications*, DOI 10.1007/s12243-010-0169-z, Apr. 2010.
- [121] R. U. Nabar and H. Bölcskei, “Space-time signal design for fading relay channels,” in *Proc. IEEE Globecom*, San Francisco, CA, Dec. 2003, vol. 4, pp. 1952–1956.
- [122] B. Talha and M. Pätzold, “On the statistical properties of equal gain combining over multiple double Rice fading channels in cooperative networks,”

- in *Proc. IEEE 72nd Semiannual Veh. Tech. Conf., VTC'10-Fall*, Ottawa, Canada, Sept. 2010, accepted for publication.
- [123] B. Talha and M. Pätzold, "Dual-hop amplify-and-forward relay systems with EGC over M2M fading channels under LOS conditions: Statistical and performance analysis," *IEEE Trans. Veh. Technol.*, to be submitted for publication, 2010.
- [124] B. Talha and M. Pätzold, "BEP analysis of M -ary PSK modulation schemes over double Rice fading channels with EGC," in *Proc. Second Workshop on Scenarios for Network Evaluation Studies, (SCENES 2010)*, San Francisco, CA, USA, Nov. 2010, accepted for publication.
- [125] C. E. Shannon, "A mathematical theory of communication," *Bell Syst. Tech. J.*, vol. 27, pp. 379–423, Jul. 1948.
- [126] C. E. Shannon, "A mathematical theory of communication," *Bell Syst. Tech. J.*, vol. 27, pp. 623–656, Oct. 1948.
- [127] A. Giorgetti, P. J. Smith, M. Shafi, and M. Chiani, "MIMO capacity, level crossing rates and fades: The impact of spatial/temporal channel correlation," *J. Commun. Net.*, vol. 5, no. 2, pp. 104–115, Jun. 2003.
- [128] H. Ge, K. D. Wong, M. Barton, and J. C. Liberti, "Statistical characterization of multiple-input multiple-output (MIMO) channel capacity," in *Proc. IEEE Wireless Communications and Networking Conference, WCNC 2002*, Mar. 2002, vol. 2, pp. 789–793.
- [129] P. J. Smith, L. M. Garth, and S. Loyka, "Exact capacity distributions for MIMO systems with small numbers of antennas," *IEEE Commun. Letter*, vol. 7, no. 10, pp. 481–483, Oct. 2003.
- [130] B. O. Hogstad and M. Pätzold, "Capacity studies of MIMO models based on the geometrical one-ring scattering model," in *Proc. 15th IEEE Int. Symp. on Personal, Indoor and Mobile Radio Communications, PIMRC 2004*, Barcelona, Spain, Sept. 2004, vol. 3, pp. 1613–1617.
- [131] B. O. Hogstad and M. Pätzold, "A study of the MIMO channel capacity when using the geometrical two-ring scattering model," in *Proc. 8th International Symposium on Wireless Personal Multimedia Communications, WPMC 2005*, Aalborg, Denmark, Sept. 2005, pp. 1790–1794.

- [132] B. O. Hogstad and M. Pätzold, “Exact closed-form expressions for the distribution, level-crossing rate, and average duration of fades of the capacity of MIMO channels,” in *Proc. 65th Semiannual Vehicular Technology Conference, IEEE VTC 2007-Spring*, Dublin, Ireland, Apr. 2007, pp. 455–460.
- [133] G. Rafiq, V. Kontorovich, and M. Pätzold, “On the statistical properties of the capacity of the spatially correlated Nakagami- m MIMO Channels,” in *Proc. IEEE 67th Vehicular Technology Conference, IEEE VTC 2008-Spring*, Marina Bay, Singapore, May 2008, pp. 500–506.
- [134] G. Rafiq and M. Pätzold, “The influence of severity of fading and shadowing on the statistical properties of the capacity of Nakagami-lognormal channels,” in *Proc. IEEE Global Communications Conference, IEEE GLOBE-COM 2008*, New Orleans, LA, USA, Nov. /Dec. 2008.
- [135] G. Rafiq and M. Pätzold, “A study of the statistical properties of the envelope and the capacity of Rice- m channels,” in *Proc. 12th International Symposium on Wireless Personal Multimedia Communications, WPMC 2009*, Sendai, Japan, Sept. 2009.
- [136] B. O. Hogstad, M. Pätzold, N. Youssef, and V. Kontorovich, “Exact closed-form expressions for the distribution, the level-crossing rate, and the average duration of fades of the capacity of OSTBC-MIMO channels,” *IEEE Trans. Veh. Technol.*, vol. 58, no. 2, pp. 1011–1016, Feb. 2009.
- [137] G. Rafiq, M. Pätzold, and V. Kontorovich, “The influence of spatial correlation and severity of fading on the statistical properties of the capacity of OSTBC Nakagami- m MIMO channels,” in *Proc. IEEE 69th Vehicular Technology Conference, IEEE VTC 2009-Spring*, Barcelona, Spain, Apr. 2009.
- [138] B. O. Hogstad, G. Rafiq, V. Kontorovich, and M. Pätzold, “Capacity studies of spatially correlated Rice MIMO channels,” in *Proc. IEEE International Symposium on Wireless Pervasive Computing, ISWPC 2010*, Modena, Italy, May 2010, accepted for publication.
- [139] V. Bhaskar, “Capacity evaluation for equal gain diversity schemes over Rayleigh fading channels,” *Int. J. Electron. Commun. AEÜ*, vol. 63, pp. 235–240, Elsevier Ltd., 2009.
- [140] G. Rafiq, V. Kontorovich, and M. Pätzold, “The influence of severity of fading on the statistical properties of the capacity of Nakagami- m channels

- with MRC and EGC,” in *Proc. European Wireless, EW 2010*, Lucca, Italy, Apr. 2010, accepted for publication.
- [141] L. C. Wang, W. C. Liu, and Y. H. Chei, “Capacity fades analysis of MIMO Rician channels in mobile and ad hoc networks,” *Performance Evaluation*, vol. 66, pp. 742–753, Elsevier Ltd., Aug. 2009.
- [142] G. Rafiq and M. Pätzold, “Statistical properties of the capacity of Rice channels with MRC and EGC,” in *IEEE Int. Conf. on Wireless Communications & Signal Processing, WCSP 2009*, Nanjing, China, Nov. 2009, DOI 10.1109/WCSP.2009.5371578.
- [143] G. Rafiq, B. O. Hogstad, and M. Pätzold, “Statistical properties of the capacity of double Nakagami- m channels,” in *Proc. IEEE International Symposium on Wireless Pervasive Computing, ISWPC 2010*, Modena, Italy, May 2010, accepted for publication.
- [144] M. Luccini, A. Shami, and S. Primak, “Cross-layer optimization of network performance over MIMO wireless mobile channels,” *IET Communications*, pp. 1–14, submitted for publication, 2010.
- [145] B. Talha and M. Pätzold, “On the statistical analysis of the channel capacity of double Rayleigh channels with equal gain combining in V2V communication systems,” in *Proc. 3rd IEEE Int. Symp. on Wireless Vehicular Communications (WiVeC’2010)*, Taipei, Taiwan, May 2010, DOI 10.1109/VETECS.2010.5494112.
- [146] M. K. Simon and M. S. Alouini, *Digital Communications over Fading Channels*. New Jersey: John Wiley & Sons, 2nd edition, 2005.
- [147] U. Charash, “Reception through Nakagami fading multipath channels with random delays,” *IEEE Trans. Commun.*, vol. 27, no. 4, pp. 657–670, Apr. 1979.
- [148] A. A. Abu-Dayya and N. C. Beaulieu, “Microdiversity on Rician fading channels,” *IEEE Trans. Commun.*, vol. 42, no. 6, pp. 2258–2267, Jun. 1994.
- [149] Q. T. Zhang, “Probability of error for equal-gain combiners over Rayleigh channels: some closed-form solutions,” *IEEE Trans. Commun.*, vol. 45, no. 3, pp. 270–273, Mar. 1997.

- [150] Y. Chen and C. Tellambura, "Performance analysis of L-branch equal gain combiners in equally correlated Rayleigh fading channels," *IEEE Communications Letters*, vol. 8, no. 3, pp. 150–152, Mar. 2004.
- [151] A. Annamalai, C. Tellambura, and V. K. Bhargava, "Equal-gain diversity receiver performance in wireless channels," *IEEE Trans. Commun.*, vol. 48, no. 10, pp. 1732–1745, Oct. 2000.
- [152] H. Samimi and P. Azmi, "An approximate analytical framework for performance analysis of equal gain combining technique over independent Nakagami, Rician and Weibull fading channels," *Wireless Personal Communications (WPC)*, vol. 43, no. 4, pp. 1399–1408, DOI 10.1007/s11277-007-9314-z, dec 2007.
- [153] D. A. Zogas, G. K. Karagiannidis, and S. A. Kotsopoulos, "Equal gain combining over Nakagami- n (Rice) and Nakagami- q (Hoyt) generalized fading channels," *IEEE Trans. Wireless Commun.*, vol. 4, no. 2, pp. 374–379, Mar. 2005.
- [154] K. Peppas, F. Lazarakis, A. Alexandridis, and K. Dangakis, "Error performance of digital modulation schemes with MRC diversity reception over $\eta - \mu$ fading channels," *IEEE Trans. Wireless Commun.*, vol. 8, no. 10, pp. 4974–4980, Oct. 2009.
- [155] Z. M. Win and H. J. Winters, "Analysis of hybrid selection/maximal-ratio combining in Rayleigh fading," *IEEE Trans. Commun.*, vol. 47, no. 12, pp. 1773–1776, Dec. 1999.
- [156] M. S. Alouini and M. K. Simon, "Dual diversity over log-normal fading channels," in *Proc. IEEE Int. Conf. Communications (ICC'01)*, Helsinki, Finland, Jun. 2001, vol. 4, pp. 1089–1093.
- [157] B. Holter and G. E. Øien, "On the amount of fading in MIMO diversity systems," *IEEE Trans. Wireless Commun.*, vol. 4, no. 5, pp. 2498–2507, Sept. 2005.
- [158] Y. Chen and C. Tellambura, "Moment analysis of the equal gain combiner output in equally correlated fading channels," *IEEE Trans. Veh. Technol.*, vol. 54, no. 6, pp. 1971–1979, Nov. 2005.

- [159] O. M. Hasna and M. S. Alouini, "End-to-end performance of transmission systems with relays over Rayleigh-fading channels," *IEEE Trans. Wireless Commun.*, vol. 2, no. 6, pp. 1126 – 1131, Nov. 2003.
- [160] O. M. Hasna and M. S. Alouini, "Harmonic mean and end-to-end performance of transmission systems with relays," *IEEE Trans. Commun.*, vol. 52, no. 1, pp. 130–135, Jan. 2004.
- [161] O. M. Hasna and M. S. Alouini, "A performance study of dual-hop transmissions with fixed gain relays," *IEEE Trans. Wireless Commun.*, vol. 3, no. 6, pp. 1963 – 1968, Nov. 2004.
- [162] P. A. Anghel and M. Kaveh, "Exact symbol error probability of a cooperative network in a Rayleigh fading environment," *IEEE Trans. Wireless Commun.*, vol. 3, no. 5, pp. 1416–1421, Sept. 2004.
- [163] L. Wu, J. Lin, K. Niu, and Z. He, "Performance of dual-hop transmissions with fixed gain relays over generalized-K fading channels," in *Proc. IEEE Int. Conf. Communications (ICC'09)*, Dresden, Germany, Jun. 2009, DOI 10.1109/ICC.2009.5199331.
- [164] T. A. Tsiftsis, G. K. Karagiannidis, and S. A. Kotsopoulos, "Dual-hop wireless communications with combined gain relays," *IEE Proc. Communications*, vol. 152, no. 5, pp. 528 – 532, Oct. 2005.
- [165] A. Ribeiro, X. Cai, and G. B. Giannakis, "Symbol error probabilities for general Cooperative links," *IEEE Trans. Wireless Commun.*, vol. 4, no. 3, pp. 1264 – 1273, May 2005.
- [166] Y. Li and S. Kishore, "Asymptotic analysis of amplify-and-forward relaying in Nakagami fading environments," *IEEE Trans. Wireless Commun.*, vol. 6, no. 12, pp. 4256–4262, Dec. 2007.
- [167] W. Su, A. K. Sadek, and K. J. R. Liu, "Cooperative communication protocols in wireless networks: Performance analysis and optimum power allocation," *Wireless Personal Communications (WPC)*, vol. 44, no. 2, pp. 181–217, Jan. 2008.
- [168] M. Di Renzo, F. Graziosi, and F. Santucci, "A comprehensive framework for performance analysis of dual-hop cooperative wireless systems with fixed-gain relays over generalized fading channels," *IEEE Trans. Wireless Commun.*, vol. 8, no. 10, pp. 5060 – 5074, Oct. 2009.

- [169] H. Suraweera, G. Karagiannidis, and P. Smith, “Performance analysis of the dual-hop asymmetric fading channel,” vol. 8, no. 6, pp. 2783 – 2788, Jun. 2009.
- [170] F. Xu, F. C. M. Lau, and D. W. Yue, “Diversity order for amplify-and-forward dual-hop systems with fixed-gain relay under Nakagami fading channels,” vol. 9, no. 1, pp. 92 – 98, Jan. 2010.
- [171] D. B. da Costa and S. Aissa, “Performance of cooperative diversity networks: Analysis of amplify-and-forward relaying under equal-gain and maximal-ratio combining,” in *Proc. IEEE Int. Conf. Communications (ICC’09)*, Dresden, Germany, Jun. 2009, pp. 1–5, DOI 10.1109/ICC.2009.5199330.
- [172] S. S. Ikki and M. H. Ahmed, “Performance of cooperative diversity using equal gain combining (EGC) over Nakagami- m fading channels,” *IEEE Trans. Wireless Commun.*, vol. 8, no. 2, pp. 557–562, Feb. 2009.
- [173] H. Q. Huynh, S. I. Husain, J. Yuan, A. Razi, and D. S. Taubman, “Performance analysis of multi-branch non-regenerative relay systems with EGC in Nakagami- m channels,” in *Proc. IEEE 70th Veh. Technol. Conf., VTC’09-Fall*, Anchorage, AK, USA, Sept. 2009, pp. 1–5, DOI 10.1109/VETECONF.2009.5378710.
- [174] H. Ilhan, M. Uysal, and I. Altunbas, “Cooperative diversity for intervehicular communication: Performance analysis and optimization,” *IEEE Trans. Veh. Technol.*, vol. 58, no. 7, pp. 3301 – 3310, Aug. 2009.
- [175] W. Wongtrairat and P. Supnithi, “Performance of digital modulation in double Nakagami- m fading channels with MRC diversity,” *IEICE Trans. Commun.*, vol. E92-B, no. 2, pp. 559–566, Feb. 2009.
- [176] B. Talha, M. Pätzold, and S. Primak, “Performance analysis of M -ary PSK modulation schemes over multiple double Rayleigh fading channels with EGC in cooperative networks,” in *Proc. IEEE Int. Conf. Communications, Workshop on Vehicular Connectivity, Veh-Con 2010*, Cape Town, South Africa, May 2010, DOI 10.1109/ICCW.2010.5503940.
- [177] D. Umansky and M. Pätzold, “Design of measurement-based wideband mobile radio channel simulators,” in *Proc. 4th IEEE International Symposium on Wireless Communication Systems, ISWCS 2007*, Trondheim, Norway, Oct. 2007, pp. 229–235.

- [178] D. Umansky and M. Pätzold, “Design of wideband mobile radio channel simulators based on real-world measurement data,” in *Proc. IEEE 67th Vehicular Technology Conference, IEEE VTC 2008-Spring*, Marina Bay, Singapore, May 2008, pp. 319–324.

Appendix A

List of Publications

The purpose of inclusion of Appendix A here is to keep a record of all the articles that are an outcome of the research work carried out by the author of this dissertation. The list of publications comprises of both submitted and already published articles. Appendix A is organized in two sections. Section A.1 and Section A.2 details those peer-reviewed articles that have and have not been replicated in the current dissertation, respectively.

A.1 Articles Included in this Dissertation

This section consists of the following articles:

- Paper I** B. Talha and M. Pätzold, A geometrical three-ring-based model for MIMO mobile-to-mobile fading channels in cooperative networks, *EURASIP Journal on Advances in Signal Processing, Special Issue on Cooperative MIMO Multicell Networks*, 2010. (submitted for publication)
- Paper II** B. Talha and M. Pätzold, On the statistical characterization of mobile-to-mobile fading channels in dual-hop distributed cooperative multi-relay systems, *12th International Symposium on Wireless Personal Multimedia Communications, WPMC 2009*, Sendai, Japan, Sept. 2009.
- Paper III** B. Talha and M. Pätzold, Level-crossing rate and average duration of fades of the envelope of mobile-to-mobile fading channels in K -parallel dual-hop relay networks, *International Conference on Wireless Communications & Signal Processing, WCSP 2009*,

Nanjing, China, Nov. 2009. DOI10.1109/WCSP.2009.5371574.

Paper IV B. Talha, S. Primak, and M. Pätzold, On the statistical properties of equal gain combining over mobile-to-mobile fading channels in cooperative networks, *IEEE International Conference on Communications, ICC 2010*, Cape Town, South Africa, May 2010. DOI10.1109/ICC.2010.5501898.

Paper V B. Talha and M. Pätzold, On the statistical properties of double Rice channels, *Proc. 10th Int. Symp. on Wireless Personal Multimedia Communications, WPMC 2007*, Jaipur, India, Dec. 2007, pp. 517–522.

Paper VI B. Talha and M. Pätzold, Statistical modeling and analysis of mobile-to-mobile fading channels in cooperative networks under line-of-sight conditions, *Wireless Personal Communications, Special Issue on “Wireless Future”*, 2009. DOI10.1007/s11277-009-9721-4.

Paper VII B. Talha and M. Pätzold, Mobile-to-mobile fading channels in amplify-and-forward relay systems under line-of-sight conditions: Statistical modeling and analysis, *Annals of Telecommunications*, April 2010. DOI 10.1007/s12243-010-0169-z.

Paper VIII B. Talha and M. Pätzold, On the statistical analysis of equal gain combining over multiple double Rice fading channels in cooperative networks, *IEEE 72nd Vehicular Technology Conference, IEEE VTC2009-Spring*, Ottawa, Canada, Sept. 2010, accepted for publication.

Paper IX B. Talha and M. Pätzold, On the statistical analysis of the channel capacity of double Rayleigh channels with equal gain combining in V2V communication systems, *3rd IEEE International Symposium on Wireless Vehicular Communications, WiVec 2010*, Taipei, Taiwan, May 2010. DOI 10.1109/VETECS.2010.5494112.

Paper X B. Talha, M. Pätzold, and S. Primak, Performance analysis of M -Ary PSK modulation schemes over multiple double Rayleigh fading channels with EGC in cooperative networks, *IEEE ICC 2010 Workshop on Vehicular Connectivity, Veh-Con 2010*, Cape Town,

South Africa, May 2010. DOI 10.1109/ICCW.2010.5503940.

Paper XI B. Talha and M. Pätzold, BEP analysis of M -Ary PSK modulation schemes over double Rice fading channels with EGC, *Second Workshop on Scenarios for Network Evaluation Studies, (SCENES 2010)*, San Francisco, CA, USA, Nov. 2010, accepted for publication.

Paper XII B. Talha and M. Pätzold, Dual-hop amplify-and-forward relay systems with EGC over M2M fading channels under LOS conditions: Statistical and performance analysis, to be submitted for publication.

The next four articles in Section A.2 have not been reproduced in this paper collection.

A.2 Articles Not Included in this Dissertation

The articles pointed out in the following are equally important compared to the ones mentioned in Section A.1. They are, however, not a part of the dissertation in order to reduce the overlap among the articles making up the final manuscript.

Paper XIII B. Talha and M. Pätzold, A geometrical channel model for MIMO mobile-to-mobile fading channels in cooperative networks, *IEEE 69th Vehicular Technology Conference, IEEE VTC2009-Spring*, Barcelona, Spain, Apr. 2009. DOI10.1109/VETECS.2009.5073296.

Paper XIV ¹B. Talha and M. Pätzold, On the statistical properties of mobile-to-mobile fading channels in cooperative networks under line-of-sight conditions, *Proc. 10th Int. Symp. on Wireless Personal Multimedia Communications, WPMC 2007*, Jaipur, India, Dec. 2007, pp. 388 - 393.

Paper XV B. Talha and M. Pätzold, A novel amplify-and-forward relay channel model for mobile-to-mobile fading channels under line-of-sight conditions, *Radio Communications, IN-TECH Education and Publishing*, Vienna, Austria, April 2010, pp. 307 - 319,

¹This article received the Best Student Paper Award at the 10th International Symposium on Wireless Personal Multimedia Communications, WPMC 2007, Jaipur, India, December 2007.

ISBN 978-953-307-091-9.

Paper XVI B. Talha and M. Pätzold, Level-crossing rate and average duration of fades of the envelope of a mobile-to-mobile fading channel in cooperative networks under line-of-sight conditions, *IEEE Global Communications Conference, IEEE GLOBECOM 2008*, New Orleans, LA, USA, Nov. /Dec. 2008. DOI10.1109/GLOCOM.2008.ECP.860.

Appendix B

Paper I

Title: A Geometrical Three-Ring-Based Model for MIMO Mobile-to-Mobile Fading Channels in Cooperative Networks

Authors: **Batool Talha** and Matthias Pätzold

Affiliation: University of Agder, Faculty of Engineering and Science, P. O. Box 509, NO-4898 Grimstad, Norway

Journal: *EURASIP Journal on Advances in Signal Processing, Special Issue on Cooperative MIMO Multicell Networks*, 2010. (submitted for publication)

A Geometrical Three-Ring-Based Model for MIMO Mobile-to-Mobile Fading Channels in Cooperative Networks

Batool Talha and Matthias Pätzold

Department of Information and Communication Technology
Faculty of Engineering and Science, Agder University College
Servicebox 509, NO-4876 Grimstad, Norway
E-mails: {batool.talha, matthias.paetzold}@uia.no

Abstract — This paper deals with the modeling and analysis of narrowband multiple-input multiple-output (MIMO) mobile-to-mobile (M2M) fading channels in relay-based cooperative networks. Non-line-of-sight (NLOS) propagation conditions are assumed in the transmission links from the source mobile station to the destination mobile station via the mobile relay. A stochastic narrowband MIMO M2M reference channel model is derived from the geometrical three-ring scattering model, where it is assumed that an infinite number of local scatterers surround the source mobile station, the mobile relay, and the destination mobile station. The complex channel gains associated with the new reference channel model are derived and their temporal as well as spatial correlation properties are explored. General analytical solutions are presented for the four-dimensional (4-D) space-time cross-correlation function (CCF), the three-dimensional (3-D) spatial CCF, the two-dimensional (2-D) source (relay, destination) correlation function (CF), and the temporal autocorrelation function (ACF). Closed-formed expressions for different CCFs under isotropic as well as non-isotropic scattering conditions are also provided in this paper. A stochastic simulation model is then derived from the reference model. It is shown that the CCFs of the simulation model closely approximate the corresponding CCFs of the reference model. The developed channel simulator is not only important for the development of future MIMO M2M cooperative communication systems, but also for analyzing the dynamic behavior of the MIMO M2M channel capacity.

Keywords—Amplify-and-forward relay links, mobile-to-mobile fading channels, MIMO channels, space-time correlation function.

I. INTRODUCTION

Recent attempts at combating multipath fading effects along with providing increased mobility support have resulted in the emergence of M2M communication systems in cooperative networks. The use of cooperative diversity protocols [6, 21, 22, 13] improves the transmission link quality and the end-to-end system's throughput, whereas M2M communication on the other hand, extends the network range (coverage area). The fundamental idea of operation in cooperative networks is to allow mobile stations in the network to relay signals to the final destination or to other mobile stations acting as relays. The development and performance investigation of such seemingly simple cooperative networks require a thorough understanding of the M2M fading channel characteristics. For this reason, there is a need of simple yet efficient M2M fading channel models, providing us with a detailed knowledge about the statistical characterization of M2M channels.

The idea of introducing M2M communication in non-cooperative networks can be traced back to the work of Akki and Haber [4, 3], which deals with the study of the statistical properties of narrowband single-input single-output (SISO) M2M fading channels under NLOS propagation conditions. Several papers dealing with M2M communication in cooperative networks can also be found in the recent literature [23, 24, 26, 25]. In various studies pertaining to M2M fading channels in relay-based cooperative networks under NLOS propagation conditions, it has been shown that a double Rayleigh process is a simple and yet a well-suited statistical channel model for such channels [8, 15]. The analysis of experimental measurement data for outdoor-to-indoor M2M fading channels presented in [12] verifies the existence of double Rayleigh processes in real-world environments. The authors of [23] have extended the double Rayleigh channel model to the double Rice channel model for LOS propagation environments. Furthermore, several other realistic M2M fading channel models based on the multiple scattering concept [5] are available in the literature for both NLOS and LOS propagation environments [20, 26, 25]. The M2M fading channel models for relay-based cooperative networks developed so far are for narrowband SISO fading channels. Meaning thereby, the source mobile station, the mobile relay, and the destination mobile station are equipped with only one antenna. However, it is a well-established fact that the gains in terms of channel capacity are larger for MIMO channels as compared to SISO channels [9, 28]. Thus, there is a need to extend SISO M2M fading channel models to MIMO M2M fading channel models to enable the investigations of the channel capacity and the system performance of cooperative networks with multiple antenna models.

Another area that requires further attention is the development of simulation

models for MIMO M2M fading channels in cooperative networks. Some techniques for simulating narrowband SISO M2M fading channels in non-cooperative networks have been proposed in [14]. Various studies have revealed that geometrical channel models are a good starting point for deriving simulation models for MIMO channels. Based on the geometrical two-ring channel models for MIMO fixed-to-mobile (F2M) and/or fixed-to-fixed (F2F) channels [7, 27], the authors of [19] proposed reference and simulation models for narrowband MIMO M2M fading channels in non-cooperative networks. Extensions of MIMO M2M reference and simulation models under LOS propagation conditions have been reported in [29]. In addition to 2-D channel models, 3-D MIMO M2M channel models based on geometrical cylinders can be found in [30]. However, to the best of the authors' knowledge, geometrical channel models for MIMO M2M communication systems in cooperative networks are an unexplored area. This in turn results in a lack of proper reference and simulation models derived from such geometrical models for MIMO M2M fading channels.

Motivated by need for proper MIMO M2M fading channel models, we are addressing in this paper modeling and simulation approaches for such channels in amplify-and-forward relay type cooperative networks. We propose a new reference model for MIMO M2M fading channels in cooperative networks and explore its temporal as well as spatial correlation properties. The scattering environment around the source mobile station, the mobile relay, and the destination mobile station is modeled by a geometrical three-ring scattering model. The proposed geometrical three-ring scattering model is an extension of the geometrical two-ring scattering model presented in [19], where the source mobile station and the destination mobile station are surrounded by rings of scatterers. However, in the proposed extension of the two-ring model to the three-ring model, we have a separate ring of scatterers around the mobile relay along with a ring each around the source mobile station and the destination mobile station. The reference model is proposed for MIMO M2M fading channels under NLOS propagation conditions. Furthermore, it is assumed that the direct transmission link between the source mobile station and the destination mobile station is blocked by obstacles. We also derive a stochastic simulation model from the developed reference model. Finally, we discuss isotropic and non-isotropic scattering scenarios and present closed-form expressions for the correlation functions of the reference model and the simulation model.

This article has the following structure: Section II introduces briefly the geometrical three-ring scattering model describing the transmission link from the source mobile station to the destination mobile station via the mobile relay. Based on

the geometrical three-ring scattering model, we develop the reference model for MIMO M2M fading channels and study its correlation properties in Section III. In Section IV, we derive the stochastic simulation model from the developed reference model. Section V deals with the derivation of closed-form expressions for the correlation functions describing the reference model under isotropic and non-isotropic scattering conditions. Section VI shows the accuracy of the stochastic simulation model by comparing its statistical properties with those of the reference model. In this section, we also confirm the validity of the closed-form expressions presented in Section V. Finally, concluding remarks are given in Section VII.

II. THE GEOMETRICAL THREE-RING MODEL

In this section, we extend the geometrical two-ring scattering model proposed in [19] to a geometrical three-ring scattering model for narrowband MIMO M2M fading channels in amplify-and-forward relay type cooperative networks. For ease of analysis, we have considered an elementary $2 \times 2 \times 2$ antenna configuration, meaning thereby, the source mobile station, the mobile relay, and the destination mobile station are equipped with two antennas each. For simplicity, we have considered non-line-of-sight (NLOS) propagation conditions in all the transmission links. It is further assumed that there is no direct transmission link from the source mobile station to the destination mobile station.

Due to high path loss, the contribution of signal power from remote scatterers to the total received power is usually negligible. Therefore, in the proposed three-ring scattering model, we have only assumed local scattering. A total number of M local scatterers, i.e., $S_s^{(m)}$ ($m = 1, 2, \dots, M$) are positioned on a ring of radius R_s around the source mobile station, whereas N local scatterers $S_d^{(n)}$ ($n = 1, 2, \dots, N$) lie around the destination mobile station on a separate ring of radius R_d . Furthermore, the local scatterers $S_r^{(k)}$ ($k = 1, 2, \dots, K$) and $S_r^{(l)}$ ($l = 1, 2, \dots, L$) are located on a third ring of radius R_r around the mobile relay. The number of local scatterers around the mobile relay is $K = L$. It should be pointed out here that $S_r^{(k)} = S_r^{(l)}$ for $k = l$. Throughout this paper, the subscripts S, R, and D represent the source mobile station, the mobile relay, and the destination mobile station. As can be seen from Fig. B.1, the symbol $\phi_s^{(m)}$ denotes the angle of departure (AOD) of the m th transmitted wave seen at the source mobile station, whereas $\phi_d^{(n)}$ represents the angle of arrival (AOA) of the n th received wave at the destination mobile station. Furthermore, the symbols $\phi_{S-R}^{(k)}$ and $\phi_{R-D}^{(l)}$ correspond to the AOA of the k th received wave and the AOD of the l th transmitted wave at the mobile relay, respectively. The mobile relay is positioned at a distance D_{S-R} and an angle γ_s with respect to the source mobile station.

While the location of the mobile relay seen from the destination mobile station can be specified by the distance D_{R-D} and the angle γ_D . Furthermore, the source mobile station and the destination mobile station are a distance D_{S-D} apart from each other. It is assumed that the inequalities $\max\{R_S, R_R\} \ll D_{S-R}$, $\max\{R_R, R_D\} \ll D_{R-D}$, and $\max\{R_S, R_D\} \ll D_{S-D}$ hold. The inter-element spacings at the source mobile station, the mobile relay, and the destination mobile station antenna arrays are labeled as δ_S , δ_R , and δ_D , respectively, where it is assumed that these quantities are smaller than the radii R_S , R_R , and R_D , i.e., $\max\{\delta_S, \delta_R, \delta_D\} \ll \min\{R_S, R_R, R_D\}$. With respect to the x -axis, the symbols β_S , β_R , and β_D describe the tilt angle of the antenna arrays at the source mobile station, the mobile relay, and the destination mobile station, respectively. It is further assumed that the source mobile station (mobile relay, destination mobile station) moves with speed v_S (v_R , v_D) in the direction determined by the angle of motion α_S (α_R , α_D).

III. THE REFERENCE MODEL

A. Derivation of the Reference Model

In this section, we develop a reference model for MIMO M2M fading channels in cooperative networks using the geometrical three-ring scattering model shown in Fig. B.1. Ignoring for the moment the geometrical details, Fig. B.1 can be simplified to Fig. B.2, in order to understand the overall MIMO channel from the source mobile station to the destination mobile station via the mobile relay. Figure B.2 shows that the complete system can be separated into two 2×2 MIMO subsystems. One of the MIMO subsystems (comprising the source mobile station and mobile relay) is denoted by the S-R MIMO subsystem. While the other MIMO subsystem (consisting of the mobile relay and the destination mobile station) is termed as the R-D MIMO subsystem. The input-output relationship of the S-R MIMO subsystem can be expressed as

$$\mathbf{X}(t) = \mathbf{H}_{S-R}(t)\mathbf{S}(t) + \mathbf{N}_R(t) \quad (1)$$

where $\mathbf{X}(t) = [X^{(1)}(t) \ X^{(2)}(t)]^T$ is a 2×1 received signal vector at the mobile relay, $\mathbf{S}(t) = [S^{(1)}(t) \ S^{(2)}(t)]^T$ is a 2×1 signal vector transmitted by the source mobile station, and $\mathbf{N}_R(t) = [N_R^{(1)}(t) \ N_R^{(2)}(t)]^T$ is a 2×1 additive white Gaussian noise (AWGN) vector. In (1), $\mathbf{H}_{S-R}(t)$ is a 2×2 channel matrix, which models the M2M fading channel between the source mobile station and the mobile relay. The

channel matrix $\mathbf{H}_{S-R}(t)$ can be expressed as

$$\mathbf{H}_{S-R}(t) = \begin{pmatrix} h_{S-R}^{(11)}(t) & h_{S-R}^{(12)}(t) \\ h_{S-R}^{(21)}(t) & h_{S-R}^{(22)}(t) \end{pmatrix}. \quad (2)$$

Here, each element $h_{S-R}^{(iq)}(t)$ ($i, q = 1, 2$) of the channel matrix represents the diffuse component of the channel describing the transmission link from the source mobile station antenna element $A_S^{(q)}$ to the mobile relay antenna element $A_R^{(i)}$. Considering the geometrical three-ring scattering model shown in Fig. B.1, it can be observed that the m th homogeneous plane wave emitted from $A_S^{(q)}$, first encounters the local scatterers $S_S^{(m)}$ around the source mobile station. Furthermore, before impinging on $A_R^{(i)}$, the plane wave is captured by the local scatterers $S_R^{(k)}$ around the mobile relay. It is worth mentioning here that the reference model is based on the assumption that the number of local scatterers, M and K , around the source mobile station and the mobile relay is infinite. Following [19], the diffuse component $h_{S-R}^{(11)}(t)$ of the transmission link from $A_S^{(1)}$ to $A_R^{(1)}$ can be approximated as

$$h_{S-R}^{(11)}(t) = \lim_{\substack{M \rightarrow \infty \\ K \rightarrow \infty}} \frac{1}{\sqrt{MK}} \sum_{m=1}^M \sum_{k=1}^K g_{S-R}^{(mk)} e^{j[2\pi(f_S^{(m)} + f_{S-R}^{(k)})t + (\theta_{S-R}^{(mk)} + \theta_{S-R})]} \quad (3)$$

with joint gains $1/\sqrt{MK}$ and joint phases $\theta_{S-R}^{(mk)}$ caused by the interaction of the local scatterers $S_S^{(m)}$ and $S_R^{(k)}$. The joint phases $\theta_{S-R}^{(mk)}$ are assumed to be independent and identically distributed (i.i.d.) random variables, each having a uniform distribution over the interval $[0, 2\pi]$. In (3),

$$g_{S-R}^{(mk)} = a_S^{(m)} b_R^{(k)} c_{S-R}^{(mk)} \quad (4a)$$

$$a_S^{(m)} = e^{j\frac{\pi}{\lambda} \delta_S \cos(\phi_S^{(m)} - \beta_S)} \quad (4b)$$

$$b_R^{(k)} = e^{j\frac{\pi}{\lambda} \delta_R \cos(\phi_{S-R}^{(k)} - \beta_R)} \quad (4c)$$

$$c_{S-R}^{(mk)} = e^{j\frac{2\pi}{\lambda} \{R_S \cos(\phi_S^{(m)} - \gamma_S) - R_R \cos(\phi_{S-R}^{(k)} - \gamma_S)\}} \quad (4d)$$

$$\theta_{S-R} = -\frac{2\pi}{\lambda} (R_S + D_{S-R} + R_R) \quad (4e)$$

$$f_S^{(m)} = f_{S_{\max}} \cos(\phi_S^{(m)} - \alpha_S) \quad (4f)$$

$$f_{S-R}^{(k)} = f_{R_{\max}} \cos(\phi_{S-R}^{(k)} - \alpha_R) \quad (4g)$$

where $f_{S_{\max}} = v_S/\lambda$ ($f_{R_{\max}} = v_R/\lambda$) is the maximum Doppler frequency caused by the motion of the source mobile station (mobile relay). Furthermore, the symbol λ denotes the carrier's wavelength. The knowledge of the position of the mobile

relay with respect to the source mobile station is incorporated in (4d). It should be pointed out here that in the reference model, the AOD $\phi_s^{(m)}$ and the AOA $\phi_{s-R}^{(k)}$ are independent random variables determined by the distribution of the local scatterers around the source mobile station and the mobile relay, respectively.

Replacing $a_s^{(m)}$ and $b_R^{(k)}$ by their complex conjugates $a_s^{(m)*}$ and $b_R^{(k)*}$ in (4b) and (4c), respectively, we can obtain the diffuse component $h_{s-R}^{(22)}(t)$ of the $A_s^{(2)} - A_R^{(2)}$ transmission link [19]. The diffuse components $h_{s-R}^{(12)}(t)$ and $h_{s-R}^{(21)}(t)$ can be obtained likewise by substituting $a_s^{(m)} \rightarrow a_s^{(m)*}$ and $b_R^{(k)} \rightarrow b_R^{(k)*}$, respectively, in (3) [19].

Similarly, as can be seen from Fig. B.2, the input-output relationship of the R-D MIMO subsystem can be written as

$$\mathbf{R}(t) = \mathbf{H}_{R-D}(t)\mathbf{X}(t) + \mathbf{N}_D(t) \quad (5)$$

where $\mathbf{R}(t) = [R^{(1)}(t) R^{(2)}(t)]^T$ is a 2×1 received signal vector at the destination mobile station, $\mathbf{X}(t) = [X^{(1)}(t) X^{(2)}(t)]^T$ is a 2×1 signal vector transmitted by the mobile relay, $\mathbf{H}_{R-D}(t)$ is a 2×2 R-D fading channel matrix, and $\mathbf{N}_D(t) = [N_D^{(1)}(t) N_D^{(2)}(t)]^T$ is a 2×1 AWGN vector. By referring to the previous discussion on the elements of the matrix $\mathbf{H}_{s-R}(t)$, one can easily show that the diffuse component $h_{R-D}^{(11)}(t)$ of the $A_R^{(1)} - A_D^{(1)}$ transmission link can be expressed as

$$h_{R-D}^{(11)}(t) = \lim_{\substack{L \rightarrow \infty \\ N \rightarrow \infty}} \frac{1}{\sqrt{LN}} \sum_{l=1}^L \sum_{n=1}^N g_{R-D}^{(ln)} e^{j[2\pi(f_{R-D}^{(l)} + f_D^{(n)})t + (\theta_{R-D}^{(ln)} + \theta_{R-D})]} \quad (6)$$

where the term $1/\sqrt{LN}$ and the symbol $\theta_{R-D}^{(ln)}$ represent the joint gains and joint phases, respectively, introduced by the local scatterers $S_R^{(l)}$ and $S_D^{(n)}$. Like the joint phases, $\theta_{s-R}^{(mk)}$, $\theta_{R-D}^{(ln)}$ are also assumed to be i.i.d. random variables, each having a uniform distribution over the interval $[0, 2\pi]$. Furthermore, in (6)

$$g_{R-D}^{(ln)} = a_R^{(l)} b_D^{(n)} c_{R-D}^{(ln)} \quad (7a)$$

$$a_R^{(l)} = e^{j\frac{\pi}{\lambda} \delta_R \cos(\phi_{R-D}^{(l)} - \beta_R)} \quad (7b)$$

$$b_D^{(n)} = e^{j\frac{\pi}{\lambda} \delta_D \cos(\phi_D^{(n)} - \beta_D)} \quad (7c)$$

$$c_{R-D}^{(ln)} = e^{j\frac{2\pi}{\lambda} \{R_D \cos(\phi_D^{(n)} - \gamma_D) - R_R \cos(\phi_{R-D}^{(l)} - \gamma_D)\}} \quad (7d)$$

$$\theta_{R-D} = -\frac{2\pi}{\lambda} (R_R + D_{R-D} + R_D) \quad (7e)$$

$$f_{R-D}^{(l)} = f_{R\max} \cos(\phi_{R-D}^{(l)} - \alpha_R) \quad (7f)$$

$$f_D^{(n)} = f_{D\max} \cos(\phi_D^{(n)} - \alpha_D) \quad (7g)$$

where $f_{D_{\max}} = v_D/\lambda$ is the maximum Doppler frequency caused by the movement of the destination mobile station. The symbol γ_D in (7d) describes the position of the mobile relay with respect to the destination mobile station [see Fig. B.1]. Furthermore, the AOD $\phi_{R-D}^{(l)}$ and the AOA $\phi_D^{(n)}$ are independent random variables determined by the distribution of the local scatterers around the mobile relay and the destination mobile station, respectively.

One can show that the diffuse components $h_{R-D}^{(iq)}(t)$ ($i, q = 1, 2$) of the remaining transmission links from the mobile relay antenna element $A_R^{(q)}$ to the destination mobile station antenna element $A_D^{(i)}$ can similarly be obtained as described for the $A_S^{(q)} - A_R^{(i)}$ transmission link.

Finally, substituting (1) in (5) allows us to identify the overall fading channel between the source mobile station and the destination mobile station as

$$\begin{aligned} \mathbf{R}(t) &= \mathbf{H}_{R-D}(t)\mathbf{H}_{S-R}(t)\mathbf{S}(t) + \mathbf{H}_{R-D}(t)\mathbf{N}_R(t) + \mathbf{N}_D(t) \\ &= \mathbf{H}_{S-R-D}(t)\mathbf{S}(t) + \mathbf{N}_{R-D}(t) \end{aligned} \quad (8)$$

where $\mathbf{N}_{R-D}(t) = \mathbf{H}_{R-D}(t)\mathbf{N}_R(t) + \mathbf{N}_D(t)$ is the total noise of the system. The symbol $\mathbf{H}_{S-R-D}(t)$ denotes the overall channel matrix, which is defined as follows

$$\begin{aligned} \mathbf{H}_{S-R-D}(t) &= \mathbf{H}_{R-D}(t)\mathbf{H}_{S-R}(t) \\ &= \begin{pmatrix} h_{R-D}^{(11)}(t) & h_{R-D}^{(12)}(t) \\ h_{R-D}^{(21)}(t) & h_{R-D}^{(22)}(t) \end{pmatrix} \begin{pmatrix} h_{S-R}^{(11)}(t) & h_{S-R}^{(12)}(t) \\ h_{S-R}^{(21)}(t) & h_{S-R}^{(22)}(t) \end{pmatrix} \\ &= \begin{pmatrix} h_{S-R-D}^{(11)}(t) & h_{S-R-D}^{(12)}(t) \\ h_{S-R-D}^{(21)}(t) & h_{S-R-D}^{(22)}(t) \end{pmatrix}. \end{aligned} \quad (9)$$

It is noteworthy that the overall channel matrix $\mathbf{H}_{S-R-D}(t)$ describes completely the reference model of the proposed geometrical three-ring MIMO M2M fading channel. Here, each element $h_{S-R-D}^{(iq)}(t)$ ($i, q = 1, 2$) of the channel matrix defines the diffuse component of the overall MIMO M2M fading channel, describing the transmission link from the source mobile station antenna element $A_S^{(q)}$ to the destination mobile station antenna element $A_D^{(i)}$ via the mobile relay antenna elements. Expanding (9) allows us to explicitly write the diffuse component $h_{S-R-D}^{(11)}(t)$ of the transmission link from the first antenna element at the source mobile station, $A_S^{(1)}$, to the first antenna element at the destination mobile station, $A_D^{(1)}$, as follows

$$h_{S-R-D}^{(11)}(t) = h_{R-D}^{(11)}(t)h_{S-R}^{(11)}(t) + h_{R-D}^{(12)}(t)h_{S-R}^{(21)}(t)$$

$$\begin{aligned}
 &= \lim_{\substack{K \rightarrow \infty \\ L \rightarrow \infty \\ M \rightarrow \infty \\ N \rightarrow \infty}} \frac{2}{\sqrt{KLMN}} \sum_{k=1}^K \sum_{l=1}^L \sum_{m=1}^M \sum_{n=1}^N a_s^{(m)} b_D^{(n)} c_{S-R}^{(mk)} c_{R-D}^{(ln)} \Re\{b_R^{(k)} a_R^{(l)}\} \\
 &\quad e^{j \left[2\pi (f_S^{(m)} + f_{S-R}^{(k)} + f_{R-D}^{(l)} + f_D^{(n)}) t + (\theta_{S-R}^{(mk)} + \theta_{R-D}^{(ln)} + \theta_{S-R} + \theta_{R-D}) \right]} \quad (10)
 \end{aligned}$$

where $\Re\{b_R^{(k)} a_R^{(l)}\}$ denotes the real part of a complex number, i.e., $2\Re\{b_R^{(k)} a_R^{(l)}\} = b_R^{(k)} a_R^{(l)} + b_R^{(k)*} a_R^{(l)*}$. Note that the phases θ_{S-R} and θ_{R-D} in (10) are constant quantities, which can be set to zero without loss of generality, since the statistical properties of the reference model are not influenced by a constant phase shift. Similarly, the diffuse component $h_{S-R-D}^{(22)}(t)$ of the $A_S^{(2)} - A_D^{(2)}$ transmission link can be expressed as

$$\begin{aligned}
 h_{S-R-D}^{(22)}(t) &= h_{R-D}^{(21)}(t) h_{S-R}^{(12)}(t) + h_{R-D}^{(22)}(t) h_{S-R}^{(22)}(t) \\
 &= \lim_{\substack{K \rightarrow \infty \\ L \rightarrow \infty \\ M \rightarrow \infty \\ N \rightarrow \infty}} \frac{2}{\sqrt{KLMN}} \sum_{k=1}^K \sum_{l=1}^L \sum_{m=1}^M \sum_{n=1}^N a_s^{(m)*} b_D^{(n)*} c_{S-R}^{(mk)} c_{R-D}^{(ln)} \Re\{b_R^{(k)} a_R^{(l)}\} \\
 &\quad e^{-j \left[2\pi (f_S^{(m)} - f_{S-R}^{(k)} + f_{R-D}^{(l)} - f_D^{(n)}) t - (\theta_{S-R}^{(mk)} + \theta_{R-D}^{(ln)} + \theta_{S-R} + \theta_{R-D}) \right]}. \quad (11)
 \end{aligned}$$

The equations (10) and (11) will be used in the next subsection to calculate the 4-D space-time CCF.

B. Correlation Properties of the Reference Model

By definition, the 4-D space-time CCF between the transmission links $A_S^{(1)} - A_D^{(1)}$ and $A_S^{(2)} - A_D^{(2)}$ is equivalent to the correlation between the diffuse components $h_{S-R-D}^{(11)}(t)$ and $h_{S-R-D}^{(22)}(t)$, i.e., [2]

$$\rho_{11,22}(\delta_S, \delta_R, \delta_D, \tau) := E \left\{ h_{S-R-D}^{(11)}(t) h_{S-R-D}^{(22)*}(t + \tau) \right\}. \quad (12)$$

It should be noticed here that the expectation operator is applied to all random variables, i.e., the random phase shifts $\{\theta_{S-R}^{(mk)}, \theta_{R-D}^{(ln)}\}$, the AODs $\{\phi_S^{(m)}, \phi_{R-D}^{(l)}\}$, and the AOAAs $\{\phi_{S-R}^{(k)}, \phi_D^{(n)}\}$. Substituting (10) and (11) in (12), the 4-D space-time CCF can be expressed as

$$\begin{aligned}
 \rho_{11,22}(\delta_S, \delta_R, \delta_D, \tau) &= \lim_{\substack{K \rightarrow \infty \\ M \rightarrow \infty \\ L \rightarrow \infty \\ N \rightarrow \infty}} \frac{4}{KLMN} \sum_{k=1}^K \sum_{l=1}^L \sum_{m=1}^M \sum_{n=1}^N \\
 &\quad E \left\{ a_s^{(m)2} b_D^{(n)2} [\Re\{b_R^{(k)} a_R^{(l)}\}]^2 e^{-j2\pi (f_S^{(m)} + f_{S-R}^{(k)} + f_{R-D}^{(l)} + f_D^{(n)}) \tau} \right\}. \quad (13)
 \end{aligned}$$

It is important to highlight here, the functions of random variables to which the expectation is applied. We can see that $\{a_s^{(m)}, f_s^{(m)}\}$ and $\{a_r^{(l)}, f_{r-D}^{(l)}\}$ are functions of the AODs $\phi_s^{(m)}$ and $\phi_{r-D}^{(l)}$, respectively. While $\{b_r^{(k)}, f_{s-R}^{(k)}\}$ and $\{b_D^{(n)}, f_D^{(n)}\}$ are functions of the AOA's $\phi_{s-R}^{(k)}$ and $\phi_D^{(n)}$, respectively [19]. If the number of local scatterers approaches infinity, i.e., $K, L, M, N \rightarrow \infty$, then the discrete random variables $\phi_s^{(m)}$, $\phi_{s-R}^{(k)}$, $\phi_{r-D}^{(l)}$, and $\phi_D^{(n)}$ become continuous random variables ϕ_s , ϕ_{s-R} , ϕ_{r-D} , and ϕ_D , each of which is characterized by a certain distribution, denoted by $p_{\phi_s}(\phi_s)$, $p_{\phi_{s-R}}(\phi_{s-R})$, $p_{\phi_{r-D}}(\phi_{r-D})$, and $p_{\phi_D}(\phi_D)$, respectively, [19]. The infinitesimal power of the diffuse components corresponding to the differential angles $d\phi_s$, $d\phi_{s-R}$, $d\phi_{r-D}$, and $d\phi_D$ is proportional to $p_{\phi_s}(\phi_s)p_{\phi_{s-R}}(\phi_{s-R})p_{\phi_{r-D}}(\phi_{r-D})p_{\phi_D}(\phi_D)d\phi_s d\phi_{s-R} d\phi_{r-D} d\phi_D$. This implies that when the number of local scatterers approaches infinity, i.e., $K, L, M, N \rightarrow \infty$, the infinitesimal power of all diffuse components becomes equal to $1/(KLMN)$, i.e.,

$$\frac{1}{KLMN} = p_{\phi_s}(\phi_s) p_{\phi_{s-R}}(\phi_{s-R}) p_{\phi_{r-D}}(\phi_{r-D}) p_{\phi_D}(\phi_D) d\phi_s d\phi_{s-R} d\phi_{r-D} d\phi_D. \quad (14)$$

Thus, we can write the 4-D space-time CCF $\rho_{11,22}(\delta_s, \delta_r, \delta_D, \tau)$ of the reference model given in (13) as

$$\rho_{11,22}(\delta_s, \delta_r, \delta_D, \tau) = \rho_s(\delta_s, \tau) \cdot \rho_r(\delta_r, \tau) \cdot \rho_D(\delta_D, \tau) \quad (15)$$

where

$$\rho_s(\delta_s, \tau) = \int_{-\pi}^{\pi} a_s^2(\delta_s, \phi_s) e^{-j2\pi f_s(\phi_s)\tau} p_{\phi_s}(\phi_s) d\phi_s \quad (16)$$

$$\begin{aligned} \rho_r(\delta_r, \tau) = & 4 \int_{-\pi}^{\pi} \int_{-\pi}^{\pi} p_{\phi_{s-R}}(\phi_{s-R}) p_{\phi_{r-D}}(\phi_{r-D}) d\phi_{s-R} d\phi_{r-D} \\ & e^{-j2\pi[f_{s-R}(\phi_{s-R}) + f_{r-D}(\phi_{r-D})]\tau} [\Re\{b_r(\delta_r, \phi_{s-R})a_r(\delta_r, \phi_{r-D})\}]^2 \end{aligned} \quad (17)$$

and

$$\rho_D(\delta_D, \tau) = \int_{-\pi}^{\pi} b_D^2(\delta_D, \phi_D) e^{-j2\pi f_D(\phi_D)\tau} p_{\phi_D}(\phi_D) d\phi_D \quad (18)$$

are the CFs at the source mobile station, mobile relay, and the destination mobile station. Here,

$$a_s(\delta_s, \phi_s) = e^{j\frac{\pi}{\lambda} \delta_s \cos(\phi_s - \beta_s)} \quad (19a)$$

$$b_{\text{R}}(\delta_{\text{R}}, \phi_{\text{S-R}}) = e^{j\frac{\pi}{\lambda} \delta_{\text{R}} \cos(\phi_{\text{S-R}} - \beta_{\text{R}})} \quad (19\text{b})$$

$$a_{\text{R}}(\delta_{\text{R}}, \phi_{\text{S-R}}) = e^{j\frac{\pi}{\lambda} \delta_{\text{R}} \cos(\phi_{\text{R-D}} - \beta_{\text{R}})} \quad (19\text{c})$$

$$b_{\text{D}}(\delta_{\text{D}}, \phi_{\text{D}}) = e^{j\frac{\pi}{\lambda} \delta_{\text{D}} \cos(\phi_{\text{D}} - \beta_{\text{D}})} \quad (19\text{d})$$

$$f_{\text{S}}(\phi_{\text{S}}) = f_{\text{Smax}} \cos(\phi_{\text{S}} - \alpha_{\text{S}}) \quad (19\text{e})$$

$$f_{\text{S-R}}(\phi_{\text{S-R}}) = f_{\text{Rmax}} \cos(\phi_{\text{S-R}} - \alpha_{\text{R}}) \quad (19\text{f})$$

$$f_{\text{R-D}}(\phi_{\text{R-D}}) = f_{\text{Rmax}} \cos(\phi_{\text{R-D}} - \alpha_{\text{R}}) \quad (19\text{g})$$

$$f_{\text{D}}(\phi_{\text{D}}) = f_{\text{Dmax}} \cos(\phi_{\text{D}} - \alpha_{\text{D}}). \quad (19\text{h})$$

In this article, we refer to the CF at the source mobile station $\rho_{\text{S}}(\delta_{\text{S}}, \tau)$ as the source CF. Similarly, the CF at the mobile relay (destination mobile station) $\rho_{\text{S}}(\delta_{\text{R}}, \tau)$ ($\rho_{\text{S}}(\delta_{\text{D}}, \tau)$) is termed as the relay CF (destination CF). Equation (15) illustrates that the 4-D space-time CCF $\rho_{11,22}(\delta_{\text{S}}, \delta_{\text{R}}, \delta_{\text{D}}, \tau)$ of the reference model can be expressed as the product of the source CF $\rho_{\text{S}}(\delta_{\text{S}}, \tau)$, the relay CF $\rho_{\text{R}}(\delta_{\text{R}}, \tau)$, and the destination CF $\rho_{\text{D}}(\delta_{\text{D}}, \tau)$. Besides, from (16) and (18), it turns out that the source mobile station and the destination mobile station are interchangeable.

The 3-D spatial CCF $\rho(\delta_{\text{S}}, \delta_{\text{R}}, \delta_{\text{D}})$, defined as $\rho(\delta_{\text{S}}, \delta_{\text{R}}, \delta_{\text{D}}) = E \left\{ h_{\text{S-R-D}}^{(11)}(t) h_{\text{S-R-D}}^{(22)*}(t) \right\}$, is equal to the 4-D space-time CCF $\rho_{11,22}(\delta_{\text{S}}, \delta_{\text{R}}, \delta_{\text{D}}, \tau)$ at $\tau = 0$, i.e.,

$$\begin{aligned} \rho(\delta_{\text{S}}, \delta_{\text{R}}, \delta_{\text{D}}) &= \rho_{11,22}(\delta_{\text{S}}, \delta_{\text{R}}, \delta_{\text{D}}, 0) \\ &= \rho_{\text{S}}(\delta_{\text{S}}, 0) \cdot \rho_{\text{R}}(\delta_{\text{R}}, 0) \cdot \rho_{\text{D}}(\delta_{\text{D}}, 0). \end{aligned} \quad (20)$$

Furthermore, the temporal autocorrelation function (ACF) $r_{h_{\text{S-R-D}}^{(iq)}}(\tau)$ of the diffuse component $h_{\text{S-R-D}}^{(iq)}(t)$ of the transmission link from the source mobile station antenna element $A_{\text{S}}^{(q)}$ to the destination mobile station antenna element $A_{\text{D}}^{(i)} \forall i, q \in \{1, 2\}$ can be given as

$$r_{h_{\text{S-R-D}}^{(iq)}}(\tau) := E \left\{ h_{\text{S-R-D}}^{(iq)}(t) h_{\text{S-R-D}}^{(iq)*}(t + \tau) \right\}. \quad (21)$$

It is not difficult to show that the temporal ACF $r_{h_{\text{S-R-D}}^{(iq)}}(\tau) \forall i, q \in \{1, 2\}$ is equal to the 4-D space-time CCF $\rho_{11,22}(\delta_{\text{S}}, \delta_{\text{R}}, \delta_{\text{D}}, \tau)$ of the reference model at $\delta_{\text{S}} = \delta_{\text{R}} = \delta_{\text{D}} = 0$, i.e.,

$$\begin{aligned} r_{h_{\text{S-R-D}}^{(iq)}}(\tau) &= \rho_{11,22}(0, 0, 0, \tau) \\ &= \rho_{\text{S}}(0, \tau) \cdot \rho_{\text{R}}(0, \tau) \cdot \rho_{\text{D}}(0, \tau). \end{aligned} \quad (22)$$

Substituting $\delta_s = 0$, $\delta_r = 0$, and $\delta_d = 0$ in (16), (17), and (18), respectively, gives $\rho_s(0, \tau)$, $\rho_r(0, \tau)$, and $\rho_d(0, \tau)$, respectively as

$$\rho_s(0, \tau) = \int_{-\pi}^{\pi} e^{-j2\pi f_s(\phi_s)\tau} p_{\phi_s}(\phi_s) d\phi_s, \quad (23)$$

$$\rho_r(0, \tau) = 4 \int_{-\pi}^{\pi} \int_{-\pi}^{\pi} e^{-j2\pi[f_{S-R}(\phi_{S-R}) + f_{R-D}(\phi_{R-D})]\tau} p_{\phi_{S-R}}(\phi_{S-R}) p_{\phi_{R-D}}(\phi_{R-D}) d\phi_{S-R} d\phi_{R-D}, \quad (24)$$

and

$$\rho_d(0, \tau) = \int_{-\pi}^{\pi} e^{-j2\pi f_d(\phi_d)\tau} p_{\phi_d}(\phi_d) d\phi_d. \quad (25)$$

IV. THE STOCHASTIC SIMULATION MODEL

The reference model developed in Section III is a theoretical model, which is based on the assumption that the number of local scatterers (K, L, M, N) around the source mobile station, the mobile relay, and the destination mobile station is infinite. The assumption of an infinite number of local scatterers prevents the realization of the reference model. However, a realizable stochastic simulation model can be derived from the reference model by: (i) using only a limited number of local scatterers $K = L, M$, and N is finite, (ii) setting the constant phase shifts θ_{S-R} and θ_{R-D} to zero in (10), and (iii) considering the discrete AOD $\phi_s^{(m)}$ and $\phi_{R-D}^{(l)}$, as well as the AOA $\phi_{S-R}^{(k)}$ and $\phi_D^{(n)}$ are constant quantities [19]. Thus, using (10), the diffuse component $\hat{h}_{S-R-D}^{(11)}(t)$ of the $A_S^{(1)} - A_D^{(1)}$ transmission link of the stochastic simulation model can be expressed as

$$\hat{h}_{S-R-D}^{(11)}(t) = \frac{2}{\sqrt{KLMN}} \sum_{k=1}^K \sum_{l=1}^L \sum_{m=1}^M \sum_{n=1}^N a_s^{(m)} b_D^{(n)} c_{S-R}^{(mk)} c_{R-D}^{(ln)} \Re\{b_R^{(k)} a_R^{(l)}\} e^{j[2\pi\{f_s^{(m)} + f_{S-R}^{(k)} + f_{R-D}^{(l)} + f_D^{(n)}\}t - \theta_{S-R}^{(mk)} - \theta_{R-D}^{(ln)}]}. \quad (26)$$

Throughout this paper, the hat symbol is used for the stochastic simulation model. Similarly, the diffuse component $\hat{h}_{S-R-D}^{(22)}(t)$ of the $A_S^{(2)} - A_D^{(2)}$ transmission link in the stochastic simulation model can be expressed as

$$\hat{h}_{S-R-D}^{(22)}(t) = \frac{2}{\sqrt{KLMN}} \sum_{k=1}^K \sum_{l=1}^L \sum_{m=1}^M \sum_{n=1}^N a_s^{(m)*} b_D^{(n)*} c_{S-R}^{(mk)} c_{R-D}^{(ln)} \Re\{b_R^{(k)} a_R^{(l)}\} e^{j[2\pi\{f_s^{(m)} + f_{S-R}^{(k)} + f_{R-D}^{(l)} + f_D^{(n)}\}t - \theta_{S-R}^{(mk)} - \theta_{R-D}^{(ln)}]}. \quad (27)$$

The 4-D space-time CCF of the diffuse components $\hat{h}_{S-R-D}^{(11)}(t)$ and $\hat{h}_{S-R-D}^{(22)}(t)$ of the stochastic simulation model is defined by

$$\hat{\rho}_{11,22}(\delta_s, \delta_r, \delta_d, \tau) := E \left\{ \hat{h}_{S-R-D}^{(11)}(t) \hat{h}_{S-R-D}^{(22)*}(t + \tau) \right\} \quad (28)$$

where the expectation operator now only applies on the random phases $\theta_{S-R}^{(mk)}$ and $\theta_{R-D}^{(ln)}$. Substitution of (26) and (27) in (28) results in the following closed-form expression

$$\begin{aligned} \hat{\rho}_{11,22}(\delta_s, \delta_r, \delta_d, \tau) &= \frac{4}{KLMN} \sum_{k=1}^K \sum_{l=1}^L \sum_{m=1}^M \sum_{n=1}^N \\ &\quad a_s^{(m)2} b_D^{(n)2} (\Re\{b_R^{(k)} a_R^{(l)}\})^2 e^{-j2\pi\{f_S^{(m)} + f_{S-R}^{(k)} + f_{R-D}^{(l)} + f_D^{(n)}\}\tau} \\ &= \hat{\rho}_S(\delta_s, \tau) \cdot \hat{\rho}_R(\delta_r, \tau) \cdot \hat{\rho}_D(\delta_d, \tau) \end{aligned} \quad (29)$$

where

$$\hat{\rho}_S(\delta_s, \tau) = \frac{1}{M} \sum_{m=1}^M a_s^{(m)2}(\delta_s) e^{-j2\pi f_S^{(m)} \tau} \quad (30)$$

$$\hat{\rho}_R(\delta_r, \tau) = \frac{4}{KL} \sum_{k=1}^K \sum_{l=1}^L (\Re\{b_R^{(k)} a_R^{(l)}\})^2 e^{-j2\pi [f_{S-R}^{(k)} + f_{R-D}^{(l)}] \tau} \quad (31)$$

and

$$\hat{\rho}_D(\delta_d, \tau) = \frac{1}{N} \sum_{n=1}^N b_D^{(n)2}(\delta_d) e^{-j2\pi f_D^{(n)} \tau} \quad (32)$$

are called the source CF, the relay CF, and the destination CF of the simulation model.

The 3-D spatial CCF $\hat{\rho}(\delta_s, \delta_r, \delta_d)$ of the simulation model, defined as

$$\hat{\rho}(\delta_s, \delta_r, \delta_d) = E \left\{ \hat{h}_{S-R-D}^{(11)}(t) \hat{h}_{S-R-D}^{(22)*}(t) \right\} \quad (33)$$

is equal to the 4-D space-time CCF $\hat{\rho}_{11,22}(\delta_s, \delta_r, \delta_d, \tau)$ at $\tau = 0$, i.e.,

$$\hat{\rho}(\delta_s, \delta_r, \delta_d) = \hat{\rho}_{11,22}(\delta_s, \delta_r, \delta_d, 0) = \hat{\rho}_S(\delta_s, 0) \cdot \hat{\rho}_R(\delta_r, 0) \cdot \hat{\rho}_D(\delta_d, 0). \quad (34)$$

In the stochastic simulation model, the temporal ACF $\hat{r}_{h_{S-R-D}^{(iq)}}(\tau)$ of the diffuse component $\hat{h}_{S-R-D}^{(iq)}(t)$ of the $A_S^{(q)} - A_D^{(i)}$ transmission link can be derived as follows

$$\hat{r}_{h_{S-R-D}^{(iq)}}(\tau) := E \left\{ \hat{h}_{S-R-D}^{(iq)}(t) \hat{h}_{S-R-D}^{(iq)*}(t + \tau) \right\}$$

$$\begin{aligned}
&= \frac{1}{KLMN} \sum_{k=1}^K \sum_{l=1}^L \sum_{m=1}^M \sum_{n=1}^N e^{-j2\pi\{f_S^{(m)} + f_{S-R}^{(k)} + f_{R-D}^{(l)} + f_D^{(n)}\}\tau} \\
&= \hat{\rho}_S(0, \tau) \cdot \hat{\rho}_R(0, \tau) \cdot \hat{\rho}_D(0, \tau) \quad \forall i, q \in \{1, 2\}. \quad (35)
\end{aligned}$$

From (35), it can be seen that the temporal ACF $\hat{r}_{h^{(iq)}_{S-R-D}}(\tau)$ is equal to the 4-D space-time CCF $\hat{\rho}_{11,22}(\delta_S, \delta_R, \delta_D, \tau)$ of the simulation model at $\delta_S = \delta_R = \delta_D = 0$, i.e., $\hat{r}_{h^{(iq)}_{S-R-D}}(\tau) = \hat{\rho}_{11,22}(0, 0, 0, \tau)$.

V. SCATTERING SCENARIOS

In this section, the correlation properties of the reference model are studied under isotropic and non-isotropic scattering conditions.

A. Isotropic Scattering Scenarios

Isotropic scattering around the source mobile station can be determined by assuming uniformly distributed AOD ϕ_S over the interval $[0, 2\pi)$, i.e.,

$$p_{\phi_S}(\phi_S) = \frac{1}{2\pi}, \quad \phi_S \in [0, 2\pi). \quad (36)$$

Similarly, isotropic scattering around the mobile relay (destination mobile station) can be characterized by a uniform distribution of the AOA ϕ_{S-R} (ϕ_D) along with a uniform distribution of the AOD ϕ_{R-D} over $[0, 2\pi)$. Hence, the distributions $p_{\phi_{S-R}}(\phi_{S-R})$, $p_{\phi_{R-D}}(\phi_{R-D})$, and $p_{\phi_D}(\phi_D)$ can be obtained by replacing the index S by S-R, R-D, and D in (36), respectively.

Substituting (36) in (16) and solving the integrals using [10, Eq. (3.338-4)] results in the following closed-form expression of the source CF

$$\rho_S(\delta_S, \tau) = J_0 \left(2\pi \sqrt{\left(\frac{\delta_S}{\lambda}\right)^2 + (f_{S_{\max}} \tau)^2 - 2\frac{\delta_S}{\lambda} f_{S_{\max}} \tau \cos(\alpha_S - \beta_S)} \right) \quad (37)$$

where $J_0(\cdot)$ is the zeroth-order Bessel function of the first kind [10]. Furthermore, the destination CF $\rho_D(\delta_D, \tau)$ can be obtained by replacing the index S by D in (37). Finally, substituting $p_{\phi_{S-R}}(\phi_{S-R})$ and $p_{\phi_{R-D}}(\phi_{R-D})$ in (17) allows us to solve the integrals using [10, Eq. (3.338-4)] and to write the relay CF $\rho_R(\delta_R, \tau)$ in a closed form as

$$\rho_R(\delta_R, \tau) = \left\{ J_0 \left(2\pi \sqrt{\left(\frac{\delta_R}{\lambda}\right)^2 + (f_{R_{\max}} \tau)^2 - 2\frac{\delta_R}{\lambda} f_{R_{\max}} \tau \cos(\alpha_R - \beta_R)} \right) \right\}^2 + \left\{ J_0 \left(2\pi \sqrt{\left(\frac{\delta_R}{\lambda}\right)^2 + (f_{R_{\max}} \tau)^2 + 2\frac{\delta_R}{\lambda} f_{R_{\max}} \tau \cos(\alpha_R - \beta_R)} \right) \right\}^2 + 2\{J_0(2\pi f_{R_{\max}} \tau)\}^2. \quad (38)$$

Substituting (37), (38), and the closed-form expression of $\rho_D(\delta_D, \tau)$ in (15) results in the 4-D space-time CCF $\rho_{11,22}(\delta_S, \delta_R, \delta_D, \tau)$ of the reference model in a closed form given in (39) as follows

$$\begin{aligned} \rho_{11,22}(\delta_S, \delta_R, \delta_D, \tau) = & \left[\left\{ J_0 \left(2\pi \sqrt{\left(\frac{\delta_R}{\lambda}\right)^2 + (f_{R_{\max}} \tau)^2 - 2\frac{\delta_R}{\lambda} f_{R_{\max}} \tau \cos(\alpha_R - \beta_R)} \right) \right\}^2 \right. \\ & \left. + \left\{ J_0 \left(2\pi \sqrt{\left(\frac{\delta_R}{\lambda}\right)^2 + (f_{R_{\max}} \tau)^2 + 2\frac{\delta_R}{\lambda} f_{R_{\max}} \tau \cos(\alpha_R - \beta_R)} \right) \right\}^2 + 2\{J_0(2\pi f_{R_{\max}} \tau)\}^2 \right] \\ & \times J_0 \left(2\pi \sqrt{\left(\frac{\delta_S}{\lambda}\right)^2 + (f_{S_{\max}} \tau)^2 - 2\frac{\delta_S}{\lambda} f_{S_{\max}} \tau \cos(\alpha_S - \beta_S)} \right) \\ & \times J_0 \left(2\pi \sqrt{\left(\frac{\delta_D}{\lambda}\right)^2 + (f_{D_{\max}} \tau)^2 - 2\frac{\delta_D}{\lambda} f_{D_{\max}} \tau \cos(\alpha_D - \beta_D)} \right). \quad (39) \end{aligned}$$

From (39), it follows that the 3-D spatial CCF $\rho(\delta_S, \delta_R, \delta_D)$ of the reference model is a product of four Bessel functions, i.e., $\rho(\delta_S, \delta_R, \delta_D) = \rho_{11,22}(\delta_S, \delta_R, \delta_D, 0) = J_0(2\pi\delta_S/\lambda) \{2J_0(2\pi\delta_R/\lambda)\}^2 J_0(2\pi\delta_D/\lambda)$. In the same way, the temporal ACF $r_{h_{S-R-D}}^{(iq)}(\tau)$ of the reference model can be written as $r_{h_{S-R-D}}^{(iq)}(\tau) = \rho_{11,22}(0, 0, 0, \tau) = J_0(2\pi f_{S_{\max}} \tau) \{2J_0(2\pi f_{R_{\max}} \tau)\}^2 J_0(2\pi f_{D_{\max}} \tau)$. A product of two Bessel functions describes the 2-D spatial CCF and the temporal ACF of the reference model derived from a geometrical two-ring scattering model [19]. For the 3-D spatial CCF and the temporal ACF of the reference model derived from a geometrical three-ring scattering model, a product of four Bessel functions is justified. Since, the geometrical three-ring scattering model is a concatenation of two separate geometrical two-ring scattering models.

B. Non-Isotropic Scattering Scenarios

In this paper, for characterizing non-isotropic scattering around the source mobile station (destination mobile station), we have assumed the von Mises distribution for the AOD ϕ_s (AOA ϕ_d), i.e.,

$$p_{\phi_s}(\phi_s) = \frac{1}{2\pi I_0(\kappa_s)} e^{\kappa_s \cos(\phi_s - \phi_s^{(0)})}, \quad \phi_s \in [0, 2\pi) \quad (40)$$

where $I_0(\cdot)$ is the modified Bessel function of the first kind of order zero, the parameter $\phi_s^{(0)}$ ($\phi_d^{(0)}$) $\in [0, 2\pi)$ is the mean AOD (AOA), and the parameter κ_s (κ_d) ≥ 0 controls the angular spread of ϕ_s (ϕ_d). The reason for using the von Mises distribution is its flexibility to closely approximate the Gaussian distribution and the cardioid distribution as well as to have the uniform distribution as a special case [1]. Substituting (40) in (16) and using [10, Eq. (3.338-4)] results in the following closed-form expression for the source CF

$$\begin{aligned} \rho_s(\delta_s, \tau) = & \frac{1}{I_0(\kappa_s)} I_0 \left(\left[\kappa_s^2 - 4\pi^2 \left\{ \left(\frac{\delta_s}{\lambda} \right)^2 + (f_{s_{\max}} \tau)^2 - 2 \frac{\delta_s}{\lambda} f_{s_{\max}} \tau \cos(\alpha_s - \beta_s) \right\} \right. \right. \\ & \left. \left. + j4\pi\kappa_s \left\{ \frac{\delta_s}{\lambda} \cos(\beta_s - \phi_s^{(0)}) - f_{s_{\max}} \tau \cos(\alpha_s - \phi_s^{(0)}) \right\} \right]^{1/2} \right). \quad (41) \end{aligned}$$

The destination CF $\rho_d(\delta_d, \tau)$ can easily be obtained by replacing the index S by D in (41).

Similarly, the von Mises distribution for the AOA ϕ_{s-R} and the AOD ϕ_{r-D} describes non-isotropic scattering conditions around the mobile relay. Substituting the von Mises distribution for the AOA ϕ_{s-R} and the AOD ϕ_{r-D} in (17) and solving the integrals using [10, Eq. (3.338-4)], provides us with the closed-form solution for relay CF $\rho_r(\delta_r, \tau)$ as given in the following

$$\begin{aligned} \rho_r(\delta_r, \tau) = & (1 / (I_0(\kappa_{s-R}) I_0(\kappa_{r-D}))) \times \\ & \left[I_0 \left(\left[\kappa_{s-R}^2 - 4\pi^2 \left\{ \left(\frac{\delta_r}{\lambda} \right)^2 + (f_{r_{\max}} \tau)^2 - 2 \frac{\delta_r}{\lambda} f_{r_{\max}} \tau \cos(\alpha_r - \beta_r) \right\} \right. \right. \right. \\ & \left. \left. + j4\pi\kappa_{s-R} \left\{ \frac{\delta_r}{\lambda} \cos(\beta_r - \phi_{s-R}^{(0)}) - f_{r_{\max}} \tau \cos(\alpha_r - \phi_{s-R}^{(0)}) \right\} \right]^{1/2} \right) \\ & I_0 \left(\left[\kappa_{r-D}^2 - 4\pi^2 \left\{ \left(\frac{\delta_r}{\lambda} \right)^2 + (f_{r_{\max}} \tau)^2 - 2 \frac{\delta_r}{\lambda} f_{r_{\max}} \tau \cos(\alpha_r - \beta_r) \right\} \right. \right. \\ & \left. \left. + j4\pi\kappa_{r-D} \left\{ \frac{\delta_r}{\lambda} \cos(\beta_r - \phi_{r-D}^{(0)}) - f_{r_{\max}} \tau \cos(\alpha_r - \phi_{r-D}^{(0)}) \right\} \right]^{1/2} \right) \end{aligned}$$

$$\begin{aligned}
 & + I_0 \left(\left[\kappa_{S-R}^2 - 4\pi^2 f_{R_{\max}}^2 \tau^2 - j4\pi \kappa_{S-R} f_{R_{\max}} \tau \cos \left(\alpha_R - \phi_{S-R}^{(0)} \right) \right]^{1/2} \right) \\
 & I_0 \left(\left[\kappa_{R-D}^2 - 4\pi^2 f_{R_{\max}}^2 \tau^2 - j4\pi \kappa_{R-D} f_{R_{\max}} \tau \cos \left(\alpha_R - \phi_{R-D}^{(0)} \right) \right]^{1/2} \right) \\
 & + I_0 \left(\left[\kappa_{S-R}^2 - 4\pi^2 \left\{ \left(\frac{\delta_R}{\lambda} \right)^2 + (f_{R_{\max}} \tau)^2 + 2 \frac{\delta_R}{\lambda} f_{R_{\max}} \tau \cos (\alpha_R - \beta_R) \right\} \right. \right. \\
 & \quad \left. \left. - j4\pi \kappa_{S-R} \left\{ \frac{\delta_R}{\lambda} \cos (\beta_R - \phi_{S-R}^{(0)}) + f_{R_{\max}} \tau \cos (\alpha_R - \phi_{S-R}^{(0)}) \right\} \right]^{1/2} \right) \\
 & I_0 \left(\left[\kappa_{R-D}^2 - 4\pi^2 \left\{ \left(\frac{\delta_R}{\lambda} \right)^2 + (f_{R_{\max}} \tau)^2 + 2 \frac{\delta_R}{\lambda} f_{R_{\max}} \tau \cos (\alpha_R - \beta_R) \right\} \right. \right. \\
 & \quad \left. \left. - j4\pi \kappa_{R-D} \left\{ \frac{\delta_R}{\lambda} \cos (\beta_R - \phi_{R-D}^{(0)}) + f_{R_{\max}} \tau \cos (\alpha_R - \phi_{R-D}^{(0)}) \right\} \right]^{1/2} \right) \Big] \\
 \end{aligned} \tag{42}$$

Note that the von Mises distribution reduces to the uniform distribution for $\kappa_S = \kappa_{S-R} = \kappa_{R-D} = \kappa_D = 0$. This implies that (41) and (42) reduce to (37) and (38), respectively, when the corresponding κ 's are set to zero.

VI. NUMERICAL RESULTS

The purpose of this section is twofold. Firstly, to illustrate the important theoretical results found for the CCFs of the reference model and the stochastic simulation model by evaluating the expressions in (16), (18), (30), and (32). Here, we focus on discussing numerical results for the transmit CFs and the relay CFs. The results for the receive CFs can easily be obtained from the transmit CFs just by replacing the index S by D. As performance criterion, we consider the absolute error $e_s(\delta_s, \tau) = |\rho_s(\delta_s, \tau) - \hat{\rho}_s(\delta_s, \tau)|$ as a measure for the quality of the approximation $\rho_s(\delta_s, \tau) \approx \hat{\rho}_s(\delta_s, \tau)$. Similarly, the absolute error $e_r(\delta_r, \tau) = |\rho_r(\delta_r, \tau) - \hat{\rho}_r(\delta_r, \tau)|$ has been introduced to study the amount of precision of the approximation $\rho_r(\delta_r, \tau) \approx \hat{\rho}_r(\delta_r, \tau)$. The selected values for the parameters influencing the CFs are: $\beta_s = \beta_r = \pi/2$, $\alpha_s = \alpha_r = \pi/4$, and $f_{s_{\max}} = f_{r_{\max}} = 91$ Hz. Furthermore, the wavelength λ was set to $\lambda = 0.15$ m.

For the stochastic simulation model, an appropriate number of discrete scatterers M and K (L) located on the rings around the source mobile station and the mobile relay, respectively, should be selected. In our simulations, we have chose $M = 40$ and $K = L = 23$. A good solution to the parameter computation problem in M2M fading channel simulators in case of isotropic scattering is proposed in [19], where the authors have suggested the extended method of exact Doppler spread

(EMEDS). Whereas, in case of non-isotropic scattering, a high-performance parameter computation method is the modified method of equal areas (MMEA) [11]. Since the MMEA reduces to the EMEDS in case of isotropic scattering [19], we have used the MMEA for computing the AODs $\phi_s^{(m)}$ and $\phi_{R-D}^{(l)}$ as well as the AOA $\phi_{S-R}^{(k)}$.

Figures B.3–B.8 present the numerical results in case of isotropic scattering. Figure B.3 shows the shape of the source CF $\rho_s(\delta_s, \tau)$ of the reference model determined by (37), whereas the simulation model's source CF $\hat{\rho}_s(\delta_s, \tau)$ is illustrated in Fig. B.4. The absolute error $e_s(\delta_s, \tau)$, presented in Fig. B.5, shows the quality of the approximation $\rho_s(\delta_s, \tau) \approx \hat{\rho}_s(\delta_s, \tau)$. Similarly, the shape of the relay CF $\rho_r(\delta_r, \tau)$ of the reference model given by (38) and the simulation model's relay CF $\hat{\rho}_r(\delta_r, \tau)$ are presented in Fig. B.6 and Fig. B.7, respectively. Carefully studying the absolute error $e_r(\delta_r, \tau)$ presented in Fig. B.8 reveals the ranges of δ_r/λ and $\tau \cdot f_{Rmax}$ with an excellent approximation $\rho_r(\delta_r, \tau) \approx \hat{\rho}_r(\delta_r, \tau)$. When δ_r/λ is confined in the range $[0, (K=L)/8]$, then the approximation $\rho_r(\delta_r, \tau) \approx \hat{\rho}_r(\delta_r, \tau)$ is very accurate. On the other hand, for $\delta_r = 0$ with $\tau \cdot f_{Rmax}$ in the range $[0, (K=L)/8]$, the absolute error $e_r(\delta_r, \tau)$ is almost zero.

Figures B.9–B.14 illustrate the results in case of non-isotropic scattering. As mentioned in Subsection V.B, the von Mises distribution has been employed to characterize non-isotropic scattering around the source mobile station (destination mobile station) and the mobile relay. In our simulations, the parameters of the von Mises distribution were set as $\phi_s^{(0)} = \phi_{S-R}^{(0)} = \phi_{R-D}^{(0)} = 60^\circ$ and $\kappa_s = \kappa_{S-R} = \kappa_{R-D} = 40$. The absolute value of the reference model's source CF $|\rho_s(\delta_s, \tau)|$ given in (41) is presented in Fig. B.9, whereas the absolute value of the simulation model's source CF $|\hat{\rho}_s(\delta_s, \tau)|$ is shown in Fig. B.10. The absolute error $e_s(\delta_s, \tau)$ is illustrated in Fig. B.11, which shows that the approximation $\rho_s(\delta_s, \tau) \approx \hat{\rho}_s(\delta_s, \tau)$ holds in case of non-isotropic scattering as well. The error function $e_s(\delta_s, \tau)$ shows a ripple behavior, where the maximum value of this error function is in the orders of $3 \cdot 10^{-2}$. It has been recommended in the literature to utilize the Lp-norm method (LPNM) [16] for computing the simulation model parameters when the AODs are non-uniformly distributed on the rings around the source mobile station [19]. The successful application of the LPNM for minimizing the error function of the one-ring model parameters and the two-ring model parameters can be found in [17] and [18], respectively. It is therefore believed that the LPNM is equally beneficial for the computation of the three-ring model parameters under non-isotropic scattering conditions. Similarly, the absolute value of the reference model's relay CF $|\rho_r(\delta_r, \tau)|$ [see (42)], and the absolute value of the simulation model's source CF $|\hat{\rho}_r(\delta_r, \tau)|$ [see (31)]

are shown in Fig. B.12 and Fig. B.13, respectively. The measure of the quality of the approximation $\rho_R(\delta_R, \tau) \approx \hat{\rho}_R(\delta_R, \tau)$, i.e., the absolute error $e_R(\delta_R, \tau)$ is illustrated in Fig. B.14. It can be seen in Fig. B.14 that the maximum value of $e_R(\delta_R, \tau)$ is less than 10^{-1} . The same arguments given for minimizing $e_S(\delta_S, \tau)$ by using the LPNM are valid for minimizing $e_R(\delta_R, \tau)$.

VII. CONCLUSION

In this paper, we have derived a reference model and a stochastic simulation model for narrowband MIMO M2M fading channels under NLOS propagation conditions. Here, we have considered a single-relay dual-hop amplify-and-forward relay type cooperative network. It is further assumed that the source mobile station, the mobile relay, and the destination mobile station are equipped with two antennas each. The starting point for deriving the reference model was the geometrical three-ring scattering model, where the local scatterers are placed on rings around the source mobile station, the mobile relay, and the destination mobile station. In addition, the suggested three-ring scattering model turned out to be a concatenation of two separate two-ring scattering models. General analytical formulas for the 4-D space-time CCF, 3-D spatial CCF, 2-D source (relay, destination) CF, and temporal ACF have been derived. Closed-form expressions for the source (destination) CF and the relay CF specific to isotropic as well as non-isotropic scattering have been presented. The results show that the various CCFs describing the simulation model closely approximate the corresponding CCFs of the reference model. It is worth mentioning that this excellent fitting of the simulation model CCFs to that of the reference model CCFs is achieved with the help of the MMEA. The MMEA indeed reduced the complexity of the designed channel simulator.

The developed channel simulator is the first of its kind to model narrowband NLOS MIMO M2M channels in relay-based cooperative communication systems. It is useful for analyzing the dynamic behavior of the MIMO channel capacity of relay-based M2M communication systems. In addition, the proposed geometrical three-ring scattering model for narrowband MIMO M2M fading channels can be considered as a starting point for the development and analysis of new channels models for wideband MIMO M2M fading channels in cooperative networks.

REFERENCES

- [1] A. Abdi, J. A. Barger, and M. Kaveh. A parametric model for the distribution of the angle of arrival and the associated correlation function and power spectrum at the mobile station. *IEEE Trans. Veh. Technol.*, 51(3):425–434, May 2002.
- [2] A. Abdi and M. Kaveh. A space-time correlation model for multielement antenna systems in mobile fading channels. *IEEE J. Select. Areas Commun.*, 20(3):550–560, April 2002.
- [3] A. S. Akki. Statistical properties of mobile-to-mobile land communication channels. *IEEE Trans. Veh. Technol.*, 43(4):826–831, November 1994.
- [4] A. S. Akki and F. Haber. A statistical model of mobile-to-mobile land communication channel. *IEEE Trans. Veh. Technol.*, 35(1):2–7, February 1986.
- [5] J. B. Andersen. Statistical distributions in mobile communications using multiple scattering. In *Proc. 27th URSI General Assembly*. Maastricht, Netherlands, August 2002.
- [6] S. Barbarossa and G. Scutari. Cooperative diversity through virtual arrays in multihop networks. In *Proc. IEEE International Conf. Acoustics, Speech, Signal Processing*, volume 4, pages 209–212. Hong Kong, China, April 2003.
- [7] G. J. Byers and F. Takawira. Spatially and temporally correlated MIMO channels: modelling and capacity analysis. *IEEE Trans. Veh. Technol.*, 53(3):634–643, May 2004.
- [8] V. Ercerg, S. J. Fortune, J. Ling, A. J. Rustako Jr., and R. A. Valenzuela. Comparison of a computer-based propagation prediction tool with experimental data collected in urban microcellular environment. *IEEE J. Select. Areas Commun.*, 15(4):677–684, May 1997.
- [9] G. J. Foschini and M. J. Gans. On limits of wireless communications in a fading environment when using multiple antennas. *Wireless Pers. Commun.*, 6:311–335, March 1998.
- [10] I. S. Gradshteyn and I. M. Ryzhik. *Table of Integrals, Series, and Products*. New York: Academic Press, 6th edition, 2000.

- [11] C. A. Gutiérrez and M. Pätzold. Sum-of-sinoids-based simulation of flat fading wireless propagation channels under non-isotropic scattering conditions. In *Proc. 50th IEEE Global Telecommunications Conference, GLOBECOM 2007*, pages 3842–3846. Washington DC, USA, November 2007.
- [12] I. Z. Kovacs, P. C. F. Eggers, K. Olesen, and L. G. Petersen. Investigations of outdoor-to-indoor mobile-to-mobile radio communication channels. In *Proc. IEEE 56th Veh. Technol. Conf., VTC'02-Fall*, volume 1, pages 430–434. Vancouver BC, Canada, September 2002.
- [13] J. N. Laneman, D. N. C. Tse, and G. W. Wornell. Cooperative diversity in wireless networks: Efficient protocols and outage behavior. *IEEE Trans. Inform. Theory*, 50(12):3062–3080, December 2004.
- [14] C. S. Patel, G. L. Stüber, and T. G. Pratt. Comparative analysis of statistical models for the simulation of Rayleigh faded cellular channels. *IEEE Trans. Commun.*, 53(6):1017–1026, June 2005.
- [15] C. S. Patel, G. L. Stüber, and T. G. Pratt. Statistical properties of amplify and forward relay fading channels. *IEEE Trans. Veh. Technol.*, 55(1):1–9, January 2006.
- [16] M. Pätzold. *Mobile Fading Channels*. Chichester: John Wiley & Sons, 2002.
- [17] M. Pätzold and B. O. Hogstad. A space-time channel simulator for MIMO channels based on the geometrical one-ring scattering model. *Wireless Communications and Mobile Computing, Special Issue on Multiple-Input Multiple-Output (MIMO) Communications*, 4(7):727–737, November 2004.
- [18] M. Pätzold and B. O. Hogstad. Design and performance of MIMO channel simulators derived from the two-ring scattering model. In *Proc. 14th IST Mobile & Communications Summit, IST 2005*. Dresden, Germany, June 2005. paper no. 121.
- [19] M. Pätzold, B. O. Hogstad, and N. Youssef. Modeling, analysis, and simulation of MIMO mobile-to-mobile fading channels. *IEEE Trans. Wireless Commun.*, 7(2):510–520, February 2008.
- [20] J. Salo, H. M. El-Sallabi, and P. Vainikainen. Statistical analysis of the multiple scattering radio channel. *IEEE Trans. Antennas Propagat.*, 54(11):3114–3124, November 2006.

- [21] A. Sendonaris, E. Erkip, and B. Aazhang. User cooperation diversity — Part I: System description. *IEEE Trans. Commun.*, 51(11):1927–1938, November 2003.
- [22] A. Sendonaris, E. Erkip, and B. Aazhang. User cooperation diversity — Part II: Implementation aspects and performance analysis. *IEEE Trans. Commun.*, 51(11):1939–1948, November 2003.
- [23] B. Talha and M. Pätzold. On the statistical properties of double Rice channels. In *Proc. 10th Int. Symp. on Wireless Personal Multimedia Communications, WPMC 2007*, pages 517–522. Jaipur, India, December 2007.
- [24] B. Talha and M. Pätzold. On the statistical properties of mobile-to-mobile fading channels in cooperative networks under line-of-sight conditions. In *Proc. 10th Int. Symp. on Wireless Personal Multimedia Communications, WPMC 2007*, pages 388–393. Jaipur, India, December 2007.
- [25] B. Talha and M. Pätzold. Level-crossing rate and average duration of fades of the envelope of mobile-to-mobile fading channels in cooperative networks under line-of-sight conditions. In *Proc. 51st IEEE Globecom 2008*, pages 1–6. New Orleans, USA, November/December 2008. DOI 10.1109/GLOCOM.2008.ECP.860.
- [26] B. Talha and M. Pätzold. A novel amplify-and-forward relay channel model for mobile-to-mobile fading channels under line-of-sight conditions. In *Proc. 19th IEEE Int. Symp. on Personal, Indoor and Mobile Radio Communications, PIMRC 2008*, pages 1–6. Cannes, France, September 2008. DOI 10.1109/PIMRC.2008.4699733.
- [27] Z. Tang and A. S. Mohan. A correlated indoor MIMO channel model. In *Canadian Conference on Electrical and Computer Engineering 2003, IEEE CCECE 2003*, volume 3, pages 1889 – 1892. Venice, Italy, May 2003.
- [28] I. E. Telatar. Capacity of multi-antenna Gaussian channels. *European Trans. Telecommun. Related Technol.*, 10:585–595, 1999.
- [29] A. G. Zajić and G. L. Stüber. Space-time correlated mobile-to-mobile channels: modelling and simulation. *IEEE Trans. Veh. Technol.*, 57(2):715–726, March 2008.

- [30] A. G. Zajić and G. L. Stüber. Three-dimensional modeling, simulation, and capacity analysis of space-time correlated mobile-to-mobile channels. *IEEE Trans. Veh. Technol.*, 57(4):2042–2054, July 2008.

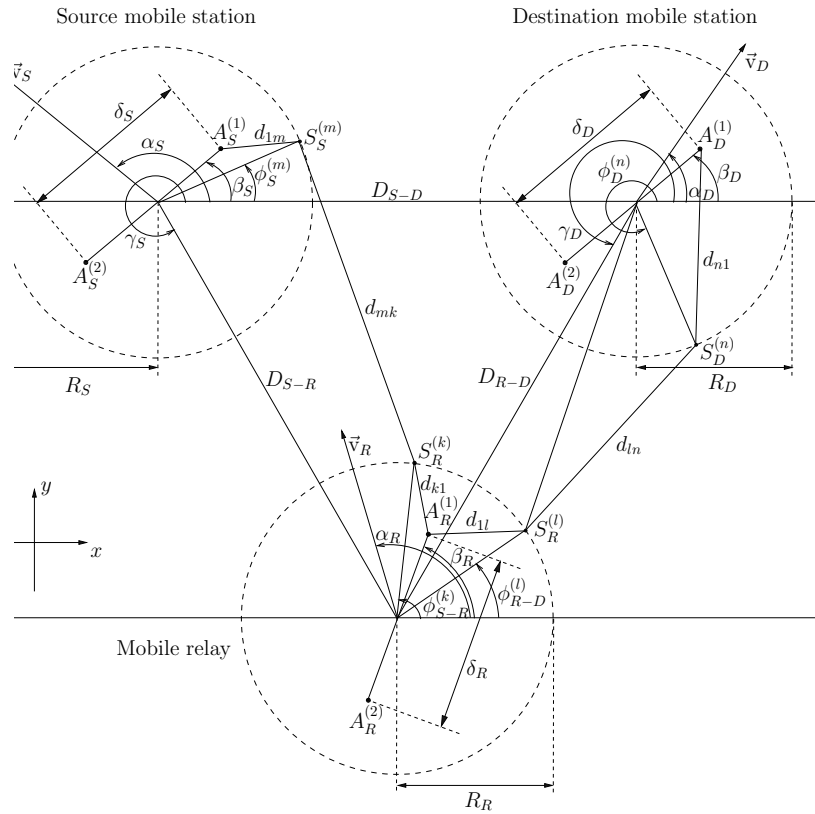


Figure B.1: The geometrical three-ring scattering model for a $2 \times 2 \times 2$ MIMO M2M channel with local scatterers on rings around the source mobile station, the mobile relay, and the destination mobile station.

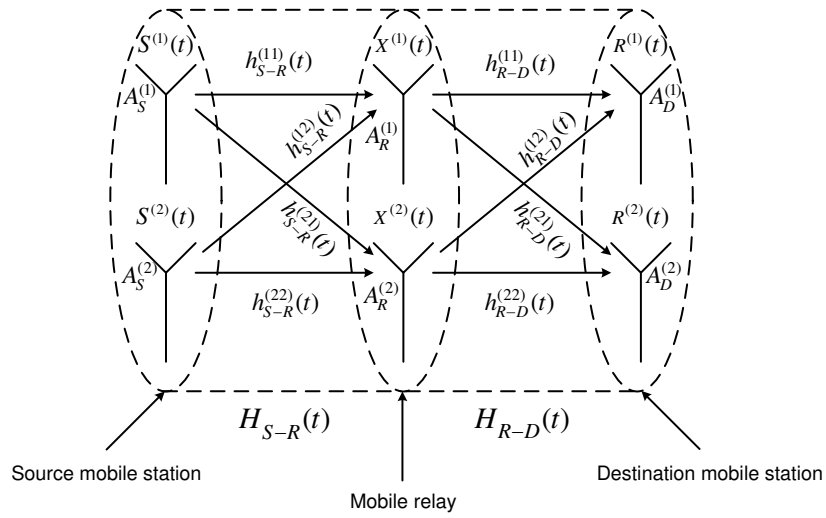


Figure B.2: A simplified diagram describing the overall MIMO M2M channel from the source mobile station to the destination mobile station via the mobile relay.

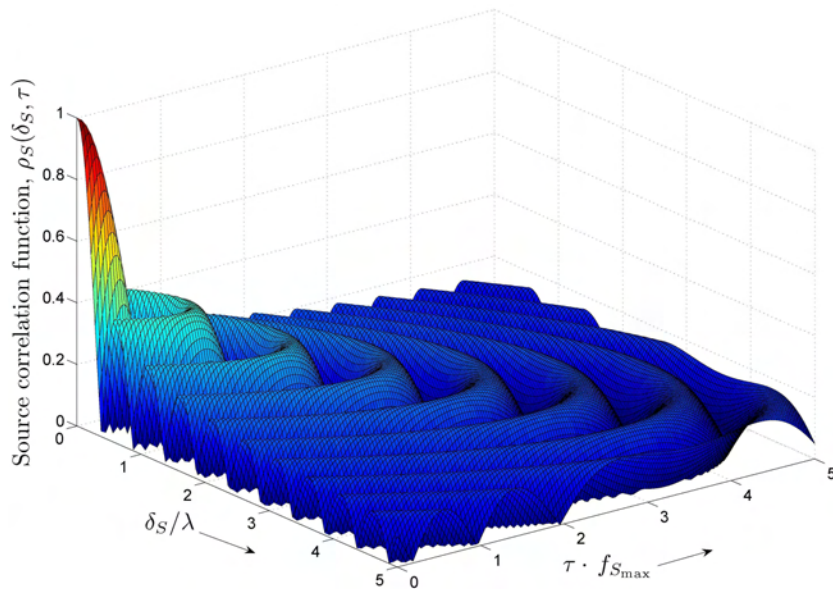


Figure B.3: The source CF $\rho_S(\delta_S, \tau)$ of the $2 \times 2 \times 2$ MIMO M2M reference channel model under isotropic scattering conditions.

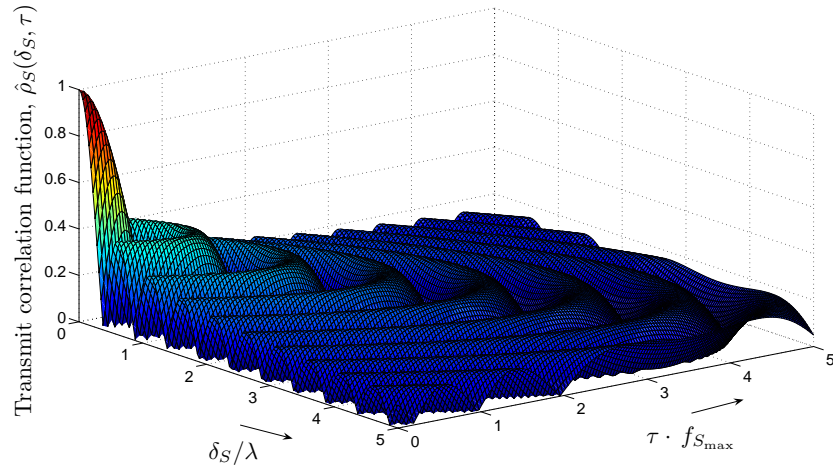


Figure B.4: The source CF $\hat{\rho}_s(\delta_s, \tau)$ of the $2 \times 2 \times 2$ MIMO M2M stochastic channel simulator under isotropic scattering conditions.

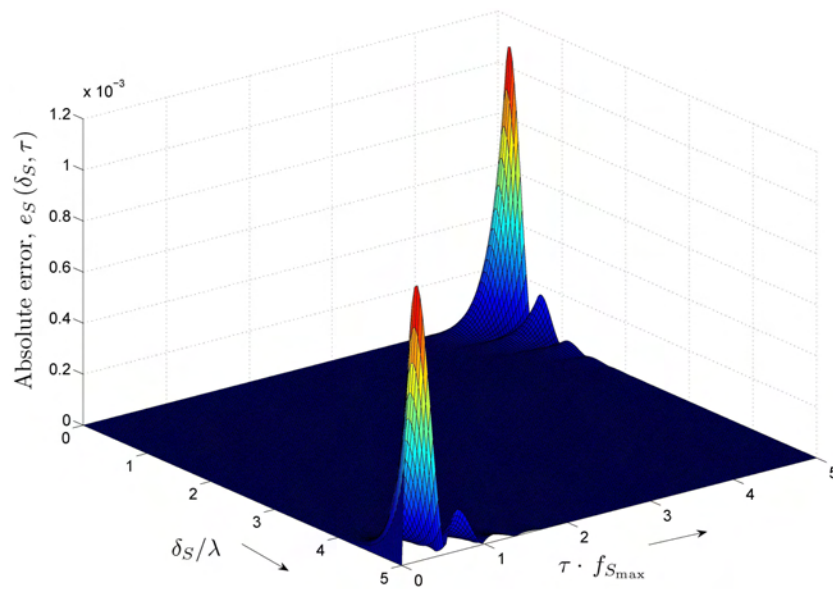


Figure B.5: Absolute error $e_s(\delta_s, \tau) = |\rho_s(\delta_s, \tau) - \hat{\rho}_s(\delta_s, \tau)|$ by using the MMEA with $M = 40$ (isotropic scattering).

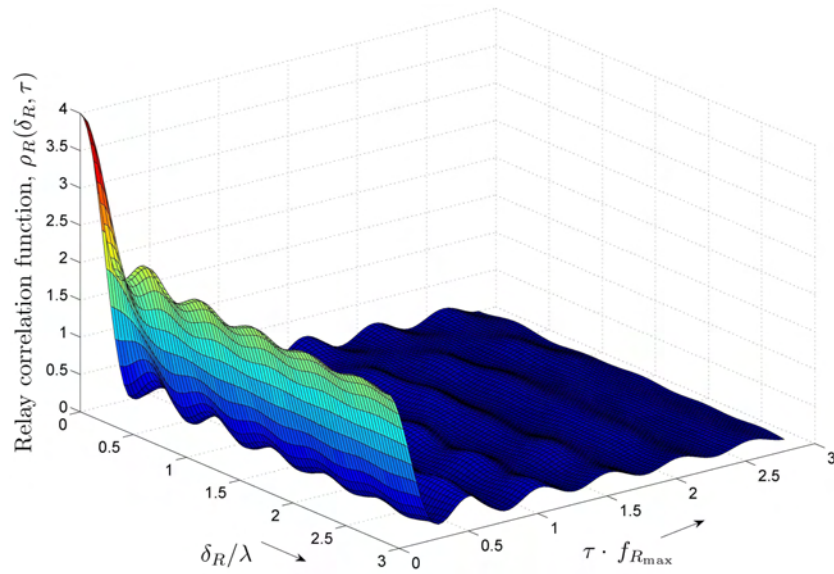


Figure B.6: The relay CF $\rho_R(\delta_R, \tau)$ of the $2 \times 2 \times 2$ MIMO M2M reference channel model under isotropic scattering conditions.

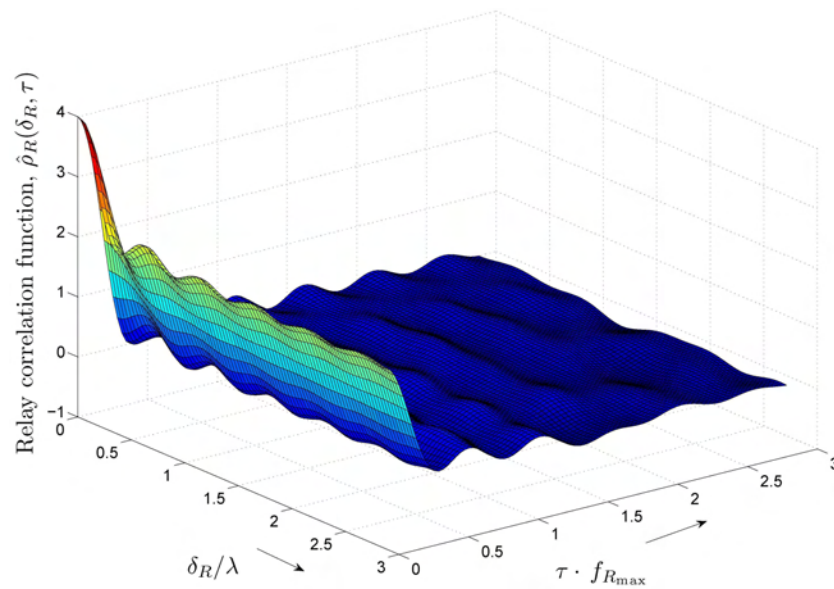


Figure B.7: The relay CF $\hat{\rho}_R(\delta_R, \tau)$ of the $2 \times 2 \times 2$ MIMO M2M stochastic channel simulator under isotropic scattering conditions.

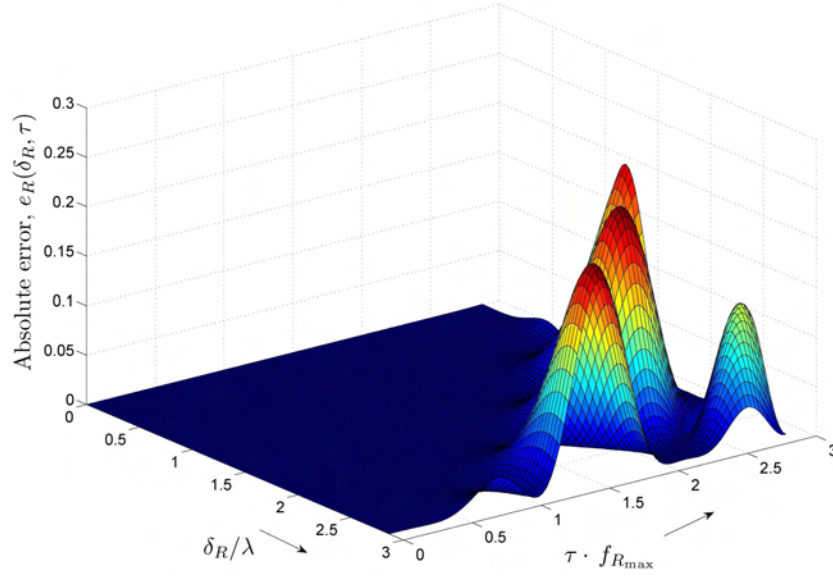


Figure B.8: Absolute error $e_R(\delta_R, \tau) = |\rho_R(\delta_R, \tau) - \hat{\rho}_R(\delta_R, \tau)|$ by using the MMEA with $K = L = 23$ (isotropic scattering).

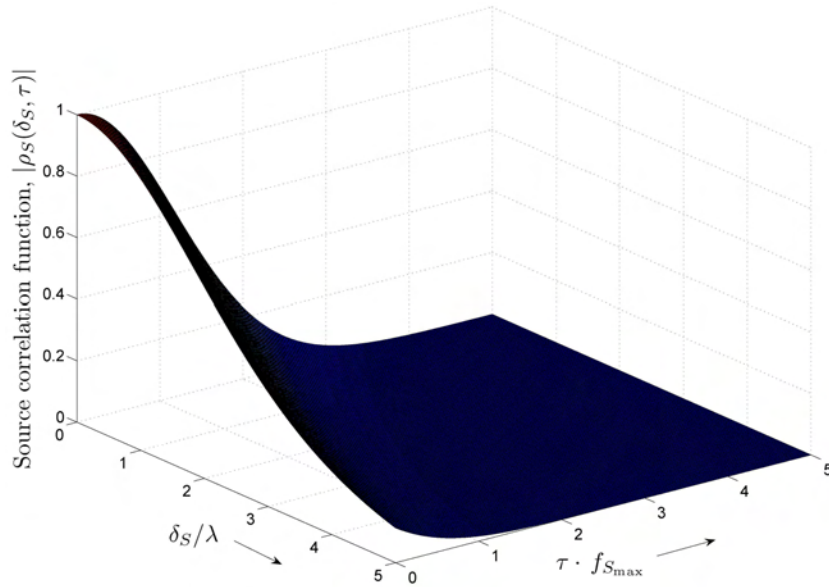


Figure B.9: Absolute value of the source CF $|\rho_S(\delta_S, \tau)|$ of the $2 \times 2 \times 2$ MIMO M2M reference channel model under non-isotropic scattering conditions (von Mises density with $\phi_s^{(0)} = 60^\circ$ and $\kappa_s = 40$).

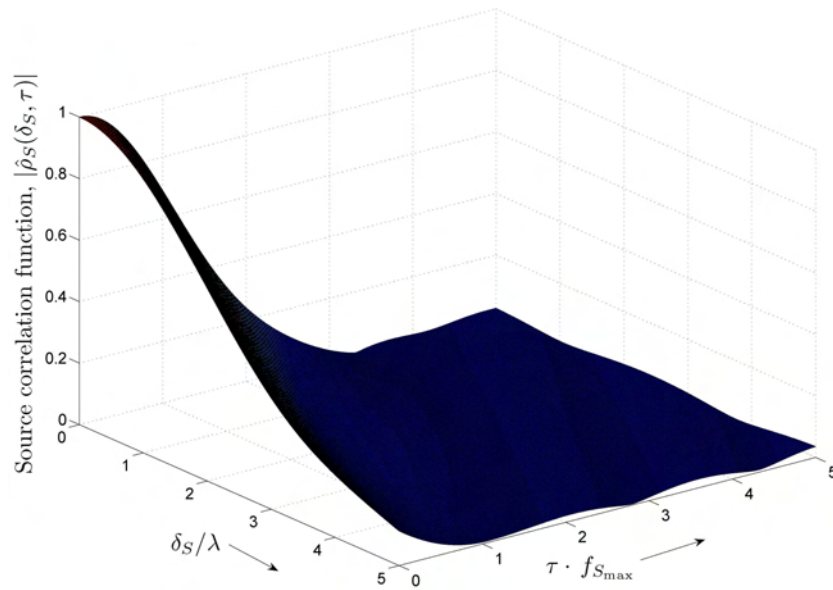


Figure B.10: Absolute value of the source CF $|\hat{\rho}_s(\delta_s, \tau)|$ of the $2 \times 2 \times 2$ MIMO M2M stochastic channel simulator designed by applying the MMEA with $M = 40$ (non-isotropic scattering, von Mises density with $\phi_s^{(0)} = 60^\circ$ and $\kappa_s = 40$).

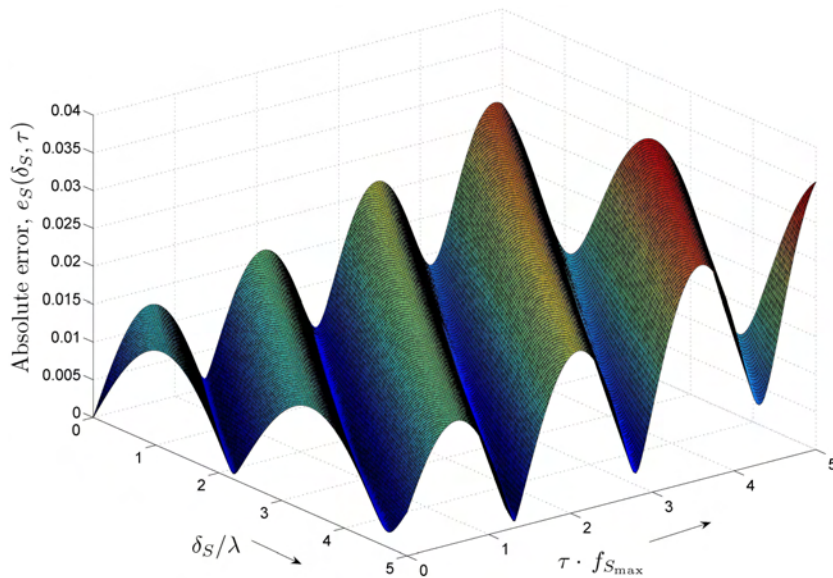


Figure B.11: Absolute error $e_s(\delta_s, \tau) = |\rho_s(\delta_s, \tau) - \hat{\rho}_s(\delta_s, \tau)|$ by using the MMEA with $M = 40$ (non-isotropic scattering, von Mises density with $\phi_s^{(0)} = 60^\circ$ and $\kappa_s = 40$).

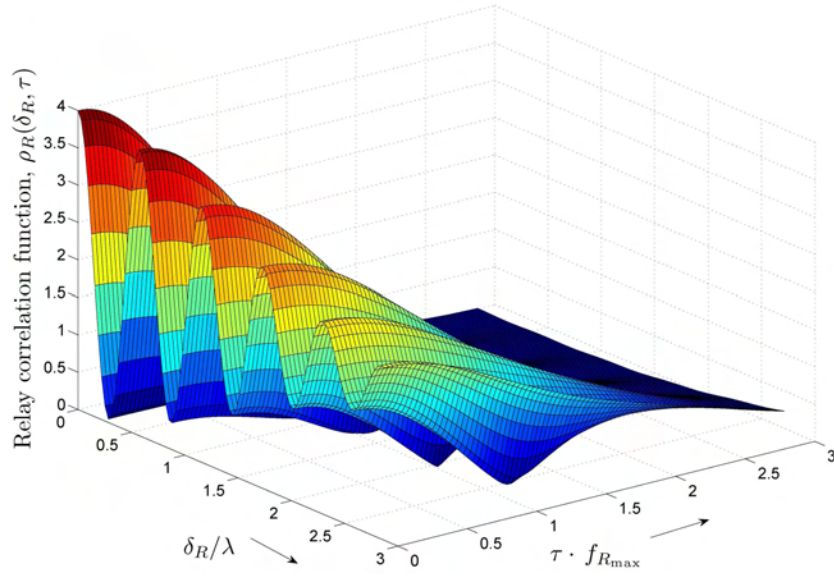


Figure B.12: Absolute value of the relay CF $|\rho_R(\delta_R, \tau)|$ of the $2 \times 2 \times 2$ MIMO M2M reference channel model under non-isotropic scattering conditions (von Mises density with $\phi_{S-R}^{(0)} = \phi_{R-D}^{(0)} = 60^\circ$ and $\kappa_{S-R} = \kappa_{R-D} = 40$).

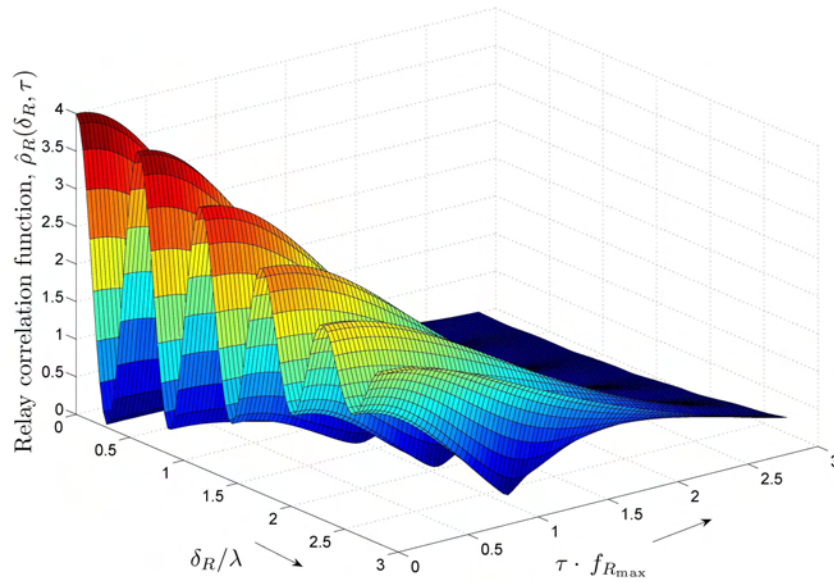


Figure B.13: Absolute value of the relay CF $|\hat{\rho}_R(\delta_R, \tau)|$ of the $2 \times 2 \times 2$ MIMO M2M stochastic channel simulator designed by applying the MMEA with $K = L = 23$ (non-isotropic scattering, von Mises density with $\phi_{S-R}^{(0)} = \phi_{R-D}^{(0)} = 60^\circ$ and $\kappa_{S-R} = \kappa_{R-D} = 40$).

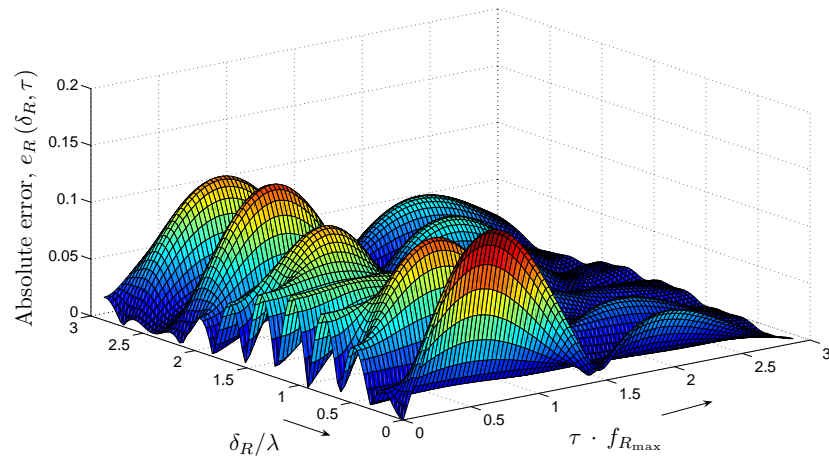


Figure B.14: Absolute error $e_R(\delta_R, \tau) = |\rho_R(\delta_R, \tau) - \hat{\rho}_R(\delta_R, \tau)|$ by using the MMEA with $K = L = 23$ (non-isotropic scattering, von Mises density with $\phi_{S-R}^{(0)} = \phi_{R-D}^{(0)} = 60^\circ$ and $\kappa_{S-R} = \kappa_{R-D} = 40$).

Appendix C

Paper II

Title: On the Statistical Characterization of Mobile-to-Mobile Fading Channels in Dual-Hop Distributed Cooperative Multi-Relay Systems

Authors: **Batool Talha** and Matthias Pätzold

Affiliation: University of Agder, Faculty of Engineering and Science, P. O. Box 509, NO-4898 Grimstad, Norway

Conference: *12th International Symposium on Wireless Personal Multimedia Communications, WPMC 2009*, Sendai, Japan, Sept. 2009.

On the Statistical Characterization of Mobile-to-Mobile Fading Channels in Dual-Hop Distributed Cooperative Multi-Relay Systems

Batool Talha and Matthias Pätzold

Department of Information and Communication Technology
Faculty of Engineering and Science, Agder University College
Servicebox 509, NO-4876 Grimstad, Norway
E-mails: {batool.talha, matthias.paetzold}@uia.no

Abstract — This paper deals with the statistical characterization of narrow-band mobile-to-mobile (M2M) fading channels in dual-hop distributed cooperative multi-relay systems under non-line-of-sight (NLOS) propagation conditions. Here, we analyze M2M fading channels in dual-hop, amplify-and-forward relay networks with K relays placed between the source mobile station and the destination mobile station in a distributed network topology. The statistical quantities, such as the characteristic function (CF), the probability density function (PDF) of the envelope as well as the phase, and the mean value along with the variance are discussed in detail. We derive analytical integral expressions of the aforementioned quantities associated with dual-hop multi-relay M2M fading channels assuming that the underlying processes making up such channels are statistically independent but not necessarily identically distributed. In addition, we also present exact closed-form expressions of these statistical quantities for independent and identically distributed (i.i.d.) processes. The validity of the presented expressions is backed-up with the help of simulations. Our studies presented in this paper can be very beneficial for performance analysis of dual-hop distributed cooperative multi-relay systems.

I. INTRODUCTION

Transmission links in mobile wireless communication systems are particularly vulnerable to the multipath fading effects. Therefore, for decades, the development of new and robust diversity techniques [19] to mitigate the adverse fading effects has been a topic of interest in the field of mobile communication systems design. The motivation of the scientists to fulfill the demands of combating fading has resulted in a new concept for achieving a spatial diversity gain. This new diversity scheme is referred to as the cooperative diversity scheme [12, 21, 22]. The spatial diversity

gain is realized in cooperative diversity systems because the single-antenna mobile stations in the network coordinate with each other to form a so-called virtual antenna array [5]. Studies pertaining to several cooperation protocols for single relay systems and their analysis can be found in the literature [8, 9, 12, 14].

The work of Akki and Haber on the statistical analysis of narrowband single-input single-output (SISO) M2M fading channels under NLOS propagation conditions [1, 2] is among the pioneering works dealing with M2M fading channels in non-cooperative communication systems. The success of cooperative diversity techniques in classical mobile communication systems recently encouraged researchers to introduce M2M communications in cooperative networks. It is known that the overall M2M fading channel in a dual-hop relay-based cooperative system having a single relay in the network can be modeled as a double Rayleigh process under NLOS propagation conditions [11, 16]. A straight-forward extension of the double Rayleigh channel model to the double Rice channel model assuming line-of-sight (LOS) propagation conditions has been presented in [23]. The authors of [20, 24, 25] have developed M2M fading channel models based on the multiple scattering concept proposed in [3] for dual-hop single-relay cooperative systems for both NLOS and LOS propagation environments. In addition to the dual-hop cooperative systems, several papers are available dealing with the statistical modeling and analysis of multi-hop cooperative systems having K relays connected in series between the source and the destination terminals in the network [7, 10].

This paper aims at the statistical characterization of M2M fading links in a dual-hop multi-relay distributed cooperative system having K mobile relays in the network. The novelty in the current M2M fading channel model lies in the fact that the K mobile relays are connected in parallel between the source mobile station and the destination mobile station. Each individual transmission link from the source mobile station to the destination mobile station via the k th relay is modeled as a complex double Gaussian process. However, the overall M2M fading channel taking into consideration K relay links is modeled as the sum of K complex double Gaussian processes. Here, we have derived analytical expressions of the CF, the PDF of the envelope as well as the phase, and the mean value along with the variance of K -parallel dual-hop relay M2M fading channels. The integral expressions of the aforementioned statistical quantities are obtained under the assumption that the underlying complex Gaussian processes are statistically independent but they might have different variances. It is shown that the integral expressions reduce to simple closed-form expressions when i.i.d. complex double Gaussian random processes are assumed.

The rest of the paper is structured as follows: In Section II, the reference model for dual-hop distributive cooperative multi-relay fading channels is developed. Section III deals with the analysis of the statistical properties of K -parallel dual-hop relay fading processes. Section IV confirms the validity of the analytical expressions presented in Section III by simulations. Finally, concluding remarks are given in Section V.

II. THE K -PARALLEL DUAL-HOP RELAY FADING CHANNEL MODEL

In this paper, we study the overall M2M fading channel in a dual-hop distributed cooperative network consisting of a source mobile station, a destination mobile station, and K mobile relays (see Fig. C.1). Time-division multiple-access (TDMA) based amplify-and-forward relay type dual-hop distributed cooperative networks are considered. Here, we have based our K -parallel dual-hop relay fading channel model on TDMA based amplify-and-forward relay protocols proposed in [4, 13, 14] in particular. Furthermore, taking into account the limitations of the physical implementation of such networks, we have assumed that the source mobile station, the destination mobile station, and the K mobile relays operate in half-duplex. The half-duplex operation ensures that all the mobile stations do not transmit and receive a signal at the same time in the same band. The K -parallel dual-hop relay fading channel model, discussed in this section, caters for frequency non-selective channels under NLOS propagation conditions in isotropic scattering environments.

The overall complex time-varying channel gain from the source mobile station to the destination mobile station via K mobile relays in K -parallel dual-hop relay fading channels can be written as

$$\chi(t) = \chi_1(t) + j\chi_2(t) = \sum_{k=1}^K \zeta^{(k)}(t) \quad (1)$$

where $\zeta^{(k)}(t)$ ($k = 1, 2, \dots, K$) describes the fading process in the k th subchannel from the source mobile station to the destination mobile station via the k th mobile relay. Furthermore, $\zeta^{(k)}(t)$ is modeled as a weighted zero-mean complex double Gaussian process, i.e.,

$$\zeta^{(k)}(t) = \zeta_1^{(k)}(t) + j\zeta_2^{(k)}(t) = A_{R(k)} \mu^{(2k-1)}(t) \mu^{(2k)}(t) \quad (2)$$

for $k = 1, 2, \dots, K$. In (2), $\mu^{(i)}(t)$ ($i = 1, 2, \dots, 2K$) is a zero-mean complex Gaussian process with variance $2\sigma_{\mu^{(i)}}^2/\sqrt{K}$. Furthermore, the Gaussian processes $\mu^{(i)}(t)$ are mutually independent, each having a symmetrical Doppler power spectral density (PSD) $S_{\mu^{(i)}\mu^{(i)}}(f)$. Note that for $i = 1, 3, \dots, (2k-1)$, the Gaussian process

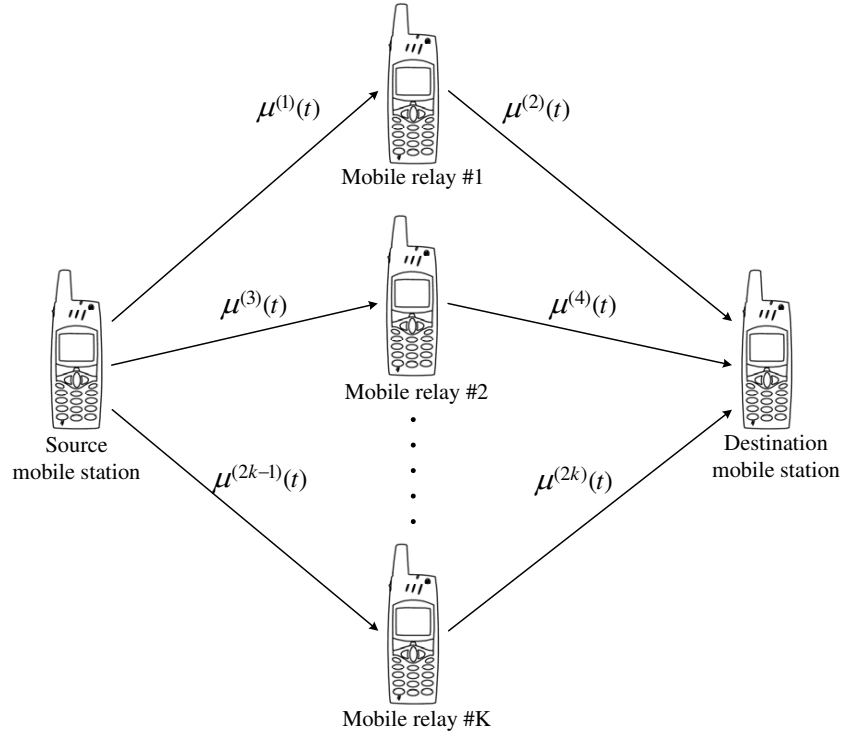


Figure C.1: The propagation scenario describing K -parallel dual-hop relay fading channels.

$\mu^{(i)}(t)$ represents the scattered component of the subchannel between the source mobile station and the k th mobile relay. Analogously, for $i = 2, 4, \dots, 2k$, the Gaussian process $\mu^{(i)}(t)$ is the scattered component of the subchannel between the k th mobile relay and the destination mobile station.

In (2), $A_{R^{(k)}}$ is referred to as the relay gain of the k th relay. It is worth mentioning here that the relay gain $A_{R^{(k)}}$ is merely a scaling factor for the variance of the complex Gaussian process $\mu^{(i)}(t)$, i.e., $\text{Var} \{A_{R^{(k)}} \mu^{(i)}(t)\} = 2(A_{R^{(k)}} \sigma_{\mu^{(i)}})^2 / \sqrt{K}$, where $i = 2, 4, \dots, 2k$ and $k = 1, 2, \dots, K$.

We define the envelope of K -parallel dual-hop relay fading channels as

$$\Xi(t) = |\chi(t)| = \left| \sum_{k=1}^K \zeta^{(k)}(t) \right|. \quad (3)$$

Furthermore, the phase associated with K -parallel dual-hop relay fading channels can be expressed as

$$\Theta(t) = \arg \{ \chi(t) \}. \quad (4)$$

The next section deals with the statistical characterization of the envelope $\Xi(t)$ and the phase $\Theta(t)$.

III. STATISTICAL ANALYSIS OF K -PARALLEL DUAL-HOP RELAY FADING CHANNELS

This section deals with the derivation of analytical expressions for the statistical properties of K -parallel dual-hop relay fading channels introduced in Section II. The important statistical quantities analyzed in this section include the CF, the PDF of the envelope as well as the phase, the mean, and the variance of K -parallel dual-hop relay fading channels.

A. CF of K -Parallel Dual-Hop Relay Fading Channels

The CF is an important statistical quantity that is useful to characterize fading channels. The importance of the CF comes from the fact that it completely defines the corresponding PDF associated with fading channels. The CF and the PDF actually form a Fourier transform pair [15].

From (1), it is evident that K -parallel dual-hop relay fading channels $\chi(t)$ can be modeled as a sum of K independent but not necessarily identical, weighted complex double Gaussian processes $\zeta^{(k)}(t)$ ($k = 1, 2, \dots, K$). Thus, we can express the joint CF $\Phi_{\chi_1 \chi_2}(\omega_1, \omega_2)$ of the inphase and quadrature components of $\chi(t)$ as a product of the joint CFs $\phi_{\zeta_1 \zeta_2}^{(k)}(\omega_1, \omega_2)$ of the inphase and quadrature components of $\zeta^{(k)}(t)$ [15] as

$$\Phi_{\chi_1 \chi_2}(\omega_1, \omega_2) = \prod_{k=1}^K \phi_{\zeta_1 \zeta_2}^{(k)}(\omega_1, \omega_2) \quad (5)$$

where

$$\phi_{\zeta_1 \zeta_2}^{(k)}(\omega_1, \omega_2) = \frac{K}{K + A_{\mathbf{R}^{(k)}}^2 \sigma_{\mu^{(2k-1)}}^2 \sigma_{\mu^{(2k)}}^2 (\omega_1^2 + \omega_2^2)}. \quad (6)$$

The joint CF $\phi_{\zeta_1 \zeta_2}^{(k)}(\omega_1, \omega_2)$ of the inphase and quadrature components of $\zeta^{(k)}(t)$ presented in (6) can be found in the literature (see, e.g., [20]).

Assuming $\zeta^{(k)}(t)$ ($k = 1, 2, \dots, K$) are i.i.d. complex double Gaussian random processes, then $\phi_{\zeta_1 \zeta_2}^{(1)}(\omega_1, \omega_2) = \phi_{\zeta_1 \zeta_2}^{(2)}(\omega_1, \omega_2) = \dots = \phi_{\zeta_1 \zeta_2}^{(K)}(\omega_1, \omega_2)$. Thus, for i.i.d. complex double Gaussian random processes such that $\sigma_{\mu^{(2k-1)}}^2 = \sigma_{\mu^{(1)}}^2$, $\sigma_{\mu^{(2k)}}^2 = \sigma_{\mu^{(2)}}^2$ with $A_{\mathbf{R}^{(k)}} = A_{\mathbf{R}} \forall k = 1, 2, \dots, K$, (5) reduces to the following closed-form expression

$$\Phi_{\chi_1 \chi_2}(\omega_1, \omega_2) = \frac{K^K}{\left\{ K + A_{\mathbf{R}}^2 \sigma_{\mu^{(1)}}^2 \sigma_{\mu^{(2)}}^2 (\omega_1^2 + \omega_2^2) \right\}^K}. \quad (7)$$

B. Joint PDF of the Envelope and Phase of K -Parallel Dual-Hop Relay Fading Channels

The PDF of the envelope and the phase are the most important statistical quan-

tities of K -parallel dual-hop relay fading channels. Therefore, we derive the joint PDF $p_{\Xi\Theta}(r, \theta)$ of the envelope and the phase of K -parallel dual-hop relay fading channels as a starting point towards finding the corresponding marginal PDFs.

As mentioned in Subsection III-A, the CF and the PDF of random processes form a Fourier transform pair. Thus, by definition, taking the (complex conjugate of the) inverse Fourier transform of the joint CF $\Phi_{\chi_1\chi_2}(\omega_1, \omega_2)$ allows us to express the joint PDF $p_{\chi_1\chi_2}(z_1, z_2)$ as [15]

$$\begin{aligned} p_{\chi_1\chi_2}(z_1, z_2) &= \mathcal{F}^{-1}\{\Phi_{\chi_1\chi_2}(\omega_1, \omega_2)\} \\ &= \frac{1}{(2\pi)^2} \int_{-\infty}^{\infty} \int_{-\infty}^{\infty} \Phi_{\chi_1\chi_2}(\omega_1, \omega_2) e^{-j(\omega_1 z_1 + \omega_2 z_2)} d\omega_1 d\omega_2. \end{aligned} \quad (8)$$

Substituting (5) in (8), doing some mathematical manipulations, and solving the resulting integrals using [6, Eq. (3.338-IV)] allows us to write the joint PDF $p_{\chi_1\chi_2}(z_1, z_2)$ as

$$p_{\chi_1\chi_2}(z_1, z_2) = \frac{1}{2\pi} \int_0^{\infty} x J_0\left(x\sqrt{z_1^2 + z_2^2}\right) g(x) dx \quad (9)$$

where

$$g(x) = \prod_{k=1}^K \frac{K}{K + A_{\mathbf{R}^{(k)}}^2 \sigma_{\mu^{(2k-1)}}^2 \sigma_{\mu^{(2k)}}^2 x^2} \quad (10)$$

and $J_0(\cdot)$ is the zeroth-order Bessel function of the first kind [6].

The joint PDF $p_{\Xi\Theta}(r, \theta)$ of the envelope and the phase of K -parallel dual-hop relay fading channels can now easily be computed by transforming the random variables in (9) from rectangular coordinates (z_1, z_2) to polar coordinates (r, θ) , i.e.,

$$p_{\Xi\Theta}(r, \theta) = J(r, \theta) p_{\chi_1\chi_2}(r \cos \theta, r \sin \theta) = \frac{r}{2\pi} \int_0^{\infty} x J_0(rx) g(x) dx \quad (11)$$

for $r \geq 0$ and $|\theta| \leq \pi$. In (11), $J(r, \theta) = r$ is the Jacobian determinant and $g(\cdot)$ is defined in (10).

1) *PDF of the Envelope:*

Integrating $p_{\Xi\Theta}(r, \theta)$ over θ from $-\pi$ to π gives the PDF $p_{\Xi}(r)$ of the envelope

$\Xi(t)$ of K -parallel dual-hop relay fading channels as follows

$$p_{\Xi}(r) = r \int_0^{\infty} x J_0(rx) g(x) dx, \quad r \geq 0. \quad (12)$$

For i.i.d. complex double Gaussian random processes $\zeta^{(k)}(t)$ ($k = 1, 2, \dots, K$), a simple closed-form expression for the PDF $p_{\Xi}(r)$ of the envelope $\Xi(t)$ can be obtained by replacing $g(x)$ in (12) by (7) and solving the integral using [6, Eq. (6.565-IV)], i.e.,

$$p_{\Xi}(r) = \frac{K^{\left(\frac{K+1}{2}\right)} r^K}{2^{(K-1)} (K-1)! \left(A_R \sigma_{\mu^{(1)}} \sigma_{\mu^{(2)}}\right)^{(K+1)}} K_{K-1} \left(\frac{r \sqrt{K}}{A_R \sigma_{\mu^{(1)}} \sigma_{\mu^{(2)}}} \right), \quad r \geq 0 \quad (13)$$

where $K_{K-1}(\cdot)$ is the $(K-1)$ th-order modified Bessel function of the second kind [6]. Note that it follows from the central limit theorem (CLT) [15] that the PDF $p_{\Xi}(r)$ of the envelope $\Xi(t)$ approaches the Rayleigh distribution for $K \rightarrow \infty$ when $\zeta^{(k)}(t)$ are i.i.d. complex double Gaussian random processes. Furthermore, it is also noteworthy that the PDF $p_{\Xi}(r)$ in (13) reduces to the double Rayleigh distribution for $K = 1$.

2) *PDF of the Phase:*

The PDF $p_{\Theta}(\theta)$ of the phase $\Theta(t)$ of K -parallel dual-hop relay fading channels can be obtained by integrating $p_{\Xi\Theta}(r, \theta)$ over r from 0 to ∞ . The resulting expression of the PDF $p_{\Theta}(\theta)$ of the phase $\Theta(t)$ is

$$p_{\Theta}(\theta) = \frac{1}{2\pi} \int_0^{\infty} \int_0^{\infty} x p J_0(rx) g(x) dx dr, \quad |\theta| \leq \pi. \quad (14)$$

It is interesting to observe that the terms on the right-hand-side of (14) are independent of θ . This implies that the PDF $p_{\Theta}(\theta)$ of the phase $\Theta(t)$ is uniformly distributed over $(-\pi, \pi)$. This statement has been confirmed by numerical investigations.

Under the assumption that $\zeta^{(k)}(t)$ ($k = 1, 2, \dots, K$) are i.i.d. complex double Gaussian processes, $g(x)$ in (14) can be replaced by (7). Thus, solving the resulting two-fold integral with the help of [6, Eqs. (6.561-XVI) and (6.565-IV)] shows that the PDF $p_{\Theta}(\theta)$ of the phase $\Theta(t)$ equals $p_{\Theta}(\theta) = 1/2\pi \forall \theta \in (-\pi, \pi)$.

III.C Mean Value and Variance of K -Parallel Dual-Hop Relay Fading Channels

Among several important statistical quantities, the expected value (mean value) and the variance of fading channels are worth mentioning, since they summarize the information provided by the PDF of the envelope of fading channels.

Using (12) and [15, Eq. (5.44)], the expected value m_{Ξ} of the envelope $\Xi(t)$ of K -parallel dual-hop relay fading channels can be expressed as

$$m_{\Xi} = E\{\Xi(t)\} = \int_0^{\infty} \int_0^{\infty} r^2 x J_0(rx) g(x) dx dr \quad (15)$$

where $E\{\cdot\}$ is the expected value operator and $g(\cdot)$ is defined in (10). Fortunately, we can obtain a simple, closed-form expression of the expected value m_{Ξ} of the envelope $\Xi(t)$ subject to the fact that $\zeta^{(k)}(t)$ ($k = 1, 2, \dots, K$) are i.i.d. complex double Gaussian processes. Thus, solving the integrals in (15) with the help of [6, Eqs. (6.561-XVI), (6.565-IV), (8.339-I), and (8.339-II)] allows us to write the final expression of m_{Ξ} as

$$m_{\Xi} = \frac{\pi}{2^K} \cdot \frac{(2K-1)!!}{(K-1)!} \cdot \frac{A_R \sigma_{\mu^{(1)}} \sigma_{\mu^{(2)}}}{\sqrt{K}} \quad (16)$$

where $(\cdot)!$ and $(\cdot)!!$ represent factorial and double factorial, respectively.

It is well known that the variance σ_{Ξ}^2 of stochastic processes (in our case, the envelope $\Xi(t)$ of K -parallel dual-hop relay fading channels) is the difference of the mean power and squared mean value of the stochastic process [6, Eq. (5.61)], i.e., $\sigma_{\Xi}^2 = m_{\Xi^2} - (m_{\Xi})^2$, where $m_{\Xi^2} = E\{\Xi^2(t)\}$ denotes the mean power of $\Xi(t)$. The mean power m_{Ξ^2} of the envelope of K -parallel dual-hop relay fading channels can easily be obtained using (12) and [15, Eq. (5.67)] as

$$m_{\Xi^2} = E\{\Xi^2(t)\} = \int_0^{\infty} \int_0^{\infty} r^3 x J_0(rx) g(x) dx dr. \quad (17)$$

The mean power m_{Ξ^2} presented in (17) can be reduced to the following closed-form expression by using [6, Eqs. (6.561-XVI) and (6.565-IV)] if $\zeta^{(k)}(t)$ ($k = 1, 2, \dots, K$) are i.i.d. complex double Gaussian processes:

$$m_{\Xi^2} = \left(2A_R \sigma_{\mu^{(1)}} \sigma_{\mu^{(2)}}\right)^2. \quad (18)$$

Finally, using (17) and (15), an integral expression of the variance σ_{Ξ}^2 can be obtained, whereas (18) and (16) result in a simple closed-form expression of σ_{Ξ}^2 .

IV. NUMERICAL RESULTS

This section illustrates the important theoretical results by evaluating the analytical expressions and the confirmation of their correctness with the help of simulations. In this paper, we have employed the concept of sum-of-sinusoids (SOS) [17] to simulate the underlying uncorrelated Gaussian noise processes making up the overall K -parallel dual-hop relay channel. The generalized method of exact Doppler spread (GMEDS₁) [18] was selected for the computation of the model parameters of the channel simulator. Each Gaussian process $\mu^{(i)}(t)$ ($i = 1, 2, \dots, 2K$) was simulated using $N_1^{(i)} = 14 + k$ and $N_2^{(i)} = 34 + k$ for $i = 1, 2, \dots, 2K$ and $k = 1, 2, \dots, K$, where $N_1^{(i)}$ and $N_2^{(i)}$ are the number of sinusoids required to simulate the inphase and quadrature components of $\mu^{(i)}(t)$, respectively. It has been shown in [17] that with $N_l^{(i)} \geq 7$, where $l = 1, 2$, the simulated distribution of $|\mu^{(i)}(t)|$ closely approximates the Rayleigh distribution. The maximum Doppler frequencies caused by the motion of the source mobile station and the destination mobile station, denoted by $f_{s_{\max}}$ and $f_{d_{\max}}$, respectively, were both set to 91 Hz. Whereas, the maximum Doppler frequencies $f_{R_{\max}^{(k)}}$ caused by the motion of $k = 1, 2, \dots, 10$ mobile relays were selected from the set $\{125, 210, 225, 165, 191, 65, 200, 137, 91, 125\}$. The variances $\sigma_{\mu^{(i)}}^2$ were chosen as $\sigma_{\mu^{(i)}}^2 = 1/\sqrt{K} \forall i = 1, 2, 3, \dots, 2K$ and the relay gains $A_{R^{(k)}}$ were set to unity $\forall k = 1, 2, 3, \dots, K$ unless stated otherwise.

The results presented in Figs. C.2–C.4 show the excellent fitting of the analytical and simulation results. Figure C.2 illustrates the PDF $p_{\Xi}(r)$ of the envelope $\Xi(t)$ of K -parallel dual-hop relay fading channels, whereas Figs. C.3 and C.4 present the mean value m_{Ξ} and the standard deviation σ_{Ξ} , respectively. It is clear from both Figs. C.2 and C.3 that there is no significant increase in the mean value of the process, while keeping the variances $\sigma_{\mu^{(i)}}^2$ and the relay gains $A_{R^{(k)}}$ constant and increasing the number of mobile relays in the network. Furthermore, increasing the relay gains $A_{R^{(k)}}$ increases the mean value and standard deviation of the process. For the sake of completeness of analysis, we have included results when $\sigma_{\mu^{(1)}}^2 \neq \sigma_{\mu^{(2)}}^2 \neq \dots \neq \sigma_{\mu^{(2K)}}^2$ and/or $A_{R^{(1)}} \neq A_{R^{(2)}} \neq \dots \neq A_{R^{(K)}}$.

V. CONCLUSION

In this paper, we have proposed a new dual-hop multi-relay fading channel model for frequency non-selective M2M fading channels under NLOS propagation conditions in isotropic scattering environments. The novelty in the model comes from the fact that K mobile relays are connected in parallel between the source mobile station and the destination mobile station. Utilizing TDMA based amplify-and-forward relay protocols, we can model the overall M2M fading channel between the source

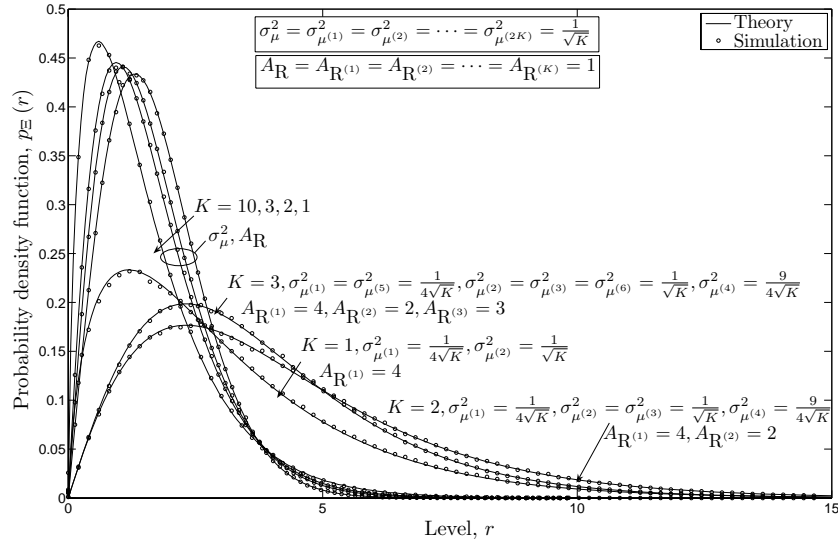


Figure C.2: The PDF $p_{\Xi}(r)$ of the envelope $\Xi(t)$ of K -parallel dual-hop relay fading channels.

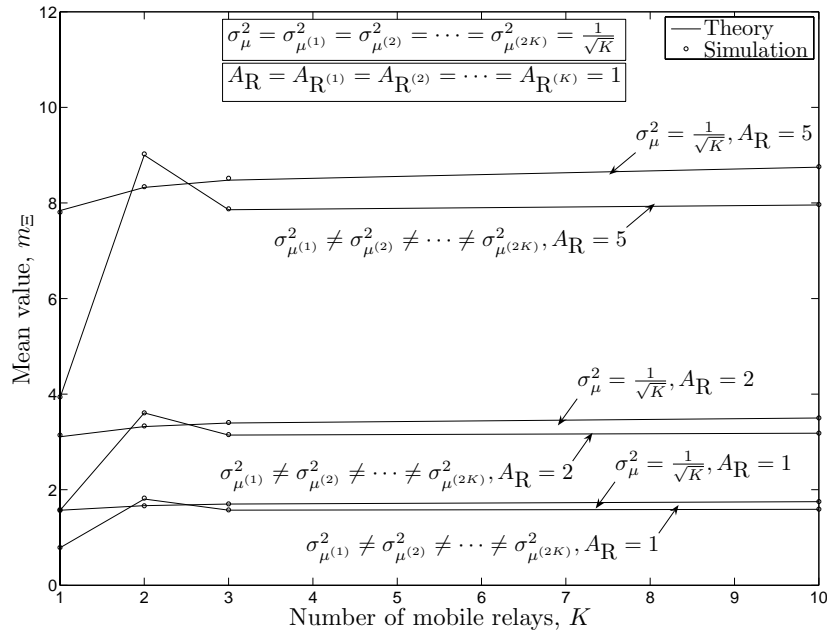


Figure C.3: The mean value m_{Ξ} of the envelope $\Xi(t)$ of K -parallel dual-hop relay fading channels.

mobile station and the destination mobile station via K independent relay links as the sum of K complex double Gaussian processes. Here, we have derived both, analytical integral and closed-form expressions of the CF, the PDF of the envelope as well as the phase, and the mean value along with the variance of K -parallel dual-hop relay M2M fading channels. The correctness of the theoretical results is backed-up

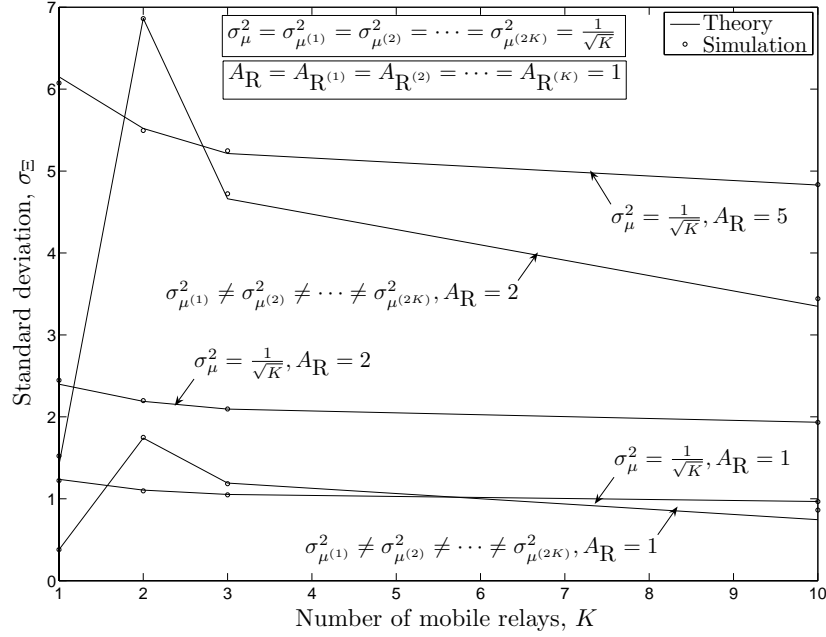


Figure C.4: The standard deviation σ_{Ξ} of the envelope $\Xi(t)$ of K -parallel dual-hop relay fading channels.

with the help of simulations. The results presented in this article, can be employed in system performance studies of dual-hop distributed cooperative multi-relay systems.

REFERENCES

- [1] A. S. Akki. Statistical properties of mobile-to-mobile land communication channels. *IEEE Trans. Veh. Technol.*, 43(4):826–831, November 1994.
- [2] A. S. Akki and F. Haber. A statistical model of mobile-to-mobile land communication channel. *IEEE Trans. Veh. Technol.*, 35(1):2–7, February 1986.
- [3] J. B. Andersen. Statistical distributions in mobile communications using multiple scattering. In *Proc. 27th URSI General Assembly*. Maastricht, Netherlands, August 2002.
- [4] K. Azarian, H. E. Gamal, and P. Schniter. On the achievable diversity-multiplexing tradeoff in half-duplex cooperative channels. *IEEE Trans. Inform. Theory*, 51(12):4152–4172, December 2005.
- [5] M. Dohler. *Virtual Antenna Arrays*. Ph.D. dissertation, King’s College, London, United Kingdom, 2003.

- [6] I. S. Gradshteyn and I. M. Ryzhik. *Table of Integrals, Series, and Products*. New York: Academic Press, 6th edition, 2000.
- [7] Z. Hadzi-Velkov, N. Zlatanov, and G. K. Karagiannidis. On the second order statistics of the multihop Rayleigh fading channel. *IEEE Trans. Commun.*, 57(6):1815–1823, June 2009.
- [8] A. Host-Madsen. On the capacity of wireless relaying. In *Proc. IEEE 56th Veh. Technol. Conf., VTC'02-Fall*, volume 3, pages 1333–1337. Vancouver BC, Canada, September 2002.
- [9] T. E. Hunter and A. Nosratinia. Cooperative diversity through coding. In *Proc. IEEE Int. Symp. Information Theory, ISIT 2002*, volume 1, page 220. Lausanne, Switzerland, June/July 2002.
- [10] G. K. Karagiannidis, N. C. Sagias, and P. T. Mathiopoulos. N*Nakagami: A novel stochastic model for cascaded fading channels. *IEEE Trans. Commun.*, 55(8):1453–1458, August 2007.
- [11] I. Z. Kovacs, P. C. F. Eggers, K. Olesen, and L. G. Petersen. Investigations of outdoor-to-indoor mobile-to-mobile radio communication channels. In *Proc. IEEE 56th Veh. Technol. Conf., VTC'02-Fall*, volume 1, pages 430–434. Vancouver BC, Canada, September 2002.
- [12] J. N. Laneman, D. N. C. Tse, and G. W. Wornell. Cooperative diversity in wireless networks: Efficient protocols and outage behavior. *IEEE Trans. Inform. Theory*, 50(12):3062–3080, December 2004.
- [13] R. U. Nabar and H. Bölcskei. Space-time signal design for fading relay channels. In *Proc. IEEE Globecom*, volume 4, pages 1952–1956. San Francisco, CA, December 2003.
- [14] R. U. Nabar, H. Bölcskei, and F. W. Kneubühler. Fading relay channels: Performance limits and space-time signal design. *IEEE J. Select. Areas Commun.*, 22(6):1099–1109, August 2004.
- [15] A. Papoulis and S. U. Pillai. *Probability, Random Variables and Stochastic Processes*. New York: McGraw-Hill, 4th edition, 2002.
- [16] C. S. Patel, G. L. Stüber, and T. G. Pratt. Statistical properties of amplify and forward relay fading channels. *IEEE Trans. Veh. Technol.*, 55(1):1–9, January 2006.

- [17] M. Pätzold. *Mobile Fading Channels*. Chichester: John Wiley & Sons, 2002.
- [18] M. Pätzold and B. O. Hogstad. Two new methods for the generation of multiple uncorrelated Rayleigh fading waveforms. In *Proc. IEEE 63rd Semi-annual Veh. Tech. Conf., VTC'06-Spring*, volume 6, pages 2782–2786. Melbourne, Australia, May 2006.
- [19] T. S. Rappaport. *Wireless Communications: Principles and Practice*. Upper Saddle River, New Jersey: Prentice-Hall, 2nd edition, 1996.
- [20] J. Salo, H. M. El-Sallabi, and P. Vainikainen. Statistical analysis of the multiple scattering radio channel. *IEEE Trans. Antennas Propagat.*, 54(11):3114–3124, November 2006.
- [21] A. Sendonaris, E. Erkip, and B. Aazhang. User cooperation diversity — Part I: System description. *IEEE Trans. Commun.*, 51(11):1927–1938, November 2003.
- [22] A. Sendonaris, E. Erkip, and B. Aazhang. User cooperation diversity — Part II: Implementation aspects and performance analysis. *IEEE Trans. Commun.*, 51(11):1939–1948, November 2003.
- [23] B. Talha and M. Pätzold. On the statistical properties of double Rice channels. In *Proc. 10th Int. Symp. on Wireless Personal Multimedia Communications, WPMC 2007*, pages 517–522. Jaipur, India, December 2007.
- [24] B. Talha and M. Pätzold. Level-crossing rate and average duration of fades of the envelope of mobile-to-mobile fading channels in cooperative networks under line-of-sight conditions. In *Proc. 51st IEEE Globecom 2008*, pages 1–6. New Orleans, USA, November/December 2008. DOI 10.1109/GLOCOM.2008.ECP.860.
- [25] B. Talha and M. Pätzold. A novel amplify-and-forward relay channel model for mobile-to-mobile fading channels under line-of-sight conditions. In *Proc. 19th IEEE Int. Symp. on Personal, Indoor and Mobile Radio Communications, PIMRC 2008*, pages 1–6. Cannes, France, September 2008. DOI 10.1109/PIMRC.2008.4699733.

Appendix D

Paper III

Title: Level-Crossing Rate and Average Duration of Fades of the Envelope of Mobile-to-Mobile Fading Channels in K-Parallel Dual-Hop Relay Networks

Authors: **Batool Talha** and Matthias Pätzold

Affiliation(s): University of Agder, Faculty of Engineering and Science, P. O. Box 509, NO-4898 Grimstad, Norway

Conference: *International Conference on Wireless Communications & Signal Processing, WCSP 2009*, Nanjing, China, Nov. 2009. DOI10.1109/WCSP.2009.5371574.

Level-Crossing Rate and Average Duration of Fades of the Envelope of Mobile-to-Mobile Fading Channels in K -Parallel Dual-Hop Relay Networks

Batool Talha and Matthias Pätzold

Department of Information and Communication Technology
Faculty of Engineering and Science, Agder University College
Servicebox 509, NO-4876 Grimstad, Norway
E-mails: {batool.talha, matthias.paetzold}@uia.no

Abstract — This paper studies the fading behavior of narrowband mobile-to-mobile (M2M) fading channels in dual-hop distributed cooperative multi-relay systems under non-line-of-sight (NLOS) propagation conditions. M2M fading channels considered here are associated with amplify-and-forward relay networks, where K mobile relays are connected in parallel between the source mobile station and the destination mobile station. Such M2M fading channels are referred to as K -parallel dual-hop relay M2M fading channels. We study the fading behavior of these channels by analyzing the level-crossing rate (LCR) and the average duration of fades (ADF) of the received signal envelope. We derive analytical integral expressions of the aforementioned quantities along with the cumulative distribution function (CDF) of the envelope. These statistical quantities are derived assuming that the underlying stochastic processes are independent but not necessarily identically distributed. In addition, the statistical analysis pertaining to the special case of independent and identically distributed (i.i.d.) processes is also presented in this paper. The validity of the presented expressions is confirmed by simulations. Our results are very beneficial for future performance analysis of overall dual-hop distributed cooperative multi-relay systems.

I. INTRODUCTION

For decades, diversity techniques have been employed in mobile wireless communication systems in order to mitigate the adverse fading effects. Among several other diversity techniques, the cooperative diversity scheme [16, 17, 9] has also gained attention for its potential to provide spatial diversity gain. A spatial diversity gain in cooperative diversity systems is achieved if several single-antenna mobile stations in the network share their antennas to form a so-called virtual antenna array [3]. The signal from the source mobile station is thus relayed to the destination mobile

station via other mobile stations in the network.

Mobile radio fading channels are usually described by statistical quantities, such as the mean value, the variance, as well as the probability density function (PDF) of the envelope and the phase of the received signal. Unfortunately, these statistical quantities do not give any information about how fast (or slow) the fading channel is changing with time. However, to cope with the problems faced in the development of cooperative diversity systems, a solid knowledge of the underlying fading behavior of the channel is inevitable. Analyzing the LCR and the ADF provides vital information regarding the fading behavior of M2M channels.

Studies pertaining to the statistical analysis of narrowband M2M fading channels under NLOS propagation conditions in a dual-hop relay-based cooperative system with a single relay in the network have shown that a double Rayleigh process is the most suitable statistical channel model for such scenarios [8, 11]. The work presented in [18] is a straight-forward extension of the double Rayleigh channel model to the double Rice channel model assuming line-of-sight (LOS) propagation conditions. Several M2M fading channel models have been developed based on the multiple scattering concept proposed in [2] for dual-hop single-relay cooperative systems for both NLOS and LOS propagation environments [15, 20, 19]. In addition to dual-hop cooperative systems, several papers dealing with the statistical modeling and analysis of multi-hop cooperative systems having K relays connected in series between the source and the destination terminals are available in the literature [7, 5].

This paper studies the fading behavior of M2M fading links in dual-hop amplify-and-forward relay networks, where K mobile relays are connected in parallel between the source mobile station and the destination mobile station. Such M2M fading channels are referred to as K -parallel dual-hop relay M2M fading channels. Each individual transmission link from the source mobile station to the destination mobile station via the k th ($k = 1, 2, \dots, K$) relay is modeled as a complex double Gaussian process. Consequently, the overall M2M fading channel taking into account K parallel relay links can be modeled as a sum of K complex double Gaussian processes. The authors of [21] have derived analytical expressions for the characteristic function (CF), the PDF of the envelope as well as the phase, and the mean value along with the variance of K -parallel dual-hop relay M2M fading channels.

In this paper, we fill the information gap regarding the LCR and the ADF of K -parallel dual-hop relay M2M fading channels. Here, we derive analytical integral expressions of these quantities along with the CDF for the envelope of K -parallel dual-hop relay M2M fading channels. The expressions for the LCR, the ADF, and

the CDF are derived assuming that the underlying stochastic processes are independent but not necessarily identically distributed. Furthermore, it is shown that the obtained formulae can be reduced to simple and closed-form expressions when i.i.d. processes are taken into account.

The organization of the remaining part of the paper is as follows: In Section II, the reference model for K -parallel dual-hop relay fading channels is developed. Section III deals with the derivation of the LCR and the ADF. Section IV validates the correctness of the obtained analytical expressions by simulations. Finally, some concluding remarks are given in Section V.

II. THE K -PARALLEL DUAL-HOP RELAY FADING CHANNEL MODEL

In this paper, we study the fading behavior of the overall M2M fading channel in a dual-hop cooperative network, where there are K mobile relays connected in parallel between the source mobile station and the destination mobile station. We refer to the resulting overall M2M fading channel as the K -parallel dual-hop relay fading channel. We aim to investigate frequency non-selective K -parallel dual-hop relay fading channels under NLOS propagation conditions in isotropic scattering conditions. Furthermore, we have considered time-division multiple-access (TDMA) based amplify-and-forward relay protocols. In addition, all the mobile stations in the network, i.e., the source mobile station, the destination mobile station, and the K mobile relays do not transmit and receive a signal at the same time in the same frequency band. The propagation scenario considered is presented in Fig. D.1. The overall complex time-varying channel gain associated with K -parallel dual-hop relay fading channels can be written as

$$\chi(t) = \chi_1(t) + j\chi_2(t) = \sum_{k=1}^K \zeta^{(k)}(t) \quad (1)$$

where $\zeta^{(k)}(t)$ ($k = 1, 2, \dots, K$) describes the fading process in the k th subchannel from the source mobile station to the destination mobile station via the k th mobile relay. Here, the fading process $\zeta^{(k)}(t)$ is modeled as a weighted zero-mean complex double Gaussian process, i.e.,

$$\zeta^{(k)}(t) = \varsigma_1^{(k)}(t) + j\varsigma_2^{(k)}(t) = A_{r(k)} \mu^{(2k-1)}(t) \mu^{(2k)}(t) \quad (2)$$

for $k = 1, 2, \dots, K$. In (2), $\mu^{(i)}(t)$ ($i = 1, 2, \dots, 2K$) is a zero-mean complex Gaussian process with variance $2\sigma_{\mu^{(i)}}^2/\sqrt{K}$.

These Gaussian processes $\mu^{(i)}(t)$ are mutually independent, where each one is described by the classical Jakes Doppler power spectral density (PSD). Note

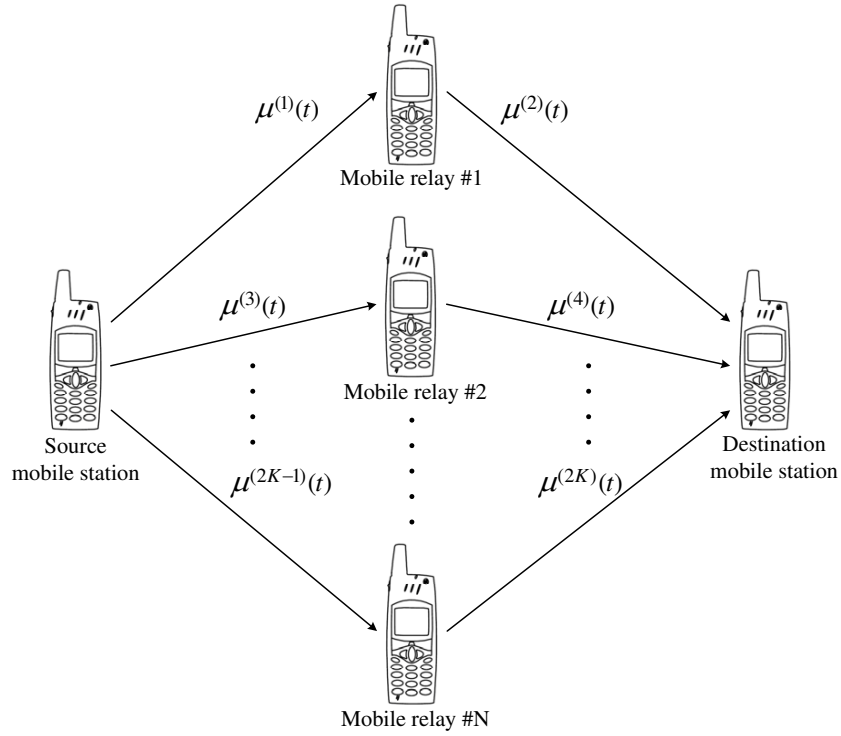


Figure D.1: The propagation scenario describing K -parallel dual-hop relay M2M fading channels.

that the Gaussian process $\mu^{(i)}(t)$ represents the corresponding scattered component of the subchannel between the source mobile station and the k th mobile relay for $i = 2k - 1 = 1, 3, \dots, (2K - 1)$. Analogously, the Gaussian process $\mu^{(i)}(t)$ defines the scattered component of the subchannel between the k th mobile relay and the destination mobile station for $i = 2k = 2, 4, \dots, 2K$. In (2), $A_{R(k)}$ is referred to as the relay gain of the k th relay. It is important to state here that the relay gain $A_{R(k)}$ is only a scaling factor for the variance of the complex Gaussian process $\mu^{(i)}(t)$, i.e., $\text{Var} \left\{ A_{R(k)} \mu^{(i)}(t) \right\} = 2(A_{R(k)} \sigma_{\mu^{(i)}})^2 / \sqrt{K}$, where $i = 2, 4, \dots, 2K$.

The absolute value of the overall complex time-varying channel gain $\chi(t)$ in (1) defines the envelope of K -parallel dual-hop relay fading channels, i.e., $\Xi(t) = |\chi(t)| = \left| \sum_{k=1}^K \zeta^{(k)}(t) \right|$.

III. LCR AND ADF OF K -PARALLEL DUAL-HOP RELAY FADING CHANNELS

This section deals with the derivation of analytical expressions for the LCR and the ADF of the envelope $\Xi(t)$ of K -parallel dual-hop relay fading channels introduced in Section II.

A. Derivation of the LCR

The LCR $N_{\Xi}(r)$ of the envelope $\Xi(t)$ describes the average number of times the process $\Xi(t)$ crosses a certain threshold level from up to down (or from down to up) per second. Mathematically, the LCR $N_{\Xi}(r)$ can be obtained using [14]

$$N_{\Xi}(r) = \int_0^{\infty} \dot{x} p_{\Xi\dot{\Xi}}(r, \dot{x}) d\dot{x} \quad (3)$$

where $p_{\Xi\dot{\Xi}}(r, \dot{x})$ is the joint PDF of the envelope $\Xi(t)$ and its time derivative $\dot{\Xi}(t)$ at the same time. Throughout this article, the overdot denotes the time derivative. Here, the main problem is to compute the joint PDF $p_{\Xi\dot{\Xi}}(r, \dot{x})$ in order to obtain the LCR $N_{\Xi}(r)$ of the envelope $\Xi(t)$.

For the sake of convenience in deriving the joint PDF $p_{\Xi\dot{\Xi}}(r, \dot{x})$, we first compute the joint CF $\Phi_{\chi_1 \chi_2 \dot{\chi}_1 \dot{\chi}_2}(\omega_1, \omega_2, \dot{\omega}_1, \dot{\omega}_2)$ of the inphase and quadrature components of $\chi(t)$ and $\dot{\chi}(t)$. From (1), it is clear that we can express this joint CF as a product of the joint CFs $\Phi_{\zeta_1^{(k)} \zeta_2^{(k)} \dot{\zeta}_1^{(k)} \dot{\zeta}_2^{(k)}}(\omega_1, \omega_2, \dot{\omega}_1, \dot{\omega}_2)$ of the inphase and quadrature components of $\zeta^{(k)}(t)$ and $\dot{\zeta}^{(k)}(t)$ [10] as

$$\Phi_{\chi_1 \chi_2 \dot{\chi}_1 \dot{\chi}_2}(\omega_1, \omega_2, \dot{\omega}_1, \dot{\omega}_2) = \prod_{k=1}^K \Phi_{\zeta_1^{(k)} \zeta_2^{(k)} \dot{\zeta}_1^{(k)} \dot{\zeta}_2^{(k)}}(\omega_1, \omega_2, \dot{\omega}_1, \dot{\omega}_2). \quad (4)$$

By definition, the CF and the PDF form a Fourier transform pair [10]. Thus, given the joint PDF $p_{\zeta_1^{(k)} \zeta_2^{(k)} \dot{\zeta}_1^{(k)} \dot{\zeta}_2^{(k)}}(y_1, y_2, \dot{y}_1, \dot{y}_2)$ of the inphase and quadrature components of $\zeta^{(k)}(t)$ and $\dot{\zeta}^{(k)}(t)$, the joint CF $\Phi_{\zeta_1^{(k)} \zeta_2^{(k)} \dot{\zeta}_1^{(k)} \dot{\zeta}_2^{(k)}}(\omega_1, \omega_2, \dot{\omega}_1, \dot{\omega}_2)$ can be expressed as

$$\begin{aligned} \Phi_{\zeta_1^{(k)} \zeta_2^{(k)} \dot{\zeta}_1^{(k)} \dot{\zeta}_2^{(k)}}(\omega_1, \omega_2, \dot{\omega}_1, \dot{\omega}_2) &= \int_{-\infty}^{\infty} \int_{-\infty}^{\infty} \int_{-\infty}^{\infty} \int_{-\infty}^{\infty} p_{\zeta_1^{(k)} \zeta_2^{(k)} \dot{\zeta}_1^{(k)} \dot{\zeta}_2^{(k)}}(y_1, y_2, \dot{y}_1, \dot{y}_2) \\ &\times e^{-j(\omega_1 y_1 + \omega_2 y_2 + \dot{\omega}_1 \dot{y}_1 + \dot{\omega}_2 \dot{y}_2)} dy_1 dy_2 d\dot{y}_1 d\dot{y}_2 \end{aligned} \quad (5)$$

where the joint PDF $p_{\zeta_1^{(k)} \zeta_2^{(k)} \dot{\zeta}_1^{(k)} \dot{\zeta}_2^{(k)}}(y_1, y_2, \dot{y}_1, \dot{y}_2)$ is given as follows [20]

$$\begin{aligned} p_{\zeta_1^{(k)} \zeta_2^{(k)} \dot{\zeta}_1^{(k)} \dot{\zeta}_2^{(k)}}(y_1, y_2, \dot{y}_1, \dot{y}_2) &= \frac{K}{(2\pi)^2 A_{R^{(k)}}^2 \sigma_{\mu^{(2k-1)}}^2 \sigma_{\mu^{(2k)}}^2} \int_0^{\infty} dv e^{-\frac{v^2 \sqrt{K}}{2A_{R^{(k)}}^2 \sigma_{\mu^{(2k)}}^2}} \\ &\times \frac{v}{\beta_{\mu^{(2k)}}(y_1^2 + y_2^2) + \beta_{\mu^{(2k-1)}} v^4} e^{-\frac{(y_1^2 + y_2^2) \sqrt{K}}{2\sigma_{\mu^{(2k-1)}}^2 v^2} - \frac{v^2 (y_1^2 + y_2^2)}{2\{\beta_{\mu^{(2k)}}(y_1^2 + y_2^2) + \beta_{\mu^{(2k-1)}} v^4\}}}. \end{aligned} \quad (6)$$

In (6), the quantity $\beta_{\mu^{(i)}} (i = 1, 2, \dots, 2K)$ is the negative curvature of the autocorrelation function of the inphase and quadrature components of $\mu^{(i)}(t)$ ($i = 1, 2, \dots, 2K$). Under isotropic scattering conditions, the quantities $\beta_{\mu^{(i)}}$ can be expressed for M2M fading channels as [1, 12]

$$\beta_{\mu^{(2k-1)}} = 2 \left(\sigma_{\mu^{(2k-1)}} \pi \right)^2 \left(f_{S_{\max}}^2 + f_{R_{\max}^{(k)}}^2 \right) / \sqrt{K} \quad (7a)$$

$$\beta_{\mu^{(2k)}} = 2 \left(A_{R^{(k)}} \sigma_{\mu^{(2k)}} \pi \right)^2 \left(f_{R_{\max}^{(k)}}^2 + f_{D_{\max}}^2 \right) / \sqrt{K} \quad (7b)$$

where $f_{S_{\max}}$, $f_{D_{\max}}$, and $f_{R_{\max}^{(k)}}$ are the maximum Doppler frequencies caused by the motion of the source mobile station, the destination mobile station, and the k th mobile relay, respectively.

After substituting (6) in (5), doing some tedious algebraic manipulations, and solving the integrals using [4, Eqs. (3.323-II), (3.338-IV), (3.478-IV), and (6.521-II)], we get the final expression for the joint CF $\Phi_{\zeta_1^{(k)} \zeta_2^{(k)} \dot{\zeta}_1^{(k)} \dot{\zeta}_2^{(k)}}(\omega_1, \omega_2, \dot{\omega}_1, \dot{\omega}_2)$ as presented in (8).

$$\begin{aligned} \phi_{\zeta_1^{(k)} \zeta_2^{(k)} \dot{\zeta}_1^{(k)} \dot{\zeta}_2^{(k)}}(\omega_1, \omega_2, \dot{\omega}_1, \dot{\omega}_2) &= K \left(A_{R^{(k)}}^2 \sigma_{\mu^{(2k-1)}}^2 \sigma_{\mu^{(2k)}}^2 (\omega_1^2 + \omega_2^2) + \right. \\ &\left. \left\{ \sqrt{K} + \sigma_{\mu^{(2k-1)}}^2 \beta_{\mu^{(2k)}} (\dot{\omega}_1^2 + \dot{\omega}_2^2) \right\} \left\{ \sqrt{K} + A_{R^{(k)}}^2 \sigma_{\mu^{(2k)}}^2 \beta_{\mu^{(2k-1)}} (\dot{\omega}_1^2 + \dot{\omega}_2^2) \right\} \right)^{-1}. \quad (8) \end{aligned}$$

Assuming $\zeta^{(k)}(t)$ ($k = 1, 2, \dots, K$) are i.i.d. complex double Gaussian random processes, which implies that $\Phi_{\zeta_1 \zeta_2 \dot{\zeta}_1 \dot{\zeta}_2}(\omega_1, \omega_2, \dot{\omega}_1, \dot{\omega}_2) = \Phi_{\zeta_1^{(k)} \zeta_2^{(k)} \dot{\zeta}_1^{(k)} \dot{\zeta}_2^{(k)}}(\omega_1, \omega_2, \dot{\omega}_1, \dot{\omega}_2)$ with $\sigma_{\mu^{(2k-1)}}^2 = \sigma_{\mu^{(1)}}^2$, $\sigma_{\mu^{(2k)}}^2 = \sigma_{\mu^{(2)}}^2$, and $A_R = A_{R^{(k)}} \forall k = 1, 2, \dots, K$. Thus, for i.i.d. complex double Gaussian random processes, (4) can simply be expressed as

$$\Phi_{\chi_1 \chi_2 \dot{\chi}_1 \dot{\chi}_2}(\omega_1, \omega_2, \dot{\omega}_1, \dot{\omega}_2) = \left[\Phi_{\zeta_1 \zeta_2 \dot{\zeta}_1 \dot{\zeta}_2}(\omega_1, \omega_2, \dot{\omega}_1, \dot{\omega}_2) \right]^K. \quad (9)$$

Given the joint CF $\Phi_{\chi_1 \chi_2 \dot{\chi}_1 \dot{\chi}_2}(\omega_1, \omega_2, \dot{\omega}_1, \dot{\omega}_2)$ of the inphase and quadrature components of $\chi(t)$ and $\dot{\chi}(t)$, we can compute the corresponding joint PDF $p_{\chi_1 \chi_2 \dot{\chi}_1 \dot{\chi}_2}(z_1, z_2, \dot{z}_1, \dot{z}_2)$ by taking the (complex conjugate of the) inverse Fourier transform of the joint CF $\Phi_{\chi_1 \chi_2 \dot{\chi}_1 \dot{\chi}_2}(\omega_1, \omega_2, \dot{\omega}_1, \dot{\omega}_2)$ [10], i.e.,

$$\begin{aligned} p_{\chi_1 \chi_2 \dot{\chi}_1 \dot{\chi}_2}(z_1, z_2, \dot{z}_1, \dot{z}_2) &= \int_{-\infty}^{\infty} \int_{-\infty}^{\infty} \int_{-\infty}^{\infty} \int_{-\infty}^{\infty} d\omega_1 d\omega_2 d\dot{\omega}_1 d\dot{\omega}_2 \\ &\times \Phi_{\chi_1 \chi_2 \dot{\chi}_1 \dot{\chi}_2}(\omega_1, \omega_2, \dot{\omega}_1, \dot{\omega}_2) \frac{e^{-j(\omega_1 z_1 + \omega_2 z_2 + \dot{\omega}_1 \dot{z}_1 + \dot{\omega}_2 \dot{z}_2)}}{(2\pi)^4}. \quad (10) \end{aligned}$$

Substituting (4) in (10), doing some mathematical manipulations, and solving the resulting integrals using [4, Eq. (3.338-IV)] gives the joint PDF $p_{\chi_1 \chi_2 \dot{\chi}_1 \dot{\chi}_2}(z_1, z_2, \dot{z}_1, \dot{z}_2)$ in the form

$$p_{\chi_1 \chi_2 \dot{\chi}_1 \dot{\chi}_2}(z_1, z_2, \dot{z}_1, \dot{z}_2) = \frac{1}{(2\pi)^3} \int_{-\infty}^{\infty} \int_{-\infty}^{\infty} \int_0^{\infty} dy d\dot{\omega}_1 d\dot{\omega}_2 \times y J_0 \left(y \sqrt{z_1^2 + z_2^2} \right) g_1(y, \dot{\omega}_1, \dot{\omega}_2) e^{-j(\dot{\omega}_1 \dot{z}_1 + \dot{\omega}_2 \dot{z}_2)} \quad (11)$$

where $g_1(\cdot, \cdot, \cdot)$ is defined below in (12)

$$g_1(y, \dot{\omega}_1, \dot{\omega}_2) = \prod_{k=1}^K K \left(A_{R^{(k)}}^2 \sigma_{\mu^{(2k-1)}}^2 \sigma_{\mu^{(2k)}}^2 y^2 + \left\{ \sqrt{K} + \sigma_{\mu^{(2k-1)}}^2 \beta_{\mu^{(2k)}} (\dot{\omega}_1^2 + \dot{\omega}_2^2) \right\} \left\{ \sqrt{K} + A_{R^{(k)}}^2 \sigma_{\mu^{(2k)}}^2 \beta_{\mu^{(2k-1)}} (\dot{\omega}_1^2 + \dot{\omega}_2^2) \right\} \right)^{-1} \quad (12)$$

and $J_0(\cdot)$ is the zeroth-order Bessel function of the first kind [4].

The joint PDF $p_{\Xi \dot{\Xi} \Theta \dot{\Theta}}(x, \dot{x}, \theta, \dot{\theta})$ of the envelope and the phase of K -parallel dual-hop relay fading channels can now easily be computed by transforming the random variables in (11) from rectangular coordinates $(z_1, z_2, \dot{z}_1, \dot{z}_2)$ to polar coordinates $(x, \dot{x}, \theta, \dot{\theta})$, which results in

$$p_{\Xi \dot{\Xi} \Theta \dot{\Theta}}(x, \dot{x}, \theta, \dot{\theta}) = \frac{x^2}{(2\pi)^3} \int_{-\infty}^{\infty} \int_{-\infty}^{\infty} \int_0^{\infty} dy d\dot{\omega}_1 d\dot{\omega}_2 y J_0(yx) \times g_1(y, \dot{\omega}_1, \dot{\omega}_2) e^{-j(\dot{\omega}_1 (\dot{x} \cos \theta - x \dot{\theta} \sin \theta) + \dot{\omega}_2 (\dot{x} \sin \theta + x \dot{\theta} \cos \theta))} \quad (13)$$

for $x \geq 0$, $|\dot{x}| < \infty$, $|\theta| \leq \pi$, and $|\dot{\theta}| < \infty$, where $g_1(\cdot, \cdot, \cdot)$ is given in (12).

Finally, integrating (13) over the undesirable variables θ and $\dot{\theta}$ using [4, Eqs. (3.338-IV), (6.596-I), and (8.464-II)], allows us to express the joint PDF $p_{\Xi \dot{\Xi}}(x, \dot{x})$ of the envelope $\Xi(t)$ and its time derivative $\dot{\Xi}(t)$ as

$$p_{\Xi \dot{\Xi}}(x, \dot{x}) = \frac{1}{\pi} \int_0^{\infty} \int_0^{\infty} dz dy y x J_0(yx) \cos(z\dot{x}) g_1(y, z \cos \psi, z \sin \psi), \quad x \geq 0, |\dot{x}| < \infty. \quad (14)$$

Substituting (14) in (3) results in the following final expression for the LCR $N_{\Xi}(r)$ of the envelope $\Xi(t)$

$$N_{\Xi}(r) = \frac{1}{\pi} \int_0^{\infty} \int_0^{\infty} \int_0^{\infty} y r \dot{x} J_0(yr) \cos(z\dot{x}) g_1(y, z \cos \psi, z \sin \psi) d\dot{x} dz dy. \quad (15)$$

For i.i.d. complex double Gaussian random processes $\zeta^{(k)}(t)$ ($k = 1, 2, \dots, K$), the integral over the variable y in (15) can be solved using [4, Eq. (6.565-IV)]. In this case, the expression of the LCR $N_{\Xi}(r)$ in (15) reduces to

$$N_{\Xi}(r) = \frac{1}{\pi} \cdot \frac{K^K}{2^{K-1} (K-1)!} \cdot \frac{r^K}{\left(A_R \sigma_{\mu(1)} \sigma_{\mu(2)}\right)^{(K+1)}} \times \int_0^{\infty} \int_0^{\infty} \frac{\dot{x} \cos(z\dot{x})}{(g_2(z))^{(K-1)}} K_{K-1} \left(\frac{r g_2(z)}{A_R \sigma_{\mu(1)} \sigma_{\mu(2)}} \right) d\dot{x} dz \quad (16)$$

where $(\cdot)!$ denotes the factorial, $K_{K-1}(\cdot)$ is the $(K-1)$ th-order modified Bessel function of the second kind [4], and

$$g_2(z) = \sqrt{\left\{ \sqrt{K} + \sigma_{\mu(1)}^2 \beta_{\mu(2)} z^2 \right\} \left\{ \sqrt{K} + A_R^2 \sigma_{\mu(2)}^2 \beta_{\mu(1)} z^2 \right\}}. \quad (17)$$

B. Derivation of the ADF

The ADF $T_{\Xi-}(r)$ of the envelope $\Xi(t)$ is the expected value of the time intervals over which the process $\Xi(t)$ remains below a certain threshold level r . The ADF $T_{\Xi-}(r)$ can be calculated by means of [6]

$$T_{\Xi-}(r) = \frac{F_{\Xi-}(r)}{N_{\Xi}(r)} \quad (18)$$

where $F_{\Xi-}(r)$ is the CDF and $N_{\Xi}(r)$ is the LCR of $\Xi(t)$.

The CDF $F_{\Xi-}(r)$ of the envelope $\Xi(t)$ is the probability that $\Xi(t)$ remains below the threshold level r (see, e.g., [10]).

The PDF $p_{\Xi}(x)$ of the envelope $\Xi(t)$ required to compute the CDF $F_{\Xi-}(r)$ can be obtained by integrating (14) over \dot{x} in the interval $(-\infty, \infty)$. With the help of the resulting PDF $p_{\Xi}(x)$, the final expression of the CDF $F_{\Xi-}(r)$ of the envelope $\Xi(t)$ can be given as

$$F_{\Xi-}(r) = 1 - \frac{2}{\pi} \int_0^{\infty} \int_0^{\infty} \int_0^{\infty} \int_r^{\infty} y x J_0(yx) \cos(z\dot{x}) g_1(y, z \cos \psi, z \sin \psi) dx d\dot{x} dz dy. \quad (19)$$

Under the assumption that $\zeta^{(k)}(t)$ ($k = 1, 2, \dots, K$) are i.i.d. complex double Gaussian processes, the product on the right-hand-side in (12) becomes $(\cdot)^K$. Then solving the integral over the variables x and y in (19) allows us to write the CDF $F_{\Xi_-}(r)$ of the envelope $\Xi(t)$ as

$$F_{\Xi_-}(r) = 1 - \frac{2}{\pi} \cdot \frac{K^K}{2^{K-1}(K-1)!} \cdot \frac{r^K}{\left(A_R \sigma_{\mu^{(1)}} \sigma_{\mu^{(2)}}\right)^K} \times \int_0^\infty \int_0^\infty \frac{\cos(z\dot{x})}{(g_2(z))^K} K_K \left(\frac{r g_2(z)}{A_R \sigma_{\mu^{(1)}} \sigma_{\mu^{(2)}}} \right) d\dot{x} dz \quad (20)$$

where $g_2(\cdot)$ is given in (17). It can be shown that (20) reduces to the following closed-form expression

$$F_{\Xi_-}(r) = 1 - \frac{K^{\frac{K}{2}} r^K K_K \left(r \sqrt{K} / (A_R \sigma_{\mu^{(1)}} \sigma_{\mu^{(2)}}) \right)}{2^{K-1}(K-1)! \left(A_R \sigma_{\mu^{(1)}} \sigma_{\mu^{(2)}}\right)^K}. \quad (21)$$

The proof of (21) is omitted here for reasons of brevity. However, in the next section, we present numerical results to illustrate that (20) and (21) are equivalent.

IV. NUMERICAL RESULTS

The purpose of this section is to illustrate the theoretical expressions presented in Section III and to validate their correctness with the help of simulations. In this paper, the underlying uncorrelated Gaussian noise processes making up the overall K -parallel dual-hop relay channel are simulated using the sum-of-sinusoids (SOS) concept[12]. The model parameters of the channel simulator were computed by using the generalized method of exact Doppler spread (GMEDS₁) [13]. Each Gaussian process $\mu^{(i)}(t)$ ($i = 1, 2, \dots, 2K$) was simulated using $N_1^{(i)} = 14 + k$ and $N_2^{(i)} = 14 + k$ for $i = 1, 2, \dots, 2K$ and $k = 1, 2, \dots, K$, where $N_1^{(i)}$ and $N_2^{(i)}$ are the number of sinusoids required to simulate the inphase and quadrature components of $\mu^{(i)}(t)$, respectively. The maximum Doppler frequencies caused by the motion of the source mobile station and the destination mobile station, denoted by $f_{s_{\max}}$ and $f_{d_{\max}}$, respectively, were both set to 91 Hz. Whereas, the maximum Doppler frequencies $f_{R_{\max}^{(k)}} = f_{R_{\max}}$ caused by the motion of K mobile relays were selected from the set $\{91 \text{ Hz}, 125 \text{ Hz}, 210 \text{ Hz}\}$. The variances of the underlying Gaussian processes are assumed to be equal, i.e., $2\sigma_{\mu^{(i)}}^2 = 2\sigma_{\mu}^2 \forall i = 1, 2, \dots, 2K$. The relay gains associated with the subchannels are also equal, i.e., $A_{R^{(k)}} = A_R \forall k = 1, 2, \dots, K$ unless stated otherwise.

The results presented in Figs. D.2–D.4 show a good fitting of the analytical and simulation results. Figure D.2 illustrates the LCR $N_{\Xi}(r)$ of the envelope $\Xi(t)$ given in (16). It can be seen from Fig. D.2 that keeping the relay gains $A_{R^{(k)}}$ and the maximum Doppler frequencies $f_{R_{\max}^{(k)}}$ associated with K mobile relays constant, the LCR $N_{\Xi}(r)$ decreases with the increase in the number of mobile relays in the network. The effect of the maximum Doppler frequencies $f_{R_{\max}^{(k)}}$ associated with K mobile relays is noticeable in Fig. D.2. In Fig. D.3, the theoretical results of the CDF $F_{\Xi_{-}}(r)$

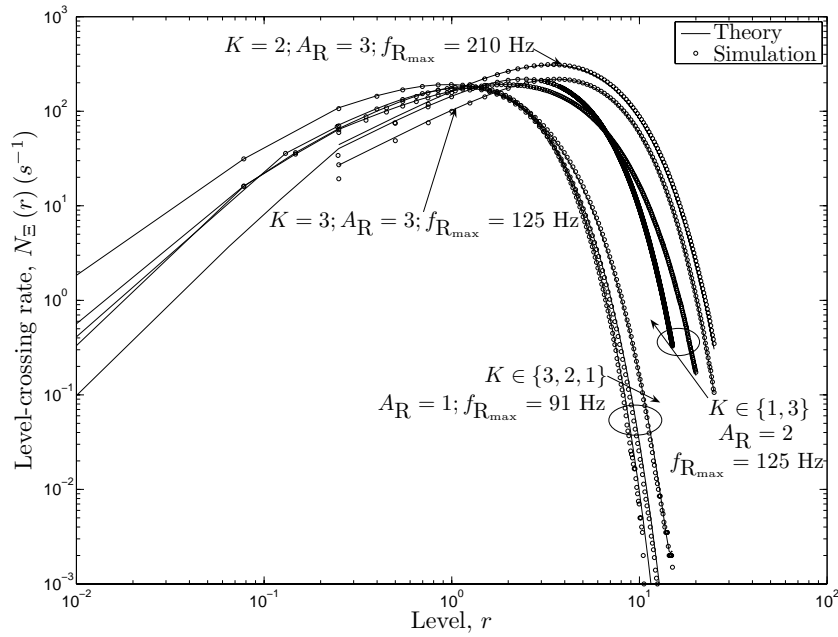


Figure D.2: The LCR $N_{\Xi}(r)$ of the envelope $\Xi(t)$ of K -parallel dual-hop relay M2M fading channels.

of the envelope $\Xi(t)$ described by (20) and (21) are presented. The presented results validate our claim that (20) and (21) are equivalent. The ADF $T_{\Xi_{-}}(r)$ of the envelope $\Xi(t)$ described by (18) is evaluated along with the simulation results in Fig. D.4. Studying the results presented in Fig. D.4 reveals that the ADF $T_{\Xi_{-}}(r)$ increases at high values of r with the increase in the number of mobile relays keeping the corresponding relay gains $A_{R^{(k)}}$ and the maximum Doppler frequencies $f_{R_{\max}^{(k)}}$ constant. At low values of r , however, the ADF $T_{\Xi_{-}}(r)$ decreases with an increase in the number of mobile relays. We can further deduce from Fig. D.4 that the relay gains $A_{R^{(k)}}$ and the maximum Doppler frequencies $f_{R_{\max}^{(k)}}$ influence the ADF $T_{\Xi_{-}}(r)$ of the envelope $\Xi(t)$ significantly.

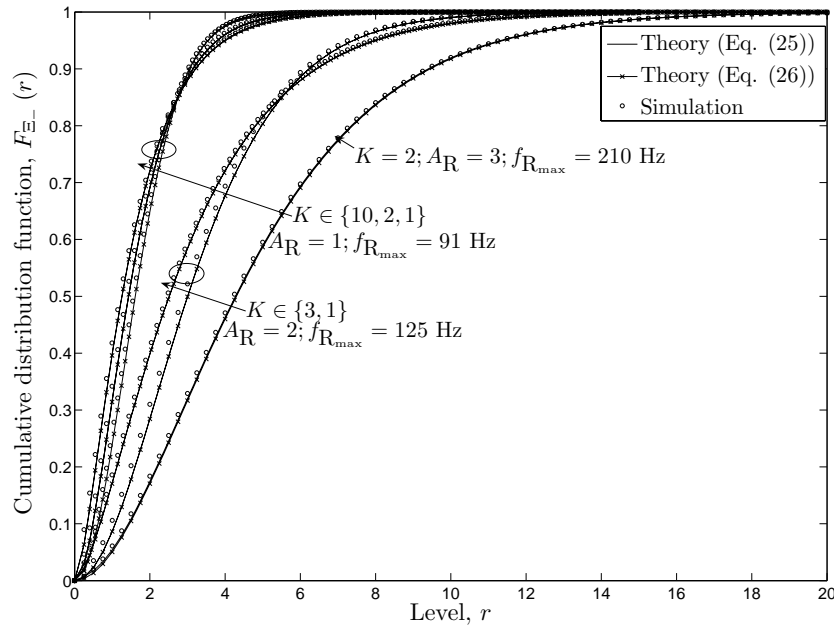


Figure D.3: The CDF $F_{\Xi_-}(r)$ of the envelope $\Xi(t)$ of K -parallel dual-hop relay M2M fading channels.

V. CONCLUSION

In this paper, we have studied the fading behavior of K -parallel dual-hop relay frequency non-selective M2M fading channels under NLOS propagation conditions in

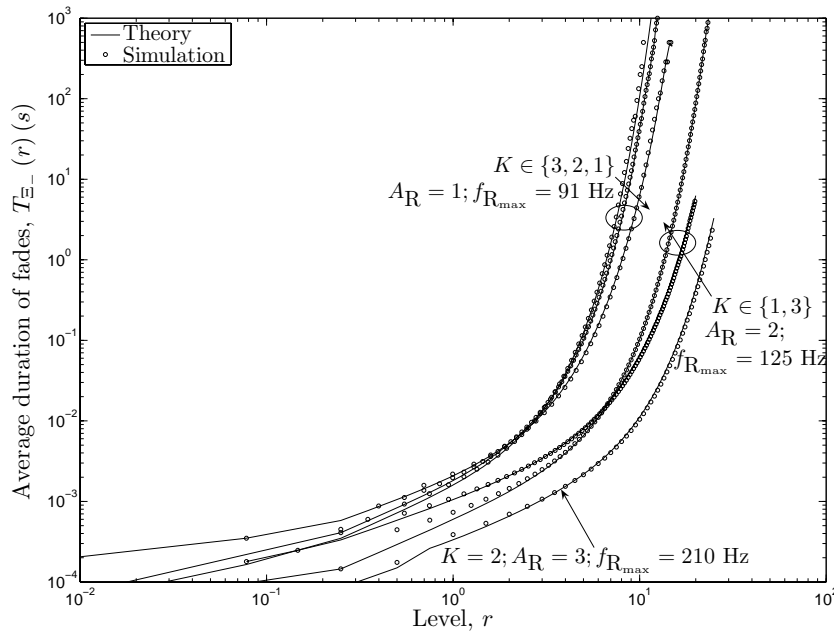


Figure D.4: The ADF $T_{\Xi_-}(r)$ of the envelope $\Xi(t)$ of K -parallel dual-hop relay M2M fading channels.

isotropic scattering environments. The fading behavior of such M2M fading channels is analyzed by evaluating the LCR and the ADF of the received signal envelope. Here, we presented analytical integral expressions of these quantities along with the CDF associated with the envelope. These expressions are derived assuming that the underlying processes making up such channels are independent but not necessarily identical as well as if they are i.i.d. processes. The theoretical results are validated by simulations. The results presented show that the number of mobile relays K in the network, the relay gains $A_{R^{(k)}}$, and the maximum Doppler frequencies $f_{R_{\max}}^{(k)}$ associated with the K mobile relays significantly influence the LCR, the ADF, and the CDF of the received signal envelope of K -parallel dual-hop relay M2M fading channels. These results are of importance to the designers of dual-hop/ multi-hop cooperative multi-relay systems.

REFERENCES

- [1] A. S. Akki. Statistical properties of mobile-to-mobile land communication channels. *IEEE Trans. Veh. Technol.*, 43(4):826–831, November 1994.
- [2] J. B. Andersen. Statistical distributions in mobile communications using multiple scattering. In *Proc. 27th URSI General Assembly*. Maastricht, Netherlands, August 2002.
- [3] M. Dohler. *Virtual Antenna Arrays*. Ph.D. dissertation, King’s College, London, United Kingdom, 2003.
- [4] I. S. Gradshteyn and I. M. Ryzhik. *Table of Integrals, Series, and Products*. New York: Academic Press, 6th edition, 2000.
- [5] Z. Hadzi-Velkov, N. Zlatanov, and G. K. Karagiannidis. On the second order statistics of the multihop Rayleigh fading channel. *IEEE Trans. Commun.*, 57(6):1815–1823, June 2009.
- [6] W. C. Jakes, editor. *Microwave Mobile Communications*. Piscataway, NJ: IEEE Press, 1994.
- [7] G. K. Karagiannidis, N. C. Sagias, and P. T. Mathiopoulos. N*Nakagami: A novel stochastic model for cascaded fading channels. *IEEE Trans. Commun.*, 55(8):1453–1458, August 2007.
- [8] I. Z. Kovacs, P. C. F. Eggers, K. Olesen, and L. G. Petersen. Investigations of outdoor-to-indoor mobile-to-mobile radio communication channels. In *Proc.*

- IEEE 56th Veh. Technol. Conf., VTC'02-Fall*, volume 1, pages 430–434. Vancouver BC, Canada, September 2002.
- [9] J. N. Laneman, D. N. C. Tse, and G. W. Wornell. Cooperative diversity in wireless networks: Efficient protocols and outage behavior. *IEEE Trans. Inform. Theory*, 50(12):3062–3080, December 2004.
- [10] A. Papoulis and S. U. Pillai. *Probability, Random Variables and Stochastic Processes*. New York: McGraw-Hill, 4th edition, 2002.
- [11] C. S. Patel, G. L. Stüber, and T. G. Pratt. Statistical properties of amplify and forward relay fading channels. *IEEE Trans. Veh. Technol.*, 55(1):1–9, January 2006.
- [12] M. Pätzold. *Mobile Fading Channels*. Chichester: John Wiley & Sons, 2002.
- [13] M. Pätzold, C. X. Wang, and B. O. Hogstad. Two new sum-of-sinusoids-based methods for the efficient generation of multiple uncorrelated Rayleigh fading waveforms. *IEEE Trans. Wireless Commun.*, 8(6):3122–3131, June 2009.
- [14] S. O. Rice. Mathematical analysis of random noise. *Bell Syst. Tech. J.*, 24:46–156, January 1945.
- [15] J. Salo, H. M. El-Sallabi, and P. Vainikainen. Statistical analysis of the multiple scattering radio channel. *IEEE Trans. Antennas Propagat.*, 54(11):3114–3124, November 2006.
- [16] A. Sendonaris, E. Erkip, and B. Aazhang. User cooperation diversity — Part I: System description. *IEEE Trans. Commun.*, 51(11):1927–1938, November 2003.
- [17] A. Sendonaris, E. Erkip, and B. Aazhang. User cooperation diversity — Part II: Implementation aspects and performance analysis. *IEEE Trans. Commun.*, 51(11):1939–1948, November 2003.
- [18] B. Talha and M. Pätzold. On the statistical properties of double Rice channels. In *Proc. 10th Int. Symp. on Wireless Personal Multimedia Communications, WPMC 2007*, pages 517–522. Jaipur, India, December 2007.
- [19] B. Talha and M. Pätzold. Level-crossing rate and average duration of fades of the envelope of mobile-to-mobile fading channels in cooperative networks under line-of-sight conditions. In *Proc. 51st IEEE Globecom 2008*, pages

- 1–6. New Orleans, USA, November/December 2008. DOI 10.1109/GLOCOM.2008.ECP.860.
- [20] B. Talha and M. Pätzold. A novel amplify-and-forward relay channel model for mobile-to-mobile fading channels under line-of-sight conditions. In *Proc. 19th IEEE Int. Symp. on Personal, Indoor and Mobile Radio Communications, PIMRC 2008*, pages 1–6. Cannes, France, September 2008. DOI 10.1109/PIMRC.2008.4699733.
- [21] B. Talha and M. Pätzold. A geometrical channel model for MIMO mobile-to-mobile fading channels in cooperative networks. In *Proc. IEEE 69th Vehicular Technology Conference, IEEE VTC 2009-Spring*. Barcelona, Spain, April 2009.

Appendix E

Paper IV

Title: On the Statistical Properties of Equal Gain Combining over Mobile-to-Mobile Fading Channels in Cooperative Networks

Authors: **Batool Talha**¹, S. Primak² and Matthias Pätzold¹

Affiliations: ¹University of Agder, Faculty of Engineering and Science, P. O. Box 509, NO-4898 Grimstad, Norway

²University of Western Ontario, Department of ECE, London, ON, N6A 5B9, Canada

Conference: *IEEE International Conference on Communications, ICC 2010*, Cape Town, South Africa, May 2010. DOI 10.1109/ICC.2010.5501898.

On the Statistical Properties of Equal Gain Combining over Mobile-to-Mobile Fading Channels in Cooperative Networks

Batool Talha¹, Serguei Primak², and Matthias Pätzold¹

¹Department of Information and Communication Technology
Faculty of Engineering and Science, Agder University College
Servicebox 509, NO-4876 Grimstad, Norway

E-mails: {batool.talha, matthias.paetzold}@uia.no

²Department of ECE, University of Western Ontario,
London, ON, N6A 5B9, Canada
Email: primak@engga.uwo.ca

Abstract — This article deals with the statistical analysis of equal gain combining (EGC) over mobile-to-mobile (M2M) fading channels in a dual-hop amplify-and-forward relay network. Here, we analyze narrowband M2M fading channels under non-line-of-sight (NLOS) propagation conditions. It is assumed that there exist K diversity branches between the source mobile station and the destination mobile station via K mobile relays. The received signal envelope at the output of the equal gain (EG) combiner is thus modeled as a sum of K double Rayleigh processes. It has been shown that the evaluation of the probability density function (PDF) of this sum process using the characteristic function (CF) is rather intractable. However, the target PDF can efficiently be approximated by the gamma distribution. Exploiting the properties of the gamma distribution, the cumulative distribution function (CDF), the level-crossing rate (LCR), and the average duration of fades (ADF) of the sum process are also approximated. The approximation of the mentioned sum process by a gamma distributed process makes it possible to provide simple and closed-form analytical expressions for the aforementioned statistical quantities. The validity of the obtained analytical expressions is confirmed by simulations.

I. INTRODUCTION

Recent studies in the field of wireless communications have demonstrated the potential of cooperative relaying to meet the high data-rate and coverage requirements of future wireless communication systems [17, 6]. The advantage of such relaying is the attainment of spatial diversity gain by utilizing the existing resources of the network. From a variety of cooperative diversity schemes [13, 25, 26], the study

presented in this article revolves around amplify-and-forward-type relaying. In this scenario, several mobile stations assist the source mobile station by amplifying and forwarding its information signal to the destination mobile station.

Here, a dual-hop amplify-and-forward configuration has been taken into account, where there exist K mobile relays between the source mobile station and the destination mobile station. Such a configuration in turn gives rise to K diversity branches. Thus, the previously mentioned spatial diversity gain is achieved by combining the signal received from the K diversity branches at the destination mobile station. Among the most important diversity combining techniques [12], maximal ratio combining (MRC) has been proved to be the optimum one [12]. It is widely acknowledged in the literature that a suboptimal and less complex combining technique, referred to as EGC, performs very close to MRC [12]. Studies regarding the statistical properties of EGC and MRC in non-cooperative networks over Rayleigh, Rice, and Nakagami fading channels are reported in [32, 5, 11]. Furthermore, performance analysis of the said schemes in terms of the bit error and outage probability over Rayleigh, Rice, and Nakagami fading channels can be found in [33, 34, 24]. In addition, the performance analysis of cooperative diversity using EGC and MRC over Rayleigh and Nakagami- m fading channels is presented in [2, 8, 9].

In recent years, M2M communications has also gained considerable attention for its potential utilization in cooperative networks, ad hoc networks, and vehicle-to-vehicle (V2V) communications. Statistical studies of M2M fading channels in [1] have revealed that such channels behave quite differently from the conventional cellular and land mobile terrestrial channels like, e.g., Rayleigh, Rice, and Suzuki channels. In relay-based cooperative networks, M2M fading channels under NLOS propagation conditions can be modeled as double Rayleigh stochastic processes [19]. Under line-of-sight (LOS) propagation conditions, double Rice processes effectively model M2M fading channels [29]. The authors of [30] have recently studied the performance of digital modulation over double Nakagami- m fading channels with MRC diversity. However, to the best of our knowledge, the statistical analysis of double Rayleigh and/or double Nakagami- m fading channels with EGC has not been carried out so far.

This article deals with the derivation and analysis of the statistical properties of EGC over M2M fading channels in cooperative networks. Although, on the one hand, the PDF can efficiently characterize a fading channel, the LCR and the ADF, on the other hand, provide vital information about how fast the fading channel is changing with time. Thus, studies pertaining to the PDF, the CDF, the LCR, and the ADF along with the CF of the received signal envelope at the output of the EG com-

biner are included in this article. The output signal of the EG combiner is modeled as a sum of K double Rayleigh processes. It has been illustrated that the computation of the PDF of the sum of K double Rayleigh processes is rather intractable when it comes to the evaluation of the inverse Fourier transform of the CF. An alternate approach is therefore presented in which the PDF is either approximated by another but a simpler expression or by a series.

Depending upon the purpose for which the approximated PDF has to be used, several methods of approximation have been proposed so far [4, 22, 16, 28]. Here, we follow the approximation approach using orthogonal series expansion. Specifically, we introduce an approximation approach based on the Laguerre series expansion [22]. It turns out that the first term in the Laguerre series equals gamma distribution. This enables us to show that the PDF of the sum of K double Rayleigh processes can efficiently be approximated by the gamma distribution. Exploiting the properties of the gamma distribution, closed-form approximations are presented for the CDF, the LCR, and the ADF of the sum process. Furthermore, the close fitting of the approximated theoretical results with those of the exact simulation results shows that the approximation approach followed here is valid. We have demonstrated the influence of the number of diversity branches K on the statistical properties of the received signal envelope at the output of the EG combiner.

The organization of the remaining part of the paper is as follows. Section II describes the M2M fading channel model associated with amplify-and-forward relay networks. Section III deals with the derivation of the analytical expressions for the CF, the PDF, the CDF, the LCR, and the ADF of the received signal envelope at the output of the EG combiner. Section IV validates the correctness of the analytical expressions presented in Section III by simulations. Finally, some concluding remarks are presented in Section V.

II. EGC OVER M2M FADING CHANNELS

In this section, we describe the system model of EGC over M2M fading channels in a dual-hop cooperative network, where there are K mobile relays connected in parallel between the source mobile station and the destination mobile station. We aim to investigate frequency non-selective M2M fading channels under NLOS propagation conditions in isotropic scattering conditions. All mobile stations in the network, i.e., the source mobile station, the destination mobile station, and the K mobile relays do not transmit and receive a signal at the same time in the same frequency band. The propagation scenario considered is illustrated in Fig. E.1, where it can be seen that the mobile relays form K diversity branches.

We have taken into account the time-division multiple-access (TDMA) based

amplify-and-forward relay protocols proposed in [14, 3]. Thus, the signals from the K diversity branches in different time slots can be combined at the destination mobile station using EGC. Assuming perfect channel state information (CSI) at the receiver, the received signal envelope at the output of an EG combiner can be written as [12]

$$\Xi(t) = \sum_{k=1}^K \left| \zeta^{(k)}(t) \right| = \sum_{k=1}^K \chi^{(k)}(t) \quad (1)$$

where $\zeta^{(k)}(t)$ ($k = 1, 2, \dots, K$) describes the fading process in the k th subchannel from the source mobile station to the destination mobile station via the k th mobile relay. Here, we model the fading process $\zeta^{(k)}(t)$ as a weighted zero-mean complex double Gaussian process, i.e.,

$$\zeta^{(k)}(t) = \zeta_1^{(k)}(t) + j\zeta_2^{(k)}(t) = A_{R^{(k)}} \mu^{(2k-1)}(t) \mu^{(2k)}(t) \quad (2)$$

for $k = 1, 2, \dots, K$. In (2), $\mu^{(i)}(t)$ ($i = 1, 2, \dots, 2K$) represents a complex circular Gaussian process with zero mean and variance $2\sigma_{\mu^{(i)}}^2$. These Gaussian processes are mutually independent, where the spectral characteristics of each one are described by the classical Jakes Doppler power spectral density. The Gaussian process $\mu^{(i)}(t)$ defines for $i = 2k - 1 = 1, 3, \dots, (2K - 1)$ the scattered component of the subchannel between the source mobile station and the k th mobile relay. Similarly, the Gaussian process $\mu^{(i)}(t)$ represents for $i = 2k = 2, 4, \dots, 2K$ the scattered component of the subchannel between the k th mobile relay and the destination mobile station. In (2), $A_{R^{(k)}}$ is the relay gain of the k th relay. It is worth mentioning that the relay gain $A_{R^{(k)}}$ can be considered as a scaling factor for the variance of the complex Gaussian process $\mu^{(i)}(t)$, i.e., $\text{Var} \left\{ A_{R^{(k)}} \mu^{(i)}(t) \right\} = 2(A_{R^{(k)}} \sigma_{\mu^{(i)}})^2$, where $i = 2, 4, \dots, 2K$. The absolute value of $\zeta^{(k)}(t)$ is denoted by $\chi^{(k)}(t)$ in (1), where each $\chi^{(k)}(t)$ is a double Rayleigh process.

III. STATISTICAL ANALYSIS OF EGC OVER M2M FADING CHANNELS

This section aims at presenting a thorough study of the statistical properties of EGC over M2M fading channels. The derivation and analysis of the closed-form analytical expressions for the CF, the PDF, the CDF, the LCR, and the ADF of $\Xi(t)$ is included in the discussion below.

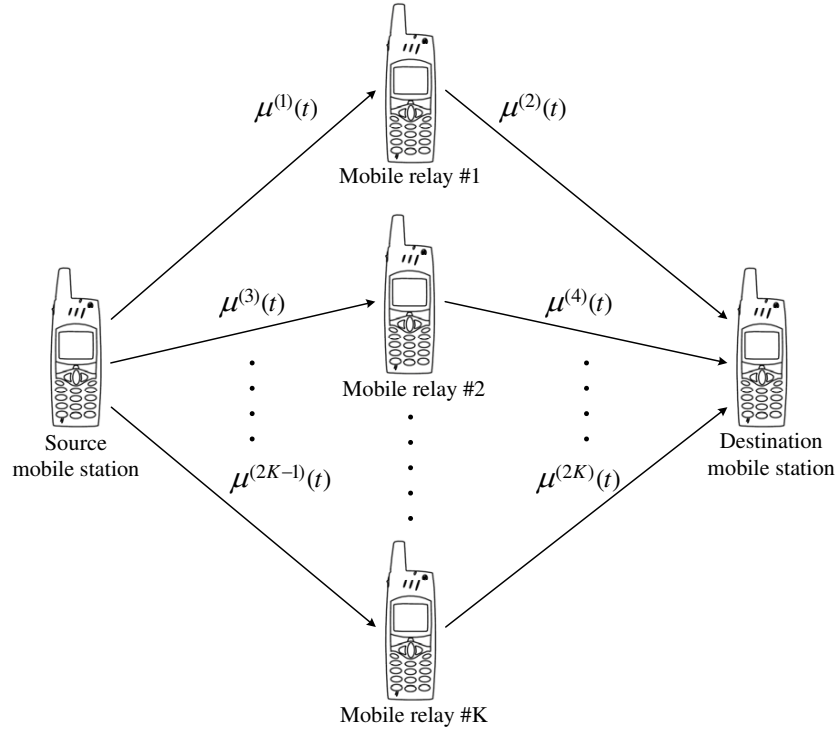


Figure E.1: The propagation scenario describing K -parallel dual-hop relay M2M fading channels.

A. PDF of a Sum of Double Rayleigh Processes

In order to express the PDF $p_{\Xi}(x)$ of $\Xi(t)$, we discuss two independent approaches, namely the CF-based exact solution and the approximate solution obtained using an orthogonal series.

1) *CF-based Exact Solution:* Mobile radio fading channels are usually characterized with the help of statistical quantities, such as the PDF of the envelope and the phase of the received signal. Another, important statistical quantity is the CF, which is related to the corresponding PDF through the Fourier transform.

Since the received signal envelope at the output of the EG combiner $\Xi(t)$ given in (1) is a sum of K independent but not necessarily identical double Rayleigh processes $\chi^{(k)}(t)$, ($k = 1, 2, \dots, K$). Therefore, we can express the CF $\Phi_{\Xi}(\omega)$ of $\Xi(t)$ as a product of the CFs $\Phi_{\chi^{(k)}}(\omega)$ of the stochastic processes $\chi^{(k)}(t)$, i.e.,

$$\Phi_{\Xi}(\omega) = \prod_{k=1}^K \Phi_{\chi^{(k)}}(\omega). \quad (3)$$

By definition, the PDF of a stochastic process and its CF are related through the Fourier transform [18] as

$$\Phi_{\chi^{(k)}}(\omega) = \int_{-\infty}^{\infty} p_{\chi^{(k)}}(x) e^{jx\omega} dx \quad (4)$$

where $p_{\chi^{(k)}}(x)$ represents the double Rayleigh distribution [19], i.e.,

$$p_{\chi^{(k)}}(x) = \frac{x}{\sigma_{\mu^{(2k-1)}}^2 \sigma_{\mu^{(2k)}}^2} K_0 \left(\frac{x}{\sigma_{\mu^{(2k-1)}} \sigma_{\mu^{(2k)}}} \right). \quad (5)$$

Substituting (5) in (4) and solving the integral over x using [7, Eq. (6.621-3)] allows us to write $\Phi_{\chi^{(k)}}(\omega)$ as [10]

$$\Phi_{\chi^{(k)}}(\omega) = \frac{4/3}{(1 - j\omega A_{R^{(k)}} \sigma_{\mu^{(2k-1)}} \sigma_{\mu^{(2k)}})^2} {}_2F_1 \left[2, \frac{1}{2}; \frac{5}{2}; \frac{-1 - j\omega A_{R^{(k)}} \sigma_{\mu^{(2k-1)}} \sigma_{\mu^{(2k)}}}{1 - j\omega A_{R^{(k)}} \sigma_{\mu^{(2k-1)}} \sigma_{\mu^{(2k)}}} \right] \quad (6)$$

$\forall k = 1, 2, \dots, K$. In (6), ${}_2F_1[\cdot, \cdot; \cdot; \cdot]$ is the Gauss hypergeometric function [7]. Finally, substituting (6) in (3) provides us with the required CF $\Phi_{\Xi}(\omega)$ of $\Xi(t)$, i.e.,

$$\Phi_{\Xi}(\omega) = \prod_{k=1}^K \frac{4/3}{(1 - j\omega A_{R^{(k)}} \sigma_{\mu^{(2k-1)}} \sigma_{\mu^{(2k)}})^2} {}_2F_1 \left[2, \frac{1}{2}; \frac{5}{2}; \frac{-1 - j\omega A_{R^{(k)}} \sigma_{\mu^{(2k-1)}} \sigma_{\mu^{(2k)}}}{1 - j\omega A_{R^{(k)}} \sigma_{\mu^{(2k-1)}} \sigma_{\mu^{(2k)}}} \right]. \quad (7)$$

Given the CF $\Phi_{\Xi}(\omega)$ of $\Xi(t)$, the corresponding PDF $p_{\Xi}(x)$ can be obtained by computing the (complex conjugate of the) inverse Fourier transform of the CF $\Phi_{\Xi}(\omega)$. Unfortunately, the complicated form of the CF $\Phi_{\Xi}(\omega)$ makes it difficult to obtain a simple and closed-form expression for the PDF $p_{\Xi}(x)$.

Assuming $\chi^{(k)}(t)$ ($k = 1, 2, \dots, K$) are independent and identically distributed (i.i.d.) stochastic processes, implies that $\Phi_{\chi}(\omega) = \Phi_{\chi^{(k)}}(\omega)$, with $\sigma_{\mu^{(2k-1)}}^2 = \sigma_{\mu^{(1)}}^2$, $\sigma_{\mu^{(2k)}}^2 = \sigma_{\mu^{(2)}}^2$, and $A_R = A_{R^{(k)}} \forall k = 1, 2, \dots, K$. This in turn allows us to express the CF $\Phi_{\Xi}(\omega)$ in (3) as

$$\Phi_{\Xi}(\omega) = \{\phi_{\chi}(\omega)\}^K = \left\{ \frac{4/3}{(1 - j\omega A_R \sigma_{\mu^{(1)}} \sigma_{\mu^{(2)}})^2} {}_2F_1 \left[2, \frac{1}{2}; \frac{5}{2}; \frac{-1 - j\omega A_R \sigma_{\mu^{(1)}} \sigma_{\mu^{(2)}}}{1 - j\omega A_R \sigma_{\mu^{(1)}} \sigma_{\mu^{(2)}}} \right] \right\}^K. \quad (8)$$

By substituting (8) in [18, Eq. (5-94)], the PDF $p_{\Xi}(x)$ can be obtained. However, note that the CF $\Phi_{\Xi}(\omega)$ in (8) is still quite complex to be evaluated using [18, Eq. (5-94)].

2) *Approximate Solution Using an Orthogonal Series Expansion:* It has been shown in Section III-A.1 that it is rather complicated to compute the PDF $p_{\Xi}(x)$ of $\Xi(t)$ by taking the inverse Fourier transform of the CF $\Phi_{\Xi}(\omega)$. An alternate approach is to approximate the PDF $p_{\Xi}(x)$ of $\Xi(t)$ either by another but a simpler expression or by a series. Here, we follow the approximation approach using orthogonal series expansion. From various options of such series, like, e.g., the Edgeworth series and the Gram-Charlier series, we apply in our analysis the Laguerre series expansion [22]. The Laguerre series provides a good approximation for PDFs that are unimodal (i.e., having single maximum) with fast decaying tails and positive defined random variables. Furthermore, the Laguerre series is often used when the first term of the series provides a good enough statistical accuracy [22].

The PDF $p_{\Xi}(x)$ of $\Xi(t)$ can then be expressed using the Laguerre series expansion as [22]

$$p_{\Xi}(x) = \sum_{n=0}^{\infty} b_n e^{-x} x^{\alpha_L} L_n^{(\alpha_L)}(x) \tag{9}$$

where

$$L_n^{(\alpha_L)}(x) = e^x x^{(-\alpha_L)} \frac{d^n}{dx^n} \left[e^{(-x)} x^{n+\alpha_L} \right], \alpha_L > -1 \tag{10}$$

denote the Laguerre polynomials. The coefficients b_n can be given as

$$b_n = \frac{n!}{\Gamma(n + \alpha_L + 1)} \int_0^{\infty} L_n^{(\alpha_L)}(x) p_{\Xi}(x) dx \tag{11}$$

where $x = y/\beta_L$ and $\Gamma(\cdot)$ is the gamma function [7].

The parameters α_L and β_L can be computed by solving the system of equations in [22, p. 21] for $b_1 = 0$ and $b_2 = 0$. The solution of the mentioned system of equations yields

$$\alpha_L = \frac{(\kappa_1^{\Xi})^2}{\kappa_2^{\Xi}} - 1, \quad \beta_L = \frac{\kappa_2^{\Xi}}{\kappa_1^{\Xi}} \tag{12a,b}$$

where κ_1^{Ξ} and κ_2^{Ξ} are the first and second cumulant, respectively, of the stochastic process $\Xi(t)$. Note that the first and second cumulant of $\Xi(t)$ are merely the mean value and the variance, respectively. Furthermore, assuming that the power of the sum process $\Xi(t)$ is normalized by the number of diversity branches K and the underlying double Rayleigh processes are i.i.d. stochastic processes, we can express

the n th cumulant of $\Xi(t)$, κ_n^Ξ , in terms of the n th cumulant of $\chi(t)$, κ_n^χ , as

$$\kappa_n^\Xi = \frac{\kappa_n^\chi}{K^{(n-1)}} \quad (13)$$

where $\chi(t)$ denotes a double Rayleigh process. The first two cumulants of $\chi(t)$ can be expressed as [27]

$$\kappa_1^\chi = \frac{A_R \sigma_{\mu(1)} \sigma_{\mu(2)} \pi}{2}, \quad \kappa_2^\chi = \frac{1}{4} A_R^2 \sigma_{\mu(1)}^2 \sigma_{\mu(2)}^2 (16 - \pi^2). \quad (14a,b)$$

Given κ_n^χ , the value of κ_n^Ξ ($n = 1, 2$) can easily be computed using (13), which directly leads to the evaluation of α_L and β_L in (12a,b). Substituting the obtained quantities α_L and β_L in the Laguerre series expansion, the first term of the series can be identified as the gamma distribution

$$p_\Gamma(x) = \frac{x^{\alpha_L}}{\beta_L^{(\alpha_L+1)} \Gamma(\alpha_L + 1)} e^{-\frac{x}{\beta_L}}. \quad (15)$$

The PDF $p_\Xi(x)$ of $\Xi(t)$ can thus be approximated as

$$p_\Xi(x) \approx p_\Gamma(x) = \frac{x^{\alpha_L}}{\beta_L^{(\alpha_L+1)} \Gamma(\alpha_L + 1)} e^{-\frac{x}{\beta_L}}. \quad (16)$$

The usefulness of the PDF $p_\Xi(x)$ of $\Xi(t)$ lies in the fact that it can be utilized in the performance analysis at the link level of EGC systems. Such performance studies require the knowledge of the PDF of the received signal-to-noise ratio (SNR). Making use of (16) and applying the concept of transformation of random variables [18, p. 244], the required PDF of the SNR can be obtained.

In the following, we derive the analytical expressions of the CDF, the LCR, and the ADF assuming that the double Rayleigh processes $\chi^{(k)}(t)$ are i.i.d. stochastic processes. In addition, we would exploit the properties of the gamma distribution.

B. CDF of a Sum of Double Rayleigh Processes

The CDF $F_{\Xi_-}(r)$ of $\Xi(t)$ is the probability that $\Xi(t)$ remains below the threshold level r [18]. Substituting (16) in $F_{\Xi_-}(r) = \int_0^r p_\Xi(x) dx$ and solving the integral over x using [7, Eq. (3.381-3)] allows us to express the CDF $F_{\Xi_-}(r)$ in closed form as

$$F_{\Xi_-}(r) \approx 1 - \frac{1}{\Gamma(\alpha_L + 1)} \Gamma\left(\alpha_L, \frac{r}{\beta_L}\right) \quad (17)$$

where $\Gamma(\cdot, \cdot)$ is the upper incomplete gamma function [7].

C. LCR of a Sum of Double Rayleigh Processes

The LCR $N_{\Xi}(r)$ of $\Xi(t)$ represents the average rate of up-crossings (or down-crossings) of the stochastic process $\Xi(t)$ per second through a certain threshold level r . The LCR $N_{\Xi}(r)$ can be computed using the formula [23]

$$N_{\Xi}(r) = \int_0^{\infty} \dot{x} p_{\Xi\dot{\Xi}}(r, \dot{x}) d\dot{x} \tag{18}$$

where $p_{\Xi\dot{\Xi}}(r, \dot{x})$ is the joint PDF of the stochastic process $\Xi(t)$ and its corresponding time derivative $\dot{\Xi}(t)$ at the same time t . Throughout this paper, the overdot represents the time derivative.

In Section III-A.2, we have shown that the PDF $p_{\Xi}(x)$ of $\Xi(t)$ can efficiently be approximated by the gamma distribution $p_{\Gamma}(x)$. Based on this fact, we assume that the joint PDF $p_{\Xi\dot{\Xi}}(r, \dot{x})$ is approximately equal to the joint PDF $p_{\Gamma\dot{\Gamma}}(r, \dot{x})$ of a gamma process and its corresponding time derivative at the same time t , i.e.,

$$p_{\Xi\dot{\Xi}}(r, \dot{x}) \approx p_{\Gamma\dot{\Gamma}}(r, \dot{x}) . \tag{19}$$

A gamma distributed process is equivalent to a squared Nakagami- m distributed process [15]. Thus, applying the concept of transformation of random variables [18, p. 244], we can express the joint PDF $p_{\Gamma\dot{\Gamma}}(x, \dot{x})$ in terms of the joint PDF $p_{NN}(y, \dot{y})$ of a Nakagami- m distributed process and its corresponding time derivative at the same time t as

$$p_{\Gamma\dot{\Gamma}}(x, \dot{x}) = \frac{1}{4x} p_{NN} \left(\sqrt{x}, \frac{\dot{x}}{2\sqrt{x}} \right) . \tag{20}$$

After substituting $p_{NN}(y, \dot{y})$ as given in [31, Eq. (13)] in (20), the joint PDF $p_{\Gamma\dot{\Gamma}}(x, \dot{x})$ can be written as

$$p_{\Gamma\dot{\Gamma}}(x, \dot{x}) = \frac{1}{2\sqrt{2\pi x \hat{\sigma}} (\Omega/m)^m \Gamma(m)} x^{(m-1)} e^{-\frac{x}{(\Omega/m)} - \frac{\dot{x}^2}{8\hat{\sigma}^2 x}} \tag{21}$$

where m , Ω , and $\hat{\sigma}$ are the parameters associated with the Nakagami- m distribution. The result in (21) can be expressed in terms of the parameters of the gamma distribution, i.e., α_L and β_L , as

$$p_{\Gamma\dot{\Gamma}}(x, \dot{x}) = \frac{1}{2\sqrt{2\pi\beta x} \beta_L^{(\alpha_L+1)} \Gamma(\alpha_L+1)} x^{\alpha_L} e^{-\frac{x}{\beta_L} - \frac{\dot{x}^2}{8\beta x}} \tag{22}$$

where $\beta = 2 \left(\pi A_R \sigma_{\mu^{(1)}} \sigma_{\mu^{(2)}} \right)^2 (f_{s_{\max}}^2 + 2f_{R_{\max}}^2 + f_{D_{\max}}^2) / K$. Here, $f_{s_{\max}}$, $f_{R_{\max}}$, and $f_{D_{\max}}$ are the maximum Doppler frequencies caused by the motion of the source mobile station, mobile relays, and the destination mobile station, respectively.

Numerical investigations show that $p_{\Xi\dot{\Xi}}(r, \dot{x}) \approx \frac{1}{\sqrt{3A_R}} p_{\Gamma\dot{\Gamma}}(r, \dot{x})$. Substituting $p_{\Xi\dot{\Xi}}(r, \dot{x})$ in (18) allows us to express the LCR $N_{\Xi}(r)$ in closed form as

$$\begin{aligned} N_{\Xi}(r) &\approx \int_0^{\infty} \frac{\dot{x}}{\sqrt{3A_R}} p_{\Gamma\dot{\Gamma}}(r, \dot{x}) d\dot{x} \\ &= \sqrt{\frac{2r\beta}{3\pi A_R}} \frac{r^{\alpha_L} e^{-\frac{r}{\beta_L}}}{\beta_L^{(\alpha_L+1)} \Gamma(\alpha_L+1)} = \sqrt{\frac{2r\beta}{3\pi A_R}} p_{\Xi}(r). \end{aligned} \quad (23)$$

D. ADF of a Sum of Double Rayleigh Processes

The ADF $T_{\Xi-}(r)$ of $\Xi(t)$ is the expected value of the time intervals over which the stochastic process $\Xi(t)$ remains below a certain threshold level r . Mathematically, the ADF $T_{\Xi-}(r)$ is defined as the ratio of the CDF $F_{\Xi-}(r)$ and the LCR $N_{\Xi}(r)$ of $\Xi(t)$ [12], i.e.,

$$T_{\Xi-}(r) = \frac{F_{\Xi-}(r)}{N_{\Xi}(r)}. \quad (24)$$

By substituting (17) and (23) in (24), we can easily obtain an approximate solution for the ADF $T_{\Xi-}(r)$.

IV. NUMERICAL RESULTS

The purpose of this section is twofold. Firstly, to illustrate the important theoretical results by evaluating the expressions in (16), (17), (23), and (24). Secondly, to validate the correctness of the theoretical results with the help of simulations. The exact simulation results have been obtained by applying the sum-of-sinusoids (SOS) concept [20] on the uncorrelated Gaussian noise processes making up the received signal envelope at the output of the EG combiner. The model parameters of the channel simulator were computed by the generalized method of exact Doppler spread (GMEDS₁) [21]. Each Gaussian process $\mu^{(i)}(t)$ ($i = 1, 2, \dots, 2K$) was simulated using $N_l^{(i)} = 14$ for $i = 1, 2, \dots, 2K$ and $l = 1, 2$, where $N_l^{(i)}$ is the number of sinusoids required to simulate the inphase ($l = 1$) and quadrature components ($l = 2$) of $\mu^{(i)}(t)$. The authors of [20] have shown that with $N_l^{(i)} \geq 7$ ($l = 1, 2$), the simulated distribution of $|\mu^{(i)}(t)|$ closely approximates the Rayleigh distribution for all $i = 1, 2, \dots, 2K$. The maximum Doppler frequencies caused by the motion of the source mobile station, the mobile relays, and the destination mobile station, denoted by $f_{s_{\max}}$, $f_{R_{\max}}$, and $f_{D_{\max}}$, respectively, were set to 91 Hz, 125 Hz, and 210 Hz.

The variances $\sigma_{\mu^{(i)}}^2$ were chosen to be $\sigma_{\mu^{(i)}}^2 = 1/K \forall i = 1, 2, \dots, 2K$. The relay gains $A_{R^{(k)}}$ were selected to be unity, i.e., $A_{R^{(k)}} = A_R = 1 \forall k = 1, 2, \dots, K$ unless stated otherwise.

The results presented in Figs. E.2–E.5 show a good fitting of the approximated analytical and the exact simulation results considered as the true results. Figure E.2 illustrates the theoretical results of the PDF $p_{\Xi}(x)$ of $\Xi(t)$ described by the approximation in (16). For the purpose of validation of the theory, the simulation results obtained by evaluating the statistics of the waveforms generated by using the SOS-based channel simulator are included in Fig. E.2. The PDF $p_{\Xi}(x)$ of $\Xi(t)$ for a different number of diversity branches K , keeping the relay gain A_R constant is shown in Fig. E.2. For $K = 1$ and $A_R = 1$, the PDF $p_{\Xi}(x)$ of $\Xi(t)$ maps to the double Rayleigh distribution, confirming that our approximation in (16) is valid. Furthermore, the PDF $p_{\Xi}(x)$ of $\Xi(t)$ tends to a Gaussian distribution if K increases. This observation is in accordance with the central limit theorem (CLT) [18].

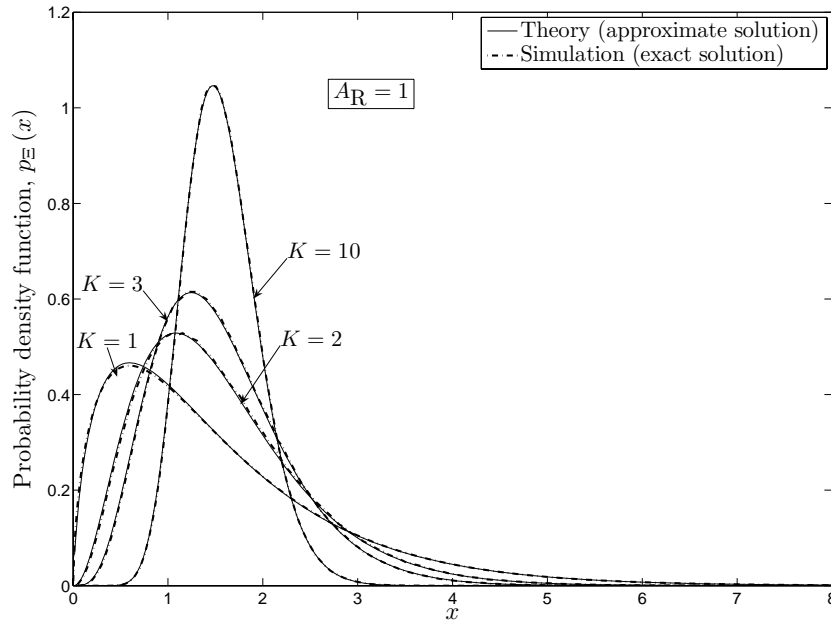


Figure E.2: The PDF $p_{\Xi}(x)$ of the received signal envelope at the output of the EG combiner $\Xi(t)$ for a different number of diversity branches K .

In Fig. E.3, the theoretical results of the CDF $F_{\Xi}(r)$ of $\Xi(t)$ described by the approximation in (17) are illustrated. Here, the CDF $F_{\Xi}(r)$ of $\Xi(t)$ for a different number of diversity branches K keeping the relay gain A_R in each branch constant is shown. A close agreement can be observed between the presented approximate solution and the exact simulation results.

The LCR $N_{\Xi}(r)$ of $\Xi(t)$ described by (23) is evaluated along with the exact simulation results in Fig. E.4. This figure illustrates the LCR $N_{\Xi}(r)$ of $\Xi(t)$ for a

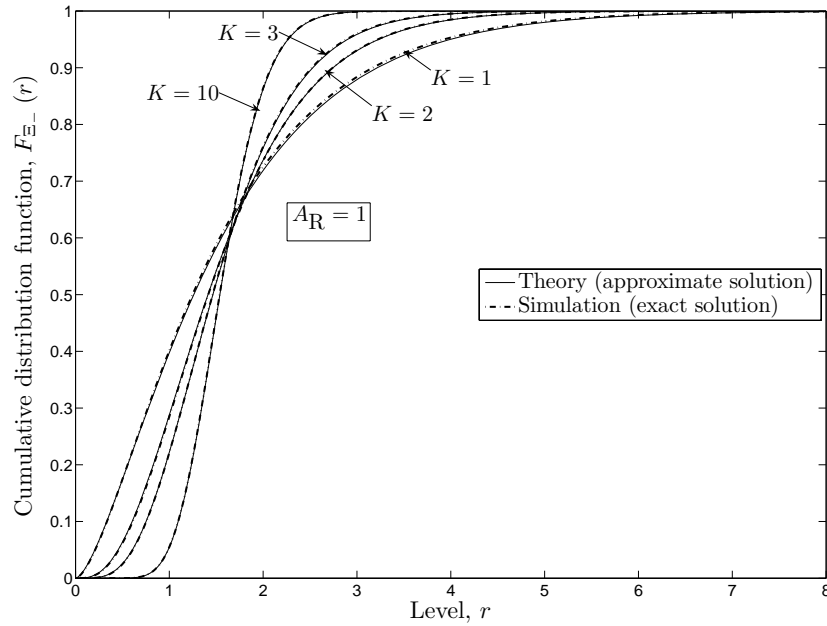


Figure E.3: The CDF $F_{\Xi_-}(r)$ of the received signal envelope at the output of the EG combiner $\Xi(t)$ for a different number of diversity branches K .

different number of diversity branches K while the relay gain A_R is kept constant. It is quite clear from the graphs that for $K = 1$ and $A_R = 1$, (23) provides us with a very close approximation to the exact LCR of a double Rayleigh distributed process given in [19]. In addition, increasing K while keeping A_R constant, result in a decrease in the LCR $N_{\Xi}(r)$ for both lower and higher signal levels r .

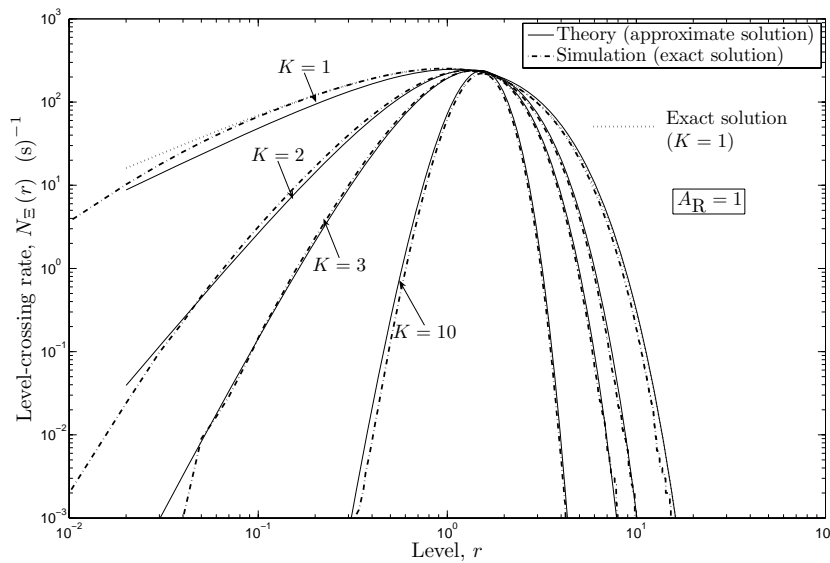


Figure E.4: The LCR $N_{\Xi}(r)$ of the received signal envelope at the output of the EG combiner $\Xi(t)$ for a different number of diversity branches K .

Figure E.5 reveals the theoretical results of the ADF $T_{\Xi_-}(r)$ of $\Xi(t)$ described by (24) along with the exact simulation results. It can be observed in Fig. E.5 that keeping the relay gain A_R constant and increasing the number of diversity branches K result in an increase of the ADF $T_{\Xi_-}(r)$ at higher values of r . However, at lower values of r , the ADF $T_{\Xi_-}(r)$ decreases with increasing K .

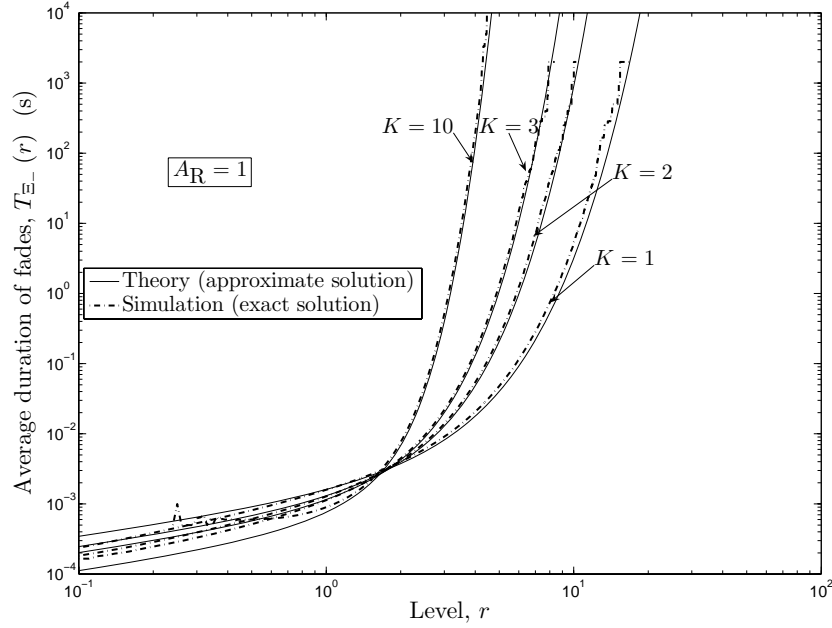


Figure E.5: The ADF $T_{\Xi_-}(r)$ of the received signal envelope at the output of the EG combiner $\Xi(t)$ for a different number of diversity branches K .

V. CONCLUSION

In this article, we have studied the statistical properties of EGC over frequency non-selective M2M fading channels under NLOS propagation conditions in a dual-hop amplify-and-forward relay network. It is assumed that K diversity branches are present between the source mobile station and the destination mobile station via K mobile relays. The received signal envelope at the output of the EG combiner has therefore been modeled as a sum of K double Rayleigh processes. Here, we have thoroughly analyzed the PDF, the CDF, the LCR, and the ADF along with the CF of this sum process. We have proposed an approximation approach using an orthogonal series expansion in the form of the Laguerre series to approximate the PDF of the sum of K double Rayleigh processes. The approximation of the target PDF using the Laguerre series makes it possible to approximate the PDF of the sum process by a gamma distribution. It has been shown that the approximation provided by the Laguerre series is remarkably good. Exploiting the properties of

the gamma distribution, the CDF, the LCR, and the ADF of the sum process are also approximated. With the help of this approximation, we are able to present simple and closed-form expressions for the aforementioned statistical quantities. Furthermore, the close agreement of the approximated theoretical results with those of the exact simulation results shows that the approximation approach followed here is valid. We have demonstrated the influence of the number of diversity branches K on the statistical properties of the received signal envelope at the output of the EG combiner. The results can easily be utilized in the performance analysis studies of EGC over relay-based M2M fading channels.

REFERENCES

- [1] A. S. Akki. Statistical properties of mobile-to-mobile land communication channels. *IEEE Trans. Veh. Technol.*, 43(4):826–831, November 1994.
- [2] P. A. Anghel and M. Kaveh. Exact symbol error probability of a cooperative network in a Rayleigh fading environment. *IEEE Trans. Wireless Commun.*, 3(5):1416–1421, September 2004.
- [3] K. Azarian, H. E. Gamal, and P. Schniter. On the achievable diversity-multiplexing tradeoff in half-duplex cooperative channels. *IEEE Trans. Inform. Theory*, 51(12):4152–4172, December 2005.
- [4] O. E. Barndorff-Nielsen and D. R. Cox. *Asymptotic Techniques for use in Statistics*. New York: Chapman and Hall, 1989.
- [5] N. C. Beaulieu and X. Dong. Level crossing rate and average fade duration of MRC and EGC diversity in Ricean fading. *IEEE Trans. Commun.*, 51(5):722–726, May 2003.
- [6] Y. Fan and J. S. Thompson. MIMO configurations for relay channels: Theory and practice. *IEEE Trans. Wireless Commun.*, 6(5):1774–1786, May 2007.
- [7] I. S. Gradshteyn and I. M. Ryzhik. *Table of Integrals, Series, and Products*. New York: Academic Press, 6th edition, 2000.
- [8] S. S. Ikki and M. H. Ahmed. Performance of cooperative diversity using equal gain combining (EGC) technique over Rayleigh fading channels. In *Proc. IEEE Int. Conf. Communications (ICC'07)*. Glasgow, Scotland, June 2007.

- [9] S. S. Ikki and M. H. Ahmed. Performance of cooperative diversity using equal gain combining (EGC) over Nakagami- m fading channels. *IEEE Trans. Wireless Commun.*, 8(2):557–562, February 2009.
- [10] R. Iskander. The characteristic function of the K -distributed interference. In *Proc. XII European Signal Processing Conf. (EUSIPCO)*, volume 1–3. Vienna, Austria, September 2004.
- [11] P. Ivanis, D. Drajić, and B. Vucetic. The second order statistics of maximal ratio combining with unbalanced branches. *IEEE Communications Letters*, 12(7):508–510, July 2008.
- [12] W. C. Jakes, editor. *Microwave Mobile Communications*. Piscataway, NJ: IEEE Press, 1994.
- [13] J. N. Laneman, D. N. C. Tse, and G. W. Wornell. Cooperative diversity in wireless networks: Efficient protocols and outage behavior. *IEEE Trans. Inform. Theory*, 50(12):3062–3080, December 2004.
- [14] R. U. Nabar, H. Bölcskei, and F. W. Kneubühler. Fading relay channels: Performance limits and space-time signal design. *IEEE J. Select. Areas Commun.*, 22(6):1099–1109, August 2004.
- [15] M. Nakagami. The m -distribution: A general formula of intensity distribution of rapid fading. In W. G. Hoffman, editor, *Statistical Methods in Radio Wave Propagation*. Oxford, UK: Pergamon Press, 1960.
- [16] A. Ord. *Families of Frequency Distributions*. London: Griffin, 1972.
- [17] R. Pabst, B. Walke, D. Schultz, et al. Relay-based deployment concepts for wireless and mobile broadband radio. *IEEE Communications Magazine*, 42(9):80–89, September 2004.
- [18] A. Papoulis and S. U. Pillai. *Probability, Random Variables and Stochastic Processes*. New York: McGraw-Hill, 4th edition, 2002.
- [19] C. S. Patel, G. L. Stüber, and T. G. Pratt. Statistical properties of amplify and forward relay fading channels. *IEEE Trans. Veh. Technol.*, 55(1):1–9, January 2006.
- [20] M. Pätzold. *Mobile Fading Channels*. Chichester: John Wiley & Sons, 2002.

- [21] M. Pätzold, C. X. Wang, and B. O. Hogstad. Two new sum-of-sinusoids-based methods for the efficient generation of multiple uncorrelated Rayleigh fading waveforms. *IEEE Trans. Wireless Commun.*, 8(6):3122–3131, June 2009.
- [22] S. Primak, V. Kontorovich, and V. Lyandres, editors. *Stochastic Methods and their Applications to Communications: Stochastic Differential Equations Approach*. Chichester: John Wiley & Sons, 2004.
- [23] S. O. Rice. Mathematical analysis of random noise. *Bell Syst. Tech. J.*, 24:46–156, January 1945.
- [24] H. Samimi and P. Azmi. An approximate analytical framework for performance analysis of equal gain combining technique over independent Nakagami, Rician and Weibull fading channels. *Wireless Personal Communications (WPC)*, 43(4):1399–1408, dec 2007. DOI 10.1007/s11277-007-9314-z.
- [25] A. Sendonaris, E. Erkip, and B. Aazhang. User cooperation diversity — Part I: System description. *IEEE Trans. Commun.*, 51(11):1927–1938, November 2003.
- [26] A. Sendonaris, E. Erkip, and B. Aazhang. User cooperation diversity — Part II: Implementation aspects and performance analysis. *IEEE Trans. Commun.*, 51(11):1939–1948, November 2003.
- [27] M. K. Simon. *Probability Distributions Involving Gaussian Random Variables: A Handbook for Engineers and Scientists*. Dordrecht: Kluwer Academic Publishers, 2002.
- [28] A. Stuart and J. K. Ord. *Kendall's Advanced Theory of Statistics*, volume I. London: Arnold, 6th edition, 1994.
- [29] B. Talha and M. Pätzold. On the statistical properties of double Rice channels. In *Proc. 10th Int. Symp. on Wireless Personal Multimedia Communications, WPMC 2007*, pages 517–522. Jaipur, India, December 2007.
- [30] W. Wongtrairat and P. Supnithi. Performance of digital modulation in double Nakagami- m fading channels with MRC diversity. *IEICE Trans. Commun.*, E92-B(2):559–566, February 2009.
- [31] M. D. Yacoub, J. E. V. Bautista, and L. G. de Rezende Guedes. On higher order statistics of the Nakagami- m distribution. *IEEE Trans. Veh. Technol.*, 48(3):790–794, May 1999.

- [32] M. D. Yacoub, C. R. C. Monterio da Silva, and J. E. V. Bautista. Second-order statistics for diversity-combining techniques in Nakagami fading channels. *IEEE Trans. Veh. Technol.*, 50(6):1464–1470, November 2001.
- [33] Q. T. Zhang. Probability of error for equal-gain combiners over Rayleigh channels: some closed-form solutions. *IEEE Trans. Commun.*, 45(3):270–273, March 1997.
- [34] D. A. Zogas, G. K. Karagiannidis, and S. A. Kotsopoulos. Equal gain combining over Nakagami- n (Rice) and Nakagami- q (Hoyt) generalized fading channels. *IEEE Trans. Wireless Commun.*, 4(2):374–379, March 2005.

Appendix F

Paper V

- Title:** On the Statistical Properties of Double Rice Channels
- Authors:** **Batool Talha** and Matthias Pätzold
- Affiliation:** University of Agder, Faculty of Engineering and Science,
P. O. Box 509, NO-4898 Grimstad, Norway
- Conference:** *Proc. 10th Int. Symp. on Wireless Personal Multimedia
Communications, WPMC 2007, Jaipur, India, Dec. 2007, pp. 517
522.*
-

On the Statistical Properties of Double Rice Channels

Batool Talha and Matthias Pätzold

Department of Information and Communication Technology
Faculty of Engineering and Science, Agder University College
Servicebox 509, NO-4876 Grimstad, Norway
E-mails: {batool.talha, matthias.paetzold}@uia.no

Abstract — In amplify-and-forward relay links, the mobile fading channel under non-line-of-sight (NLOS) conditions is usually modeled as a double Rayleigh channel. In our paper, we are taking into consideration the existence of line-of-sight (LOS) components in the amplify-and-forward relay links. As a result, we have modeled the overall mobile fading channel as a double Rice channel. The purpose of this paper is also to give analytical expressions for the main statistical quantities like the mean value, variance, probability density functions (PDF), level-crossing rate (LCR), and average duration of fades (ADF) of double Rice channels. The validity of the derived analytical expressions is confirmed by simulations.

Keywords—Cooperative diversity, amplify-and-forward relay fading channels, mobile-to-mobile channels, double Rayleigh fading, probability density function, level-crossing rate, average duration of fades.

I. INTRODUCTION

In wireless and mobile communication networks, the capacity of the entire system, its throughput, and the quality of service (QoS) are the key performance parameters. Multipath propagation and fading adversely affects these performance parameters. Thus, in order to have a better link quality, which would in turn increase the overall capacity of the system, several diversity techniques have been proposed [14]. Recently, a diversity scheme called the cooperative diversity [17, 18, 7] has gained much attention. In cooperative diversity systems, single-antenna mobiles share their antennas with other mobile antennas in the network in a so-called virtual multiple-antenna configuration [3]. Cooperative diversity protocols proposed in [7] include fixed relaying, selection relaying, and incremental relaying. Furthermore, an amplify-and-forward type of relaying that is being studied in this paper has been introduced as a fixed relaying scenario in [7]. In such a system, a relay (R) amplifies and retransmits the signal received from a transmitter (Tx) towards the destination

receiver (Rx). Depending upon the type of relay, i.e., stationary or mobile, applications of cooperative diversity schemes can be found in cellular networks and mobile ad hoc networks.

Considering NLOS propagation, the amplify-and-forward relay fading channel can be modeled in the equivalent complex baseband as a double Gaussian channel with zero mean, i.e., the product of two zero-mean complex Gaussian channels [3],[9]. Hence, the envelope of the amplify-and-forward relay fading channel follows the double Rayleigh distribution. Studies have shown [16] that such a double Rayleigh channel also results when the wave propagation is taking place via diffracting edges such as street corners in typical urban environments. Moreover, the relay channels of mobile ad hoc networks are statistically identical to mobile-to-mobile fading channels under the assumption that the distance between the transmitter and the receiver is sufficiently large [6],[11]. The PDF of the envelope of double Rayleigh fading channels is readily available in the literature [9],[6]. Unfortunately, much less information can be found for other important statistical properties like the autocorrelation function, LCR, and ADF. These properties have only been studied in [9] for amplify-and-forward relay fading channels under NLOS propagation conditions. This paper is aimed at analyzing the statistics of amplify-and-forward relay fading channels in the presence of LOS components.

Our amplify-and-forward relay fading channel is similar to that proposed in [9], which is a combination of fixed-to-mobile [5] and mobile-to-mobile channels [2]. However, the novelty in our approach is that we model the envelope of the amplify-and-forward relay fading channel as a double Rice channel, i.e., the product of two Rice channels because of the presence of a direct LOS component in both the Tx-R and R-Rx links. In this paper, we present exact expressions for the mean value and the variance of double Rice fading processes. Furthermore, integral expressions for the envelope PDF, phase PDF, LCR, and ADF of the double Rice fading process are also derived. The simulation results presented in this paper closely fit the numerical solutions of our integral expressions.

The rest of the paper is structured as follows: Some communication scenarios, where the double Rice fading comes into play, are described in Section II. In Section III, the reference model for the amplify-and-forward double Rice fading channel is developed. Section IV provides a detailed analysis of the statistical properties of double Rice fading processes. The analytical expressions presented in Section IV are verified with the help of simulations in Section V. Finally, concluding remarks are given in Section VI.

II. DOUBLE RICE FADING SCENARIOS

In this paper, we have modeled the amplify-and-forward relay fading channel under LOS conditions as the product of two non-zero-mean complex Gaussian processes. Thereby, the individual complex Gaussian processes model the fading behavior in the Tx–R and R–Rx links. The Tx–R and R–Rx links can also be termed as fixed-to-mobile [5], mobile-to-fixed [5], and mobile-to-mobile [2] channels depending upon the nature of Tx, R, and Rx used. In the following, we will briefly discuss two typical communication scenarios. In the first scenario, the overall relay fading channel is modeled as a concatenation of fixed-to-mobile and mobile-to-mobile fading channels, whereas in the second scenario, the overall mobile fading channel is considered to be a concatenation of mobile-to-fixed and fixed-to-mobile fading channels. It should be noted here that both scenarios are based on LOS propagation, thus giving rise to the double Rice fading channel.

Scenario A: Double Rice fading channel — A concatenation of fixed-to-mobile and mobile-to-mobile fading channels

In Scenario A, the overall Tx–R–Rx link corresponds to the downlink from the base station (BS) to the destination mobile station (MS) via a mobile relay (MR) as shown in Fig. F.1. Since an MR is considered in the system, the channel from the BS to the MR is analogous to the fixed-to-mobile fading channel, whereas from the MR to the MS, it is a mobile-to-mobile fading channel.

Scenario B: Double Rice fading channel — A concatenation of mobile-to-fixed and fixed-to-mobile fading channels

In Scenario B, the Tx–R and R–Rx links correspond to the uplink from the MS to the BS and the downlink from the BS to another MS, respectively, as shown in Fig. F.2. Since the BS is considered to be a stationary relay, it can be seen that the overall relay fading channel from the first MS to the second MS via the BS is a concatenation of mobile-to-fixed and fixed-to-mobile fading channels. Throughout this paper, we are dealing with Scenario A. However, for some particular results, Scenario B is also considered in the analysis.

III. THE DOUBLE RICE CHANNEL

In this section, we develop the reference model based on Scenario A discussed in Section II. We have assumed that the channel is frequency-nonselctive. Moreover, fixed gain relays are considered in our model. It should be kept in mind that we are considering the effect of the direct LOS components existing in the links from the BS to the MR and from the MR to the destination MS.

As stated for Scenario A, the channel from the BS to the MR is analogous to the

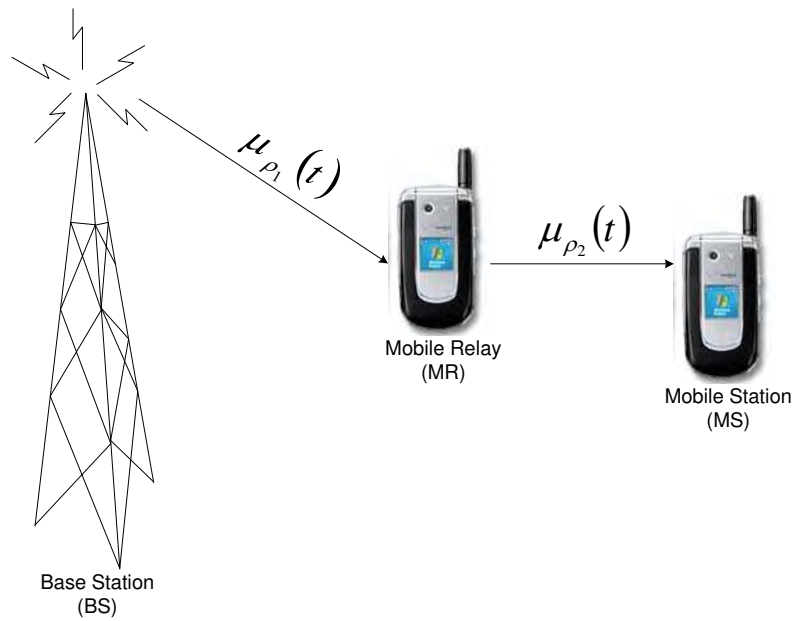


Figure F.1: Scenario A: The overall mobile fading channel as a result of a concatenation of fixed-to-mobile and mobile-to-mobile fading channels.

land mobile terrestrial (fixed-to-mobile) channel with an LOS component [5]. Let us denote the signal transmitted by the BS as $s(t)$. Then, the signal $r_1(t)$ received

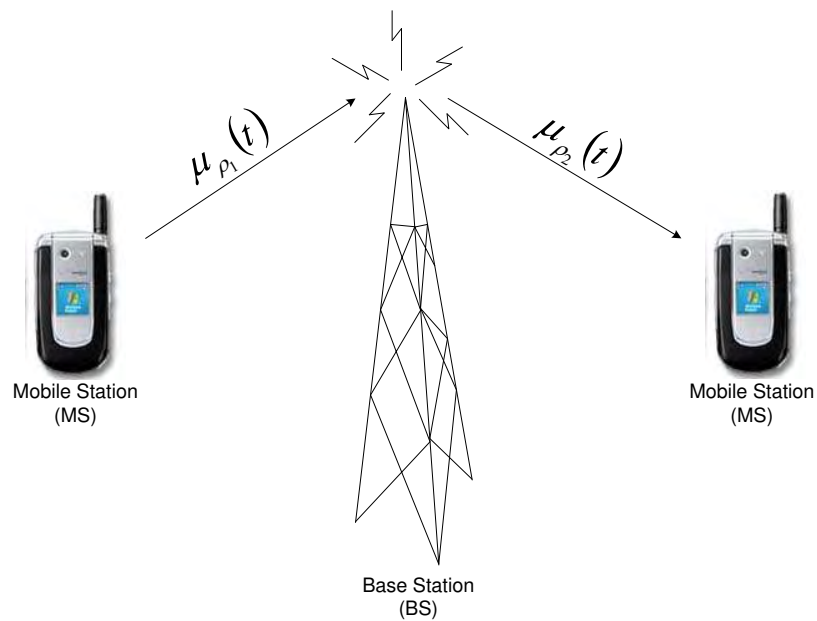


Figure F.2: Scenario B: The overall mobile fading channel as a result of a concatenation of mobile-to-fixed and fixed-to-mobile fading channels.

by the MR can be expressed as

$$r_1(t) = \mu_{\rho_1}(t) s(t) + n_1(t) \quad (1)$$

where $\mu_{\rho_1}(t)$ is a complex Gaussian process and $n_1(t)$ denotes additive white Gaussian noise (AWGN). The complex Gaussian process $\mu_{\rho_1}(t)$ models the fading channel between the BS and the MR. It represents the sum of the scattered component $\mu_1(t)$ and the LOS component $m_1(t)$, i.e., $\mu_{\rho_1}(t) = \mu_1(t) + m_1(t)$. The scattered component is modeled by a zero-mean complex Gaussian process $\mu_1(t) = \mu_{11}(t) + j\mu_{12}(t)$ with variance $2\sigma_1^2$. The LOS component $m_1(t) = \rho_1 e^{j(2\pi f_{\rho_1} t + \theta_{\rho_1})}$ has amplitude ρ_1 , Doppler frequency f_{ρ_1} , and phase θ_{ρ_1} . The Doppler frequency f_{ρ_1} is the Doppler frequency $f_{\rho_{MR}}$ of the MR, i.e., $f_{\rho_1} = f_{\rho_{MR}}$. The MR then amplifies $r_1(t)$ and retransmits it to the MS. Thus, the signal $r_2(t)$ received by the MS is

$$\begin{aligned} r_2(t) &= A\mu_{\rho_2}(t) r_1(t) + n_2(t) \\ &= A\mu_{\rho_2}(t) \mu_{\rho_1}(t) s(t) + A\mu_{\rho_2}(t) n_1(t) + n_2(t) \\ &= A\chi(t) s(t) + A\mu_{\rho_2}(t) n_1(t) + n_2(t) \end{aligned} \quad (2)$$

where A is the amplification factor, $\mu_{\rho_2}(t)$ is the second complex Gaussian process, and $n_2(t)$ denotes AWGN. Since we are dealing with fixed gain relays, the amplification factor A is a real constant. The complex Gaussian process $\mu_{\rho_2}(t)$ describes the fading channel from the MR to the MS. It is the sum of the scattered component $\mu_2(t)$ and the LOS component $m_2(t)$, i.e., $\mu_{\rho_2}(t) = \mu_2(t) + m_2(t)$. Again the scattered component is modeled as a zero-mean complex Gaussian process $\mu_2(t) = \mu_{21}(t) + j\mu_{22}(t)$ with variance $2\sigma_2^2$. The LOS component $m_2(t) = \rho_2 e^{j(2\pi f_{\rho_2} t + \theta_{\rho_2})}$ has amplitude ρ_2 , Doppler frequency f_{ρ_2} , and phase θ_{ρ_2} . It should be noted here that the Doppler frequency f_{ρ_2} corresponds to the sum of the Doppler frequencies $f_{\rho_{MR}}$ and $f_{\rho_{MS}}$ of the MR and the MS, respectively, i.e., $f_{\rho_2} = f_{\rho_{MR}} + f_{\rho_{MS}}$. Since both the MR and the MS are mobile, the transmission link between them can be modeled as a mobile-to-mobile fading channel. It can be seen in (2) that the overall channel from the BS to the destination MS via the MR can be modeled as the product of two independent complex Gaussian processes $\mu_{\rho_1}(t)$ and $\mu_{\rho_2}(t)$, i.e., $\chi(t) = \mu_{\rho_1}(t) \mu_{\rho_2}(t)$. Thus, the absolute value of $\chi(t)$ gives rise to a double Rice process

$$\eta(t) = |\chi(t)| = \xi_1(t) \xi_2(t) \quad (3)$$

where $\xi_i(t) = |\mu_{\rho_i}(t)|$ ($i = 1, 2$) denotes the classical Rice process [15].

IV. ANALYSIS OF THE DOUBLE RICE CHANNEL

In this section, we present the analytical expressions for the statistical properties of the double Rice channel introduced in Section III.

A. Mean Value and Variance

In our double Rice fading channel model, we have assumed that the two underlying classical Rice processes are statistically independent. Therefore, the expected value $E\{\eta(t)\}$ of the double Rice process $\eta(t)$ is the product of the expected values of the individual Rice processes $\xi_1(t)$ and $\xi_2(t)$ [8], i.e.,

$$E\{\eta(t)\} = E\{\xi_1(t)\}E\{\xi_2(t)\} \quad (4)$$

where $E\{\cdot\}$ denotes the expected value operator.

After substituting the mean values $E\{\xi_i(t)\}$ ($i = 1, 2$) of the individual Rice processes [19] in (4), the final expression for the mean value of the double Rice process $\eta(t)$ can be given as

$$E\{\eta(t)\} = \frac{\sigma_1\sigma_2}{2}\pi {}_1F_1\left(-\frac{1}{2}; 1; -\frac{\rho_1^2}{2\sigma_1^2}\right) {}_1F_1\left(-\frac{1}{2}; 1; -\frac{\rho_2^2}{2\sigma_2^2}\right) \quad (5)$$

where ${}_1F_1\left(-\frac{1}{2}; 1; -\frac{\rho_i^2}{2\sigma_i^2}\right)$ is the hypergeometric function [4, eq. (9.14.1)]

$${}_1F_1\left(-\frac{1}{2}; 1; -\frac{\rho_i^2}{2\sigma_i^2}\right) = e^{-\frac{\rho_i^2}{4\sigma_i^2}} \left[\left(1 + \frac{\rho_i^2}{2\sigma_i^2}\right) I_0\left(\frac{\rho_i^2}{4\sigma_i^2}\right) + \frac{\rho_i^2}{2\sigma_i^2} I_1\left(\frac{\rho_i^2}{4\sigma_i^2}\right) \right], i = 1, 2 \quad (6)$$

In (6), $I_0(\cdot)$ and $I_1(\cdot)$ denote the zeroth and the first order modified Bessel function of the first kind, respectively.

The variance $\text{Var}\{\eta(t)\}$ of the double Rice process $\eta(t)$ can be expressed as the difference of its mean power $E\{\eta^2(t)\}$ and its squared mean value $[E\{\eta(t)\}]^2$ [8], i.e.,

$$\text{Var}\{\eta(t)\} = E\{\eta^2(t)\} - [E\{\eta(t)\}]^2. \quad (7)$$

The assumption that the two Rice processes $\xi_1(t)$ and $\xi_2(t)$ are statistically independent allows us to write $E\{\eta^2(t)\} = E\{\xi_1^2(t)\}E\{\xi_2^2(t)\}$. Thus, using the expression of the mean power $E\{\xi_i^2(t)\}$ ($i = 1, 2$) of the classical Rice process given in [19], enables us to compute the mean power of the double Rice process $\eta(t)$ as

$$E\{\eta^2(t)\} = 4\sigma_1^2\sigma_2^2 {}_1F_1\left(-1; 1; -\frac{\rho_1^2}{2\sigma_1^2}\right) {}_1F_1\left(-1; 1; -\frac{\rho_2^2}{2\sigma_2^2}\right) \quad (8)$$

where the hypergeometric function ${}_1F_1\left(-1; 1; -\frac{\rho_i^2}{2\sigma_i^2}\right)$ can be expanded as [4, eq. (9.14.1)]

$${}_1F_1\left(-1; 1; -\frac{\rho_i^2}{2\sigma_i^2}\right) = 1 + \frac{\rho_i^2}{2\sigma_i^2}, i = 1, 2. \quad (9)$$

Hence, using (9) and substituting (8) and (5) in (7) results in

$$\begin{aligned} \text{Var}\{\eta(t)\} = & -\left(\sigma_1\sigma_2\frac{\pi}{2}\right)^2 \left[{}_1F_1\left(-\frac{1}{2}; 1; -\frac{\rho_1^2}{2\sigma_1^2}\right){}_1F_1\left(-\frac{1}{2}; 1; -\frac{\rho_2^2}{2\sigma_2^2}\right)\right]^2 \\ & + 4\sigma_1^2\sigma_2^2 \left(1 + \frac{\rho_1^2}{2\sigma_1^2}\right) \left(1 + \frac{\rho_2^2}{2\sigma_2^2}\right). \end{aligned} \quad (10)$$

Note that the expressions for the mean value (5) and the variance (10) of the double Rice process $\eta(t)$ are equally valid for both Scenarios A and B.

B. Probability Density Function of the Envelope and Phase

The PDF $p_\eta(z)$ of the envelope of the double Rice process $\eta(t)$ can be derived using the relation [8]

$$p_\eta(z) = \int_{-\infty}^{\infty} \frac{1}{|y|} p_{\xi_1\xi_2}\left(\frac{z}{y}, y\right) dy \quad (11)$$

where $p_{\xi_1\xi_2}(x, y)$ is the joint PDF of the envelopes $\xi_1(t)$ and $\xi_2(t)$ at the same time t . Taking into account that the two Rice processes $\xi_1(t)$ and $\xi_2(t)$ are statistically independent allows us to write $p_{\xi_1\xi_2}(x, y) = p_{\xi_1}(x) \cdot p_{\xi_2}(y)$. Thus, using the PDF of the classical Rice process (see, e.g., [15], [8]), (11) can be written as follows

$$p_\eta(z) = \frac{z}{\sigma_1^2\sigma_2^2} \int_0^{\infty} \frac{1}{y} e^{-\frac{(z/y)^2 + \rho_1^2}{2\sigma_1^2}} e^{-\frac{y^2 + \rho_2^2}{2\sigma_2^2}} I_0\left(\frac{z\rho_1}{y\sigma_1^2}\right) I_0\left(\frac{y\rho_2}{\sigma_2^2}\right) dy, z \geq 0. \quad (12)$$

It should be noted that the envelope of the double Rice process follows the distribution given in (12) for both Scenarios A and B.

Considering the special case when $\rho_i = 0$ ($i = 1, 2$), then the PDF of the double Rice process given in (12) reduces to the PDF of the double Rayleigh process [6], i.e.,

$$p_\eta(z) = \frac{z}{\sigma_1^2\sigma_2^2} K_0\left(\frac{z}{\sigma_1\sigma_2}\right), z \geq 0 \quad (13)$$

where $K_0(\cdot)$ is the zeroth order modified Bessel function of the second kind.

The PDF of the phase $p_\vartheta(\theta)$ of the double Rice process $\eta(t)$ can be derived

using the relation [8]

$$p_{\vartheta}(\theta) = \int_{-\infty}^{\infty} p_{\vartheta_1\vartheta_2}(\theta - \psi, \psi) d\psi \quad (14)$$

where $p_{\vartheta_1\vartheta_2}(\nu, \psi)$ is the joint PDF of the phase of $\mu_{\rho_1}(t)$ and $\mu_{\rho_2}(t)$ at the same time t . Since $\mu_{\rho_1}(t)$ and $\mu_{\rho_2}(t)$ are statistically independent, it follows that the phase processes $\vartheta_1(t) = \arg\{\mu_{\rho_1}(t)\}$ and $\vartheta_2(t) = \arg\{\mu_{\rho_2}(t)\}$ are also statistically independent, i.e., $p_{\vartheta_1\vartheta_2}(\nu, \psi) = p_{\vartheta_1}(\nu) \cdot p_{\vartheta_2}(\psi)$. Thus, using the PDF of the phase of the classical Rice process defined in [15], (14) can be written as follows

$$p_{\vartheta}(\theta; t) = \frac{1}{(2\pi)^2} e^{-\frac{\rho_1^2}{2\sigma_1^2}} e^{-\frac{\rho_2^2}{2\sigma_2^2}} \int_{-\pi}^{\pi} P_1(\nu_1(\theta, \psi), f_{\rho_1}) P_2(\nu_2(\theta, \psi), f_{\rho_2}) d\psi \quad (15)$$

for $-\pi < \theta \leq \pi$, where

$$P_i(\nu_i(\theta, \psi), f_{\rho_i}) = 1 + \sqrt{\pi} L_i(\nu_i(\theta, \psi), f_{\rho_i}) e^{L_i^2(\nu_i(\theta, \psi), f_{\rho_i})} [1 + \Phi(\nu_i(\theta, \psi), f_{\rho_i})] \quad (16)$$

$$L_i(\nu_i(\theta, \psi), f_{\rho_i}) = \frac{\rho_i}{\sqrt{2}\sigma_i} \cos(\nu_i - 2\pi f_{\rho_i} t - \theta_{\rho_i}) \quad (17)$$

$$\nu_i = \begin{cases} \theta - \psi & \text{if } i = 1, \\ \psi & \text{if } i = 2. \end{cases} \quad (18)$$

In (16), $\Phi(\cdot)$ is the error function [4, eq. (8.250.1)].

Replacing f_{ρ_1} and f_{ρ_2} with the Doppler frequencies $f_{\rho_{MS_1}}$ and $f_{\rho_{MS_2}}$ associated with the LOS component of the first MS and the second MS, respectively, makes it possible to use (15) for Scenario B.

It is interesting to note that for $\rho_i = 0$ ($i = 1, 2$), the PDF given in (15) reduces to the PDF of the phase of the double Rayleigh process and the classical Rice process, which is a uniform distribution

$$p_{\vartheta}(\theta) = \frac{1}{2\pi}, \quad -\pi < \theta \leq \pi. \quad (19)$$

C. Level-Crossing Rate

The rate at which the double Rice process $\eta(t)$ crosses a given level r from up to down or vice versa defines the LCR $N_{\eta}(r)$. The expression for the LCR can be

obtained by using [15]

$$N_{\eta}(r) = \int_0^{\infty} \dot{z} p_{\eta\dot{\eta}}(r, \dot{z}) d\dot{z} \quad (20)$$

where $p_{\eta\dot{\eta}}(z, \dot{z})$ is the joint PDF of the double Rice process $\eta(t)$ and its corresponding time derivative $\dot{\eta}(t)$ at the same time t . The joint PDF $p_{\eta\dot{\eta}}(z, \dot{z})$ can be derived using the relation [13]

$$p_{\eta\dot{\eta}}(z, \dot{z}) = \int_{-\infty}^{\infty} \int_{-\infty}^{\infty} \frac{1}{y^2} p_{\xi_1 \dot{\xi}_1} \left(\frac{z}{y}, \frac{\dot{z}}{y} - \frac{z}{y^2} \dot{y} \right) p_{\xi_2 \dot{\xi}_2}(y, \dot{y}) dy \dot{y}, \quad z \geq 0, |\dot{z}| < \infty \quad (21)$$

where $p_{\xi_i \dot{\xi}_i}(x, \dot{x})$ ($i = 1, 2$) denotes the joint PDF of the classical Rice process $\xi_i(t)$ and its time derivative $\dot{\xi}_i(t)$ at the same time t . The integral expression for the joint PDF $p_{\xi_i \dot{\xi}_i}(x, \dot{x})$ ($i = 1, 2$) can be found in the literature (see, e.g., [10]). Thus, substituting this integral expression in (21) and doing some lengthy computations results in

$$p_{\eta\dot{\eta}}(z, \dot{z}) = \frac{z}{(2\pi)^{\frac{5}{2}} \sigma_1^2 \sigma_2^2} \int_0^{\infty} \frac{1}{\sqrt{\beta_1 y^4 + \beta_2 z^2}} e^{-\frac{(z/y)^2 + \rho_1^2}{2\sigma_1^2} - \frac{y^2 + \rho_2^2}{2\sigma_2^2}} \int_{-\pi}^{\pi} e^{\frac{(z/y)\rho_1 \cos \theta_1}{\sigma_1^2}} \int_{-\pi}^{\pi} e^{\frac{y\rho_2 \cos \theta_2}{\sigma_2^2}} \times e^{-\frac{1}{2}K^2(z, y, \theta_1, \theta_2)} e^{-\frac{(y\dot{z})^2}{2(\beta_1 y^4 + \beta_2 z^2)}} e^{-\frac{y\dot{z}}{\sqrt{\beta_1 y^4 + \beta_2 z^2}} K(z, y, \theta_1, \theta_2)} d\theta_2 d\theta_1 dy \quad (22)$$

for $z \geq 0, |\dot{z}| < \infty$, where

$$K(z, y, \theta_1, \theta_2) = \frac{y^2 \sqrt{2\beta_1} \alpha_1 \rho_1 \sin \theta_1 + z \sqrt{2\beta_2} \alpha_2 \rho_2 \sin \theta_2}{\sqrt{\beta_1 y^4 + \beta_2 z^2}} \quad (23)$$

$$\alpha_1 = \frac{2\pi f_{\rho_1}}{\sqrt{2\beta_1}}, \quad \alpha_2 = \frac{2\pi f_{\rho_2}}{\sqrt{2\beta_2}}, \quad (24a, b)$$

$$\beta_1 = 2(\sigma_1 \pi f_{\max_1})^2, \quad \beta_2 = 2(\sigma_2 \pi)^2 (f_{\max_1}^2 + f_{\max_2}^2). \quad (25a, b)$$

In (25a,b), the symbols f_{\max_1} and f_{\max_2} denote the maximum Doppler frequency of the MR and the MS, respectively. It should be noted here that under isotropic scattering conditions, β_i ($i = 1, 2$) corresponds to the negative curvature of the autocorrelation function of the inphase and quadrature components of $\mu_{\rho_i}(t)$ ($i = 1, 2$) at the origin. Furthermore, β_1 is the characteristic quantity corresponding to a fixed-to-mobile fading process [5], whereas β_2 is indicating a mobile-to-mobile fading process [1].

Finally, after substituting (22) in (20) and doing some extensive mathematical

manipulations, the LCR $N_\eta(r)$ of the double Rice process $\eta(t)$ can be expressed as follows

$$N_\eta(r) = \frac{r/(2\pi)^{\frac{5}{2}}}{\sigma_1^2 \sigma_2^2} \int_0^\infty \frac{dy}{y} \sqrt{\beta_1 y^2 + \beta_2 (r/y)^2} e^{-\frac{(r/y)^2 + \rho_1^2}{2\sigma_1^2}} e^{-\frac{y^2 + \rho_2^2}{2\sigma_2^2}} \int_{-\pi}^{\pi} d\theta_1 e^{\frac{(r/y)\rho_1 \cos \theta_1}{\sigma_1^2}} \int_{-\pi}^{\pi} d\theta_2 e^{\frac{y\rho_2 \cos \theta_2}{\sigma_2^2}} e^{-\frac{1}{2}K^2(r,y,\theta_1,\theta_2)} \left(1 + \sqrt{\frac{\pi}{2}} K(r,y,\theta_1,\theta_2) e^{\frac{1}{2}K^2(r,y,\theta_1,\theta_2)} \left\{ 1 + \Phi\left(\frac{K(r,y,\theta_1,\theta_2)}{2}\right) \right\} \right) \quad (26)$$

where $K(\cdot, \cdot, \cdot, \cdot)$ is the function defined in (23). The quantities α_1 , α_2 and β_1 , β_2 are the same as those given in (24a,b) and (25a,b), respectively.

It is important to mention here that (26) is a valid expression for both Scenarios A and B. However, for Scenario B, the quantities α_1 , α_2 and β_1 , β_2 are given as follows

$$\alpha_1 = \frac{2\pi f_{\rho_{MS1}}}{\sqrt{2\beta_1}}, \quad \alpha_2 = \frac{2\pi f_{\rho_{MS2}}}{\sqrt{2\beta_2}}, \quad (27a,b)$$

$$\beta_1 = 2(\sigma_1 \pi f_{\max_1})^2, \quad \beta_2 = 2(\sigma_2 \pi f_{\max_2})^2 \quad (28a,b)$$

where $f_{\rho_{MS1}}$ and $f_{\rho_{MS2}}$ are the Doppler frequencies of the LOS component associated with the first and the second MS, respectively. Similarly, f_{\max_1} and f_{\max_2} are the maximum Doppler frequencies of the first and the second MS, respectively. Note that both β_1 and β_2 in (28a,b) are the characteristic quantities corresponding to the fixed-to-mobile (or vice versa) fading channels in isotropic scattering environments.

Considering the special case when $\rho_i = 0$ ($i = 1, 2$), then (26) reduces to the LCR of the double Rayleigh process given in [9] as

$$N_\eta(r) = \frac{r}{\sqrt{2\pi} \sigma_1^2 \sigma_2^2} \int_0^\infty \frac{1}{y} \sqrt{\beta_1 y^2 + \beta_2 (r/y)^2} e^{-\frac{(r/y)^2}{2\sigma_1^2}} e^{-\frac{y^2}{2\sigma_2^2}} dy. \quad (29)$$

D. Average Duration of Fades

Apart from the mean value, variance, PDF, and LCR, the ADF is another important statistical property describing the fading behavior of a stochastic process. The ADF is defined as the expected value of the length of the time intervals in which the stochastic process is below a given level r [15].

Considering the double Rice process $\eta(t)$, the ADF $T_{\eta_-}(r)$ can be expressed using the relation [15]

$$T_{\eta_-}(r) = \frac{F_{\eta_-}(r)}{N_\eta(r)} \quad (30)$$

where $F_{\eta_-}(r)$ is the cumulative distribution function (CDF), and $N_{\eta}(r)$ is the LCR of the double Rice process $\eta(t)$ [see (26)]. The CDF $F_{\eta_-}(r)$ of the double Rice process $\eta(t)$ can be written as

$$F_{\eta_-}(r) = 1 - \int_0^{\infty} Q_1\left(\frac{\rho_1}{\sigma_1}, \frac{r}{y\sigma_1}\right) p_{\xi}(y) dy, \quad r \geq 0 \quad (31)$$

where $Q_m(a, b)$ is the Marcum Q-function, which is defined as follows [10]

$$Q_m(a, b) = \int_b^{\infty} z \left(\frac{z}{a}\right)^{m-1} e^{-\frac{z^2+a^2}{2}} I_{m-1}(az) dz \quad (32)$$

and $p_{\xi}(y)$ is the PDF of the classical Rice process.

Finally, substituting (31) and (26) in (30) gives the ADF $T_{\eta_-}(r)$ of the double Rice process $\eta(t)$.

For the special case where $\rho_i = 0$ ($i = 1, 2$), the CDF given in (31) reduces to the CDF of the double Rayleigh process [6]

$$F_{\eta_-}(r) = 1 - \frac{r}{\sigma_1\sigma_2} K_1\left(\frac{r}{\sigma_1\sigma_2}\right), \quad r \geq 0 \quad (33)$$

where $K_1(\cdot)$ is the first order modified Bessel function of the second kind. Thus, the ADF given in (30) can easily be reduced to the ADF of the double Rayleigh process using (33) and (29).

V. NUMERICAL RESULTS

The validity of the analytical expressions presented in Section IV is confirmed by simulations in the current section. Using the sum-of-sinusoids model [10], uncorrelated complex Gaussian processes that make up the overall double Rice process are simulated. The parameters of the simulation model are designed using the generalized method of exact Doppler spread (GMEDS_q) proposed in [12] with $q = 1$, i.e., GMEDS₁. The number of sinusoids (N_1 and N_2) considered in the GMEDS₁ is $N_1 = N_2 = 20$. The maximum Doppler frequency f_{\max_1} of the MR is taken to be 91 Hz, whereas that of the MS (i.e., f_{\max_2}) is equal to 125 Hz. Furthermore, the amplitudes ρ_1 and ρ_2 of the LOS components are considered to be equal, i.e., $\rho_1 = \rho_2 = \rho$ unless stated otherwise.

The results presented in Figs. F.3–F.8 show an excellent fitting of the analytical and simulation results. In Fig. F.3, a comparison of the envelope PDF $p_{\eta}(z)$ of the double Rice process $\eta(t)$ and that of the classical Rice process $\xi(t)$ is presented for

different values of ρ , keeping $f_{\rho_{MR}}$ and $f_{\rho_{MS}}$ constant equal to zero. A few cases for which $\rho_1 \neq \rho_2 \neq \rho$ are also included in Fig. F.3. For $\rho = 0$, it can be seen that the PDF of the double Rice process $\eta(t)$ is following the PDF of the double Rayleigh process. Furthermore, the PDFs corresponding to the classical Rice process $\xi(t)$ have higher maxima and narrower spreads as compared to those of the double Rice process $\eta(t)$ for same value of ρ . Similarly, Fig. F.4 compares the phase PDF $p_{\vartheta}(\theta)$ of the double Rice process $\eta(t)$ with the phase PDF of the classical Rice process $\xi(t)$ for different values of ρ , where $f_{\rho_{MR}}$ and $f_{\rho_{MS}}$ are kept to zero. Figures F.5 and F.6 correspond to the study of the LCR of the double Rice process $\eta(t)$. It is evident from these figures that the spread of the LCR of the double Rice process $\eta(t)$ increases with the increase of ρ . A similar trend can be observed when unequal amplitudes of the LOS components, i.e., $\rho_1 \neq \rho_2 \neq \rho$ are considered. On the other hand, keeping ρ constant and changing $f_{\rho_{MR}}$ and $f_{\rho_{MS}}$, produces a visible difference in the maximum of the LCR. The spread of the LCR is also changed in this case. Finally, some plots of the ADF for different values of ρ , $f_{\rho_{MR}}$, and $f_{\rho_{MS}}$ are presented in Figs. F.7 and F.8, respectively.

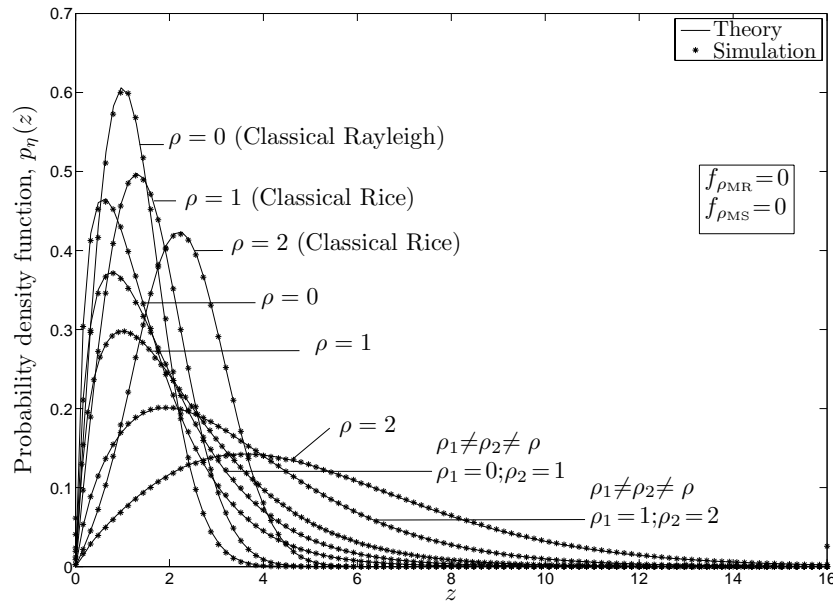


Figure F.3: The PDF $p_{\eta}(z)$ of the envelope of the double Rice process $\eta(t)$.

VI. CONCLUSION

In this paper, we have described two different scenarios where double Rice fading comes into play. It has been shown that such a fading channel can be modeled as a product of fixed-to-mobile and mobile-to-mobile Rice channels. On the other

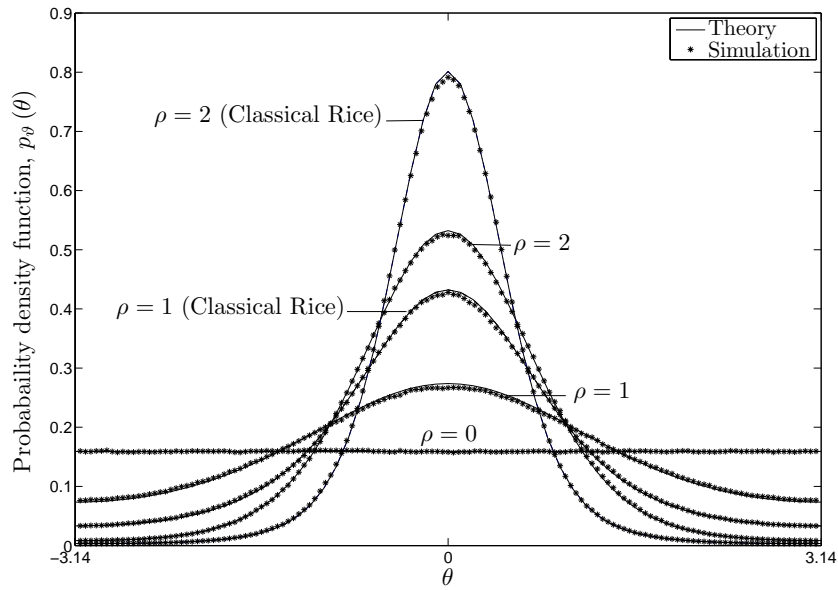


Figure F.4: The PDF $p_{\vartheta}(\theta)$ of the phase of the double Rice process $\eta(t)$.

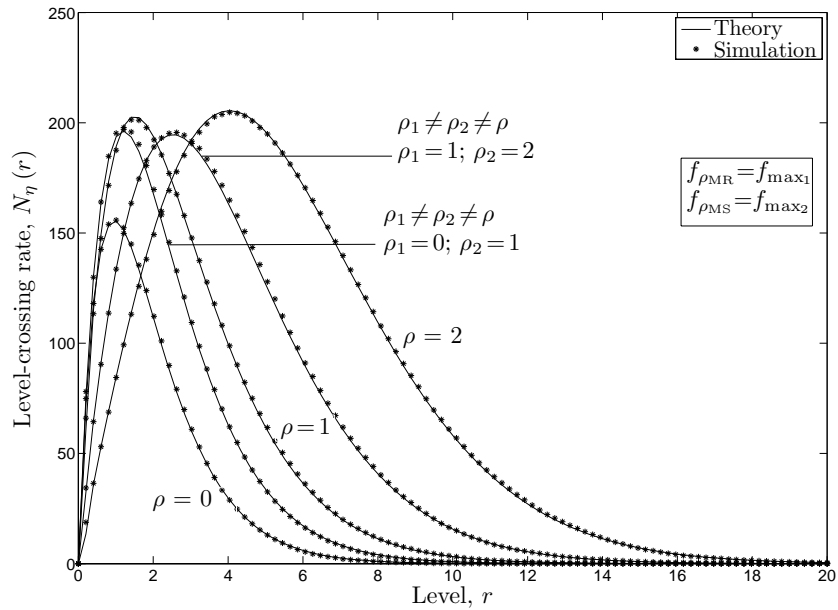


Figure F.5: The LCR $N_{\eta}(r)$ of the double Rice process $\eta(t)$ for various values of ρ .

hand, it can also be considered as the concatenation of mobile-to-fixed and fixed-to-mobile Rice channels.

We have thoroughly studied the statistical properties of double Rice fading channels. The statistical properties investigated include the mean value, variance, envelope PDF, phase PDF, LCR, and ADF. We have shown that our expressions are valid for the two types of double Rice fading scenarios discussed in this paper.

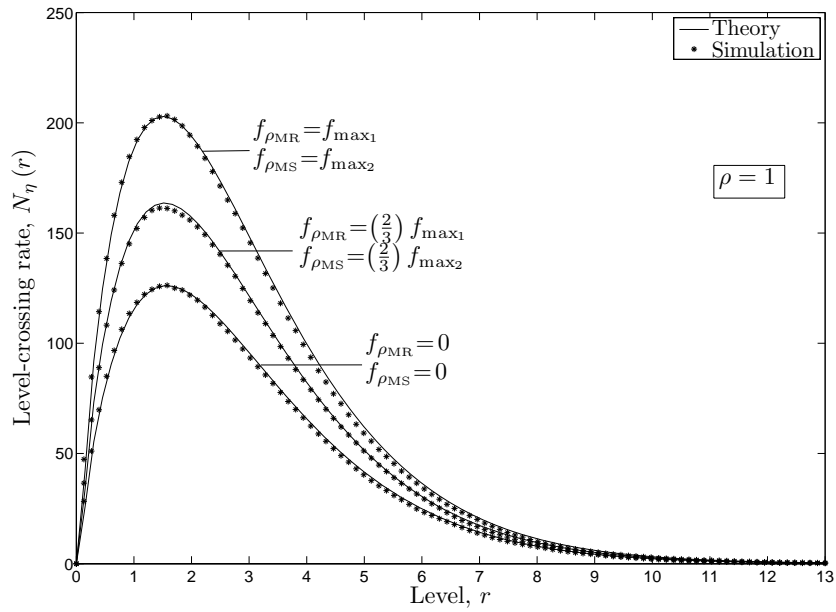


Figure F.6: The LCR $N_{\eta}(r)$ of the double Rice process $\eta(t)$ for various values of $f_{\rho_{MR}}$ and $f_{\rho_{MS}}$.

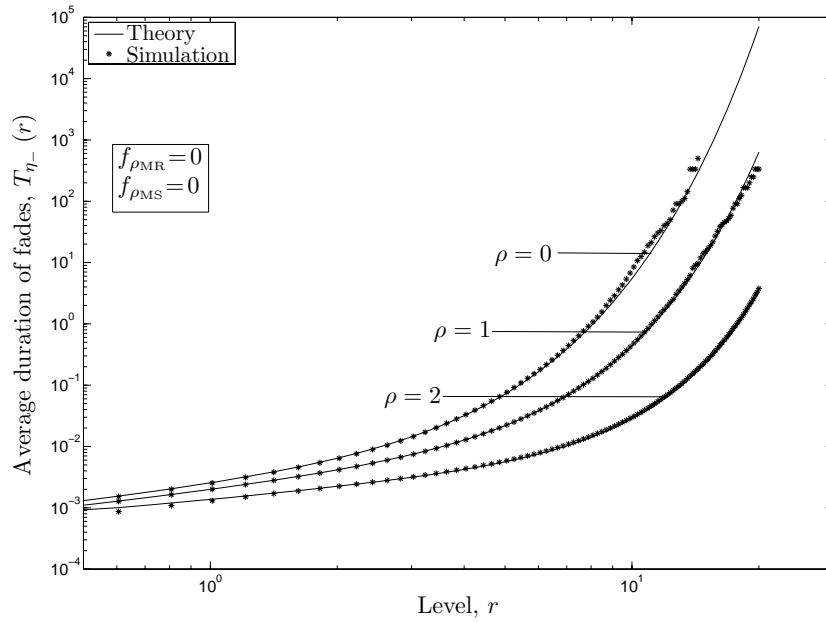


Figure F.7: The ADF $T_{\eta-}(r)$ of the double Rice process $\eta(t)$ for various values of ρ .

All numerical solutions of the integral expressions of the PDFs (envelope and phase), LCR, and ADF were verified through simulation. The obtained simulation results show that theory and simulation are in accordance with each other. The results presented in this paper provide sufficient evidence that the properties of the

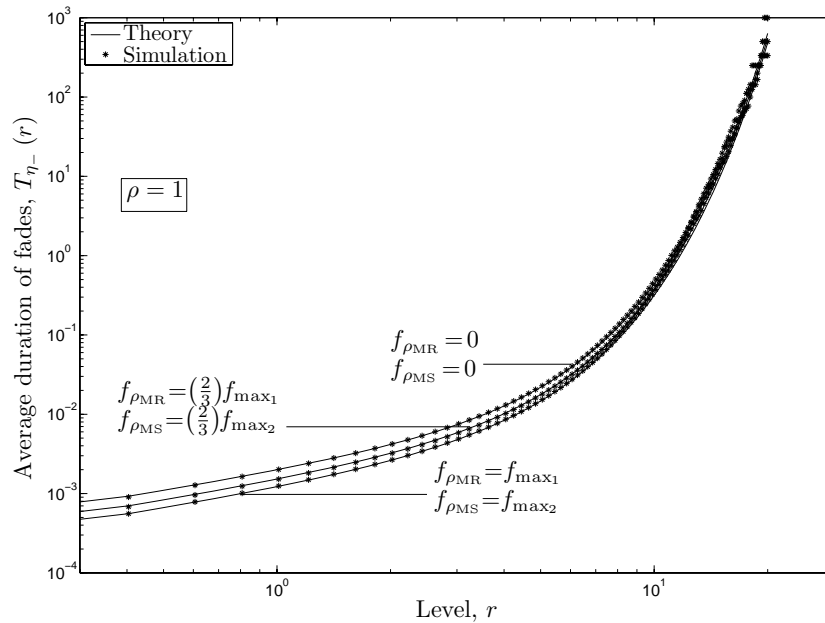


Figure F.8: The ADF $T_{\eta_-}(r)$ of the double Rice process $\eta(t)$ for various values of $f_{\rho_{MR}}$ and $f_{\rho_{MS}}$.

double Rice fading channels are quite different from the classical Rice fading channels. Furthermore, we have shown that the double Rice distribution reduces to the double Rayleigh distribution when the LOS component is set to zero.

REFERENCES

- [1] A. S. Akki. Statistical properties of mobile-to-mobile land communication channels. *IEEE Trans. Veh. Technol.*, 43(4):826–831, November 1994.
- [2] A. S. Akki and F. Haber. A statistical model of mobile-to-mobile land communication channel. *IEEE Trans. Veh. Technol.*, 35(1):2–7, February 1986.
- [3] M. Dohler. *Virtual Antenna Arrays*. Ph.D. dissertation, King’s College, London, United Kingdom, 2003.
- [4] I. S. Gradshteyn and I. M. Ryzhik. *Tables of Series, Products, and Integrals*, volume I and II. Frankfurt: Harri Deutsch, 5th edition, 1981.
- [5] W. C. Jakes, editor. *Microwave Mobile Communications*. Piscataway, NJ: IEEE Press, 1994.
- [6] I. Z. Kovacs, P. C. F. Eggers, K. Olesen, and L. G. Petersen. Investigations of outdoor-to-indoor mobile-to-mobile radio communication channels. In *Proc.*

- IEEE 56th Veh. Technol. Conf., VTC'02-Fall*, volume 1, pages 430–434. Vancouver BC, Canada, September 2002.
- [7] J. N. Laneman, D. N. C. Tse, and G. W. Wornell. Cooperative diversity in wireless networks: Efficient protocols and outage behavior. *IEEE Trans. Inform. Theory*, 50(12):3062–3080, December 2004.
- [8] A. Papoulis and S. U. Pillai. *Probability, Random Variables and Stochastic Processes*. New York: McGraw-Hill, 4th edition, 2002.
- [9] C. S. Patel, G. L. Stüber, and T. G. Pratt. Statistical properties of amplify and forward relay fading channels. *IEEE Trans. Veh. Technol.*, 55(1):1–9, January 2006.
- [10] M. Pätzold. *Mobile Fading Channels*. Chichester: John Wiley & Sons, 2002.
- [11] M. Pätzold and B. O. Hogstad. Design and performance of MIMO channel simulators derived from the two-ring scattering model. In *Proc. 14th IST Mobile & Communications Summit, IST 2005*. Dresden, Germany, June 2005. paper no. 121.
- [12] M. Pätzold and B. O. Hogstad. Two new methods for the generation of multiple uncorrelated Rayleigh fading waveforms. In *Proc. IEEE 63rd Semi-annual Veh. Tech. Conf., VTC'06-Spring*, volume 6, pages 2782–2786. Melbourne, Australia, May 2006.
- [13] M. Pätzold, U. Killat, and F. Laue. An extended Suzuki model for land mobile satellite channels and its statistical properties. *IEEE Trans. Veh. Technol.*, 47(2):617–630, May 1998.
- [14] T. S. Rappaport. *Wireless Communications: Principles and Practice*. Upper Saddle River, New Jersey: Prentice-Hall, 2nd edition, 1996.
- [15] S. O. Rice. Mathematical analysis of random noise. *Bell Syst. Tech. J.*, 24:46–156, January 1945.
- [16] J. Salo, H. M. El-Sallabi, and P. Vainikainen. Impact of double-rayleigh fading on system performance. In *Proc. 1st IEEE Int. Symp. on Wireless Pervasive Computing, ISWPC 2006*. Phuket, Thailand, January 2006. 0-7803-9410-0/10.1109/ISWPC.2006.1613574.

- [17] A. Sendonaris, E. Erkip, and B. Aazhang. User cooperation diversity — Part I: System description. *IEEE Trans. Commun.*, 51(11):1927–1938, November 2003.
- [18] A. Sendonaris, E. Erkip, and B. Aazhang. User cooperation diversity — Part II: Implementation aspects and performance analysis. *IEEE Trans. Commun.*, 51(11):1939–1948, November 2003.
- [19] D. Wolf, T. Munakata, and J. Wehhofer. Die Verteilungsdichte der Pegelunterschreitungszeitintervalle bei Rayleigh-Fadingkanälen. *NTG-Fachberichte 84*, pages 23–32, 1983.

Appendix G

Paper VI

Title: Statistical Modeling and Analysis of Mobile-to-Mobile Fading Channels in Cooperative Networks Under Line-of-Sight Conditions

Authors: **Batool Talha** and Matthias Pätzold

Affiliation: University of Agder, Faculty of Engineering and Science, P. O. Box 509, NO-4898 Grimstad, Norway

Journal: *Wireless Personal Communications, Special Issue on “Wireless Future”*, 2009. DOI10.1007/s11277-009-9721-4.

Statistical Modeling and Analysis of Mobile-to-Mobile Fading Channels in Cooperative Networks Under Line-of-Sight Conditions

Batool Talha and Matthias Pätzold

Department of Information and Communication Technology
Faculty of Engineering and Science, Agder University College
Servicebox 509, NO-4876 Grimstad, Norway
E-mails: {batool.talha, matthias.paetzold}@uia.no

Abstract — Recently, mobile-to-mobile (M2M) cooperative network technology has gained considerable attention for its promise of enhanced system performance with increased mobility support. As this is a new research field, little is known about the statistical properties of M2M fading channels in cooperative networks. So far, M2M fading channels have mainly been modeled under the assumption of non-line-of-sight (NLOS) conditions. In this paper¹, we propose a new model for M2M fading channels in amplify-and-forward relay links, where it is assumed that a line-of-sight (LOS) component exists in the direct link between the source mobile station and the destination mobile station. Analytical expressions will be derived for the main statistical quantities of the channel envelope, such as the mean value, variance, probability density function (PDF), level-crossing rate (LCR), and average duration of fades (ADF) as well as the channel phase. Our results show that the statistical properties of the proposed M2M channel are quite different from those of double Rayleigh and double Rice channels. In addition, a high-performance channel simulator will be presented for the new M2M channel model. The developed channel simulator is used to confirm the correctness of all obtained theoretical results by simulations.

Keywords—Mobile-to-mobile fading channels, cooperative networks, amplify-and-forward relaying, channel modeling, level-crossing rate, average duration of fades.

¹The material in this paper is based on “On the Statistical Properties of Mobile-to-Mobile Fading Channels in Cooperative Networks Under Line-of-Sight Conditions”, by Batool Talha and Matthias Pätzold which appeared in the proceedings of the 10th International Symposium on Wireless Personal Multimedia Communications, WPMC 2007, Jaipur, India, December 2007.

I. INTRODUCTION

M2M communication in cooperative wireless networks is an emerging technology. Combining the advantages of cooperative diversity [16, 17, 8] with the features of M2M communication systems [2] makes it possible to fulfill the consumer demands of enhanced quality of service (QoS) with greater mobility support. M2M cooperative wireless networks exploit the fact that single-antenna mobile stations can share their antennas to create a virtual multiple-input multiple-output (MIMO) system in a multi-user scenario [4]. Thus, such wireless networks permit mobile stations to relay signals using other mobile stations in the network to a final destination [3]. Furthermore, the mobile relays can either decode and retransmit the received signal or simply amplify and forward the signal [8]. This paper focuses on amplify-and-forward relay type M2M cooperative wireless networks.

Since M2M cooperative network technology is a rather new concept, there are only some few results available, which describe the multipath fading channel characteristics under some specific communication scenarios. Studies on the statistical properties of amplify-and-forward relay fading channels under NLOS conditions can be found in [10]. The authors of [10] have modeled the amplify-and-forward relay channel in the equivalent complex baseband as a zero-mean complex double Gaussian channel, i.e., the product of two zero-mean complex Gaussian channels. Hence, the envelope of the overall amplify-and-forward relay fading channel follows the double Rayleigh distribution [7]. Questions like how does the double Rayleigh fading impact the systems' performance are answered in [14]. However, there is still a lack of information about amplify-and-forward relay fading channels under LOS conditions. Thus, the purpose of this paper is to fill this gap by analyzing the statistical properties of amplify-and-forward relay fading channels under LOS conditions.

An LOS component can either exist only in the direct link between the source mobile station and the destination mobile station or only in the link between the source mobile station and the destination mobile station via a mobile relay (i.e., the double Rice fading scenario)[19] or in both links. Our amplify-and-forward relay fading channel model takes into consideration the LOS component only in the direct link between the source mobile station and the destination mobile station. The novelty in our approach is that we model the envelope of the amplify-and-forward relay channel as a single-LOS double-scattering (SLDS) fading channel, i.e., the superposition of a deterministic LOS component and a zero-mean complex double Gaussian process. The PDF of the envelope of SLDS fading channels has been derived in [15]. However, other important statistical quantities like the PDF of the

phase, LCR, and ADF have not been studied so far. Here, we present the integral expressions for these statistical quantities. Furthermore, the validity of the analytical expressions is confirmed with the help of a high-performance channel simulator. In addition, the results presented in this paper will provide sufficient evidence that the properties of SLDS fading channels are quite different from those of double Rayleigh and double Rice channels.

The rest of the paper is structured as follows: In Section II, the reference model for amplify-and-forward SLDS fading channels is developed. Section III deals with the analysis of the statistical properties of SLDS fading processes. Section IV confirms the validity of the analytical expressions presented in Section III by simulations. Finally, concluding remarks are given in Section V.

II. THE SLDS FADING CHANNEL

In this section, we will develop a reference channel model for SLDS fading channels under the assumption of flat fading. It is important to note that SLDS fading channels are M2M fading channels in the amplify-and-forward relay links, where an LOS component exists only in the direct transmission link between the source mobile station and the destination mobile station. The communication scenario associated with SLDS fading channels is presented in Fig. G.1.

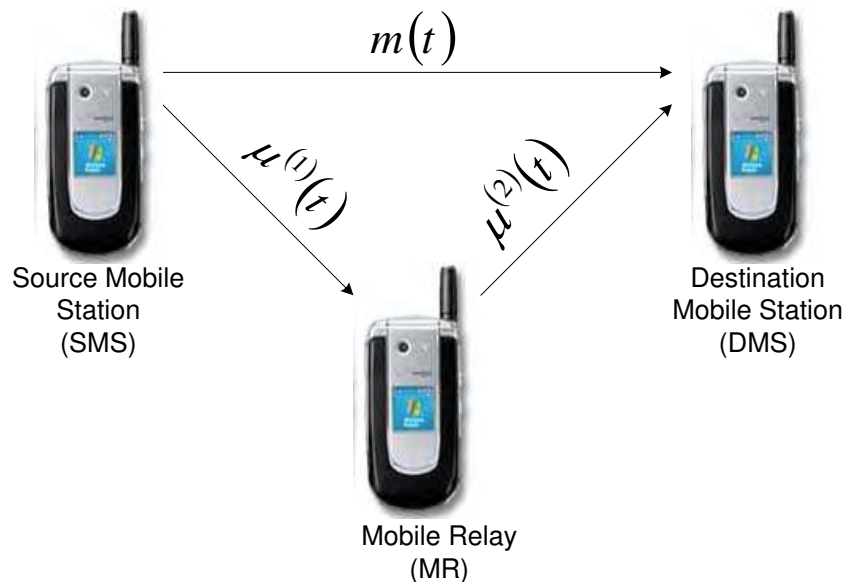


Figure G.1: The propagation scenario behind single-LOS double-scattering fading channels.

Let us denote the transmission link between the source mobile station and the destination mobile station via the mobile relay as L_{S-R-D} . The signal transmitted by the

source mobile station is $s(t)$. Furthermore, the deterministic LOS component, $m(t)$ defined as

$$m(t) = m_r(t) + jm_i(t) = \rho e^{j(2\pi f_\rho t + \theta_\rho)} \quad (1)$$

assumes fixed values for the amplitude ρ , Doppler frequency f_ρ , and phase θ_ρ . The Doppler frequency f_ρ of the LOS component corresponds to the sum of the Doppler frequencies f_{ρ_s} and f_{ρ_d} caused by the motion of the source mobile station and the destination mobile station, respectively, i.e., $f_\rho = f_{\rho_s} + f_{\rho_d}$. Throughout this paper, we will use subscripts r and i to indicate the real and the imaginary part, respectively, of a complex number. The transmitted signal $s(t)$ following the link L_{S-R-D} reaches the destination mobile station in two steps. First, the signal $s(t)$ arrives through multipath propagation at the mobile relay, and then it is retransmitted to the destination mobile station. The signal $r_r(t)$ received by the mobile relay can be expressed as

$$r_r(t) = \mu^{(1)}(t)s(t) + n_1(t) \quad (2)$$

where $\mu^{(1)}(t)$ is a scattered component that describes the fading in the link between the source mobile station and the mobile relay (i.e., L_{S-R}), and $n_1(t)$ is an additive white Gaussian noise (AWGN) process. Here, the scattered component $\mu^{(1)}(t)$ is modeled as a zero-mean complex Gaussian process having $2\sigma_1^2$ variance, i.e., $\mu^{(1)}(t) = \mu_r^{(1)}(t) + j\mu_i^{(1)}(t)$. The mobile relay then amplifies the signal $r_r(t)$ and retransmits it to the destination mobile station. Thus, the total signal $r_d(t)$ received at the destination mobile station can be written as

$$\begin{aligned} r_d(t) &= m(t)s(t) + A_R \mu^{(2)}(t)r_r(t) + n_2(t) \\ &= m(t)s(t) + A_R \mu^{(2)}(t)\mu^{(1)}(t)s(t) + A_R \mu^{(2)}(t)n_1(t) + n_2(t) \\ &= \left(m(t) + A_R \mu^{(2)}(t)\mu^{(1)}(t)\right)s(t) + A_R \mu^{(2)}(t)n_1(t) + n_2(t) \\ &= (m(t) + A_R \zeta(t))s(t) + A_R \mu^{(2)}(t)n_1(t) + n_2(t) \end{aligned} \quad (3)$$

where A_R is referred to as the relay gain, $\mu^{(2)}(t)$ is the second scattered component, $\zeta(t)$ corresponds to the double scattered component, and $n_2(t)$ is the second AWGN process. We have assumed fixed gain relays in our model, meaning that the relay gain A_R is a real constant. The scattered component $\mu^{(2)}(t)$ is a zero-mean complex Gaussian process with variance $2\sigma_2^2$, i.e., $\mu^{(2)}(t) = \mu_r^{(2)}(t) + j\mu_i^{(2)}(t)$. This process models the fading channel in the link between the mobile relay and the destination mobile station (i.e., L_{R-D}). The double scattered component $\zeta(t)$ defines the overall fading channel in the link L_{S-R-D} . It represents a zero-mean complex double Gaussian process, which is modeled as the product of two independent, zero-mean complex

Gaussian processes $\mu^{(1)}(t)$ and $\mu^{(2)}(t)$, i.e., $\zeta(t) = \varsigma_r(t) + j\varsigma_i(t) = \mu^{(1)}(t)\mu^{(2)}(t)$. It should be pointed out here that the relay gain A_R acts as a scaling factor for the variance of $\mu^{(2)}(t)$, i.e., $2\sigma_{A_R}^2 = \text{Var}\{A_R\mu^{(2)}(t)\} = 2(A_R\sigma_2)^2$. In (3), the sum of the double scattered component $\zeta(t)$ and the LOS component $m(t)$ results in a non-zero-mean complex double Gaussian process $\chi(t)$, i.e., $\chi(t) = \chi_r(t) + j\chi_i(t) = A_R\zeta(t) + m(t)$. This process $\chi(t)$ models the overall fading channel between the source mobile station and the destination mobile station. The absolute value of $\chi(t)$ gives rise to an SLDS process $\Xi(t)$, i.e.,

$$\Xi(t) = |\chi(t)|. \quad (4)$$

Furthermore, the argument of $\chi(t)$ defines the phase process $\Theta(t)$, i.e.,

$$\Theta(t) = \arg\{\chi(t)\}. \quad (5)$$

III. STATISTICAL ANALYSIS OF SLDS FADING CHANNELS

In this section, we derive the analytical expressions for the statistical properties of SLDS channels introduced in Section II. Main statistical quantities of interest include the mean value, variance, PDF of the envelope as well as the phase, LCR and ADF.

A. Joint PDF of SLDS Processes

The starting point for the derivation of the statistics of SLDS processes is the computation of the joint PDF $p_{\chi_r\chi_i\dot{\chi}_r\dot{\chi}_i}(u_r, u_i, \dot{u}_r, \dot{u}_i)$ of the stationary processes $\chi_r(t)$, $\chi_i(t)$, $\dot{\chi}_r(t)$, and $\dot{\chi}_i(t)$ at the same time t . Throughout this paper, the overdot indicates the time derivative. Applying the concept of transformation of random variables [9], we can write the joint PDF $p_{\chi_r\chi_i\dot{\chi}_r\dot{\chi}_i}(u_r, u_i, \dot{u}_r, \dot{u}_i)$ as follows

$$\begin{aligned} p_{\chi_r\chi_i\dot{\chi}_r\dot{\chi}_i}(u_r, u_i, \dot{u}_r, \dot{u}_i) &= \int_{-\infty}^{\infty} \int_{-\infty}^{\infty} \int_{-\infty}^{\infty} \int_{-\infty}^{\infty} d\dot{y}_i d\dot{y}_r dy_i dy_r |J|^{-1} \\ &\times P_{\mu_r^{(1)}\mu_i^{(1)}\dot{\mu}_r^{(1)}\dot{\mu}_i^{(1)}\mu_r^{(2)}\mu_i^{(2)}\dot{\mu}_r^{(2)}\dot{\mu}_i^{(2)}}(x_r, x_i, \dot{x}_r, \dot{x}_i, y_r, y_i, \dot{y}_r, \dot{y}_i) \end{aligned} \quad (6)$$

where $p_{\mu_r^{(1)}\mu_i^{(1)}\dot{\mu}_r^{(1)}\dot{\mu}_i^{(1)}\mu_r^{(2)}\mu_i^{(2)}\dot{\mu}_r^{(2)}\dot{\mu}_i^{(2)}}(x_r, x_i, \dot{x}_r, \dot{x}_i, y_r, y_i, \dot{y}_r, \dot{y}_i)$ is the joint PDF of the real and imaginary parts of $\mu^{(k)}(t)$ as well as their respective time derivatives $\dot{\mu}^{(k)}(t)$ ($k = 1, 2$). The quantity x_l is a function of y_r, y_i, u_r , and u_i , with \dot{x}_l as a function of $\dot{y}_r, \dot{y}_i, \dot{u}_r$, and \dot{u}_i for $l = r, i$. In (6), J denotes the Jacobian determinant. It is worth mentioning here that the processes $\chi_l(t)$, $\dot{\chi}_l(t)$, $\mu_l^{(1)}(t)$, $\dot{\mu}_l^{(1)}(t)$, $\mu_l^{(2)}(t)$, and $\dot{\mu}_l^{(2)}(t)$ ($l = r, i$) are uncorrelated in pairs. Taking into account that the underlying Gaussian processes and their time derivatives, i.e., $\mu_l^{(k)}(t)$, and

$\dot{\mu}_l^{(k)}(t)$ ($k = 1, 2; l = r, i$) are statistically independent allows us to write $P_{\mu_r^{(1)} \mu_i^{(1)} \dot{\mu}_r^{(1)} \dot{\mu}_i^{(1)} \mu_r^{(2)} \mu_i^{(2)} \dot{\mu}_r^{(2)} \dot{\mu}_i^{(2)}}(x_r, x_i, \dot{x}_r, \dot{x}_i, y_r, y_i, \dot{y}_r, \dot{y}_i)$ as a product of $P_{\mu_r^{(1)} \mu_i^{(1)} \dot{\mu}_r^{(1)} \dot{\mu}_i^{(1)}}(x_r, x_i, \dot{x}_r, \dot{x}_i)$ and $P_{\mu_r^{(2)} \mu_i^{(2)} \dot{\mu}_r^{(2)} \dot{\mu}_i^{(2)}}(y_r, y_i, \dot{y}_r, \dot{y}_i)$. Furthermore, $P_{\mu_r^{(1)} \mu_i^{(1)} \dot{\mu}_r^{(1)} \dot{\mu}_i^{(1)}}(x_r, x_i, \dot{x}_r, \dot{x}_i)$ and $P_{\mu_r^{(2)} \mu_i^{(2)} \dot{\mu}_r^{(2)} \dot{\mu}_i^{(2)}}(y_r, y_i, \dot{y}_r, \dot{y}_i)$ can be expressed by the multivariate Gaussian distribution (see, e.g., [18, eq. (3.2)]). Thus, substituting $P_{\mu_r^{(1)} \mu_i^{(1)} \dot{\mu}_r^{(1)} \dot{\mu}_i^{(1)}}(x_r, x_i, \dot{x}_r, \dot{x}_i)$ and $P_{\mu_r^{(2)} \mu_i^{(2)} \dot{\mu}_r^{(2)} \dot{\mu}_i^{(2)}}(y_r, y_i, \dot{y}_r, \dot{y}_i)$ in (6) and doing some lengthy algebraic computations results in

$$P_{\chi_r \chi_i \dot{\chi}_r \dot{\chi}_i}(u_r, u_i, \dot{u}_r, \dot{u}_i) = \frac{1}{(2\pi)^2 \sigma_1^2 \sigma_{A_R}^2} \int_0^\infty v e^{-\frac{1}{2\sigma_1^2} \left(\frac{g_1(u_r, u_i, \rho)}{v^2} \right)} e^{\frac{\beta_2}{2\beta_1} \left(\frac{g_1(u_r, u_i, \rho)}{v^2} \frac{g_2(\dot{u}_r, \dot{u}_i, \rho)}{v^2} \right)} e^{-\frac{1}{2\sigma_{A_R}^2} v^2} e^{-\frac{1}{2\beta_1} \left(\frac{g_2(\dot{u}_r, \dot{u}_i, \rho)}{v^2} \right)} \times \frac{dv}{\beta_2 g_1(u_r, u_i, \rho) + \beta_1 v^4} \quad (7)$$

where

$$g_1(u_r, u_i, \rho) = u_r^2 + u_i^2 + \rho^2 - 2\rho u_r \cos(2\pi f_\rho t + \theta_\rho) - 2\rho u_i \sin(2\pi f_\rho t + \theta_\rho) \quad (8a)$$

$$g_2(\dot{u}_r, \dot{u}_i, \rho) = \dot{u}_r^2 + \dot{u}_i^2 + (2\pi f_\rho \rho)^2 - 4\pi f_\rho \rho \dot{u}_i \cos(2\pi f_\rho t + \theta_\rho) + 4\pi f_\rho \rho \dot{u}_r \sin(2\pi f_\rho t + \theta_\rho) \quad (8b)$$

and

$$\beta_1 = 2(\sigma_1 \pi)^2 (f_{\max_S}^2 + f_{\max_R}^2), \quad \beta_2 = 2(\sigma_{A_R} \pi)^2 (f_{\max_R}^2 + f_{\max_D}^2). \quad (9a,b)$$

In (9a,b), the quantity β_k ($k = 1, 2$) is the negative curvature of the autocorrelation function of the real and imaginary parts of $\mu^{(k)}(t)$ ($k = 1, 2$) presented here for the case of isotropic scattering [11]. Furthermore, β_k ($k = 1, 2$) is the characteristic quantity corresponding to M2M fading process [1]. The symbols f_{\max_S} , f_{\max_R} , and f_{\max_D} appearing in (9a,b) correspond to the maximum Doppler frequency caused by the motion of the source mobile station, the mobile relay, and the destination mobile station, respectively.

Starting from (7), the transformation of the Cartesian coordinates (u_r, u_i) into polar coordinates (z, θ) by means of $z = \sqrt{u_r^2 + u_i^2}$ and $\theta = \arctan(u_i/u_r)$ results

after some lengthy algebraic manipulations in

$$\begin{aligned}
 p_{\Xi\dot{\Xi}\Theta\dot{\Theta}}(z, \dot{z}, \theta, \dot{\theta}; t) &= \frac{z^2 / (2\pi)^2}{\sigma_1^2 \sigma_{A_R}^2} \int_0^\infty v e^{-\frac{1}{2\sigma_1^2} \left(\frac{z^2 + \rho^2}{v^2} \right)} e^{-\frac{v^2}{2\sigma_{A_R}^2} \frac{z\rho \cos(\theta - 2\pi f\rho t - \theta\rho)}{\sigma_1^2 v^2}} \\
 &\times e^{-\frac{1}{2} \left(\frac{v^2 (\dot{z}^2 + (z\dot{\theta})^2) + (2\pi f\rho v)^2}{\beta_2 g_3(z, \rho, \theta) + \beta_1 v^4} \right)} e^{\frac{2\pi f\rho v^2 (z \sin(\theta - 2\pi f\rho t - \theta\rho) + z\dot{\theta} \cos(\theta - 2\pi f\rho t - \theta\rho))}{\beta_2 g_3(z, \rho, \theta) + \beta_1 v^4}} dv \quad (10)
 \end{aligned}$$

for $z \geq 0$, $|\theta| \leq \pi$, $|\dot{z}| < \infty$, and $|\dot{\theta}| < \infty$. In (10), the function $g_3(\cdot, \cdot, \cdot)$ can be expressed as follows

$$g_3(z, \rho, \theta) = z^2 + \rho^2 - 2z\rho \cos(\theta - 2\pi f\rho t - \theta\rho). \quad (11)$$

The joint PDF $p_{\Xi\dot{\Xi}\Theta\dot{\Theta}}(z, \dot{z}, \theta, \dot{\theta}; t)$ in (10) is a fundamental equation, because it provides the basis for the computation of the PDF, LCR, and ADF of SLDS processes $\Xi(t)$, as well as the PDF of the phase process $\Theta(t)$. We will provide sufficient evidence in rest of the current section to support our argument by deriving integral expressions for the PDFs, LCR, and ADF using (10).

B. PDF of SLDS Processes

The PDF $p_\Xi(z)$ of SLDS processes $\Xi(t)$ can be derived from (10) by solving the integrals over the joint PDF $p_{\Xi\dot{\Xi}\Theta\dot{\Theta}}(z, \dot{z}, \theta, \dot{\theta}; t)$ according to

$$p_\Xi(z) = \int_{-\pi}^{\pi} \int_{-\infty}^{\infty} \int_{-\infty}^{\infty} p_{\Xi\dot{\Xi}\Theta\dot{\Theta}}(z, \dot{z}, \theta, \dot{\theta}; t) d\dot{\theta} d\dot{z} d\theta, \quad z \geq 0. \quad (12)$$

The closed-form solution of (12) can be given as

$$p_\Xi(z) = \begin{cases} \frac{z}{\sigma_1^2 \sigma_{A_R}^2} I_0 \left(\frac{z}{\sigma_1 \sigma_{A_R}} \right) K_0(\kappa), & z < \rho \\ \frac{z}{\sigma_1^2 \sigma_{A_R}^2} K_0 \left(\frac{z}{\sigma_1 \sigma_{A_R}} \right) I_0(\kappa), & z \geq \rho \end{cases} \quad (13)$$

where $\kappa = \rho / (\sigma_1 \sigma_{A_R})$, $I_0(\cdot)$ and $K_0(\cdot)$ are denoting the zeroth-order modified Bessel function of the first kind and the second kind [5], respectively. The PDF $p_\Xi(z)$ of SLDS processes $\Xi(t)$ presented in (13) can be verified from the literature (see, e.g., [15]).

The condition $\rho = 0$ indicates absence of the LOS component in the direct link from the source mobile station to the destination mobile station. The PDF $p_\Xi(z)$ of SLDS processes $\Xi(t)$ given in (13) then reduces to the PDF of the envelope of

double Rayleigh processes [7], i.e.,

$$p_{\Xi}(z) |_{\rho=0} = \frac{z}{\sigma_1^2 \sigma_{A_R}^2} K_0 \left(\frac{z}{\sigma_1 \sigma_{A_R}} \right), \quad z \geq 0. \quad (14)$$

Furthermore, using the asymptotic expansions of the zeroth-order modified Bessel function of the first kind and the second kind, i.e., $I_0(\cdot)$ and $K_0(\cdot)$, respectively [20], the PDF $p_{\Xi}(z)$ of SLDS processes $\Xi(t)$ in (13) can be approximated for large values of κ as the Laplace distribution [6], i.e.,

$$p_{\Xi}(z) |_{\kappa \gg 1} \approx \sqrt{\frac{z}{\rho}} \frac{1}{2\sigma_1 \sigma_{A_R}} e^{-\frac{|z-\rho|}{\sigma_1 \sigma_{A_R}}} \approx \sqrt{\frac{z}{\rho}} p_o(z), \quad z \geq 0 \quad (15)$$

where $p_o(z)$ represents the Laplace distribution having the mean value ρ and the variance $\sigma_1^2 \sigma_{A_R}^2$. It is important to note here that the approximation in (15) is valid if $\kappa \gg 1$, i.e., the ratio of the power of the LOS component to the power of the scattered components is large. Otherwise, in the presence of a very strong LOS component, i.e., $\rho \gg 1$, when the power of the scattered components is constant, κ acquires a large value.

C. Mean Value and Variance of SLDS Processes

The expected value and the variance of a stochastic process are important statistical parameters, since they summarize the information provided by the PDF. The expected value m_{Ξ} of SLDS processes $\Xi(t)$ can be obtained using [9]

$$m_{\Xi} = E\{\Xi(t)\} = \int_{-\infty}^{\infty} z p_{\Xi}(z) dz \quad (16)$$

where $E\{\cdot\}$ is the expected value operator. Substituting (13) in (16) results in the following final expression

$$m_{\Xi} = \kappa K_0(\kappa) \left[\rho I_1(\kappa) + \frac{\pi}{2} \sigma_1 \sigma_{A_R} \{I_0(\kappa) L_1(\kappa) - I_1(\kappa) L_0(\kappa)\} \right] + \frac{1}{(\sigma_1 \sigma_{A_R})^2} I_0(\kappa) g_4(z) \quad (17)$$

where

$$g_4(z) = \int_{\rho}^{\infty} z^2 K_0 \left(\frac{z}{\sigma_1 \sigma_{A_R}} \right) dz. \quad (18)$$

In (17), $I_n(\cdot)$ and $K_n(\cdot)$ denote the n th-order modified Bessel functions of the first and the second kind [5], respectively, and $L_n(\cdot)$ designates the n th-order modified

Struve function [5].

The difference of the mean power m_{Ξ^2} and the squared mean value $(m_{\Xi})^2$ of SLDS processes $\Xi(t)$ defines its variance σ_{Ξ}^2 [9], i.e.,

$$\sigma_{\Xi}^2 = \text{Var}\{\Xi(t)\} = m_{\Xi^2} - (m_{\Xi})^2 . \quad (19)$$

By using (13) and [9, eq. (5.67)], the mean power m_{Ξ^2} of SLDS processes $\Xi(t)$ can be expressed as

$$\begin{aligned} m_{\Xi^2} = E\{\Xi^2(t)\} &= \int_{-\infty}^{\infty} z^2 p_{\Xi}(z) dz \\ &= 2\rho^2 K_0(\kappa) \left(I_2(\kappa) + \frac{\kappa}{2} I_3(\kappa) \right) + \frac{I_0(\kappa)}{(\sigma_1 \sigma_{A_R})^2} g_5(z) \end{aligned} \quad (20)$$

where the function $g_5(\cdot)$ is defined as follows

$$g_5(z) = \int_{\rho}^{\infty} z^3 K_0\left(\frac{z}{\sigma_1 \sigma_{A_R}}\right) dz . \quad (21)$$

From (17), (20), and by using (19), the variance σ_{Ξ}^2 of SLDS processes $\Xi(t)$ can easily be calculated.

D. PDF of Phase Processes

The PDF $p_{\Theta}(\theta;t)$ of phase processes $\Theta(t)$ can be derived from (10) by solving the integrals over the joint PDF $p_{\Xi\dot{\Xi}\Theta\dot{\Theta}}(z, \dot{z}, \theta, \dot{\theta};t)$ according to

$$p_{\Theta}(\theta;t) = \int_0^{\infty} \int_{-\infty}^{\infty} \int_{-\infty}^{\infty} p_{\Xi\dot{\Xi}\Theta\dot{\Theta}}(z, \dot{z}, \theta, \dot{\theta};t) d\dot{\theta} d\dot{z} dz, \quad |\theta| \leq \pi. \quad (22)$$

This results in the following final expression

$$\begin{aligned} p_{\Theta}(\theta;t) &= \frac{1}{2\pi} \int_0^{\infty} \left[1 + \sqrt{\frac{\pi}{2}} g_6(x, \rho, f_{\rho}, \theta) e^{\frac{1}{2} g_6(x, \rho, f_{\rho}, \theta)^2} \left\{ 1 + \Phi\left(\frac{g_6(x, \rho, f_{\rho}, \theta)}{\sqrt{2}}\right) \right\} \right] \\ &\quad \times e^{-x - \frac{1}{x} \left(\frac{\rho}{2\sigma_1 \sigma_{A_R}}\right)^2} dx \end{aligned} \quad (23)$$

for $|\theta| \leq \pi$ and

$$g_6(x, \rho, \theta) = \frac{\rho \cos(\theta - 2\pi f_{\rho} t - \theta_{\rho})}{\sigma_1 \sigma_{A_R} \sqrt{2x}} . \quad (24)$$

Furthermore, in (23), $\Phi(\cdot)$ represents the error function [5, eq. (8.250.1)]. From (23), it is obvious that the phase process $\Theta(t)$ is not stationary in a strict sense since $p_{\Theta}(\theta; t) \neq p_{\Theta}(\theta)$. This time dependency of the PDF $p_{\Theta}(\theta; t)$ is due the Doppler frequency f_{ρ} of the LOS component $m(t)$. However, for the special case that $f_{\rho} = 0$ ($\rho \neq 0$), the phase process $\Theta(t)$ is a strict sense stationary process.

As $\rho \rightarrow 0$, it follows $\Xi(t) = |\zeta(t) + m(t)| \rightarrow |\zeta(t)|$, and from (23), we obtain the uniform distribution

$$p_{\Theta}(\theta) \Big|_{\rho=0} = \frac{1}{2\pi}, \quad -\pi < \theta \leq \pi. \quad (25)$$

E. LCR of SLDS Processes

The LCR of the envelope of mobile fading channels is a measure to describe the average number of times the envelope crosses a certain threshold level r from up to down (or vice versa) per second. The LCR $N_{\Xi}(r)$ of SLDS processes $\Xi(t)$ can be obtained using [13]

$$N_{\Xi}(r) = \int_0^{\infty} \dot{z} p_{\Xi\dot{\Xi}}(r, \dot{z}) d\dot{z} \quad (26)$$

where $p_{\Xi\dot{\Xi}}(r, \dot{z})$ is the joint PDF of SLDS processes $\Xi(t)$ and its corresponding time derivative $\dot{\Xi}(t)$ at the same time t . The joint PDF $p_{\Xi\dot{\Xi}}(z, \dot{z})$ can be derived from (10) by solving the integrals over the joint PDF $p_{\Xi\dot{\Xi}\Theta\dot{\Theta}}(z, \dot{z}, \theta, \dot{\theta}; t)$ according to

$$p_{\Xi\dot{\Xi}}(z, \dot{z}) = \int_{-\pi-\infty}^{\pi} \int_0^{\infty} p_{\Xi\dot{\Xi}\Theta\dot{\Theta}}(z, \dot{z}, \theta, \dot{\theta}; t) d\dot{\theta} d\theta, \quad z \geq 0, |\dot{z}| \leq \infty. \quad (27)$$

After doing some lengthy computations, the joint PDF in (27) results in the following expression

$$p_{\Xi\dot{\Xi}}(z, \dot{z}) = \frac{(2\pi)^{-\frac{3}{2}} z}{\sigma_1^2 \sigma_{A_R}^2} \int_0^{\infty} \int_{-\pi}^{\pi} \frac{e^{-\frac{1}{2\sigma_1^2} \left(\frac{z^2 + \rho^2}{v^2} \right)} e^{-\frac{v^2}{2\sigma_{A_R}^2}} e^{-\frac{z\rho \cos \theta}{v^2 \sigma_1^2}}}{\sqrt{\beta_2 g_7(z, \rho, \theta) + \beta_1 v^4}} \times e^{-\frac{2(\pi f_{\rho} \rho v \sin \theta)^2}{\beta_2 g_7(z, \rho, \theta) + \beta_1 v^4}} e^{-\frac{1}{2} \left(\frac{(v\dot{z})^2 - 4\pi f_{\rho} \rho v^2 \dot{z} \sin \theta}{\beta_2 g_7(z, \rho, \theta) + \beta_1 v^4} \right)} d\theta dv \quad (28)$$

for $z \geq 0, |\dot{z}| \leq \infty$, where

$$g_7(z, \rho, \theta) = z^2 + \rho^2 - 2z\rho \cos \theta. \quad (29)$$

Finally, after substituting (28) in (26) and doing some extensive mathematical manipulations, the LCR $N_{\Xi}(r)$ of SLDS processes $\Xi(t)$ can be expressed as follows

$$N_{\Xi}(r) = \frac{\sqrt{2\pi}r}{(2\pi)^2 \sigma_1^2 \sigma_{AR}^2} \int_{-\pi}^{\pi} \int_0^{\infty} d\theta dv \frac{\sqrt{\beta_2 g_7(r, \rho, \theta) + \beta_1 v^4}}{v^2} e^{-\frac{v^2}{2\sigma_{AR}^2}} e^{-\frac{g_7(r, \rho, \theta)}{2v^2 \sigma_1^2}} \times \left(e^{-\frac{1}{2}g_8^2(r, \nu, \rho, \theta)} + \sqrt{\frac{\pi}{2}} g_8(r, \nu, \rho, \theta) \left\{ 1 + \Phi \left(\frac{g_8(r, \nu, \rho, \theta)}{\sqrt{2}} \right) \right\} \right) \quad (30)$$

where

$$g_8(r, \nu, \rho, \theta) = \frac{2\pi f_{\rho} \rho \nu \sin \theta}{\sqrt{\beta_2 g_7(r, \rho, \theta) + \beta_1 \nu^4}}. \quad (31)$$

The quantities β_1 and β_2 are the same as those defined in (9a,b). Furthermore, $g_7(\cdot, \cdot, \cdot)$ is the function defined in (29).

Considering the special case when $\rho = 0$, (30) reduces to the expression of the LCR for double Rayleigh processes given in [10] as

$$N_{\Xi}(r) |_{\rho=0} = \frac{r}{\sqrt{2\pi} \sigma_1^2 \sigma_{AR}^2} \int_0^{\infty} \frac{\sqrt{\beta_2 r^2 + \beta_1 v^4}}{v^2} e^{-\frac{(r/v)^2}{2\sigma_1^2}} e^{-\frac{v^2}{2\sigma_{AR}^2}} dv. \quad (32)$$

F. ADF of SLDS Processes

We will conclude Section III with the discussion on the ADF. The ADF $T_{\Xi_-}(r)$ of SLDS processes $\Xi(t)$ can be defined as the ratio of the CDF $F_{\Xi_-}(r)$ of $\Xi(t)$ and its LCR $N_{\Xi}(r)$, i.e.,

$$T_{\Xi_-}(r) = \frac{F_{\Xi_-}(r)}{N_{\Xi}(r)}. \quad (33)$$

The CDF $F_{\Xi_-}(r)$ of SLDS processes $\Xi(t)$ can be expressed using (13) as follows

$$F_{\Xi_-}(r) = \int_0^r p_{\Xi}(z) dz = \begin{cases} \frac{r}{\sigma_1 \sigma_{AR}} K_0(\kappa) I_1 \left(\frac{r}{\sigma_1 \sigma_{AR}} \right), & r < \rho \\ 1 - \frac{r}{\sigma_1 \sigma_{AR}} I_0(\kappa) K_1 \left(\frac{r}{\sigma_1 \sigma_{AR}} \right), & r \geq \rho. \end{cases} \quad (34)$$

From (34), (30), and by using (33), the ADF $T_{\Xi_-}(r)$ of SLDS processes $\Xi(t)$ can easily be computed.

It is quite obvious from (34) that as $\rho \rightarrow 0$, (34) reduces to

$$F_{\Xi_-}(r) |_{\rho=0} = 1 - \frac{r}{\sigma_1 \sigma_{AR}} K_1 \left(\frac{r}{\sigma_1 \sigma_{AR}} \right). \quad (35)$$

The resulting CDF $F_{\Xi}(r)$ in (35) corresponds to the CDF of double Rayleigh processes [7]. Thus, substituting (35) and (32) in (33) gives the ADF of double Rayleigh processes.

IV. NUMERICAL RESULTS

In this section, we will confirm the correctness of the analytical expressions presented in Section III with the help of simulations. Furthermore, for a detailed analysis the results for SLDS processes are compared with those of classical Rayleigh, classical Rice, double Rayleigh, and double Rice processes. It is important to note that the double Rice process is defined as the product of two independent classical Rice processes, i.e., $\Xi(t) = \left| \mu^{(1)}(t) + \rho_1 \right| \left| \mu^{(2)}(t) + \rho_2 \right|$. To simplify matters, the amplitudes ρ_1 and ρ_2 of the LOS components of the double Rice process are considered to be equal, i.e., $\rho_1 = \rho_2 = \rho$. The concept of sum-of-sinusoids (SOS) [11] is used to simulate uncorrelated complex Gaussian processes $\mu^{(k)}(t)$ that make up the overall SLDS process. For simulating Gaussian processes $\mu^{(k)}(t)$, $N_l^{(k)} = 20$ ($k = 1, 2; l = r, i$) is used. Here $N_r^{(k)}$ and $N_i^{(k)}$ denote the number of sinusoids required to generate the real and the imaginary parts of $\mu^{(k)}(t)$, respectively. It is readily available in the literature that $N_l^{(k)} \geq 7$ is a sufficient number to approximate the simulated distribution of $\left| \mu^{(k)}(t) \right|$ very close to the Rayleigh distribution [11]. For computation of the model parameters, we selected the generalized method of exact Doppler spread (GMEDS_q) proposed in [12] for $q = 1$. The values for the maximum Doppler frequencies f_{\max_S} , f_{\max_R} , and f_{\max_D} were set to 91 Hz, 75 Hz, and 110 Hz, respectively. The relay gain A_R as well as the parameters σ_1 and σ_2 were selected to be 1, unless stated otherwise.

The results presented in Figs. G.2–G.9 show an excellent fitting of the analytical and the simulation results. In Fig. G.2, the PDF $p_{\Xi}(z)$ of SLDS processes $\Xi(t)$ is being compared with those of classical Rice and double Rice processes for different values of ρ , where f_{ρ} was set to zero. It can be observed that the maximum value of the PDF $p_{\Xi}(z)$ of SLDS processes $\Xi(t)$ is higher than that of classical Rice and double Rice processes for same value of ρ . On the other hand, the spread of the PDF $p_{\Xi}(z)$ of SLDS processes $\Xi(t)$ follows the same trend as that of classical Rayleigh, classical Rice, and double Rayleigh processes. However, the PDF $p_{\Xi}(z)$ of the SLDS process $\Xi(t)$ has a narrower spread when compared to the spread of double Rice processes for the same value of ρ .

Figure G.3 demonstrates the fact that for increasing values of κ , the PDF $p_{\Xi}(z)$ of SLDS processes $\Xi(t)$ approaches the symmetrical Laplace distribution. Furthermore, the right shift of the PDF $p_{\Xi}(z)$ of SLDS processes $\Xi(t)$ with increasing values of ρ is merely due to the fact that ρ contributes towards the mean value of

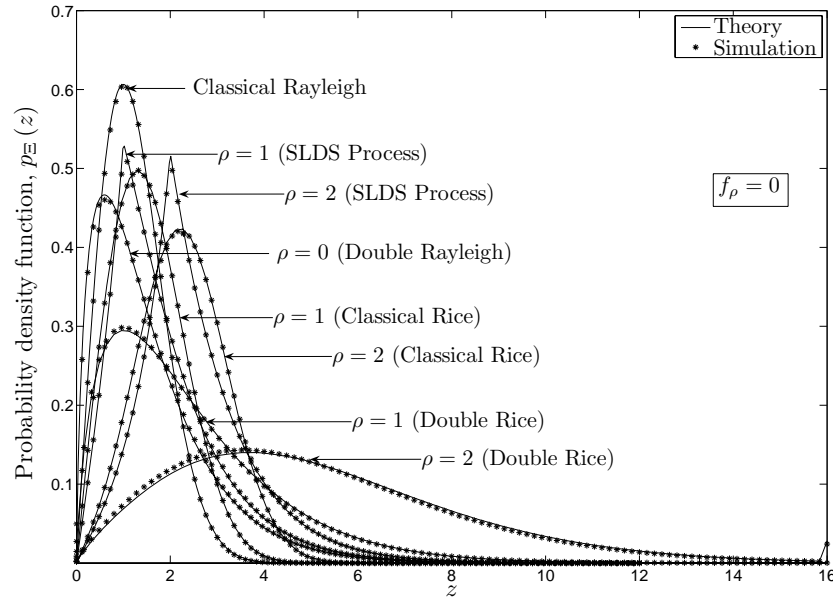


Figure G.2: A comparison of the PDF $p_{\Xi}(z)$ of SLDS processes $\Xi(t)$ with that of various other stochastic processes.

SLDS processes. The mean value of SLDS processes for different values of ρ is presented in Fig. G.4 along with the mean value of classical Rice and double Rice processes. It is obvious from Fig. G.4 that the increase in the mean value of classical Rice and SLDS processes is proportional to ρ , whereas for double Rice processes it is proportional to the squared value of ρ .

The observation that the PDF $p_{\Xi}(z)$ of SLDS processes $\Xi(t)$ has a narrower spread when compared to the spread of double Rice processes is more explicitly shown in Fig. G.5. In Fig. G.5, the standard deviation σ_{Ξ} of SLDS processes $\Xi(t)$ for different values of ρ is presented along with the standard deviation of classical Rice and double Rice processes. It can be seen from Fig. G.5 that for a particular value of ρ the standard deviation corresponding to double Rice processes is greater than that of classical Rice and SLDS processes. Furthermore, when the standard deviation σ_{Ξ} of various stochastic processes, i.e., the classical Rice, the double Rice, and the SLDS process is self-compared for different values of ρ , it can be observed in Fig. G.5 that there is no noticeable difference in the standard deviation σ_{Ξ} of classical Rice and SLDS processes with increasing values of ρ . However, the increase in the standard deviation of double Rice processes, meaning thereby an increase in the spread of the PDF of these processes with increasing ρ is quite obvious. Similarly, Fig. G.6 presents the CDF $F_{\Xi}(r)$ of SLDS processes $\Xi(t)$ evaluated by using (34).

A comparison of the PDF $p_{\Theta}(\theta)$ of the phase process $\Theta(t)$ with that of the cor-

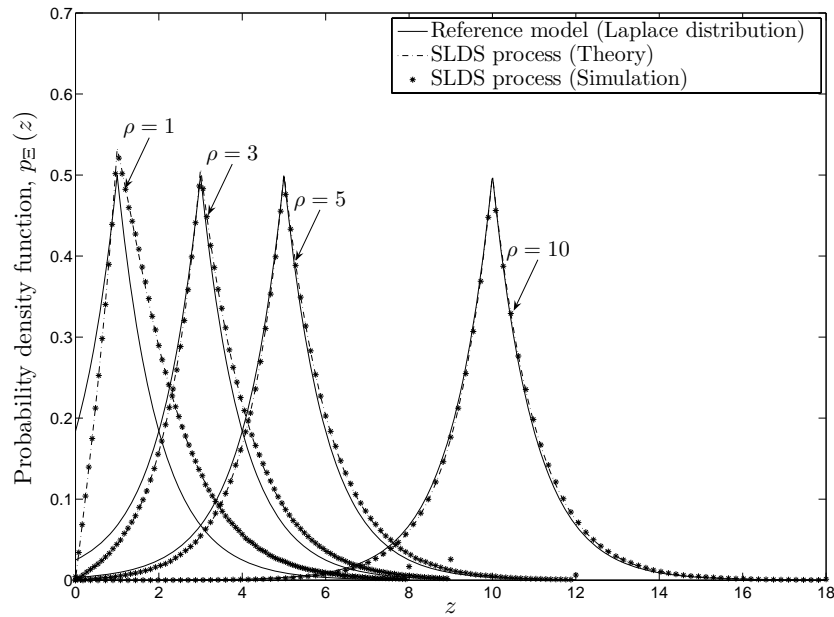


Figure G.3: Approximation of the PDF $p_{\Xi}(z)$ of SLDS processes $\Xi(t)$ to the Laplace distribution.

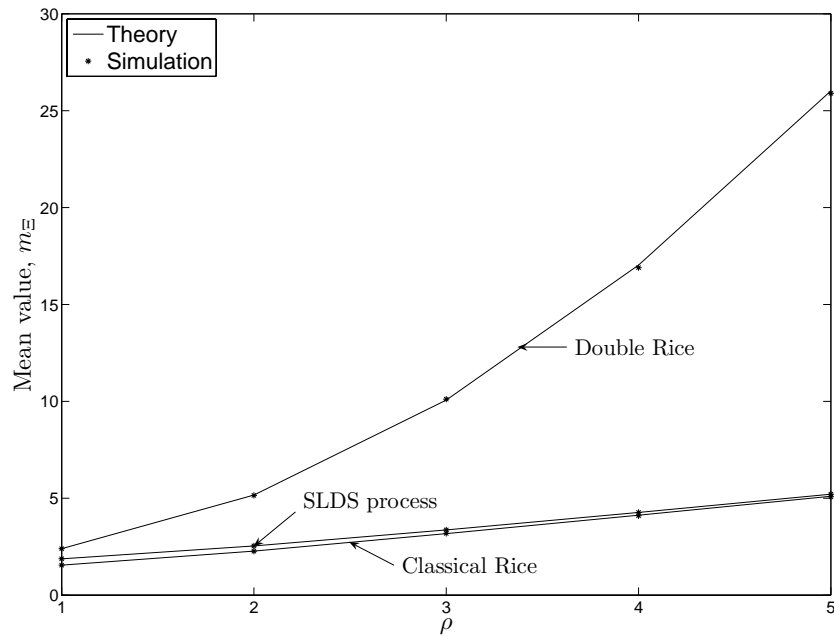


Figure G.4: A comparison of the mean value m_{Ξ} of SLDS processes $\Xi(t)$ with that of various other stochastic processes.

responding classical Rice and double Rice phase processes is shown in Fig. G.7. It is clear from Fig. G.7 that the PDF $p_{\Theta}(\theta)$ of the phase process $\Theta(t)$ has a higher peak and narrow spread when compared with the PDF of the phase process associated with classical Rice and double Rice processes for a specific value of ρ .

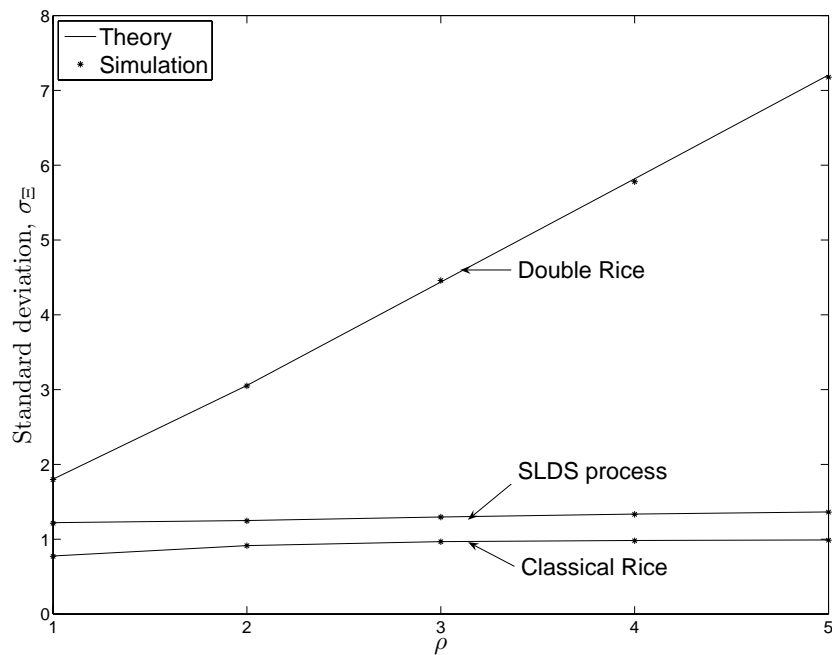


Figure G.5: A comparison of the standard deviation σ_{Ξ} of SLDS processes $\Xi(t)$ with that of various other stochastic processes.

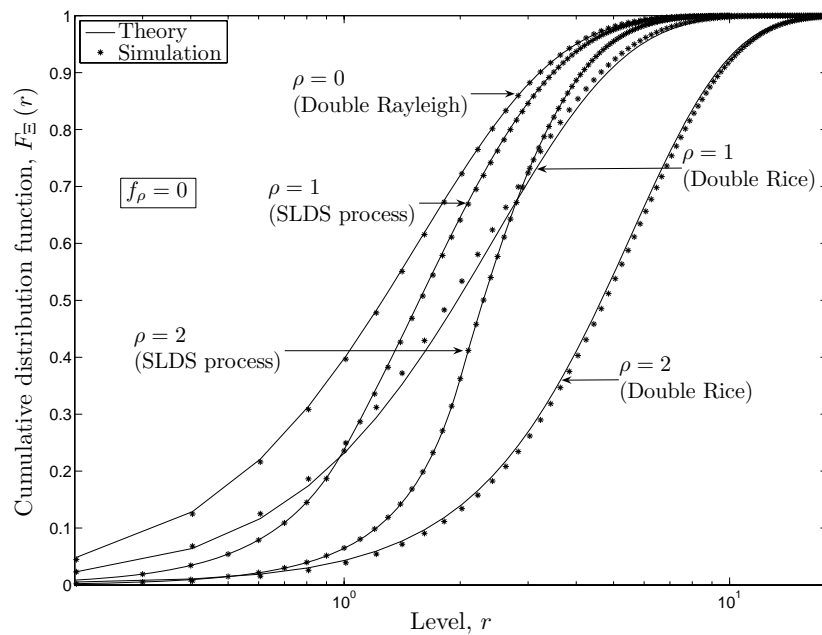


Figure G.6: A comparison of the CDF $F_{\Xi}(r)$ of SLDS processes $\Xi(t)$ with that of various other stochastic processes.

Figure G.8 shows that at low signal levels, the LCR $N_{\Xi}(r)$ of SLDS processes $\Xi(t)$ decreases with an increase in ρ , keeping f_{ρ} constant. While, $N_{\Xi}(r)$ increases at medium and high levels with increasing ρ . Furthermore, as ρ increases the LCR

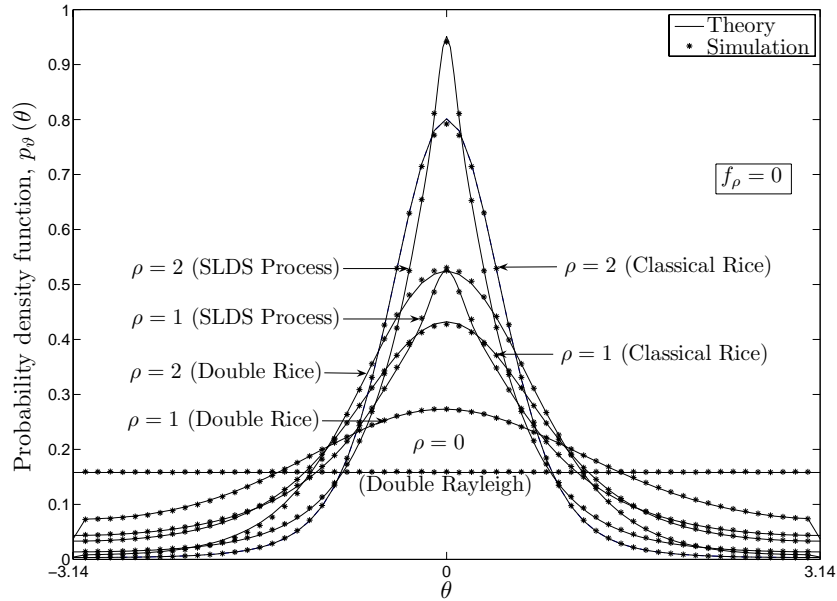


Figure G.7: A comparison of the PDF $p_{\Theta}(\theta)$ of the phase process $\Theta(t)$ with that of various other stochastic processes.

$N_{\Xi}(r)$ of SLDS processes $\Xi(t)$ becomes greater than that of double Rice processes at low signal levels. However, at medium and high signal levels, the LCR $N_{\Xi}(r)$ of SLDS processes $\Xi(t)$ is lower than the LCR of double Rice processes for the same value of ρ . Similarly, Fig. G.9 compares the ADF $T_{\Xi-}(r)$ of SLDS processes $\Xi(t)$ with that of double Rice processes for different values of ρ keeping f_{ρ} equal to zero.

V. CONCLUSION

In this paper, we have studied the statistics of M2M fading channels in cooperative wireless networks under LOS conditions. Considering the amplify-and-forward relay type systems, the existence of an LOS component in the direct transmission link between the source mobile station and the destination mobile station results in SLDS fading channels. Here, we have modeled the NLOS link of the system as a zero-mean complex double Gaussian channel. Thus, the overall SLDS fading channel is modeled as the superposition of a deterministic LOS component and the zero-mean complex double Gaussian channel.

Statistical properties of SLDS fading channels are thoroughly investigated in this paper. We have derived analytical expressions for the mean, variance, PDFs, LCR, and ADF. Furthermore, we have verified our analytical expressions using numerical techniques in simulations. The close fitting of the presented theoretical and simulation results proves correctness of our analytical expressions. It has been

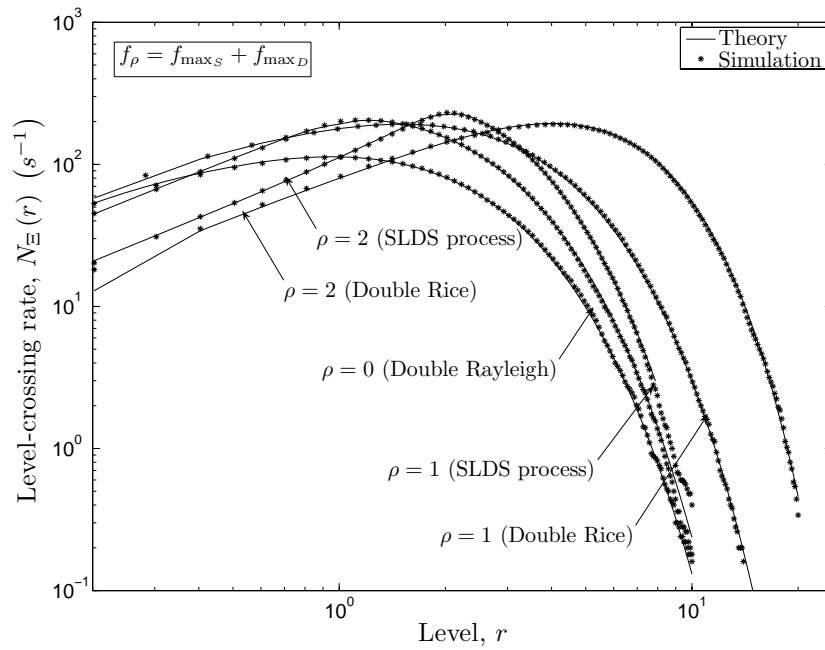


Figure G.8: A comparison of the LCR $N_{\Xi}(r)$ of SLDS processes $\Xi(t)$ for various values of ρ with that of various other stochastic processes.

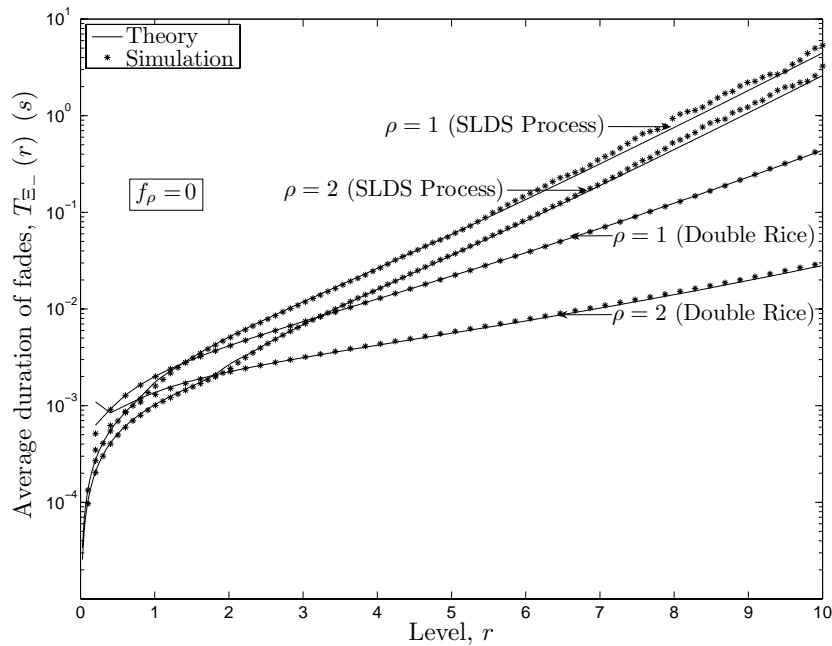


Figure G.9: A comparison of the ADF $T_{\Xi-}(r)$ of SLDS processes $\Xi(t)$ for various values of ρ with that of various other stochastic processes.

shown that the properties of SLDS processes are quite different from both double Rayleigh and the double Rice processes. For example, the PDF of SDLS processes approaches the symmetrical Laplace distribution when the amplitude of the LOS

component increases. Furthermore, the PDF of SLDS processes has a higher maximum value as compared to various other stochastic processes. On the other hand, for a particular value of ρ the spread of the PDF of SLDS processes follow the same trend as that of classical Rayleigh and classical Rice processes. However, the PDF of SLDS processes has a narrower spread as compared to the spread of double Rice processes. With increasing values of ρ the PDF of the phase process associated with SLDS processes acquires a higher maximum value and narrow spread. A thorough analysis of the LCR of SLDS processes reveals that at low signal levels, the LCR of SLDS processes decreases when ρ increases. However, the LCR of SLDS processes increases with increasing ρ at low signal levels, when compared with the LCR of double Rice processes. At medium and high signal levels, the LCR of SLDS processes is always lower than that of double Rice processes for the same value of ρ . The ADF of SLDS processes shows a behavior opposite to the LCR of SLDS processes. We have also provided sufficient evidence in this paper that SLDS processes reduces to double Rayleigh processes in the absence of the LOS component.

The theoretical analysis presented in this paper is useful for the researchers and designers of the physical layer for mobile-to-mobile communication systems. Our study provides an insight into the dynamics of SLDS fading channels, which can be exploited to develop robust modulation and coding schemes for such fading environments. Furthermore, with the help of the designed channel simulator, the overall performance of the system can also be evaluated by simulation for different kinds of SLDS fading environments.

REFERENCES

- [1] A. S. Akki. Statistical properties of mobile-to-mobile land communication channels. *IEEE Trans. Veh. Technol.*, 43(4):826–831, November 1994.
- [2] A. S. Akki and F. Haber. A statistical model of mobile-to-mobile land communication channel. *IEEE Trans. Veh. Technol.*, 35(1):2–7, February 1986.
- [3] S. Barbarossa and G. Scutari. Cooperative diversity through virtual arrays in multihop networks. In *Proc. IEEE International Conf. Acoustics, Speech, Signal Processing*, volume 4, pages 209–212. Hong Kong, China, April 2003.
- [4] M. Dohler. *Virtual Antenna Arrays*. Ph.D. dissertation, King's College, London, United Kingdom, 2003.
- [5] I. S. Gradshteyn and I. M. Ryzhik. *Table of Integrals, Series, and Products*. New York: Academic Press, 6th edition, 2000.

- [6] S. Kotz, T. J. Kozubowski, and K. Podgórski, editors. *The Laplace Distribution and Generalizations: A Revisit with Applications to Communications, Economics, Engineering, and Finance*. Boston: Birkhäuser, 2001.
- [7] I. Z. Kovacs, P. C. F. Eggers, K. Olesen, and L. G. Petersen. Investigations of outdoor-to-indoor mobile-to-mobile radio communication channels. In *Proc. IEEE 56th Veh. Technol. Conf., VTC'02-Fall*, volume 1, pages 430–434. Vancouver BC, Canada, September 2002.
- [8] J. N. Laneman, D. N. C. Tse, and G. W. Wornell. Cooperative diversity in wireless networks: Efficient protocols and outage behavior. *IEEE Trans. Inform. Theory*, 50(12):3062–3080, December 2004.
- [9] A. Papoulis and S. U. Pillai. *Probability, Random Variables and Stochastic Processes*. New York: McGraw-Hill, 4th edition, 2002.
- [10] C. S. Patel, G. L. Stüber, and T. G. Pratt. Statistical properties of amplify and forward relay fading channels. *IEEE Trans. Veh. Technol.*, 55(1):1–9, January 2006.
- [11] M. Pätzold. *Mobile Fading Channels*. Chichester: John Wiley & Sons, 2002.
- [12] M. Pätzold and B. O. Hogstad. Two new methods for the generation of multiple uncorrelated Rayleigh fading waveforms. In *Proc. IEEE 63rd Semi-annual Veh. Tech. Conf., VTC'06-Spring*, volume 6, pages 2782–2786. Melbourne, Australia, May 2006.
- [13] S. O. Rice. Mathematical analysis of random noise. *Bell Syst. Tech. J.*, 24:46–156, January 1945.
- [14] J. Salo, H. M. El-Sallabi, and P. Vainikainen. Impact of double-rayleigh fading on system performance. In *Proc. 1st IEEE Int. Symp. on Wireless Pervasive Computing, ISWPC 2006*. Phuket, Thailand, January 2006. 0-7803-9410-0/10.1109/ISWPC.2006.1613574.
- [15] J. Salo, H. M. El-Sallabi, and P. Vainikainen. Statistical analysis of the multiple scattering radio channel. *IEEE Trans. Antennas Propagat.*, 54(11):3114–3124, November 2006.
- [16] A. Sendonaris, E. Erkip, and B. Aazhang. User cooperation diversity — Part I: System description. *IEEE Trans. Commun.*, 51(11):1927–1938, November 2003.

- [17] A. Sendonaris, E. Erkip, and B. Aazhang. User cooperation diversity — Part II: Implementation aspects and performance analysis. *IEEE Trans. Commun.*, 51(11):1939–1948, November 2003.
- [18] M. K. Simon. *Probability Distributions Involving Gaussian Random Variables: A Handbook for Engineers and Scientists*. Dordrecht: Kluwer Academic Publishers, 2002.
- [19] B. Talha and M. Pätzold. On the statistical properties of double Rice channels. In *Proc. 10th Int. Symp. on Wireless Personal Multimedia Communications, WPMC 2007*, pages 517–522. Jaipur, India, December 2007.
- [20] G. N. Watson. *A Treatise on the Theory of Bessel Functions*. Bentley House, London: Cambridge University Press, 2nd edition, 1966.

Appendix H

Paper VII

Title: Mobile-to-Mobile Fading Channels in Amplify-and-Forward Relay Systems Under Line-of-Sight Conditions: Statistical Modeling and Analysis

Authors: **Batool Talha** and Matthias Pätzold

Affiliation: University of Agder, Faculty of Engineering and Science, P. O. Box 509, NO-4898 Grimstad, Norway

Journal: *Annals of Telecommunications*, April 2010. DOI 10.1007/s12243-010-0169-z.

Mobile-to-Mobile Fading Channels in Amplify-and-Forward Relay Systems Under Line-of-Sight Conditions: Statistical Modeling and Analysis

Batool Talha and Matthias Pätzold

Department of Information and Communication Technology
Faculty of Engineering and Science, Agder University College
Servicebox 509, NO-4876 Grimstad, Norway
E-mails: {batool.talha, matthias.paetzold}@uia.no

Abstract — This paper deals with the modeling and analysis of narrowband mobile-to-mobile (M2M) fading channels for amplify-and-forward relay links under line-of-sight (LOS) conditions. It is assumed that a LOS component exists in the direct link between the source mobile station (SMS) and the destination mobile station (DMS) as well as in the links via the mobile relay (MR). The proposed channel model is referred to as the multiple-LOS second-order scattering (MLSS) channel model^{1,2}. The MLSS channel model is derived from a second-order scattering process, where the received signal is modeled in the complex baseband as the sum of a single and a double scattered components. Analytical expressions are derived for the mean value, variance, probability density function (PDF), cumulative distribution function (CDF), level-crossing rate (LCR), and average duration of fades (ADF) of the received envelope of MLSS channels. The PDF of the channel phase is also investigated. It is observed that the LOS components and the relay gain have a significant influence on the statistics of MLSS channels. It is also shown that MLSS channels include various other channel models as special cases, e.g., double Rayleigh channels, double Rice channels, single-LOS double-scattering (SLDS) channels, non-line-of-sight (NLOS) second-order scattering (NLSS) channels, and single-LOS second-order scattering (SLSS) channels. The correctness of all analytical results is confirmed by simulations using a high performance channel simulator. Our novel MLSS channel model is of significant importance for

¹The material in this paper was presented in part at the 19th IEEE International Symposium on Personal, Indoor and Mobile Radio Communications, PIMRC 2008, Cannes, France, September 2008.

²The material in this paper has been published in part in the proceedings of the 51st IEEE Globecom 2008, New Orleans, USA, December 2008.

the system level performance evaluation of M2M communication systems in different M2M propagation scenarios. Furthermore, our studies pertaining to the fading behavior of MLSS channels are useful for the design and development of relay-based cooperative wireless networks.

Keywords—Amplify-and-forward relay systems, mobile-to-mobile fading channels, double Rayleigh process, double Rice process, probability density function, level-crossing rate, average duration of fades.

I. INTRODUCTION

Among several upcoming new wireless technologies, M2M communication [2] in cooperative networks has gained considerable attention in recent years. The driving force behind merging M2M communication into cooperative networks is its promise to provide a better link quality (higher diversity gain), an improved network range, and an overall increase in the system capacity. M2M cooperative wireless networks exploit the fact that single-antenna mobile stations cooperate with each other to share their antennas in order to form a virtual multiple-input multiple-output (MIMO) system in a multi-user scenario [8]. Thus, in such networks, cooperative diversity [6, 40, 41, 15] is achieved by relaying the signal transmitted from a mobile station to the final destination using other mobile stations in the network. However, to cope with the problems faced within the development of such systems, a solid knowledge of the underlying multipath fading channel characteristics is essential.

M2M fading channels in cooperative networks can be modeled as a sum of multiplicative fading channels. This sum of multiplicative fading channels is also called the multiple scattering radio propagation channel [4]. In a multiple scattering radio propagation environment, the received signal is composed of single, double, and in general multiple scattered components [4]. The multiple scattering concept provides a starting point for modeling the signal envelope fluctuations of various types of M2M channels, so that their statistical properties are in good agreement with measurement data [9, 4, 14]. In terms of statistics, M2M fading channels for relay-based cooperative networks are usually characterized by the mean, variance, and probability density function (PDF) of the envelope and phase of the received signal. Unfortunately, the envelope and phase distributions do not provide any information pertaining to the rate of fading of the channel. However, a detailed knowledge of the fading behavior of M2M fading channels is indispensable to the development, performance analysis, and test of cooperative wireless networks. The LCR of the envelope of fading channels is an important statistical quantity, revealing information about how fast the received signal changes with time. It is basically a measure

to describe the average number of times the signal envelope crosses a certain threshold level from up to down (or from down to up) per second. Another important statistical quantity is the ADF, which is defined as the expected value of the time intervals over which the fading signal envelope remains below a certain threshold level.

Studies pertaining to the statistical properties of M2M fading channels under NLOS propagation conditions in non-cooperative single-input single-output (SISO) systems can be found in [2, 1]. Real-world measurement data for narrowband M2M fading channels are studied in [16]. Analysis of correlation properties in the form of autocorrelation functions (ACFs) and cross-correlation functions (CCFs) for M2M fading channels in non-cooperative MIMO systems are available in [29, 50]. A variety of M2M propagation scenarios in relay-based cooperative networks however exist. Several models have therefore been proposed so far to characterize the fading statistics of M2M fading channels in such networks. Under NLOS propagation conditions, the M2M amplify-and-forward relay fading channel can be modeled as a double Rayleigh process [9, 14, 24]. Experimental measurements of outdoor-to-indoor M2M fading channels analyzed in [14] provide us with a solid ground to believe that double Rayleigh processes are well suited to model such channels. A detailed analysis on the statistics of double Rayleigh channels is presented in [24]. The authors of [37] have addressed the impact of double Rayleigh fading on the systems performance. Furthermore, motivated by the studies of double Rayleigh fading channels for keyhole channels [3], the so-called double Nakagami-m and cascaded Weibull fading channels have been proposed in [42] and [36], respectively. From the physical point of view it is reasonable to extend the double Rayleigh channel model to the double Rice channel model for M2M amplify-and-forward relay fading channels under LOS propagations conditions [44]. The double Rice channels come into play when LOS components exist in the transmission links from the SMS to the DMS via the relay. A thorough study pertaining to the dynamic behavior of double Rice channels is presented in [44]. In amplify-and-forward relay systems, profiting from cooperative diversity schemes require a further extension of the double Rayleigh channel model by adding a direct link from the SMS to the DMS. The resulting channel, obtained by combining the SMS-MR-DMS link and the SMS-DMS link is named as the NLSS channel model. The signal received after traversing through NLSS channels is composed of a sum of a single and a double scattered component [39, 38]. Studies conducted for NLSS channels provide us with a thorough analysis of the PDF and CDF of NLSS channels. However, there is a lack of information regarding the LCR and ADF of NLSS channels in the literature. Exten-

sions of NLSS fading channel models when a significant LOS component is present between the direct SMS-DMS link results in SLSS channels [39, 38]. SLSS channels have only been partially analyzed so far just as NLSS channels. A detailed analysis of the statistical properties of a physically non-realistic channel called the SLDS channel is presented in [45]. SLDS channel models can not be justified physically, since the scattered component of the direct SMS-DMS link is ignored while modeling the M2M fading channels.

In this paper, we propose a novel channel model referred to as the MLSS fading channel for amplify-and-forward relay channels under LOS conditions [46]. This model is specifically developed for such relay-based cooperative networks where time-division multiple-access (TDMA) based amplify-and-forward relay protocols [19, 5, 18] are employed. Furthermore, MLSS fading channels belong to the class of second-order scattering channels, where the received signal is modeled in the complex baseband as a sum of the single and the double scattered component. We have assumed that a LOS component is present in the direct link between the SMS and the DMS (i.e., the SMS-DMS link) as well as in the two links via the MR (i.e., the SMS-MR link and the MR-DMS link). For this new class of MLSS channels, we derive analytical expressions for the mean value, variance, PDF, CDF, LCR, and ADF of the received envelope as well as for the PDF of the channel phase assuming isotropic scattering conditions. We also show that the derived analytical expressions for MLSS processes include the corresponding expressions for double Rayleigh, double Rice, SLDS, NLSS, and SLSS processes as special cases. The correctness of all analytical results is confirmed by simulations using a high-performance channel simulator. Notice, that problems pertaining to the protocol level and system level implementation of amplify-and-forward relay networks is out of scope of the current paper. However, the analytical results presented in this article are important for the development and performance evaluation of relay-based cooperative networks in different M2M propagation environments under LOS and NLOS conditions.

The rest of the paper is structured as follows: In Section II, the reference model for amplify-and-forward MLSS fading channels is developed. Section III deals with the analysis of the statistical properties of MLSS fading processes. Special cases of MLSS fading channels are discussed in detail in Section IV. Section V confirms the validity of the analytical expressions presented in Section III by simulations. Finally, concluding remarks are given in Section VI.

II. THE MLSS FADING CHANNEL

Taking into consideration the limitations on the physical implementation of the mobile stations, i.e., the SMS, the mobile relay, and the DMS in an amplify-and-

forward relay communication system, the mentioned mobile stations mostly operate in half-duplex. This means that the mobile stations cannot transmit and receive a signal in the same frequency band at the same time. Here, it is assumed that the SMS continuously communicates with the DMS, i.e., the signal transmitted by the SMS in each time slot is received by the DMS. The MR however, receives a signal from the SMS in the first time slot and re-transmits it to the DMS in the second time slot [19, 5, 18]. The considered communication scenario determined by an SMS, a DMS, and an MR is shown in Fig. H.1.

In general, under NLOS conditions, the complex time-varying channel gain of the multiple scattering radio propagation channel proposed in [4] can be written as

$$\chi(t) = \alpha_1 \mu^{(1)}(t) + \alpha_2 \mu^{(2)}(t) \mu^{(3)}(t) + \alpha_3 \mu^{(4)}(t) \mu^{(5)}(t) \mu^{(6)}(t) + \dots \quad (1)$$

where $\mu^{(i)}(t)$ ($i = 1, 2, 3, \dots$) is a zero-mean complex Gaussian process that represents the scattered component of the i th link and α_i ($i = 1, 2, 3, \dots$) is a real-valued constant that determines the contribution of the i th scattered component. In (1), the Gaussian processes $\mu^{(i)}(t)$ are mutually independent. However, when the fading channel is modeled by taking into account only the first two terms of (1), the resulting channel is referred to as the NLSS channel [39, 38]. Here, we are presenting an extension of the NLSS channel to the MLSS channel by incorporating a LOS component in all transmission links.

Starting from (1), ignoring $\mu^{(i)}(t) \forall i \geq 4$, and replacing $\mu^{(i)}(t)$ by $\mu_\rho^{(i)}(t)$ for $i = 1, 2, 3$, results in

$$\chi_\rho(t) = \mu_\rho^{(1)}(t) + A_{\text{MR}} \mu_\rho^{(2)}(t) \mu_\rho^{(3)}(t) \quad (2)$$

where $\alpha_1 = 1$ and $\alpha_2 = A_{\text{MR}}$. The signal model in (2) represents well the considered propagation scenario, where the direct transmission link from the SMS to the DMS and the link via the MR coexist every second time slot.

In (2), the quantity A_{MR} is called the relay gain, which is a real constant quantity. In (2), $\mu_\rho^{(1)}(t)$, $\mu_\rho^{(2)}(t)$, and $\mu_\rho^{(3)}(t)$ are statistically independent non-zero-mean complex Gaussian processes, which model the subchannels in the SMS-DMS, SMS-MR, and MR-DMS links, respectively (see Fig. H.1). Each complex Gaussian process $\mu_\rho^{(i)}(t) = \mu_{\rho_1}^{(i)}(t) + j\mu_{\rho_2}^{(i)}(t)$ represents the sum of a scattered component $\mu^{(i)}(t)$ and a LOS component $m^{(i)}(t)$, i.e., $\mu_\rho^{(i)}(t) = \mu^{(i)}(t) + m^{(i)}(t)$. The scattered component $\mu^{(i)}(t) = \mu_1^{(i)}(t) + j\mu_2^{(i)}(t)$ is modeled by a zero-mean complex Gaussian process with variance $2\sigma_i^2$. Furthermore, the power spectral density (PSD) $S_{\mu^{(i)}\mu^{(i)}}(f)$ can be proved to be symmetrical for isotropic scattering condi-

tions [13]. The LOS component $m^{(i)}(t) = \rho_i e^{j(2\pi f_{\rho_i} t + \theta_{\rho_i})}$ assumes a fixed amplitude ρ_i , a constant Doppler frequency f_{ρ_i} , and a constant phase θ_{ρ_i} for $i = 1, 2, 3$. Let us denote the second term in (2), which is a weighted non-zero-mean complex double Gaussian process, as $\zeta_\rho(t) = \zeta_{\rho_1}(t) + j\zeta_{\rho_2}(t) = A_{\text{MR}} \mu_\rho^{(2)}(t) \mu_\rho^{(3)}(t)$. From Fig. H.1, we can realize that $\zeta_\rho(t)$ models the overall fading in the SMS-MR-DMS link. It is worth mentioning here that the relay gain A_{MR} is just a scaling factor for the mean and variance of the complex Gaussian process $\mu_\rho^{(3)}(t)$, i.e., $m^{(3)}(t) = E\{A_{\text{MR}} \mu_\rho^{(3)}(t)\} = \rho_{A_{\text{MR}}} e^{j(2\pi f_{\rho_3} t + \theta_{\rho_3})}$, where $\rho_{A_{\text{MR}}} = A_{\text{MR}} \rho_3$ and $2\sigma_{A_{\text{MR}}}^2 = \text{Var}\{A_{\text{MR}} \mu_\rho^{(3)}(t)\} = 2(A_{\text{MR}} \sigma_3)^2$. Finally, the overall fading process that takes into account the direct SMS-DMS link and the SMS-DMS link via the MR results in the complex process $\chi_\rho(t) = \chi_{\rho_1}(t) + j\chi_{\rho_2}(t)$ introduced in (2). The absolute value of $\chi_\rho(t)$ defines the MLSS process

$$\Xi(t) = |\chi_\rho(t)| = |\mu_\rho^{(1)}(t) + \zeta_\rho(t)|. \quad (3)$$

Furthermore, the argument of $\chi_\rho(t)$ introduces the phase process $\Theta(t)$

$$\Theta(t) = \arg\{\chi_\rho(t)\}. \quad (4)$$

It is important to point out here that the signal reaching the DMS via the mobile relay is delayed by one time slot. However, we have not introduced this time delay in (2). One of the reasons behind this is that the time delay is meaningless in channel modeling and system performance analysis. Notice, a time delay only introduces a phase shift in the signal. Thus, this delay does not affect the envelope related statistical properties of the channel, like for example, PDF, LCR, and ADF. Besides, it is assumed that the subchannels in the SMS-DMS, SMS-MR, and MR-DMS links are uncorrelated (see Section III). It can be shown that the correlation properties of a channel, such as the cross-correlation function (CCF), are independent of the time delay. Meaning thereby, the observed delay here would not influence the correlation properties of the overall channel.

If there is no delay, then the received signal is like a superposition of different multipath components. These multipath components can be single-, double-, triple-scattered components as shown in [4]. In our system, the transmitted signal arrives at the DMS after crossing two links. One of the links can be modeled as a single scattered component and the other link corresponds to double scattered component. The superposition of the multipath components is given in (2).

III. ANALYSIS OF THE MLSS FADING CHANNEL

In this section, we analyze the statistical properties of MLSS fading channels introduced in Section II. The starting point for the derivation of the analytical expressions of the most important statistical quantities like the mean value, variance, PDF, LCR, and ADF of MLSS fading channels, as well as the PDF of the corresponding phase process is the computation of the joint PDF $p_{\chi_{\rho_1} \chi_{\rho_2} \dot{\chi}_{\rho_1} \dot{\chi}_{\rho_2}}(u_1, u_2, \dot{u}_1, \dot{u}_2; t)$ of the stochastic processes $\chi_{\rho_1}(t)$, $\chi_{\rho_2}(t)$, $\dot{\chi}_{\rho_1}(t)$, and $\dot{\chi}_{\rho_2}(t)$ at the same time t . Throughout this paper, the overdot indicates the time derivative. The joint PDF $p_{\chi_{\rho_1} \chi_{\rho_2} \dot{\chi}_{\rho_1} \dot{\chi}_{\rho_2}}(u_1, u_2, \dot{u}_1, \dot{u}_2; t)$ can be expressed in terms of a 4-dimensional (4D) convolution integral as

$$p_{\chi_{\rho_1} \chi_{\rho_2} \dot{\chi}_{\rho_1} \dot{\chi}_{\rho_2}}(u_1, u_2, \dot{u}_1, \dot{u}_2; t) = \int_{-\infty}^{\infty} \int_{-\infty}^{\infty} \int_{-\infty}^{\infty} \int_{-\infty}^{\infty} d\dot{y}_2 d\dot{y}_1 dy_2 dy_1 \times p_{\varsigma_{\rho_1} \varsigma_{\rho_2} \dot{\varsigma}_{\rho_1} \dot{\varsigma}_{\rho_2} \mu_{\rho_1}^{(1)} \mu_{\rho_2}^{(1)} \dot{\mu}_{\rho_1}^{(1)} \dot{\mu}_{\rho_2}^{(1)}}(y_1, y_2, \dot{y}_1, \dot{y}_2, u_1 - y_1, u_2 - y_2, \dot{u}_1 - \dot{y}_1, \dot{u}_2 - \dot{y}_2; t) \quad (5)$$

where $p_{\varsigma_{\rho_1} \varsigma_{\rho_2} \dot{\varsigma}_{\rho_1} \dot{\varsigma}_{\rho_2} \mu_{\rho_1}^{(1)} \mu_{\rho_2}^{(1)} \dot{\mu}_{\rho_1}^{(1)} \dot{\mu}_{\rho_2}^{(1)}}(y_1, y_2, \dot{y}_1, \dot{y}_2, u_1, u_2, \dot{u}_1, \dot{u}_2; t)$ is the joint PDF of the processes $\mu_{\rho_1}^{(1)}(t)$, $\mu_{\rho_2}^{(1)}(t)$, $\dot{\mu}_{\rho_1}^{(1)}(t)$, $\dot{\mu}_{\rho_2}^{(1)}(t)$, $\varsigma_{\rho_1}(t)$, $\varsigma_{\rho_2}(t)$, $\dot{\varsigma}_{\rho_1}(t)$, and $\dot{\varsigma}_{\rho_2}(t)$ at the same time t . It is important to note that the processes $\mu_{\rho_i}^{(1)}(t)$, $\dot{\mu}_{\rho_i}^{(1)}(t)$, $\varsigma_{\rho_i}(t)$, and $\dot{\varsigma}_{\rho_i}(t)$ ($i = 1, 2$) are mutually uncorrelated³. Furthermore, the statistically independent nature of the process pairs $\{\mu_{\rho_i}^{(1)}(t), \dot{\mu}_{\rho_i}^{(1)}(t)\}$ and $\{\varsigma_{\rho_i}(t), \dot{\varsigma}_{\rho_i}(t)\}$ ($i = 1, 2$) allows us to write $p_{\varsigma_{\rho_1} \varsigma_{\rho_2} \dot{\varsigma}_{\rho_1} \dot{\varsigma}_{\rho_2} \mu_{\rho_1}^{(1)} \mu_{\rho_2}^{(1)} \dot{\mu}_{\rho_1}^{(1)} \dot{\mu}_{\rho_2}^{(1)}}(y_1, y_2, \dot{y}_1, \dot{y}_2, u_1, u_2, \dot{u}_1, \dot{u}_2; t)$ as a product of the joint PDFs $p_{\mu_{\rho_1}^{(1)} \mu_{\rho_2}^{(1)} \dot{\mu}_{\rho_1}^{(1)} \dot{\mu}_{\rho_2}^{(1)}}(u_1, u_2, \dot{u}_1, \dot{u}_2; t)$ and $p_{\varsigma_{\rho_1} \varsigma_{\rho_2} \dot{\varsigma}_{\rho_1} \dot{\varsigma}_{\rho_2}}(y_1, y_2, \dot{y}_1, \dot{y}_2; t)$. Hence, (5) becomes

$$p_{\chi_{\rho_1} \chi_{\rho_2} \dot{\chi}_{\rho_1} \dot{\chi}_{\rho_2}}(u_1, u_2, \dot{u}_1, \dot{u}_2; t) = \int_{-\infty}^{\infty} \int_{-\infty}^{\infty} \int_{-\infty}^{\infty} \int_{-\infty}^{\infty} d\dot{y}_2 d\dot{y}_1 dy_2 dy_1 p_{\varsigma_{\rho_1} \varsigma_{\rho_2} \dot{\varsigma}_{\rho_1} \dot{\varsigma}_{\rho_2}}(y_1, y_2, \dot{y}_1, \dot{y}_2; t) \times p_{\mu_{\rho_1}^{(1)} \mu_{\rho_2}^{(1)} \dot{\mu}_{\rho_1}^{(1)} \dot{\mu}_{\rho_2}^{(1)}}(u_1 - y_1, u_2 - y_2, \dot{u}_1 - \dot{y}_1, \dot{u}_2 - \dot{y}_2; t) \quad (6)$$

where $p_{\mu_{\rho_1}^{(1)} \mu_{\rho_2}^{(1)} \dot{\mu}_{\rho_1}^{(1)} \dot{\mu}_{\rho_2}^{(1)}}(u_1, u_2, \dot{u}_1, \dot{u}_2; t)$ is the joint PDF of the processes $\mu_{\rho_i}^{(1)}(t)$ and $\dot{\mu}_{\rho_i}^{(1)}(t)$ ($i = 1, 2$) at the same time t . Using the multivariate Gaussian distribution

³The PSD $S_{\mu^{(i)} \mu^{(i)}}(f)$ is an even function. Then, $\mu^{(i)}(t)$ and $\dot{\mu}^{(i)}(t)$ are uncorrelated at the same point in time, because $r_{\mu^{(i)} \mu^{(i)}}(0) = -\frac{d}{d\tau} r_{\mu^{(i)} \mu^{(i)}}(\tau) \big|_0 = -j2\pi \int_{-\infty}^{\infty} f S_{\mu^{(i)} \mu^{(i)}}(f) d\tau = 0$. Since, $\mu^{(i)}(t)$ and $\dot{\mu}^{(i)}(t)$ are uncorrelated Gaussian processes, it follows that $\mu^{(i)}(t)$ and $\dot{\mu}^{(i)}(t)$ are also independent [22].

(see, e.g., [43, Eq. (3.2)]), this joint PDF can be written as

$$p_{\mu_{\rho_1}^{(1)} \mu_{\rho_2}^{(1)} \dot{\mu}_{\rho_1}^{(1)} \dot{\mu}_{\rho_2}^{(1)}}(u_1, u_2, \dot{u}_1, \dot{u}_2; t) = \frac{1}{(2\pi)^2 \sigma_1^2 \beta_1} e^{-\frac{(u_1 - m_1^{(1)}(t))^2 + (u_2 - m_2^{(1)}(t))^2}{2\sigma_1^2}} \times e^{-\frac{(\dot{u}_1 - \dot{m}_1^{(1)}(t))^2 + (\dot{u}_2 - \dot{m}_2^{(1)}(t))^2}{2\beta_1}}. \quad (7)$$

Similarly, $p_{\varsigma_{\rho_1} \varsigma_{\rho_2} \dot{\varsigma}_{\rho_1} \dot{\varsigma}_{\rho_2}}(y_1, y_2, \dot{y}_1, \dot{y}_2; t)$ in (6), represents the joint PDF of the processes $\varsigma_{\rho_i}(t)$ and $\dot{\varsigma}_{\rho_i}(t)$ ($i = 1, 2$) at the same time t . Recall that the stochastic process $\varsigma_{\rho}(t)$ is a product process, i.e., $\varsigma_{\rho}(t) = A_{\text{MR}} \mu_{\rho}^{(2)}(t) \mu_{\rho}^{(3)}(t)$. Thus, exploiting the statistical independent nature of the underlying complex Gaussian processes, i.e., $\mu_{\rho}^{(2)}(t)$ and $\mu_{\rho}^{(3)}(t)$ we can write the joint PDF $p_{\varsigma_{\rho_1} \varsigma_{\rho_2} \dot{\varsigma}_{\rho_1} \dot{\varsigma}_{\rho_2}}(y_1, y_2, \dot{y}_1, \dot{y}_2; t)$ as follows

$$p_{\varsigma_{\rho_1} \varsigma_{\rho_2} \dot{\varsigma}_{\rho_1} \dot{\varsigma}_{\rho_2}}(y_1, y_2, \dot{y}_1, \dot{y}_2; t) = \int_{-\infty}^{\infty} \int_{-\infty}^{\infty} \int_{-\infty}^{\infty} \int_{-\infty}^{\infty} |J|^{-1} p_{\mu_{\rho_1}^{(2)} \mu_{\rho_2}^{(2)} \dot{\mu}_{\rho_1}^{(2)} \dot{\mu}_{\rho_2}^{(2)}}(z_1, z_2, \dot{z}_1, \dot{z}_2; t) \times p_{\mu_{\rho_1}^{(3)} \mu_{\rho_2}^{(3)} \dot{\mu}_{\rho_1}^{(3)} \dot{\mu}_{\rho_2}^{(3)}}\left(\frac{y_1}{z_1}, \frac{y_2}{z_2}, \frac{\dot{y}_1}{\dot{z}_1}, \frac{\dot{y}_2}{\dot{z}_2}; t\right) dz_2 dz_1 dz_2 dz_1 \quad (8)$$

where $|J| = (z_1^2 + z_2^2)^2$ denotes the Jacobian determinant and $p_{\mu_{\rho_1}^{(i)} \mu_{\rho_2}^{(i)} \dot{\mu}_{\rho_1}^{(i)} \dot{\mu}_{\rho_2}^{(i)}}(z_1, z_2, \dot{z}_1, \dot{z}_2; t)$ ($i = 2, 3$) is the multivariate Gaussian distribution [43, Eq. (3.2)]. The solution of (8) is as follows

$$p_{\varsigma_{\rho_1} \varsigma_{\rho_2} \dot{\varsigma}_{\rho_1} \dot{\varsigma}_{\rho_2}}(y_1, y_2, \dot{y}_1, \dot{y}_2; t) = \int_{-\infty}^{\infty} \int_{-\infty}^{\infty} dz_2 dz_1 \frac{e^{-\frac{(z_1 - m_1^{(3)}(t))^2 + (z_2 - m_2^{(3)}(t))^2}{2\sigma_{A_{\text{MR}}}^2}} e^{-\frac{(m_1^{(3)}(t))^2 + (m_2^{(3)}(t))^2}{2\beta_3}}}{(2\pi)^3 \sigma_2^2 \sigma_{A_{\text{MR}}}^2 [\beta_3 (y_1^2 + y_2^2) + \beta_2 (z_1^2 + z_2^2)^2]} \times e^{\frac{\beta_2 (z_1^2 + z_2^2)^2 \left\{ (m_1^{(3)}(t))^2 + (m_2^{(3)}(t))^2 \right\} + \beta_3 (y_1^2 + y_2^2) (m_1^{(2)}(t) y_2 z_1 + m_2^{(2)}(t) y_1 z_1)}{2\beta_2 \left\{ \beta_3 (y_1^2 + y_2^2) + \beta_2 (z_1^2 + z_2^2)^2 \right\}}} \times e^{\frac{z_1 m_2^{(3)}(t) (-y_2 \dot{y}_1 + y_1 \dot{y}_2 - \dot{m}_2^{(2)}(t) y_1 z_1 + \dot{m}_1^{(2)}(t) y_2 z_1)}{\beta_3 (y_1^2 + y_2^2) + \beta_2 (z_1^2 + z_2^2)^2}} \times e^{-\frac{y_1^2 + y_2^2 - 2(y_2 m_2^{(2)}(t) + y_1 m_1^{(2)}(t)) z_1 - 2(y_2 m_1^{(2)}(t) - y_1 m_2^{(2)}(t)) z_2 + \left\{ (m_1^{(2)}(t))^2 + (m_2^{(2)}(t))^2 \right\} (z_1^2 + z_2^2)}{2\sigma_2^2 (z_1^2 + z_2^2)}} \times e^{-\frac{y_1^2 + y_2^2 - 2(\dot{y}_2 \dot{m}_2^{(2)}(t) + \dot{y}_1 \dot{m}_1^{(2)}(t)) z_1 - 2(\dot{y}_2 \dot{m}_1^{(2)}(t) - \dot{y}_1 \dot{m}_2^{(2)}(t)) z_2 + \left\{ (\dot{m}_1^{(2)}(t))^2 + (\dot{m}_2^{(2)}(t))^2 \right\} (z_1^2 + z_2^2)}{2\beta_2 (z_1^2 + z_2^2)}} \times e^{\frac{2\beta_2 z_2 (z_1^2 + z_2^2) \left\{ m_1^{(3)}(t) (y_2 \dot{y}_1 - y_1 \dot{y}_2 + 2\dot{m}_2^{(2)}(t) y_1 z_1 - 2\dot{m}_1^{(2)}(t) y_2 z_1) + \dot{m}_2^{(3)}(t) (y_1 \dot{y}_1 + y_2 \dot{y}_2 - 2\dot{m}_1^{(2)}(t) y_1 z_1 - 2\dot{m}_2^{(2)}(t) y_2 z_1) \right\} + \beta_3 (y_1^2 + y_2^2) (y_1^2 + y_2^2)}{2\beta_2 (z_1^2 + z_2^2) \left\{ \beta_3 (y_1^2 + y_2^2) + \beta_2 (z_1^2 + z_2^2)^2 \right\}}} \times e^{\frac{\beta_3 (y_1^2 + y_2^2) [-2\dot{y}_2 (\dot{m}_2^{(2)}(t) z_1 + \dot{m}_1^{(2)}(t) z_2) + 2\dot{y}_1 (-\dot{m}_1^{(2)}(t) z_1 + \dot{m}_2^{(2)}(t) z_2)]}{2\beta_2 (z_1^2 + z_2^2) \left\{ \beta_3 (y_1^2 + y_2^2) + \beta_2 (z_1^2 + z_2^2)^2 \right\}}} \times e^{\frac{z_1 m_1^{(3)}(t) (y_1 \dot{y}_1 + y_2 \dot{y}_2 - \dot{m}_1^{(2)}(t) y_1 z_1 + \dot{m}_2^{(2)}(t) y_2 z_1)}{\beta_3 (y_1^2 + y_2^2) + \beta_2 (z_1^2 + z_2^2)^2}}$$

$$\times e^{-\frac{z_2^2 \left\{ m_1^{(2)}(t) m_1^{(3)}(t) y_1 + m_2^{(2)}(t) m_2^{(3)}(t) y_1 + m_2^{(2)}(t) m_1^{(3)}(t) y_2 - m_1^{(2)}(t) m_2^{(3)}(t) y_2 \right\}}{\beta_3 (y_1^2 + y_2^2) + \beta_2 (z_1^2 + z_2^2)^2}} \quad (9)$$

It should be pointed out here that the joint densities $p_{\mu_{\rho_1}^{(1)} \mu_{\rho_2}^{(1)} \dot{\mu}_{\rho_1}^{(1)} \dot{\mu}_{\rho_2}^{(1)}}(u_1, u_2, \dot{u}_1, \dot{u}_2; t)$ and $p_{\varsigma_{\rho_1} \varsigma_{\rho_2} \dot{\varsigma}_{\rho_1} \dot{\varsigma}_{\rho_2}}(y_1, y_2, \dot{y}_1, \dot{y}_2; t)$ are functions of time t because of the Doppler frequency f_{ρ_i} of the LOS component $m^{(i)}(t)$ ($i = 1, 2, 3$). Only for the special case when $f_{\rho_i} = 0 \quad \forall i = 1, 2, 3$, the joint densities $p_{\mu_{\rho_1}^{(1)} \mu_{\rho_2}^{(1)} \dot{\mu}_{\rho_1}^{(1)} \dot{\mu}_{\rho_2}^{(1)}}(u_1, u_2, \dot{u}_1, \dot{u}_2)$ and $p_{\varsigma_{\rho_1} \varsigma_{\rho_2} \dot{\varsigma}_{\rho_1} \dot{\varsigma}_{\rho_2}}(y_1, y_2, \dot{y}_1, \dot{y}_2)$ become independent of time t . Furthermore, in (7) and (9), the quantity β_i ($i = 1, 2, 3$) is the negative curvature of the autocorrelation function of the inphase and quadrature components of $\mu^{(i)}(t)$ ($i = 1, 2, 3$). Under isotropic scattering conditions, the quantities β_i ($i = 1, 2, 3$) can be expressed for M2M fading channels as [1, 25]

$$\beta_1 = 2(\sigma_1 \pi)^2 (f_{\text{SMS}_{\max}}^2 + f_{\text{DMS}_{\max}}^2) \quad (10a)$$

$$\beta_2 = 2(\sigma_2 \pi)^2 (f_{\text{SMS}_{\max}}^2 + f_{\text{MR}_{\max}}^2) \quad (10b)$$

$$\beta_3 = 2(\sigma_{\text{AMR}} \pi)^2 (f_{\text{MR}_{\max}}^2 + f_{\text{DMS}_{\max}}^2) \quad (10c)$$

where the symbols $f_{\text{SMS}_{\max}}$, $f_{\text{MR}_{\max}}$, and $f_{\text{DMS}_{\max}}$ denote the maximum Doppler frequency caused by the motion of the SMS, the MR, and the DMS, respectively. Note that the maximum Doppler frequencies associated with the individual M2M subchannels in the SMS-DMS, SMS-MR, and MR-DMS links, i.e., $f_{\text{SMS-DMS}_{\max}}$, $f_{\text{SMS-MR}_{\max}}$, and $f_{\text{MR-DMS}_{\max}}$ are greater than maximum Doppler frequencies $f_{\text{SMS}_{\max}}$, $f_{\text{MR}_{\max}}$, and $f_{\text{DMS}_{\max}}$. Substituting (7) and (9) in (6), applying the concept of transformation of random variables [22], and doing tedious algebraic manipulations, allows us to express the joint PDF $p_{\Xi \dot{\Xi} \Theta \dot{\Theta}}(x, \dot{x}, \theta, \dot{\theta}; t)$ of the MLSS process $\Xi(t)$, and the phase process $\Theta(t)$ as well as their respective time derivatives $\dot{\Xi}(t)$ and $\dot{\Theta}(t)$ as shown in (11) below

$$\begin{aligned} p_{\Xi \dot{\Xi} \Theta \dot{\Theta}}(x, \dot{x}, \theta, \dot{\theta}; t) &= \frac{x^2 e^{-\frac{x^2}{2\sigma_1^2}} e^{-\frac{(m_1^{(2)}(t))^2 + (m_2^{(2)}(t))^2}{2\beta_2}} e^{-\frac{(m_1^{(3)}(t))^2 + (m_2^{(3)}(t))^2}{2\beta_3}} e^{-\frac{(m_1^{(1)}(t))^2 + (m_2^{(1)}(t))^2}{2\beta_1}}}{(2\pi)^4 \sigma_1^2 \sigma_2^2 \sigma_{\text{AMR}}^2} \\ &\times \int_{-\infty}^{\infty} \int_{-\infty}^{\infty} \int_{-\infty}^{\infty} \int_{-\infty}^{\infty} dz_2 dz_1 dy_2 dy_1 \frac{e^{-\frac{(z_1 - m_1^{(3)}(t))^2 + (z_2 - m_2^{(3)}(t))^2}{2\sigma_{\text{AMR}}^2}} e^{-\frac{(y_1 + m_1^{(1)}(t))^2 + (y_2 + m_2^{(1)}(t))^2}{2\sigma_1^2}}}{\beta_1 (z_1^2 + z_2^2) + \beta_3 (y_1^2 + y_2^2) + \beta_2 (z_1^2 + z_2^2)^2} \\ &\times e^{-\frac{y_1^2 + y_2^2 - 2(y_2 m_2^{(2)}(t) + y_1 m_1^{(2)}(t)) z_1 - 2(y_2 m_1^{(2)}(t) - y_1 m_2^{(2)}(t)) z_2 + \left\{ (m_1^{(2)}(t))^2 + (m_2^{(2)}(t))^2 \right\} (z_1^2 + z_2^2)}{2\sigma_2^2 (z_1^2 + z_2^2)}} \frac{\beta_3 (y_1^2 + y_2^2) \left\{ (m_1^{(1)}(t))^2 + (m_2^{(1)}(t))^2 \right\}}{e^{2\beta_1 \left\{ \beta_1 (z_1^2 + z_2^2) + \beta_3 (y_1^2 + y_2^2) + \beta_2 (z_1^2 + z_2^2)^2 \right\}}} \\ &\times e^{-\frac{\beta_2^2 (z_1^2 + z_2^2)^2 \left[\beta_3 \left\{ (m_1^{(1)}(t))^2 + (m_2^{(1)}(t))^2 \right\} + \beta_1 \left\{ (m_1^{(3)}(t))^2 + (m_2^{(3)}(t))^2 \right\} + \beta_3 \beta_1 \left\{ (m_1^{(2)}(t))^2 + (m_2^{(2)}(t))^2 \right\} \right] \left[\beta_3 (y_1^2 + y_2^2) + \beta_1 (z_1^2 + z_2^2) \right]}{2\beta_3 \beta_2 \beta_1 \left\{ \beta_1 (z_1^2 + z_2^2) + \beta_3 (y_1^2 + y_2^2) + \beta_2 (z_1^2 + z_2^2)^2 \right\}}} \end{aligned}$$

$$\begin{aligned}
& \frac{z_2^2 \left\{ \dot{m}_1^{(2)}(t) \dot{m}_1^{(3)}(t) y_1 + \dot{m}_2^{(2)}(t) \dot{m}_2^{(3)}(t) y_1 + \dot{m}_2^{(2)}(t) \dot{m}_1^{(3)}(t) y_2 - \dot{m}_1^{(2)}(t) \dot{m}_2^{(3)}(t) y_2 - z_1 \left(\dot{m}_1^{(1)}(t) \dot{m}_1^{(2)}(t) + \dot{m}_2^{(1)}(t) \dot{m}_2^{(2)}(t) \right) - z_2 \left(\dot{m}_2^{(1)}(t) \dot{m}_1^{(2)}(t) - \dot{m}_1^{(1)}(t) \dot{m}_2^{(2)}(t) \right) \right\}}{\beta_1 (z_1^2 + z_2^2) + \beta_3 (y_1^2 + y_2^2) + \beta_2 (z_1^2 + z_2^2)^2} \\
& \times e \\
& \frac{z_2 \left\{ 2z_1 \left(\dot{m}_2^{(2)}(t) \dot{m}_1^{(3)}(t) y_1 - \dot{m}_1^{(2)}(t) \dot{m}_2^{(3)}(t) y_1 - \dot{m}_1^{(2)}(t) \dot{m}_1^{(3)}(t) y_2 - \dot{m}_2^{(2)}(t) \dot{m}_2^{(3)}(t) y_2 \right) - z_1^2 \left(\dot{m}_2^{(1)}(t) \dot{m}_1^{(2)}(t) - \dot{m}_1^{(1)}(t) \dot{m}_2^{(2)}(t) \right) + \left(\dot{m}_2^{(1)}(t) \dot{m}_1^{(3)}(t) - \dot{m}_1^{(1)}(t) \dot{m}_2^{(3)}(t) \right) y_1 \right\}}{\beta_1 (z_1^2 + z_2^2) + \beta_3 (y_1^2 + y_2^2) + \beta_2 (z_1^2 + z_2^2)^2} \\
& \times e \\
& \frac{z_1^2 \left(\dot{m}_1^{(2)}(t) \dot{m}_2^{(3)}(t) y_2 - \dot{m}_1^{(2)}(t) \dot{m}_1^{(3)}(t) y_1 - \dot{m}_2^{(2)}(t) \dot{m}_2^{(3)}(t) y_1 - \dot{m}_2^{(2)}(t) \dot{m}_1^{(3)}(t) y_2 \right) - z_1 \left(\dot{m}_1^{(1)}(t) \dot{m}_1^{(3)}(t) y_1 + \dot{m}_2^{(1)}(t) \dot{m}_2^{(3)}(t) y_1 + \dot{m}_2^{(1)}(t) \dot{m}_1^{(3)}(t) y_2 - \dot{m}_1^{(1)}(t) \dot{m}_2^{(3)}(t) y_2 \right)}{\beta_1 (z_1^2 + z_2^2) + \beta_3 (y_1^2 + y_2^2) + \beta_2 (z_1^2 + z_2^2)^2} \\
& \times e \\
& \frac{z_1^3 \left(\dot{m}_1^{(1)}(t) \dot{m}_1^{(2)}(t) + \dot{m}_2^{(1)}(t) \dot{m}_2^{(2)}(t) \right) + \left\{ \dot{m}_1^{(3)}(t) (y_2 z_1 - y_1 z_2) + \dot{m}_2^{(3)}(t) (y_1 z_1 + y_2 z_2) + \left(\dot{m}_2^{(1)}(t) + \dot{m}_2^{(2)}(t) z_1 + \dot{m}_1^{(2)}(t) z_2 \right) (z_1^2 + z_2^2) \right\} (x \dot{\theta} \cos \theta + \dot{x} \sin \theta)}{\beta_1 (z_1^2 + z_2^2) + \beta_3 (y_1^2 + y_2^2) + \beta_2 (z_1^2 + z_2^2)^2} \\
& \times e \\
& \frac{\left\{ \dot{m}_2^{(3)}(t) (y_1 z_2 - y_2 z_1) + \dot{m}_1^{(3)}(t) (y_1 z_1 + y_2 z_2) + \left(\dot{m}_1^{(1)}(t) + \dot{m}_1^{(2)}(t) z_1 - \dot{m}_2^{(2)}(t) z_2 \right) (z_1^2 + z_2^2) \right\} (x \cos \theta - x \dot{\theta} \sin \theta) - \left\{ \dot{m}_2^{(1)}(t) \dot{m}_2^{(3)}(t) + \dot{m}_1^{(1)}(t) \dot{m}_1^{(3)}(t) \right\} y_2 z_2}{\beta_1 (z_1^2 + z_2^2) + \beta_3 (y_1^2 + y_2^2) + \beta_2 (z_1^2 + z_2^2)^2} \\
& \times e \\
& \frac{\beta_1 (z_1^2 + z_2^2) \left\{ \left(\dot{m}_1^{(3)}(t) \right)^2 + \left(\dot{m}_2^{(3)}(t) \right)^2 \right\}}{2 \beta_3 \left\{ \beta_1 (z_1^2 + z_2^2) + \beta_3 (y_1^2 + y_2^2) + \beta_2 (z_1^2 + z_2^2)^2 \right\}} e^{-\frac{(z_1^2 + z_2^2) \{ x^2 + (x \dot{\theta})^2 \}}{2 \left\{ \beta_1 (z_1^2 + z_2^2) + \beta_3 (y_1^2 + y_2^2) + \beta_2 (z_1^2 + z_2^2)^2 \right\}}} \frac{r (y_1 + \dot{m}_1^{(1)}(t)) \cos \theta + r (y_2 + \dot{m}_2^{(1)}(t)) \sin \theta}{\sigma_1^2} \\
& \times e \tag{11}
\end{aligned}$$

for $x \geq 0$, $|\dot{x}| < \infty$, $|\theta| \leq \pi$, and $|\dot{\theta}| < \infty$. The resulting joint PDF $p_{\Xi \dot{\Xi} \Theta \dot{\Theta}}(x, \dot{x}, \theta, \dot{\theta}; t)$ is of fundamental importance, because it provides the basis for the computation of the PDF, LCR, and ADF of MLSS processes $\Xi(t)$ as well as the PDF of the corresponding phase processes $\Theta(t)$.

A. PDF of MLSS Processes

The joint PDF $p_{\Xi \Theta}(x, \theta; t)$ of the MLSS process $\Xi(t)$ and the corresponding phase process $\Theta(t)$ can be obtained by solving the integrals over the joint PDF $p_{\Xi \dot{\Xi} \Theta \dot{\Theta}}(x, \dot{x}, \theta, \dot{\theta}; t)$ according to

$$p_{\Xi \Theta}(x, \theta; t) = \int_{-\infty}^{\infty} \int_{-\infty}^{\infty} p_{\Xi \dot{\Xi} \Theta \dot{\Theta}}(x, \dot{x}, \theta, \dot{\theta}; t) d\dot{\theta} d\dot{x} \tag{12}$$

for $x \geq 0$ and $|\theta| \leq \pi$. Substituting (11) in (12) results in the following expression

$$\begin{aligned}
p_{\Xi \Theta}(x, \theta; t) &= \frac{x e^{\frac{x^2}{2\sigma_1^2}}}{(2\pi)^2 \sigma_1^2 \sigma_2^2 \sigma_{A_{MR}}^2} \int_0^{\infty} \int_0^{\infty} \int_{-\pi}^{\pi} d\psi d\omega dv \frac{\omega}{v} e^{-\frac{(\omega/v)^2 + \rho_2^2}{2\sigma_2^2}} e^{-\frac{v^2 + \rho_{A_{MR}}^2}{2\sigma_{A_{MR}}^2}} e^{-\frac{g_1(\omega, \psi; t)}{2\sigma_1^2}} \\
&\times e^{-\frac{x g_3(\omega, \theta, \psi; t)}{\sigma_1}} I_0 \left(\sqrt{g_2(\omega, v, \psi; t)} \right), \quad x \geq 0, |\theta| \leq \pi \tag{13}
\end{aligned}$$

where

$$\begin{aligned}
g_1(\omega, \psi; t) &= \omega^2 + \rho_1^2 + 2\rho_1 \omega \cos(\psi - 2\pi f_{\rho_1} t - \theta_{\rho_1}) \tag{14a} \\
g_2(\omega, v, \psi; t) &= \frac{2\rho_2 \rho_{A_{MR}} \omega}{\sigma_2^2 \sigma_{A_{MR}}^2} \cos[\psi - 2\pi(f_{\rho_2} + f_{\rho_3})t - (\theta_{\rho_2} + \theta_{\rho_3})]
\end{aligned}$$

$$+ \left(\frac{\rho_2 \omega}{\sigma_2^2} \right)^2 + \left(\frac{\rho_{A_{MR}} v}{\sigma_{A_{MR}}^2} \right)^2 \quad (14b)$$

$$g_3(\omega, \theta, \psi; t) = \frac{\rho_1 \cos(\theta - 2\pi f_{\rho_1} t - \theta_{\rho_1}) + \omega \cos(\theta - \psi)}{\sigma_1}. \quad (14c)$$

In (13), $I_0(\cdot)$ is the zeroth-order modified Bessel function of the first kind [10].

The PDF $p_{\Xi}(x)$ of MLSS processes $\Xi(t)$ can be obtained by integrating (13) over θ in the interval $[-\pi, \pi]$. Hence,

$$p_{\Xi}(x) = \frac{x e^{-\frac{x^2}{2\sigma_1^2}}}{2\pi \sigma_1^2 \sigma_2^2 \sigma_{A_{MR}}^2} \int_0^{\infty} \int_0^{\infty} dv d\omega \frac{\omega}{v} e^{-\frac{(\omega/v)^2 + \rho_2^2}{2\sigma_2^2}} e^{-\frac{v^2 + \rho_{A_{MR}}^2}{2\sigma_{A_{MR}}^2}} \times \int_{-\pi}^{\pi} d\psi e^{-\frac{g_4(\omega, \psi)}{2\sigma_1^2}} I_0\left(\frac{x}{\sigma_1^2} \sqrt{g_4(\omega, \psi)}\right) I_0\left(\sqrt{g_5(\omega, v, \psi)}\right) \quad (15)$$

for $x \geq 0$, where

$$g_4(\omega, \psi) = \omega^2 + \rho_1^2 + 2\rho_1 \omega \cos(\psi) \quad (16a)$$

$$g_5(\omega, v, \psi) = \left(\frac{\rho_2 \omega}{\sigma_2^2} \right)^2 + \left(\frac{\rho_{A_{MR}} v}{\sigma_{A_{MR}}^2} \right)^2 + \frac{2\rho_2 \rho_{A_{MR}} \omega}{\sigma_2^2 \sigma_{A_{MR}}^2} \cos(\psi). \quad (16b)$$

It is worth mentioning that the joint PDF $p_{\Xi\Theta}(x, \theta; t)$ in (13) is dependent on time t . Nevertheless, the PDF $p_{\Xi}(x)$ in (15) is independent of time t showing that MLSS processes $\Xi(t)$ are first order stationary.

The significance of the PDF $p_{\Xi}(x)$ lies in the fact that it can easily be utilized in the link level performance analysis of relay-based M2M communication systems. The bit error probability (BEP) or the symbol error probability (SEP) and the channel capacity are a few measures to evaluate the performance of communication systems at the link level. The evaluation of the BEP, the SEP, and the channel capacity usually requires the knowledge of the PDF of the signal-to-noise ratio (SNR). Thus, given the PDF $p_{\Xi}(x)$ of $\Xi(t)$, the computation of the PDF of the SNR is nothing but transformation of random variables.

Integrating (13) over x in the interval $[0, \infty)$ results in the following expression for the PDF $p_{\Theta}(\theta; t)$ of the phase process $\Theta(t)$

$$p_{\Theta}(\theta; t) = \int_0^{\infty} \int_0^{\infty} \int_{-\pi}^{\pi} d\psi d\omega dv \frac{\omega}{v} \frac{e^{-\frac{(\omega/v)^2 + \rho_2^2}{2\sigma_2^2}} e^{-\frac{v^2 + \rho_{A_{MR}}^2}{2\sigma_{A_{MR}}^2}}}{(2\pi)^2 \sigma_2^2 \sigma_{A_{MR}}^2} e^{-\frac{g_1(\omega, \psi; t)}{2\sigma_1^2}} I_0\left(\sqrt{g_2(\omega, v, \psi; t)}\right)$$

$$\times \left[1 + \sqrt{\frac{\pi}{2}} g_3(\omega, \theta, \psi; t) e^{\frac{1}{2} g_3^2(\omega, \theta, \psi; t)} \left\{ 1 + \Phi \left(\frac{g_3(\omega, \theta, \psi; t)}{\sqrt{2}} \right) \right\} \right] \quad (17)$$

for $|\theta| \leq \pi$, where $g_1(\cdot, \cdot; t)$, $g_2(\cdot, \cdot, \cdot; t)$, and $g_3(\cdot, \cdot, \cdot; t)$ are defined in (14a), (14b), and (14c), respectively. In (17), $\Phi(\cdot)$ represents the error function [10, Eq. (8.250.1)]. From (17), it is obvious that the phase process $\Theta(t)$ is not strict sense stationary, because the density $p_{\Theta}(\theta; t)$ is a function of time t . This time dependency of the PDF $p_{\Theta}(\theta; t)$ is due the Doppler frequency f_{ρ_i} of the LOS component $m^{(i)}(t)$ ($i = 1, 2, 3$). However, for the special case when $f_{\rho_i} = 0$, $\rho_i \neq 0$ ($i = 1, 2, 3$), the phase process $\Theta(t)$ becomes a first order stationary process.

B. CDF of MLSS Processes

The CDF $F_{\Xi_-}(r)$ of MLSS processes $\Xi(t)$ can be obtained by using [22, Eqs. (4.1), (4.6), (4.16)]

$$F_{\Xi_-}(r) = \int_{-\infty}^r p_{\Xi}(x) dx = 1 - \int_r^{\infty} p_{\Xi}(x) dx, \quad r \geq 0 \quad (18)$$

where $p_{\Xi}(x)$ is the PDF as given by (15). Substituting (15) in (18), allows us to write the final expression of the CDF $F_{\Xi_-}(r)$ of MLSS processes $\Xi(t)$ as

$$F_{\Xi_-}(r) = 1 - \frac{1}{(2\pi)^2 \sigma_2^2 \sigma_{A_{MR}}^2} \int_0^{\infty} \int_0^{\infty} \int_{-\pi}^{\pi} d\psi d\omega dv \frac{\omega}{v} e^{-\frac{(\omega/v)^2 + \rho_2^2}{2\sigma_2^2}} e^{-\frac{v^2 + \rho_{A_{MR}}^2}{2\sigma_{A_{MR}}^2}} \times Q_1 \left(\frac{\sqrt{g_4(\omega, \psi)}}{\sigma_1}, \frac{r}{\sigma_1} \right) I_0(\sqrt{g_5(\omega, v, \psi)}) \quad (19)$$

for $r \geq 0$. In (19), $g_4(\cdot, \cdot)$ and $g_5(\cdot, \cdot, \cdot)$ are the functions defined in (16a) and (16b), respectively, whereas $Q_m(a, b)$ is the generalized Marcum Q-function [25].

C. Mean Value and Variance of MLSS Processes

The PDF of a stochastic process plays a vital role in characterizing the process. However, the information provided by the PDF can also be summarized with the help of the expected value (mean value) and the variance of the stochastic process. The expected value m_{Ξ} of MLSS processes $\Xi(t)$ can be obtained by substituting (15) in [22, Eq. (5.44)] and performing some mathematical manipulations, i.e.,

$$m_{\Xi} = \sqrt{\frac{\pi}{2}} \frac{\sigma_1}{(2\pi)^2 \sigma_2^2 \sigma_{A_{MR}}^2} \int_0^{\infty} \int_0^{\infty} \int_{-\pi}^{\pi} d\psi d\omega dv \frac{\omega}{v} e^{-\frac{(\omega/v)^2 + \rho_2^2}{2\sigma_2^2}} e^{-\frac{\omega^2 + \rho_{A_{MR}}^2}{2\sigma_{A_{MR}}^2}} e^{-\frac{1}{2} \left(\frac{g_4(\omega, \psi)}{2\sigma_1^2} \right)} \times \left\{ \left(1 + \frac{g_4(\omega, \psi)}{2\sigma_1^2} \right) I_0 \left(\frac{g_4(\omega, \psi)}{4\sigma_1^2} \right) + \left(\frac{g_4(\omega, \psi)}{2\sigma_1^2} \right) I_1 \left(\frac{g_4(\omega, \psi)}{4\sigma_1^2} \right) \right\} I_0(\sqrt{g_5(\omega, v, \psi)})$$

$$(20)$$

where $g_4(\cdot, \cdot)$ and $g_5(\cdot, \cdot, \cdot)$ are defined in (16a) and (16b), respectively.

The difference of the mean power $E\{\Xi^2(t)\}$ and the squared mean value m_{Ξ}^2 of MLSS processes $\Xi(t)$ defines its variance σ_{Ξ}^2 [22, Eq. (5.61)], i.e., $\sigma_{\Xi}^2 = E\{\Xi^2(t)\} - m_{\Xi}^2$. Note that $E\{\cdot\}$ is the expected value operator. Using (15) and [22, Eq. (5.67)], the mean power $E\{\Xi^2(t)\}$ of MLSS processes $\Xi(t)$ can be expressed as

$$\begin{aligned} E\{\Xi^2(t)\} &= \int_0^{\infty} x^2 p_{\Xi}(x) dx \\ &= \frac{(2\pi)^{-1}}{\sigma_2^2 \sigma_{A_{MR}}^2} \int_0^{\infty} \int_0^{\infty} \frac{\omega}{v} e^{-\frac{(\omega/v)^2 + \rho_2^2}{2\sigma_2^2}} e^{-\frac{v^2 + \rho_{A_{MR}}^2}{2\sigma_{A_{MR}}^2}} \int_{-\pi}^{\pi} \{2\sigma_1^2 + g_4(\omega, \psi)\} I_0\left(\sqrt{g_5(\omega, v, \psi)}\right) d\psi d\omega dv. \end{aligned} \quad (21)$$

Thus, the variance σ_{Ξ}^2 of MLSS processes $\Xi(t)$ can be computed by using (21) and (20).

D. LCR of MLSS Processes

The LCR of the received envelope of mobile fading channels is a measure to describe the average number of times the envelope crosses a certain threshold level r from up to down (or vice versa) per second. The LCR $N_{\Xi}(r)$ of MLSS processes $\Xi(t)$ can be obtained using [35]

$$N_{\Xi}(r) = \int_0^{\infty} \dot{x} p_{\Xi\dot{\Xi}}(r, \dot{x}) d\dot{x} \quad (22)$$

where $p_{\Xi\dot{\Xi}}(x, \dot{x})$ is the joint PDF of the MLSS process $\Xi(t)$ and its corresponding time derivative $\dot{\Xi}(t)$ at the same time t . From (11), the joint PDF $p_{\Xi\dot{\Xi}}(x, \dot{x})$ can be obtained by integrating over the undesirable variables θ and $\dot{\theta}$, i.e.,

$$p_{\Xi\dot{\Xi}}(x, \dot{x}) = \int_{-\pi-\infty}^{\pi} \int_0^{\infty} p_{\Xi\dot{\Xi}\theta\dot{\theta}}(x, \dot{x}, \theta, \dot{\theta}; t) d\dot{\theta} d\theta, \quad x \geq 0, |\dot{x}| < \infty. \quad (23)$$

In (11), after performing transformation of random variables from rectangular to polar coordinates, substituting the values of $m_k^{(i)}(t)$ as well as $\dot{m}_k^{(i)}(t)$ ($i = 1, 2, 3$ and $k = 1, 2$), and doing some lengthy computations, the joint PDF $p_{\Xi\dot{\Xi}}(x, \dot{x})$ results in

the following expression

$$p_{\Xi\dot{\Xi}}(x, \dot{x}) = \frac{(2\pi)^{-\frac{7}{2}} x e^{-\frac{x^2}{2\sigma_1^2}}}{\sigma_1^2 \sigma_2^2 \sigma_{A_{MR}}^2} \int_0^\infty \int_0^\infty \int_{-\pi}^\pi \int_{-\pi}^\pi \int_{-\pi}^\pi d\theta d\psi d\phi d\omega dv \frac{\omega e^{-\frac{g_4(\omega, \psi)}{2\sigma_1^2}} e^{\frac{x g_6(\omega, \theta, \psi)}{\sigma_1^2}} e^{-\frac{g_8(v, \phi)}{2\sigma_{A_{MR}}^2}}}{\sqrt{\beta(\omega, v)}} \times e^{-\frac{g_7(\omega, v, \psi, \phi)}{2\sigma_2^2}} e^{-\frac{1}{2} g_9(\omega, v, \theta, \psi, \phi)} e^{-\frac{x^2 v^2}{2\beta(\omega, v)}} e^{-\frac{xv}{\sqrt{\beta(\omega, v)}} g_9(\omega, v, \theta, \psi, \phi)}, \quad x \geq 0, |\dot{x}| < \infty \quad (24)$$

where

$$\beta(\omega, v) = \beta_1 v^2 + \beta_3 \omega^2 + \beta_2 v^4 \quad (25a)$$

$$g_6(\omega, \theta, \psi) = \rho_1 \cos(\theta) + \omega \cos(\theta - \psi) \quad (25b)$$

$$g_7(\omega, v, \psi, \phi) = (\omega/v)^2 - 2(\omega/v) \rho_2 \cos(\psi - \phi) + \rho_2^2 \quad (25c)$$

$$g_8(v, \phi) = v^2 - 2v \rho_{A_{MR}} \cos(\phi) + \rho_{A_{MR}}^2 \quad (25d)$$

$$g_9(\omega, v, \theta, \psi, \phi) = \frac{2\pi f_{\rho_2} \rho_2 v^2 \sin(\theta - \phi) + 2\pi f_{\rho_1} \rho_1 v \sin(\theta)}{\sqrt{\beta(\omega, v)}} + \frac{2\pi f_{\rho_3} \rho_{A_{MR}} \omega \sin(\theta - \psi + \phi)}{\sqrt{\beta(\omega, v)}}. \quad (25e)$$

Substituting (24) in (22) and further doing some tedious mathematical manipulations, the LCR $N_{\Xi}(r)$ of MLSS processes $\Xi(t)$ can be expressed as

$$N_{\Xi}(r) = \frac{(2\pi)^{-\frac{7}{2}} r e^{-\frac{r^2}{2\sigma_1^2}}}{\sigma_1^2 \sigma_2^2 \sigma_{A_{MR}}^2} \int_0^\infty \int_0^\infty \int_{-\pi}^\pi \int_{-\pi}^\pi \int_{-\pi}^\pi \sqrt{\beta(\omega, v)} \frac{\omega}{v^2} e^{\frac{r g_6(\omega, \theta, \psi)}{\sigma_1^2}} e^{-\frac{g_4(\omega, \psi)}{2\sigma_1^2}} e^{-\frac{g_7(\omega, v, \psi, \phi)}{2\sigma_2^2}} \times \left[e^{-\frac{1}{2} g_9(\omega, v, \theta, \psi, \phi)} + \sqrt{\frac{\pi}{2}} g_9(\omega, v, \theta, \psi, \phi) \left\{ 1 + \Phi\left(\frac{g_9(\omega, v, \theta, \psi, \phi)}{\sqrt{2}}\right) \right\} \right] \times e^{-\frac{g_8(v, \phi)}{2\sigma_{A_{MR}}^2}} d\theta d\psi d\phi d\omega dv \quad (26)$$

where $g_4(\cdot, \cdot)$, $\beta(\cdot, \cdot)$, $g_6(\cdot, \cdot, \cdot)$, $g_7(\cdot, \cdot, \cdot, \cdot)$, $g_8(\cdot, \cdot)$, and $g_9(\cdot, \cdot, \cdot, \cdot, \cdot)$ are defined in (16a) and (25a) – (25e), respectively.

E. ADF of MLSS Processes

The ADF of mobile fading channels is a measure to quantify how long the received envelope remains in average below a certain threshold level r . The ADF $T_{\Xi}(r)$ of MLSS processes $\Xi(t)$ can be obtained from the ratio of the CDF $F_{\Xi}(r)$ and the LCR $N_{\Xi}(r)$ [35], i.e.,

$$T_{\Xi}(r) = \frac{F_{\Xi}(r)}{N_{\Xi}(r)}. \quad (27)$$

The ADF $T_{\Xi}(r)$ of MLSS processes $\Xi(t)$ can easily be computed by substituting (19) and (26) in (27).

Note that MLSS fading channels belong to the class of time-variant multipath propagation and fading channels. Such channels exhibit bursty error characteristics [33]. The fading channel often causes the signal to fall below a certain threshold noise level, which in turn results in error bursts. The error bursts produced as a consequence of fading can be combated by using interleaving techniques [33, 47] and coding techniques [7, 17]. The PDF $p_{\Xi}(x)$ of $\Xi(t)$ is insufficient to be utilized in developing robust interleaving and coding schemes, as it does not give any insight into the rate of fading. The statistical quantities such as the LCR $N_{\Xi}(r)$ and the ADF $T_{\Xi}(r)$ describe the fading behavior of MLSS processes $\Xi(t)$. Studies pertaining to the LCR $N_{\Xi}(r)$ and the ADF $T_{\Xi}(r)$ of $\Xi(t)$ are thus quite useful in the design as well as optimization of coding and interleaving schemes for M2M fading channels in the relay links in cooperative networks.

IV. SPECIAL CASES OF MLSS CHANNELS

The MLSS fading channel model developed in Section II incorporates at least five other fading processes as special cases. These special cases include double Rice [44], double Rayleigh [14, 24], SLDS [45], SLSS [39, 38], and NLSS [39, 38] fading channels. In this section, we will discuss the conditions under which MLSS fading processes reduce to any of the embedded processes. Furthermore, in order to demonstrate the flexibility of the analytical expression presented in Section III, the expressions for the PDF, CDF, and LCR of all the above mentioned processes are also presented in this section. The proofs for the reduction of the PDF of MLSS processes to that of the stochastic processes mentioned above are included in Appendices H.A–H.E.

A. The Double Rice Process

The double Rice process is obtained by removing the direct SMS-DMS transmission link and considering LOS propagation conditions in the SMS-MR-DMS transmission link [44]. Thus, under the consideration when $\mu_{\rho_1}^{(1)}(t) \rightarrow 0$, i.e., $\rho_1 = 0$ and $\sigma_1^2 \rightarrow 0$, and choosing without loss of generality $A_{MR} = 1$ the MLSS process in (2) reduces to

$$\chi_{\rho}(t) \Big|_{\substack{\rho_1=0 \\ A_{MR}=1 \\ \sigma_1^2 \rightarrow 0}} = \mu_{\rho}^{(2)}(t) \mu_{\rho}^{(3)}(t). \quad (28)$$

Note that even though the direct SMS-DMS transmission link is not present, still the transmitted signal is available at the DMS every second time slot according to the

amplify-and-forward relay protocol considered. The absolute value of the stochastic process in (28) defines the double Rice process, i.e.,

$$\Xi(t) \Big|_{\substack{\rho_1=0 \\ A_{MR}=1 \\ \sigma_1^2 \rightarrow 0}} = \left| \chi_\rho(t) \Big|_{\substack{\rho_1=0 \\ A_{MR}=1 \\ \sigma_1^2 \rightarrow 0}} \right| = \left| \mu_\rho^{(2)}(t) \mu_\rho^{(3)}(t) \right|. \quad (29)$$

Substituting $\rho_1 = 0$ and $A_{MR} = 1$ in (15), (19), and (26) and taking the limit $\sigma_1^2 \rightarrow 0$, reduces the PDF, LCR, and ADF of the MLSS processes to the following corresponding expressions for double Rice processes:

$$p_\Xi(x) \Big|_{\substack{\rho_1=0 \\ A_{MR}=1 \\ \sigma_1^2 \rightarrow 0}} = \frac{x}{\sigma_2^2 \sigma_{A_{MR}}^2} \int_0^\infty \frac{1}{v} e^{-\frac{(x/v)^2 + \rho_2^2}{2\sigma_2^2} - \frac{v^2 + \rho_{A_{MR}}^2}{2\sigma_{A_{MR}}^2}} I_0\left(\frac{x\rho_2}{v\sigma_2^2}\right) I_0\left(\frac{v\rho_{A_{MR}}}{\sigma_{A_{MR}}^2}\right) dv, \quad x \geq 0 \quad (30)$$

$$F_{\Xi-}(r) \Big|_{\substack{\rho_1=0 \\ A_{MR}=1 \\ \sigma_1^2 \rightarrow 0}} = 1 - \int_0^\infty \frac{v}{\sigma_{A_{MR}}^2} e^{-\frac{v^2 + \rho_{A_{MR}}^2}{2\sigma_{A_{MR}}^2}} I_0\left(\frac{v\rho_{A_{MR}}}{\sigma_{A_{MR}}^2}\right) Q_1\left(\frac{\rho_2}{\sigma_2}, \frac{r}{v\sigma_2}\right) dv, \quad r \geq 0 \quad (31)$$

$$N_\Xi(r) \Big|_{\substack{\rho_1=0 \\ A_{MR}=1 \\ \sigma_1^2 \rightarrow 0}} = \frac{(2\pi)^{-\frac{5}{2}} r}{\sigma_2^2 \sigma_{A_{MR}}^2} \int_0^\infty \frac{dv}{v^2} \sqrt{\beta_2 v^4 + \beta_3 r^2} e^{-\frac{(r/v)^2 + \rho_2^2}{2\sigma_2^2} - \frac{v^2 + \rho_{A_{MR}}^2}{2\sigma_{A_{MR}}^2}} \int_{-\pi}^{\pi} d\phi e^{\frac{(r/v)\rho_2 \cos(\phi - \psi)}{\sigma_2^2}} \\ \times \int_{-\pi}^{\pi} e^{\frac{v\rho_{A_{MR}} \cos \phi}{\sigma_{A_{MR}}^2}} \left(e^{-\frac{1}{2} g_{10}(r, v, \phi, \psi)} + \sqrt{\frac{\pi}{2}} g_{10}(r, v, \phi, \psi) \left\{ 1 + \Phi\left(\frac{g_{10}(r, v, \phi, \psi)}{2}\right) \right\} \right) d\psi \quad (32)$$

where

$$g_{10}(r, v, \phi, \psi) = \frac{2\pi f \rho_3 r \rho_3 \sin(\phi - \psi) - 2\pi f \rho_2 v^2 \rho_2 \sin \phi}{\sqrt{\beta_2 v^4 + \beta_3 r^2}}. \quad (33)$$

The proof of (30) can be found in Appendix H.A, whereas the proofs of (31) and (32) have been omitted for reasons of brevity. We notice that the results in (30)–(33) have first been presented in the study conducted for double Rice processes in [44].

B. The Double Rayleigh Process

Considering NLOS propagation conditions in the SMS-MR-DMS link, when there is no direct transmission link between the SMS and the DMS, a double Rayleigh process comes into play. Thus, substituting $\rho_2 = \rho_3 = 0$ in (29), results in

the double Rayleigh process

$$\Xi(t) \left| \begin{array}{l} \rho_1, \rho_2, \rho_3=0 \\ A_{MR}=1 \\ \sigma_1^2 \rightarrow 0 \end{array} \right. = \left| \chi_\rho(t) \left| \begin{array}{l} \rho_1, \rho_2, \rho_3=0 \\ A_{MR}=1 \\ \sigma_1^2 \rightarrow 0 \end{array} \right. \right| = |\mu^{(2)}(t) \mu^{(3)}(t)|. \quad (34)$$

Applying the same conditions mentioned above on (15), (19), and (26) allows us to obtain the PDF, CDF, and LCR of double Rayleigh processes as follows:

$$p_\Xi(x) \left| \begin{array}{l} \rho_1, \rho_2, \rho_3=0 \\ A_{MR}=1 \\ \sigma_1^2 \rightarrow 0 \end{array} \right. = \frac{x}{\sigma_2^2 \sigma_{AMR}^2} K_0 \left(\frac{x}{\sigma_2 \sigma_{AMR}} \right), \quad x \geq 0 \quad (35)$$

$$F_{\Xi-}(r) \left| \begin{array}{l} \rho_1, \rho_2, \rho_3=0 \\ A_{MR}=1 \\ \sigma_1^2 \rightarrow 0 \end{array} \right. = 1 - \frac{r}{\sigma_2 \sigma_3} K_1 \left(\frac{r}{\sigma_2 \sigma_3} \right) \quad r \geq 0 \quad (36)$$

$$N_\Xi(r) \left| \begin{array}{l} \rho_1, \rho_2, \rho_3=0 \\ A_{MR}=1 \\ \sigma_1^2 \rightarrow 0 \end{array} \right. = \frac{r}{\sqrt{2\pi} \sigma_2^2 \sigma_{AMR}^2} \int_0^\infty \frac{\sqrt{\beta_3 r^2 + \beta_2 v^4}}{v^2} e^{-\frac{(r/v)^2}{2\sigma_2^2}} e^{-\frac{v^2}{2\sigma_{AMR}^2}} dv. \quad (37)$$

The proof of (35) can be found in Appendix H.B. The expressions presented in (35) – (37) can be found in the literature (see, e.g., [14, 24]).

C. The SLDS Process

The MLSS fading process tends to the SLDS fading process if a LOS component is considered only in the direct transmission link from the SMS to the DMS, ignoring the scattered component of the link [45]. The stochastic process associated with SLDS processes can be expressed by substituting $\rho_2 = \rho_3 = 0$, $A_{MR} = 1$, and taking the limit $\sigma_1^2 \rightarrow 0$ in (2) as follows

$$\chi_\rho(t) \left| \begin{array}{l} \rho_2, \rho_3=0 \\ A_{MR}=1 \\ \sigma_1^2 \rightarrow 0 \end{array} \right. = m^{(1)}(t) + \mu^{(2)}(t) \mu^{(3)}(t). \quad (38)$$

The absolute value of the stochastic process in (38) defines the SLDS process, i.e.,

$$\Xi(t) \left| \begin{array}{l} \rho_2, \rho_3=0 \\ A_{MR}=1 \\ \sigma_1^2 \rightarrow 0 \end{array} \right. = \left| \chi_\rho(t) \left| \begin{array}{l} \rho_2, \rho_3=0 \\ A_{MR}=1 \\ \sigma_1^2 \rightarrow 0 \end{array} \right. \right| = |m^{(1)}(t) + \mu^{(2)}(t) \mu^{(3)}(t)|. \quad (39)$$

Substituting $\rho_2 = \rho_3 = 0$, $A_{MR} = 1$, and taking the limit $\sigma_1^2 \rightarrow 0$ in (15), (19), and (26), allows us to obtain the PDF, CDF, and LCR of SLDS processes in the form [45]

$$p_{\Xi}(x) \Big|_{\substack{\rho_2, \rho_3=0 \\ A_{MR}=1 \\ \sigma_1^2 \rightarrow 0}} = \begin{cases} \frac{x}{\sigma_2^2 \sigma_{A_{MR}}^2} I_0\left(\frac{x}{\sigma_2 \sigma_{A_{MR}}}\right) K_0\left(\frac{\rho_1}{\sigma_2 \sigma_{A_{MR}}}\right), & x < \rho_1 \\ \frac{x}{\sigma_2^2 \sigma_{A_{MR}}^2} K_0\left(\frac{x}{\sigma_2 \sigma_{A_{MR}}}\right) I_0\left(\frac{\rho_1}{\sigma_2 \sigma_{A_{MR}}}\right), & x \geq \rho_1 \end{cases} \quad (40)$$

$$F_{\Xi}(r) \Big|_{\substack{\rho_2, \rho_3=0 \\ A_{MR}=1 \\ \sigma_1^2 \rightarrow 0}} = \begin{cases} \frac{r}{\sigma_2 \sigma_3} K_0\left(\frac{\rho_1}{\sigma_2 \sigma_3}\right) I_1\left(\frac{r}{\sigma_2 \sigma_3}\right), & r < \rho_1 \\ 1 - \frac{r}{\sigma_1 \sigma_2} I_0\left(\frac{\rho_1}{\sigma_2 \sigma_3}\right) K_1\left(\frac{r}{\sigma_2 \sigma_3}\right), & r \geq \rho_1 \end{cases} \quad (41)$$

$$N_{\Xi}(r) \Big|_{\substack{\rho_2, \rho_3=0 \\ A_{MR}=1 \\ \sigma_1^2 \rightarrow 0}} = \frac{\sqrt{2\pi} r}{(2\pi)^2 \sigma_2^2 \sigma_{A_{MR}}^2} \int_0^{\infty} \int_{-\pi}^{\pi} d\theta dv \frac{\sqrt{\beta_3 g_{11}(r, \theta) + \beta_2 v^4}}{v^2} e^{-\frac{v^2}{2\sigma_{A_{MR}}^2}} e^{-\frac{g_{11}(r, \theta)}{2v^2 \sigma_2^2}} \\ \times \left(e^{-\frac{1}{2} g_{12}^2(v, \theta)} + \sqrt{\frac{\pi}{2}} g_{12}(v, \theta) \left\{ 1 + \Phi\left(\frac{g_{12}(v, \theta)}{\sqrt{2}}\right) \right\} \right) \quad (42)$$

respectively, where

$$g_{11}(r, \theta) = r^2 + \rho_1^2 - 2r\rho_1 \cos \theta \quad \text{and} \quad g_{12}(v, \theta) = \frac{2\pi f \rho_1 \rho_1 v \sin \theta}{\sqrt{\beta_3 g_{11}(r, \theta) + \beta_2 v^4}}. \quad (43a, b)$$

The proof of (40) is given in Appendix H.C.

D. The SLSS Process

The MLSS process tends to the SLSS process if NLOS propagation conditions are assumed in the transmission link between the SMS and the DMS via the MR. Thus, for $\rho_2 = \rho_3 = 0$ and $A_{MR} = 1$, (2) reduces to the stochastic process given by

$$\chi_{\rho}(t) \Big|_{A_{MR}=1}^{\rho_2, \rho_3=0} = \mu_{\rho}^{(1)}(t) + \mu^{(2)}(t) \mu^{(3)}(t). \quad (44)$$

Taking the absolute value of the stochastic process in (44) is referred to as the SLSS process, i.e.,

$$\Xi(t) \Big|_{A_{MR}=1}^{\rho_2, \rho_3=0} = \left| \chi_{\rho}(t) \Big|_{A_{MR}=1}^{\rho_2, \rho_3=0} \right| = \left| \mu_{\rho}^{(1)}(t) + \mu^{(2)}(t) \mu^{(3)}(t) \right|. \quad (45)$$

The PDF, CDF, and LCR of SLSS processes can be obtained by substituting $\rho_2, \rho_3 = 0$ and $A_{MR} = 1$ in (15), (19), and (26), respectively, i.e.,

$$p_{\Xi}(x) \Big|_{\substack{\rho_2, \rho_3=0 \\ A_{MR}=1}} = \frac{x}{2\pi \sigma_1^2 \sigma_2^2 \sigma_{A_{MR}0}^2} \int_0^{\infty} \int_{-\pi}^{\pi} d\theta d\omega \omega e^{-\frac{\omega^2}{2\sigma_1^2} - \frac{g_{11}(x, \theta)}{2\sigma_1^2}} \times K_0\left(\frac{\omega}{\sigma_2 \sigma_{A_{MR}}}\right) I_0\left(\frac{\omega}{\sigma_1^2} \sqrt{g_{11}(x, \theta)}\right), \quad x \geq 0 \quad (46)$$

$$F_{\Xi}(r) \Big|_{\substack{\rho_2, \rho_3=0 \\ A_{MR}=1}} = 1 - \frac{1}{2\pi \sigma_2^2 \sigma_3^2 \sigma_1^2} \int_0^{\infty} d\omega \omega e^{-\frac{\omega^2}{2\sigma_1^2}} K_0\left(\frac{\omega}{\sigma_2 \sigma_3}\right) \int_{-\pi}^{\pi} d\theta \times \int_r^{\infty} dx x e^{-\frac{g_{11}(x, \theta)}{2\sigma_1^2}} I_0\left(\frac{\omega}{\sigma_1^2} \sqrt{g_{11}(x, \theta)}\right), \quad (47)$$

$$N_{\Xi}(r) \Big|_{\substack{\rho_2, \rho_3=0 \\ A_{MR}=1}} = \frac{(2\pi)^{-\frac{3}{2}} r}{\sigma_1^2 \sigma_2^2 \sigma_{A_{MR}}^2} \int_0^{\infty} \int_0^{\infty} \int_{-\pi}^{\pi} d\theta d\omega dv \frac{\omega}{v^2} \sqrt{\beta(\omega, v)} e^{-\frac{v^2}{2\sigma_{A_{MR}}^2} - \frac{\omega^2 + g_{11}(r, \theta)}{2\sigma_1^2} - \frac{(\omega/v)^2}{2\sigma_2^2}} \times I_0\left(\frac{\omega}{\sigma_1^2} \sqrt{g_{11}(r, \theta)}\right) \left[e^{-\frac{1}{2} g_{13}^2(\omega, v, \theta)} + \sqrt{\frac{\pi}{2}} g_{13}(\omega, v, \theta) \left\{ 1 + \Phi\left(\frac{g_{13}(\omega, v, \theta)}{\sqrt{2}}\right) \right\} \right] \quad (48)$$

where

$$g_{13}(\omega, v, \theta) = \frac{2\pi f_{\rho_1} \rho_1 v \sin \theta}{\sqrt{\beta(\omega, v)}}. \quad (49)$$

The proof of (46) is given in Appendix H.D. The expressions for the PDF and CDF of the SLSS process presented in (46) and (47), respectively, can be found in the literature [39, 38]. However, the expression for the LCR of the SLSS process given in (48) is one of our side results.

E. The NLSS Process

The NLSS process assumes NLOS propagation conditions in both the transmission links, i.e., the direct SMS-DMS link and the SMS-MR-DMS link. This implies that $\rho_1 = \rho_2 = \rho_3 = 0$ and $A_{MR} = 1$. Substituting $\rho_1 = 0$ in (45) gives the NLSS process, i.e.,

$$\Xi(t) \Big|_{\substack{\rho_1, \rho_2, \rho_3=0 \\ A_{MR}=1}} = \left| \chi_{\rho}(t) \Big|_{\substack{\rho_1, \rho_2, \rho_3=0 \\ A_{MR}=1}} \right| = \left| \mu^{(1)}(t) + \mu^{(2)}(t) \mu^{(3)}(t) \right|. \quad (50)$$

The PDF, CDF, and LCR of NLSS processes can be derived from the PDF, CDF, and LCR of MLSS processes by solving (15), (19), and (26), respectively, for $\rho_1 =$

$\rho_2 = \rho_3 = 0$ and $A_{MR} = 1$, i.e.,

$$p_{\Xi}(x) \Big|_{\substack{\rho_1, \rho_2, \rho_3=0 \\ A_{MR}=1}} = \frac{x e^{-\frac{x^2}{2\sigma_1^2}}}{\sigma_1^2 \sigma_2^2 \sigma_{A_{MR}}^2} \int_0^{\infty} \omega e^{-\frac{\omega^2}{2\sigma_1^2}} K_0\left(\frac{\omega}{\sigma_2 \sigma_{A_{MR}}}\right) I_0\left(\frac{\omega}{\sigma_1^2} x\right) d\omega, \quad x \geq 0 \quad (51)$$

$$F_{\Xi}(r) \Big|_{\substack{\rho_1, \rho_2, \rho_3=0 \\ A_{MR}=1}} = 1 - \frac{1}{\sigma_2^2 \sigma_3^2} \int_0^{\infty} \omega K_0\left(\frac{\omega}{\sigma_2 \sigma_3}\right) Q_1\left(\frac{\omega}{\sigma_1}, \frac{r}{\sigma_1}\right) d\omega, \quad r \geq 0 \quad (52)$$

$$N_{\Xi}(r) \Big|_{\substack{\rho_1, \rho_2, \rho_3=0 \\ A_{MR}=1}} = \frac{(2\pi)^{-\frac{3}{2}} r e^{-\frac{r^2}{2\sigma_1^2}}}{\sigma_1^2 \sigma_2^2 \sigma_{A_{MR}}^2} \int_0^{\infty} \int_0^{\infty} \int_{-\pi}^{\pi} d\theta \frac{\omega}{v^2} \sqrt{\beta(\omega, v)} e^{-\frac{v^2}{2\sigma_{A_{MR}}^2}} e^{-\frac{\omega^2}{2\sigma_1^2}} \\ \times e^{-\frac{(\omega/v)^2}{2\sigma_2^2}} I_0\left(\frac{r\omega}{\sigma_1^2}\right) d\omega dv \quad r \geq 0. \quad (53)$$

The proof of (51) is given in Appendix H.E. To the best of our knowledge, analytical expressions for the LCR of NLSS processes have not yet been published. However, the PDF and CDF of NLSS processes are well-studied functions (see, e.g., [39, 38]).

V. NUMERICAL RESULTS

The purpose of this section is twofold. Firstly, to illustrate the important theoretical results by evaluating the expressions in (15), (17), (19), (26), and (27). Secondly, we will confirm the correctness of the theoretical results with the help of simulations. The concept of sum-of-sinusoids (SOS) [34, 35] was exploited to simulate the underlying uncorrelated Gaussian noise processes of the overall MLSS process. The motivation to select an SOS-based channel simulator is that such simulators are widely acknowledged to be simple but efficient to model mobile radio fading channels under isotropic scattering conditions [25]. In addition, the concept of SOS has found its application in the design of channel simulators for temporally correlated frequency-nonselctive channels [25, 23], frequency-selective channels [12, 49], and space-selective channels [11, 32, 26, 29]. However, in order to reproduce the desired channel characteristics in simulations, a careful selection of the simulator parameters is essential. For this reason, several methods for an accurate computation of the model parameters of SOS simulators have been developed [30, 31, 12, 51, 49, 28]. One such method for the parameter computation, which is referred to as the generalized method of exact Doppler spread (GMEDS₁) [27], has been employed in this work. Using the GMEDS₁, it is possible to generate

any number of uncorrelated Gaussian waveforms without increasing the complexity of the channel simulator. Each Gaussian process $\mu^{(i)}(t)$ was simulated using $N_1^{(i)} = 20$ and $N_2^{(i)} = 21$, where $N_1^{(i)}$ and $N_2^{(i)}$ are the number of sinusoids required to simulate the inphase and quadrature components of $\mu^{(i)}(t)$, respectively. It has been shown in [25] that with $N_l^{(i)} \geq 7$ where $l = 1, 2$, the simulated distribution of $|\mu^{(i)}(t)|$ closely approximates the Rayleigh distribution. The variance of the inphase and quadrature components of $\mu^{(i)}(t)$ is equal to $\sigma_i^2 = 1$ for $i = 1, 2, 3$, unless stated otherwise. The Doppler frequencies, i.e., $f_{\text{SMS}_{\max}}$, $f_{\text{MR}_{\max}}$, and $f_{\text{DMS}_{\max}}$, were set to 91 Hz, 75 Hz, and 110 Hz, respectively. Whereas, the Doppler frequencies of the three LOS components, i.e., f_{ρ_1} , f_{ρ_2} , and f_{ρ_3} , were set to 166 Hz, 185 Hz, and 201 Hz, respectively. For simplicity, the amplitudes of the three LOS components ρ_1 , ρ_2 , and ρ_3 are assumed to be equal, i.e., $\rho_1 = \rho_2 = \rho_3 = \rho$ and the relay gain $A_{\text{MR}} = 1$, unless stated otherwise.

In the following, the theory is verified for many different propagation scenarios and the results presented in Figs. H.2–H.6 show a good fit between the analytical and simulation results. These results illustrate that the statistics of MLSS fading channels corresponding to various propagation scenarios vary in a wide range. This in turn leads to the fact that the proposed model is highly flexible, since we expect that its statistics can be fitted to measurement data.

The PDF $p_{\Xi}(x)$ of MLSS processes $\Xi(t)$ described by (15) is presented in Fig. H.2 as well as the simulation results obtained by evaluating the statistics of the waveforms generated by using the SOS-based channel simulator. Figure H.2 also shows several special cases of the PDF $p_{\Xi}(x)$ of MLSS processes $\Xi(t)$ that can be obtained by selecting appropriate values of ρ_1 , ρ_2 , ρ_3 , and σ_1^2 in (15). The presented results show an excellent fitting between the analytical and simulation results. Studying the PDF $p_{\Xi}(x)$ of MLSS processes $\Xi(t)$ shows that the mean value m_{Ξ} and the variance σ_{Ξ}^2 of $\Xi(t)$ are greater than the mean values and the variances of the above mentioned processes for the same value of ρ . The same trend can be seen when different values of ρ_i ($i = 1, 2, 3$) are selected. Furthermore, increasing the value of the relay gain A_{MR} causes an increase in the spread of the PDF $p_{\Xi}(x)$ of MLSS processes $\Xi(t)$. Similarly, Fig. H.3 illustrates the theoretical results of the CDF $F_{\Xi}(r)$ of MLSS processes $\Xi(t)$ described by (19) along with the simulation results.

Figure H.4 presents a comparison of the PDF $p_{\Theta}(\theta)$ of the phase process $\Theta(t)$ with that of the phase processes corresponding to classical Rayleigh, classical Rice, double Rayleigh, double Rice, SLDS, NLSS, and SLSS processes for $\rho = 1$. It should be noted that the results presented in Fig. H.4 are valid for the case when

f_{ρ_i} ($i = 1, 2, 3$) is set to zero. It can be observed that the PDF of the phase process corresponding to the SLDS process has the smallest variance. The PDF $p_{\Theta}(\theta)$ follows the same trend in terms of the maximum value and the spread as that of the classical Rice process for the same value of ρ . Furthermore, it is interesting to note that for the phase process $\Theta(t)$ with ρ_i ($i = 1, 2, 3$) being selected as $\rho_1 = \rho_3 = 0.5$ and $\rho_2 = 1$, the PDF $p_{\Theta}(\theta)$ is almost the same as that of the double Rice process for $\rho = 1$. In addition, conclusions can be drawn about the influence of the relay gain A_{MR} on the PDF $p_{\Theta}(\theta)$ of the phase process $\Theta(t)$ from Fig. H.4 like, e.g., as A_{MR} increases, the variance of the phase process $\Theta(t)$ increases.

The LCR $N_{\Xi}(r)$ of MLSS processes $\Xi(t)$ described by (26) is shown in Fig. H.5. Like Figs. H.2–H.4, Fig. H.5 also presents a comparison of the LCR $N_{\Xi}(r)$ of MLSS processes $\Xi(t)$ with that of the LCR of several special cases, e.g., double Rayleigh, double Rice, SLDS, NLSS, and SLSS processes for some values of ρ . Studying the results presented in Fig. H.5 show that at low signal levels r , the LCR $N_{\Xi}(r)$ of MLSS processes $\Xi(t)$ is lower as compared to that of the special cases. This is in contrast to the behavior at medium and high levels, where the LCR $N_{\Xi}(r)$ of $\Xi(t)$ is higher than that of the LCR of the special cases. Furthermore, increasing the value of A_{MR} results in a decrease in the LCR $N_{\Xi}(r)$ at low signal levels r and in an increase in the LCR $N_{\Xi}(r)$ at medium and high signal levels.

The ADF $T_{\Xi_{-}}(r)$ of MLSS processes $\Xi(t)$ described by (27) is evaluated along with the simulation results in Fig. H.6. For comparative purposes, the ADF of double Rayleigh, double Rice, SLDS, NLSS, and SLSS processes for some values of ρ is also presented in Fig. H.6 along with the ADF $T_{\Xi_{-}}(r)$ of MLSS processes $\Xi(t)$. It can be observed that the ADF $T_{\Xi_{-}}(r)$ of MLSS processes $\Xi(t)$ is lower than the ADF of the mentioned stochastic processes. Furthermore, the decrease in the ADF $T_{\Xi_{-}}(r)$ as a consequence of an increase in the value of the relay gain A_{MR} is also visible in Fig. H.6.

The qualitative description of the figures presented above is to put emphasis on the correctness of the derived analytical expressions. The quantitative analysis however is imperative to show how the channel and system parameters such as A_{MR} , ρ , f_{ρ} , etc. effect the statistics of the channel and to what extent. Thus, classifying the studied fading channels as NLOS M2M channels (i.e., double Rayleigh and NLSS channels) and LOS M2M channels (i.e., double Rice, SLDS, SLSS, and MLSS channels) we can conclude that LOS M2M channels have higher mean values and variances compared NLOS M2M channels. Furthermore, the fading behavior of LOS M2M channels can be described by a higher LCR at higher signal levels (a lower LCR at lower signal levels) but a lower ADF when compared to that of

NLOS M2M channels. The relay gain A_{MR} influences the statistics of both NLOS and LOS M2M fading channels in the same way, i.e., increasing A_{MR} increases the mean value, the variance, and the LCR of M2M fading channels. An increase in A_{MR} on the other hand decreases the ADF of the channels under discussion.

VI. CONCLUSION

In this paper, we have proposed a new flexible M2M amplify-and-forward relay fading channel model under LOS conditions. The novelty in the model is that we are considering the LOS components in all transmission links, i.e., the direct link between the SMS and the DSM as well as the two links via the MR. Thus, by analogy to multiple scattering radio propagation channels, we have introduced a new narrowband M2M channel referred to as the MLSS channel. The flexibility of the MLSS fading channel model comes from the fact that it includes several other channel models as special cases, e.g., double Rayleigh, double Rice, SLDS, NLSS, and SLSS channel models.

This paper presents a deep analysis pertaining to the statistical behavior of MLSS channels. Analytical expressions for the most important statistical properties like the mean, variance, PDF, CDF, LCR, and ADF of MLSS fading channels along with the PDF of the corresponding phase process are derived. The obtained theoretical results have complicated integral forms, which is inherent in the nature of the problem. However, that is not a serious drawback since, nowadays there are several efficient ways to solve multi-fold integrals numerically. Modern day computers and computer programmes such as Matlab can give very accurate numerical results of integrals. Furthermore, using functions available in Matlab for numerical integration such as *trapz*, we managed to evaluate the derived analytical expressions with high accuracy and precision. An excellent fitting between the theoretical and simulation results confirms the correctness of the derived analytical expressions. It has been shown that under certain assumptions, the derived analytical expressions for the PDF, CDF, and LCR of MLSS processes reduce to the corresponding expressions of double Rayleigh, double Rice, SLDS, NLSS, and SLSS processes. The same is true for the ADF of MLSS processes as well as for the PDF of the corresponding phase processes. The presented results show that the PDF of MLSS processes has lower maximum value and higher spread in comparison to various special cases. Furthermore, at low signal levels, the LCR of MLSS processes is lower compared to that of several special cases. While, at medium and high signal levels, the LCR of MLSS processes is higher than that of the included special cases. A significant impact of the relay gain on different statistical properties of MLSS

processes has also been observed. An increase in the relay gain decreases the maximum value of the PDF of MLSS processes and increases its spread. Similarly, an increase in the relay gain decreases the LCR of MLSS process at low signal levels, whereas the LCR at medium and high signal levels increases. The opposite is true for the ADF of MLSS processes.

Our novel M2M channel model is useful for the system level performance evaluation of M2M communication systems in different M2M propagation scenarios. Furthermore, the theoretical results presented in this paper are beneficial for designers of the physical layer of M2M cooperative wireless networks. Based on our studies about the dynamics of MLSS fading channels, robust modulation, coding, and interleaving schemes can be developed and analyzed for M2M communication systems under LOS and NLOS propagation conditions.

H.A Proof of (30)

For $\rho_1 = 0$, $A_{MR} = 1$, and $\sigma_1^2 \rightarrow 0$, (15) reduces to

$$p_{\Xi}(x) \Bigg|_{\substack{\rho_1=0 \\ A_{MR}=1 \\ \sigma_1^2 \rightarrow 0}} = \frac{x/(2\pi)}{\sigma_2^2 \sigma_{A_{MR}0}^2} \int_0^\infty \int_{-\pi}^\pi d\psi dv d\omega \frac{\omega}{v} e^{-\frac{(\omega/v)^2 + \rho_2^2}{2\sigma_2^2}} e^{-\frac{v^2 + \rho_{A_{MR}}^2}{2\sigma_{A_{MR}}^2}} I_0\left(\sqrt{g_5(\omega, v, \psi)}\right) \times \underbrace{\lim_{\sigma_1^2 \rightarrow 0} \frac{e^{-\frac{x^2 + \omega^2}{2\sigma_1^2}} I_0\left(\frac{x\omega}{\sigma_1^2}\right)}{\sigma_1^2}}_{X_1} \tag{A.1}$$

for $x \geq 0$. Furthermore, using the asymptotic expansions of the zeroth-order modified Bessel function of the first kind $I_0(\cdot)$ [48, Sec. (7.23), Eq. (2)], allows us to write X_1 as

$$X_1 = \lim_{\sigma_1^2 \rightarrow 0} \frac{e^{-\frac{x^2 + \omega^2}{2\sigma_1^2}}}{\sigma_1^2} \frac{e^{\frac{x\omega}{\sigma_1^2}}}{\sqrt{2\pi x\omega}} = \frac{1}{\sqrt{x\omega}} \lim_{\sigma_1^2 \rightarrow 0} \frac{e^{-\frac{x^2 + \omega^2 - 2x\omega}{2\sigma_1^2}}}{\sqrt{2\pi}\sigma_1} = \frac{1}{\sqrt{x\omega}} \delta(\omega - x) . \tag{A.2}$$

Substituting (A.2) in (A.1) gives

$$p_{\Xi}(x) \Bigg|_{\substack{\rho_1=0 \\ A_{MR}=1 \\ \sigma_1^2 \rightarrow 0}} = \frac{x/(2\pi)}{\sigma_2^2 \sigma_{A_{MR}0}^2} \int dv \frac{1}{v} e^{-\frac{v^2 + \rho_{A_{MR}}^2}{2\sigma_{A_{MR}}^2}} \int_{-\pi}^\pi d\psi \int_0^\infty d\omega \sqrt{\frac{\omega}{x}} e^{-\frac{(\omega/v)^2 + \rho_2^2}{2\sigma_2^2}} \times I_0\left(\sqrt{g_5(\omega, v, \psi)}\right) \delta(\omega - x) \tag{A.3}$$

for $x \geq 0$. Applying the sifting property of the delta function [20] on (A.3) gives

$$p_{\Xi}(x) \Bigg|_{\substack{\rho_1=0 \\ A_{MR}=1 \\ \sigma_1^2 \rightarrow 0}} = \frac{x}{2\pi \sigma_2^2 \sigma_{A_{MR}0}^2} \int dv \frac{1}{v} e^{-\frac{(x/v)^2 + \rho_2^2}{2\sigma_2^2}} e^{-\frac{v^2 + \rho_{A_{MR}}^2}{2\sigma_{A_{MR}}^2}} \underbrace{\int_{-\pi}^\pi I_0\left(\sqrt{g_5(x, v, \psi)}\right) d\psi}_{X_2} \tag{A.4}$$

for $x \geq 0$. Numerical investigations show that it is possible to approximate X_2 in (A.4) as

$$X_2 = (2\pi) I_0\left(\frac{x\rho_2}{v\sigma_2^2}\right) I_0\left(\frac{v\rho_{A_{MR}}}{\sigma_{A_{MR}}^2}\right) . \tag{A.5}$$

Thus, replacing (A.5) in (A.4) gives (30).

H.B Proof of (35)

Substituting $\rho_1 = \rho_2 = \rho_3 = 0$ and $A_{MR} = 1$ in (15), we can express $p_{\Xi}(x) \Big|_{\substack{\rho_1, \rho_2, \rho_3=0 \\ A_{MR}=1}}$ as follows

$$p_{\Xi}(x) \Big|_{\substack{\rho_1, \rho_2, \rho_3=0 \\ A_{MR}=1}} = \frac{x e^{-\frac{x^2}{2\sigma_1^2}} / (2\pi)}{\sigma_1^2 \sigma_2^2 \sigma_{A_{MR}}^2} \int_0^{\infty} d\omega \omega e^{-\frac{\omega^2}{2\sigma_1^2}} I_0\left(\frac{x\omega}{\sigma_1^2}\right) \underbrace{\int_0^{\infty} \frac{1}{v} e^{-\frac{(\omega/v)^2}{2\sigma_2^2}} e^{-\frac{v^2}{2\sigma_{A_{MR}}^2}} dv}_{X_3 = K_0\left(\frac{\omega}{\sigma_2 \sigma_{A_{MR}}}\right)} \times \underbrace{\int_{-\pi}^{\pi} d\psi}_{X_4 = 2\pi}, \quad x \geq 0 \quad (\text{B.1})$$

where X_3 is obtained by using [10, Eq. (3.478.4)]. Taking the limit $\sigma_1^2 \rightarrow 0$, (B.1) can be written as

$$p_{\Xi}(x) \Big|_{\substack{\rho_1, \rho_2, \rho_3=0 \\ A_{MR}=1 \\ \sigma_1^2 \rightarrow 0}} = \frac{x}{\sigma_2^2 \sigma_{A_{MR}}^2} \int_0^{\infty} d\omega \omega K_0\left(\frac{\omega}{\sigma_2 \sigma_{A_{MR}}}\right) \lim_{\sigma_1^2 \rightarrow 0} \frac{e^{-\frac{x^2 + \omega^2}{2\sigma_1^2}}}{\sigma_1^2} I_0\left(\frac{\omega}{\sigma_1^2} x\right) \quad (\text{B.2})$$

for $x \geq 0$. Using the asymptotic expansions of the zeroth-order modified Bessel function of the first kind $I_0(\cdot)$ [48, Sec. (7.23), Eq. (2)], (B.2) can be expressed as

$$p_{\Xi}(x) \Big|_{\substack{\rho_1, \rho_2, \rho_3=0 \\ A_{MR}=1 \\ \sigma_1^2 \rightarrow 0}} = \frac{x}{\sigma_2^2 \sigma_{A_{MR}}^2} \int_0^{\infty} d\omega \omega K_0\left(\frac{\omega}{\sigma_2 \sigma_{A_{MR}}}\right) \lim_{\sigma_1^2 \rightarrow 0} \frac{e^{-\frac{x^2 + \omega^2}{2\sigma_1^2}}}{\sigma_1^2} \frac{e^{\frac{x\omega}{\sigma_1^2}} \sigma_1}{\sqrt{2\pi x \omega}} \\ = \frac{x}{\sigma_2^2 \sigma_{A_{MR}}^2} \int_0^{\infty} d\omega \sqrt{\frac{\omega}{x}} K_0\left(\frac{\omega}{\sigma_2 \sigma_{A_{MR}}}\right) \underbrace{\lim_{\sigma_1^2 \rightarrow 0} \frac{e^{-\frac{x^2 + \omega^2 - 2x\omega}{2\sigma_1^2}}}{\sqrt{2\pi \sigma_1}}}_{X_5}, \quad x \geq 0 \quad (\text{B.3})$$

where $X_5 = \delta(\omega - x)$ by definition of the delta function [21]. Thus, (B.3) can be written as

$$p_{\Xi}(x) \Big|_{\substack{\rho_1, \rho_2, \rho_3=0 \\ A_{MR}=1 \\ \sigma_1^2 \rightarrow 0}} = \frac{x}{\sigma_2^2 \sigma_{A_{MR}}^2} \int_0^{\infty} d\omega \sqrt{\frac{\omega}{x}} K_0\left(\frac{\omega}{\sigma_2 \sigma_{A_{MR}}}\right) \delta(\omega - x), \quad x \geq 0. \quad (\text{B.4})$$

Applying the sifting property of the delta function [20] on (B.4), results in (35).

H.C Proof of (40)

Substituting $\rho_2 = \rho_3 = 0$ as well as $A_{MR} = 1$ and integrating (13) over θ from $-\pi$ to π allows us to write $p_{\Xi}(x) \Big|_{\substack{\rho_2, \rho_3=0 \\ A_{MR}=1}}$ as

$$\begin{aligned}
 p_{\Xi}(x) \Big|_{\substack{\rho_2, \rho_3=0 \\ A_{MR}=1}} &= \frac{x/(2\pi)^2}{\sigma_2^2 \sigma_{A_{MR}}^2} \int_0^{\infty} \int_{-\pi}^{\pi} d\theta d\omega \underbrace{\int_0^{\infty} dv \frac{\omega}{v} e^{-\frac{(\omega/v)^2}{2\sigma_2^2}} e^{-\frac{v^2}{2\sigma_{A_{MR}}^2}} e^{-\frac{g_{11}(x,\theta)}{2\sigma_1^2}}}_{X_6=K_0\left(\frac{\omega}{\sigma_2 \sigma_{A_{MR}}}\right)} \\
 &\times \underbrace{\int_{-\pi}^{\pi} e^{-\frac{\omega\{\rho_1 \cos(\theta)+x \cos(\theta-\psi)\}}{\sigma_1^2}} d\psi}_{X_7=(2\pi)I_0\left(\frac{\omega}{\sigma_1^2} \sqrt{g_{11}(x,\theta)}\right)} \quad (C.1)
 \end{aligned}$$

for $x \geq 0$. In (C.1), X_6 is evaluated using [10, Eq. (3.478.4)], whereas X_7 with the help of [10, Eq. (3.338.4)]. Taking the limit $\sigma_1^2 \rightarrow 0$ in (C.1), allows us to write

$$\begin{aligned}
 p_{\Xi}(x) \Big|_{\substack{\rho_2, \rho_3=0 \\ A_{MR}=1 \\ \sigma_1^2 \rightarrow 0}} &= \frac{x/(2\pi)}{\sigma_2^2 \sigma_{A_{MR}}^2} \int_0^{\infty} \int_0^{\infty} \int_{-\pi}^{\pi} d\theta dv d\omega \frac{\omega}{v} e^{-\frac{(\omega/v)^2}{2\sigma_2^2}} e^{-\frac{v^2}{2\sigma_{A_{MR}}^2}} \\
 &\times \lim_{\sigma_1^2 \rightarrow 0} \frac{e^{-\frac{\omega^2}{2\sigma_1^2}} e^{-\frac{g_{11}(x,\theta)}{2\sigma_1^2}}}{\sigma_1^2} I_0\left(\frac{\omega}{\sigma_1^2} \sqrt{g_{11}(x,\theta)}\right) \quad (C.2)
 \end{aligned}$$

for $x \geq 0$. Using the asymptotic expansions of the zeroth-order modified Bessel function of the first kind $I_0(\cdot)$ [48, Sec. (7.23), Eq. (2)], (C.2) can be expressed as

$$\begin{aligned}
 p_{\Xi}(x) \Big|_{\substack{\rho_2, \rho_3=0 \\ A_{MR}=1 \\ \sigma_1^2 \rightarrow 0}} &= \frac{x/(2\pi)}{\sigma_2^2 \sigma_{A_{MR}}^2} \int_0^{\infty} \int_0^{\infty} \int_{-\pi}^{\pi} d\theta dv d\omega \frac{\omega}{v} e^{-\frac{(\omega/v)^2}{2\sigma_2^2}} e^{-\frac{v^2}{2\sigma_{A_{MR}}^2}} \\
 &\times \lim_{\sigma_1^2 \rightarrow 0} \frac{e^{-\frac{\omega^2}{2\sigma_1^2}} e^{-\frac{g_{11}(x,\theta)}{2\sigma_1^2}}}{\sigma_1^2} \frac{e^{\frac{\omega}{\sigma_1^2} \sqrt{g_{11}(x,\theta)}} \sigma_1}{\sqrt{2\pi \omega g_{11}(x,\theta)}} \\
 &\frac{x/(2\pi)}{\sigma_2^2 \sigma_{A_{MR}}^2} \int_0^{\infty} \int_0^{\infty} \int_{-\pi}^{\pi} d\theta dv d\omega \frac{\sqrt{\omega}}{v g_{11}(x,\theta)} e^{-\frac{(\omega/v)^2}{2\sigma_2^2}} e^{-\frac{v^2}{2\sigma_{A_{MR}}^2}}
 \end{aligned}$$

$$\times \underbrace{\lim_{\sigma_1^2 \rightarrow 0} \frac{e^{-\frac{\omega^2 + (\sqrt{g_{11}(x,\theta)})^2 - 2\omega\sqrt{g_{11}(x,\theta)}}{2\sigma_1^2}}}{\sqrt{2\pi\sigma_1}}}_{X_8} \quad (C.3)$$

for $x \geq 0$. In (C.3), $X_8 = \delta(\omega - g_{11}(x, \theta))$ by definition of the delta function [21]. Thus, (C.3) can be written as

$$p_{\Xi}(x) \Big|_{\substack{\rho_2, \rho_3=0 \\ A_{MR}=1 \\ \sigma_1^2 \rightarrow 0}} = \frac{x}{2\pi\sigma_2^2\sigma_{A_{MR}}^2} \int_0^{\infty} \int_{-\pi}^{\pi} d\theta dv d\omega \frac{\sqrt{\omega}}{v g_{11}(x, \theta)} e^{-\frac{(\omega/v)^2}{2\sigma_2^2}} e^{-\frac{v^2}{2\sigma_{A_{MR}}^2}} \times \delta\left(\omega - \sqrt{g_{11}(x, \theta)}\right) \quad (C.4)$$

for $x \geq 0$. Applying the sifting property of the delta function [20] on (C.5) results in

$$p_{\Xi}(x) \Big|_{\substack{\rho_2, \rho_3=0 \\ A_{MR}=1 \\ \sigma_1^2 \rightarrow 0}} = \frac{x}{2\pi\sigma_2^2\sigma_{A_{MR}}^2} \int_{-\pi}^{\pi} d\theta \underbrace{\int_0^{\infty} \frac{e^{-\frac{g_{11}^2(x,\theta)}{2\sigma_2^2 v^2}} e^{-\frac{v^2}{2\sigma_{A_{MR}}^2}}}{v} dv}_{X_9 = K_0\left(\frac{\sqrt{g_{11}(x,\theta)}}{\sigma_2\sigma_{A_{MR}}}\right)} dv, x \geq 0. \quad (C.5)$$

where X_9 is evaluated using [10, Eq. (3.478.4)]. Thus, integrating (C.5) over θ from $-\pi$ to π results in the final expression given in (40).

H.D Proof of (46)

Substituting $\rho_2 = \rho_3 = 0$ as well as $A_{MR} = 1$ and integrating (13) over θ from $-\pi$ to π allows us to write $p_{\Xi}(x) \Big|_{A_{MR}=1}$ as

$$p_{\Xi}(x) \Big|_{A_{MR}=1} = \frac{x/(2\pi)^2}{\sigma_2^2\sigma_{A_{MR}}^2} \int_0^{\infty} \int_{-\pi}^{\pi} d\theta d\omega \underbrace{\int_0^{\infty} \frac{\omega}{v} e^{-\frac{(\omega/v)^2}{2\sigma_2^2}} e^{-\frac{v^2}{2\sigma_{A_{MR}}^2}} e^{-\frac{g_{11}(x,\theta)}{2\sigma_1^2}}}_{X_{10} = K_0\left(\frac{\omega}{\sigma_2\sigma_{A_{MR}}}\right)} dv \times \underbrace{\int_{-\pi}^{\pi} e^{-\frac{\omega\{\rho_1 \cos(\theta) + x \cos(\theta - \psi)\}}{\sigma_1^2}} d\psi}_{X_{11} = (2\pi)I_0\left(\frac{\omega}{\sigma_1} \sqrt{g_{11}(x,\theta)}\right)} \quad (D.1)$$

for $x \geq 0$. In (D.1), X_{10} and X_{11} are evaluated using [10, Eq. (3.478.4)] and [10, Eq. (3.338.4)], respectively. Thus, replacing X_{10} and X_{11} in (D.1) results in (46).

H.E Proof of (51)

Substituting $\rho_1 = \rho_2 = \rho_3 = 0$ and $A_{MR} = 1$ in (15), we can express $p_{\Xi}(x) \Big|_{\substack{\rho_1, \rho_2, \rho_3=0 \\ A_{MR}=1}}$ as follows

$$\begin{aligned}
 p_{\Xi}(x) \Big|_{\substack{\rho_1, \rho_2, \rho_3=0 \\ A_{MR}=1}} &= \frac{x e^{-\frac{x^2}{2\sigma_1^2}} / (2\pi)}{\sigma_1^2 \sigma_2^2 \sigma_{A_{MR}}^2} \int_0^{\infty} d\omega \omega e^{-\frac{\omega^2}{2\sigma_1^2}} I_0\left(\frac{x\omega}{\sigma_1^2}\right) \\
 &\times \underbrace{\int_0^{\infty} \frac{1}{v} e^{-\frac{(\omega/v)^2}{2\sigma_2^2}} e^{-\frac{v^2}{2\sigma_{A_{MR}}^2}} dv}_{X_{12}=K_0\left(\frac{w}{\sigma_2 \sigma_{A_{MR}}}\right)} \underbrace{\int_{-\pi}^{\pi} d\psi}_{X_{13}=2\pi}, \quad x \geq 0 \quad (E.1)
 \end{aligned}$$

where X_{12} is evaluated using [10, Eq. (3.478.4)]. Thus, replacing X_{12} and X_{13} in (E.1) gives (51).

REFERENCES

- [1] A. S. Akki. Statistical properties of mobile-to-mobile land communication channels. *IEEE Trans. Veh. Technol.*, 43(4):826–831, November 1994.
- [2] A. S. Akki and F. Haber. A statistical model of mobile-to-mobile land communication channel. *IEEE Trans. Veh. Technol.*, 35(1):2–7, February 1986.
- [3] P. Almers, F. Tufvesson, and A. F. Molisch. Keyhole effect in MIMO wireless channels: measurements and theory. *IEEE Trans. Wireless Commun.*, 5(12):3596–3604, December 2006.
- [4] J. B. Andersen. Statistical distributions in mobile communications using multiple scattering. In *Proc. 27th URSI General Assembly*. Maastricht, Netherlands, August 2002.
- [5] K. Azarian, H. E. Gamal, and P. Schniter. On the achievable diversity-multiplexing tradeoff in half-duplex cooperative channels. *IEEE Trans. Inform. Theory*, 51(12):4152–4172, December 2005.

- [6] S. Barbarossa and G. Scutari. Cooperative diversity through virtual arrays in multihop networks. In *Proc. IEEE International Conf. Acoustics, Speech, Signal Processing*, volume 4, pages 209–212. Hong Kong, China, April 2003.
- [7] E. Biglieri, D. Divsalar, P. J. McLane, and M. K. Simon. *Introduction to Trellis-Coded Modulation with Applications*. New York: Macmillan Publishing Company, 1991.
- [8] M. Dohler. *Virtual Antenna Arrays*. Ph.D. dissertation, King's College, London, United Kingdom, 2003.
- [9] V. Ercerg, S. J. Fortune, J. Ling, A. J. Rustako Jr., and R. A. Valenzuela. Comparison of a computer-based propagation prediction tool with experimental data collected in urban microcellular environment. *IEEE J. Select. Areas Commun.*, 15(4):677–684, May 1997.
- [10] I. S. Gradshteyn and I. M. Ryzhik. *Table of Integrals, Series, and Products*. New York: Academic Press, 6th edition, 2000.
- [11] J. K. Han, J. G. Yook, and H. K. Park. A deterministic channel simulation model for spatially correlated Rayleigh fading. *IEEE Communications Letters*, 6(2):58–60, February 2002.
- [12] P. Höher. A statistical discrete-time model for the WSSUS multipath channel. *IEEE Trans. Veh. Technol.*, 41(4):461–468, November 1992.
- [13] W. C. Jakes, editor. *Microwave Mobile Communications*. Piscataway, NJ: IEEE Press, 1994.
- [14] I. Z. Kovacs, P. C. F. Eggers, K. Olesen, and L. G. Petersen. Investigations of outdoor-to-indoor mobile-to-mobile radio communication channels. In *Proc. IEEE 56th Veh. Technol. Conf., VTC'02-Fall*, volume 1, pages 430–434. Vancouver BC, Canada, September 2002.
- [15] J. N. Laneman, D. N. C. Tse, and G. W. Wornell. Cooperative diversity in wireless networks: Efficient protocols and outage behavior. *IEEE Trans. Inform. Theory*, 50(12):3062–3080, December 2004.
- [16] J. Maurer, T. Fügen, and W. Wiesbeck. Narrow-band measurement and analysis of the inter-vehicle transmission channel at 5.2 GHz. In *Proc. IEEE 55th Semiannual Veh. Technol. Conf., VTC'02-Spring*, volume 3, pages 1274–1278. Birmingham, Alabama, May 2002.

- [17] J. M. Morris. Burst error statistics of simulated Viterbi decoded BPSK on fading and scintillating channels. *IEEE Trans. Commun.*, 40(1):34–41, January 1992.
- [18] R. U. Nabar and H. Bölcskei. Space-time signal design for fading relay channels. In *Proc. IEEE Globecom*, volume 4, pages 1952–1956. San Francisco, CA, December 2003.
- [19] R. U. Nabar, H. Bölcskei, and F. W. Kneubühler. Fading relay channels: Performance limits and space-time signal design. *IEEE J. Select. Areas Commun.*, 22(6):1099–1109, August 2004.
- [20] A. V. Oppenheim and A. S. Willsky with S. Hamid. *Signals & Systems*. New Jersey: Prentice-Hall, Inc., 2nd edition, 1996.
- [21] A. Papoulis. *Signal Analysis*. Auckland: McGraw-Hill, 3rd edition, 1977.
- [22] A. Papoulis and S. U. Pillai. *Probability, Random Variables and Stochastic Processes*. New York: McGraw-Hill, 4th edition, 2002.
- [23] C. S. Patel, G. L. Stüber, and T. G. Pratt. Comparative analysis of statistical models for the simulation of Rayleigh faded cellular channels. *IEEE Trans. Commun.*, 53(6):1017–1026, June 2005.
- [24] C. S. Patel, G. L. Stüber, and T. G. Pratt. Statistical properties of amplify and forward relay fading channels. *IEEE Trans. Veh. Technol.*, 55(1):1–9, January 2006.
- [25] M. Pätzold. *Mobile Fading Channels*. Chichester: John Wiley & Sons, 2002.
- [26] M. Pätzold and B. O. Hogstad. A space-time channel simulator for MIMO channels based on the geometrical one-ring scattering model. *Wireless Communications and Mobile Computing, Special Issue on Multiple-Input Multiple-Output (MIMO) Communications*, 4(7):727–737, November 2004.
- [27] M. Pätzold and B. O. Hogstad. Two new methods for the generation of multiple uncorrelated Rayleigh fading waveforms. In *Proc. IEEE 63rd Semi-annual Veh. Tech. Conf., VTC'06-Spring*, volume 6, pages 2782–2786. Melbourne, Australia, May 2006.
- [28] M. Pätzold, B. O. Hogstad, and D. Kim. A new design concept for high-performance fading channel simulators using set partitioning. *Wireless Personal Communications (WPC)*, 40(2):267–279, February 2007.

- [29] M. Pätzold, B. O. Hogstad, and N. Youssef. Modeling, analysis, and simulation of MIMO mobile-to-mobile fading channels. *IEEE Trans. Wireless Commun.*, 7(2):510–520, February 2008.
- [30] M. Pätzold, U. Killat, and F. Laue. A deterministic digital simulation model for Suzuki processes with application to a shadowed Rayleigh land mobile radio channel. *IEEE Trans. Veh. Technol.*, 45(2):318–331, May 1996.
- [31] M. Pätzold, U. Killat, F. Laue, and Y. Li. On the statistical properties of deterministic simulation models for mobile fading channels. *IEEE Trans. Veh. Technol.*, 47(1):254–269, February 1998.
- [32] M. Pätzold and N. Youssef. Modelling and simulation of direction-selective and frequency-selective mobile radio channels. *International Journal of Electronics and Communications*, AEÜ-55(6):433–442, November 2001.
- [33] J. Proakis and M. Salehi. *Digital Communications*. New York: McGraw-Hill, 5th edition, 2008.
- [34] S. O. Rice. Mathematical analysis of random noise. *Bell Syst. Tech. J.*, 23:282–332, July 1944.
- [35] S. O. Rice. Mathematical analysis of random noise. *Bell Syst. Tech. J.*, 24:46–156, January 1945.
- [36] N. C. Sagias and G. S. Tombras. On the cascaded Weibull fading channel model. *J. Franklin Inst.*, 344:1–11, January 2007.
- [37] J. Salo, H. M. El-Sallabi, and P. Vainikainen. Impact of double-rayleigh fading on system performance. In *Proc. 1st IEEE Int. Symp. on Wireless Pervasive Computing, ISWPC 2006*. Phuket, Thailand, January 2006. 0-7803-9410-0/10.1109/ISWPC.2006.1613574.
- [38] J. Salo, H. M. El-Sallabi, and P. Vainikainen. Statistical analysis of the multiple scattering radio channel. *IEEE Trans. Antennas Propagat.*, 54(11):3114–3124, November 2006.
- [39] J. Salo, J. Salmi, and P. Vainikainen. Distribution of the amplitude of a sum of singly and doubly scattered fading radio signal. In *Proc. IEEE 61st Semi-annual Veh. Tech. Conf., VTC'05-Spring*, volume 1, pages 87–91. Stockholm, Sweden, May/June 2005.

- [40] A. Sendonaris, E. Erkip, and B. Aazhang. User cooperation diversity — Part I: System description. *IEEE Trans. Commun.*, 51(11):1927–1938, November 2003.
- [41] A. Sendonaris, E. Erkip, and B. Aazhang. User cooperation diversity — Part II: Implementation aspects and performance analysis. *IEEE Trans. Commun.*, 51(11):1939–1948, November 2003.
- [42] H. Shin and J. H. Lee. Performance analysis of space-time block codes over keyhole Nakagami-m fading channels. *IEEE Trans. Veh. Technol.*, 53(2):351–362, March 2004.
- [43] M. K. Simon. *Probability Distributions Involving Gaussian Random Variables: A Handbook for Engineers and Scientists*. Dordrecht: Kluwer Academic Publishers, 2002.
- [44] B. Talha and M. Pätzold. On the statistical properties of double Rice channels. In *Proc. 10th Int. Symp. on Wireless Personal Multimedia Communications, WPMC 2007*, pages 517–522. Jaipur, India, December 2007.
- [45] B. Talha and M. Pätzold. On the statistical properties of mobile-to-mobile fading channels in cooperative networks under line-of-sight conditions. In *Proc. 10th Int. Symp. on Wireless Personal Multimedia Communications, WPMC 2007*, pages 388–393. Jaipur, India, December 2007.
- [46] B. Talha and M. Pätzold. A novel amplify-and-forward relay channel model for mobile-to-mobile fading channels under line-of-sight conditions. In *Proc. 19th IEEE Int. Symp. on Personal, Indoor and Mobile Radio Communications, PIMRC 2008*, pages 1–6. Cannes, France, September 2008. DOI 10.1109/PIMRC.2008.4699733.
- [47] K. Y. Tsie, P. Fines, and A. H. Aghvami. Concatenated code and interleaver design for data transmission over fading channels. In *Proc. 9th International Conference on Digital Satellite Communications, ICDS-9*, pages 253–259. Copenhagen, Denmark, May 1992.
- [48] G. N. Watson. *A Treatise on the Theory of Bessel Functions*. Bentley House, London: Cambridge University Press, 2nd edition, 1995.
- [49] K. W. Yip and T. S. Ng. Efficient simulation of digital transmission over WSSUS channels. *IEEE Trans. Commun.*, 43(12):2907–2913, December 1995.

- [50] A. G. Zajić and G. L. Stüber. Space-time correlated mobile-to-mobile channels: modelling and simulation. *IEEE Trans. Veh. Technol.*, 57(2):715–726, March 2008.
- [51] Y. R. Zheng and C. Xiao. Improved models for the generation of multiple uncorrelated Rayleigh fading waveforms. *IEEE Communications Letters*, 6(6):256–258, June 2002.

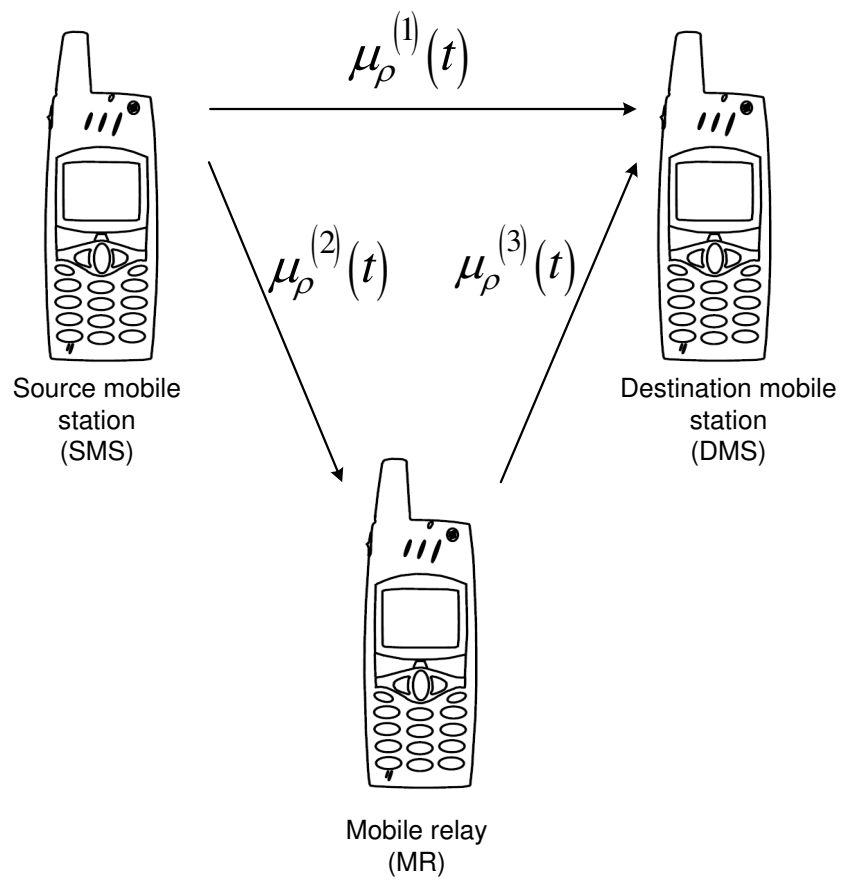


Figure H.1: The propagation scenario describing MLSS fading channels.

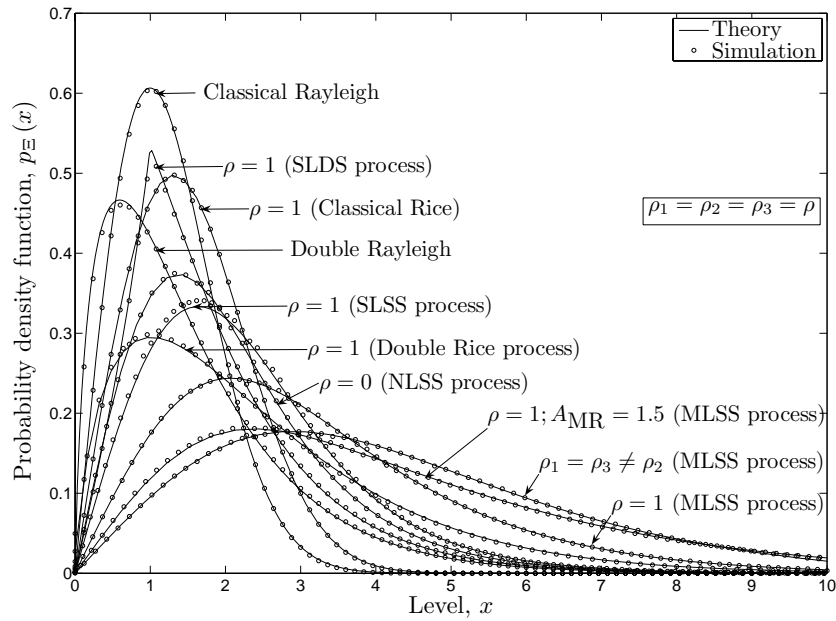


Figure H.2: A comparison of the PDF $p_{\Xi}(x)$ of the MLSS process $\Xi(t)$ with that of various other stochastic processes.

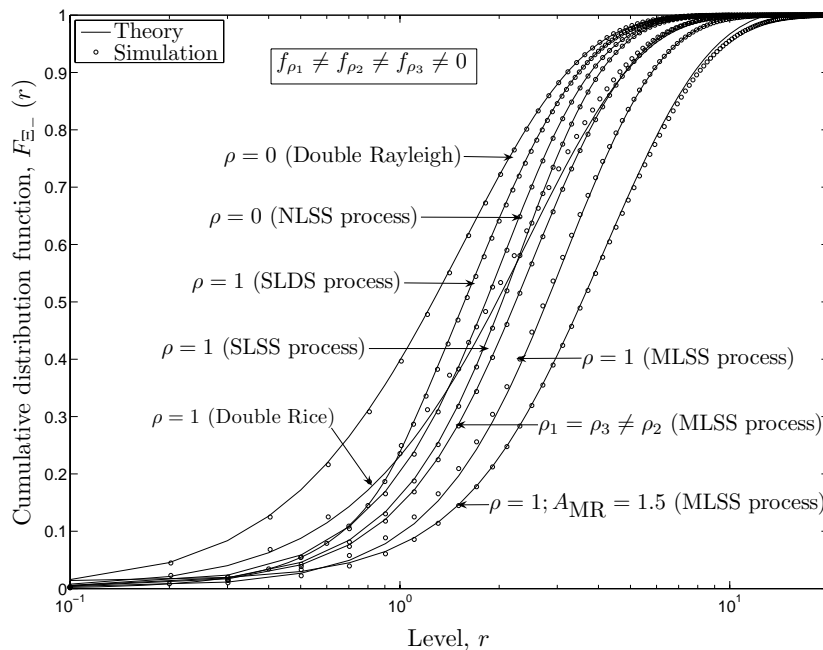


Figure H.3: A comparison of the CDF $p_{\Xi}(r)$ of the MLSS process $\Xi(t)$ with that of various other stochastic processes.

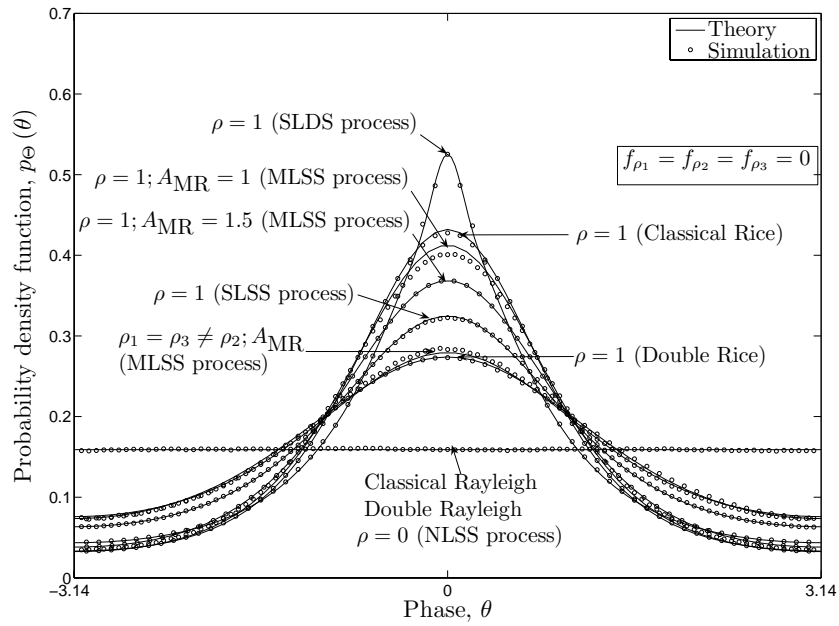


Figure H.4: A comparison of the PDF $p_{\Theta}(\theta)$ of the phase of the MLSS process $\Theta(t)$ with that of various other stochastic processes.

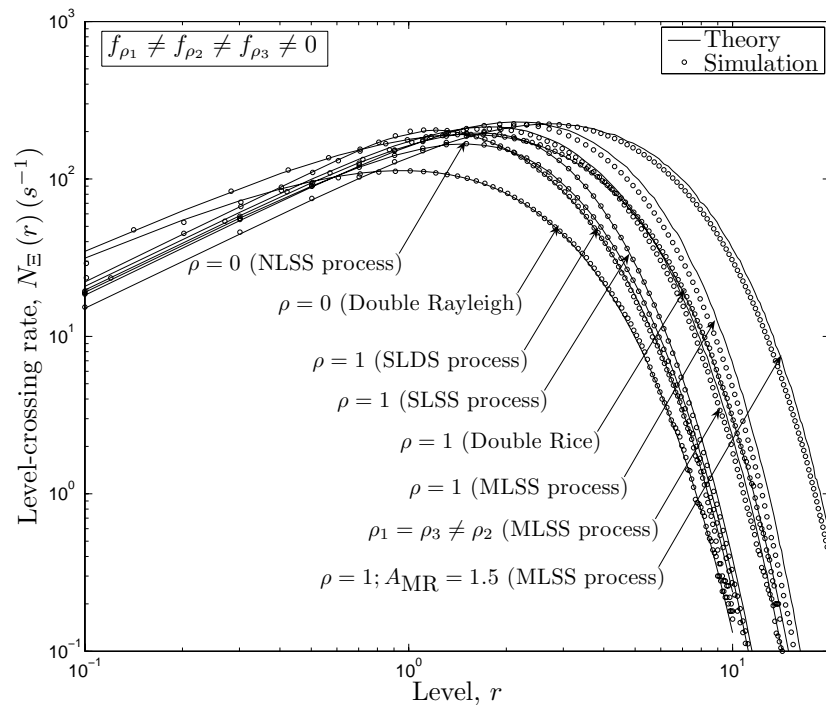


Figure H.5: A comparison of the LCR $N_{\Xi}(r)$ of the MLSS process $\Xi(t)$ with that of various other stochastic processes.

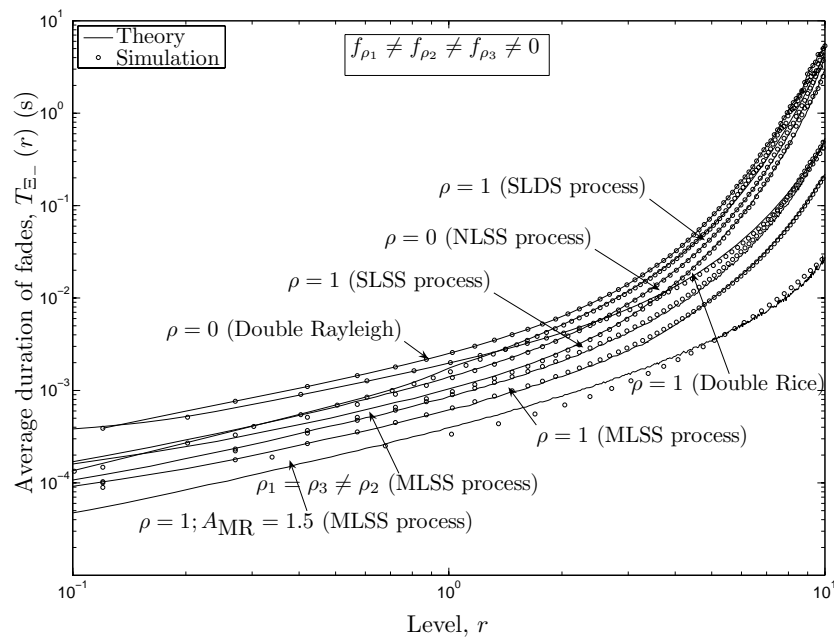


Figure H.6: A comparison of the ADF $T_{\Xi}(r)$ of the MLSS process $\Xi(t)$ with that of various other stochastic processes.

Appendix I

Paper VIII

Title: On the Statistical Analysis of Equal Gain Combining over Multiple Double Rice Fading Channels in Cooperative Networks

Authors: **Batool Talha** and Matthias Pätzold

Affiliation: University of Agder, Faculty of Engineering and Science, P. O. Box 509, NO-4898 Grimstad, Norway

Conference: *IEEE 72nd Vehicular Technology Conference, IEEE VTC2009-Spring, Ottawa, Canada, Sept. 2010, accepted for publication.*

On the Statistical Analysis of Equal Gain Combining over Multiple Double Rice Fading Channels in Cooperative Networks

Batool Talha and Matthias Pätzold

Department of Information and Communication Technology
Faculty of Engineering and Science, Agder University College
Servicebox 509, NO-4876 Grimstad, Norway
E-mails: {batool.talha, matthias.paetzold}@uia.no

Abstract — This article analyzes the statistical properties of narrowband mobile-to-mobile (M2M) fading channels with equal gain combining (EGC) under line-of-sight (LOS) propagation conditions. Here, we study a dual-hop amplify-and-forward relay network. It is assumed that there can exist LOS components in the transmission links between the source mobile station and the destination mobile station via K mobile relays. In order to cater for asymmetric fading conditions in the relay links, the received signal envelope at the output of the equal gain (EG) combiner is thus modeled as a sum of K double Rice processes. These processes are considered to be independent but not necessarily identically distributed. Simple and closed-form analytical approximations are derived for the probability density function (PDF), the cumulative distribution function (CDF), the level-crossing rate (LCR), and the average duration of fades (ADF) of the sum process by exploiting the properties of gamma processes. The correctness of the derived analytical approximations is verified by simulations. The presented results are easily utilizable in the system performance analysis and optimization of relay-based cooperative networks, where EGC is deployed at the destination mobile station.

I. INTRODUCTION

In recent years, cooperative relaying has secured a prominent position in the wireless communications' research community. The reason is that it promises high data-rate, improved link quality, and increased network coverage [13, 5, 4]. Furthermore, in cooperative networks, the link quality is enhanced by realizing a spatial diversity gain with the help of existing resources (i.e., the mobile stations) of the network. From several different cooperative diversity techniques proposed to date [11, 20, 21], amplify-and-forward relaying is the simplest. In this kind of relaying,

several mobile stations work together with the source mobile station, where they amplify and then forward the information signal to the destination mobile station.

In this work, we study a dual-hop amplify-and-forward relay network, where EGC [9] is deployed at the destination mobile station. The system under consideration contains K mobile relays that are connected in parallel between the source mobile station and the destination mobile station. It is widely acknowledged that EGC is a suboptimal combining technique, which is less complex but performs very close to the optimal maximal ratio combining (MRC) schemes [9]. Studies pertaining to the statistical characterization as well as the performance analysis of EGC along with MRC over Rayleigh, Rice, and Nakagami channels are readily available in the literature, see, e.g., [26, 3, 8, 27]. In addition, quite a few works have studied the performance of cooperative diversity using EGC along with MRC over Rayleigh and Nakagami- m fading channels [1, 7].

Rayleigh and Rice distributions efficiently describe the multipath propagation in classical cellular networks under non-line-of-sight (NLOS) and LOS conditions, respectively. These distributions are however not appropriate to effectively characterize the fading in M2M cooperative communication systems. Under NLOS propagation conditions, the distribution that models best, the fading in relay-based M2M networks is referred to as the double Rayleigh distribution [10, 15]. An extension from the double Rayleigh channel model to the double Rice channel model has been proposed in [22]. The statistics of EGC over multiple double Rayleigh fading channels have been explored recently in [24]. Furthermore, the performance of digital modulations over double Rayleigh as well as double Nakagami- m fading channels with EGC and MRC diversity has already been studied [23, 25]. At present, there is a lack in information regarding the propagation channel characteristics under LOS conditions in relay-based M2M networks with EGC.

Here, the statistical properties of EGC over M2M fading channels under LOS propagation conditions in relay-based networks are thoroughly investigated. In many practical propagation scenarios, asymmetric fading conditions can be observed in different relay links. Meaning thereby, LOS components can exist in only some few transmission links between the source mobile station and the destination mobile station via K mobile relays. Thus, in order to accommodate unbalanced relay links, the received signal envelope at the output of the EG combiner is modeled as a sum of K double Rice processes. Furthermore, these double Rice processes are independent but not necessarily identically distributed. Analytical approximations are derived for the PDF, the CDF, the LCR, and the ADF of the sum process. Analysis of these statistical quantities give us a complete picture of the fading channel,

since the PDF can well characterize the channel, and the LCR along with the ADF provide an insight into the fading behavior of the channel. This work includes a discussion on the influence of the number of diversity branches K as well as the presence of LOS components in the transmission links on the statistics of double Rice processes with EGC. In addition, the obtained results can easily be used in the system performance analysis and optimization of relay-based cooperative networks, where EGC is deployed at the destination mobile station.

This article has the following structure. In Section II, we present the system model for EGC over M2M fading channels under LOS propagation conditions in amplify-and-forward relay networks. Section III deals with the derivation and analysis of approximations for the PDF, the CDF, the LCR, and the ADF of the received signal envelope at the output of the EG combiner. The correctness of the derived analytical approximations is verified by simulations in Section IV. Section V summarizes and concludes the article.

II. EGC OVER DOUBLE RICE FADING CHANNELS

This section aims at describing the system model of EGC over M2M fading channels in a dual-hop cooperative network. The M2M channels explored here are flat fading channels in isotropic scattering environments under LOS propagation conditions. It is further assumed that there exist K diversity branches due to the presence of K mobile relays. These mobile relays are connected in parallel between the source mobile station and the destination mobile station (see Fig. I.1). In addition, considering the limitations on the technical implementation of the mobile stations, we suppose that all mobile stations in the network operate in half-duplex. Time-division multiple-access (TDMA) based amplify-and-forward relay protocols proposed in [12, 2] have been employed in the system under consideration. Thus, the signals from the K diversity branches in different time slots can be combined at the destination mobile station using EGC. This allows us to express the received signal envelope at the output of the EG combiner as [9]

$$\Xi_{\rho}(t) = \sum_{k=1}^K \left| \zeta_{\rho}^{(k)}(t) \right| = \sum_{k=1}^K \chi_{\rho}^{(k)}(t) \quad (1)$$

where it is assumed that perfect channel state information (CSI) is available at the receiver, i.e., the destination mobile station.

In (1), the process $\zeta_{\rho}^{(k)}(t)$ ($k = 1, 2, \dots, K$) represents the complex channel gain of the k th subchannel from the source mobile station to the destination mobile station via the k th mobile relay under LOS propagation conditions. Here, each fading

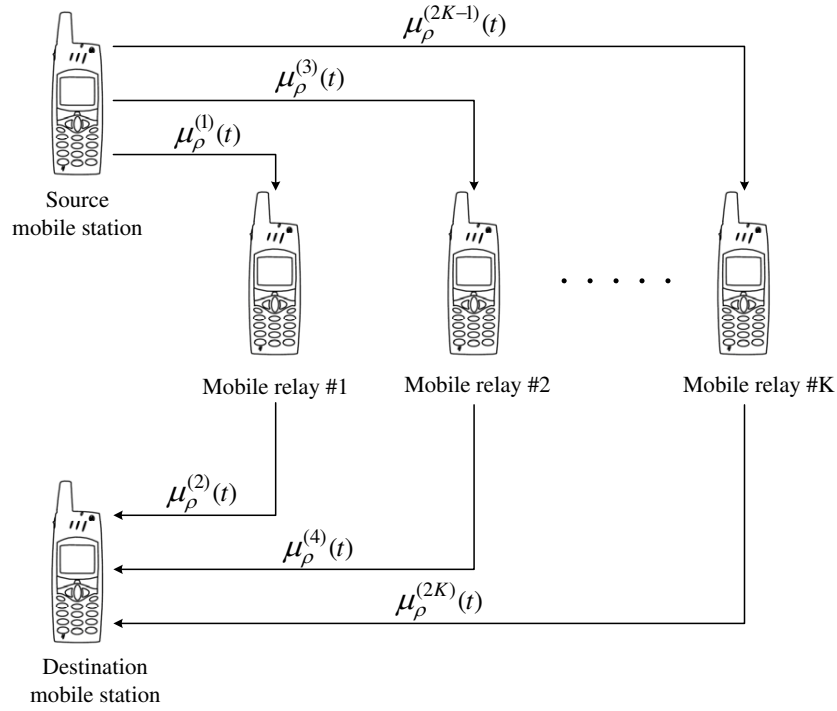


Figure I.1: The propagation scenario illustrating K -parallel dual-hop relay M2M fading channels.

process $\zeta_{\rho}^{(k)}(t)$ is modeled as a weighted non-zero-mean complex double Gaussian process, i.e.,

$$\zeta_{\rho}^{(k)}(t) = \zeta_{\rho_1}^{(k)}(t) + j\zeta_{\rho_2}^{(k)}(t) = A_k \mu_{\rho}^{(2k-1)}(t) \mu_{\rho}^{(2k)}(t) \quad (2)$$

for $k = 1, 2, \dots, K$. For $i = 2k - 1 = 1, 3, \dots, (2K - 1)$, the non-zero-mean complex Gaussian process $\mu_{\rho}^{(i)}(t)$ in (2) is the sum of the scattered component $\mu^{(i)}(t)$ and the LOS component $m^{(i)}(t)$ of the subchannel between the source mobile station and the k th mobile relay, i.e., $\mu_{\rho}^{(i)}(t) = \mu^{(i)}(t) + m^{(i)}(t)$. Similarly, for $i = 2k = 2, 4, \dots, 2K$, the Gaussian process $\mu_{\rho}^{(i)}(t)$ denotes the sum of the scattered component $\mu^{(i)}(t)$ and the LOS component $m^{(i)}(t)$ of the subchannel between the k th mobile relay and the destination mobile station. Each scattered component $\mu^{(i)}(t)$ is modeled by a zero-mean complex Gaussian process with variance $2\sigma_i^2$. In addition, these Gaussian processes are mutually independent, where the classical Jakes Doppler power spectral density describes the spectral characteristics of each process. The corresponding LOS component $m^{(i)}(t) = \rho_i \exp\{j(2\pi f_{\rho}^{(i)} t + \theta_{\rho}^{(i)})\}$ possesses a fixed amplitude ρ_i , a constant Doppler frequency $f_{\rho}^{(i)}$, and a constant phase $\theta_{\rho}^{(i)}$. In (2), A_k is the relay gain of the k th relay. It is interesting to note that the relay gain A_k is nothing but a scaling factor of the mean (i.e.,

$E\{A_k \mu_\rho^{(i)}(t)\} = \rho_i^{(k)} \exp\{j(2\pi f_\rho^{(i)} t + \theta_\rho^{(i)})\}$, where $\rho_i^{(k)} = A_k \rho_i$ and the variance (i.e., $\text{Var}\{A_k \mu_\rho^{(i)}(t)\} = 2(A_k \sigma_i)^2$) of the complex Gaussian process $\mu_\rho^{(i)}(t) \forall i = 2k - 1 = 1, 3, \dots, (2K - 1)$. The absolute value of $\zeta_\rho^{(k)}(t)$ is denoted by $\chi_\rho^{(k)}(t)$ in (1), where each $\chi_\rho^{(k)}(t)$ is a double Rice process.

III. STATISTICAL ANALYSIS OF EGC OVER DOUBLE RICE FADING CHANNELS

In this section, we analyze the statistical properties of EGC over M2M fading channels under LOS propagation conditions. The statistical quantities of interest include the PDF, the CDF, the LCR, and the ADF of double Rice processes $\Xi_\rho(t)$ with EGC.

A. PDF of a Sum of Double Rice Processes

Under LOS propagation conditions, the received signal envelope $\Xi_\rho(t)$ at the output of the EG combiner is modeled as a sum of K independent but not necessarily identically distributed double Rice processes. The PDF $p_{\Xi_\rho}(x)$ of $\Xi_\rho(t)$ can be obtained by solving a K -dimensional convolution integral. The computation of this convolution integral is however quite tedious. It can further be shown that the evaluation of the inverse Fourier transform of the characteristic function (CF) does not lead to a simple and closed-form expression for the PDF $p_{\Xi_\rho}(x)$. Thus, we propose to approximate the PDF $p_{\Xi_\rho}(x)$ by the gamma distribution. This gamma distribution in fact appears as the first term in the Laguerre series expansion [18], i.e.,

$$p_{\Xi_\rho}(x) \approx p_\Gamma(x) = \frac{x^{\alpha_L}}{\beta_L^{(\alpha_L+1)} \Gamma(\alpha_L+1)} e^{-\frac{x}{\beta_L}} \quad (3)$$

where $\Gamma(\cdot)$ is the gamma function [6]. The parameters α_L and β_L can be obtained by following the steps in [18, p. 21], which yields in

$$\alpha_L = [\kappa_1^2 / \kappa_2] - 1, \quad \beta_L = \kappa_2 / \kappa_1 \quad (4a,b)$$

where κ_1 corresponds to the first cumulant (i.e., the mean value) and κ_2 represents the second cumulant (i.e., the variance) of the stochastic process $\Xi_\rho(t)$. Mathematically, κ_1 and κ_2 can be expressed as

$$\kappa_n = \sum_{k=1}^K \kappa_n^{(k)}, \quad n = 1, 2 \quad (5)$$

where $\kappa_n^{(k)}$ describes the cumulants associated with the double Rice process $\chi_\rho^{(k)}(t)$. The first two cumulants of $\chi_\rho^{(k)}(t)$ originally reported in [22] are as follows

$$\begin{aligned} \kappa_1^{(k)} &= A_k \sigma_{(2k-1)} \sigma_{(2k)} \frac{\pi}{2} {}_1F_1\left(-\frac{1}{2}; 1; -\rho_{(2k-1)}^2/2\sigma_{(2k-1)}^2\right) \\ &\quad \times {}_1F_1\left(-\frac{1}{2}; 1; -\rho_{(2k)}^2/2\sigma_{(2k)}^2\right) \end{aligned} \quad (6a)$$

$$\begin{aligned} \kappa_2^{(k)} &= A_k^2 \left(2\sigma_{(2k-1)}^2 + \rho_{(2k-1)}^2\right) \left(2\sigma_{(2k)}^2 + \rho_{(2k)}^2\right) - \left(A_k \sigma_{(2k-1)} \sigma_{(2k)} \frac{\pi}{2}\right)^2 \\ &\quad \times \left[{}_1F_1\left(-\frac{1}{2}; 1; -\rho_{(2k-1)}^2/2\sigma_{(2k-1)}^2\right) {}_1F_1\left(-\frac{1}{2}; 1; -\rho_{(2k)}^2/2\sigma_{(2k)}^2\right) \right]^2. \end{aligned} \quad (6b)$$

where ${}_1F_1(\cdot; \cdot; \cdot)$ is the hypergeometric function [6].

The evaluation of κ_n in (5) is rather straightforward once we have $\kappa_n^{(k)}$ ($n = 1, 2$) for all $\chi_\rho^{(k)}(t)$. Given κ_n , the quantities α_L and β_L can easily be computed using (4a,b). Substitution of α_L and β_L in (3) leads to the approximate solution for the PDF $p_{\Xi_\rho}(x)$.

The motivation behind deriving an expression for the PDF $p_{\Xi_\rho}(x)$ of $\Xi_\rho(t)$ is that it can be utilized with ease in the link level performance analysis of dual-hop cooperative networks with EGC.

B. CDF of a Sum of Double Rice Processes

The probability that $\Xi_\rho(t)$ remains below a threshold level r defines the CDF $F_{\Xi_\rho}(r)$ of $\Xi_\rho(t)$ [14]. After substituting (3) in $F_{\Xi_\rho}(r) = 1 - \int_r^\infty p_{\Xi_\rho}(x) dx$ and solving the integral over x using [6, Eq. (3.381-3)], we can approximate $F_{\Xi_\rho}(r)$ in closed form as

$$F_{\Xi_\rho}(r) \approx 1 - \frac{1}{\Gamma(\alpha_L + 1)} \Gamma\left(\alpha_L, \frac{r}{\beta_L}\right) \quad (7)$$

where $\Gamma(\cdot, \cdot)$ is the upper incomplete gamma function [6].

C. LCR of a Sum of Double Rice Processes

The LCR $N_{\Xi_\rho}(r)$ of $\Xi_\rho(t)$ is a measure to describe the average number of times the stochastic process $\Xi_\rho(t)$ crosses a particular threshold level r from up to down (or from down to up) within one second. The LCR $N_{\Xi_\rho}(r)$ can be computed using the formula [19]

$$N_{\Xi_\rho}(r) = \int_0^\infty \dot{x} p_{\Xi_\rho, \dot{\Xi}_\rho}(r, \dot{x}) d\dot{x} \quad (8)$$

where $p_{\Xi_\rho, \dot{\Xi}_\rho}(r, \dot{x})$ is the joint PDF of the stochastic process $\Xi_\rho(t)$ and its corresponding time derivative $\dot{\Xi}_\rho(t)$ at the same time t . Throughout this paper, the overdot represents the time derivative. The task at hand is to find the joint PDF

$p_{\Xi_\rho, \dot{\Xi}_\rho}(r, \dot{x})$. Here, we proceed to solve this problem by approximating the joint PDF $p_{\Xi_\rho, \dot{\Xi}_\rho}(r, \dot{x})$ by the joint PDF $p_{\Gamma\dot{\Gamma}}(r, \dot{x})$ of a gamma process and its corresponding time derivative at the same time t , i.e.,

$$p_{\Xi_\rho, \dot{\Xi}_\rho}(r, \dot{x}) \approx p_{\Gamma\dot{\Gamma}}(r, \dot{x}) \quad (9)$$

where $p_{\Gamma\dot{\Gamma}}(r, \dot{x})$ can be expressed in terms of α_L and β_L , as

$$p_{\Gamma\dot{\Gamma}}(x, \dot{x}) = \frac{1}{2\sqrt{2\pi\beta x}} \frac{x^{\alpha_L}}{\beta_L^{(\alpha_L+1)}\Gamma(\alpha_L+1)} e^{-\frac{x}{\beta_L} - \frac{\dot{x}^2}{8\beta x}} \quad (10)$$

with $\beta = \pi^2\beta_L(f_{s_{\max}}^2 + 2f_{R_{\max}}^2 + f_{D_{\max}}^2)$. The quantities $f_{s_{\max}}$ and $f_{D_{\max}}$ represent the maximum Doppler frequencies caused by the motion of the source mobile station and the destination mobile station, respectively. In addition, the maximum Doppler frequencies caused by the motion of mobile relays are assumed to be equal such that $f_{R_{\max}}^{(1)} = f_{R_{\max}}^{(2)} = \dots = f_{R_{\max}}^{(K)} = f_{R_{\max}}$.

Finally, substituting $p_{\Xi_\rho, \dot{\Xi}_\rho}(r, \dot{x})$ in (8) and solving the integral over \dot{x} using [6, Eq. (3.326-2)], we reach the following closed-form approximation for the LCR $N_{\Xi_\rho}(r)$

$$\begin{aligned} N_{\Xi_\rho}(r) &\approx \int_0^\infty \dot{x} p_{\Gamma\dot{\Gamma}}(r, \dot{x}) d\dot{x} \\ &= \sqrt{\frac{2r\beta}{\pi}} \frac{r^{\alpha_L} e^{-\frac{r}{\beta_L}}}{\beta_L^{(\alpha_L+1)}\Gamma(\alpha_L+1)} = \sqrt{\frac{2r\beta}{\pi}} p_{\Xi_\rho}(r). \end{aligned} \quad (11)$$

D. ADF of a Sum of Double Rice Processes

The ADF $T_{\Xi_\rho}(r)$ of $\Xi_\rho(t)$ is the expected value of the time intervals over which the stochastic process $\Xi_\rho(t)$ remains below a certain threshold level r . Mathematically, the ADF $T_{\Xi_\rho}(r)$ is defined as the ratio of the CDF $F_{\Xi_\rho}(r)$ and the LCR $N_{\Xi_\rho}(r)$ of $\Xi_\rho(t)$ [9], i.e.,

$$T_{\Xi_\rho}(r) = \frac{F_{\Xi_\rho}(r)}{N_{\Xi_\rho}(r)}. \quad (12)$$

By substituting (7) and (11) in (12), we can easily obtain an approximate solution for the ADF $T_{\Xi_\rho}(r)$.

The significance of studying the LCR $N_{\Xi_\rho}(r)$ and the ADF $T_{\Xi_\rho}(r)$ of $\Xi_\rho(t)$ lies in the fact that they provide insight into the rate of fading of the stochastic process $\Xi_\rho(t)$. Knowledge about the rate of fading is beneficial in both the design as well as the optimization of coding and interleaving schemes to combat fading in the relay

links of cooperative networks.

IV. NUMERICAL RESULTS

This section deals with the illustration of important theoretical results by evaluating the approximations in (3), (11), and (12). In addition, here the correctness of the theoretical results is verified with the help of simulations. The sum-of-sinusoids (SOS) concept [16] has been applied on the uncorrelated Gaussian noise processes making up the received signal envelope at the output of the EG combiner in order to obtain the exact simulation results. The model parameters of the channel simulator were computed by employing the generalized method of exact Doppler spread (GMEDS₁) [17]. Each Gaussian process $\mu^{(i)}(t)$ ($i = 1, 2, \dots, 2K$) was simulated with $N_l^{(i)} = 14$ for $i = 1, 2, \dots, 2K$ and $l = 1, 2$, where $N_l^{(i)}$ is the number of sinusoids used to simulate the inphase ($l = 1$) and quadrature components ($l = 2$) of $\mu^{(i)}(t)$. The simulated waveforms $\tilde{\mu}^{(i)}(t)$ have a distribution which closely approximates the Rayleigh distribution if $N_l^{(i)} \geq 7$ ($l = 1, 2$) for all $i = 1, 2, \dots, 2K$ [16]. Thus, by choosing $N_l^{(i)} = 14$, we make sure the waveforms $\tilde{\mu}^{(i)}(t)$ have the desired Gaussian distribution. The maximum Doppler frequencies caused by the motion of the source mobile station, K mobile relays, and the destination mobile station, denoted by $f_{s_{\max}}$, $f_{r_{\max}}$, and $f_{d_{\max}}$, respectively, were set to 91 Hz, 125 Hz, and 110 Hz. The variances σ_i^2 , the amplitudes of the LOS components ρ_i , and the relay gains A_k were selected to be unity for all $i = 1, 2, \dots, 2K$ and $k = 1, 2, \dots, K$ unless stated otherwise.

In Figs. I.2–I.4, we have presented the PDF, the LCR, and the ADF of $\Xi_\rho(t)$ considering the full-LOS (FLOS) and partial-LOS (PLOS) propagation scenarios. We have referred to the scenario as FLOS propagation where LOS components exist in all the transmission links between the source mobile station and the destination mobile station via K mobile relays. In PLOS propagation scenario, the LOS components are present only in the links from the source mobile station to the k -th mobile relay. The presented results illustrate a good fit of the approximated analytical and the exact simulation results.

Figure I.2 demonstrates the theoretical approximation for the PDF $p_{\Xi_\rho}(x)$ of $\Xi_\rho(t)$ described in (3). The simulation results obtained by evaluating the statistics of the waveforms generated by using the SOS-based channel simulator are included in this figure for confirming the correctness of the theory. Studying the PDFs $p_{\Xi_\rho}(x)$ for a different number of diversity branches K reveal that increasing K increases the mean value whereas the variance of $\Xi_\rho(t)$ decreases under both FLOS and PLOS propagation conditions. Furthermore, for $K = 1$, $\rho_i = 1$ ($i = 1, 2$), and $A_k = 1$, the

PDF $p_{\Xi_\rho}(x)$ of $\Xi_\rho(t)$ maps to the double Rice distribution, verifying the correctness of our approximation in (3).

The LCR $N_{\Xi_\rho}(r)$ of $\Xi_\rho(t)$ described by (11) is evaluated along with the exact simulation results in Fig. I.3. This figure presents the LCR $N_{\Xi_\rho}(r)$ for a different number of diversity branches K for FLOS and PLOS propagation conditions. For $K = 1$, $\rho_i = 1$ ($i = 1, 2$), and $A_k = 1$, it is quite clear from the graphs that at higher signal levels r , (11) provides us with a very close approximation to the exact LCR of a double Rice process given in [22]. Under FLOS propagation conditions, increasing K while keeping ρ_i and A_k constant, results in a decrease in the LCR $N_{\Xi_\rho}(r)$ at lower signal levels r . However, the LCR $N_{\Xi_\rho}(r)$ increases at higher signal levels r for increasing K with constant ρ_i and A_k . Figure I.3 also shows that for a particular value of K with constant A_k , the LCR $N_{\Xi_\rho}(r)$ assumes a lower value at lower signal levels r under PLOS propagation conditions and vice versa.

In Fig. I.4, the analytical approximate results of the ADF $T_{\Xi_\rho}(r)$ of $\Xi_\rho(t)$ described by (12) along with the exact simulation results are displayed. These results clearly indicate that under both FLOS and PLOS propagation conditions, increasing the number of diversity branches K results in a decrease of the ADF $T_{\Xi_\rho}(r)$ for all signal levels r . It can also be observed in Fig. I.4 that the presence of the LOS components in all the transmission links lowers the ADF $T_{\Xi_\rho}(r)$ at all signal levels r for any number K .

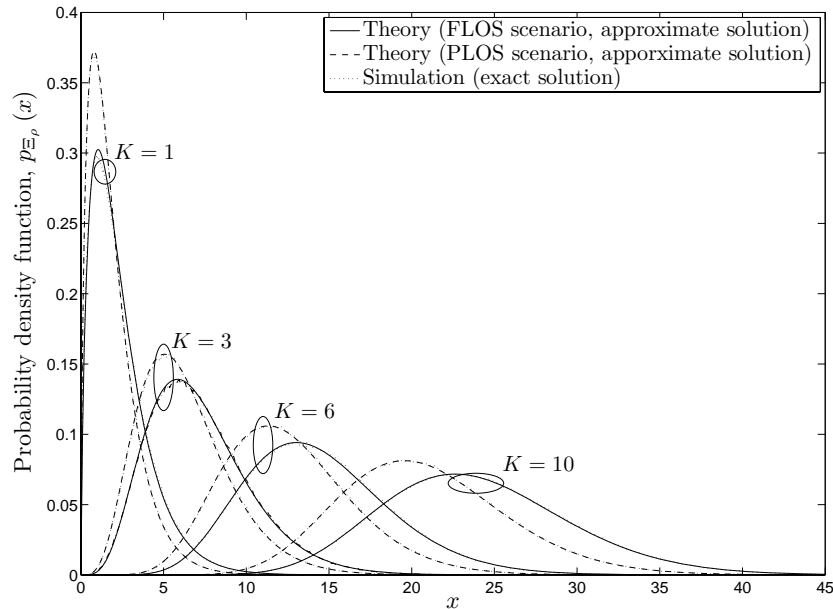


Figure I.2: The PDF $p_{\Xi_\rho}(x)$ of the received signal envelope $\Xi_\rho(t)$ at the output of the EG combiner for a different number of diversity branches K .

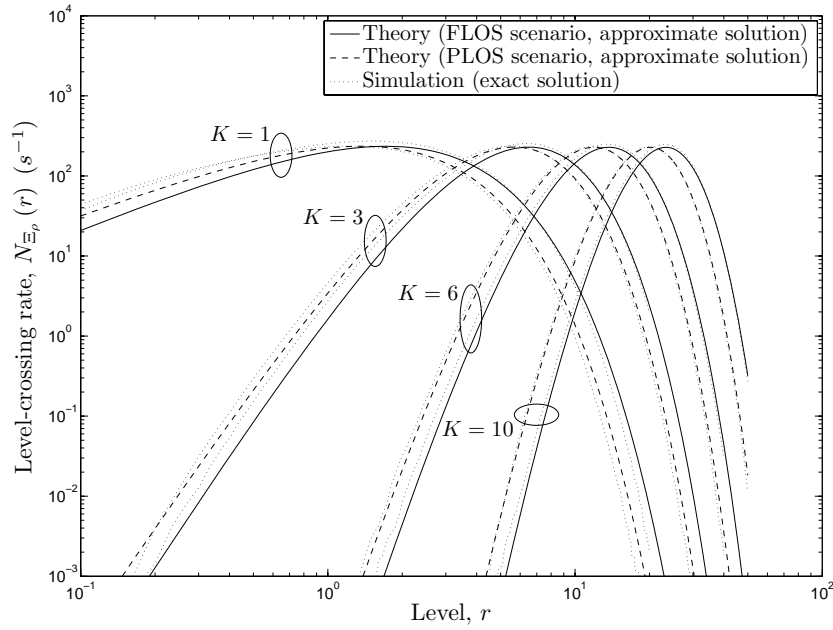


Figure I.3: The LCR $N_{\Xi_\rho}(r)$ of the received signal envelope $\Xi_\rho(t)$ at the output of the EG combiner for a different number of diversity branches K .

V. CONCLUSION

This article is focused on the statistical analysis of EGC over narrowband M2M fading channels under LOS propagation conditions. The system under investiga-

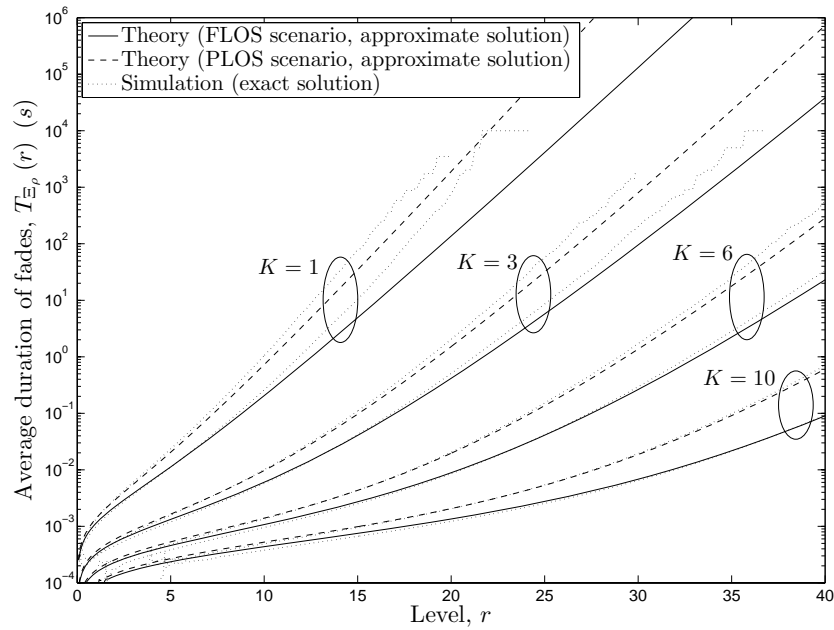


Figure I.4: The ADF $T_{\Xi_\rho}(r)$ of the received signal envelope $\Xi_\rho(t)$ at the output of the EG combiner for a different number of diversity branches K .

tion is a dual-hop amplify-and-forward relay communication system, where there exist K mobile relays between the source mobile station and the destination mobile station. Such a system configuration gives rise to K diversity branches. The signals received from the K diversity branches are then combined at the destination mobile station to achieve the spatial diversity gain. We have modeled the received signal envelope at the output of the EG combiner as a sum of K independent but not necessarily identically distributed double Rice processes. Simple and closed-form analytical approximations for the channel statistics such as the PDF, the CDF, the LCR, and the ADF are derived. Here, the gamma distribution has been employed to approximate with reasonable accuracy the PDF of a sum of K double Rice processes. The CDF, the LCR, and the ADF of the sum process are also approximated by exploiting the properties of a gamma distributed process. Furthermore, the presented results demonstrate that the approximated theoretical results fit closely to the exact simulation results. For this reason, we believe that the proposed approximation approach followed in this study is valid. In addition to studying the impact of the number of diversity branches K , we have investigated the influence of the existence of the LOS components in the transmission links on the statistical properties of EGC over M2M channels. Designers of the physical layer of M2M cooperative wireless networks can take advantage of this work by utilizing our results in system performance analysis and optimization.

REFERENCES

- [1] P. A. Anghel and M. Kaveh. Exact symbol error probability of a cooperative network in a Rayleigh fading environment. *IEEE Trans. Wireless Commun.*, 3(5):1416–1421, September 2004.
- [2] K. Azarian, H. E. Gamal, and P. Schniter. On the achievable diversity-multiplexing tradeoff in half-duplex cooperative channels. *IEEE Trans. Inform. Theory*, 51(12):4152–4172, December 2005.
- [3] N. C. Beaulieu and X. Dong. Level crossing rate and average fade duration of MRC and EGC diversity in Ricean fading. *IEEE Trans. Commun.*, 51(5):722–726, May 2003.
- [4] M. Dohler and Y. Li. *Cooperative Communications: Hardware, Channel, and PHY*. Chichester: John Wiley & Sons, 1st edition, 2010.
- [5] Y. Fan and J. S. Thompson. MIMO configurations for relay channels: Theory and practice. *IEEE Trans. Wireless Commun.*, 6(5):1774–1786, May 2007.

- [6] I. S. Gradshteyn and I. M. Ryzhik. *Table of Integrals, Series, and Products*. New York: Academic Press, 6th edition, 2000.
- [7] S. S. Ikki and M. H. Ahmed. Performance of cooperative diversity using equal gain combining (EGC) over Nakagami- m fading channels. *IEEE Trans. Wireless Commun.*, 8(2):557–562, February 2009.
- [8] P. Ivanis, D. Drajić, and B. Vucetic. The second order statistics of maximal ratio combining with unbalanced branches. *IEEE Communications Letters*, 12(7):508–510, July 2008.
- [9] W. C. Jakes, editor. *Microwave Mobile Communications*. Piscataway, NJ: IEEE Press, 1994.
- [10] I. Z. Kovacs, P. C. F. Eggers, K. Olesen, and L. G. Petersen. Investigations of outdoor-to-indoor mobile-to-mobile radio communication channels. In *Proc. IEEE 56th Veh. Technol. Conf., VTC'02-Fall*, volume 1, pages 430–434. Vancouver BC, Canada, September 2002.
- [11] J. N. Laneman, D. N. C. Tse, and G. W. Wornell. Cooperative diversity in wireless networks: Efficient protocols and outage behavior. *IEEE Trans. Inform. Theory*, 50(12):3062–3080, December 2004.
- [12] R. U. Nabar, H. Bölcskei, and F. W. Kneubühler. Fading relay channels: Performance limits and space-time signal design. *IEEE J. Select. Areas Commun.*, 22(6):1099–1109, August 2004.
- [13] R. Pabst, B. Walke, D. Schultz, et al. Relay-based deployment concepts for wireless and mobile broadband radio. *IEEE Communications Magazine*, 42(9):80–89, September 2004.
- [14] A. Papoulis and S. U. Pillai. *Probability, Random Variables and Stochastic Processes*. New York: McGraw-Hill, 4th edition, 2002.
- [15] C. S. Patel, G. L. Stüber, and T. G. Pratt. Statistical properties of amplify and forward relay fading channels. *IEEE Trans. Veh. Technol.*, 55(1):1–9, January 2006.
- [16] M. Pätzold. *Mobile Fading Channels*. Chichester: John Wiley & Sons, 2002.
- [17] M. Pätzold, C. X. Wang, and B. O. Hogstad. Two new sum-of-sinusoids-based methods for the efficient generation of multiple uncorrelated Rayleigh fading waveforms. *IEEE Trans. Wireless Commun.*, 8(6):3122–3131, June 2009.

- [18] S. Primak, V. Kontorovich, and V. Lyandres, editors. *Stochastic Methods and their Applications to Communications: Stochastic Differential Equations Approach*. Chichester: John Wiley & Sons, 2004.
- [19] S. O. Rice. Mathematical analysis of random noise. *Bell Syst. Tech. J.*, 24:46–156, January 1945.
- [20] A. Sendonaris, E. Erkip, and B. Aazhang. User cooperation diversity — Part I: System description. *IEEE Trans. Commun.*, 51(11):1927–1938, November 2003.
- [21] A. Sendonaris, E. Erkip, and B. Aazhang. User cooperation diversity — Part II: Implementation aspects and performance analysis. *IEEE Trans. Commun.*, 51(11):1939–1948, November 2003.
- [22] B. Talha and M. Pätzold. On the statistical properties of double Rice channels. In *Proc. 10th Int. Symp. on Wireless Personal Multimedia Communications, WPMC 2007*, pages 517–522. Jaipur, India, December 2007.
- [23] B. Talha, M. Pätzold, and S. Primak. Performance analysis of M -ary PSK modulation schemes over multiple double Rayleigh fading channels with EGC in cooperative networks. In *Proc. IEEE Int. Conf. Communications, Workshop on Vehicular Connectivity, Veh-Con 2010*. Cape Town, South Africa, May 2010. DOI 10.1109/ICCW.2010.5503940.
- [24] B. Talha, S. Primak, and M. Pätzold. On the statistical properties of equal gain combining over mobile-to-mobile fading channels in cooperative networks. In *Proc. IEEE Int. Conf. Communications (ICC'10)*. Cape Town, South Africa, May 2010. DOI 10.1109/ICC.2010.5501898.
- [25] W. Wongtrairat and P. Supnithi. Performance of digital modulation in double Nakagami- m fading channels with MRC diversity. *IEICE Trans. Commun.*, E92-B(2):559–566, February 2009.
- [26] M. D. Yacoub, C. R. C. Monterio da Silva, and J. E. V. Bautista. Second-order statistics for diversity-combining techniques in Nakagami fading channels. *IEEE Trans. Veh. Technol.*, 50(6):1464–1470, November 2001.
- [27] D. A. Zogas, G. K. Karagiannidis, and S. A. Kotsopoulos. Equal gain combining over Nakagami- n (Rice) and Nakagami- q (Hoyt) generalized fading channels. *IEEE Trans. Wireless Commun.*, 4(2):374–379, March 2005.

Appendix J

Paper IX

Title: On the Statistical Analysis of the Channel Capacity of Double Rayleigh Channels with Equal Gain Combining in V2V Communication Systems

Authors: **Batool Talha** and Matthias Pätzold

Affiliation: University of Agder, Faculty of Engineering and Science, P. O. Box 509, NO-4898 Grimstad, Norway

Conference: *3rd IEEE International Symposium on Wireless Vehicular Communications, WiVec 2010*, Taipei, Taiwan, May 2010. DOI 10.1109/VETECS.2010.5494112.

On the Statistical Analysis of the Channel Capacity of Double Rayleigh Channels with Equal Gain Combining in V2V Communication Systems

Batool Talha and Matthias Pätzold

Department of Information and Communication Technology
Faculty of Engineering and Science, Agder University College
Servicebox 509, NO-4876 Grimstad, Norway
E-mails: {batool.talha, matthias.paetzold}@uia.no

Abstract — In this article, we present a detailed study on the statistical properties of the channel capacity of vehicle-to-vehicle (V2V) fading channels with equal gain combining (EGC). Assuming perfect channel state information (CSI) at the receiver, we have modeled the received signal envelope at the output of the equal gain (EG) combiner as a sum of double Rayleigh processes. These double Rayleigh processes are assumed to be independent but not necessarily identical processes. It is illustrated that the PDF of this sum process can efficiently be approximated using the gamma distribution. Furthermore, exploiting the properties of the gamma distribution, other statistical properties of the sum process are also evaluated. Thus, given the analytical approximations for the statistical properties of the received signal envelope at the output of the EG combiner, the theoretical results associated the statistics of the channel capacity just involves transformation of random variables. Here, simple and closed-form analytical approximations for the probability density function (PDF), the cumulative distribution function (CDF), the level-crossing rate (LCR), and the average duration of fades (ADF) of the channel capacity are derived. The correctness of the theoretical results is validated by simulations. The presented results can be utilized to optimize the performance of spatial diversity receivers employed in the forthcoming V2V multiple-input multiple-output (MIMO) wireless communication systems.

I. INTRODUCTION

V2V wireless communications has recently gained a fair share of attention by researchers, standardization bodies, and industrial companies, since it offers many applications. These applications are targeted to reduce traffic accidents and to facilitate the flow of traffic [36, 7]. The development of V2V communication systems

requires the knowledge of the propagation channel characteristics. It is well-known that the multipath propagation channel in any mobile and wireless communication system can efficiently be described with the help of proper statistical models. For example, the Rayleigh distribution is considered to be a suitable distribution to model the fading channel under non line-of-sight (NLOS) propagation conditions in classical cellular networks [34, 15, 16], a Suzuki process represents a reasonable model for land mobile terrestrial channels [20, 31] and the generalized- K distribution is widely accepted in radar systems [5, 28]. To model fading channels under NLOS propagation conditions in V2V communication systems, the double Rayleigh distribution is the appropriate choice (see, e.g., [14, 19] and the references therein). Motivated by the applications of the double Rayleigh channel model, a generalized channel model referred to as the N^* Nakagami channel model has been proposed in [12].

Inter-vehicle communication can be considered as a kind of mobile-to-mobile (M2M) communication. In M2M communication systems both the source (transmitter) and the destination (receiver) are mobile stations. If the destination mobile station is equipped with K receive antennas, then the signals reaching the destination mobile station through K diversity branches can be combined in order to mitigate the adverse multipath fading effects. Among other diversity combining techniques [24] aiming to combat the undesirable fading effects, the spatial diversity combining is a well-studied topic in the field of wireless communications. Selection combining (SC) [11], maximal ratio combining (MRC) [11], and EGC [11] are to name a few such combining schemes that provide a spatial diversity gain. MRC has been proved to be the optimum scheme, while the suboptimal EGC scheme is more popular for its simplicity in implementation [11]. Studies pertaining to the statistical properties as well as the performance analysis of both EGC and MRC over Rayleigh, Rice, and Nakagami channels can be found in the literature, see, e.g., [33, 4, 10, 35, 37, 26]. In a recent work [32], the performance of digital modulation over double Nakagami- m fading channels with MRC diversity is investigated.

In addition to the knowledge about the propagation channel characteristics, a sound understanding of the channel capacity is also indispensable to meet the data rate requirements of future mobile communication systems. For this reason, researchers are currently devoting their time and efforts in investigating the various aspects of the channel capacity. A study on the capacity of Rayleigh and Rice channels with MRC diversity is presented in [3, 13, 9]. The authors of [23] have analyzed the statistical properties of the channel capacity of Rice fading channels with EGC and MRC. However, to the best of the authors' knowledge, the analysis

of the statistical properties of the channel capacity of double Rayleigh fading channels with EGC in V2V communication systems is still an open problem that calls for further work.

This article analyzes the statistical properties of the channel capacity of double Rayleigh fading channels with EGC. The statistical quantities included in our study are the PDF, the CDF, the LCR, and the ADF of the channel capacity. The derived expression for the PDF of the channel capacity allows us to deduce the mean channel capacity and the capacity variance. To obtain an insight into the temporal variations of the channel capacity, an analysis of the LCR and the ADF of the channel capacity is inevitable [6]. We have derived simple and closed-form approximations for all these statistical quantities. The obtained approximate analytical results are compared with the exact simulation results that are considered to be the true results. This allows us to confirm the correctness and to study the accuracy of our approximate solution. Lastly, the influence of the number of diversity branches K on the statistical properties of the channel capacity of double Rayleigh fading channels with EGC has been investigated in detail.

The rest of the article is comprised of five parts. First, a brief review of EGC over double Rayleigh fading channels is given in Section II. In Section III, we discuss the statistical properties of EGC over double Rayleigh fading channels. Section IV deals with the derivation and analysis of the PDF, the CDF, the LCR, and the ADF of the channel capacity of double Rayleigh fading channels with EGC. In Section V, we compare the obtained analytical results with simulation results to validate the correctness of the theory. Finally, we conclude the article in Section VI.

II. EGC OVER DOUBLE RAYLEIGH FADING CHANNELS

The instantaneous signal-to-noise ratio (SNR) per symbol $\gamma_{\text{EGC}}(t)$ at the output of the EG combiner can be defined as [30, 27]

$$\gamma_{\text{EGC}}(t) = \frac{\Xi^2(t)}{E\{N^2(t)\}} E_s = \frac{\Xi^2(t)}{KN_0} E_s = \gamma_s \Xi^2(t) \quad (1)$$

where $E\{\cdot\}$ is the expectation operator. The quantity $\gamma_s = E_s/(KN_0)$ denotes the average received SNR where E_s gives the energy (in joules) per symbol, K is the total number of diversity branches, and N_0 is the total noise power. The process $\Xi(t)$ corresponds to the total received signal envelope at the output of the EG combiner, and $N(t)$ represents the total received noise, i.e., $N(t) = \sum_{k=1}^K n^{(k)}(t)$. Here, $n^{(k)}(t)$ ($k = 1, 2, \dots, K$) refers to the additive white Gaussian noise (AWGN) in the k th diversity branch. The AWGN is a zero-mean Gaussian process with variance

$N_0/2$.

Assuming perfect CSI at the destination mobile station, the received signal envelope $\Xi(t)$ at the output of an EG combiner can be written as [11]

$$\Xi(t) = \sum_{k=1}^K \left| \zeta^{(k)}(t) \right| = \sum_{k=1}^K \chi^{(k)}(t) \quad (2)$$

where $\zeta^{(k)}(t)$ describes the fading process in the k th diversity branch between the source mobile station and the destination mobile station. We model the fading process $\zeta^{(k)}(t)$ as a zero-mean complex double Gaussian process, i.e.,

$$\zeta^{(k)}(t) = \zeta_1^{(k)}(t) + j\zeta_2^{(k)}(t) = \mu^{(2k-1)}(t) \mu^{(2k)}(t) \quad (3)$$

for $k = 1, 2, \dots, K$. In (3), $\mu^{(i)}(t)$ ($i = 1, 2, \dots, 2K$) represents a zero-mean complex circular Gaussian process having variance $2\sigma_{\mu^{(i)}}^2$. These Gaussian processes $\mu^{(i)}(t)$ are mutually independent, where each one is characterized by the classical Jakes Doppler power spectral density. The absolute value of $\zeta^{(k)}(t)$ is denoted by $\chi^{(k)}(t)$ in (2), where each $\chi^{(k)}(t)$ is a double Rayleigh process.

III. STATISTICAL ANALYSIS OF EGC OVER DOUBLE RAYLEIGH FADING CHANNELS

In order to conduct a statistical analysis of the channel capacity, the knowledge of the statistics of the channel itself is imperative. Thus, this section is devoted to briefly discuss the statistical properties of EGC over double Rayleigh fading channels.

In the previous section, we modeled the received signal envelope $\Xi(t)$ at the output of the EG combiner as a sum of K independent but not necessarily identical double Rayleigh processes. Thus, the derivation of the PDF $p_{\Xi}(x)$ of $\Xi(t)$ involves the computation of a K -dimensional convolution integral. This computation is however quite tedious but still simple as well as closed-form result is not obtained. Here, we follow an approximation approach based on the Laguerre series expansion [22]. The Laguerre series is known to provide a reasonably good approximation for PDFs that have single maximum and fast decaying tails. In addition, the Laguerre series is often used when the first term in the expansion gives a simple approximation of high accuracy [22]. We can thus start by expressing the PDF $p_{\Xi}(x)$ of $\Xi(t)$ using the Laguerre series expansion as [22]

$$p_{\Xi}(x) = \sum_{n=0}^{\infty} b_n e^{-x} x^{\alpha_L} L_n^{(\alpha_L)}(x) \quad (4)$$

where

$$L_n^{(\alpha_L)}(x) = e^x \frac{x^{(-\alpha_L)} d^n}{x! dx^n} \left[e^{(-x)} x^{n+\alpha_L} \right], \alpha_L > -1 \quad (5)$$

represent the Laguerre polynomials. The coefficients b_n can be computed as

$$b_n = \frac{n!}{\Gamma(n + \alpha_L + 1)} \int_0^\infty L_n^{(\alpha_L)}(x) p_\Xi(x) dx \quad (6)$$

where $x = y/\beta_L$ and $\Gamma(\cdot)$ is the gamma function [8].

By solving the system of equations in [22, p. 21] for $b_1 = 0$ and $b_2 = 0$, the parameters α_L and β_L can easily be obtained. The solution of the said system of equations results in

$$\alpha_L = \frac{(\kappa_1^\Xi)^2}{\kappa_2^\Xi} - 1, \quad \beta_L = \frac{\kappa_2^\Xi}{\kappa_1^\Xi} \quad (7a,b)$$

where κ_1^Ξ denotes the first cumulant (i.e., the mean value) of the stochastic process $\Xi(t)$ and κ_2^Ξ is the second cumulant (i.e., the variance) of $\Xi(t)$. Mathematically, κ_1^Ξ and κ_2^Ξ can be expressed as

$$\kappa_1^\Xi = \sum_{k=1}^K \kappa_1^{\chi^{(k)}}, \quad \kappa_2^\Xi = \sum_{k=1}^K \kappa_2^{\chi^{(k)}} \quad (8a,b)$$

where $\kappa_n^{\chi^{(k)}}$ ($n = 1, 2$) represents the n th cumulant associated with the double Rayleigh process $\chi^{(k)}(t)$. The first two cumulants of $\chi^{(k)}(t)$ can be given as [29]

$$\kappa_1^{\chi^{(k)}} = \frac{\sigma_{\mu^{(2k-1)}} \sigma_{\mu^{(2k)}} \pi}{2}, \quad \kappa_2^{\chi^{(k)}} = \frac{1}{4} \sigma_{\mu^{(2k-1)}}^2 \sigma_{\mu^{(2k)}}^2 (16 - \pi^2). \quad (9a,b)$$

Once the cumulants $\kappa_n^{\chi^{(k)}}$ ($n = 1, 2$) are obtained for all $\chi^{(k)}(t)$ using (9a,b), it is not difficult to compute κ_n^Ξ in (8a,b). In addition, given κ_n^Ξ , the required quantities α_L and β_L can be found with the help of (7a,b). After substituting α_L and β_L in the Laguerre series expansion, the first term of the series turns out to be the gamma distribution $p_\Gamma(x)$ [22]. This allows us to approximate the PDF $p_\Xi(x)$ of $\Xi(t)$ as

$$p_\Xi(x) \approx p_\Gamma(x) = \frac{x^{\alpha_L}}{\beta_L^{(\alpha_L+1)} \Gamma(\alpha_L + 1)} e^{-\frac{x}{\beta_L}}, x \geq 0. \quad (10)$$

The PDF $p_{\Xi^2}(x)$ of the squared received signal envelope $\Xi^2(t)$ at the output of the EG combiner can be obtained by a simple transformation of the random

variables [17, p. 244] as follows:

$$\begin{aligned} p_{\Xi^2}(x) &= \frac{1}{2\sqrt{x}} p_{\Xi}(\sqrt{x}) \\ &\approx \frac{1}{2\beta_L^{(\alpha_L+1)}\Gamma(\alpha_L+1)} x^{\left(\frac{\alpha_L-1}{2}\right)} e^{-\frac{\sqrt{x}}{\beta_L}} \end{aligned} \quad (11)$$

for $x \geq 0$. This PDF $p_{\Xi^2}(x)$ of $\Xi^2(t)$ will be used in the following section for computing the PDF of the channel capacity.

The derivation of the analytical expression for the LCR of a stochastic process involves the evaluation of the joint PDF of that process and its time derivative at the same time t . Thus, similar to the approximation of the PDF $p_{\Xi}(x)$ of $\Xi(t)$, here the joint PDF $p_{\Xi\dot{\Xi}}(x, \dot{x})$ of $\Xi(t)$ and $\dot{\Xi}(t)$ ¹ is approximated by the joint PDF $p_{\Gamma\dot{\Gamma}}(x, \dot{x})$ of a gamma process and its corresponding time derivative at the same time t . Numerical investigations have shown that $p_{\Xi\dot{\Xi}}(r, \dot{x}) \approx \frac{1}{\sqrt{3}} p_{\Gamma\dot{\Gamma}}(x, \dot{x})$, where

$$p_{\Gamma\dot{\Gamma}}(x, \dot{x}) = \frac{1}{2\sqrt{2\pi\beta x} \beta_L^{(\alpha_L+1)}\Gamma(\alpha_L+1)} x^{\alpha_L} e^{-\frac{x}{\beta_L} - \frac{\dot{x}^2}{8\beta x}} \quad (12)$$

for $x \geq 0$ and $|\dot{x}| < \infty$. Furthermore, for the isotropic scattering conditions, the quantity β equals $2\pi^2\beta_L(f_{s_{\max}}^2 + f_{d_{\max}}^2)$ [2, 1]. Here, $f_{s_{\max}}$ and $f_{d_{\max}}$ correspond to the maximum Doppler frequencies caused by the motion of the source mobile station and the destination mobile station, respectively.

Finally, making use of the joint PDF $p_{\Xi\dot{\Xi}}(x, \dot{x})$ and applying the concept of transformation of random variables [17, p. 244] allows us to express the joint PDF $p_{\Xi^2\dot{\Xi}^2}(x, \dot{x})$ as

$$\begin{aligned} p_{\Xi^2\dot{\Xi}^2}(x, \dot{x}) &= \frac{1}{4x} p_{\Xi\dot{\Xi}}\left(\sqrt{x}, \frac{\dot{x}}{2\sqrt{x}}\right) \approx \frac{1}{4\sqrt{3}x} p_{\Gamma\dot{\Gamma}}\left(\sqrt{x}, \frac{\dot{x}}{2\sqrt{x}}\right) \\ &= \frac{1}{8\sqrt{6\pi\beta} \beta_L^{(\alpha_L+1)}\Gamma(\alpha_L+1)} x^{\left(\frac{2\alpha_L-5}{4}\right)} e^{-\frac{\sqrt{x}}{\beta_L} - \frac{\dot{x}^2}{32\beta x^{3/2}}} \end{aligned} \quad (13)$$

for $x \geq 0$ and $|\dot{x}| < \infty$. In (13), $p_{\Xi^2\dot{\Xi}^2}(x, \dot{x})$ represents the joint PDF of the squared received envelope $\Xi^2(t)$ and its corresponding time derivative $\dot{\Xi}^2(t)$ at the same time t . The joint PDF $p_{\Xi^2\dot{\Xi}^2}(x, \dot{x})$ will be utilized in the derivation of the LCR of the channel capacity in the next section.

¹Throughout this paper, the overdot represents the time derivative.

IV. STATISTICAL ANALYSIS OF THE CHANNEL CAPACITY OF DOUBLE RAYLEIGH FADING CHANNELS WITH EGC

In this section, we present a statistical analysis of the channel capacity of double Rayleigh fading channels with EGC. The statistical quantities studied here include the PDF, the CDF, the LCR, and the ADF of the channel capacity.

The instantaneous channel capacity $C(t)$ of double Rayleigh fading channels with EGC is defined as

$$C(t) = \log_2(1 + \gamma_{\text{EGC}}(t)) \text{ (bits/s/Hz)} \quad (14)$$

where $\gamma_{\text{EGC}}(t)$ introduced in (1) is the instantaneous SNR per symbol. Equation (14) illustrates the mapping of the instantaneous SNR $\gamma_{\text{EGC}}(t)$ on the channel capacity $C(t)$. This mapping makes it possible to derive the analytical expressions for the statistical properties of the channel capacity $C(t)$ with the help of those associated with $\gamma_{\text{EGC}}(t)$.

We start the statistical analysis of the channel capacity $C(t)$ by deriving an expression for the PDF $p_C(r)$ of $C(t)$. However, in order to proceed with this derivation, we require the PDF $p_{\gamma_{\text{EGC}}}(z)$ of $\gamma_{\text{EGC}}(t)$. The PDF $p_{\gamma_{\text{EGC}}}(z)$ can be obtained using the relation $p_{\gamma_{\text{EGC}}}(z) = (1/\gamma_s) p_{\Xi^2}(z/\gamma_s)$, where $p_{\Xi^2}(z)$ is presented in (11). Using the concept of transformation of random variables [17, p. 244], the PDF $p_C(r)$ of $C(t)$ can be expressed in closed form as

$$\begin{aligned} p_C(r) &= 2^r \ln(2) p_{\gamma_{\text{EGC}}}(2^r - 1) \\ &\approx \frac{2^{r-1} \ln(2) (2^r - 1)^{\left(\frac{\alpha_L - 1}{2}\right)} e^{-\frac{\sqrt{(2^r - 1)/\gamma_s}}{\beta_L}}}{\gamma_s^{\left(\frac{\alpha_L + 1}{2}\right)} \beta_L^{(\alpha_L + 1)} \Gamma(\alpha_L + 1)}, \quad r \geq 0. \end{aligned} \quad (15)$$

The probability that the channel capacity $C(t)$ remains below a certain threshold level r defines the CDF $F_C(r)$ of $C(t)$ [17]. Substituting (15) in $F_C(r) = 1 - \int_r^\infty p_C(z) dz$ results in the following approximation

$$F_C(r) = 1 - \frac{0.5 \ln(2) \gamma_s^{-\left(\frac{\alpha_L + 1}{2}\right)}}{\beta_L^{(\alpha_L + 1)} \Gamma(\alpha_L + 1)} \int_r^\infty 2^z (2^z - 1)^{\left(\frac{\alpha_L - 1}{2}\right)} e^{-\frac{\sqrt{(2^z - 1)/\gamma_s}}{\beta_L}} dz, \quad r \geq 0. \quad (16)$$

The LCR $N_C(r)$ of $C(t)$ describes the average number of times the channel capacity $C(t)$ crosses a certain threshold level r from up to down (or from down to up) per second. Mathematically, the LCR $N_C(r)$ of $C(t)$ can be expressed as [25]

$$N_C(r) = \int_0^{\infty} \dot{z} p_{C\dot{C}}(r, \dot{z}) d\dot{z}, \quad r \geq 0 \quad (17)$$

where $p_{C\dot{C}}(r, \dot{z})$ is the joint PDF of the stochastic process $C(t)$ and its corresponding time derivative $\dot{C}(t)$ at the same time t . Here, we first need to find the joint PDF $p_{\gamma_{\text{EGC}}\dot{\gamma}_{\text{EGC}}}(z, \dot{z})$ of $\gamma_{\text{EGC}}(t)$ and $\dot{\gamma}_{\text{EGC}}(t)$ at the same time t . The joint PDF $p_{\gamma_{\text{EGC}}\dot{\gamma}_{\text{EGC}}}(z, \dot{z})$ can be found using the relation $p_{\gamma_{\text{EGC}}\dot{\gamma}_{\text{EGC}}}(z, \dot{z}) = (1/\gamma_s)^2 p_{\Xi^2\dot{\Xi}^2}(z/\gamma_s, \dot{z}/\gamma_s)$ along with (13). Thus, given the joint PDF $p_{\gamma_{\text{EGC}}\dot{\gamma}_{\text{EGC}}}(z, \dot{z})$ and using the concept of transformation of random variables [17, p. 244], the joint PDF $p_{C\dot{C}}(r, \dot{z})$ can be expressed as

$$\begin{aligned} p_{C\dot{C}}(z, \dot{z}) &= (2^z \ln(2))^2 p_{\gamma_{\text{EGC}}\dot{\gamma}_{\text{EGC}}}(2^z - 1, 2^z \dot{z} \ln(2)) \\ &\approx \frac{(2^z \ln(2))^2}{8\sqrt{6\pi\beta}\gamma_s^{\left(\frac{2\alpha_L+3}{4}\right)}} \frac{(2^z - 1)^{\left(\frac{2\alpha_L-5}{4}\right)}}{\beta_L^{(\alpha_L+1)}\Gamma(\alpha_L+1)} e^{-\frac{\sqrt{(2^z-1)/\gamma_s}}{\beta_L} - \frac{(2^z \dot{z} \ln(2))^2/\sqrt{\gamma_s}}{32\beta(2^z-1)^{3/2}}} \end{aligned} \quad (18)$$

for $z \geq 0$, $|\dot{z}| < \infty$.

Finally, substituting (18) in (17) and solving the integral over \dot{z} using [8, Eq. (3.326-2)] leads to a closed-form approximation for the LCR $N_C(r)$ of $C(t)$ in the form

$$N_C(r) \approx \sqrt{\frac{2}{3\pi}} \beta \frac{(2^r - 1)^{\left(\frac{2\alpha_L+1}{4}\right)} e^{-\frac{\sqrt{(2^r-1)/\gamma_s}}{\beta_L}}}{\gamma_s^{\left(\frac{2\alpha_L+1}{4}\right)} \beta_L^{(\alpha_L+1)} \Gamma(\alpha_L+1)}, \quad r \geq 0. \quad (19)$$

The ADF $T_C(r)$ of the channel capacity $C(t)$ is the expected value of the time intervals over which $C(t)$ remains below a certain threshold level r . The ADF $T_C(r)$ of $C(t)$ can be computed by evaluating the ratio of the CDF $F_C(r)$ and the LCR $N_C(r)$ of $C(t)$ [11], i.e.,

$$T_C(r) = \frac{F_C(r)}{N_C(r)}. \quad (20)$$

Thus, the substitution of (16) and (19) in (20) results in an approximation for the ADF $T_C(r)$ of $C(t)$.

V. NUMERICAL RESULTS

This section illustrates the important theoretical results by evaluating the expressions in (10), (15), (16), (19), and (20). The correctness of the approximations is then validated by simulations. Here, the simulation results are considered as the true results. A sum-of-sinusoids (SOS) channel simulator [18] has been employed to obtain the simulation results. Meaning thereby, the SOS concept has been exploited to simulate the uncorrelated Gaussian noise processes making up the received signal envelope at the output of the EG combiner. The model parameters of the channel simulator are computed by utilizing the generalized method of exact Doppler spread (GMEDS₁) [21]. Each Gaussian process $\mu^{(i)}(t)$ was simulated using $N_l^{(i)} = 14$ for $i = 1, 2, \dots, 2K$ and $l = 1, 2$, where $N_l^{(i)}$ is the number of sinusoids required to simulate the inphase ($l = 1$) and quadrature components ($l = 2$) of $\mu^{(i)}(t)$. It is required that the simulated distribution of $|\hat{\mu}^{(i)}(t)|^2$ closely approximates the Rayleigh distribution for all $i = 1, 2, \dots, 2K$. Furthermore, it has been shown in [18] that any value of $N_l^{(i)} \geq 7$ ($l = 1, 2$) serves this purpose. Thus, our selection of $N_l^{(i)} = 14$ for $i = 1, 2, \dots, 2K$ and $l = 1, 2$ provides us with the waveforms having the desired distribution. The maximum Doppler frequencies caused by the motion of the source mobile station and the destination mobile station, denoted by $f_{s\max}$ and $f_{d\max}$, respectively, were selected as 154 Hz and 273 Hz. The variances $\sigma_{\mu^{(i)}}^2$ were set to unity $\forall i = 1, 2, \dots, 2K$ unless stated otherwise. In addition, the analysis of the statistical properties of the channel capacity $C(t)$ is carried out for an SNR γ_s of 15 dB.

The results presented in Figs. J.1-J.5 show a good fitting of the approximated analytical and the exact simulation results considered as the true results. Figure J.1 illustrates the theoretical results of the PDF $p_{\Xi}(x)$ of $\Xi(t)$ described by the approximation in (10) as well as the simulation results obtained by evaluating the statistics of the waveforms generated by using the SOS-based channel simulator. This figure shows the influence of the number of diversity branches K on the behavior of the PDF $p_{\Xi}(x)$. It can be observed that as the number of diversity branches K increases, the mean value and the variance of the stochastic process $\Xi(t)$ increases. Furthermore, for $K = 1$, the PDF $p_{\Xi}(x)$ of $\Xi(t)$ reduces to the double Rayleigh distribution. This result confirms the validity of the approximation in (10).

The closed-form approximate expression of the PDF $p_C(r)$ of the channel capacity $C(t)$ given in (15) is presented in Fig. J.2 along with the simulation results. A close agreement can be seen between the approximate solution and the exact (simulation) results. Figure J.2 also compares the PDF $p_C(r)$ of $C(t)$ for a different number of diversity branches K . It is obvious that increasing K , increases the mean

²The process $\hat{\mu}^{(i)}(t)$ denotes a simulated Gaussian process.

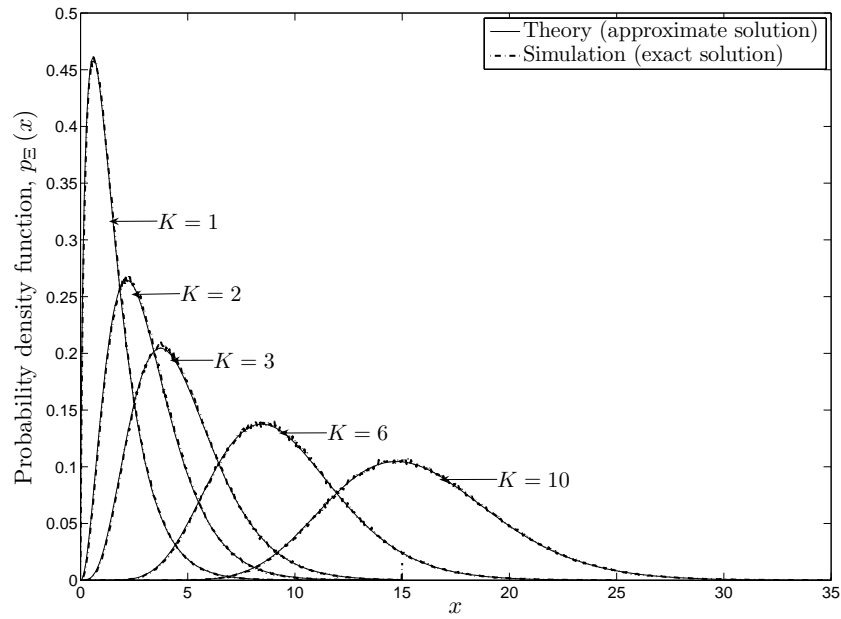


Figure J.1: The PDF $p_{\Xi}(x)$ of the received signal envelope at the output of the EG combiner $\Xi(t)$ for a different number K of diversity branches.

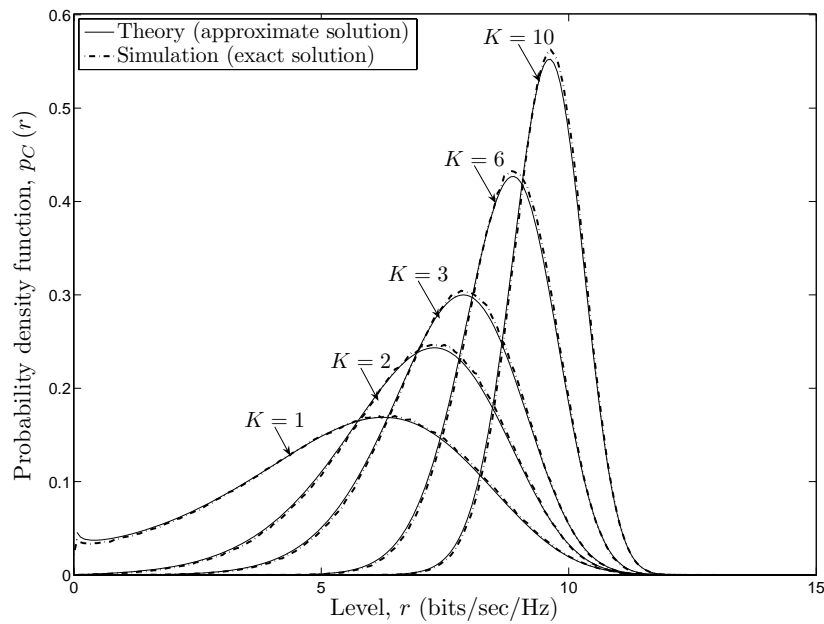


Figure J.2: The PDF $p_C(r)$ of the channel capacity $C(t)$ of the double Rayleigh fading channels with EGC for a different number K of diversity branches.

channel capacity, whereas the variance of $C(t)$ decreases. Similarly, in Fig. J.3, the theoretical results of the CDF $F_C(r)$ of $C(t)$ described by the approximation in (16) are illustrated.

The LCR $N_C(r)$ of the channel capacity $C(t)$ described by the closed-form ap-

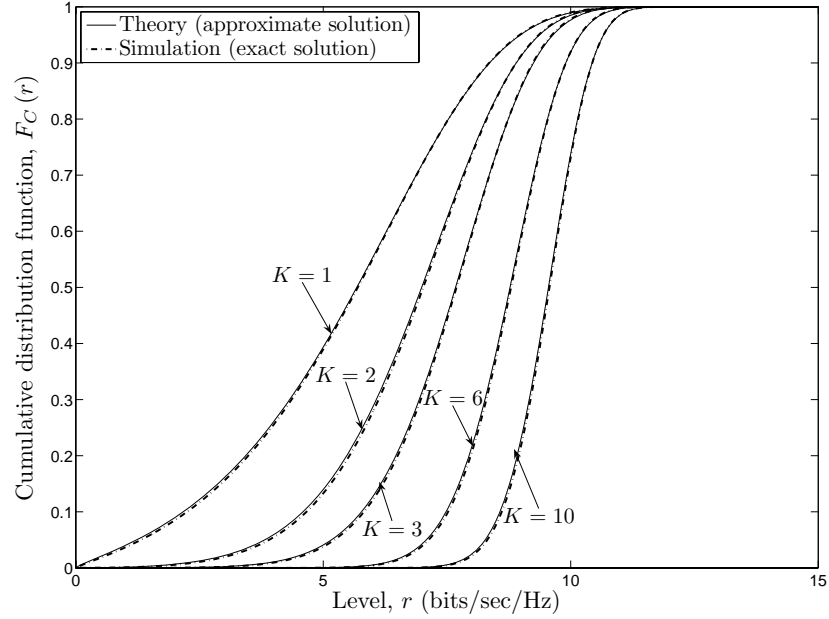


Figure J.3: The CDF $F_C(r)$ of the channel capacity $C(t)$ of the double Rayleigh fading channels with EGC for a different number K of diversity branches.

proximate expression in (19) is evaluated together with the exact (simulation) results in Fig. J.4. This figure depicts the LCR $N_C(r)$ of $C(t)$ for a different number of diversity branches K . Studying the graphs shows that increasing the value of K results in a drastic decrease in the LCR $N_C(r)$ at low signal levels r . The LCR $N_C(r)$ at higher signal levels r is however the same for all values of K . Furthermore, a very good fitting of the approximate solution and the exact simulation results can be witnessed for any number of diversity branches $K > 1$.

Figure J.5 displays the ADF $T_C(r)$ of the channel capacity $C(t)$ given in (20) for a different number of diversity branches K . For the purpose of validation of the obtained approximate solution, the exact (simulation) results are also plotted in Fig. J.5. The presented results reveal the fact that the ADF $T_C(r)$ of $C(t)$ decreases with the increase in the number of diversity branches K .

VI. CONCLUSION

In this article, we present a thorough analysis of the statistical properties of the channel capacity of double Rayleigh fading channels with EGC. A V2V communication system is considered here, where the destination mobile station is equipped with K receive antennas. The signal reaching the destination mobile station through K diversity branches is then combined using EGC. Simple and close-form analytical approximations for the PDF, the CDF, the LCR, and the ADF of the channel

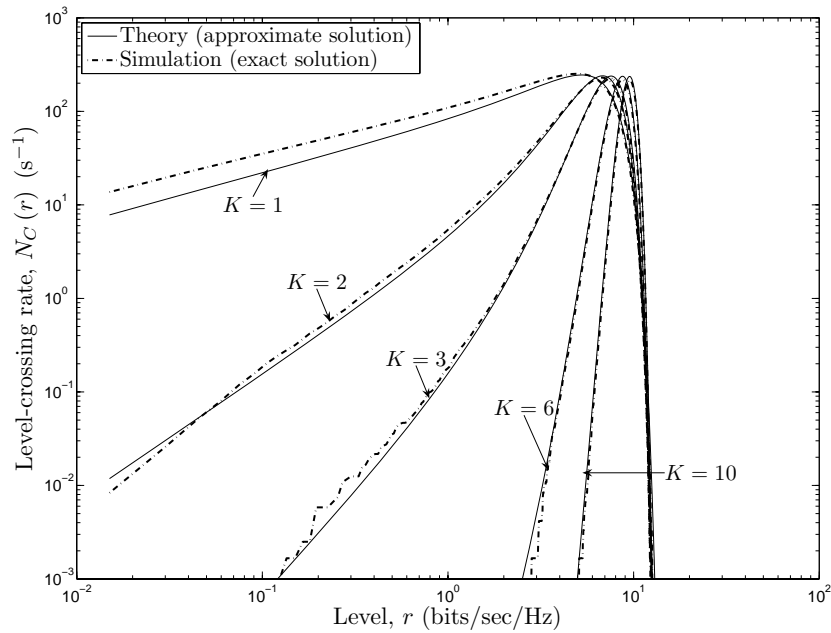


Figure J.4: The LCR $N_C(r)$ of the channel capacity $C(t)$ of the double Rayleigh fading channels with EGC for a different number K of diversity branches.

capacity of double Rayleigh fading channels with EGC have been derived. We have modeled the received signal envelope at the output of the EG combiner as a sum of K independent but not necessarily identical double Rayleigh processes. With the

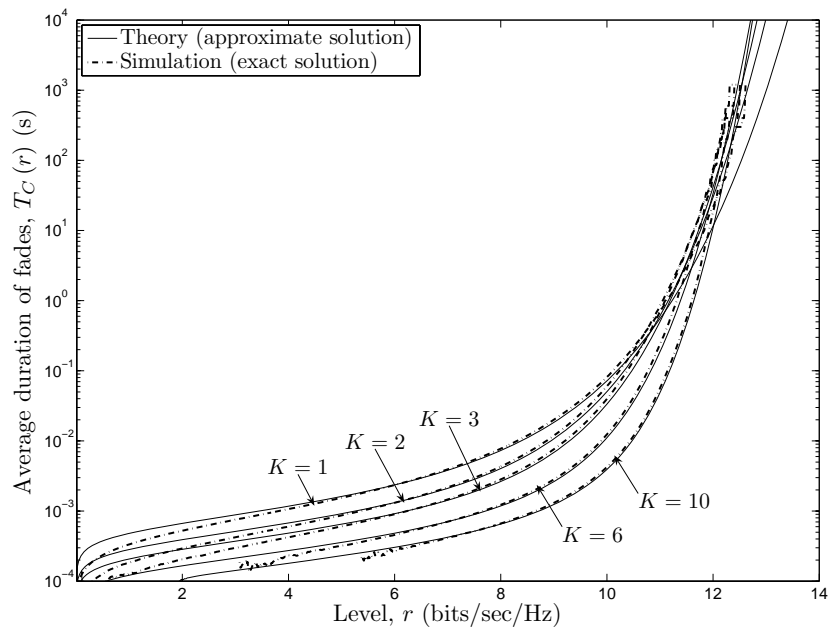


Figure J.5: The ADF $T_C(r)$ of the channel capacity $C(t)$ of the double Rayleigh fading channels with EGC for a different number K of diversity branches.

help of the Laguerre series expansion, the PDF of this sum process can be approximated by the gamma distribution. Furthermore, making use of the properties of the gamma distribution, other statistical properties of the sum process can also be evaluated. Once the analytical expressions for the statistical properties of the received signal envelope at the output of the EG combiner are obtained, the computation of the theoretical results associated with the statistics of the channel capacity can be performed using the concept of transformation of random variables. The correctness of the approximate theoretical results are then validated by simulations. We have presented the results demonstrating the influence of the number of diversity branches K on the PDF, the CDF, the LCR, and the ADF of the channel capacity of double Rayleigh fading channels with EGC. It has been shown that the mean channel capacity increases and the capacity variance decreases with an increase in the number of diversity branches K . In addition, at low signal levels r , the LCR of the channel capacity decreases as the value of K increases. The LCR however remains the same at high signal levels r for all values of K . A decrease in the ADF of the channel capacity can be observed if the number of diversity branches K increases. The results presented in this article can be utilized to optimize the spatial diversity receivers employed in the future V2V MIMO communication systems.

REFERENCES

- [1] A. S. Akki. Statistical properties of mobile-to-mobile land communication channels. *IEEE Trans. Veh. Technol.*, 43(4):826–831, November 1994.
- [2] A. S. Akki and F. Haber. A statistical model of mobile-to-mobile land communication channel. *IEEE Trans. Veh. Technol.*, 35(1):2–7, February 1986.
- [3] M. S. Alouini and A. J. Goldsmith. Capacity of Rayleigh fading channels under different adaptive transmission and diversity-combining techniques. *IEEE Trans. Veh. Technol.*, 48(4):1165–1181, July 1999.
- [4] N. C. Beaulieu and X. Dong. Level crossing rate and average fade duration of MRC and EGC diversity in Ricean fading. *IEEE Trans. Commun.*, 51(5):722–726, May 2003.
- [5] S. Chitroub, A. Houacine, and B. Sansal. Statistical characterisation and modelling of SAR images. *Elsevier, Signal Processing*, 82(1):69–92, January 2002. DOI [http://dx.doi.org/10.1016/S0165-1684\(01\)00158-X](http://dx.doi.org/10.1016/S0165-1684(01)00158-X).

- [6] A. Giorgetti, P. J. Smith, M. Shafi, and M. Chiani. MIMO capacity, level crossing rates and fades: The impact of spatial/temporal channel correlation. *J. Commun. Net.*, 5(2):104–115, June 2003.
- [7] V. Gradinescu et al. Adaptive traffic lights using car-to-car communication. In *Proc. IEEE 65th Veh. Technol. Conf., VTC'07-Spring*, pages 21–25. Dublin, Ireland, April 2007. DOI 10.1109/VETECS.2007.17.
- [8] I. S. Gradshteyn and I. M. Ryzhik. *Table of Integrals, Series, and Products*. New York: Academic Press, 6th edition, 2000.
- [9] K. A. Hamdi. Capacity of MRC on correlated Rician fading channels. *IEEE Trans. Commun.*, 56(5):708–711, May 2008.
- [10] P. Ivanis, D. Drajić, and B. Vucetic. The second order statistics of maximal ratio combining with unbalanced branches. *IEEE Communications Letters*, 12(7):508–510, July 2008.
- [11] W. C. Jakes, editor. *Microwave Mobile Communications*. Piscataway, NJ: IEEE Press, 1994.
- [12] G. K. Karagiannidis, N. C. Sagias, and P. T. Mathiopoulos. N*Nakagami: A novel stochastic model for cascaded fading channels. *IEEE Trans. Commun.*, 55(8):1453–1458, August 2007.
- [13] S. Khatalin and J. P. Fonseka. On the channel capacity in Rician and Hoyt fading environments with MRC diversity. *IEEE Trans. Veh. Technol.*, 55(1):137–141, January 2006.
- [14] I. Z. Kovacs, P. C. F. Eggers, K. Olesen, and L. G. Petersen. Investigations of outdoor-to-indoor mobile-to-mobile radio communication channels. In *Proc. IEEE 56th Veh. Technol. Conf., VTC'02-Fall*, volume 1, pages 430–434. Vancouver BC, Canada, September 2002.
- [15] H. W. Nylund. Characteristics of small-area signal fading on mobile circuits in the 150 MHz band. *IEEE Trans. Veh. Technol.*, 17:24–30, October 1968.
- [16] Y. Okumura, E. Ohmori, T. Kawano, and K. Fukuda. Field strength and its variability in VHF and UHF land mobile radio services. *Rev. Elec. Commun. Lab.*, 16:825–873, September/October 1968.
- [17] A. Papoulis and S. U. Pillai. *Probability, Random Variables and Stochastic Processes*. New York: McGraw-Hill, 4th edition, 2002.

- [18] M. Pätzold. *Mobile Fading Channels*. Chichester: John Wiley & Sons, 2002.
- [19] M. Pätzold, B. O. Hogstad, and N. Youssef. Modeling, analysis, and simulation of MIMO mobile-to-mobile fading channels. *IEEE Trans. Wireless Commun.*, 7(2):510–520, February 2008.
- [20] M. Pätzold, U. Killat, and F. Laue. An extended Suzuki model for land mobile satellite channels and its statistical properties. *IEEE Trans. Veh. Technol.*, 47(2):617–630, May 1998.
- [21] M. Pätzold, C. X. Wang, and B. O. Hogstad. Two new sum-of-sinusoids-based methods for the efficient generation of multiple uncorrelated Rayleigh fading waveforms. *IEEE Trans. Wireless Commun.*, 8(6):3122–3131, June 2009.
- [22] S. Primak, V. Kontorovich, and V. Lyandres, editors. *Stochastic Methods and their Applications to Communications: Stochastic Differential Equations Approach*. Chichester: John Wiley & Sons, 2004.
- [23] G. Rafiq and M. Pätzold. Statistical properties of the capacity of Rice channels with MRC and EGC. In *IEEE Int. Conf. on Wireless Communications & Signal Processing, WCSP 2009*. Nanjing, China, November 2009. DOI 10.1109/WCSP.2009.5371578.
- [24] T. S. Rappaport. *Wireless Communications: Principles and Practice*. Upper Saddle River, New Jersey: Prentice-Hall, 2nd edition, 1996.
- [25] S. O. Rice. Mathematical analysis of random noise. *Bell Syst. Tech. J.*, 24:46–156, January 1945.
- [26] H. Samimi and P. Azmi. An approximate analytical framework for performance analysis of equal gain combining technique over independent Nakagami, Rician and Weibull fading channels. *Wireless Personal Communications (WPC)*, 43(4):1399–1408, dec 2007. DOI 10.1007/s11277-007-9314-z.
- [27] M. Schwartz, W. R. Bennett, and S. Stein. *Communication Systems and Techniques*, volume 4. New York: McGraw Hill, 1966.
- [28] P. M. Shankar. Error rates in generalized shadowed fading channels. *Wireless Personal Communications (WPC)*, 28(3):233–238, February 2004. DOI <http://dx.doi.org/10.1023/B:wire.0000032253.68423.86>.

- [29] M. K. Simon. *Probability Distributions Involving Gaussian Random Variables: A Handbook for Engineers and Scientists*. Dordrecht: Kluwer Academic Publishers, 2002.
- [30] M. K. Simon and M. S. Alouini. *Digital Communications over Fading Channels*. New Jersey: John Wiley & Sons, 2nd edition, 2005.
- [31] H. Suzuki. A statistical model for urban radio propagation. *IEEE Trans. Commun.*, 25(7):673–680, July 1977.
- [32] W. Wongtrairat and P. Supnithi. Performance of digital modulation in double Nakagami- m fading channels with MRC diversity. *IEICE Trans. Commun.*, E92-B(2):559–566, February 2009.
- [33] M. D. Yacoub, C. R. C. Monterio da Silva, and J. E. V. Bautista. Second-order statistics for diversity-combining techniques in Nakagami fading channels. *IEEE Trans. Veh. Technol.*, 50(6):1464–1470, November 2001.
- [34] W. R. Young. Comparison of mobile radio transmission at 150, 450, 900, and 3700 MHz. 31:1068–1085, November 1952.
- [35] Q. T. Zhang. Probability of error for equal-gain combiners over Rayleigh channels: some closed-form solutions. *IEEE Trans. Commun.*, 45(3):270–273, March 1997.
- [36] J. Zhu and S. Roy. MAC for dedicated short range communications in intelligent transport system. *IEEE Communications Magazine*, 41(12):60–67, December 2003.
- [37] D. A. Zogas, G. K. Karagiannidis, and S. A. Kotsopoulos. Equal gain combining over Nakagami- n (Rice) and Nakagami- q (Hoyt) generalized fading channels. *IEEE Trans. Wireless Commun.*, 4(2):374–379, March 2005.

Appendix K

Paper X

Title: Performance Analysis of M -Ary PSK Modulation Schemes over Multiple Double Rayleigh Fading Channels with EGC in Cooperative Networks

Authors: **Batool Talha**¹, Matthias Pätzold¹, and S. Primak²

Affiliations: ¹University of Agder, Faculty of Engineering and Science, P. O. Box 509, NO-4898 Grimstad, Norway

²University of Western Ontario, Department of ECE, London, ON, N6A 5B9, Canada

Conference: *IEEE ICC 2010 Workshop on Vehicular Connectivity, Veh-Con 2010*, Cape Town, South Africa, May 2010. DOI 10.1109/ICCW.2010.5503940.

Performance Analysis of M -Ary PSK Modulation Schemes over Multiple Double Rayleigh Fading Channels with EGC in Cooperative Networks

Batool Talha¹, Matthias Pätzold¹, and Serguei Primak²

¹Department of Information and Communication Technology
Faculty of Engineering and Science, Agder University College
Servicebox 509, NO-4876 Grimstad, Norway

E-mails: {batool.talha, matthias.paetzold}@uia.no

²Department of ECE, University of Western Ontario,
London, ON, N6A 5B9, Canada
Email: primak@engga.uwo.ca

Abstract — This article studies the performance of M -ary phase shift keying (PSK) modulation schemes over mobile-to-mobile (M2M) fading channels with equal gain combining (EGC) in cooperative networks. The frequency-nonselctive M2M fading channels are modeled assuming non-line-of-sight (NLOS) propagation conditions. Furthermore, a dual-hop amplify-and-forward relay type cooperative network is taken into consideration here. It is assumed that K diversity branches are present between the source mobile station and the destination mobile station via K mobile relays. The performance of M -ary PSK modulation schemes is analyzed by evaluating the average bit error probability (BEP). We have derived a simple analytical approximation for the average BEP of M -ary PSK modulation schemes over relay-based M2M fading channels with EGC. The validity and accuracy of the analytical approximation is confirmed by simulations. The presented results show that in a dual-hop relay system with EGC, there is a remarkable improvement in the diversity gain as the number of diversity branches K increases.

I. INTRODUCTION

Recently, cooperative relaying has emerged as an attractive technology in the field of wireless communications. Since it is capable of fulfilling the ever-increasing demand of high data-rates with improved coverage that is imposed by the consumers [14, 5]. Such relaying makes it possible to achieve a spatial diversity gain by exploiting the existing resources (i.e., the mobile stations) of the network. So far several cooperative diversity schemes have been proposed [12, 22, 23]. However, in all these schemes, the network resources assist the source mobile station by relaying

its information signal to the destination mobile station.

In this article, a dual-hop amplify-and-forward relay type cooperative network has been considered. It is assumed that K mobile relays are connected in parallel between the source mobile station and the destination mobile. Consequently, this kind of configuration gives rise to K diversity branches. The signals received from these K diversity branches can then be combined with each other at the destination mobile station, thus providing the desirable spatial diversity gain. Selection combining (SC) [11], EGC [11], and maximal ratio combining (MRC) [11] are those diversity combining techniques that have been studied since decades. Studies pertaining to the statistical and the performance analysis of EGC along with MRC in non-cooperative networks over Rayleigh, Rice as well as Nakagami fading channels are reported in [28, 4, 10] and [29, 30, 20], respectively. In addition, the authors of [2, 8, 9] have analyzed the performance of cooperative diversity using EGC and MRC over Rayleigh and Nakagami- m fading channels.

Like cooperative relaying, M2M communications is also an emerging technology that has demonstrated its potential application in cooperative networks, ad hoc networks, and vehicle-to-vehicle (V2V) communications. It is widely acknowledged now that M2M fading channels [1] are statistically quite different from conventional cellular and land mobile terrestrial channels like, e.g., Rayleigh, Rice, and Suzuki channels. Under NLOS propagation conditions, M2M fading channels in relay-based cooperative networks can effectively be modeled as double Rayleigh stochastic processes [15]. A straightforward extension of the double Rayleigh channel model to the double Rice channel model for relay-based M2M fading channels under line-of-sight (LOS) propagation conditions is presented in [26]. A study on the performance of digital modulation schemes over double Nakagami- m fading channels with MRC diversity is available in [27]. However, there is a lack of information in the literature regarding the performance of digital modulation schemes over double Rayleigh and/or double Nakagami- m fading channels with EGC. Thus, we aim to fill in this gap by studying the performance of M -ary PSK modulation schemes over double Rayleigh fading channels with EGC assuming K diversity branches (mobile relays).

Here, the performance of M -ary PSK modulation schemes is analyzed by evaluating the average BEP. We have derived a simple analytical approximation for the average BEP of M -ary PSK modulation schemes over M2M fading channels with EGC. The derivation of the approximation requires the knowledge of the probability density function (PDF) of the received signal envelope at the output of the equal gain (EG) combiner. The output of the EG combiner is modeled as a sum of K

statistically independent but not necessarily identical double Rayleigh fading channels. Furthermore, we approximate the PDF of this sum process with the help of an orthogonal series expansion. Depending upon the purpose of use of the approximated PDF and the amount of accuracy required, there are various orthogonal series to choose from. The Edgeworth series, the Gram-Charlier series, and the Laguerre series expansion [18] are just to name a few. To obtain a simple and closed-form approximate expression for the PDF of the sum process, we have employed the Laguerre series expansion. It turns out that the first term in the Laguerre series equals the gamma distribution, which provides a simple approximation of high accuracy. The average BEP computed by making use of the approximate PDF of the sum process is validated by simulations. A good fitting of the approximate theoretical results with those of the exact results obtained by simulations confirms the correctness of our approach. The presented results illustrate that in a dual-hop relay system with EGC, there is a significant improvement in the diversity gain as the number of diversity branches K increases.

The remaining part of the paper is organized as follows. Section II describes the system model for EGC over M2M fading channels in amplify-and-forward relay networks. The PDF of the received signal envelope at the output of the EG combiner is derived in Section III. Section IV deals with the derivation of the average BEP of M -ary PSK modulation schemes over relay-based M2M fading channels with EGC. Verification of the analytical expressions by simulations and a detailed discussion on the presented results are included in Section V. Finally, the article is concluded in Section VI.

II. EGC OVER M2M FADING CHANNELS

In this section, we describe the system model for EGC over M2M fading channels in a K -parallel dual-hop cooperative network. Here, the K mobile relays in the network are connected in parallel between the source mobile station and the destination mobile station, as illustrated in Fig. K.1. We target to study frequency-nonselective M2M fading channels under NLOS propagation conditions. Furthermore, the system model has been developed assuming isotropic scattering conditions. The mode of operation of all the mobile stations in the network, i.e., the source mobile station, the destination mobile station, and the K mobile relays is considered to be half-duplex. This means that the mobile stations do not transmit and receive a signal at the same time in the same frequency band.

The time-division multiple-access (TDMA) based amplify-and-forward relay protocols proposed in [13, 3] are taken into account here. Thus, the signals from

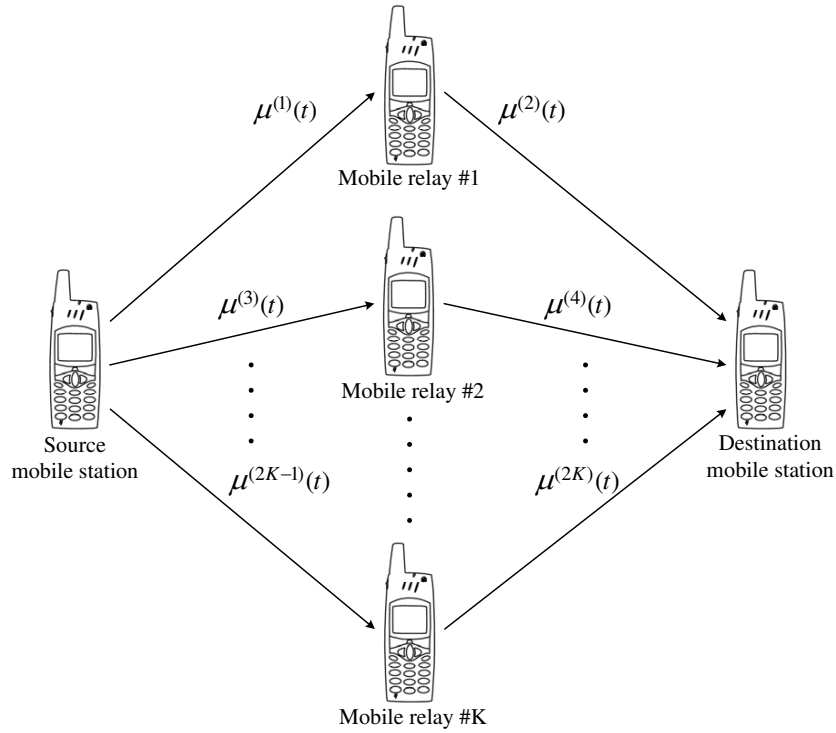


Figure K.1: The propagation scenario describing K -parallel dual-hop relay M2M fading channels.

the K diversity branches in different time slots can be combined at the destination mobile station using EGC. Let $s(t)$ denote the signal transmitted by the source mobile station. Then, the signal $r^{(k)}(t)$ received from the k th diversity branch at the destination mobile station can be expressed as

$$r^{(k)}(t) = \zeta^{(k)}(t) s(t) + n^{(k)}(t) \quad (1)$$

where $\zeta^{(k)}(t)$ and $n^{(k)}(t)$ ($k = 1, 2, \dots, K$) describe the fading process from the source mobile station to the destination mobile station via the k th mobile relay and the additive white Gaussian noise (AWGN) in the k th subchannel, respectively. The AWGN is a zero-mean stochastic process having variance $N_0/2$, where N_0 is the noise power spectral density.

In (1), we model the fading process $\zeta^{(k)}(t)$ as a weighted zero-mean complex double Gaussian process, i.e.,

$$\zeta^{(k)}(t) = \zeta_1^{(k)}(t) + j\zeta_2^{(k)}(t) = A_{r^{(k)}} \mu^{(2k-1)}(t) \mu^{(2k)}(t) \quad (2)$$

for $k = 1, 2, \dots, K$. In (2), $\mu^{(i)}(t)$ ($i = 1, 2, \dots, 2K$) represents a zero-mean complex circular Gaussian process having variance $2\sigma_{\mu^{(i)}}^2$. These Gaussian processes $\mu^{(i)}(t)$

are mutually independent, where each one is characterized by the classical Jakes Doppler power spectral density. The Gaussian process $\mu^{(i)}(t)$ for $i = 2k - 1 = 1, 3, \dots, (2K - 1)$ corresponds to the scattered component of the subchannel between the source mobile station and the k th mobile relay. Likewise, the Gaussian process $\mu^{(i)}(t)$ for $i = 2k = 2, 4, \dots, 2K$ describes the scattered component of the subchannel between the k th mobile relay and the destination mobile station. In (2), $A_{R^{(k)}}$ is the relay gain of the k th relay. It is noteworthy that the relay gain $A_{R^{(k)}}$ is only a scaling factor for the variance of the complex Gaussian process $\mu^{(i)}(t)$, i.e., $\text{Var} \left\{ A_{R^{(k)}} \mu^{(i)}(t) \right\} = 2(A_{R^{(k)}} \sigma_{\mu^{(i)}})^2$, where $i = 2, 4, \dots, 2K$.

It is imperative to stress that in a real amplify-and-forward relay system, the total noise $n_T^{(k)}(t)$ in the k th relay link is in fact given as follows

$$n_T^{(k)}(t) = A_{R^{(k)}} \mu^{(2k)}(t) n^{(2k-1)}(t) + n^{(2k)}(t) \tag{3}$$

for all $k = 1, 2, \dots, K$. However, for reasons of simplicity, we have considered the total noise $n_T^{(k)}(t)$ in the link from the source mobile station to the destination mobile station via the k th mobile relay to be AWGN, i.e., $n^{(k)}(t)$.

Finally, the total signal $r(t)$ at the destination mobile station, after combining the signals $r^{(k)}(t)$ received from the k th diversity branch can be given as

$$r(t) = \sum_{k=1}^K r^{(k)}(t) = \Xi(t) s(t) + N(t) \tag{4}$$

under the assumption of perfect channel state information (CSI) at the destination mobile station. In (4), $\Xi(t)$ represents the fading envelope at the output of the EG combiner, which can be written as [11]

$$\Xi(t) = \sum_{k=1}^K \chi^{(k)}(t) \tag{5}$$

where $\chi^{(k)}(t)$ is the absolute value of $\zeta^{(k)}(t)$. Thus, each $\chi^{(k)}(t)$ is a double Rayleigh process. In (4), $N(t)$ is the total received noise, i.e., $N(t) = \sum_{k=1}^K n^{(k)}(t)$.

III. PDF OF A SUM OF DOUBLE RAYLEIGH PROCESSES

In this section, we approximate the PDF $p_{\Xi}(x)$ of a sum of double Rayleigh processes $\Xi(t)$ by making use of an orthogonal series expansion. Depending upon the purpose of use of the approximated PDF and the amount of accuracy required, one can choose from various options of such series, like, e.g., the Edgeworth series, the Gram-Charlier series, and the Laguerre series expansion [18]. In our study, we em-

ploy the Laguerre series since it provides a good enough statistical accuracy even when only the first term of this series is used [18].

The PDF $p_{\Xi}(x)$ of $\Xi(t)$ can be expressed using the Laguerre series expansion as [18]

$$p_{\Xi}(x) = \sum_{n=0}^{\infty} b_n e^{-x} x^{\alpha_L} L_n^{(\alpha_L)}(x) \quad (6)$$

where

$$L_n^{(\alpha_L)}(x) = e^x \frac{x^{(-\alpha_L)} d^n}{x! dx^n} \left[e^{(-x)} x^{n+\alpha_L} \right], \quad \alpha_L > -1 \quad (7)$$

denote the Laguerre polynomials. The coefficients b_n can be given as

$$b_n = \frac{n!}{\Gamma(n + \alpha_L + 1)} \int_0^{\infty} L_n^{(\alpha_L)}(x) p_{\Xi}(x) dx \quad (8)$$

where $x = y/\beta_L$ and $\Gamma(\cdot)$ is the gamma function [7].

The parameters α_L and β_L can be computed by solving the system of equations in [18, p. 21] for $b_1 = 0$ and $b_2 = 0$, which yields

$$\alpha_L = \frac{(\kappa_1^{\Xi})^2}{\kappa_2^{\Xi}} - 1, \quad \beta_L = \frac{\kappa_2^{\Xi}}{\kappa_1^{\Xi}} \quad (9a,b)$$

where κ_1^{Ξ} is the first and κ_2^{Ξ} is the second cumulant of the stochastic process $\Xi(t)$. It is important to understand here that the first and second cumulant of $\Xi(t)$ are merely the mean value and the variance, respectively. Mathematically, κ_1^{Ξ} and κ_2^{Ξ} can be expressed as

$$\kappa_1^{\Xi} = \sum_{k=1}^K \kappa_1^{\chi^{(k)}}, \quad \kappa_2^{\Xi} = \sum_{k=1}^K \kappa_2^{\chi^{(k)}} \quad (10a,b)$$

where $\kappa_n^{\chi^{(k)}} (n = 1, 2)$ denotes the cumulants associated with the double Rayleigh process $\chi^{(k)}(t)$. The first two cumulants of $\chi^{(k)}(t)$ are [24]

$$\kappa_1^{\chi^{(k)}} = \frac{A_{R^{(k)}} \sigma_{\mu^{(2k-1)}} \sigma_{\mu^{(2k)}} \pi}{2}, \quad (11a)$$

$$\kappa_2^{\chi^{(k)}} = \frac{1}{4} A_{R^{(k)}}^2 \sigma_{\mu^{(2k-1)}}^2 \sigma_{\mu^{(2k)}}^2 (16 - \pi^2). \quad (11b)$$

Given $\kappa_n^{\chi^{(k)}} (n = 1, 2)$ for all $\chi^{(k)}(t)$, leads to a straightforward evaluation of κ_n^{Ξ} using (10a,b). This in turn allows an easy computation of α_L and β_L in (9a,b). Substituting the obtained quantities α_L and β_L in the Laguerre series expansion provides an exact solution for the PDF $p_{\Xi}(x)$. The first term of the series can be

identified as the gamma distribution, i.e.,

$$p_{\Gamma}(x) = \frac{x^{\alpha_L}}{\beta_L^{(\alpha_L+1)}\Gamma(\alpha_L + 1)} e^{-\frac{x}{\beta_L}}. \quad (12)$$

The PDF $p_{\Xi}(x)$ of $\Xi(t)$ can thus be approximated as

$$p_{\Xi}(x) \approx p_{\Gamma}(x) = \frac{x^{\alpha_L}}{\beta_L^{(\alpha_L+1)}\Gamma(\alpha_L + 1)} e^{-\frac{x}{\beta_L}}. \quad (13)$$

The approximation in (13) will be used in the following section for deriving the average BEP of M -ary PSK modulation schemes over double Rayleigh processes with EGC.

IV. PERFORMANCE ANALYSIS OF M -ARY PSK MODULATION SCHEMES OVER DOUBLE RAYLEIGH FADING CHANNELS WITH EGC

In Section II, we derived the total received signal envelope at the output of the EG combiner, $\Xi(t)$, and the total received noise, $N(t)$. This makes it possible to define the instantaneous signal-to-noise ratio per bit $\gamma_{\text{EGC}}(t)$ at the output of the EG combiner as [25, 21]

$$\gamma_{\text{EGC}}(t) = \frac{\Xi^2(t)}{E\{N^2(t)\}} E_b = \frac{\Xi^2(t)}{K N_0} E_b \quad (14)$$

where E_b is the energy (in joules) per bit and $E\{\cdot\}$ is the expectation operator.

The average BEP P_b over the fading channel statistics at the output of the EG combiner can be given as [25]

$$P_b = \int_0^{\infty} p_{\Xi}(x) P_{b|\Xi}(x) dx \quad (15)$$

where $P_{b|\Xi}(x)$ is the BEP of M -ary PSK modulation schemes conditioned on the fading amplitudes $\{x_k\}_{k=1}^K$, and $x = \sum_{k=1}^K x_k$. It is important to keep in mind that the fading amplitudes $\{x_k\}_{k=1}^K$ follow the double Rayleigh distribution.

The conditional BEP $P_{b|\Xi}(x)$ of M -ary PSK modulation schemes is known to be equal to [6]

$$\begin{aligned} P_{b|\Xi}(x) &\approx \frac{a}{\log_2 M} Q\left(\sqrt{2g \log_2 M \gamma_{\text{EGC}}(x)}\right) \\ &\approx \frac{a}{\log_2 M} Q\left(\sqrt{\frac{2g \log_2 M E_b}{K N_0} x^2}\right) \end{aligned} \quad (16)$$

where $M = 2^b$ with b as the number of bits per symbol and $Q(\cdot)$ is the error function [19]. The parameter a equals 1 or 2 for M -ary PSK modulation schemes when $M = 2$ or $M > 2$, respectively, whereas for all M -ary PSK modulation schemes $g = \sin^2(\pi/M)$ [27].

Substituting (13) and (16) in (15) allows us to approximate the required average BEP P_b as

$$P_b \approx \frac{a}{\log_2 M} \frac{1}{\beta_L^{(\alpha_L+1)} \Gamma(\alpha_L+1)} \int_0^\infty x^{\alpha_L} e^{-\frac{x}{\beta_L}} Q\left(\sqrt{\frac{2g \log_2 M E_b}{K N_0} x^2}\right) dx. \quad (17)$$

V. NUMERICAL RESULTS

This section deals with the evaluation of the derived theoretical results and their verification. The correctness and accuracy of the approximations in (13) and (17) are validated with the help of simulations. In order to obtain the simulation results, which are the true results, the sum-of-sinusoids (SOS) concept [16] has been exploited. Meaning thereby, the SOS concept has been applied on the uncorrelated Gaussian noise processes making up the received signal envelope at the output of the EG combiner. The generalized method of exact Doppler spread (GMEDS₁) [17] has been employed for the computation of the model parameters of the channel simulator. Each Gaussian process $\mu^{(i)}(t)$ was simulated using $N_l^{(i)} = 14$ for $i = 1, 2, \dots, 2K$ and $l = 1, 2$, where $N_l^{(i)}$ is the number of sinusoids chosen to simulate the inphase ($l = 1$) and quadrature components ($l = 2$) of $\mu^{(i)}(t)$. The selection of $N_l^{(i)}$ is based on the fact that the simulated distribution of $|\mu^{(i)}(t)|$ closely approximates the Rayleigh distribution when $N_l^{(i)} \geq 7$ ($l = 1, 2$) [16]. The maximum Doppler frequencies caused by the motion of the source mobile station and the destination mobile station were set to 91 Hz. However, the maximum Doppler frequencies caused by the motion of K mobile relays were chosen to be 125 Hz. The variances $\sigma_{\mu^{(i)}}^2$ were selected from the set $\{0.25, 0.5, 0.75, 1, 1.25, 1.5, 1.75\} \forall i = 1, 2, \dots, 2K$. The relay gains $A_{R^{(k)}}$ were set to be unity, i.e., $A_{R^{(k)}} = A_R = 1 \forall k = 1, 2, \dots, K$ unless stated otherwise. The total number of symbols used for a reliable generation of the BEP

curves was 10^6 .

The results presented in Figs. K.2–K.5 show a good fitting of the approximated analytical and the exact (simulation) results. Figures K.2 and K.3 demonstrate the theoretical results of the PDF $p_{\Xi}(x)$ of $\Xi(t)$ described by (13). As an evidence of the correctness of the approximated analytical results, the simulation results obtained by evaluating the statistics of the waveforms generated by using the SOS-based channel simulator are included in Figs. K.2 and K.3. Keeping the relay gain A_R constant, the PDF $p_{\Xi}(x)$ of $\Xi(t)$ for a different number of diversity branches K , having the same and different variances is shown in Fig. K.2 and Fig. K.3, respectively. For $K = 1$ and $A_R = 1$, the PDF $p_{\Xi}(x)$ of $\Xi(t)$ reduces to the double Rayleigh distribution validating that our approximation in (13) is very accurate.

The average BEP P_b of M -ary PSK modulation schemes over double Rayleigh processes with EGC described by (15) is presented in Fig. K.4. In this figure, a comparison of the average BEP P_b of quadrature PSK (QPSK), 8-PSK, and 16-PSK modulation schemes is shown and a different number diversity branches K is considered for each modulation scheme. Here, the average BEP P_b is evaluated while keeping the variances $\sigma_{\mu^{(i)}}^2$ equal to unity. For all modulation schemes, a remarkable improvement in the diversity gain can be observed when the number of diversity branches increases from $K = 1$ to $K = 6$. See, e.g., at $P_b = 10^{-3}$, a diversity gain of ≈ 26 dB can be achieved when K increases from $K = 1$ to $K = 6$. It can also be seen in Fig. K.4 that the average BEP P_b curve associated with QPSK modulation shifts to the right when 8-PSK or 16-PSK modulation schemes are employed in the system. This shift that higher-order modulation schemes are more prone to errors. However, they have a higher data rate.

For the sake of completeness of our performance analysis, we have included in Fig. K.5 the average BEP P_b curves when MRC is deployed at the destination mobile station. Keeping the number of diversity branches K constant, i.e., $K = 3$, the average BEP P_b of QPSK, 8-PSK, and 16-PSK modulation schemes is evaluated. By studying the curves in Fig. K.5, a diversity gain of ≈ 1 dB can be observed when MRC is used instead of EGC. This gain however comes at the cost of increased complexity of the receiver.

VI. CONCLUSION

In this article, we have analyzed the performance of M -ary PSK modulation schemes over M2M fading channels with EGC in a dual-hop amplify-and-forward relay network. The narrowband M2M fading channels are modeled assuming NLOS propagation conditions. It is further assumed that there exist K diversity branches between

the source mobile station and the destination mobile station. The performance of M -ary PSK modulation schemes is studied by computing the average BEP. A simple analytical expression for the average BEP of M -ary PSK modulation schemes over double Rayleigh fading channels with EGC is derived. The derivation of this expression however, requires the knowledge of the PDF of the received signal envelope at the output of the EG combiner. Here, the output of the EG combiner is modeled as a sum of K independent, but not necessarily identical double Rayleigh fading channels. Furthermore, exploiting the properties of the Laguerre series expansion made it possible to approximate the PDF of the sum of double Rayleigh processes by a gamma distribution. Utilizing this approximation of the target PDF allowed us to evaluate with ease the required average BEP. The validity of all the obtained analytical expressions is confirmed by simulations. Note that the simulation results are the true results here. We have included in our discussion the results demonstrating the influence of the number of diversity branches K on the average BEP of different M -ary PSK modulation schemes. These results illustrate a remarkable improvement in the diversity gain as the number of diversity branches K increases.

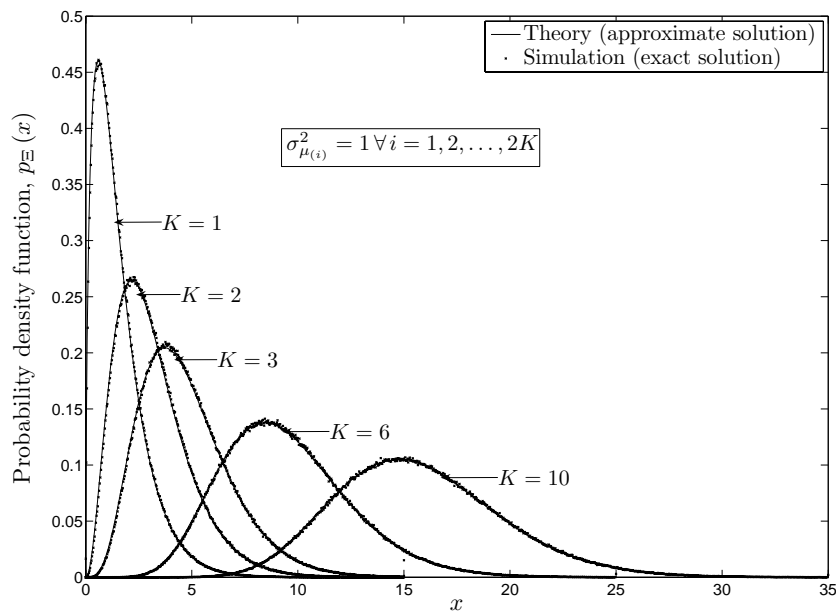


Figure K.2: The PDF $p_{\Xi}(x)$ of the received signal envelope $\Xi(t)$ at the output of the EG combiner for a different number of diversity branches K having the same variance.

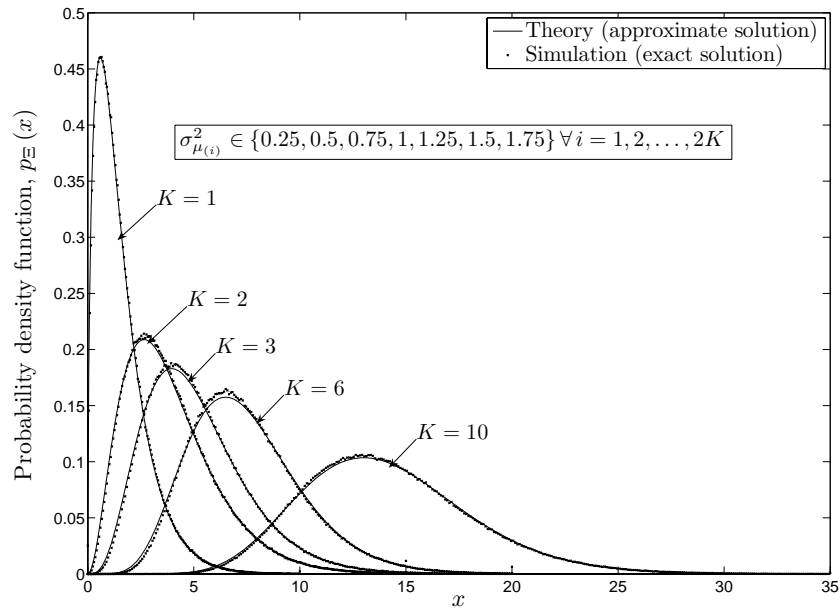


Figure K.3: The PDF $p_{\Xi}(x)$ of the received signal envelope $\Xi(t)$ at the output of the EG combiner for a different number of diversity branches K having different variances.

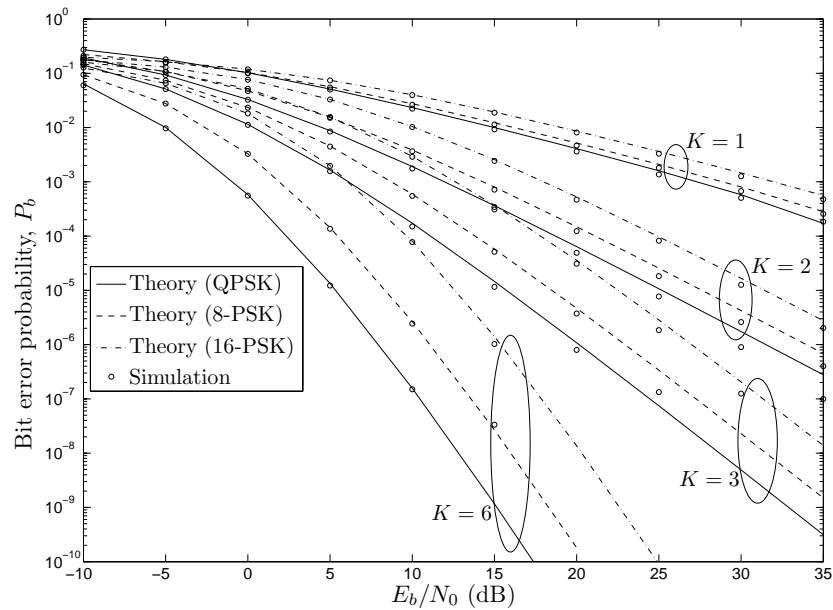


Figure K.4: The average BEP P_b of M -ary PSK modulation schemes over double Rayleigh processes with EGC.

REFERENCES

[1] A. S. Akki. Statistical properties of mobile-to-mobile land communication channels. *IEEE Trans. Veh. Technol.*, 43(4):826–831, November 1994.

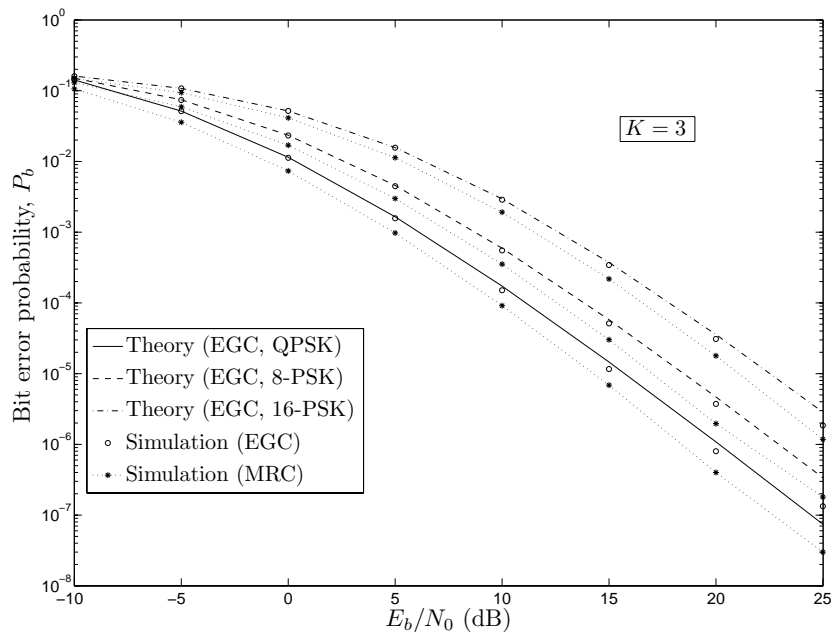


Figure K.5: A comparison of the average BEP P_b of M -ary PSK modulation schemes over double Rayleigh processes with EGC and MRC.

- [2] P. A. Anghel and M. Kaveh. Exact symbol error probability of a cooperative network in a Rayleigh fading environment. *IEEE Trans. Wireless Commun.*, 3(5):1416–1421, September 2004.
- [3] K. Azarian, H. E. Gamal, and P. Schniter. On the achievable diversity-multiplexing tradeoff in half-duplex cooperative channels. *IEEE Trans. Inform. Theory*, 51(12):4152–4172, December 2005.
- [4] N. C. Beaulieu and X. Dong. Level crossing rate and average fade duration of MRC and EGC diversity in Ricean fading. *IEEE Trans. Commun.*, 51(5):722–726, May 2003.
- [5] Y. Fan and J. S. Thompson. MIMO configurations for relay channels: Theory and practice. *IEEE Trans. Wireless Commun.*, 6(5):1774–1786, May 2007.
- [6] A. Goldsmith. *Wireless Communications*. New York: Cambridge University Press, 2005.
- [7] I. S. Gradshteyn and I. M. Ryzhik. *Table of Integrals, Series, and Products*. New York: Academic Press, 6th edition, 2000.

- [8] S. S. Ikki and M. H. Ahmed. Performance of cooperative diversity using equal gain combining (EGC) technique over Rayleigh fading channels. In *Proc. IEEE Int. Conf. Communications (ICC'07)*. Glasgow, Scotland, June 2007.
- [9] S. S. Ikki and M. H. Ahmed. Performance of cooperative diversity using equal gain combining (EGC) over Nakagami- m fading channels. *IEEE Trans. Wireless Commun.*, 8(2):557–562, February 2009.
- [10] P. Ivanis, D. Drajić, and B. Vucetic. The second order statistics of maximal ratio combining with unbalanced branches. *IEEE Communications Letters*, 12(7):508–510, July 2008.
- [11] W. C. Jakes, editor. *Microwave Mobile Communications*. Piscataway, NJ: IEEE Press, 1994.
- [12] J. N. Laneman, D. N. C. Tse, and G. W. Wornell. Cooperative diversity in wireless networks: Efficient protocols and outage behavior. *IEEE Trans. Inform. Theory*, 50(12):3062–3080, December 2004.
- [13] R. U. Nabar, H. Bölcskei, and F. W. Kneubühler. Fading relay channels: Performance limits and space-time signal design. *IEEE J. Select. Areas Commun.*, 22(6):1099–1109, August 2004.
- [14] R. Pabst, B. Walke, D. Schultz, et al. Relay-based deployment concepts for wireless and mobile broadband radio. *IEEE Communications Magazine*, 42(9):80–89, September 2004.
- [15] C. S. Patel, G. L. Stüber, and T. G. Pratt. Statistical properties of amplify and forward relay fading channels. *IEEE Trans. Veh. Technol.*, 55(1):1–9, January 2006.
- [16] M. Pätzold. *Mobile Fading Channels*. Chichester: John Wiley & Sons, 2002.
- [17] M. Pätzold, C. X. Wang, and B. O. Hogstad. Two new sum-of-sinusoids-based methods for the efficient generation of multiple uncorrelated Rayleigh fading waveforms. *IEEE Trans. Wireless Commun.*, 8(6):3122–3131, June 2009.
- [18] S. Primak, V. Kontorovich, and V. Lyandres, editors. *Stochastic Methods and their Applications to Communications: Stochastic Differential Equations Approach*. Chichester: John Wiley & Sons, 2004.
- [19] J. Proakis and M. Salehi. *Digital Communications*. New York: McGraw-Hill, 5th edition, 2008.

- [20] H. Samimi and P. Azmi. An approximate analytical framework for performance analysis of equal gain combining technique over independent Nakagami, Rician and Weibull fading channels. *Wireless Personal Communications (WPC)*, 43(4):1399–1408, dec 2007. DOI 10.1007/s11277-007-9314-z.
- [21] M. Schwartz, W. R. Bennett, and S. Stein. *Communication Systems and Techniques*, volume 4. New York: McGraw Hill, 1966.
- [22] A. Sendonaris, E. Erkip, and B. Aazhang. User cooperation diversity — Part I: System description. *IEEE Trans. Commun.*, 51(11):1927–1938, November 2003.
- [23] A. Sendonaris, E. Erkip, and B. Aazhang. User cooperation diversity — Part II: Implementation aspects and performance analysis. *IEEE Trans. Commun.*, 51(11):1939–1948, November 2003.
- [24] M. K. Simon. *Probability Distributions Involving Gaussian Random Variables: A Handbook for Engineers and Scientists*. Dordrecht: Kluwer Academic Publishers, 2002.
- [25] M. K. Simon and M. S. Alouini. *Digital Communications over Fading Channels*. New Jersey: John Wiley & Sons, 2nd edition, 2005.
- [26] B. Talha and M. Pätzold. On the statistical properties of double Rice channels. In *Proc. 10th Int. Symp. on Wireless Personal Multimedia Communications, WPMC 2007*, pages 517–522. Jaipur, India, December 2007.
- [27] W. Wongtrairat and P. Supnithi. Performance of digital modulation in double Nakagami-m fading channels with MRC diversity. *IEICE Trans. Commun.*, E92-B(2):559–566, February 2009.
- [28] M. D. Yacoub, C. R. C. Monterio da Silva, and J. E. V. Bautista. Second-order statistics for diversity-combining techniques in Nakagami fading channels. *IEEE Trans. Veh. Technol.*, 50(6):1464–1470, November 2001.
- [29] Q. T. Zhang. Probability of error for equal-gain combiners over Rayleigh channels: some closed-form solutions. *IEEE Trans. Commun.*, 45(3):270–273, March 1997.
- [30] D. A. Zogas, G. K. Karagiannidis, and S. A. Kotsopoulos. Equal gain combining over Nakagami- n (Rice) and Nakagami- q (Hoyt) generalized fading channels. *IEEE Trans. Wireless Commun.*, 4(2):374–379, March 2005.

Appendix L

Paper XI

Title: BEP Analysis of M -Ary PSK Modulation Schemes over Double Rice Fading Channels with EGC

Authors: **Batool Talha** and Matthias Pätzold

Affiliation: University of Agder, Faculty of Engineering and Science, P. O. Box 509, NO-4898 Grimstad, Norway

Conference: *Second Workshop on Scenarios for Network Evaluation Studies, (SCENES 2010)*, San Francisco, CA, USA, Nov. 2010, accepted for publication.

BEP Analysis of M -Ary PSK Modulation Schemes over Double Rice Fading Channels with EGC

Batool Talha and Matthias Pätzold

Department of Information and Communication Technology
Faculty of Engineering and Science, Agder University College
Servicebox 509, NO-4876 Grimstad, Norway
E-mails: {batool.talha, matthias.paetzold}@uia.no

Abstract — In this article, the performance of M -ary phase shift keying (PSK) modulation schemes over mobile-to-mobile (M2M) fading channels with equal gain combining (EGC) in cooperative networks is analyzed. Narrow-band M2M fading channels under line-of-sight (LOS) propagation conditions are modeled as double Rice processes. A dual-hop amplify-and-forward relay network, where LOS components can exist in the transmission links between the source mobile station and the destination mobile station via K mobile relays, is studied. Here, the average bit error probability (BEP) is utilized to evaluate the performance of M -ary PSK modulation schemes. A simple analytical approximation for the average BEP of M -ary PSK modulations over relay-based M2M fading channels with EGC is derived. The accuracy of the approximation is assessed by simulations. The presented results show that in a dual-hop relay system with EGC, the presence of LOS components in the relay links improves the systems' performance. In addition, a significant enhancement in the diversity gain can be achieved as the number of diversity branches K increases.

I. INTRODUCTION

The recently growing popularity of cooperative diversity [25, 26, 14] in wireless networks is due to its ability to mitigate the deleterious fading effects. Without any extra cost resulting from the deployment of a new infrastructure and by utilizing the existing resources of the network, a spatial diversity gain can be achieved. The fundamental principle of cooperative relaying is that several mobile stations in the network collaborate together to relay the signal from the source mobile station to the destination mobile station. In the simplest mode of operation, the relay nodes just amplify the received signal and forward it towards the destination mobile station. They can also first decode the received signal, encode it again and then forward it. In both cases, multiple copies of the same signal reach the destination mobile

station, which allows us to achieve a diversity gain by exploiting the virtual antenna array. In addition to the spatial diversity gain, cooperative relaying promises increased capacity, improved connectivity, and a larger coverage range [17, 8, 7].

During the last decade, a large number of researchers devoted their efforts to analyzing the performance of cooperative networks. For example, the performance of dual-hop amplify-and-forward relay networks has extensively been investigated for different types of fading channels in [10, 33, 23, 15, 28, 6, 29, 35, 5, 11]. A performance analysis in terms of the average BEP as well as the outage probability of single-relay dual-hop configuration over Rayleigh and generalized- K fading channels is presented in [10] and [33], respectively. Studies pertaining to the asymptotic outage behavior of amplify-and-forward dual-hop multi-relay systems with Nakagami fading channels is available in [15], whereas the diversity order is addressed in [35]. The common denominator in the works [23, 15, 28, 6, 29, 35, 5] is that they consider maximal ratio combining (MRC) at the destination mobile station, where the authors of [5] have also included in their analysis results when EGC is deployed.

The success story of cooperative relaying in cellular networks has motivated the wireless communications' research community to explore the possibilities to utilize it in M2M communication systems. It is widely acknowledged now that the statistical characteristics of M2M fading channels [2] are quite different from those of conventional cellular channels, such as Rayleigh and Rice channels. Additionally, in relay-based cooperative networks, M2M fading channels under non-line-of-sight (NLOS) and LOS propagation conditions can be modeled as double Rayleigh [18] and double Rice processes [30], respectively. The authors of [12] have explored the performance of intervehicular cooperative schemes and they proposed optimum power allocation strategies assuming cascaded Nakagami fading. The performance of several digital modulation schemes over double Nakagami- m channels with MRC diversity has been studied in [32], whereas the BEP analysis of M -ary PSK modulated signals over double Rayleigh channels with EGC can be found in [31].

This article focuses on analyzing the performance of M -ary PSK modulation schemes over M2M fading channels under LOS conditions with EGC. As far as the authors are aware, the performance analysis of digital modulation schemes over M2M channels with EGC assuming LOS propagation conditions has not been carried out yet. Here, we study a multi-relay dual-hop amplify-and-forward cooperative network. It is assumed that LOS components can exist in all or just in some few transmission links between the source mobile station and the destination mobile station via K mobile relays. Thus, in order to cater for the unbalanced conditions in the relay links, we have modeled the received signal envelope at the output of the

EG combiner as a sum of K independent but not necessarily identically distributed double Rice processes. Furthermore, the criterion for the performance analysis of M -ary PSK modulation schemes is the evaluation of the average BEP for which a simple analytical approximation is derived. The approximate analytical results for the average BEP are compared with those of the exact simulation results to validate the correctness of the proposed approach. From the presented results, it can be concluded that the performance of relay-based cooperative systems improves with the presence of LOS components in the relay links. In addition, if the number K of diversity branches K increases, the better is the system performance.

This article has the following structure. The system model for EGC over M2M channels under LOS conditions in amplify-and-forward relay networks is presented in Section II. In Section III, the PDF of the received signal envelope at the output of the EG combiner is derived. Section IV deals with the derivation of the average BEP of M -ary PSK modulation schemes over double Rice channels with EGC. Section V studies the accuracy of the analytical approximations by simulations along with a detailed discussion on the obtained results. Finally, the article is concluded in Section VI.

II. EGC OVER DOUBLE RICE FADING CHANNELS

In this section, we describe the system model for EGC over narrowband M2M fading channels under isotropic scattering conditions with LOS components in a dual-hop cooperative network. In the considered system, we have K mobile relays, which are connected in parallel between the source mobile station and the destination mobile station, as illustrated in Fig. L.1.

It is assumed that all mobile stations in the network, i.e., the source mobile station, the destination mobile station, and the K mobile relays do not transmit and receive a signal at the same time in the same frequency band. This can be achieved by using the time-division multiple-access (TDMA) based amplify-and-forward relay protocols proposed in [16, 4]. Thus, the signals from the K diversity branches in different time slots can be combined at the destination mobile station using EGC.

Let us denote the signal transmitted by the source mobile station as $s(t)$. Then, the signal $r^{(k)}(t)$ received from the k th diversity branch at the destination mobile station can be expressed as

$$r^{(k)}(t) = \zeta_p^{(k)}(t) s(t) + n^{(k)}(t) \quad (1)$$

where $\zeta_p^{(k)}(t)$ ($k = 1, 2, \dots, K$) represents the complex channel gain of the k th sub-channel from the source mobile station to the destination mobile station via the

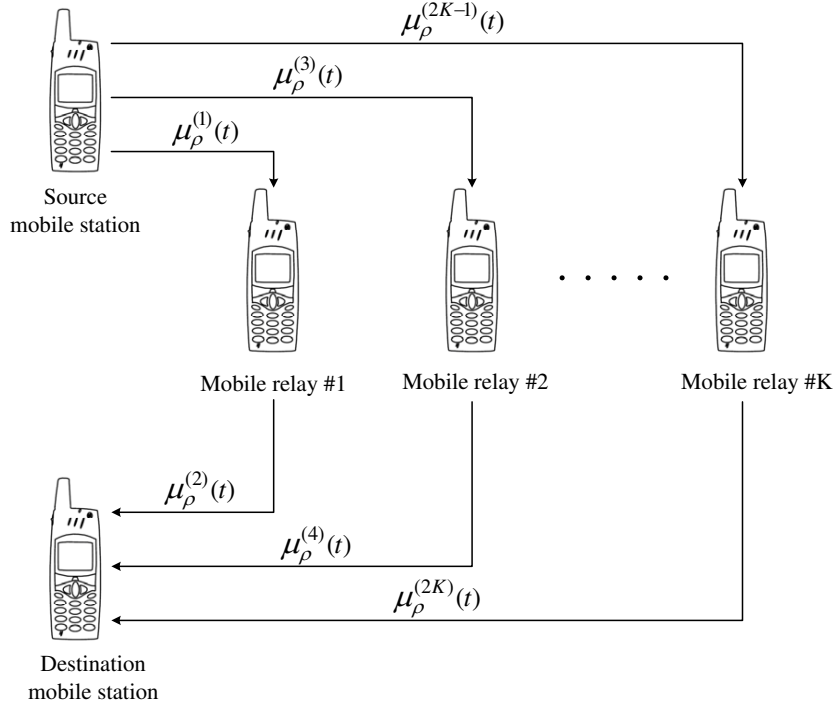


Figure L.1: The propagation scenario describing K -parallel dual-hop relay M2M fading channels.

k th mobile relay under LOS propagation conditions. In addition, $n^{(k)}(t) \forall k = 1, 2, \dots, K$ denotes the zero-mean additive white Gaussian noise (AWGN) process with variance $N_0/2$, where N_0 is the noise power spectral density.

Each fading process $\zeta_\rho^{(k)}(t)$ in (1) is modeled as a weighted non-zero-mean complex double Gaussian process of the form

$$\zeta_\rho^{(k)}(t) = \zeta_{\rho_1}^{(k)}(t) + j\zeta_{\rho_2}^{(k)}(t) = A_k \mu_\rho^{(2k-1)}(t) \mu_\rho^{(2k)}(t) \quad (2)$$

for $k = 1, 2, \dots, K$. In (2), each $\mu_\rho^{(i)}(t)$ is a non-zero-mean complex Gaussian process. For all odd superscripts i , i.e., $i = 2k - 1 = 1, 3, \dots, (2K - 1)$, the Gaussian process $\mu_\rho^{(i)}(t)$ describes the sum of the scattered component $\mu^{(i)}(t)$ and the LOS component $m^{(i)}(t)$ of the i th subchannel between the source mobile station and the k th mobile relay, i.e., $\mu_\rho^{(i)}(t) = \mu^{(i)}(t) + m^{(i)}(t)$. Whereas, for all even superscripts i , i.e., $i = 2k = 2, 4, \dots, 2K$, the Gaussian process $\mu_\rho^{(i)}(t)$ denotes the sum of the scattered component $\mu^{(i)}(t)$ and the LOS component $m^{(i)}(t)$ of the i th subchannel between the k th mobile relay and the destination mobile station. Each scattered component $\mu^{(i)}(t)$ is modeled by a zero-mean complex Gaussian process with variance $2\sigma_i^2$. Furthermore, these Gaussian processes are mutually independent, where the spectral properties of each process are characterized by the

classical Jakes Doppler power spectral density. The corresponding LOS component $m^{(i)}(t) = \rho_i \exp\{j(2\pi f_\rho^{(i)}t + \theta_\rho^{(i)})\}$ assumes a fixed amplitude ρ_i , a constant Doppler frequency $f_\rho^{(i)}$, and a constant phase $\theta_\rho^{(i)}$.

In (2), A_k is called the relay gain of the k th relay. In order to achieve the optimum performance in a relay-based system, the selection of the relay gain A_k is of critical importance. For fixed-gain relays under NLOS propagation conditions, A_k is usually selected to be [16]

$$A_k = \frac{1}{\sqrt{E \left\{ \left| \mu_{\rho \rightarrow 0}^{(2k-1)}(t) \right|^2 \right\} + N_0}} \tag{3}$$

where $E \{ \cdot \}$ is the expectation operator. Thus, $E \{ |\cdot|^2 \} = 2\sigma_{(2k-1)}^2$ represents the mean power of the NLOS fading channel between the source mobile station and the k th mobile relay. Replacing $\mu_{\rho \rightarrow 0}^{(2k-1)}(t)$ with $\mu_\rho^{(2k-1)}(t)$ in (3) allows us to express the relay gain A_k associated with LOS propagation scenarios as

$$A_k = \frac{1}{\sqrt{E \left\{ \left| \mu_\rho^{(2k-1)}(t) \right|^2 \right\} + N_0}} = \frac{1}{\sqrt{2\sigma_{(2k-1)}^2 + \rho_{(2k-1)}^2 + N_0}}. \tag{4}$$

In a practical amplify-and-forward relay system, the total noise $n_r^{(k)}(t)$ in the link from the source mobile station to the destination mobile station via the k th mobile relay has the following form

$$n_r^{(k)}(t) = A_k \mu_\rho^{(2k)}(t) n^{(2k-1)}(t) + n^{(2k)}(t) \tag{5}$$

for all $k = 1, 2, \dots, K$. It is known from the literature (see, e.g., [34] and the references therein) that the total noise $n_r^{(k)}(t)$ can be described under NLOS propagation conditions by a zero-mean complex Gaussian process with variance $N_0 + 2\sigma_{(2k)}^2 N_0 / (2\sigma_{(2k-1)}^2 + N_0)$. It can also be shown that under LOS propagation conditions, the noise process $n_r^{(k)}(t)$ is still a zero-mean complex Gaussian process, its variance changes to $N_0 + (2\sigma_{(2k)}^2 + \rho_{(2k)}^2) N_0 / (2\sigma_{(2k-1)}^2 + \rho_{(2k-1)}^2 + N_0)$.

Finally, the total signal $r(t)$ at the destination mobile station, obtained after combining the signals $r^{(k)}(t)$ received from K diversity branches, can be expressed as

$$r(t) = \sum_{k=1}^K r^{(k)}(t) = \Xi_\rho(t) s(t) + N(t). \tag{6}$$

This result is valid under the assumption of perfect channel state information (CSI) at the destination mobile station. In (6), $\Xi_\rho(t)$ represents the fading envelope at the output of the EG combiner, which can be written as [13]

$$\Xi_\rho(t) = \sum_{k=1}^K \chi_\rho^{(k)}(t) \quad (7)$$

where $\chi_\rho^{(k)}(t)$ is the absolute value of $\zeta_\rho^{(k)}(t)$. Thus, each $\chi_\rho^{(k)}(t)$ is a double Rice process. In (6), $N(t)$ is the total received noise is given by $N(t) = \sum_{k=1}^K n_r^{(k)}(t)$.

III. PDF OF A SUM OF DOUBLE RICE PROCESSES

Under LOS propagation conditions, the received signal envelope $\Xi_\rho(t)$ at the output of the EG combiner is modeled as a sum of K independent but not necessarily identically distributed double Rice processes. The computation of the PDF $p_{\Xi_\rho}(x)$ of $\Xi_\rho(t)$ involves the evaluation of a $(K-1)$ -dimensional convolution integral. The solution of this convolution integral demands plenty of time and long mathematical manipulations. It is however possible to avoid the complicated mathematics by following the less demanding approach of approximation. Depending upon the purpose of use, it is possible to approximate the PDF $p_{\Xi_\rho}(x)$ either by another but simpler expression or by a series. Here, we suggest to approximate the PDF $p_{\Xi_\rho}(x)$ by the gamma distribution. It has demonstrated the potential to approximate other distributions with reasonable accuracy, including the lognormal distribution [1] and the generalized- K distribution [3]. It also appears as the first term in the Laguerre series expansion [21]. Therefore, we write

$$p_{\Xi_\rho}(x) \approx p_\Gamma(x) = \frac{x^{\alpha_L}}{\beta_L^{(\alpha_L+1)} \Gamma(\alpha_L+1)} e^{-\frac{x}{\beta_L}} \quad (8)$$

where $\Gamma(\cdot)$ is the gamma function [22]. The Laguerre series parameters α_L and β_L can be obtained by following the steps in [21, p. 21], which results in

$$\alpha_L = [\kappa_1^2/\kappa_2] - 1, \quad \beta_L = \kappa_2/\kappa_1 \quad (9a,b)$$

where κ_1 corresponds to the first cumulant (i.e., the mean value) and κ_2 represents the second cumulant (i.e., the variance) of the stochastic process $\Xi_\rho(t)$. Mathematically, we can express κ_n ($n = 1, 2$) as

$$\kappa_n = \sum_{k=1}^K \kappa_n^{(k)} \quad (10)$$

where $\kappa_n^{(k)}$ are the cumulants associated with the double Rice process $\chi_\rho^{(k)}(t)$. The mean value and the variance of $\chi_\rho^{(k)}(t)$ [30] are presented in the following, i.e.,

$$\begin{aligned} \kappa_1^{(k)} &= A_k \sigma_{(2k-1)} \sigma_{(2k)} \frac{\pi}{2} {}_1F_1\left(-\frac{1}{2}; 1; -\rho_{(2k-1)}^2 / 2\sigma_{(2k-1)}^2\right) \\ &\quad \times {}_1F_1\left(-\frac{1}{2}; 1; -\rho_{(2k)}^2 / 2\sigma_{(2k)}^2\right) \end{aligned} \quad (11a)$$

$$\begin{aligned} \kappa_2^{(k)} &= A_k^2 \left(2\sigma_{(2k-1)}^2 + \rho_{(2k-1)}^2\right) \left(2\sigma_{(2k)}^2 + \rho_{(2k)}^2\right) - \left(A_k \sigma_{(2k-1)} \sigma_{(2k)} \frac{\pi}{2}\right)^2 \\ &\quad \times \left[{}_1F_1\left(-\frac{1}{2}; 1; -\rho_{(2k-1)}^2 / 2\sigma_{(2k-1)}^2\right) {}_1F_1\left(-\frac{1}{2}; 1; -\rho_{(2k)}^2 / 2\sigma_{(2k)}^2\right) \right]^2 \end{aligned} \quad (11b)$$

where ${}_1F_1(\cdot; \cdot; \cdot)$ is the hypergeometric function [22]. It is imperative to stress that here $\kappa_n^{(k)}$ is computed using the expression for A_k given in (4).

Once we have computed $\kappa_n^{(k)}$ ($n = 1, 2$) for all $k = 1, 2, \dots, K$, then the evaluation of κ_n in (10) is straightforward. Given κ_n , the quantities α_L and β_L can easily be calculated with the help of (9a,b). Finally, the substitution of α_L and β_L in (8) yields the approximate solution for the PDF $p_{\Xi_\rho}(x)$. The approximation in (8) will be used in the following section for deriving the average BEP of M -ary PSK modulation schemes over double Rice processes with EGC.

IV. PERFORMANCE ANALYSIS OF M -ARY PSK MODULATION SCHEMES OVER DOUBLE RICE FADING CHANNELS WITH EGC

We computed the total received signal envelope at the output of the EG combiner $\Xi_\rho(t)$, and the total received noise $N(t)$ in Section II. Using these results, we can now express the instantaneous signal-to-noise ratio per bit at the output of the EG combiner as [27, 24]

$$\gamma_{\text{EGC}}(t) = \frac{\Xi_\rho^2(t)}{E\{N^2(t)\}} E_b \quad (12)$$

where E_b is the energy (in joules) per bit and $E\{N^2(t)\}$ is the mean power of the total received noise. The mean value of the total noise power can be given as

$$\begin{aligned} E\{N^2(t)\} &= E\left\{ \left(\sum_{k=1}^K n_\tau^{(k)}(t) \right)^2 \right\} \\ &= K N_0 + \sum_{k=1}^K \frac{2\sigma_{(2k)}^2 + \rho_{(2k)}^2}{2\sigma_{(2k-1)}^2 + \rho_{(2k-1)}^2 + N_0} N_0. \end{aligned} \quad (13)$$

The average BEP P_b over the fading channel statistics at the output of the EG combiner can be obtained using the formula [27]

$$P_b = \int_0^{\infty} p_{\Xi_\rho}(x) P_{b|\Xi_\rho}(x) dx \quad (14)$$

where $P_{b|\Xi_\rho}(x)$ is the BEP of M -ary PSK modulation schemes conditioned on the fading amplitudes $\{x_k\}_{k=1}^K$, and $x = \sum_{k=1}^K x_k$. Here, the fading amplitudes $\{x_k\}_{k=1}^K$ follow the double Rice distribution.

The conditional BEP $P_{b|\Xi_\rho}(x)$ of M -ary PSK modulation schemes can be approximated as [9]

$$\begin{aligned} P_{b|\Xi_\rho}(x) &\approx \frac{a}{\log_2 M} Q\left(\sqrt{2g \log_2 M \gamma_{\text{EGC}}(x)}\right) \\ &\approx \frac{a}{\log_2 M} Q\left(\sqrt{\frac{2g \log_2 M E_b}{E\{N^2(t)\}} x^2}\right) \end{aligned} \quad (15)$$

where $M = 2^b$ with b as the number of bits per symbol, $Q(\cdot)$ is the error function [22], and $E\{N^2(t)\}$ is given in (13). The parameter a equals 1 or 2 for M -ary PSK modulation schemes when $M = 2$ or $M > 2$, respectively, whereas for all M -ary PSK modulation schemes $g = \sin^2(\pi/M)$ [32].

Substituting (8) and (15) in (14) leads to the approximate solution for the average BEP P_b , i.e.,

$$P_b \approx \frac{a}{\log_2 M} \frac{1}{\beta_L^{(\alpha_L+1)} \Gamma(\alpha_L+1)} \int_0^{\infty} x^{\alpha_L} e^{-\frac{x}{\beta_L}} Q\left(\sqrt{\frac{2g \log_2 M E_b}{E\{N^2(t)\}} x^2}\right) dx. \quad (16)$$

V. NUMERICAL RESULTS

The aim of this section is to evaluate and to illustrate the derived theoretical approximations given in (8) and (16) as well as to investigate their accuracy. The correctness of the approximated analytical results is confirmed by evaluating the statistics of the waveforms generated by utilizing the sum-of-sinusoids (SOS) method [19]. These simulation results correspond to the true (exact) results here. The waveforms $\tilde{\mu}^{(i)}(t)$ obtained from the designed SOS-based channel simulator are considered as an appropriate model for the uncorrelated Gaussian noise processes $\mu^{(i)}(t)$ making up the received signal envelope at the output of the EG combiner. The model parameters of the channel simulator have been computed by using the generalized method of exact Doppler spread (GMEDS₁) [20]. Each waveform $\tilde{\mu}^{(i)}(t)$ was generated

with $N_l^{(i)} = 14$ for $i = 1, 2, \dots, 2K$ and $l = 1, 2$, where $N_l^{(i)}$ is the number of sinusoids chosen to simulate the inphase ($l = 1$) and quadrature ($l = 2$) components of $\tilde{\mu}^{(i)}(t)$. It is widely acknowledged that the distribution of the simulated waveforms $|\tilde{\mu}^{(i)}(t)|$ closely approximates the Rayleigh distribution if $N_l^{(i)} \geq 7$ ($l = 1, 2$) [19]. Thus, by selecting $N_l^{(i)} = 14$, we ensure that the waveforms $\tilde{\mu}^{(i)}(t)$ have the required Gaussian distribution. The variance of the inphase and quadrature component of $\mu^{(i)}(t)$ ($\tilde{\mu}^{(i)}(t)$) is equal to $\sigma_i^2 = 1 \forall i = 1, 2, \dots, 2K$, unless stated otherwise. The maximum Doppler frequencies caused by the motion of the source mobile station, K mobile relays, and the destination mobile station were set to 91 Hz, 125 Hz, and 110 Hz, respectively. The total number of symbols used for a reliable generation of the BEP curves was 10^7 .

In this section, we have attempted to highlight the influence of an LOS component on the systems' performance by considering three propagation scenarios called the full-LOS (FLOS), the partial-LOS (PLOS), and the NLOS scenario. In the FLOS scenario, we have LOS components in all the transmission links between the source mobile station and the destination mobile station via K mobile relays. The scenario in which LOS components are present only in the links from the source mobile station to K mobile relays is referred to as the PLOS scenario. When LOS components do not exist in any of the transmission links, we have the NLOS scenario. Whenever, there exists a LOS component in any of the transmission links, its amplitude ρ_i is taken to be unity. The presented results in Figs. L.2–L.5 display a good fit of the approximated analytical and the exact simulation results.

Figure L.2 illustrates the analytical results of the PDF $p_{\Xi_\rho}(x)$ of $\Xi_\rho(t)$ described by (8). This figure contains the PDF $p_{\Xi_\rho}(x)$ of $\Xi_\rho(t)$ considering the FLOS, the PLOS, and the NLOS propagation conditions for a different number of diversity branches K . It is quite obvious from the figure that for any value of K , the presence of LOS components increases both the mean value and the variance of $\Xi_\rho(t)$. A close agreement between the approximated theoretical and the exact simulation results confirms the correctness of our approximation.

The average BEP P_b of M -ary PSK modulation schemes over double Rice processes with EGC described by (16) is presented in Fig. L.3. In this figure, a comparison of the average BEP P_b of quadrature PSK (QPSK), 8-PSK, as well as 16-PSK modulation schemes is shown by taking into account a different number diversity branches K for each modulation scheme. Here, the average BEP P_b is evaluated for the FLOS scenario, i.e., $\rho_i = 1 \forall i = 1, 2, \dots, 2K$. For all modulation schemes, a significant enhancement in the diversity gain can be observed when the number of diversity branches increases from $K = 1$ to $K = 6$. See, e.g., at $P_b = 10^{-3}$, it is pos-

sible to attain a diversity gain of approximately 26 dB by increasing K from $K = 1$ to $K = 6$. Provision of higher data rates is the characteristic feature of higher-order modulation schemes. These modulations are however known to be more prone to errors. This sensitivity of higher-order modulations towards errors is visible in Fig. L.3 as the average BEP P_b curve associated with QPSK modulation shifts to the right when 8-PSK or 16-PSK modulation schemes are deployed.

Figure L.4 demonstrates the impact of the existence of LOS components in the relay links on the average BEP P_b of M -ary PSK modulation schemes. Keeping the number of diversity branches K constant, e.g., $K = 3$, the average BEP P_b of QPSK and 16-PSK modulation schemes is evaluated for the FLOS, PLOS, and NLOS scenarios. For both QPSK and 16-PSK modulations, there is a noticeable gain in the performance when going from the NLOS scenario to the FLOS scenario. See, e.g., at $P_b = 10^{-4}$, a gain of approximately 1.5 dB is achieved when we have the PLOS scenario compared to the NLOS scenario. A further increase of $\approx 1.5 - 2$ dB in the gain can be seen under FLOS propagation conditions are available.

In order to complete our performance analysis, we have included in Fig. L.5 the average BEP P_b curves when MRC is utilized at the destination mobile station. Assuming FLOS propagation conditions, the average BEP P_b of QPSK, 8-PSK, and 16-PSK modulation schemes is evaluated for $K = 3$. The curves presented in Fig. L.5 show that when MRC is used instead of EGC, a diversity gain of around 1 dB can be obtained. The price to pay for this gain is however the increased complexity of the receiver.

VI. CONCLUSION

This article deals with the analysis of the performance of M -ary PSK modulation schemes over narrowband M2M fading channels with EGC in a dual-hop amplify-and-forward relay network. It is assumed that there can exist LOS components in the relay links between the source mobile station and the destination mobile station via K mobile relays. Thus, the received signal envelope at the output of the EG combiner is modeled as a sum of K independent, but not necessarily identically distributed double Rice processes. The performance of M -ary PSK modulation schemes is studied by evaluating the average BEP. An analytical approximation for the average BEP of M -ary PSK modulation schemes over double Rice fading channels with EGC is derived. The validity of the obtained analytical approximation is confirmed by simulations. We have included in our discussion results demonstrating the influence of LOS components present in the relay links as well as the number of diversity branches K on the average BEP of different M -ary PSK modulation schemes. These results illustrate that the existence of LOS components in

the relay links improves the systems' performance. Furthermore, we can achieve a significant enhancement in the diversity gain as the number of diversity branches K increases.

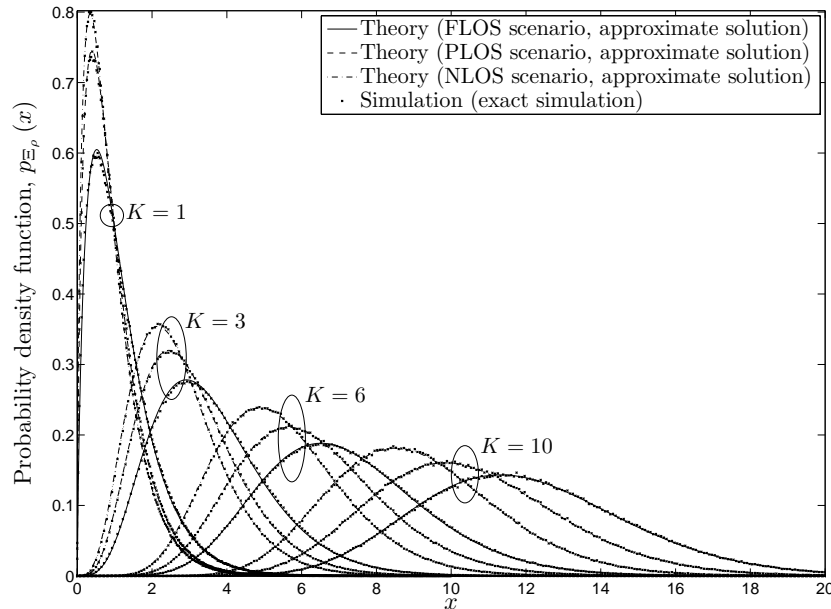


Figure L.2: The PDF $p_{\Xi_\rho}(x)$ of the received signal envelope $\Xi_\rho(t)$ at the output of the EG combiner for a different number of diversity branches K under FLOS, PLOS, and NLOS propagation conditions.

REFERENCES

- [1] A. Abdi and M. Kaveh. On the utility of gamma PDF in modeling shadow fading (slow fading). In *Proc. IEEE 49th Veh. Technol. Conf., VTC 1999*, pages 2308 – 2312. Houston, USA, May 1999.
- [2] A. S. Akki. Statistical properties of mobile-to-mobile land communication channels. *IEEE Trans. Veh. Technol.*, 43(4):826–831, November 1994.
- [3] S. Al-Ahmadi and H. Yanikomeroglu. On the approximation of the generalized-K distribution by a gamma distribution for modeling composite fading channels. *IEEE Trans. Wireless Commun.*, 9(2):706–713, February 2010.
- [4] K. Azarian, H. E. Gamal, and P. Schniter. On the achievable diversity-multiplexing tradeoff in half-duplex cooperative channels. *IEEE Trans. Inform. Theory*, 51(12):4152–4172, December 2005.

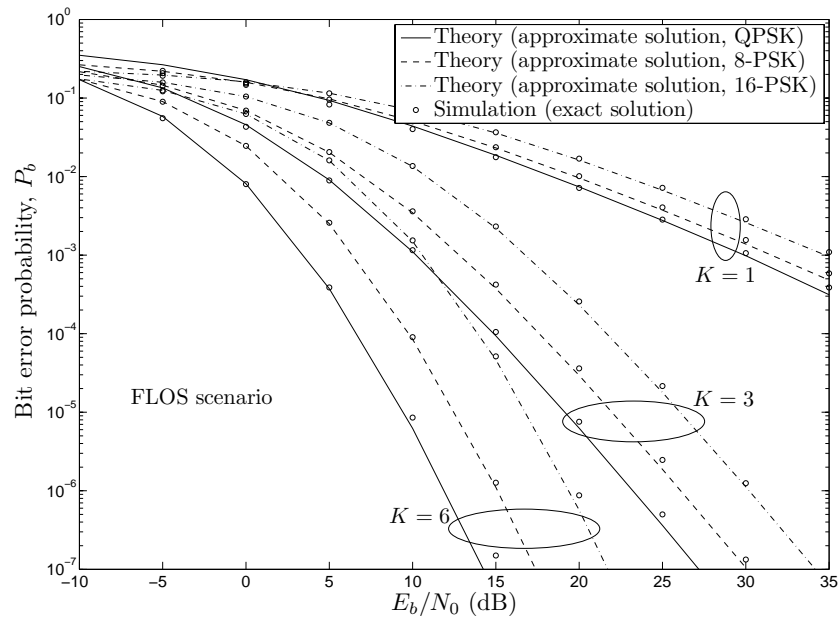


Figure L.3: The average BEP P_b of M -ary PSK modulation schemes over double Rice processes with EGC under FLOS propagation conditions.

- [5] D. B. da Costa and S. Aissa. Performance of cooperative diversity networks: Analysis of amplify-and-forward relaying under equal-gain and maximal-ratio combining. In *Proc. IEEE Int. Conf. Communications (ICC'09)*, pages 1–5.

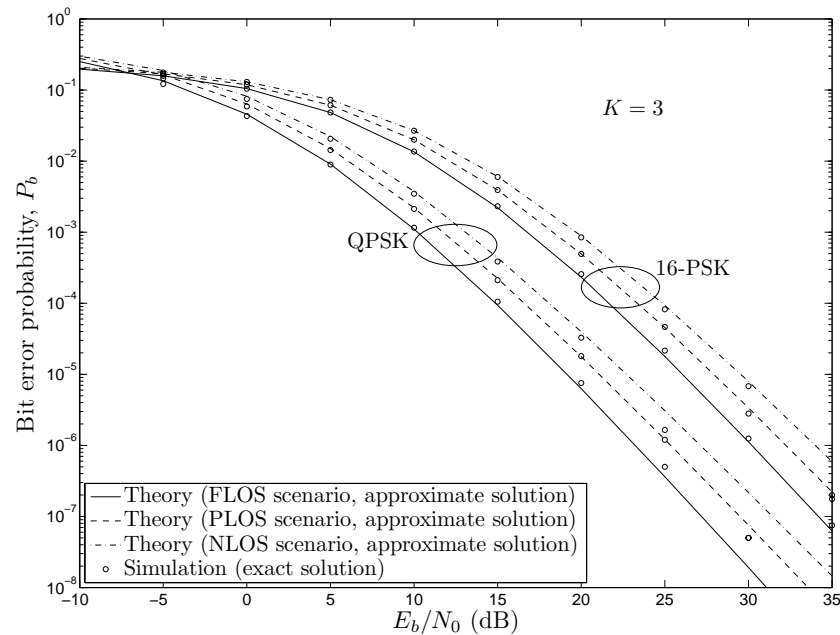


Figure L.4: The average BEP P_b of M -ary PSK modulation schemes over M2M fading channels with EGC under FLOS, PLOS, and NLOS propagation conditions.

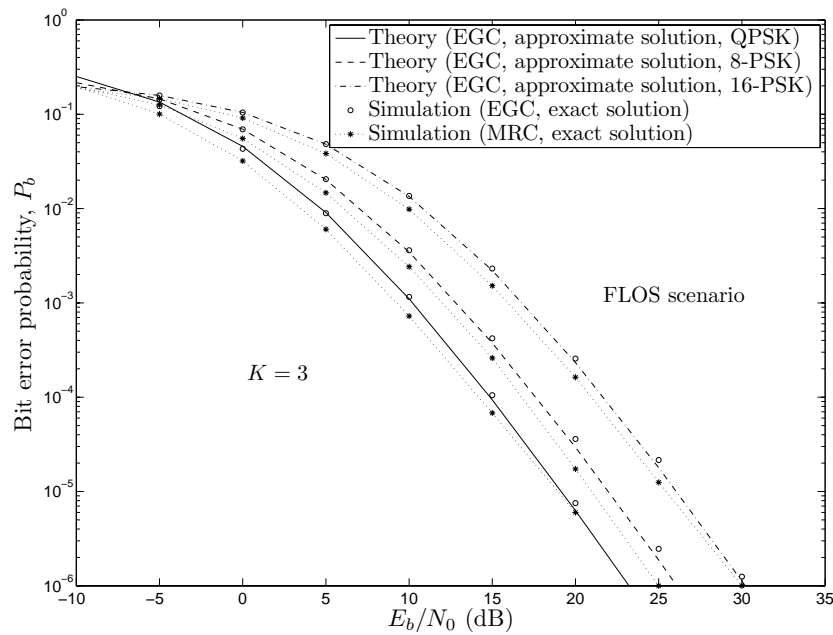


Figure L.5: The average BEP P_b of M -ary PSK modulation schemes over double Rice processes with EGC and MRC under FLOS propagation conditions.

Dresden, Germany, June 2009. DOI 10.1109/ICC.2009.5199330.

- [6] M. Di Renzo, F. Graziosi, and F. Santucci. A comprehensive framework for performance analysis of dual-hop cooperative wireless systems with fixed-gain relays over generalized fading channels. *IEEE Trans. Wireless Commun.*, 8(10):5060 – 5074, October 2009.
- [7] M. Dohler and Y. Li. *Cooperative Communications: Hardware, Channel, and PHY*. Chichester: John Wiley & Sons, 1st edition, 2010.
- [8] Y. Fan and J. S. Thompson. MIMO configurations for relay channels: Theory and practice. *IEEE Trans. Wireless Commun.*, 6(5):1774–1786, May 2007.
- [9] A. Goldsmith. *Wireless Communications*. New York: Cambridge University Press, 2005.
- [10] O. M. Hasna and M. S. Alouini. End-to-end performance of transmission systems with relays over Rayleigh-fading channels. *IEEE Trans. Wireless Commun.*, 2(6):1126 – 1131, November 2003.
- [11] S. S. Ikki and M. H. Ahmed. Performance of cooperative diversity using equal gain combining (EGC) over Nakagami- m fading channels. *IEEE Trans. Wireless Commun.*, 8(2):557–562, February 2009.

- [12] H. Ilhan, M. Uysal, and I. Altunbas. Cooperative diversity for intervehicular communication: Performance analysis and optimization. *IEEE Trans. Veh. Technol.*, 58(7):3301 – 3310, August 2009.
- [13] W. C. Jakes, editor. *Microwave Mobile Communications*. Piscataway, NJ: IEEE Press, 1994.
- [14] J. N. Laneman, D. N. C. Tse, and G. W. Wornell. Cooperative diversity in wireless networks: Efficient protocols and outage behavior. *IEEE Trans. Inform. Theory*, 50(12):3062–3080, December 2004.
- [15] Y. Li and S. Kishore. Asymptotic analysis of amplify-and-forward relaying in Nakagami fading environments. *IEEE Trans. Wireless Commun.*, 6(12):4256–4262, December 2007.
- [16] R. U. Nabar, H. Bölcskei, and F. W. Kneubühler. Fading relay channels: Performance limits and space-time signal design. *IEEE J. Select. Areas Commun.*, 22(6):1099–1109, August 2004.
- [17] R. Pabst, B. Walke, D. Schultz, et al. Relay-based deployment concepts for wireless and mobile broadband radio. *IEEE Communications Magazine*, 42(9):80–89, September 2004.
- [18] C. S. Patel, G. L. Stüber, and T. G. Pratt. Statistical properties of amplify and forward relay fading channels. *IEEE Trans. Veh. Technol.*, 55(1):1–9, January 2006.
- [19] M. Pätzold. *Mobile Fading Channels*. Chichester: John Wiley & Sons, 2002.
- [20] M. Pätzold, C. X. Wang, and B. O. Hogstad. Two new sum-of-sinusoids-based methods for the efficient generation of multiple uncorrelated Rayleigh fading waveforms. *IEEE Trans. Wireless Commun.*, 8(6):3122–3131, June 2009.
- [21] S. Primak, V. Kontorovich, and V. Lyandres, editors. *Stochastic Methods and their Applications to Communications: Stochastic Differential Equations Approach*. Chichester: John Wiley & Sons, 2004.
- [22] J. Proakis and M. Salehi. *Digital Communications*. New York: McGraw-Hill, 5th edition, 2008.
- [23] A. Ribeiro, X. Cai, and G. B. Giannakis. Symbol error probabilities for general cooperative links. *IEEE Trans. Wireless Commun.*, 4(3):1264 – 1273, May 2005.

- [24] M. Schwartz, W. R. Bennett, and S. Stein. *Communication Systems and Techniques*, volume 4. New York: McGraw Hill, 1966.
- [25] A. Sendonaris, E. Erkip, and B. Aazhang. User cooperation diversity — Part I: System description. *IEEE Trans. Commun.*, 51(11):1927–1938, November 2003.
- [26] A. Sendonaris, E. Erkip, and B. Aazhang. User cooperation diversity — Part II: Implementation aspects and performance analysis. *IEEE Trans. Commun.*, 51(11):1939–1948, November 2003.
- [27] M. K. Simon and M. S. Alouini. *Digital Communications over Fading Channels*. New Jersey: John Wiley & Sons, 2nd edition, 2005.
- [28] W. Su, A. K. Sadek, and K. J. R. Liu. Cooperative communication protocols in wireless networks: Performance analysis and optimum power allocation. *Wireless Personal Communications (WPC)*, 44(2):181–217, January 2008.
- [29] H. Suraweera, G. Karagiannidis, and P. Smith. Performance analysis of the dual-hop asymmetric fading channel. 8(6):2783 – 2788, June 2009.
- [30] B. Talha and M. Pätzold. On the statistical properties of double Rice channels. In *Proc. 10th Int. Symp. on Wireless Personal Multimedia Communications, WPMC 2007*, pages 517–522. Jaipur, India, December 2007.
- [31] B. Talha, M. Pätzold, and S. Primak. Performance analysis of M -ary PSK modulation schemes over multiple double Rayleigh fading channels with EGC in cooperative networks. In *Proc. IEEE Int. Conf. Communications, Workshop on Vehicular Connectivity, Veh-Con 2010*. Cape Town, South Africa, May 2010. DOI 10.1109/ICCW.2010.5503940.
- [32] W. Wongtrairat and P. Supnithi. Performance of digital modulation in double Nakagami- m fading channels with MRC diversity. *IEICE Trans. Commun.*, E92-B(2):559–566, February 2009.
- [33] L. Wu, J. Lin, K. Niu, and Z. He. Performance of dual-hop transmissions with fixed gain relays over generalized- K fading channels. In *Proc. IEEE Int. Conf. Communications (ICC'09)*. Dresden, Germany, June 2009. DOI 10.1109/ICC.2009.5199331.
- [34] Y. Wu and M. Pätzold. Parameter optimization for amplify-and-forward relaying systems with pilot symbol assisted modulation scheme. *Wireless Sensor Networks (WSN)*, 1(1):15–21, April 2009. DOI 10.4236/wsn.2009.11003.

- [35] F. Xu, F. C. M. Lau, and D. W. Yue. Diversity order for amplify-and-forward dual-hop systems with fixed-gain relay under Nakagami fading channels. 9(1):92 – 98, January 2010.

Appendix M

Paper XII

Title: Dual-Hop Amplify-and-Forward Relay Systems with EGC over M2M Fading Channels under LOS Conditions: Statistical and Performance Analysis

Authors: **Batool Talha** and Matthias Pätzold

Affiliation: University of Agder, Faculty of Engineering and Science, P. O. Box 509, NO-4898 Grimstad, Norway

Journal: to be submitted for publication.

Dual-Hop Amplify-and-Forward Relay Systems with EGC over M2M Fading Channels under LOS Conditions: Statistical and Performance Analysis

Abstract — This article analyzes the statistical properties of narrowband mobile-to-mobile (M2M) fading channels with equal gain combining (EGC) under line-of-sight (LOS) propagation conditions. Here, we study a dual-hop amplify-and-forward relay network and its performance in such channels is also evaluated. It is assumed that there can exist LOS components in the transmission links between the source mobile station and the destination mobile station via K mobile relays in addition to the direct source-destination link. In order to cater for asymmetric fading conditions in the relay transmission, the received signal envelope at the output of the equal gain (EG) combiner is thus modeled as a sum of a classical Rice process and K double Rice processes. Furthermore, the classical Rice process and double Rice processes are independent. Besides, these double Rice processes are independent but not necessarily identically distributed. Simple and closed-form analytical approximations are derived for the probability density function (PDF), the cumulative distribution function (CDF), the level-crossing rate (LCR), and the average duration of fades (ADF) of the sum process by exploiting the properties of a gamma process¹. The analytical approximations for the statistical properties of the sum process, especially the approximated PDF, are then employed in our performance studies. Several performance measures inclusive of the statistics of the instantaneous signal-to-noise ratio (SNR), amount of fading (AOF), average bit error probability (BEP)², and outage probability are explored in detail. The correctness of the derived analytical approximations is verified as well as their accuracy is assessed by simulations. It can be concluded from the presented results that generally, in a dual-hop relay system with EGC, the presence of LOS components in the transmission links improves the systems' performance.

Keywords—Amplify-and-forward relay systems, mobile-to-mobile fading channels, double Rayleigh process, double Rice process, probability density function, level-crossing rate, average duration of fades.

¹The material in this paper was presented in part at International Conference on Communications, ICC 2010, Cape Town, South Africa, May 2010.

²The material in this paper is submitted for publication in part in the proceedings of IEEE Global Communications Conference, IEEE GLOBECOM 2010, Miami, FL, USA, Dec. 2010.

I. INTRODUCTION

The recently growing popularity of cooperative diversity [38, 39, 20] in wireless networks is due to its ability to mitigate the deleterious fading effects. Without any extra cost resulting from the deployment of a new infrastructure and by utilizing the existing resources of the network, a spatial diversity gain can be achieved. The fundamental principle of cooperative relaying is that several mobile stations in the network collaborate together to relay the signal from the source mobile station to the destination mobile station. In the simplest mode of operation, the relay nodes just amplify the received signal and forward it towards the destination mobile station. They can also first decode the received signal, encode it again and then forward it. In both cases, multiple copies of the same signal reach the destination mobile station, which allows us to achieve a diversity gain by exploiting the virtual antenna array. In addition to the spatial diversity gain, cooperative relaying promises increased capacity, improved connectivity, and a larger coverage range [26, 9, 8].

Here, a dual-hop amplify-and-forward configuration has been taken into account, where there exist K mobile relays between the source mobile station and the destination mobile station. Furthermore, the direct link from the source mobile station to the destination mobile station is also present. Such a configuration in turn gives rise to $K + 1$ diversity branches. Thus, the previously mentioned spatial diversity gain is achieved by combining the signal received from the $K + 1$ diversity branches at the destination mobile station. Among the most important diversity combining techniques [17], maximal ratio combining (MRC) has been proved to be the optimum one [17]. It is widely acknowledged in the literature that a sub-optimal and less complex combining technique, referred to as EGC, performs very close to MRC [17]. Studies regarding the statistical properties of EGC and MRC in non-cooperative networks over Rayleigh, Rice, and Nakagami fading channels are reported in [53, 3, 16]. Furthermore, performance analysis of the said schemes in terms of the bit error and outage probability over Rayleigh, Rice, and Nakagami fading channels can be found in [55, 56, 36]. During the last decade, a large number of researchers devoted their efforts to analyzing the performance of cooperative networks. For example, the performance of dual-hop amplify-and-forward relay networks has extensively been investigated for different types of fading channels in [12, 1, 49, 47, 34, 21, 42, 7, 43, 51, 6, 14, 13]. A performance analysis in terms of the average BEP as well as the outage probability of single-relay dual-hop configuration over Rayleigh and generalized- K fading channels is presented in [12] and [49], respectively. Studies pertaining to the asymptotic outage behavior of amplify-and-forward dual-hop multi-relay systems with Nakagami fading channels is available

in [21], whereas the diversity order is addressed in [51]. The common denominator in the works [1, 34, 47, 21, 42, 7, 43, 51, 6] is that they consider maximal ratio combining (MRC) at the destination mobile station, where the authors of [6] have also included in their analysis results when EGC is deployed. Performance related issues in multi-relay dual-hop non-regenerative relay systems with EGC over Nakagami- m channels are investigated in [14, 13].

The success story of cooperative relaying in cellular networks has motivated the wireless communications' research community to explore the possibilities to utilize it in M2M communication systems. The development of relay-based M2M communication systems requires the knowledge of the propagation channel characteristics. It is well-known that the multipath propagation channel in any mobile and wireless communication system can efficiently be described with the help of proper statistical models. For example, the Rayleigh distribution is considered to be a suitable distribution to model the fading channel under non line-of-sight (NLOS) propagation conditions in classical cellular networks [54, 24, 25], a Suzuki process represents a reasonable model for land mobile terrestrial channels [31, 44] and the generalized- K distribution is widely accepted in radar systems [5, 40]. To model fading channels under NLOS propagation conditions in relay-based M2M communication systems, the double Rayleigh distribution is the appropriate choice (see, e.g., [19, 30] and the references therein). Motivated by the applications of the double Rayleigh channel model, a generalized channel model referred to as the N *Nakagami channel model has been proposed in [18]. Furthermore, an extension from the double Rayleigh channel model to the double Rice channel model for LOS propagation conditions has been proposed in [45]. The authors of [15] have explored the performance of intervehicular cooperative schemes and they proposed optimum power allocation strategies assuming cascaded Nakagami fading. The performance of several digital modulation schemes over double Nakagami- m channels with MRC diversity has been studied in [48], whereas the BEP analysis of M -ary PSK modulated signals over double Rayleigh channels with EGC can be found in [46].

This article focuses on analyzing the statistical properties of EGC over M2M fading channels under LOS propagation conditions as well as the performance of relay-based networks in such channels. As far as the authors are aware, the statistical analysis of EGC over M2M channels assuming LOS propagation conditions has not been carried out yet. In addition, the performance analysis of multi-relay dual-hop amplify-and-forward cooperative networks in such fading channels is also an open problem that calls for further work. In many practical propagation scenarios, asymmetric fading conditions can be observed in different relay links. Meaning

thereby, LOS components can exist in all or just in some few transmission links between the source mobile station and the destination mobile station via K mobile relays. Similarly, the LOS component can be present in the direct link from the source mobile station to the destination mobile station. Thus, in order to accommodate the direct link along with the unbalanced relay links, the received signal envelope at the output of the EG combiner is modeled as a sum of a classical Rice process and K double Rice processes. Furthermore, the classical Rice process and double Rice processes are independent. Note that these double Rice processes are independent but not necessarily identically distributed. Analytical approximations are derived for the PDF, CDF, LCR, and ADF of the sum process. Analysis of these statistical quantities give us a complete picture of the fading channel, since the PDF can well characterize the channel, and the LCR along with the ADF provide an insight into the fading behavior of the channel. Several performance evaluation measures such as the statistics of the instantaneous SNR at the output of the EG combiner, AOF, the average BEP, and the outage probability are thoroughly investigated. This work includes a discussion on the influence of the number of diversity branches $K + 1$ as well as the presence of LOS components in the transmission links on the statistics of M2M fading channels with EGC. The approximate analytical results for the PDF, CDF, LCR, ADF, the average BEP, and the outage probability are compared with those of the exact simulation results to validate the correctness of the proposed approach. From the presented results, it can be concluded that the performance of relay-based cooperative systems improves with the presence of LOS components in the relay links. In addition, if the number $K + 1$ of diversity branches increases, the better is the system performance.

This article has the following structure. In Section II, we present the system model for EGC over M2M fading channels under LOS propagation conditions in amplify-and-forward relay networks. Section III deals with the derivation and analysis of approximations for the PDF, CDF, LCR, and ADF of the received signal envelope at the output of the EG combiner. In Section IV, analytical approximations for the PDF as well as the moments of the SNR the output of the EG combiner, the average BEP, and the outage probability are derived and analyzed. Section V studies the accuracy of the analytical approximations by simulations and present a detailed discussion on the obtained results. Finally, the article is concluded in Section VI.

II. EGC OVER M2M FADING CHANNELS WITH LOS COMPONENTS

In this section, we describe the system model for EGC over narrowband M2M fading channels under isotropic scattering conditions with LOS components in a dual-hop cooperative network. In the considered system, we have K mobile relays, which

are connected in parallel between the source mobile station and the destination mobile station, as illustrated in Fig. M.1. It can be seen in Fig. M.1 that the direct transmission link from the source mobile station to the destination mobile station is also unobstructed.

It is assumed that all mobile stations in the network, i.e., the source mobile station, the destination mobile station, and the K mobile relays do not transmit and receive a signal at the same time in the same frequency band. This can be achieved by using the time-division multiple-access (TDMA) based amplify-and-forward relay protocols proposed in [22, 2]. Thus, the signals from the $K + 1$ diversity branches in different time slots can be combined at the destination mobile station using EGC.

Let us denote the signal transmitted by the source mobile station as $s(t)$. Then, the signal $r^{(0)}(t)$ received at the destination mobile station from the direct transmission link between the source mobile station and the destination mobile station can be given as

$$r^{(0)}(t) = \mu_\rho^{(0)}(t) s(t) + n^{(0)}(t) \tag{1}$$

where $\mu_\rho^{(0)}(t)$ models the complex channel gain of the fading channel from the source mobile station to the destination mobile station under LOS propagation conditions. The non-zero-mean complex Gaussian process $\mu_\rho^{(0)}(t)$ comprises the sum of the scattered component $\mu^{(0)}(t)$ and the LOS component $m^{(0)}(t)$ in the direct transmission link from the source mobile station to the destination mobile station, i.e., $\mu_\rho^{(0)}(t) = \mu^{(0)}(t) + m^{(0)}(t)$. In addition, $n^{(0)}(t)$ denotes the zero-mean additive white Gaussian noise (AWGN) process with variance $N_0/2$, where N_0 is the noise power spectral density.

Similarly, we can express the signal $r^{(k)}(t)$ received from the k th diversity branch at the destination mobile station as

$$r^{(k)}(t) = \zeta_\rho^{(k)}(t) s(t) + n^{(k)}(t) \tag{2}$$

where $\zeta_\rho^{(k)}(t)$ ($k = 1, 2, \dots, K$) represents the complex channel gain of the k th sub-channel from the source mobile station to the destination mobile station via the k th mobile relay under LOS propagation conditions. Furthermore, $n^{(k)}(t) \forall k = 1, 2, \dots, K$ is the zero-mean AWGN process with variance $N_0/2$.

Each fading process $\zeta_\rho^{(k)}(t)$ in (2) is modeled as a weighted non-zero-mean complex double Gaussian process of the form

$$\zeta_\rho^{(k)}(t) = \zeta_{\rho_1}^{(k)}(t) + j\zeta_{\rho_2}^{(k)}(t) = A_k \mu_\rho^{(2k-1)}(t) \mu_\rho^{(2k)}(t) \tag{3}$$

for $k = 1, 2, \dots, K$. In (3), each $\mu_\rho^{(i)}(t)$ is a non-zero-mean complex Gaussian process. For all odd superscripts i , i.e., $i = 2k - 1 = 1, 3, \dots, (2K - 1)$, the Gaussian process $\mu_\rho^{(i)}(t)$ describes the sum of the scattered component $\mu^{(i)}(t)$ and the LOS component $m^{(i)}(t)$ of the i th subchannel between the source mobile station and the k th mobile relay, i.e., $\mu_\rho^{(i)}(t) = \mu^{(i)}(t) + m^{(i)}(t)$. Whereas, for all even superscripts i , i.e., $i = 2k = 2, 4, \dots, 2K$, the Gaussian process $\mu_\rho^{(i)}(t)$ denotes the sum of the scattered component $\mu^{(i)}(t)$ and the LOS component $m^{(i)}(t)$ of the i th subchannel between the k th mobile relay and the destination mobile station. Each scattered component $\mu^{(i)}(t)$ ($i = 0, 1, 2, \dots, 2K$) is modeled by a zero-mean complex Gaussian process with variance $2\sigma_i^2$. Furthermore, these Gaussian processes are mutually independent, where the spectral properties of each process are characterized by the classical Jakes Doppler power spectral density. The corresponding LOS component $m^{(i)}(t) = \rho_i \exp\{j(2\pi f_\rho^{(i)} t + \theta_\rho^{(i)})\}$ assumes a fixed amplitude ρ_i , a constant Doppler frequency $f_\rho^{(i)}$, and a constant phase $\theta_\rho^{(i)}$.

In (3), A_k is called the relay gain of the k th relay. In order to achieve the optimum performance in a relay-based system, the selection of the relay gain A_k is of critical importance. For fixed-gain relays under NLOS propagation conditions, A_k is usually selected to be [22]

$$A_k = \frac{1}{\sqrt{E \left\{ \left| \mu_{\rho \rightarrow 0}^{(2k-1)}(t) \right|^2 \right\} + N_0}} \quad (4)$$

where $E\{\cdot\}$ is the expectation operator. Thus, $E\{|\cdot|^2\} = 2\sigma_{(2k-1)}^2$ represents the mean power of the NLOS fading channel between the source mobile station and the k th mobile relay. Replacing $\mu_{\rho \rightarrow 0}^{(2k-1)}(t)$ with $\mu_\rho^{(2k-1)}(t)$ in (4) allows us to express the relay gain A_k associated with LOS propagation scenarios as

$$\begin{aligned} A_k &= \frac{1}{\sqrt{E \left\{ \left| \mu_\rho^{(2k-1)}(t) \right|^2 \right\} + N_0}} \\ &= \frac{1}{\sqrt{2\sigma_{(2k-1)}^2 + \rho_{(2k-1)}^2 + N_0}}. \end{aligned} \quad (5)$$

In a practical amplify-and-forward relay system, the total noise $n_r^{(k)}(t)$ in the link from the source mobile station to the destination mobile station via the k th mobile

relay has the following form

$$n_{\text{r}}^{(k)}(t) = A_k \mu_{\rho}^{(2k)}(t) n^{(2k-1)}(t) + n^{(2k)}(t) \tag{6}$$

for all $k = 1, 2, \dots, K$. It is known from the literature (see, e.g., [50] and the references therein) that the total noise $n_{\text{r}}^{(k)}(t)$ can be described under NLOS propagation conditions by a zero-mean complex Gaussian process with variance $N_0 + 2\sigma_{(2k)}^2 N_0 / (2\sigma_{(2k-1)}^2 + N_0)$. It can also be shown that under LOS propagation conditions, the noise process $n_{\text{r}}^{(k)}(t)$ is still a zero-mean complex Gaussian process, its variance changes to $N_0 + (2\sigma_{(2k)}^2 + \rho_{(2k)}^2) N_0 / (2\sigma_{(2k-1)}^2 + \rho_{(2k-1)}^2 + N_0)$.

Finally, the total signal $r(t)$ at the destination mobile station, obtained after combining the signals $r^{(k)}(t)$ received from $K + 1$ diversity branches, can be expressed as

$$r(t) = r^{(0)}(t) + \sum_{k=1}^K r^{(k)}(t) = \Xi_{\rho}(t) s(t) + N(t). \tag{7}$$

This result is valid under the assumption of perfect channel state information (CSI) at the destination mobile station. In (7), $\Xi_{\rho}(t)$ represents the fading envelope at the output of the EG combiner, which can be written as [17]

$$\Xi_{\rho}(t) = \xi(t) + \sum_{k=1}^K \chi_{\rho}^{(k)}(t) = \left| \mu_{\rho}^{(0)}(t) \right| + \sum_{k=1}^K \left| \zeta_{\rho}^{(k)}(t) \right| \tag{8}$$

where $\xi(t)$ and $\chi_{\rho}^{(k)}(t)$ are absolute values of $\mu_{\rho}^{(0)}(t)$ and $\zeta_{\rho}^{(k)}(t)$, respectively. Thus, $\xi(t)$ is the classical Rice process whereas each $\chi_{\rho}^{(k)}(t)$ is a double Rice process. In (7), $N(t)$ is the total received noise is given by $N(t) = n^{(0)}(t) + \sum_{k=1}^K n_{\text{r}}^{(k)}(t)$.

III. STATISTICAL ANALYSIS OF EGC OVER M2M FADING CHANNELS WITH LOS COMPONENTS

In this section, we analyze the statistical properties of EGC over M2M fading channels under LOS propagation conditions. Statistical quantities of interest include the PDF, the CDF, the LCR, and the ADF of double Rice processes with EGC $\Xi_{\rho}(t)$.

A. PDF of a Sum of M2M Fading Processes with LOS Components

Under LOS propagation conditions, the received signal envelope $\Xi_{\rho}(t)$ at the output of the EG combiner is modeled as a sum of a classical Rice process and of a classical Rice process and K independent but not necessarily identical double Rice processes. The PDF $p_{\Xi_{\rho}}(x)$ of this sum process can be obtained by solving

a $(K + 1)$ -dimensional convolution integral. The computation of this convolution integral is however quite tedious. It can further be shown that the evaluation of the inverse Fourier transform of the characteristic function (CF) does not lead to a simple and closed-form expression for the PDF $p_{\Xi_\rho}(x)$ of this sum process. An alternate approach is to approximate the PDF $p_{\Xi}(x)$ of $\Xi(t)$ either by another but a simpler expression or by a series. Here, we follow the approximation approach using orthogonal series expansion. From various options of such series, like, e.g., the Edgeworth series and the Gram-Charlier series, we apply in our analysis the Laguerre series expansion [33]. The Laguerre series provides a good approximation for PDFs that are unimodal (i.e., having single maximum) with fast decaying tails and positive defined random variables. Furthermore, the Laguerre series is often used when the first term of the series provides a good enough statistical accuracy [33].

The PDF $p_{\Xi_\rho}(x)$ of $\Xi_\rho(t)$ can then be expressed using the Laguerre series expansion as [33]

$$p_{\Xi_\rho}(x) = \sum_{n=0}^{\infty} b_n e^{-x} x^{\alpha_L} L_n^{(\alpha_L)}(x) \quad (9)$$

where

$$L_n^{(\alpha_L)}(x) = e^x \frac{x^{(-\alpha_L)} d^n}{x! dx^n} \left[e^{(-x)} x^{n+\alpha_L} \right], \alpha_L > -1 \quad (10)$$

denote the Laguerre polynomials. The coefficients b_n can be given as

$$b_n = \frac{n!}{\Gamma(n + \alpha_L + 1)} \int_0^{\infty} L_n^{(\alpha_L)}(x) p_{\Xi_\rho}(x) dx \quad (11)$$

where $x = y/\beta_L$ and $\Gamma(\cdot)$ is the gamma function [11].

Furthermore, we can obtain the parameters α_L and β_L by solving the system of equations in [33, p. 21] for $b_1 = 0$ and $b_2 = 0$, which yields

$$\alpha_L = \left[\kappa_1^2 / \kappa_2 \right] - 1, \quad \beta_L = \kappa_2 / \kappa_1 \quad (12a,b)$$

where κ_1 corresponds to the first cumulant (i.e., the mean value) and κ_2 represents the second cumulant (i.e., the variance) of the stochastic process $\Xi_\rho(t)$. Mathematically, we can express κ_n ($n = 1, 2$) as

$$\kappa_n = \kappa_n^{(0)} + \sum_{k=1}^K \kappa_n^{(k)} \quad (13)$$

where $\kappa_n^{(0)}$ are the cumulants associated with the classical Rice process $\xi(t)$. The cumulants $\kappa_n^{(0)}$ are equal to [29]

$$\kappa_1^{(0)} = \sigma_0 \sqrt{\frac{\pi}{2}} {}_1F_1\left(-\frac{1}{2}; 1; -\rho_0^2/2\sigma_0^2\right) \tag{14a}$$

$$\kappa_2^{(0)} = 2\sigma_0^2 (1 + \rho_0^2/2\sigma_0^2) - \frac{\pi}{2}\sigma_0^2 \left[{}_1F_1\left(-\frac{1}{2}; 1; -\rho_0^2/2\sigma_0^2\right) \right]^2. \tag{14b}$$

In (13), $\kappa_n^{(k)}$ ($k = 1, 2, \dots, K$) denote the cumulants of the double Rice process $\chi_\rho^{(k)}(t)$. The mean value and the variance of $\chi_\rho^{(k)}(t)$ are as follows [45]

$$\begin{aligned} \kappa_1^{(k)} &= A_k \sigma_{(2k-1)} \sigma_{(2k)} \frac{\pi}{2} {}_1F_1\left(-\frac{1}{2}; 1; -\rho_{(2k-1)}^2/2\sigma_{(2k-1)}^2\right) \\ &\quad \times {}_1F_1\left(-\frac{1}{2}; 1; -\rho_{(2k)}^2/2\sigma_{(2k)}^2\right) \end{aligned} \tag{15a}$$

$$\begin{aligned} \kappa_2^{(k)} &= A_k^2 \left(2\sigma_{(2k-1)}^2 + \rho_{(2k-1)}^2\right) \left(2\sigma_{(2k)}^2 + \rho_{(2k)}^2\right) - \left(A_k \sigma_{(2k-1)} \sigma_{(2k)} \frac{\pi}{2}\right)^2 \\ &\quad \times \left[{}_1F_1\left(-\frac{1}{2}; 1; -\rho_{(2k-1)}^2/2\sigma_{(2k-1)}^2\right) {}_1F_1\left(-\frac{1}{2}; 1; -\rho_{(2k)}^2/2\sigma_{(2k)}^2\right) \right]^2. \end{aligned} \tag{15b}$$

It is imperative to stress that here $\kappa_n^{(k)}$ is computed using the expression for A_k given in (5). In (14a) – (15b), ${}_1F_1(\cdot; \cdot; \cdot)$ is the hypergeometric function [11], which can be expanded as

$${}_1F_1\left(-\frac{1}{2}; 1; -\frac{\rho_{(i)}^2}{2\sigma_{(i)}^2}\right) = e^{-\frac{\rho_{(i)}^2}{4\sigma_{(i)}^2}} \left[\left(1 + \frac{\rho_{(i)}^2}{2\sigma_{(i)}^2}\right) I_0\left(\frac{\rho_{(i)}^2}{4\sigma_{(i)}^2}\right) + \frac{\rho_{(i)}^2}{2\sigma_{(i)}^2} I_1\left(\frac{\rho_{(i)}^2}{4\sigma_{(i)}^2}\right) \right] \tag{16}$$

where $I_n(\cdot)$ is the n th order modified bessel function of first kind [11].

The evaluation of κ_n in (13) is rather straightforward once we have $\kappa_n^{(0)}$ and $\kappa_n^{(k)}$ ($n = 1, 2$) for $\xi(t)$ and all $\chi_\rho^{(k)}(t)$, respectively. Given κ_n , the quantities α_L and β_L can easily be computed using (12a,b). Substitution of α_L and β_L in the Laguerre series expansion leads to the exact solution for the PDF $p_{\Xi_\rho}(x)$. Note that the first term of the Laguerre series can be identified as the gamma distribution $p_\Gamma(x)$ [33]. This makes it possible for us to approximate the PDF $p_{\Xi_\rho}(x)$ of $\Xi_\rho(t)$ to the gamma distribution $p_\Gamma(x)$, i.e.,

$$p_{\Xi_\rho}(x) \approx p_\Gamma(x) = \frac{x^{\alpha_L}}{\beta_L^{(\alpha_L+1)} \Gamma(\alpha_L+1)} e^{-\frac{x}{\beta_L}}. \tag{17}$$

The motivation behind deriving an expression for the PDF $p_{\Xi_\rho}(x)$ of $\Xi_\rho(t)$ is that it can be utilized with ease in the link level performance analysis of dual-hop cooperative networks with EGC. This performance analysis is presented in Section IV.

B. CDF of a Sum of M2M Fading Processes with LOS Components

The probability that $\Xi_\rho(t)$ remains below the threshold level r defines the CDF $F_{\Xi_\rho}(r)$ of $\Xi_\rho(t)$ [27]. After substituting (17) in $F_{\Xi_\rho}(r) = 1 - \int_r^\infty p_{\Xi_\rho}(x) dx$ and solving the integral over x using [11, Eq. (3.381-3)], we can write the CDF $F_{\Xi_\rho}(r)$ in closed form as

$$F_{\Xi_\rho}(r) \approx 1 - \frac{1}{\Gamma(\alpha_L + 1)} \Gamma\left(\alpha_L, \frac{r}{\beta_L}\right) \quad (18)$$

where $\Gamma(\cdot, \cdot)$ is the upper incomplete gamma function [11].

C. LCR of a Sum of M2M Fading Processes with LOS Components

The LCR $N_{\Xi_\rho}(r)$ of $\Xi_\rho(t)$ is a measure to describe the average number of times the stochastic process $\Xi_\rho(t)$ crosses a particular threshold level r from up to down (or from down to up) in a second. The LCR $N_{\Xi_\rho}(r)$ can be computed using the formula [35]

$$N_{\Xi_\rho}(r) = \int_0^\infty \dot{x} p_{\Xi_\rho, \dot{\Xi}_\rho}(r, \dot{x}) d\dot{x} \quad (19)$$

where $p_{\Xi_\rho, \dot{\Xi}_\rho}(r, \dot{x})$ is the joint PDF of the stochastic process $\Xi_\rho(t)$ and its corresponding time derivative $\dot{\Xi}_\rho(t)$ at the same time t . Throughout this paper, the overdot represents the time derivative. The task at hand is to find the joint PDF $p_{\Xi_\rho, \dot{\Xi}_\rho}(r, \dot{x})$. In Section ??, we have shown that the PDF $p_\Xi(x)$ of $\Xi(t)$ can efficiently be approximated by the gamma distribution $p_\Gamma(x)$. Based on this fact, we assume that the joint PDF $p_{\Xi, \dot{\Xi}}(r, \dot{x})$ is approximately equal to the joint PDF $p_{\Gamma, \dot{\Gamma}}(r, \dot{x})$ of a gamma process and its corresponding time derivative at the same time t , i.e.,

$$p_{\Xi_\rho, \dot{\Xi}_\rho}(r, \dot{x}) \approx p_{\Gamma, \dot{\Gamma}}(r, \dot{x}). \quad (20)$$

A gamma distributed process is equivalent to a squared Nakagami- m distributed process [23]. Thus, applying the concept of transformation of random variables [27, p. 244], we can express the joint PDF $p_{\Gamma, \dot{\Gamma}}(x, \dot{x})$ in terms of the joint PDF $p_{NN}(y, \dot{y})$ of a Nakagami- m distributed process and its corresponding time derivative at the same time t as

$$p_{\Gamma, \dot{\Gamma}}(x, \dot{x}) = \frac{1}{4x} p_{NN}\left(\sqrt{x}, \frac{\dot{x}}{2\sqrt{x}}\right). \quad (21)$$

After substituting $p_{NN}(y, \dot{y})$ as given in [52, Eq. (13)] in (21), the joint PDF $p_{\Gamma\dot{\Gamma}}(x, \dot{x})$ can be written as

$$p_{\Gamma\dot{\Gamma}}(x, \dot{x}) = \frac{1}{2\sqrt{2\pi x \dot{\sigma}}} \frac{x^{(m-1)}}{(\Omega/m)^m \Gamma(m)} e^{-\frac{x}{(\Omega/m)} - \frac{\dot{x}^2}{8\dot{\sigma}^2 x}} \quad (22)$$

where m , Ω , and $\dot{\sigma}$ are the parameters associated with the Nakagami- m distribution. The result in (22) can be expressed in terms of the parameters of the gamma distribution, i.e., α_L and β_L , as

$$p_{\Gamma\dot{\Gamma}}(x, \dot{x}) = \frac{1}{2\sqrt{2\pi\beta x}} \frac{x^{\alpha_L}}{\beta_L^{(\alpha_L+1)} \Gamma(\alpha_L + 1)} e^{-\frac{x}{\beta_L} - \frac{\dot{x}^2}{8\beta x}} \quad (23)$$

with $\beta = \pi^2 \left(\kappa_n^{(0)} / \kappa_n^{(0)} \right) (f_{s_{\max}}^2 + f_{d_{\max}}^2) + \pi^2 \left(\sum_{k=1}^K \kappa_2^{(k)} / \sum_{k=1}^K \kappa_1^{(k)} \right) (f_{s_{\max}}^2 + 2f_{r_{\max}}^2 + f_{d_{\max}}^2)$. The quantities $f_{s_{\max}}$ and $f_{d_{\max}}$ represent the maximum Doppler frequencies caused by the motion of the source mobile station and the destination mobile station, respectively. In addition, the maximum Doppler frequencies caused by the motion of mobile relays are assumed to be equal such that $f_{r_{\max}}^{(1)} = f_{r_{\max}}^{(2)} = \dots = f_{r_{\max}}^{(K)} = f_{r_{\max}}$.

Finally, substituting $p_{\Xi\rho\dot{\Xi}\rho}(r, \dot{x})$ in (19) and solving the integral over \dot{x} using [11, Eq. (3.326-2)], we reach a closed-form solution for the LCR $N_{\Xi\rho}(r)$, i.e.,

$$N_{\Xi\rho}(r) \approx \int_0^\infty \dot{x} p_{\Gamma\dot{\Gamma}}(r, \dot{x}) d\dot{x} = \sqrt{\frac{2r\beta}{\pi}} \frac{r^{\alpha_L} e^{-\frac{r}{\beta_L}}}{\beta_L^{(\alpha_L+1)} \Gamma(\alpha_L + 1)} = \sqrt{\frac{2r\beta}{\pi}} p_{\Xi\rho}(r). \quad (24)$$

D. ADF of a Sum of M2M Fading Processes with LOS Components

The ADF $T_{\Xi\rho-}(r)$ of $\Xi\rho(t)$ is the expected value of the time intervals over which the stochastic process $\Xi\rho(t)$ remains below a certain threshold level r . Mathematically, the ADF $T_{\Xi\rho-}(r)$ is defined as the ratio of the CDF $F_{\Xi\rho-}(r)$ and the LCR $N_{\Xi\rho}(r)$ of $\Xi\rho(t)$ [17], i.e.,

$$T_{\Xi\rho-}(r) = \frac{F_{\Xi\rho-}(r)}{N_{\Xi\rho}(r)}. \quad (25)$$

By substituting (18) and (24) in (25), we can easily obtain an approximate solution for the ADF $T_{\Xi\rho-}(r)$.

The significance of studying the LCR $N_{\Xi\rho}(r)$ and the ADF $T_{\Xi\rho-}(r)$ of $\Xi\rho(t)$ lies in the fact that they provide insight into the rate of fading of the stochastic process $\Xi\rho(t)$. Knowledge about the rate of fading is beneficial in both the design as well as optimization of coding and interleaving schemes to combat M2M fading in the relay links in cooperative networks.

IV. PERFORMANCE ANALYSIS IN M2M FADING CHANNELS WITH LOS COMPONENTS AND EGC

This section is dedicated to the systems' performance analysis in M2M fading channels with EGC under LOS propagation conditions. The performance evaluation measures of interest include the PDF as well as the moments of the SNR, AOF, the average BEP, and the outage probability.

A. Analysis of the SNR

1) *Derivation of the Instantaneous SNR Expression:* We computed the total received signal envelope at the output of the EG combiner $\Xi_\rho(t)$ and the total received noise $N(t)$ in Section II. Using these results, we can now express the instantaneous SNR per bit $\gamma_{\text{EGC}}(t)$ at the output of the EG combiner as [41, 37]

$$\gamma_{\text{EGC}}(t) = \frac{\Xi_\rho^2(t)}{E\{N^2(t)\}} E_b \quad (26)$$

where E_b is the energy (in joules) per bit and $E\{N^2(t)\}$ is the mean power of the total received noise. The mean value of the total noise power can be given as

$$\begin{aligned} E\{N^2(t)\} &= E \left\{ \left(n^{(0)}(t) + \sum_{k=1}^K n_\tau^{(k)}(t) \right)^2 \right\} \\ &= (K+1)N_0 + \sum_{k=1}^K \frac{2\sigma_{(2k)}^2 + \rho_{(2k)}^2}{2\sigma_{(2k-1)}^2 + \rho_{(2k-1)}^2 + N_0} N_0. \end{aligned} \quad (27)$$

2) *PDF of the SNR:* The PDF $p_{\gamma_{\text{EGC}}}(z)$ of $\gamma_{\text{EGC}}(t)$ can be obtained using the relation

$$p_{\gamma_{\text{EGC}}}(z) = \frac{1}{(E_b/E\{N^2(t)\})} p_{\Xi_\rho^2} \left(\frac{z}{E_b/E\{N^2(t)\}} \right) \quad (28)$$

where $p_{\Xi_\rho^2}(z)$ is the squared received signal envelope $\Xi_\rho^2(t)$ at the output of the EG combiner, which can be obtained by a simple transformation of the random variables [27, p. 244] as follows:

$$\begin{aligned} p_{\Xi_\rho^2}(z) &= \frac{1}{2\sqrt{z}} p_{\Xi_\rho}(\sqrt{z}) \\ &\approx \frac{1}{2\beta_L^{(\alpha_L+1)} \Gamma(\alpha_L+1)} z^{\left(\frac{\alpha_L-1}{2}\right)} e^{-\frac{\sqrt{z}}{\beta_L}}, \quad z \geq 0. \end{aligned} \quad (29)$$

The substitution of (29) in (28) leads us to the closed-form approximation for the PDF $p_{\gamma_{\text{EGC}}}(z)$ of $\gamma_{\text{EGC}}(t)$, i.e.,

$$p_{\gamma_{\text{EGC}}}(z) \approx \frac{1}{2(E_b/E\{N^2(t)\})^{(\frac{\alpha_L+1}{2})} \beta_L^{(\alpha_L+1)} \Gamma(\alpha_L+1)} z^{(\frac{\alpha_L-1}{2})} e^{-\frac{\sqrt{z}}{\beta_L \sqrt{E_b/E\{N^2(t)\}}}}. \quad (30)$$

3) *Moments of the SNR*: Substituting (30) in $m_{\gamma_{\text{EGC}}}^{(n)} = \int_{-\infty}^{\infty} z^n p_{\gamma_{\text{EGC}}}(z) dz$ and solving the integral over z using [11, Eq. (3.478-1)] allows us to express the n th moment of the SNR $\gamma_{\text{EGC}}(t)$ in a closed form as

$$m_{\gamma_{\text{EGC}}}^{(n)} \approx \beta_L^{2n} \left(\frac{E_b}{E\{N^2(t)\}} \right)^n \frac{\Gamma(\alpha_L + 2n + 1)}{\Gamma(\alpha_L + 1)}. \quad (31)$$

4) *Amount of Fading*: The AOF is defined as the ratio of the variance $\sigma_{\gamma_{\text{EGC}}}^2$ and the squared mean value $m_{\gamma_{\text{EGC}}}^{(1)}$ of the SNR $\gamma_{\text{EGC}}(t)$, i.e., [4, 13]

$$AOF = \frac{\sigma_{\gamma_{\text{EGC}}}^2}{(m_{\gamma_{\text{EGC}}}^{(1)})^2} = \frac{m_{\gamma_{\text{EGC}}}^{(2)} - (m_{\gamma_{\text{EGC}}}^{(1)})^2}{(m_{\gamma_{\text{EGC}}}^{(1)})^2}. \quad (32)$$

Computing the first two moments of $\gamma_{\text{EGC}}(t)$ using (31) and substituting the results in (32) yields the following closed-form approximation for the AOF

$$AOF \approx (\alpha_L^2 + 7\alpha_L + 12) \beta_L^2 \Gamma(\alpha_L + 1) - 1. \quad (33)$$

B. Average BEP

The average BEP P_b over the fading channel statistics at the output of the EG combiner can be obtained using the formula [41]

$$P_b = \int_0^{\infty} p_{\Xi_\rho}(x) P_{b|\Xi_\rho}(x) dx \quad (34)$$

where $P_{b|\Xi_\rho}(x)$ is the BEP of M -ary PSK modulation schemes conditioned on the fading amplitudes $\{x_k\}_{k=0}^K$, and $x = \sum_{k=0}^K x_k$. Here, the fading amplitude x_0 follows the classical Rice distribution. Furthermore, the fading amplitudes $\{x_k\}_{k=1}^K$ possess the double Rice distribution.

The conditional BEP $P_{b|\Xi_\rho}(x)$ of M -ary PSK modulation schemes can be ap-

proximated as [10]

$$\begin{aligned} P_{b|\Xi_p}(x) &\approx \frac{a}{\log_2 M} Q\left(\sqrt{2g \log_2 M \gamma_{\text{EGC}}(x)}\right) \\ &\approx \frac{a}{\log_2 M} Q\left(\sqrt{\frac{2g \log_2 M E_b}{E\{N^2(t)\}} x^2}\right) \end{aligned} \quad (35)$$

where $M = 2^b$ with b as the number of bits per symbol, $Q(\cdot)$ is the error function [11]. The parameter a equals 1 or 2 for M -ary PSK modulation schemes when $M = 2$ or $M > 2$, respectively, whereas for all M -ary PSK modulation schemes $g = \sin^2(\pi/M)$ [48].

Substituting (17) and (35) in (34) leads to the approximate solution for the average BEP P_b , i.e.,

$$P_b \approx \frac{a}{\log_2 M} \frac{1}{\beta_L^{(\alpha_L+1)} \Gamma(\alpha_L+1)} \int_0^\infty x^{\alpha_L} e^{-\frac{x}{\beta_L}} Q\left(\sqrt{\frac{2g \log_2 M E_b}{E\{N^2(t)\}} x^2}\right) dx. \quad (36)$$

C. Outage Probability

The outage probability $P_{out}(\gamma_{th})$ is defined as the probability that the SNR $\gamma_{\text{EGC}}(t)$ at the output of the EG combiner falls below a certain threshold level γ_{th} . Substituting (30) in $P_{out}(\gamma_{th}) = Pr\{\gamma_{\text{EGC}} \leq \gamma_{th}\} = 1 - \int_{\gamma_{th}}^\infty p_{\gamma_{\text{EGC}}}(z) dz$

$$P_{out}(\gamma_{th}) \approx 1 - \frac{1}{\Gamma(\alpha_L+1)} \Gamma\left(\alpha_L+1, \frac{\sqrt{\gamma_{th}}}{\beta_L \sqrt{E_b/E\{N^2(t)\}}}\right). \quad (37)$$

V. NUMERICAL RESULTS

The aim of this section is to evaluate and to illustrate the derived theoretical approximations given in (17), (24), (25), (36), and (37) as well as to investigate their accuracy. The correctness of the approximated analytical results is confirmed by evaluating the statistics of the waveforms generated by utilizing the sum-of-sinusoids (SOS) method [29]. These simulation results correspond to the true (exact) results here. The waveforms $\tilde{\mu}^{(i)}(t)$ obtained from the designed SOS-based channel simulator are considered as an appropriate model for the uncorrelated Gaussian noise processes $\mu^{(i)}(t)$ making up the received signal envelope at the output of the EG combiner. The model parameters of the channel simulator have been computed by using the generalized method of exact Doppler spread (GMEDS₁) [32]. Each waveform $\tilde{\mu}^{(i)}(t)$ was generated with $N_l^{(i)} = 14$ for $i = 0, 1, 2, \dots, 2K$ and $l = 1, 2$, where $N_l^{(i)}$ is the number of sinusoids chosen to simulate the inphase

($l = 1$) and quadrature ($l = 2$) components of $\tilde{\mu}^{(i)}(t)$. It is widely acknowledged that the distribution of the simulated waveforms $|\tilde{\mu}^{(i)}(t)|$ closely approximates the Rayleigh distribution if $N_l^{(i)} \geq 7$ ($l = 1, 2$) [29]. Thus, by selecting $N_l^{(i)} = 14$, we ensure that the waveforms $\tilde{\mu}^{(i)}(t)$ have the required Gaussian distribution. The variance of the inphase and quadrature component of $\mu^{(i)}(t)$ ($\tilde{\mu}^{(i)}(t)$) is equal to $\sigma_i^2 = 1 \forall i = 0, 1, 2, \dots, 2K$, unless stated otherwise. The maximum Doppler frequencies caused by the motion of the source mobile station, K mobile relays, and the destination mobile station, denoted by $f_{s_{\max}}$, $f_{r_{\max}}$, and $f_{d_{\max}}$, respectively, were set to 91 Hz, 125 Hz, and 110 Hz. The total number of symbols used for a reliable generation of BEP curves was 10^7 .

In this section, we have attempted to highlight the influence of a LOS component on the statistics of the received signal envelope at the output of the EG combiner and the systems' overall performance. This is done by considering three propagation scenarios called the full-LOS, the partial-LOS, and the NLOS scenario, denoted by $LOS_{K,K}$, $LOS_{K,0}$ ($LOS_{0,K}$), and $LOS_{0,0}$, respectively. Here, K corresponds to the number of mobile relays in the network. In the full-LOS scenario, we have LOS components in the direct link as well as all the transmission links between the source mobile station and the destination mobile station via K mobile relays. The scenario in which LOS components are present only in some few links from the source mobile station to the destination mobile station via K mobile relays is referred to as the partial-LOS scenario. When LOS components do not exist in any of the transmission links, we have the NLOS scenario. Whenever, there exists a LOS component in any of the transmission links, its amplitude ρ_i is taken to be unity. It is necessary to keep in mind that there is a direct link between the source mobile station and the destination mobile station, in addition to the links via K mobile relays. Therefore, the total number of diversity branches available is $K + 1$. The presented results in Figs. M.2–M.8 display a good fit of the approximated analytical and the exact simulation results.

Figure M.2 demonstrates the theoretical approximation for the PDF $p_{\Xi_\rho}(x)$ of $\Xi_\rho(t)$ described in (17). This figure contains the PDF $p_{\Xi_\rho}(x)$ of $\Xi_\rho(t)$ under full-LOS, partial-LOS, and NLOS propagation conditions considering a different number of mobile relays K . It is quite obvious from the figure that for any value of K , the presence of LOS components increases both the mean value and the variance of $\Xi_\rho(t)$. Furthermore, for $LOS_{K,K}$ when $K = 1$, as $\sigma_0^2 \rightarrow 0$ the PDF $p_{\Xi_\rho}(x)$ of $\Xi_\rho(t)$ maps to the double Rice distribution, whereas it reduces to the double Rayleigh distribution for $LOS_{0,0}$. Another important result is that the PDF $p_{\Xi_\rho}(x)$ of $\Xi_\rho(t)$ tends to a Gaussian distribution if K increases. This observation is in accordance

with the central limit theorem (CLT) [27]. A close agreement between the approximated theoretical and the exact simulation results confirms the correctness of our approximation.

The LCR $N_{\Xi_\rho}(r)$ of $\Xi_\rho(t)$ described by (24) is evaluated along with the exact simulation results in Fig. M.3. This figure presents the LCR $N_{\Xi_\rho}(r)$ of $\Xi_\rho(t)$ corresponding to $LOS_{K,K}$, $LOS_{K,0}$ ($LOS_{0,K}$), and $LOS_{0,0}$ scenarios considering a different number of mobile relays K in the system. It can be observed that in general, for any value of K , at low signal levels r , LOS components facilitate in decreasing $N_{\Xi_\rho}(r)$. However, at high signal levels r , the presence of LOS components contributes towards the increase in $N_{\Xi_\rho}(r)$. These results also illustrate that for all the three considered propagation scenarios, at any signal level r , (24) closely approximates the exact simulation results when $K > 1$. This is in contrast with when $K = 1$, where (24) holds only for high values of r . We can further deduce from these results that by increasing K , $N_{\Xi_\rho}(r)$ can be reduced for lower values of r , whereas it increases for higher values of r . It is also worth noticing that at higher values of r , for $LOS_{K,K}$ when $K = 1$, as $\sigma_0^2 \rightarrow 0$, (24) provides us with a very close approximation to the exact LCR of a double Rice process given in [45], whereas it approximates well to the exact LCR of a double Rayleigh process for $LOS_{0,0}$ [28].

In Fig. M.4, the analytical approximate results of the ADF $T_{\Xi_{\rho-}}(r)$ of $\Xi_\rho(t)$ described by (25) along with the exact simulation results are displayed. These results clearly indicate that for all propagation scenarios, i.e., $LOS_{K,K}$, $LOS_{K,0}$ ($LOS_{0,K}$), and $LOS_{0,0}$ scenarios, increasing K results in a decrease of $T_{\Xi_{\rho-}}(r)$ at all signal levels r . It can also be observed in Fig. M.4 that the presence of the LOS components in all the transmission links lowers $T_{\Xi_{\rho-}}(r)$ for all signal levels r and any number K .

The average BEP P_b of M -ary PSK modulation schemes over M2M fading channels with LOS components and EGC described by (36) is presented in Fig. M.5. In this figure, a comparison of the average BEP P_b of quadrature PSK (QPSK), 8-PSK, as well as 16-PSK modulation schemes is shown by taking into account $K + 1$ diversity branches for each modulation scheme. The average BEP P_b curves associated with the aforementioned modulation schemes in double Rice channels are also included in Fig. M.5. Here, the average BEP P_b is evaluated for $LOS_{K,K}$, i.e., $\rho_i = 1 \forall i = 0, 1, 2, \dots, 2K$. For all modulation schemes, when $K = 1$, a significant enhancement in the diversity gain can be observed with the availability of just one extra transmission link. See, e.g., when the direct link from the source mobile station to the destination mobile station is not blocked by obstacles and there is one relay present in the system, then at $P_b = 10^{-3}$, it is possible to attain a diversity gain

of approximately 21 dB. Increasing the number, K , of mobile relays in the system, in turn increases the number of diversity branches and hence improves performance. Provision of higher data rates is the characteristic feature of higher-order modulation schemes. These modulations are however known to be more prone to errors. This sensitivity of higher-order modulations towards errors is visible in Fig. M.5 as the average BEP P_b curve associated with QPSK modulation shifts to the right when 8-PSK or 16-PSK modulation schemes are deployed.

An EG combiner installed at the destination mobile station makes a receiver diversity system. In addition to the diversity gain, such systems offer array gain as well [10]. The array gain in fact results from coherent combining of multiple received signals. In the context of EGC, the array gain allows the receiver diversity system in a fading channel to achieve better performance than a system without diversity in an AWGN channel with the same average SNR [10]. Figure M.6 includes the theoretical results of the average BEP P_b of QPSK under full-LOS propagation conditions (i.e., the $LOS_{K,K}$ scenario) with increasing number of diversity branches. In the presented results, $K \geq 10$ implies that we have ≥ 11 diversity branches. Note that in Fig. M.6, for $K \geq 10$, the dual-hop amplify-and-forward system with M2M fading channels has a lower error probability than a system in an AWGN channel with the same SNR. This improved performance is due to the array gain of the EG combiner.

Figure M.7 illustrates the impact of the existence of LOS components in the relay links on the average BEP P_b of M -ary PSK modulation schemes. Keeping the number of diversity branches constant, e.g., for $K = 3$, the average BEP P_b of QPSK and 16-PSK modulation schemes is evaluated for the $LOS_{K,K}$, $LOS_{K,0}$ ($LOS_{0,K}$), and $LOS_{0,0}$ scenarios. For both QPSK and 16-PSK modulations, there is a noticeable gain in the performance when going from $LOS_{0,0}$ to $LOS_{K,K}$. See, e.g., at $P_b = 10^{-4}$, a gain of approximately 1.5 dB is achieved when we have $LOS_{K,0}$ ($LOS_{0,K}$) compared to $LOS_{0,0}$. A further increase of ≈ 1 dB in the gain can be seen if $LOS_{K,K}$ conditions are available.

Finally, the outage probability $P_{out}(\gamma_{th})$ described by (37) is evaluated along with the exact simulation results in Fig. M.8. Under full-LOS propagation conditions with QPSK modulation scheme employed in our analysis, $P_{out}(\gamma_{th})$ for a different number of diversity branches is obtained. The presented results show a decrease in $P_{out}(\gamma_{th})$, which is due to EGC deployed at the destination mobile station and the resulting performance advantage is the diversity gain.

VI. CONCLUSION

This article provides a profound study pertaining to the statistical properties of EGC over M2M fading channels under LOS propagation conditions in relay-based networks. In addition, vital information about the performance of relay-based cooperative systems in such channels is made available. The system under investigation is a dual-hop amplify-and-forward relay communication system, where K mobile relays are arranged in parallel between the source mobile station and the destination mobile station. It is further assumed that the direct link from the source mobile station to the destination mobile station is not blocked by any obstacles. Such a configuration gives rise to $K + 1$ diversity branches. The signals received from the $K + 1$ diversity branches are then combined at the destination mobile station to achieve the spatial diversity gain. In order to accommodate the direct link along with the unbalanced relay links, we have modeled the received signal envelope at the output of the EG combiner as a sum of a classical Rice process and K double Rice processes. Furthermore, the classical Rice process and double Rice processes are independent. Besides, the double Rice processes are independent but not necessarily identically distributed.

In order to achieve the optimum performance in relay-based systems, the selection of the relay gain is of critical importance. Therefore, we have derived and verified the optimal relay gain associated with LOS propagation scenarios. Utilizing the derived relay gain in the statistical analysis simple and closed-form analytical approximations for the channel statistics such as the PDF, CDF, LCR, and ADF are derived. Here, the Laguerre series expansion has been employed to approximate the PDF of the sum of classical Rice and K double Rice processes. The advantage of using the Laguerre series is that this makes it possible to approximate the PDF of the sum process by a gamma distribution with reasonable accuracy. The CDF, LCR, and ADF of the sum process are also approximated by exploiting the properties of a gamma distributed process. Furthermore, the presented results demonstrate that the approximated theoretical results fit closely to the exact simulation results. This thus provides us with a reason to believe that the approximation approach followed in this study is valid. In addition to studying the impact of the number of diversity branches, we have included in our discussion the influence of the existence of the LOS components in the transmission links on the statistical properties of EGC over M2M channels.

The utilization of the presented statistical analysis is then demonstrated in performance evaluation of dual-hop multi-relay cooperative systems. In this work, the performance assessment measures of interest are the PDF as well as the mo-

ments of the instantaneous SNR, AOF, average BEP, and outage probability. The required SNR can be expressed as the ratio of the squared received signal envelope at the output of EG combiner and the total received noise. Furthermore, the total received noise is modeled as a sum of the noise component inherently existing in the transmission link between the k th mobile relay and the destination mobile (i.e., AWGN) and the noise component that is amplified by the k th mobile relay and then is forwarded. The PDF of the instantaneous SNR can, thus, be obtained from the previously derived PDF of the sum process by a simply transformation of random variables. Given the PDF of the instantaneous SNR, the computation of the moments of SNR, AOF, and outage probability is rather straightforward. It can be concluded from the presented results that generally, in a dual-hop relay system with EGC, the presence of LOS components in the transmission links improves the systems' performance.

REFERENCES

- [1] P. A. Anghel and M. Kaveh. Exact symbol error probability of a cooperative network in a Rayleigh fading environment. *IEEE Trans. Wireless Commun.*, 3(5):1416–1421, September 2004.
- [2] K. Azarian, H. E. Gamal, and P. Schniter. On the achievable diversity-multiplexing tradeoff in half-duplex cooperative channels. *IEEE Trans. Inform. Theory*, 51(12):4152–4172, December 2005.
- [3] N. C. Beaulieu and X. Dong. Level crossing rate and average fade duration of MRC and EGC diversity in Ricean fading. *IEEE Trans. Commun.*, 51(5):722–726, May 2003.
- [4] U. Charash. Reception through Nakagami fading multipath channels with random delays. *IEEE Trans. Commun.*, 27(4):657–670, April 1979.
- [5] S. Chitroub, A. Houacine, and B. Sansal. Statistical characterisation and modelling of SAR images. *Elsevier, Signal Processing*, 82(1):69–92, January 2002. DOI [http://dx.doi.org/10.1016/S0165-1684\(01\)00158-X](http://dx.doi.org/10.1016/S0165-1684(01)00158-X).
- [6] D. B. da Costa and S. Aissa. Performance of cooperative diversity networks: Analysis of amplify-and-forward relaying under equal-gain and maximal-ratio combining. In *Proc. IEEE Int. Conf. Communications (ICC'09)*, pages 1–5. Dresden, Germany, June 2009. DOI 10.1109/ICC.2009.5199330.

- [7] M. Di Renzo, F. Graziosi, and F. Santucci. A comprehensive framework for performance analysis of dual-hop cooperative wireless systems with fixed-gain relays over generalized fading channels. *IEEE Trans. Wireless Commun.*, 8(10):5060 – 5074, October 2009.
- [8] M. Dohler and Y. Li. *Cooperative Communications: Hardware, Channel, and PHY*. Chichester: John Wiley & Sons, 1st edition, 2010.
- [9] Y. Fan and J. S. Thompson. MIMO configurations for relay channels: Theory and practice. *IEEE Trans. Wireless Commun.*, 6(5):1774–1786, May 2007.
- [10] A. Goldsmith. *Wireless Communications*. New York: Cambridge University Press, 2005.
- [11] I. S. Gradshteyn and I. M. Ryzhik. *Table of Integrals, Series, and Products*. New York: Academic Press, 6th edition, 2000.
- [12] O. M. Hasna and M. S. Alouini. End-to-end performance of transmission systems with relays over Rayleigh-fading channels. *IEEE Trans. Wireless Commun.*, 2(6):1126 – 1131, November 2003.
- [13] H. Q. Huynh, S. I. Husain, J. Yuan, A. Razi, and D. S. Taubman. Performance analysis of multi-branch non-regenerative relay systems with EGC in Nakagami- m channels. In *Proc. IEEE 70th Veh. Technol. Conf., VTC'09-Fall*, pages 1–5. Anchorage, AK, USA, September 2009. DOI 10.1109/VETEFCF.2009.5378710.
- [14] S. S. Ikki and M. H. Ahmed. Performance of cooperative diversity using equal gain combining (EGC) over Nakagami- m fading channels. *IEEE Trans. Wireless Commun.*, 8(2):557–562, February 2009.
- [15] H. Ilhan, M. Uysal, and I. Altunbas. Cooperative diversity for intervehicular communication: Performance analysis and optimization. *IEEE Trans. Veh. Technol.*, 58(7):3301 – 3310, August 2009.
- [16] P. Ivanis, D. Drajić, and B. Vucetic. The second order statistics of maximal ratio combining with unbalanced branches. *IEEE Communications Letters*, 12(7):508–510, July 2008.
- [17] W. C. Jakes, editor. *Microwave Mobile Communications*. Piscataway, NJ: IEEE Press, 1994.

- [18] G. K. Karagiannidis, N. C. Sagias, and P. T. Mathiopoulos. N*Nakagami: A novel stochastic model for cascaded fading channels. *IEEE Trans. Commun.*, 55(8):1453–1458, August 2007.
- [19] I. Z. Kovacs, P. C. F. Eggers, K. Olesen, and L. G. Petersen. Investigations of outdoor-to-indoor mobile-to-mobile radio communication channels. In *Proc. IEEE 56th Veh. Technol. Conf., VTC'02-Fall*, volume 1, pages 430–434. Vancouver BC, Canada, September 2002.
- [20] J. N. Laneman, D. N. C. Tse, and G. W. Wornell. Cooperative diversity in wireless networks: Efficient protocols and outage behavior. *IEEE Trans. Inform. Theory*, 50(12):3062–3080, December 2004.
- [21] Y. Li and S. Kishore. Asymptotic analysis of amplify-and-forward relaying in Nakagami fading environments. *IEEE Trans. Wireless Commun.*, 6(12):4256–4262, December 2007.
- [22] R. U. Nabar, H. Bölcskei, and F. W. Kneubühler. Fading relay channels: Performance limits and space-time signal design. *IEEE J. Select. Areas Commun.*, 22(6):1099–1109, August 2004.
- [23] M. Nakagami. The m -distribution: A general formula of intensity distribution of rapid fading. In W. G. Hoffman, editor, *Statistical Methods in Radio Wave Propagation*. Oxford, UK: Pergamon Press, 1960.
- [24] H. W. Nylund. Characteristics of small-area signal fading on mobile circuits in the 150 MHz band. *IEEE Trans. Veh. Technol.*, 17:24–30, October 1968.
- [25] Y. Okumura, E. Ohmori, T. Kawano, and K. Fukuda. Field strength and its variability in VHF and UHF land mobile radio services. *Rev. Elec. Commun. Lab.*, 16:825–873, September/October 1968.
- [26] R. Pabst, B. Walke, D. Schultz, et al. Relay-based deployment concepts for wireless and mobile broadband radio. *IEEE Communications Magazine*, 42(9):80–89, September 2004.
- [27] A. Papoulis and S. U. Pillai. *Probability, Random Variables and Stochastic Processes*. New York: McGraw-Hill, 4th edition, 2002.
- [28] C. S. Patel, G. L. Stüber, and T. G. Pratt. Statistical properties of amplify and forward relay fading channels. *IEEE Trans. Veh. Technol.*, 55(1):1–9, January 2006.

- [29] M. Pätzold. *Mobile Fading Channels*. Chichester: John Wiley & Sons, 2002.
- [30] M. Pätzold, B. O. Hogstad, and N. Youssef. Modeling, analysis, and simulation of MIMO mobile-to-mobile fading channels. *IEEE Trans. Wireless Commun.*, 7(2):510–520, February 2008.
- [31] M. Pätzold, U. Killat, and F. Laue. An extended Suzuki model for land mobile satellite channels and its statistical properties. *IEEE Trans. Veh. Technol.*, 47(2):617–630, May 1998.
- [32] M. Pätzold, C. X. Wang, and B. O. Hogstad. Two new sum-of-sinusoids-based methods for the efficient generation of multiple uncorrelated Rayleigh fading waveforms. *IEEE Trans. Wireless Commun.*, 8(6):3122–3131, June 2009.
- [33] S. Primak, V. Kontorovich, and V. Lyandres, editors. *Stochastic Methods and their Applications to Communications: Stochastic Differential Equations Approach*. Chichester: John Wiley & Sons, 2004.
- [34] A. Ribeiro, X. Cai, and G. B. Giannakis. Symbol error probabilities for general cooperative links. *IEEE Trans. Wireless Commun.*, 4(3):1264 – 1273, May 2005.
- [35] S. O. Rice. Mathematical analysis of random noise. *Bell Syst. Tech. J.*, 24:46–156, January 1945.
- [36] H. Samimi and P. Azmi. An approximate analytical framework for performance analysis of equal gain combining technique over independent Nakagami, Rician and Weibull fading channels. *Wireless Personal Communications (WPC)*, 43(4):1399–1408, dec 2007. DOI 10.1007/s11277-007-9314-z.
- [37] M. Schwartz, W. R. Bennett, and S. Stein. *Communication Systems and Techniques*, volume 4. New York: McGraw Hill, 1966.
- [38] A. Sendonaris, E. Erkip, and B. Aazhang. User cooperation diversity — Part I: System description. *IEEE Trans. Commun.*, 51(11):1927–1938, November 2003.
- [39] A. Sendonaris, E. Erkip, and B. Aazhang. User cooperation diversity — Part II: Implementation aspects and performance analysis. *IEEE Trans. Commun.*, 51(11):1939–1948, November 2003.

- [40] P. M. Shankar. Error rates in generalized shadowed fading channels. *Wireless Personal Communications (WPC)*, 28(3):233–238, February 2004. DOI <http://dx.doi.org/10.1023/B:wire.0000032253.68423.86>.
- [41] M. K. Simon and M. S. Alouini. *Digital Communications over Fading Channels*. New Jersey: John Wiley & Sons, 2nd edition, 2005.
- [42] W. Su, A. K. Sadek, and K. J. R. Liu. Cooperative communication protocols in wireless networks: Performance analysis and optimum power allocation. *Wireless Personal Communications (WPC)*, 44(2):181–217, January 2008.
- [43] H. Suraweera, G. Karagiannidis, and P. Smith. Performance analysis of the dual-hop asymmetric fading channel. 8(6):2783 – 2788, June 2009.
- [44] H. Suzuki. A statistical model for urban radio propagation. *IEEE Trans. Commun.*, 25(7):673–680, July 1977.
- [45] B. Talha and M. Pätzold. On the statistical properties of double Rice channels. In *Proc. 10th Int. Symp. on Wireless Personal Multimedia Communications, WPMC 2007*, pages 517–522. Jaipur, India, December 2007.
- [46] B. Talha, M. Pätzold, and S. Primak. Performance analysis of M -ary PSK modulation schemes over multiple double Rayleigh fading channels with EGC in cooperative networks. In *Proc. IEEE Int. Conf. Communications, Workshop on Vehicular Connectivity, Veh-Con 2010*. Cape Town, South Africa, May 2010. DOI 10.1109/ICCW.2010.5503940.
- [47] T. A. Tsiftsis, G. K. Karagiannidis, and S. A. Kotsopoulos. Dual-hop wireless communications with combined gain relays. *IEE Proc. Communications*, 152(5):528 – 532, October 2005.
- [48] W. Wongtrairat and P. Supnithi. Performance of digital modulation in double Nakagami- m fading channels with MRC diversity. *IEICE Trans. Commun.*, E92-B(2):559–566, February 2009.
- [49] L. Wu, J. Lin, K. Niu, and Z. He. Performance of dual-hop transmissions with fixed gain relays over generalized- K fading channels. In *Proc. IEEE Int. Conf. Communications (ICC'09)*. Dresden, Germany, June 2009. DOI 10.1109/ICC.2009.5199331.
- [50] Y. Wu and M. Pätzold. Parameter optimization for amplify-and-forward relaying systems with pilot symbol assisted modulation scheme. *Wireless Sensor Networks (WSN)*, 1(1):15–21, April 2009. DOI 10.4236/wsn.2009.11003.

- [51] F. Xu, F. C. M. Lau, and D. W. Yue. Diversity order for amplify-and-forward dual-hop systems with fixed-gain relay under Nakagami fading channels. 9(1):92 – 98, January 2010.
- [52] M. D. Yacoub, J. E. V. Bautista, and L. G. de Rezende Guedes. On higher order statistics of the Nakagami- m distribution. *IEEE Trans. Veh. Technol.*, 48(3):790–794, May 1999.
- [53] M. D. Yacoub, C. R. C. Monterio da Silva, and J. E. V. Bautista. Second-order statistics for diversity-combining techniques in Nakagami fading channels. *IEEE Trans. Veh. Technol.*, 50(6):1464–1470, November 2001.
- [54] W. R. Young. Comparison of mobile radio transmission at 150, 450, 900, and 3700 MHz. 31:1068–1085, November 1952.
- [55] Q. T. Zhang. Probability of error for equal-gain combiners over Rayleigh channels: some closed-form solutions. *IEEE Trans. Commun.*, 45(3):270–273, March 1997.
- [56] D. A. Zogas, G. K. Karagiannidis, and S. A. Kotsopoulos. Equal gain combining over Nakagami- n (Rice) and Nakagami- q (Hoyt) generalized fading channels. *IEEE Trans. Wireless Commun.*, 4(2):374–379, March 2005.

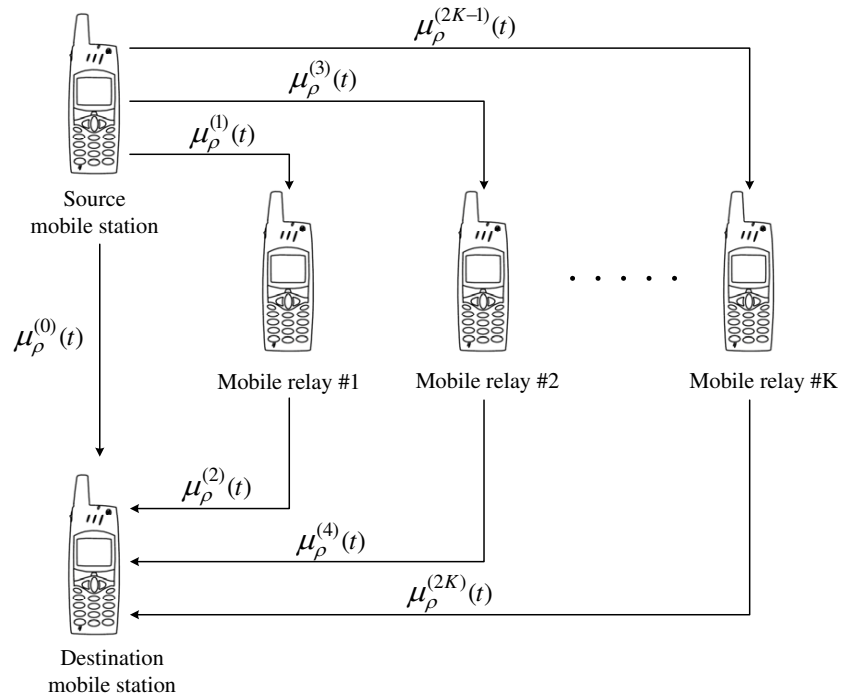


Figure M.1: The propagation scenario describing K -parallel dual-hop relay M2M fading channels.

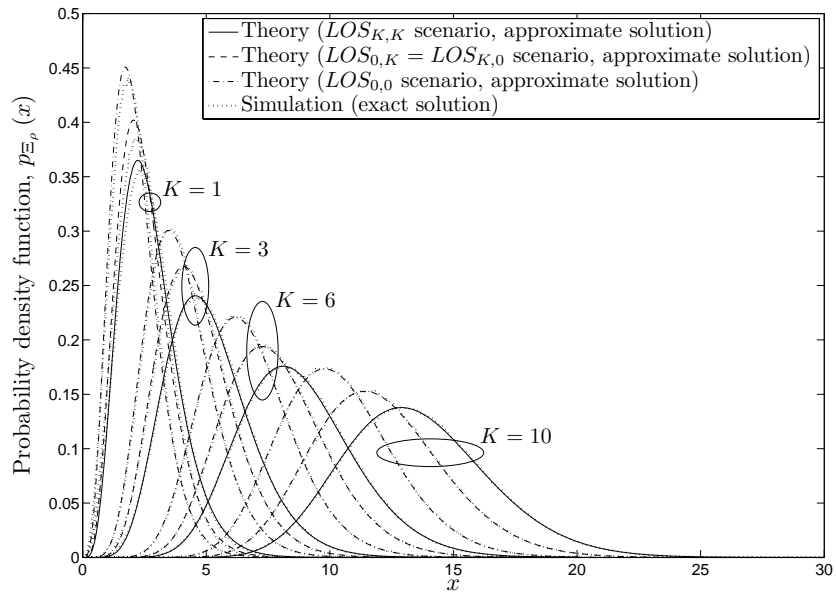


Figure M.2: The PDF $p_{\Xi_\rho}(x)$ of the received signal envelope at the output of the EG combiner $\Xi_\rho(t)$ for $K + 1$ diversity branches under different propagation conditions.

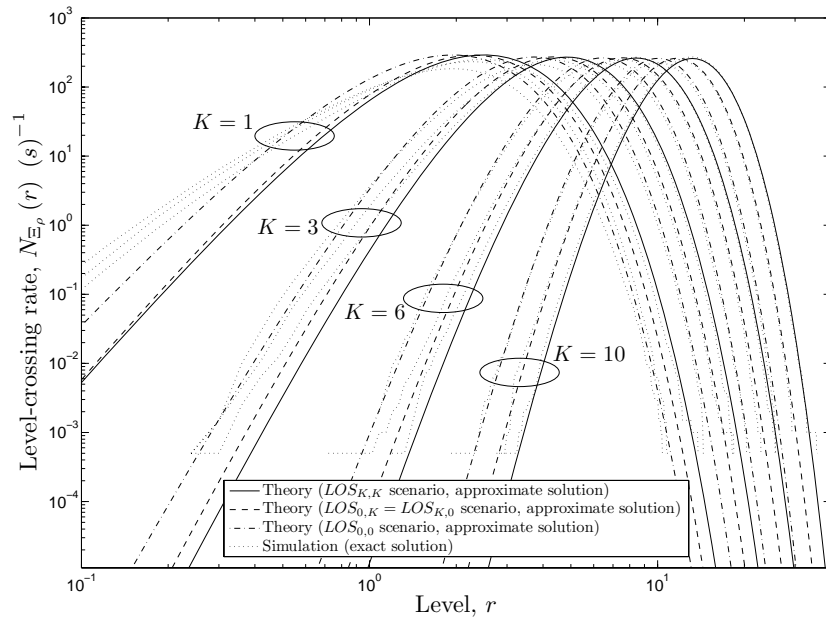


Figure M.3: The LCR $N_{E_{\rho}}(r)$ of the received signal envelope at the output of the EG combiner $E_{\rho}(t)$ for $K + 1$ diversity branches under different propagation conditions.

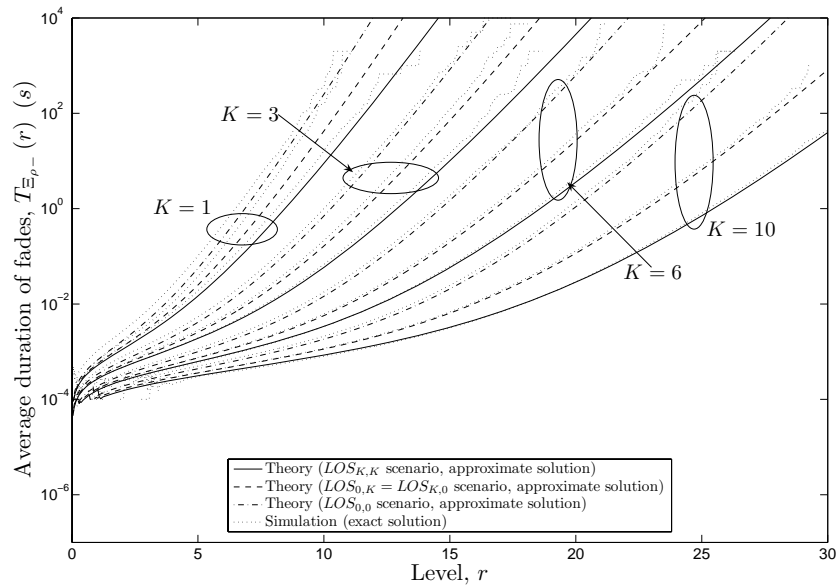


Figure M.4: The ADF $T_{E_{\rho}}(r)$ of the received signal envelope at the output of the EG combiner $E_{\rho}(t)$ for $K + 1$ diversity branches under different propagation conditions.

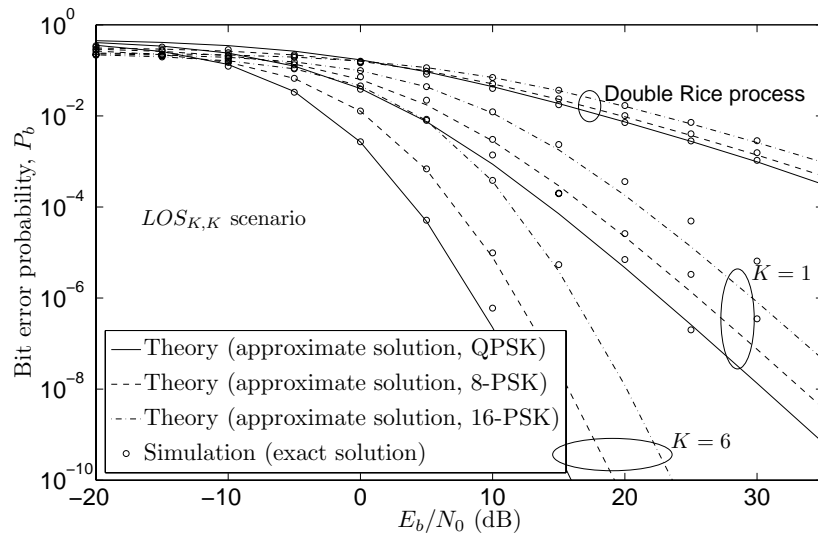


Figure M.5: The average BEP P_b of M -ary PSK modulation schemes over M2M fading channels with EGC under full-LOS propagation conditions.

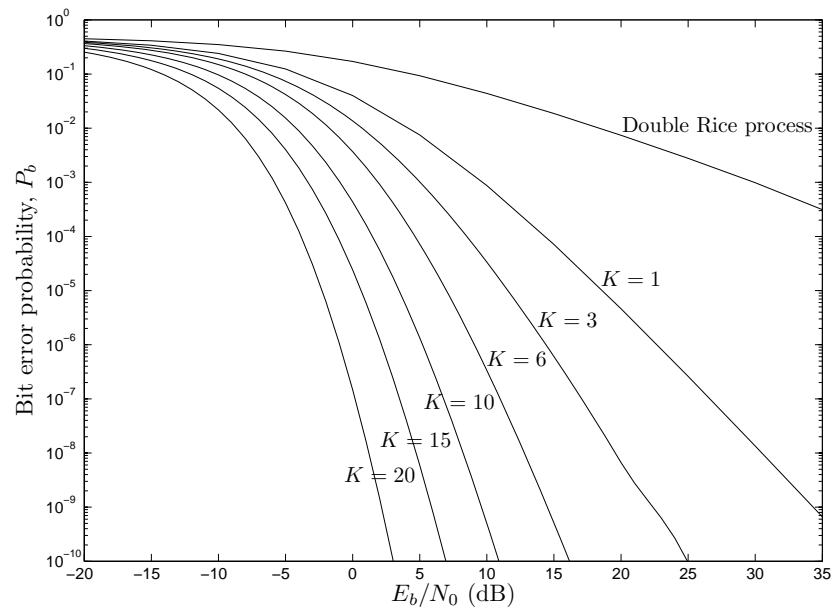


Figure M.6: The average BEP P_b of M -ary PSK modulation schemes over M2M fading channels with EGC for $LOS_{K,K}$ scenario.

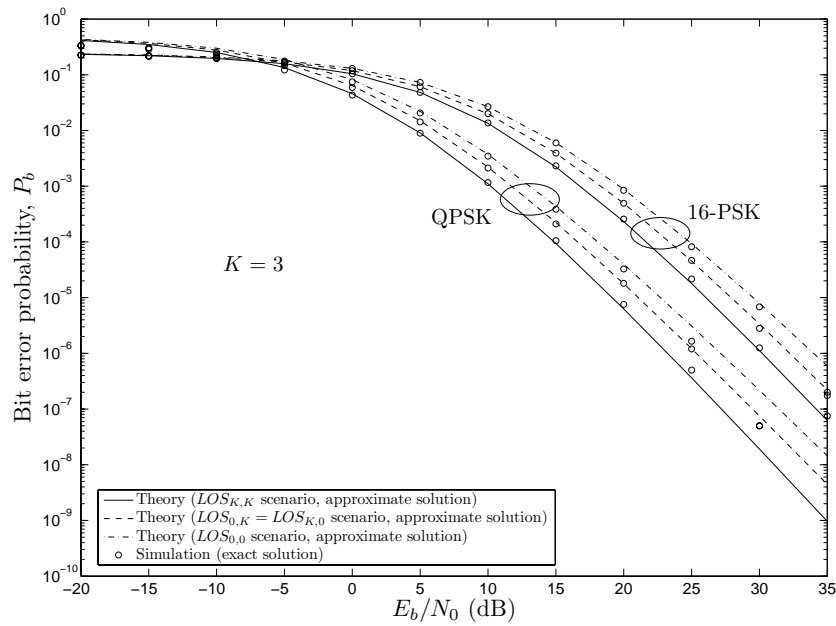


Figure M.7: The average BEP P_b of M -ary PSK modulation schemes over M2M fading channels with EGC under different propagation conditions.

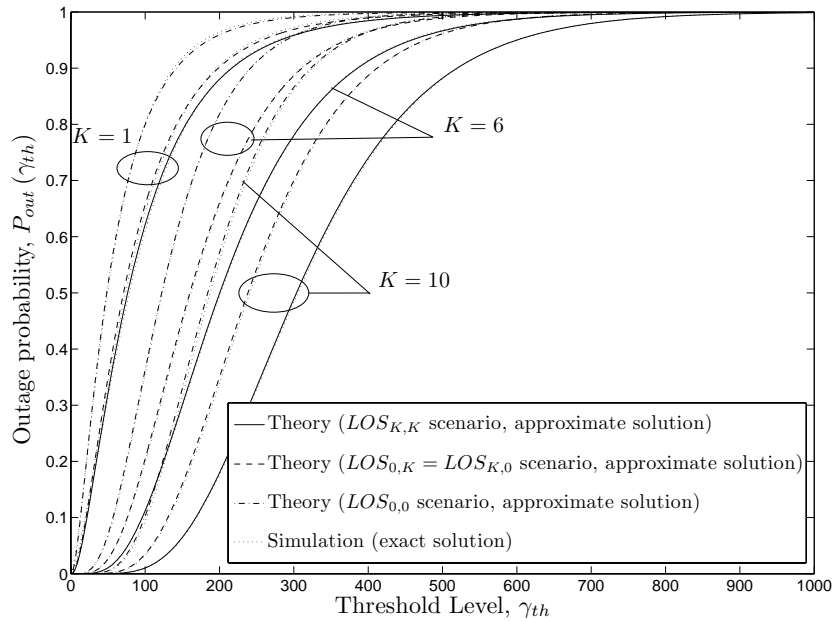


Figure M.8: The outage probability $P_{out}(\gamma_{th})$ in M2M fading channels with EGC under different propagation conditions.

